Indiana Department of Transportation – Research Division
NATIONAL POOLED FUND STUDY NO. 176

VALIDATION OF SHRP ASPHALT MIXTURE SPECIFICATIONS USING ACCELERATED TESTING

Final Report

By:
James L. Stiady
Adam J. T. Hand
A. Samy Noureldin
Khaled Galal
Jiangfeng Hua
Thomas D. White

Edited by:
Tommy E. Nantung

February 2003

TABLE OF CONTENTS

Page

Page

Page

Page

Page

PREFACE

The National Pooled Fund Study No. 176, "Validation of SHRP Asphalt Mixture Specifiactions Using Accelerated Testing", was initiated in 1997 and it incorporated two phases. The purpose of Phase I was to evaluate the sensitivity of tests to changes in certain factors within the framework of the Superpave specifications. The purpose of Phase II was to provide data for analysis of the effects of the primary factors of the study. The principal investigators of the study were Dr. Thomas D. White, Dr. Brian J. Coree, Dr. John Haddock, Dr. A. Samy Noureldin, and Dr. Adam J. T. Hand.

The overall objectives of this study were to validate various HMA aggregate specifications and volumetric relationships established by Superpave. Specifically, the study addressed the effects of voids in mineral aggregate (VMA), fine aggregate angularity (FAA), and HMA mixture gradation on the rutting performance of mixtures designed in accordance with the Superpave volumetric mixture design procedure (N-design of 96).

Mixture designs were conducted using a single neat PG64-22 binder, two nominal maximum aggregate sizes (19 and 9.5mm), two coarse aggregate types (limestone and granite), three fine aggregate types possessing FAA values of 39, 44, and 50, and three gradation types (above, through, and below the restricted zone). The rutting performance of the mixtures were evaluated using the INDOT/Purdue Accelerated Pavement Test Facility (APT), the Purdue Laboratory Wheel Track Test Device (PURWheel), and the Superpave Shear Tester (SST). In addition, triaxial testing was utilized to identify critical VMA.

Test results indicate that APT, PURWheel, SST, and Triaxial test are sensitivite to material property changes. The observed VMA associated with rutting was higher than the Superpave minimum VMA requirements. VMA could not be correlated with performance data. Film thickness was identified as a robust mixture property that correlated better with rutting performance than traditional volumetric properties. Fine aggregate angularity was found to correlate with performance, but incorporating very

high fine aggregate angularity did not necessarily provide better performance. Gradation influences APT, PURWheel, SST, and triaxial test results. However, the restricted zone may not be adequate to characterize gradation to ensure acceptable performance. The asphalt binder content corresponding to optimum triaxial strength and PURWheel rutting performance ranged from 0.0 to 0.5 percent less than the Superpave design asphalt binder content for most mixtures.

Based on all test results and analyses, it is suggested that film thickness be included in mixture design procedures with an acceptable range of 7 to 9 microns. Despite the importance of VMA in describing the HMA structure, stringent VMA criteria are not suggested because many factors can impact VMA process, such as asphalt binder content and density. These factors could deceive the essence of VMA as a durability or HMA structure parameter. The use of a typical value of FAA (≈ 45) is suggested for acceptable rutting performance. The mixture design and performance data suggest that achieving 4.0 percent air voids, the level at which the design asphalt binder content is selected in the Superpave mixture design process, when using high FAA (≈ 50) blends can lead to excess asphalt and thus poor rutting performance. Despite the importance of gradation in building aggregate structure, the selection of gradation with respect to the Superpave restricted zone as a requirement for performance is not suggested because equally adequate performance was observed with gradations plotting above, through, and below the restricted zone. Finally, a range of dust proportion of 0.9 to 1.7 is suggested for optimum rutting performance.

ACKNOWLEDGMENTS

The authors would like to acknowledge the support and guidance of the agencies and individuals involved in this research. The National Pooled Fund Study No. 176, "Validation of SHRP Asphalt Mixture Specifications Using Accelerated Testing" was supported by twenty-seven State Departments of Transportation: Arkansas, California, Connecticut, Florida, Georgia, Kansas, Illinois, Indiana, Iowa, Maine, Massachusetts, Michigan, Minnesota, Mississippi, Nebraska, New Jersey, North Carolina, North Dakota, Ohio, Oklahoma, Oregon, Pennsylvania, South Carolina, Texas, Virginia, Washington, and Wisconsin.

Representatives of fifteen of twenty-seven states served as Technical Advisory Committee (TAC) members. They represented California, Connecticut, Florida, Georgia, Illinois, Indiana, Iowa, Michigan, Minnesota, New Jersey, Ohio, Oregon, Pennsylvania, South Carolina, and Virginia. The Indiana Department of Transportation was the lead state and along with the Federal Highway Administration provided support and project administration.

Professor Thomas Kuczek of Purdue University was the statistic consultant for this project., Dr. Changlin Pan, and Dr. Aiwen Feng were actively involved in Phase I of the project. Dr. Khaled Galal was the manager of INDOT/Purdue APT facility and Dr. Tommy E. Nantung was the INDOT project manager for the project.

Professor Thomas L. Robertson and Charlie Crow of Purdue University were electrical and mechanical consultants, respectively, in troubleshooting equipment. Calvin C. Reck was the INDOT/Purdue APT operator. Kevin Brower was the INDOT laboratory technician who provided tremendous support in conducting the experiments. Joe Walters and Janet Lovell of Purdue University were laboratory supervisors who also provided support in conducting the experiments.

LIST OF TABLES

Page

Page

Page

Page

Page

Page

Page

Page

LIST OF FIGURES

Page

Page

Page

Page

Page

Page

Page

Page

Page

Page

Page

Page

1 INTRODUCTION

1.1. Background

In 1987, an ambitious five-year, $150 million research program began in the United States to benefit the nation's streets and highways. This research effort was known as the Strategic Highway Research Program (SHRP). Fifty of the $150 million specifically was dedicated to research aimed at improving the technologies associated with, and the understanding of, asphalt binders and hot mix asphalt (HMA) mixtures. The result of the SHRP asphalt research program was a performance-based system of specifying and testing asphalt binders and HMA mixtures. This system has since become known as Superior Performing Asphalt Pavements, or Superpave.

With the aid of the Federal Highway Administration (FHWA), SHRP provided an "implementable" Superpave asphalt mixture design and analysis system. Corresponding test equipment and procedures are part of this package. The Superpave system is performance-based and has promise for long-term improvement of the highway infrastructure. However, in spite of the effort and resources that have been applied to its genesis, it contains a number of factors that are of some concern to many of the agencies seeking to implement the system.

As Superpave exists today, it consists of tests and specifications for asphalt binders and an HMA mixture design method. The Superpave mixture design method can be applied solely as a volumetric design process, or the volumetric design can be coupled with either an intermediate or complete analysis of the mixture. The mixture analysis component of Superpave is sophisticated and complicated, in both the equipment used and the performance-based algorithms employed. These are of concern to many states, and are still under review by various Technical Working Groups and Expert Task Groups working under the aegis of the FHWA Office of Technology Applications. The

Superpave volumetric design method on the other hand, has evolved from the more conventional design and evaluation methods familiar to most practicing highway professionals.

Although the Superpave volumetric mixture design procedure is generally well understood, some aspects of the new specifications, the fine aggregate angularity requirements for example, are not achieving immediate or universal acceptance. With increased experience from implementing Superpave, many State Departments of Transportation (DOT's) have questioned the validity and practicality of some of the specifications and/or methods used. While wide-scale laboratory testing has been completed on some aspects of Superpave, some elements remain relatively untested. For this reason, a study was proposed to use accelerated pavement testing for validation of critical Superpave factors. From this suggestion eventually sprang the National Pooled Fund Study Number 176.

1.2. Objective

The overall objectives of this study are to validate various HMA aggregate specifications and volumetric relationships established by Superpave. Specifically, the study addresses the effects of voids in mineral aggregate (VMA), fine aggregate angularity (FAA), and HMA mixture gradation on rutting performance of mixtures designed using the Superpave volumetric design procedure. The interrelationships of these three variables will also be explored.

1.3. General Problem Statement

Although the volumetric mixture design method proposed by Superpave is familiar to many, there is some reluctance to adopt it without further study. This feeling may stem from the effective exclusion by the new specifications of mixtures, which are

known to perform acceptably under local conditions, or from the difficulty of some agencies to meet and/or exceed the new requirements. Three high priority factors of the Superpave volumetric design procedure were identified for investigation in this project. These topics are:

- Effect of voids in the mineral aggregate on rutting performance,
- Effect of fine aggregate angularity on rutting performance, and
- Effect of gradation on rutting performance.

The three topics relate largely to the Superpave "consensus aggregate properties" and to aggregate effects on mixture performance.

1.3.1. Effect of VMA on Rutting Performance

The Superpave definition of VMA is "...the sum of the volume of air voids and effective (unabsorbed) binder in a compacted sample" (McGennis, et al., 1995). Minimum VMA values are specified at the design air void content of four percent as a function of nominal maximum aggregate size. It is to be noted that there are thus two attributes of VMA:

- that which can be measured in a mixture and which provides a measure of the state of a mixture, and
- some critical VMA which defines a threshold between acceptable and unacceptable performance.

This definition and specification may be traced directly back to a paper by McLeod (McLeod, 1959) in which he proposed "... a suggested relationship between minimum VMA and nominal maximum aggregate size. This relationship is intended to ensure that the VMA values of dense-graded bituminous paving mixtures will be large enough to provide sufficient space for the quantity of bitumen needed for durability, together with the minimum air voids required to prevent flushing or bleeding ... (and) is subject to modification as further experience and additional test data are accumulated."

In fact, McLeod's originally proposed relationship between minimum VMA and nominal maximum aggregate size has remained essentially unmodified over the intervening thirty-seven years; the only adjustments appear to have been occasional redefinition of nominal maximum aggregate size.

Some State agencies have expressed reservations about the Superpave VMA criteria. There is a question related to the gradation. McLeod's proposed definition was specifically related to dense-graded bituminous paving mixtures, while Superpave specified gradations specifically exclude dense-graded mixtures as defined by McLeod (Fuller/Weymouth maximum density gradations). There is a further question, which addresses the validity of the implication that minimum VMA is a function of nominal maximum aggregate size alone. There is published data (Kallas, 1957 and Lefebvre, 1957) which suggest that the critical VMA of identically graded aggregates may be significantly influenced by the textural quality of the aggregate, more specifically of the fine aggregate (sand) fraction. A further question remains as to the constancy of the critical VMA when different gradations with the same nominal maximum aggregate gradations are used. Thus, three questions can be addressed in reference to critical VMA:

- Is the Superpave VMA vs. nominal maximum aggregate size relationship valid (i.e., does it adequately differentiate between stable and unstable mixtures)?,
- Is this relationship independent of fine aggregate angularity?, and
- Is this relationship independent of gradation relative to a given maximum density line?

As stated above the VMA criteria was adopted to maximize the amount of asphalt binder for durability short of flushing and bleeding. Continued use of the criteria, specifically for mixtures other than dense graded mixtures, may produce design asphalt binder contents that are excessive. The result of continued use might be mixtures with a high propensity for rutting. It is for this reason that the current study incorporates tests that examine strength and rutting potential. Results of these tests will help to support continued use or adjustment of the VMA criteria.

1.3.2. Effect of Fine Aggregate Angularity on Rutting Performance

Superpave defines fine aggregate angularity as "the percent air voids present in loosely compacted aggregates smaller than 2.36 mm (McGennis, et al., 1995)," and specifies three levels (less than 40, 40, and 45 percent) depending upon the amount of traffic and proximity of the layer to the pavement surface (Table 1.1). These fine aggregate angularity criteria are intended "to ensure a high degree of fine aggregate internal friction and rutting resistance (McGennis, et al., 1995)."

A number of participating state agencies have expressed concern with the fine aggregate angularity requirements in that:

- they may experience difficulties in meeting the Superpave requirements with local materials, or
- they have evidence of local materials which do not meet the Superpave specification but have provided what they, the given state agency, consider acceptable performance.

While there is evidence indicating the benefit of fine aggregate angularity on mixture rutting performance, the question remains as to the validity of the levels defined by Superpave on actual rutting performance.

1.3.3. Effect of Mixture Gradation on Rutting Performance

It is felt by many in the hot mix asphalt (HMA) industry that more rut-resistant mixtures are obtained by selecting a gradation falling below the Superpave restricted zone. However, an alternative opinion does exist that gradations above the Superpave restricted zone might provide equally rut-resistant performance. It was suggested that this study include a comparison between the performance of mixtures above, through, and below the restricted zone. However, a single such comparison would likely prove to be inconclusive since it is effectively impossible to design such mixtures in which the only

point of departure is gradation. The interrelationships between gradation, aggregate properties, and volumetrics are such that this type of comparison is difficult.

1.4. Specific Problem Statement

With the above discussion in mind, this project is designed to provide answers to the following specific questions:

- Does the Superpave minimum VMA vs. nominal maximum aggregate size relationship adequately define the threshold between stable and unstable mixtures?
- Is the Superpave minimum VMA vs. nominal maximum aggregate size relationship independent of fine aggregate angularity (FAA)?
- Is the Superpave minimum VMA vs. nominal maximum aggregate size relationship independent of the shape of gradation?
- What effect does fine aggregate angularity have on the performance of otherwise identical mixtures?
- What effect does gradation, above, through, and below the restricted zone, have on the performance of similar mixtures?

The research was designed to answer these questions as well as provide data defining effects of the various factors.

Table 1.1 Fine Aggregate Angularity Criteria.

Traffic (ESAL)	Depth from Surface	
	<100 mm	>100 mm
$<3 \times 10^5$	-	-
$<1 \times 10^6$	40	-
$<3 \times 10^6$	40	40
$<3 \times 10^7$	45	40
$<1 \times 10^8$	45	45
$>1 \times 10^8$	45	45

2 TEST PLAN

A total of nine tasks were identified by the Study Technical Advisory Committee to effectively address the objectives of this research. These tasks included:

Task 1 – Methodology;

Task 2 - Determine Sensitivity of Test Methods;

Task 3 - Complete Mixture Designs;

Task 4 - Measure Critical VMA;

Task 5 - Interim Report;

Task 6 - PURWheel Testing;

Task 7 - APT Testing;

Task 8 - Superpave Mixture Analysis; and

Task 9 - Final Report.

2.1 Task 1- Methodology

The quickest approach to obtain an indication of pavement performance is through the use of accelerated loading methods. The Indiana DOT/Purdue University Accelerated Pavement Test (APT) Facility is one of several accelerated loading facilities. Other commonly known prototype scale facilities are the FHWA Accelerated Loading Facilities (ALF), South African Heavy Vehicle Simulator (HVS), Texas Mobile Load Simulator (MLS), and full-scale test tracks such as the AASHO Road Test, WASHO Road Test, MnRoad, Penn State Test Track (PTI), and WesTrack (Metcalf, 1996).

Accelerated test facilities are not only attractive because they provide performance data in time periods which are much shorter than that of a typical pavement life, but also because they are small enough that thorough materials investigations may be conducted (Hand, 1998).

The current Superpave volumetric mixture design method lacks strength and/or performance tests. In fact there is currently no mechanical test in the method to assess potential performance. This has left agencies with the need for a tool to estimate rutting performance in the mixture design process. Committee A2DO5 of the Transportation Research Board identified laboratory evaluation of mixtures for rutting potential as a major deficiency in the Superpave volumetric mixture design system. The Purdue laboratory wheel track test device (PURWheel) is one of several laboratory wheel testing devices being utilized in the U.S. Other devices include the Laboratoire Central des Ponts et Chaussees (LCPC) French Rutting Tester, the Asphalt Pavement Analyzer formerly known as the Georgia Loaded Wheel Tester (GLWT), and the Hamburg Steel Wheel Tracking (HSWT) Device. The ability of these devices to provide an indication of field performance has been questioned. This issue could be answered by comparing laboratory wheel test results with full-scale pavement performance under controlled conditioned.

Comparison between INDOT/Purdue APT and PURWheel tests was developed to investigate more aspects of HMA mixture properties efficiently. Comparison between French Rutting Tester (LCPC), Georgia Loaded Wheel Tester, Hamburg Steel Wheel Tracking, and PURWheel tests and observed performance at WesTrack has been conducted using samples cut from WesTrack field sections with good correlation (Williams, et al, 1999 and Huber, et al., 1999). However, preliminary study indicates that compaction and mixture preparation methods significantly impact the comparison (Haddock, et al., 1998). Therefore, the comparison between INDOT/Purdue APT and PURWheel tests was developed giving extensive consideration to the effect of compaction and mixture preparation methods.

Simple tests are needed to determine material properties accurately and precisely. A simple test can determine material properties directly, while a non-simple test must

determine the material properties by inverse analysis of the measurements. A triaxial test is believed to have the desired simple test capability for HMA (Lytton, 2000). Although triaxial tests are commonly utilized in geotechnical engineering, triaxial tests have been employed in HMA mixture testing since the 1950's. In this study, triaxial tests were employed to identify the mixture transition from the stable to unstable condition over a range of asphalt binder contents following Monismith and Valerga's work conducted in 1956 REF. Like other laboratory tests, the ability of the triaxial test to identify HMA mixture performance is questioned. This issue was addressed by comparing triaxial and PURWheel test results with performance in the APT.

The Superpave Shear Tester (SST) was employed for permanent deformation evaluation of the mixtures. Also, two SST modes were selected; frequency sweep test at constant height (FSCH) and repeated shear test at constant height (RSCH). Comparison between APT and SST results was made by testing the same mixtures.

Finite element analysis (FEA) was employed to model HMA mixture rutting performance. The model was calibrated using APT and PURWheel test results. A calibrated model could be utilized to extend and explain effects of material, load, and construction factors on asphalt mixture rutting performance. FEA was employed to correlate APT and PURWheel results.

2.2 Task 2- Determine Sensitivity of Test Methods

The sensitivity of a test method to HMA material and mixture characteristics determines its usefulness. The repeatability of APT, PURWheel, and triaxial test methods are difficult to evaluate because of their destructive nature. It is almost impossible to reproduce the exact properties of mixtures tested especially for APT and PURWheel tests. Therefore, sensitivity of the APT and PURWheel were evaluated by testing several mixtures having distinct properties.

The mixtures were designed in accordance with the Superpave volumetric mixture design protocol. Because fine aggregate is believed to strongly influence rutting performance, the mixtures were selected from a 19mm limestone coarse aggregate in combination with three fine aggregates having different FAA values (39, 44, and 50) and gradations plotting above and below the restricted zone. The mixtures that were tested to evaluate the sensitivity of APT and PURWheel are marked with a √ symbol in Table 2.1. The sensitivity of the SST was also evaluated using the same mixtures.

The sensitivity of the triaxial test was evaluated more rigorously by combining two nominal maximum aggregate sizes (19 and 9.5mm), three gradations with respect to the restricted zone (plotting above, through, and below), and one fine aggregate (FAA of 44). The mixtures that were tested to evaluate the sensitivity of triaxial test are marked with a √ symbol in Table 2.1.

2.3 Task 3- Complete Mixture Designs

As previously stated, the objectives of this study were to evaluate the effects of voids in mineral aggregate (VMA), fine aggregate angularity (FAA), and gradation relative to a given maximum density on HMA performance. However, there are several factors that may influence VMA, for example gradation, fine aggregate angularity, particle shape and surface, texture, nominal maximum size, and coarse aggregate type. Fine aggregate angularity is believed to encompass fine aggregate particle shape and surface texture. In order to evaluate a wide range of VMA and FAA, two nominal maximum aggregate sizes, two coarse aggregate types, three gradations with respect to the restricted zone, and three fine aggregate sources having three levels of fine aggregate angularity were used in the study. A single neat PG 64-22 asphalt binder was used.

2.3.1 Subtask 1- Obtain Necessary Materials

All the required aggregate materials for the project were manufactured and stockpiled at one time, thereby ensuring material uniformity throughout the project. These materials were stored on-site by the aggregate manufacturer. Adequate quantities of materials were shipped to the laboratory and/or hot mix plant as needed. The fine aggregates used in the study were selected to have low, intermediate, and high values of FAA. The fine aggregates used exhibited FAA values of 39, 44, and 50. These sands were a natural sand (FAA = 39), a limestone sand (FAA=44), and a granite sand (FAA=50). Coarse aggregates used for the project were a limestone and a granite from the same sources. The selected aggregates also satisfied a goal to include materials typically used in asphalt mixtures throughout the U.S.

A single neat binder, PG 64-22, was used for the study. However, it was not feasible to obtain a sufficient quantity of PG 64-22 asphalt binder at the start of the work to ensure a consistent supply throughout the project. This issue arises from the logistics of producing mixture for the APT. As an alternative, at the outset of the project, a sufficient amount of PG 64-22 was obtained for all laboratory testing. When binder was required for production of APT mixtures, the PG 64-22 was obtained from the same supplier. The binder used for both the laboratory and the APT testing was refined from the same crude source using identical processes. In all cases, the binder was stored in such a manner as to minimize aging effects during storage.

2.3.2 Subtask 2- Characterize Materials

The materials obtained in Subtask 1 (2.3.1) were subjected to a full characterization using Superpave protocols. Coarse aggregate testing consisted of washed gradation analysis, Los Angeles abrasion, deleterious materials, sodium sulfate soundness, specific gravity and water absorption, fracture face identification, and flat elongated particle tests. Fine aggregate testing consisted of washed gradation analysis, specific gravity and water absorption, fine aggregate singularity, and sand equivalency

tests. The asphalt binder was tested according to AASHTO PP6, "Practice for Grading or Verifying the Performance Grade of an Asphalt Binder" to ensure that it met the desired grade.

2.3.3 Subtask 3- Mixture Designs

A total of twenty-one mixture designs were conducted in accordance with AASHTO MP2, "Standard Specification for Superpave Mix Design" REF. They were performed nearly simultaneously with PURWheel and APT testings. For the sake of time and materials efficiency, not all combinations of all experimental factors were designed. For example, it was expected that the mixtures incorporating natural sand with FAA of 39 would provide poor rutting performance, accordingly only two mixtures were designed with the natural sand (FAA of 39).

A Pine Instruments Superpave Gyratory Compactor (SGC) was used to compact all specimens. For the purposes of this research $N_{initial}$, N_{design}, and $N_{maximum}$, were 8, 96, and 152 revolutions, respectively. This was the compactive effort specified in Superpave for a traffic level of 3-10 million Equivalent Single Axle Loads (ESAL) and an average design high air temperature of less than 39^0C at the time the project was initiated.

2.4 Task 4- Measure Critical VMA

Many researchers believe that achieving the minimum VMA requirements is the most difficult step in the Superpave mixture design process (Anderson and Bahia, 1997) and that it is too restrictive for economical mixtures with acceptable performance properties (Hinrichsen and Heggen, 1996). Others have recommended that average asphalt film thickness be considered in the Superpave volumetric mix design system (Hinrichsen, et al, 1996 and Kandhal, et al, 1998). Review of the asphalt literature reveals that asphalt technologists have debated these issues for decades (Coree, 1999).

In this study, critical VMA was evaluated from rutting performance. Mixtures having extremely low and high design VMA were selected and tested in the APT. Some of the mixtures with low design VMA did not quite meet Superpave requirements but were tested in the APT. The hypothesis behind this decision was that if minimum VMA correlates with rutting performance, mixtures that violated minimum VMA requirements would exhibit unacceptable rutting performance. Because VMA is influenced by density and AC, some of the mixtures tested in the APT were constructed at both high and low density levels, while the others were constructed at the design as well as design plus and minus 0.5 percent.

Once the correlation between APT and PURWheel tests was developed, the critical VMA could be identified further by testing more mixtures using the PURWheel. The purpose of testing more mixtures using the PURWheel was to establish the relationship between PURWheel rutting performance and VMA. This relationship would be utilized to identify the critical VMA corresponding to unacceptable rutting performance.

Comparing PURWheel and triaxial test results would allow critical VMA be evaluated using triaxial tests. The correlation between triaxial and PURWheel test results would be utilized to identify triaxial response corresponding to PURWheel rutting performance. Then, the relationship between triaxial test result and VMA would be established. Combining a triaxial and PURWheel correlation with a triaxial test result and VMA relationship would allow critical VMA be evaluated using triaxial tests. Another approach to identifying critical VMA using the triaxial test is to identify the VMA corresponding to mixture transition from the stable to unstable condition. The mixture transition could be identified by testing specimens over a range of AC.

2.5 Task 5- Interim Report

The project interim report provided a summary of preliminary results of this study. They are summarized as follows (Haddock, et al., 1998):

- APT and PURWheel are sensitive to fine aggregate angularity, gradation, and density.
- The triaxial test is sensitive to gradation, compaction energy, and AC level.
- There is an indication that correlation between APT and PURWheel is influenced by compaction and mixture preparation methods.
- Rutting performance of mixtures incorporating the natural sand fine aggregate were obviously unacceptable in APT and PURWheel tests. Accordingly, there is no need to include mixtures incorporating natural sand as the fine aggregate in further study.
- APT, PURWheel, and Triaxial test results indicate that mixtures with gradations plotting above the restricted zone exhibit better performance than those with gradations plotting through and below the restricted zone. Consequently, further study concentrates on mixtures with gradations plotting through and below the restricted zone.

2.6 Task 6- PURWheel Testing

In this study, the sensitivity of the PURWheel to changes in Superpave material and mixture properties was evaluated. It was also correlated with APT tests, utilized to evaluate Superpave mixture properties, and correlated with Triaxial tests. Several studies have indicated that PURWheel test results are sensitive to mixture properties (Haberman, 1994, Pan, 1997, and Lee, 1998). Sensitivity to Superpave mixture properties was expected and evaluated in the beginning of this study. The mixtures that were tested in

order to evaluate sensitivity of PURWheel are summarized and marked with a √ symbol in Table 2.1.

Correlation between APT and PURWheel test results was developed considering the effects of compaction and mixture preparation methods. Three types of PURWheel specimens were utilized, i.e. field mixed-field compacted (FMFC), field mixed-laboratory compacted (FMLC), and laboratory mixed-laboratory compacted to field observed properties (LMLCDF) specimens. Field mixed field compacted (FMFC) specimens were slabs cut from APT test sections prior to traffic loading. Field mixed laboratory compacted (FMLC) specimens were slabs that were made from loose mixture sampled behind the paver and compacted using the Purdue Linear Compactor in the laboratory. Laboratory mixed-laboratory compacted at field observed properties (LMLCF) specimens were slabs that were made of laboratory prepared mixtures compacted using the Purdue Linear Compactor. It was expected that FMFC specimens would provide the best correlation between APT and PURWheel test results. Correlating APT and PURWheel FMLC test results would reveal the effects of compaction method. Correlating APT and PURWheel LMLCF test results would reveal the effects of both compaction and mixture preparation methods. For correlation purposes, PURWheel specimens were tested at the same temperature the APT testing (50^0 C) was conducted.

Evaluating Superpave mixture properties in the PURWheel and correlating triaxial and PURWheel tests could be conducted simultaneously. PURWheel specimens were prepared to have similar properties to triaxial specimens. Both PURWheel and triaxial tests were conducted at the same temperature (60^0 C).

2.7 Task 7- APT Testing

In this study, it was hypothesized that rutting performance in the APT was representative of field mixture performance. The sensitivity of APT test results was evaluated first by testing mixtures having distinct properties as marked with a √ symbol

in Table 2.1. The sensitivity of the APT tests to mixture density was evaluated by constructing low and high density lanes. Similarly, sensitivity of APT tests to mixture AC level was evaluated by constructing low and high AC lanes.

In order to identify critical VMA, mixtures with low and high design VMA were selected and tested in the APT. Construction of low to high density and low to high AC level test sections allowed for a broader range of VMA be evaluated.

During APT test section construction, mixture density was carefully controlled. Cores (102 mm or 4 in. diameter) were taken prior traffic loading or from out-of-wheel path locations to measure initial density. After loading, in-wheel path cores were taken to assess the density after testing. Theoretical maximum specific gravity, asphalt content by extraction, and washed gradation analyses were performed for quality control.

2.8 Task 8- Superpave Mixture Analysis

The effects of aggregate material properties on Superpave mixture design properties (volumetric) were analyzed, for example the effect of nominal maximum aggregate size on VMA. The material properties considered were nominal maximum aggregate size, coarse aggregate type, fine aggregate angularity, and gradation type. The Superpave mixture design properties analyzed were asphalt binder content (AC), voids in mineral aggregate (VMA), voids filled with asphalt (VFA), dust proportion (DP), percent Gmm at $N_{initial}$ (%Gmm@$N_{initial}$), and percent Gmm at $N_{maximum}$ (%Gmm@$N_{maximum}$). Film thickness was also analyzed.

The rutting performance of Superpave mixtures was evaluated using APT, PURWheel, Triaxial and SST tests. It is emphasized that the construction process influenced the rutting performance of the mixtures in APT tests. The rutting performance of the design and as built mixtures could be evaluated with the PURWheel. Using SGC prepared specimens for triaxial test specimens is convenient because it allows for evaluating the SGC specimens directly at specific compaction energy. However, using one SGC sample size leads to height to diameter ratio issues. The issue was addressed by stacking two SGC samples. Stacking two samples created a horizontal discontinuity plane in the specimen. The effect of discontinuity plane orientation is a classic issue in rock

mechanics. It was found that the horizontal discontinuity plane did not affect the measurement of intact specimen properties (Goodman, 1976).

2.9 Task 9- Final Report

This final report is organized into eight chapters. Chapter 1 provides a description of the background, objectives, and problem statement. Chapter 2 provides a description of the study approach, overall test plan, and critical decisions made during the study. Chapter 3 provides a description of materials and mixture designs details. The results of mixture design and statistical analyses are presented in Appendices A and B, respectively. INDOT/Purdue APT test results are discussed in Chapter 4. The statistical analysis of APT data, in-place mixture property data, and APT rutting data are summarized in Appendix C. Chapter 5 provides a discussion of PURWheel test results. Details of the PURWheel test procedure, summary of PURWheel mixture property data, and details of statistical analyses of PURWheel test results are presented in Appendices D1, D2, and D3, respectively. Triaxial test results are discussed in Chapter 6. Details of the triaxial test procedure, summary of PURWheel test data, and details of statistical analysis of PURWheel test results are presented in Appendices E1, E2, and E3, respectively. Chapter 7 provides a discussion of SST test results. Chapter 8 provides a discussion of conducted finite element analyses. Chapter 9 represents a summary of the discussion of Chapters 3 through 7. Conclusions and recommendations of the study are presented in Chapter 10.

Table 2.1 Summary of Test Plan.

FAA	Gradation	9.5 mm Nominal Max. Size								19 mm Nominal Max. Size							
		Limestone				Granite				Limestone				Granite			
		A	P	T	M	A	P	T	M	A	P	T	M	A	P	T	M
39	Above										√		X				
	Below									√	√		X				
44	Above		X	√	X					√	√	√	X				
	Through	X	X	√	X		X	X	X		X	√	X		X	X	X
	Below		X	√	X	X	X	X	X	√	√	√	X	X	X	X	X
50	Above									√	√	X	X				
	Through	X	X	X	X		X	X	X		X	X	X	X	X	X	X
	Below		X	X	X	X	X	X	X		X	X	X		X	X	X

Note: A = INDOT/Purdue APT tests
P = PURWheel tests
T = Dry Triaxial tests
M = Mixture designs
√ = to determine sensitivity of test methods
X = to evaluate HMA mixture properties

3 MATERIALS AND MIXTURE DESIGNS

3.1. Introduction

This chapter provides a description of the HMA raw materials employed and the Superpave volumetric mixture design results. Mixture designs were conducted with limestone and granite coarse aggregates and three fine aggregates; natural sand, crushed limestone sand, and crushed granite sand. The designs included both 19.0 and 9.5mm nominal maximum aggregate size mixtures with gradations plotting above, through, and below the restricted zone. A single neat PG64-22 binder was used in all of the mixtures. A summary of the combinations of coarse and fine aggregate types, nominal maximum aggregate sizes, gradation types, and fine aggregate angularity values associated with each of the twenty-one mixture designs conducted is presented in Table 3.1. The following example is used to describe the material characteristics incorporated in a given mixture design. The mixture associated with X^* in Table 3.1 is a 9.5mm nominal maximum size mixture composed of granite coarse aggregate and limestone fine aggregate with a FAA of 44 and the gradation plots through the Superpave restricted zone.

3.2. Materials Properties

3.2.1. Asphalt Binder Properties

The asphalt binder used in the study was a neat PG 64-22. The binder grade was verified in accordance with AASHTO PP6, "Practice for Grading or Verifying the Performance Grade of an Asphalt Binder." Table 3.2 shows the binder test results.

Following Superpave mix design requirements (McGennis, et.al, 1995), mixing and compaction temperatures were selected at temperatures corresponding to rotational viscosities of 0.17±0.02 and 0.28±0.03 Pa-s, respectively. The resulting mixing and compaction temperatures were 155±3^{0}C and 140±3^{0}C, respectively.

3.2.2. Coarse and Fine Aggregate Properties

Aggregates used for the study included two coarse aggregates; limestone and granite. The nominal maximum aggregate sizes of the coarse aggregates were 19 and 9.5mm for both the limestone and granite. The coarse aggregate properties are shown in Table 3.3. Three fine aggregates having fine aggregate angularities (FAA) of 39, 44, and 50 were used to determine the effect of FAA on HMA mixture properties and performance. The fine aggregate with the FAA value of 39 was a natural sand while the fine aggregates with FAA values of 44 and 50 were crushed limestone sand and granite sand, respectively. As noted previously, the fine aggregates were intentionally selected to have high, low and intermediate values of FAA. Small percentages of these materials are retained on the 2.36mm sieve, thus they are fine aggregates by ASTM definition (ASTM D1073), but slightly deviate from the SHRP definition which states that a fine aggregate has one hundred percent passes the 2.36mm sieve (SHRP A-407). They also satisfied the goal of including a wide range of materials typically used in asphalt mixtures with a geographic distribution within the US. A limestone filler was also employed. The fine aggregate and filler properties are presented in Table 3.4.

The coarse and fine aggregates meet all of the Superpave concensus aggregate property requirements for the design traffic (3-10X10^6 ESALs) and surface mixture conditions (within 100mm of pavement surface) with the exception of FAA in some cases. This was intentional and the obvious reason for it is one of the research objectives was to investigate the FAA specification limits. Thus fine aggregates with a range of FAA which bracketed the specification of 45 were used.

3.3. Hot Mix Asphalt Mixture Properties

Twenty-one HMA mixture designs were conducted for the study. They included nine 9.5mm nominal maximum size mixtures and twelve 19.0mm nominal maximum size mixtures. The mixture gradations are presented in Figures 3.1 through 3.4. These plots show that the gradations pass above (A), through (T), and below (B) the restricted zone. The figure legends indicate the FAA associated with the gradations as well as the location of the gradations relative to the Superpave restricted zone. For example, the legend 39B indicates that the FAA of the mixture was 39 and it plotted below the restricted zone. The volumetric properties at the design AC, associated with each mixture design are given in Tables 3.5 through 3.8. Complete mix design details can be found in Appendix A.

All mixture designs were conducted in accordance with Superpave volumetric design procedures as specified in AASHTO PP28-97, "Practice for Superpave Volumetric Design for Hot Mix Asphalt (HMA)" (AASHTO, June 1997). Specimens were compacted with a Pine Instruments Superpave Gyratory Compactor (SGC). $N_{initial}$, N_{design}, $N_{maximum}$ of 8, 96, and 152 gyrations, respectively were employed. This level of SGC compaction corresponds to traffic a level of 3-10 million Equivalent Single Axle Loads (ESAL) and an average design high air temperature of less than 39^0C. Other Superpave mixture design criteria for these conditions include minimum voids in the mineral aggregate (VMA) of 15 and 13 percent for 9.5 and 19mm mixtures, respectively; voids filled with asphalt (VFA) of 65 to 75 percent; dust to asphalt ratio of 0.6 to 1.2; and maximum percent compaction of 89 and 98 percent at $N_{initial}$ and $N_{maximum}$, respectively.

3.4. Material Property Effects on Mix Design Properties

The effects of coarse aggregate type, fine aggregate angularity, and gradation on HMA properties are presented in this section. The mix design data are presented and analyzed in the following manner. The individual volumetric properties obtained for each of the twenty-one mixtures are summarized in individual tables such that the overall

effects of aggregate characteristics may be assessed. General observations and trends are stated based on the tabulated data. At that point the effects of coarse aggregate type, fine aggregate angularity, and gradation on the volumetric properties are further analyzed using paired t-tests, with a significance level of five percent, for whatever paired data was available. Further conclusions are then stated based on the statistical analyses.

This statistical method is designed to determine the difference in main factors by replicate observations. The method allows main factors (eg. nominal maximum aggregate size) to be analyzed independently. The "paired data" that is employed is the difference in a given volumetric property (eg. %AC) for paired combinations of other main factors. This is best explained by example. Paired data combinations that would be used to assess the effect of nominal maximum aggregate size on design asphalt content for example are identified in Table 3.9. Each pair of circled asphalt content values connected by a line represent a paired data set. A total of nine pairs are identified in the table. Note that the for each pair of design asphalt content values, FAA, gradation type and coarse aggregate type are the same. The differences in each paired data set are then pooled to perform the t-test to determine the effect of nominal maximum aggregate size on design asphalt content. Because the replicates (paired data) are not true replications of the experiment, the effects of other factors are included in the calculations. These effects reduce the ability of the method to detect significance difference. Therefore, if the method does not detect a significance difference, it is not possible to determine whether the compared factors are not statistically different or the other factors have caused the insignificance. Detailed calculations and results of all paired t-tests discussed in this section are presented in Appendix B.

3.4.1. Asphalt Binder Content (AC).

The design asphalt binder contents for all mix designs are summarized in Table 3.9. General observation suggests that the design AC of 9.5mm nominal maximum size mixtures was higher than that of 19 mm nominal maximum size mixtures. The design AC

of limestone mixtures was higher than that of granite mixtures. The design AC of mixtures with FAA of 39 was approximately equal to that of mixtures with FAA of 44. However, the design AC of mixtures with FAA of 50 appears to be higher than that of mixtures with FAA of 44. There is no clear indication that the design AC of mixtures with gradations plotting above the restricted zone was higher that those with gradations plotting through or below the restricted zone. The design AC of mixtures with gradations plotting through the restricted zone was higher than that of mixtures with gradations plotting below the restricted zone.

The effects of nominal maximum aggregate size, coarse aggregate type, fine aggregate angularity, and gradation on asphalt binder content (AC) were assessed using paired t-tests. Results are summarized in Table 3.10. Several tests (mean comparisons) are presented along with an indication of whether or not statistically significant differences were observed. The design AC of 19mm mixtures was significantly greater than the design AC of 9.5mm mixtures. The design AC of limestone mixtures was significantly higher than that of granite mixtures. This conclusion is reasonable because the water absorption of limestone is typically greater than that of granite. The design AC of mixtures with FAA of 50 was greater than that of mixtures with an FAA of 44. The mixtures with FAA of 50 were more difficult to compact, therefore in order to achieve four percent air voids at the design number of gyrations a greater amount of asphalt was required. The hypothesis is that the aggregates essentially locked-up and the only way to reduce the level of air voids, under a given level of compaction was to fill the voids with asphalt. The design AC for mixtures with gradations plotting through the Superpave restricted zone were higher than those with gradations plotting below it. Similar statistical comparisons with respect to the lower FAA mixtures (FAA=39) and mixtures with gradations plotting above the restricted zone could not be made because insufficient paired data were available to obtain statistically valid comparisons.

A plot of FAA versus design AC for all twenty-one mixtures is presented in Figure 3.5. The relationship tends to suggest that design AC increased with increasing FAA. This is simply because the mixtures with very high FAA (≈50) were difficult to

compact, therefore they required more asphalt in order to achieve four percent air voids under the design level of compaction (N_{design} = 96).

3.4.2. Voids in Mineral Aggregate (VMA)

Voids in mineral aggregate (VMA) values at the design asphalt content for all the mixtures are summarized in Table 3.11. One of the 19mm and two of the 9.5mm mixtures slightly violate the minimum Superpave VMA specifications as noted in the table. Several general observations can be drawn from the data. The VMA of 9.5mm nominal maximum size mixtures was higher than that of 19mm nominal maximum size mixtures as expected. The VMA of limestone mixtures was higher than that of granite mixtures. The VMA of mixtures with FAA of 39 was approximately the same as the VMA of mixtures with FAA of 44. However the VMA of mixtures with FAA of 50 were higher than the VMA of mixtures with a FAA of 44. The VMA of mixtures with gradations plotting above the restricted zone was lower the VMA of mixtures with gradations plotting through or below the restricted zone. The VMA of mixtures with gradations plotting through the restricted zone was higher than that of mixtures with gradations plotting below it. This was not expected, but a plausible explanation is provided below.

Another important aspect of VMA is the typical U-shape of the VMA versus AC relationship. The typical U-shape is well observed in Marshall mix design (Roberts et.al, 1991). The shapes of the relationship at N_{design} for each mixture are summarized in Table 3.12. Only eight of twenty-one mixtures exhibited the typical U-shape. The others exhibited either flat or inverted U-shaped relationships. It is believed that mixtures which exhibited relationships other than the typical U-shape were difficult to compact. In otherwords, a non U-shaped relationship is indicative of a mixture which is difficult to compact or never densifies to a maximum aggregate packing (minimum VMA) under the level of compaction applied. The difficulty may result from mixture characteristics and/or compaction equipment. If a mixture is difficult to compact, then it should be compacted to a greater degree if greater compaction energy is applied (eg. from N_{design} to $N_{maximum}$).

If this is true, more than eight U-shaped VMA curves would be expected after $N_{maximum}$ gyrations for the given twenty-one mixtures. The shapes of VMA versus AC relationships at $N_{maximum}$are summarized in Table 3.13. Thirteen of twenty-one mixtures exhibit the U-shape. This indicates that some mixtures required more energy in order to become well enough compacted that the maximum aggregate packing or minimum VMA could be identified. This further suggests that if the typical U-shaped relationship is not observed for a given mixture under the design level of compaction (N_{design}) changes should be made in the blend (proportioning) of materials or the materials themselves such that the maximum aggregate packing or minimum VMA may be observed under the specified compaction level. This is very important because a design asphalt content should not be specified which corresponds to VMA that is on the "wet" side of the VMA curve (MS-2). Although it is not specified in the Superpave mix design method it is well established that this practice should be followed.

The positions of design AC with respect to AC at the minimum VMA for the twenty-one mixtures are summarized in Table 3.14. When the design AC is less than the AC at the minimum VMA, the position is said to be on the "dry" side of the VMA curve. When it is greater than the minimum, the position is referred to as being on the "wet" side of the VMA curve. The design AC was located on the dry side of the VMA curve for twelve of twenty-one mixtures. In general when the typical U-shape VMA versus AC relationship was observed, the design AC lay on the dry side.

The effects of nominal maximum aggregate size, coarse aggregate type, fine aggregate angularity, and gradation on void in mineral aggregate (VMA) were assessed using the paired t-test. Results are summarized in Table 3.15. As expected, the VMA of 9.5mm mixtures was significantly greater than that of 19mm mixtures. The VMA of limestone mixtures was higher than that of granite mixtures. A significant difference in VMA was observed between the mixtures with FAA of 50 and FAA of 44, with the higher FAA mixtures having higher VMA. This suggests that the higher FAA mixtures were more difficult to compact. This is also consistent with the design AC of the higher FAA mixtures being greater as previously discussed, assuming the design AC lay on the dry side of the VMA curve. The VMA of mixtures with gradations plotting through the

restricted zone was higher than the VMA of those plotting below the restricted zone. Similar observation is also reported (Kandhal, et al. 1998). Initially, this would appear to be an illogical result, and it would be if a single aggregate source of both coarse and fine aggregates were blended to produce gradations plotting below and through the restricted zone (Huber, 1992). However, the different gradation types were created by blending coarse and fine aggregates from the same source in some cases and coarse and fine aggregates from different sources in other cases. This also provides an explanation for the observation that the design AC of mixtures with gradations plotting through the restricted zone was higher than the design AC of mixtures with gradations plotting below the restricted zone. Similar statistical comparisons with respect to the lower FAA (39) mixtures and mixtures with gradations plotting above the restricted zone could not be made because insufficient paired data were available.

The relationship between VMA and design AC based on all twenty-one mixtures is presented in Figure 3.6. The positive linear relationship suggests that as VMA increases the amount of asphalt required to reduce air voids to four percent under a given level of compaction increases. This is very reasonable for a given aggregate source assuming the design asphalt contents all corresponded to the dry side of the VMA curves. However, a similar conclusion drawn from the data in Figure 3.6 could be misleading because course and fine aggregates from different sources were blended and the location of the design AC relative to the minimum VMA could not be clearly identified due to the fact that several of the VMA curves did not exhibit the typical U-shape.

The relationship between FAA and VMA is presented in Figure 3.7 for the mixtures. The relationship suggests that mixtures produced using fine aggregates with higher FAA resulted in higher VMA. Figure 3.6 suggests that as VMA increased design AC also increased. Therefore the data suggests that increasing FAA will result in increased VMA which will in turn will result in higher design AC levels. The relationship between FAA and VMA is consistent with fine aggregate angularity study using PURWheel (Lee, 1998).

3.4.3. Voids Filled with Asphalt (VFA)

The voids filled with asphalt (VFA) values for all the mix designs at the design AC level are summarized in Table 3.16. All values satisfy the Superpave criteria. General observation suggests that the VFA of 9.5mm nominal maximum size mixtures was higher than that of 19 mm nominal maximum size mixtures. The VFA of limestone mixtures was higher than that of granite mixtures. The VFA of mixtures with FAA of 39 was approximately equal to the VFA of mixtures with FAA of 44. The VFA of mixtures with FAA of 50 was higher than that the mixtures with FAA of 44. There is no clear indication that the VFA of mixtures with gradations plotting above the restricted zone was lower than that of mixtures with gradations plotting through or below the restricted zone. The VFA of mixtures with gradations plotting through the restricted zone was higher than that of mixtures with gradations plotting below the restricted zone.

The effects of nominal maximum aggregate size, coarse aggregate type, fine aggregate angularity, and gradation on voids filled with asphalt (VFA) were also evaluated using paired t-tests. Results are shown in Table 3.17. The VFA of 9.5 mm mixtures was higher than that of 19 mm mixtures. The VFA of limestone mixtures was higher than that of granite mixtures. The VFA of mixtures with FAA of 50 was higher than that of mixtures with FAA of 44. The VFA of mixtures with gradations plotting through the restricted zone was higher than that of mixtures with gradations plotting below the restricted zone. Similar statistical comparisons with respect to the lower FAA (39) mixtures and mixtures with gradations plotting above the restricted zone could not be made.

3.4.4. Dust Proportion (DP)

Dust proportion (DP) values for all the mix designs at their respective design AC are summarized in Table 3.18. The DP of eight of twenty-one mixtures did not fall within the Superpave specification of 0.6 to 1.2 in place at the time the mixture designs were

conducted. Most of the mixtures having gradations above and through the restricted zone did not meet the requirement. It was expected that this would be the case when the research was initiated. The recently recommended change in DP criteria to 0.8-1.6 for mixtures with gradations plotting below the restricted zone would only have impact on three of the mixtures (Brown et. al, 1999 and AASHTO, 1999).

The data in Table 3.18 suggests that the DP of 9.5mm nominal maximum size mixtures was approximately the same as that of 19mm nominal maximum size mixtures. The DP of granite mixtures was higher than that of limestone mixtures. The DP of mixtures with gradations plotting above the restricted zone was higher that of mixtures with gradations plotting through or below the restricted zone. The DP of mixtures with gradations plotting through the restricted zone was higher than that of mixtures with gradations plotting below it.

The paired t-test was used to assess the effects of nominal maximum aggregate size, coarse aggregate type, fine aggregate angularity, and gradation on dust proportion (DP). Results are shown in Table 3.19. The DP of mixtures with gradations plotting above the restricted zone was higher than that of mixtures with gradations plotting below the restricted zone. Although some comparison on gradations did not yield significant conclusion, there was a clear indication that as gradation type moves from below to above the restricted zone DP increased as expected. No significant conclusions could be drawn as to the effects of nominal maximum aggregate size, coarse aggregate type, and fine aggregate angularity on DP.

The relationship between FAA and dust proportion is presented in Figure 3.8. There does not appear to be any relationship between FAA and DP.

3.4.5. Film Thickness (FT)

Calculated film thickness (FT) values for each mixture design at the design AC are summarized in Table 3.20. FT was determined in accordance with the techniques

incorporated in the Hveem mix design method (Roberts, et al, 1991). The unit of FT is microns (10^{-6} m). Similar ranges of FT values were observed for 9.5 and 19mm nominal maximum size mixtures. The FT of limestone mixtures was greater than that of granite mixtures. The range of FT associated with mixtures produced using fine aggregates with FAA of 39, 44, and 50 were similar. The FT of mixtures with gradations plotting below the restricted zone was higher that the FT of mixtures with gradations plotting through or above the restricted zone. The FT of mixtures with gradations plotting through the restricted zone was higher than the FT of mixtures with gradations plotting above it.

The results of paired t-tests used to assess the effects of nominal maximum aggregate size, coarse aggregate type, fine aggregate angularity, and gradation on FT are summarized in Table 3.21. The FT of limestone mixtures was significantly greater than the FT of granite mixtures. This is consistent with the limestone mixtures having higher design AC, VMA, and VFA than the granite mixtures. The FT of 19mm mixtures with FAA of 50 was greater than the FT of 19mm mixtures with FAA of 44. The same observation is not drawn for 9.5mm mixtures. This indicates that although mixtures with FAA of 50 had higher design AC than those with FAA of 44 mixtures, other factors, especially nominal maximum aggregate size affect FT. The FT of below the restricted zone mixtures was greater than through and above the restricted zone mixtures.

Figure 3.9 represents the relationship between FT and FAA. The relationship suggests that FAA did not affect film thickness, although mixtures with high FAA required higher design AC. However, as previously discussed, the combination of nominal maximum aggregate size and FAA played an important role in determining film thickness.

3.4.6. Percent Gmm at $N_{initial}$ (%Gmm@N_{ini})

The percent Gmm at $N_{initial}$ (%Gmm@N_{ini}) values for all the mix designs at their respective design AC are summarized in Table 3.22. Within the context of Superpave,

%Gmm@N_{-ini} is used to identify mixtures, which could have the tendency to be tender (Kennedy, et al., 1994 or SHRP-A-410). One could also interpret this property as an indication of the workability of a mixture. A more readily compactible mixture would exhibit a higher %Gmm@N_{ini} value. General observation based on the data in Table 3.22 suggests that %Gmm@N_{ini} of 19mm nominal maximum size mixtures was greater than that of 9.5mm nominal maximum size mixtures. The %Gmm@N_{ini} of limestone mixtures was less than that observed for granite mixtures. As FAA increased from 39 to 44 to 50, %Gmm@N_{ini} decreased. The %Gmm@N_{ini} of mixtures with gradations plotting above the restricted zone was higher that of mixtures with gradations plotting through or below the restricted zone. The %Gmm@N_{ini} of through the restricted zone mixtures was higher than that of below the restricted zone mixtures.

Table 3.23 summarizes the results of paired t-tests used to assess the effects of nominal maximum aggregate size, coarse aggregate type, fine aggregate angularity, and gradation type on %Gmm@N_{ini}. The %Gmm@N_{ini} of limestone mixtures was less than that of granite mixtures. The %Gmm@N_{ini} of mixtures with FAA of 44 was higher than that of mixtures with FAA of 50. In general, as FAA increased %Gmm@N_{ini} decreased as expected indicating that mixtures with higher FAA values are more resistant to compaction. The %Gmm@N_{ini} of mixtures with gradations plotting above the restricted zone was higher than that of mixtures with gradations plotting below it. However, comparisons of mixtures with gradations plotting above and through, as well as through and below the restricted zone did not yield significant differences.

The relationship between percent Gmm at $N_{initial}$ and FAA is presented in Figure 3.10. As noted above, the relationship suggests that mixtures with higher FAA were slightly more difficult to compact and this was reflected by lower %Gmm@N_{ini}.

3.4.7. Percent Gmm at $N_{maximum}$ (%Gmm@N_{max})

Table 3.24 is a summary of percent Gmm at $N_{maximum}$ (%Gmm@N_{max}) values at the design AC level. The %Gmm@N_{max} specification is used to insure that a mixture will not compact excessively under the anticipated traffic, become plastic, and lead to permanent deformation (Kennedy, et al., 1994 or SHRP-A-410). The data in Table 3.24 suggests that %Gmm@N_{max} of 19mm nominal maximum size mixtures was higher than that of 9.5mm nominal maximum size mixtures. The %Gmm@N_{max} of limestone and granite mixtures were approximately equal. FAA does not appear to have an effect on %Gmm@N_{max}.The %Gmm@N_{max} of below the restricted zone mixtures was higher that of through or above the restricted zone mixtures. The %Gmm@N_{max} of mixtures with gradations plotting above the restricted zone was higher than that of mixtures with gradations plotting through it.

The paired t-test results used to assess the effects of nominal maximum aggregate size, coarse aggregate type, fine aggregate angularity, and gradation on %Gmm@N_{max} are summarized in Table 3.25. The %Gmm@N_{max} of 19mm mixtures was higher than that of 9.5mm mixtures. Similar statistical comparisons with respect to coarse aggregate type, fine aggregate angularity and gradations plotting above, through, and below the restricted zone did not yield significant conclusions.

Table 3.1 Summary of Twenty-one Mixture Design Combinations.

Fine Aggregate Type	FAA	Gradation	Coarse Aggregate Type			
			9.5 mm Nominal Max. Size		19 mm Nominal Max. Size	
			Limestone	Granite	Limestone	Granite
Natural sand	39	Above			X	
		Below			X	
Crushed Limestone	44	Above	X		X	
		Through	X	X*	X	X
		Below	X	X	X	X
Crushed Granite	50	Above			X	
		Through	X	X	X	X
		Below	X	X	X	X

Table 3.2 Asphalt Binder Properties (PG 64-22).

Original Binder			
Property	Test Method	Result	Specifications
Flash Point (^{0}C)	AASHTO T 48	230+	230 Min.
Rotational Viscosity @ 135^{0}C (Pa-s)	ASTM D 4402	0.40	3.0 Max.
G*/sin∗ @ 64^{0}C (kPa)	AASHTO TP 5	1.30	1.0 Min.
Rolling Thin Film Oven (AASHTO T 240)			
Mass Loss (%)	AASHTO T 240	0.25	1.0 Max.
G*/sin∗ @ 64^{0}C (kPa)	AASHTO TP 5	3.05	2.20 Min.
Pressure Aging Vessel Residue (AASHTO PP 1)			
Pressure Aging Temp (^{0}C)	AASHTO PP 1	–	100
G*×sin∗ @ 25^{0}C (kPa)	AASHTO TP 5	4120	5000 Max.
Creep Stiffness @ -12^{0}C (MPa)	AASHTO TP 1	184	300 Max.
m-value @ -12^{0}C	AASHTO TP 1	0.32	0.30 Min.

Table 3.3 Coarse Aggregate Properties.

Aggregate Type	Limestone		Granite	
Source Location	Indiana		North Carolina	
Nominal Max. Size (mm)	19.0	9.5	19.0	9.5
Sieve Size (mm)	Percent Passing			
25	100		100	
19	88		98	100
12.5	49	100	61	99
9.5	29	97	29	90
4.75	9	50	5	23
2.36	2	11	2	4
1.18	2	5	1.5	3
0.60	1	2	1	2
0.30	1	1	1	1
0.15	1	1	0.8	1
0.075	1.1	0.6	0.6	0.5
L. A. Wear Loss (%)	23.4	21.7	17.2	18.1
Deleterious Materials (%)	0.0	0.0	0.0	0.0
Soft & Non-durable Particles (%)	0.57	0.0	N/A	N/A
Chert (%)	0.0	0.86	N/A	N/A
Bulk Specific Gravity	2.656	2.640	2.649	2.674
Apparent Specific Gravity	2.738	2.747	2.705	2.694
Water Absorption (%)	1.1	1.5	0.78	0.28
One Fracture Face (%)	100	100	100	100
Two Fracture Faces (%)	95.5	95.2	95.8	99.1
Flat, Elongated Particle (Caliper 5:1)(%)	0.0	0.0	0.0	0.0

Table 3.4 Fine Aggregate and Mineral Filler Properties.

	Fine Aggregate			Filler
Fine Aggregate Angularity	39	44	50	
Source Location	Indiana	Iowa	North Carolina	Indiana
Type of Materials	Natural Sand	Limestone Sand	Granite Sand	Limestone Filler
Sieve Size (mm)	Percent Passing			
9.5			100	
4.75	100	100	99	
2.36	94	77	83	
1.18	73	43	57	
0.60	46	25	40	
0.30	15	13	27	100
0.15	2	5	19	85
0.075	1.0	2.8	13.0	57.0
Fineness Modulus	2.9	3.1	2.8	N/A
Bulk Specific Gravity	2.632	2.640	2.639	N/A
Apparent Specific Gravity	2.719	2.702	2.689	2.700
Water Absorption (%)	1.2	0.87	0.7	N/A
Sand Equivalent	N/A	94	75	N/A

Table 3.5 19mm Limestone Mixture Design Parameters.

Fine Aggregate	39		44		
Sieve Size (mm)	Mixture Gradation		Mixture Gradation		
	Above	Below	Above	Through	Below
25.0	100	100	100	100	100
19.0	97	97	96	97	94
12.5	88	88	81	87	76
9.5	83	82	73	82	66
4.75	65	53	65	67	47
2.36	49	30	49	46	29
1.18	39	22	31	28	18
0.600	27	15	21	18	13
0.300	14	8	14	12	9
0.150	7	5	9	8	6
0.075	4.8	3.1	5.9	4.6	4.3
Design AC (%)	4.7	5.5	4.6	5.4	4.6
VMA (%)	13.2	15.7	13.0	14.8	13.1
VFA (%)	70.4	74.6	68.3	72.6	69.5
Dust Proportion	1.2	0.6	1.6	1.0	1.1
%Gmm@N_{ini}	88.5	85.8	87.4	86.2	85.7
%Gmm@N_{max}	97.0	97.6	97.3	97.4	97.8
Film Thickness (μm)	6.6	13.3	6.0	8.6	8.9
Gmb	2.407	2.359	2.420	2.385	2.414
Slope	0.085	0.116	0.098	0.111	0.117

Table 3.5 19mm Limestone Mixture Design Parameters. (continue)

Fine Aggregate	50		
Sieve Size (mm)	Mixture Gradation		
	Above	Through	Below
25.0	100	100	100
19.0	98	96	94
12.5	90	85	73
9.5	85	78	61
4.75	66	57	42
2.36	45	37	26
1.18	30	25	18
0.600	21	17	12
0.300	14	12	8
0.150	10	8	6
0.075	6.9	5.7	4.3
Design AC (%)	5.9	5.9	5.5
VMA (%)	15.8	15.8	15.1
VFA (%)	74.7	74.6	72.8
Dust Proportion	1.4	1.1	0.9
%Gmm@N_{ini}	85.0	85.3	84.8
%Gmm@N_{max}	97.5	97.4	97.5
Film Thickness (μm)	7.8	9.2	11.4
Gmb	2.365	2.367	2.379
Slope	0.125	0.122	0.127

Table 3.6 19mm Granite Mixture Design Parameters.

Fine Aggregate	44		50	
Sieve Size (mm)	Mixture Gradation		Mixture Gradation	
	Through	Below	Through	Below
25.0	100	100	100	100
19.0	99	99	99	99
12.5	88	78	93	82
9.5	77	59	83	66
4.75	56	38	52	42
2.36	41	28	37	31
1.18	24	18	24	20
0.600	16	13	17	14
0.300	11	10	11	10
0.150	7	7	8	7
0.075	4.1	4.2	5.5	4.6
Design AC (%)	4.8	4.4	5.3	4.8
VMA (%)	13.6	13.0	15.9	15.1
VFA (%)	70.5	69.3	75.0	73.6
Dust Proportion	1.0	1.1	1.1	1.0
%Gmm@N_{ini}	86.5	85.6	85.7	86.3
%Gmm@N_{max}	97.2	97.5	97.5	97.6
Film Thickness (μm)	8.5	8.7	9.8	10.1
Gmb	2.403	2.410	2.347	2.367
Slope	0.108	0.118	0.117	0.110

Table 3.7 9.5mm Limestone Mixture Design Parameters.

Fine Aggregate	44			50	
Sieve Size (mm)	Mixture Gradation			Mixture Gradation	
	Above	Through	Below	Through	Below
12.5	100	100	100	100	100
9.5	99	99	98	99	98
4.75	88	83	71	76	70
2.36	64	56	40	48	41
1.18	40	33	24	32	27
0.600	28	22	15	22	18
0.300	20	14	10	15	13
0.150	13	8	7	10	9
0.075	8.2	5.3	4.2	7.0	6.1
Design AC (%)	5.6	6.2	6.2	6.6	6.7
VMA (%)	15.1	17.0	16.9	17.5	17.9
VFA (%)	73.6	75.4	75.1	75.4	75.4
Dust Proportion	1.7	0.9	0.8	1.2	1.0
%Gmm@N_{ini}	86.1	84.8	84.2	84.2	84.3
%Gmm@N_{max}	97.4	97.2	97.6	97.2	97.2
Film Thickness (μm)	5.7	9.4	11.7	9.8	10.0
Gmb	2.379	2.342	2.347	2.340	2.333
Slope	0.113	0.127	0.134	0.134	0.133

Table 3.8 9.5mm Granite Mixture Design Parameters.

Fine Aggregate	44		50	
Sieve Size (mm)	Mixture Gradation		Mixture Gradation	
	Through	Below	Through	Below
12.5	100	100	100	100
9.5	97	95	96	95
4.75	75	62	66	59
2.36	56	42	49	41
1.18	34	25	33	27
0.600	23	17	23	19
0.300	16	12	15	13
0.150	10	7	11	9
0.075	6.2	4.7	7.4	6.1
Design AC (%)	5.3	5.2	6.0	5.6
VMA (%)	14.6	14.5	16.0	15.2
VFA (%)	72.5	71.7	75.0	73.8
Dust Proportion	1.4	1.1	1.4	1.3
%Gmm@N_{ini}	87.0	86.4	85.7	85.9
%Gmm@N_{max}	97.3	97.2	97.5	97.4
Film Thickness (μm)	6.7	8.7	7.3	8.1
Gmb	2.388	2.390	2.362	2.373
Slope	0.102	0.109	0.117	0.115

Table 3.9 Summary of Design AC values.

FAA	Gradation	9.5 mm Nominal Max. Size		19 mm Nominal Max. Size	
		Limestone	Granite	Limestone	Granite
39	Above			4.7	
	Below			5.5	
44	Above	5.6		4.6	
	Through	6.2	5.3	5.4	4.8
	Below	6.2	5.2	4.6	4.4
50	Above			5.9	
	Through	6.6	6.0	5.9	5.3
	Below	6.7	5.6	5.5	4.8

Table 3.10 Summary of Statistical Analysis of Experimental Variable Effects on Design AC.

Comparison	Significance	p value
AC of 19 mm mixtures > AC of 9.5 mm mixtures	Yes	3.5e-5
AC of limestone mixtures > AC of granite mixtures	Yes	0.0002
AC of FAA of 44 mixtures < AC of FAA of 50 mixtures	Yes	0.0003
AC of above gradation mixtures > AC of through gradation mixtures	No	0.1917
AC of above gradation mixtures > AC of below gradation mixtures	No	0.4309
AC of through gradation mixtures > AC of below gradation mixtures	Yes	0.0200

Table 3.11 Summary of VMA Values at Design AC.

FAA	Gradation	9.5 mm Nominal Max. Size		19 mm Nominal Max. Size	
		Limestone	Granite	Limestone	Granite
39	Above			13.3	
	Below			15.7	
44	Above	15.1		12.9	
	Through	16.9	14.5	14.8	13.6
	Below	16.7	14.4	13.1	13.0
50	Above			15.8	
	Through	17.2	16.0	15.7	15.9
	Below	17.6	15.2	15.0	14.8

do not meet Superpave criteria

Table 3.12 VMA Curve Shapes after N_{design} (96 Gyrations).

FAA	Gradation	9.5 mm Nominal Max. Size		19 mm Nominal Max. Size	
		Limestone	Granite	Limestone	Granite
39	Above			∪	
	Below			∩	
44	Above	∪		∪	
	Through	\	\	—	\
	Below	∩	∪	∪	~
50	Above			~	
	Through	\	~	~	∪
	Below	~	∪	~	∪

Note: Obtained from VMA versus Design AC relationships at N_{design}

Table 3.13 VMA Curve Shapes at $N_{maximum}$ (152 Gyrations).

FAA	Gradation	9.5 mm Nominal Max. Size		19 mm Nominal Max. Size	
		Limestone	Granite	Limestone	Granite
39	Above			∪	
	Below			∪	
44	Above	∪		∪	
	Through	~	∪	—	~
	Below	∩	∪	∪	∪
50	Above			~	
	Through	∪	∪	∩	∪
	Below	~	∪	~	∪

Note: Obtained from VMA versus AC relationships at $N_{maximum}$

Table 3.14 Location of Design AC on VMA Curve at N_{design} Gyrations.

FAA	Gradation	9.5 mm Nominal Max. Size		19 mm Nominal Max. Size	
		Limestone	Granite	Limestone	Granite
39	Above			Dry Side	
	Below			Not Clear	
44	Above	Dry Side		Dry Side	
	Through	Dry Side	Dry Side	Not Clear	Dry Side
	Below	Not Clear	Dry Side	Dry Side	Dry Side
50	Above			Not Clear	
	Through	Dry Side	Not Clear	Not Clear	Dry Side
	Below	Not Clear	Dry Side	Not Clear	Dry Side

Table 3.15 Summary of Statistical Analysis of Experimental Variable Effects on VMA.

Comparison	Significance	p value
VMA of 19 mm mixtures < VMA of 9.5 mm mixtures	Yes	0.0021
VMA of limestone mixtures > VMA of granite mixtures	Yes	0.0167
VMA of FAA of 44 mixtures < VMA of FAA of 50 mixtures	Yes	0.0007
VMA of above gradation mixtures < VMA of through gradation mixtures	No	0.2064
VMA of above gradation mixtures > VMA of below gradation mixtures	No	0.3192
VMA of through gradation mixtures > VMA of below gradation mixtures	Yes	0.0340

Table 3.16 VFA Values at Design AC.

FAA	Gradation	9.5 mm Nominal Max. Size		19 mm Nominal Max. Size	
		Limestone	Granite	Limestone	Granite
39	Above			69.8	
	Below			74.6	
44	Above	73.6		69.0	
	Through	76.3	72.5	72.9	70.5
	Below	76.0	72.2	69.5	69.3
50	Above			74.7	
	Through	76.7	75.0	74.6	74.9
	Below	77.2	73.8	73.3	73.0

Note: the Superpave VFA criteria is 65% - 75% for traffic < 1 x10^7 ESALs

Table 3.17 Summary of Statistical Analysis of Experimental Variable Effects on VFA.

Comparison	Significance	p value
VFA of 19 mm mixtures < VFA of 9.5 mm mixtures	Yes	0.0021
VFA of limestone mixtures > VFA of granite mixtures	Yes	0.0151
VFA of FAA of 44 mixtures < VFA of FAA of 50 mixtures	Yes	0.0013
VFA of above gradation mixtures < VFA of through gradation mixtures	No	0.2090
VFA of above gradation mixtures < VFA of below gradation mixtures	No	0.3203
VFA of through gradation mixtures > VFA of below gradation mixtures	Yes	0.0299

Table 3.18 Dust Proportion Values at Design AC.

FAA	Gradation	9.5 mm Nominal Max. Size		19 mm Nominal Max. Size	
		Limestone	Granite	Limestone	Granite
39	Above			1.22	
	Below			0.61	
44	Above	1.72		1.57	
	Through	0.94	1.38	1.00	1.01
	Below	0.76	1.06	1.12	1.09
50	Above			1.36	
	Through	1.22	1.43	1.13	1.05
	Below	1.03	1.26	0.91	0.98

Violate Superpave criteria of 0.6-1.2%.

Table 3.19 Summary of Statistical Analysis of Experimental Variable Effects on Dust Proportion.

Comparison	Significance	p value
DP of 19 mm mixtures < DP of 9.5 mm mixtures	No	0.2186
DP of limestone mixtures < DP of granite mixtures	No	0.0588
DP of FAA of 44 mixtures < DP of FAA of 50 mixtures	No	0.4641
DP of above gradation mixtures > DP of through gradation mixtures	No	0.0814
DP of above gradation mixtures > DP of below gradation mixtures	Yes	0.0143
DP of through gradation mixtures > DP of below gradation mixtures	No	0.0624

Table 3.20 Film Thickness Values at Design AC.

FAA	Gradation	9.5 mm Nominal Max. Size		19 mm Nominal Max. Size	
		Limestone	Granite	Limestone	Granite
39	Above			6.63	
	Below			13.27	
44	Above	5.73		6.02	
	Through	9.40	6.68	8.62	8.46
	Below	11.69	8.66	8.94	8.68
50	Above			7.76	
	Through	9.81	7.35	9.23	9.77
	Below	10.05	8.12	11.45	10.09

Note: unit of film thickness is micron (10^{-6} m).

Table 3.21 Summary of Statistical Analysis of Experimental Variable Effects on Film Thickness.

Comparison	Significance	p value
FT of 19 mm mixtures > FT of 9.5 mm mixtures	No	0.4691
FT of limestone mixtures > FT of granite mixtures	Yes	0.0193
FT of 19mm with FAA of 44 mixtures < 19mm with FT of FAA of 50 mixtures	Yes	0.0080
FT of 9.5mm with FAA of 44 mixtures < 9.5mm with FT of FAA of 50 mixtures	No	0.6361
FT of above gradation mixtures < FT of through gradation mixtures	No	0.0556
FT of above gradation mixtures < FT of below gradation mixtures	Yes	0.0125
FT of through gradation mixtures < FT of below gradation mixtures	Yes	0.0167

Table 3.22 Percent Gmm at $N_{initial}$ Values Summary.

FAA	Gradation	9.5 mm Nominal Max. Size		19 mm Nominal Max. Size	
		Limestone	Granite	Limestone	Granite
39	Above			88.48	
	Below			85.80	
44	Above	86.12		87.44	
	Through	84.82	87.04	86.16	86.48
	Below	84.16	86.40	85.72	85.64
50	Above			85.04	
	Through	84.24	85.68	85.32	85.70
	Below	84.26	85.88	84.80	86.32

Note: Superpave specification is %Gmm at $N_{initial} \leq 89\%$.

Table 3.23 Summary of Statistical Analysis of Experimental Variable Effects on Percent Gmm at $N_{initial}$.

Comparison	Significance	p value
%Gmm@N_{ini} of 19 mm mixtures > %Gmm@N_{ini} of 9.5 mm mixtures	No	0.0861
%Gmm@N_{ini} of limestone mixtures < %Gmm@N_{ini} of granite mixtures	Yes	0.0064
%Gmm@N_{ini} of FAA of 44 mixtures > %Gmm@N_{ini} of FAA of 50 mixtures	Yes	0.0341
%Gmm@N_{ini} of above gradation mixtures > %Gmm@N_{ini} of through gradation mixtures	No	0.2806
%Gmm@N_{ini} of above gradation mixtures > %Gmm@N_{ini} of below gradation mixtures	Yes	0.0486
%Gmm@N_{ini} of through gradation mixtures > %Gmm@N_{ini} of below gradation mixtures	No	0.1592

Table 3.24 Percent Gmm at $N_{maximum}$ Values Summary.

FAA	Gradation	9.5 mm Nominal Max. Size		19 mm Nominal Max. Size	
		Limestone	Granite	Limestone	Granite
39	Above			97.00	
	Below			97.60	
44	Above	97.38		97.34	
	Through	97.18	97.34	97.36	97.20
	Below	97.58	97.22	97.76	97.50
50	Above			97.48	
	Through	97.18	97.50	97.36	97.50
	Below	97.18	97.44	97.50	97.62

Note: Superpave specification is %Gmm at $N_{maximum} \leq$ 98%.

Table 3.25 Summary of Statistical Analysis of Experimental Variable Effects on Percent Gmm at $N_{maximum}$.

Comparison	Significance	p value
%Gmm@N_{max} of 19 mm mixtures > %Gmm@N_{max} of 9.5 mm mixtures	Yes	0.0379
%Gmm@N_{max} of limestone mixtures < %Gmm@N_{max} of granite mixtures	No	0.7670
%Gmm@N_{max} of FAA of 44 mixtures < %Gmm@N_{max} of FAA of 50 mixtures	No	0.6934
%Gmm@N_{max} of above gradation mixtures > %Gmm@N_{max} of through gradation mixtures	No	0.2601
%Gmm@N_{max} of above gradation mixtures < %Gmm@N_{max} of below gradation mixtures	No	0.0918
%Gmm@N_{max} of through gradation mixtures < %Gmm@N_{max} of below gradation mixtures	No	0.0787

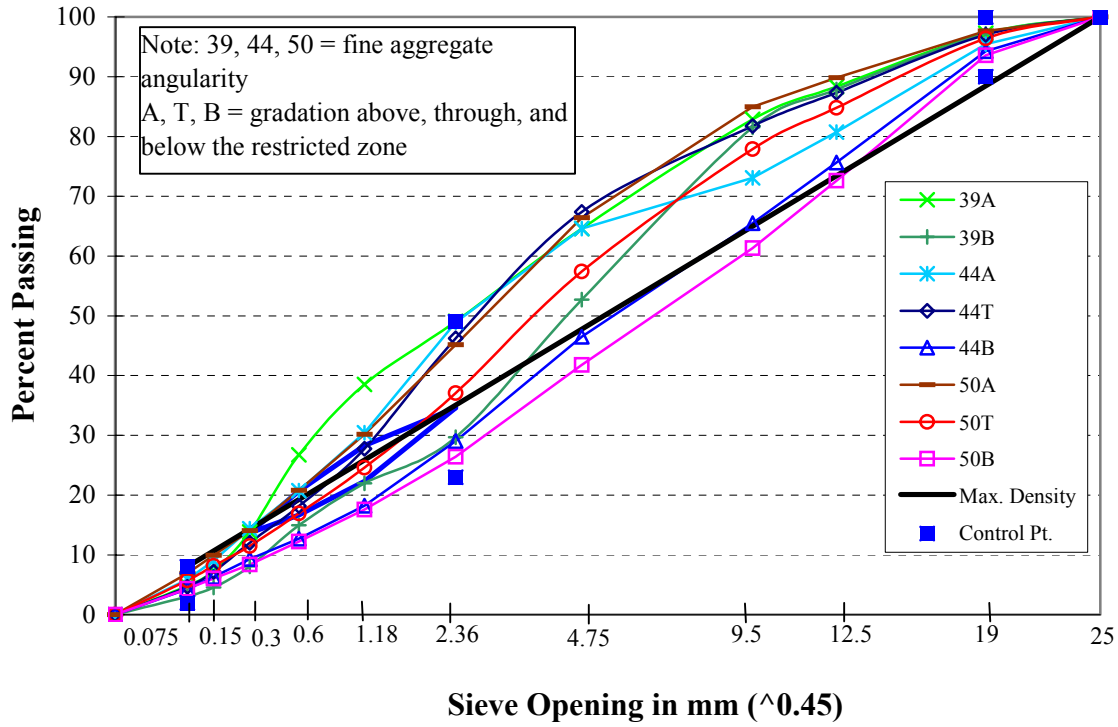

Figure 3.1 Gradations for the 19-mm Limestone Mixtures.

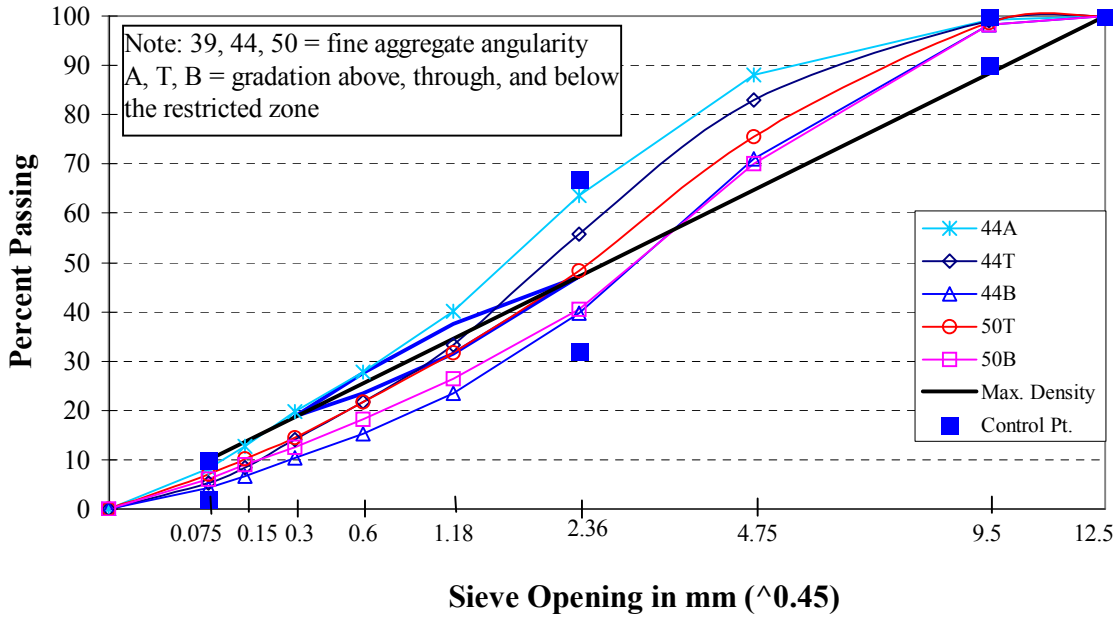

Figure 3.2 Gradations for the 9.5-mm Limestone Mixtures.

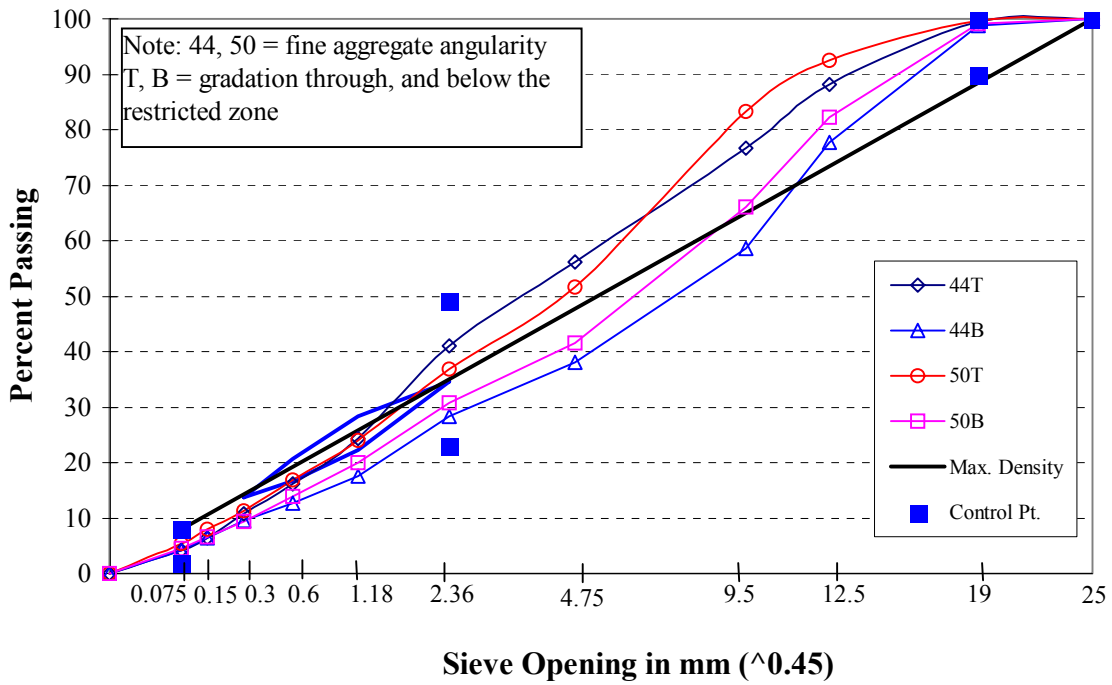

Figure 3.3 Gradations for the 19-mm Granite Coarse Aggregate Mixtures.

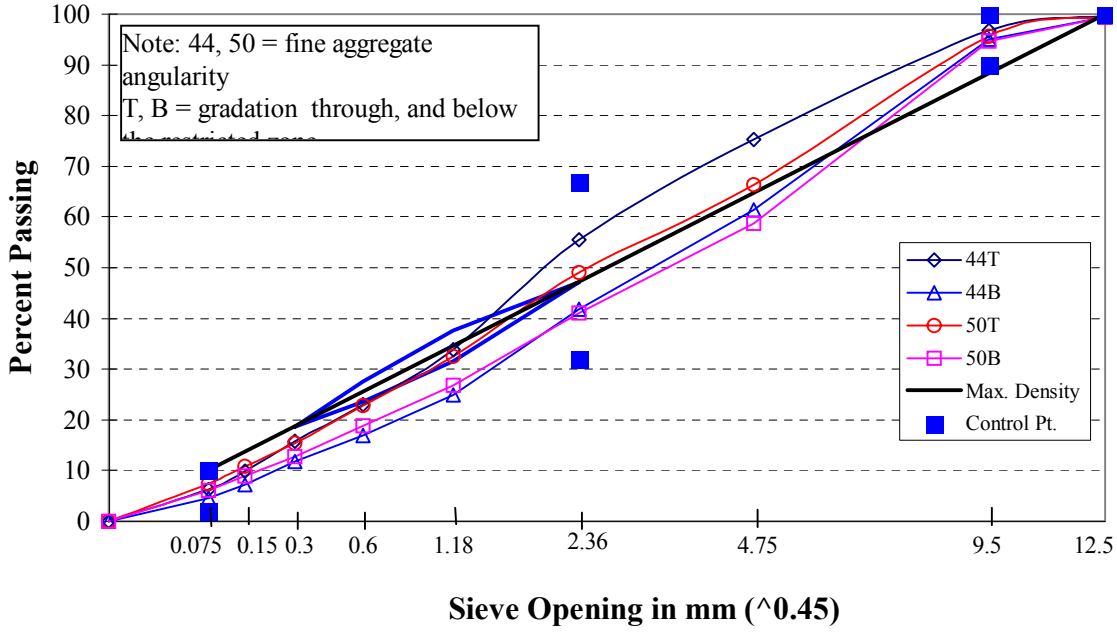

Figure 3.4 Gradations for the 9.5-mm Granite Coarse Aggregate Mixtures.

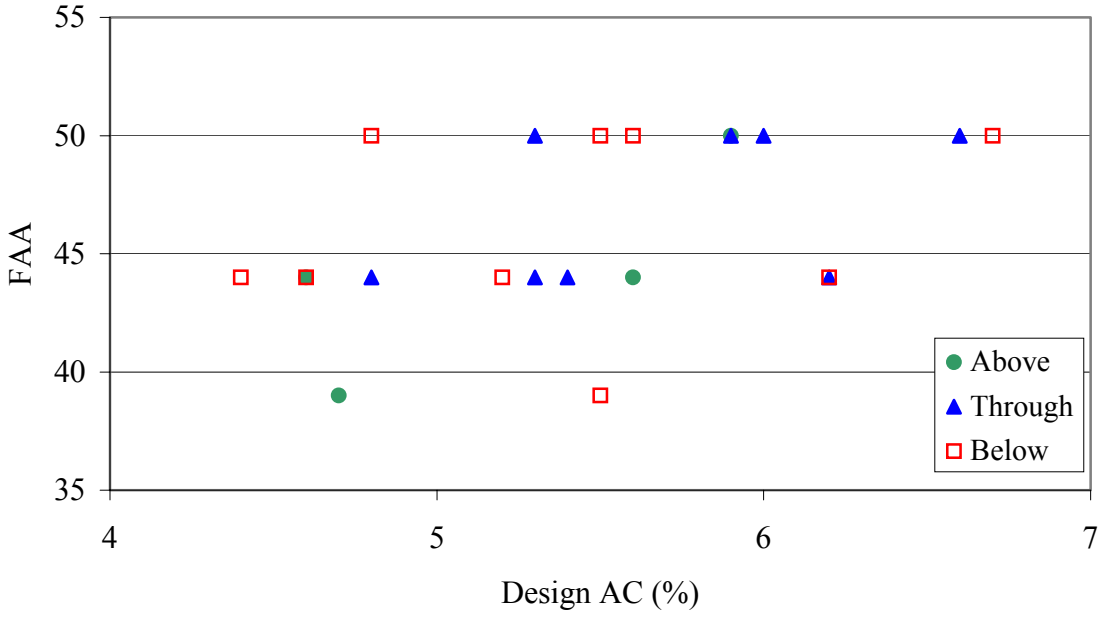

Figure 3.5 FAA and AC Relationship.

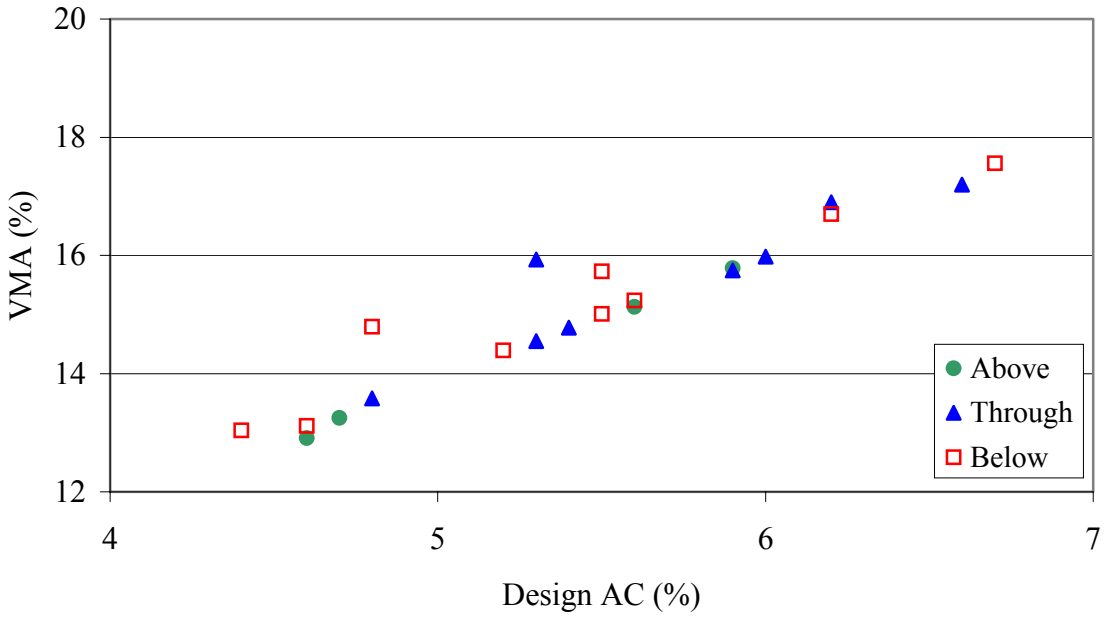

Figure 3.6 VMA and AC Relationship.

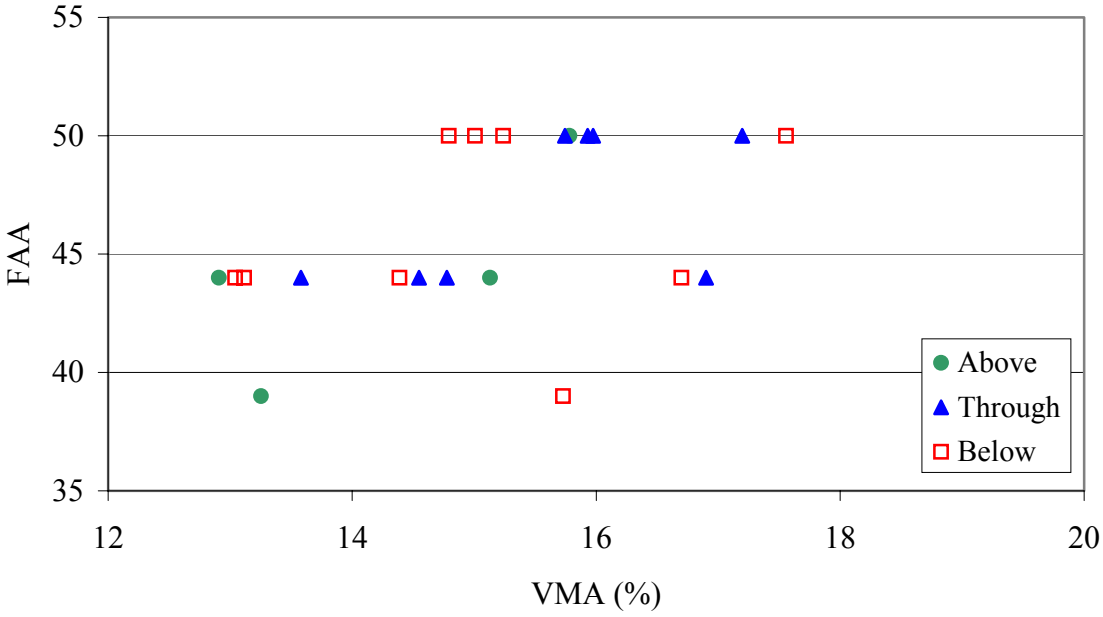

Figure 3.7 FAA and VMA Relationship.

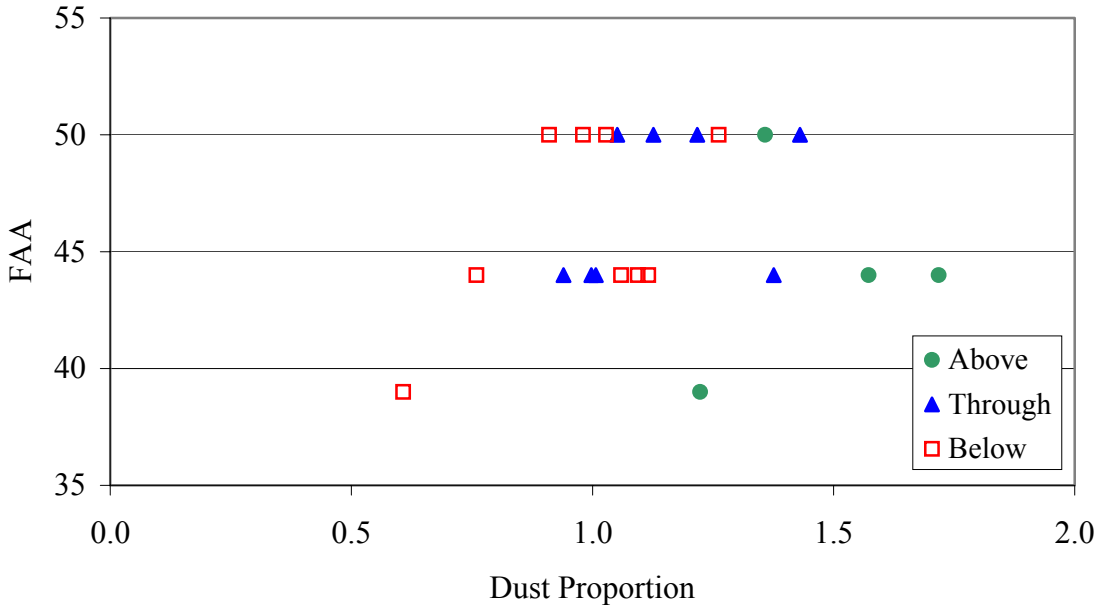

Figure 3.8 FAA and Dust Proportion Relationship.

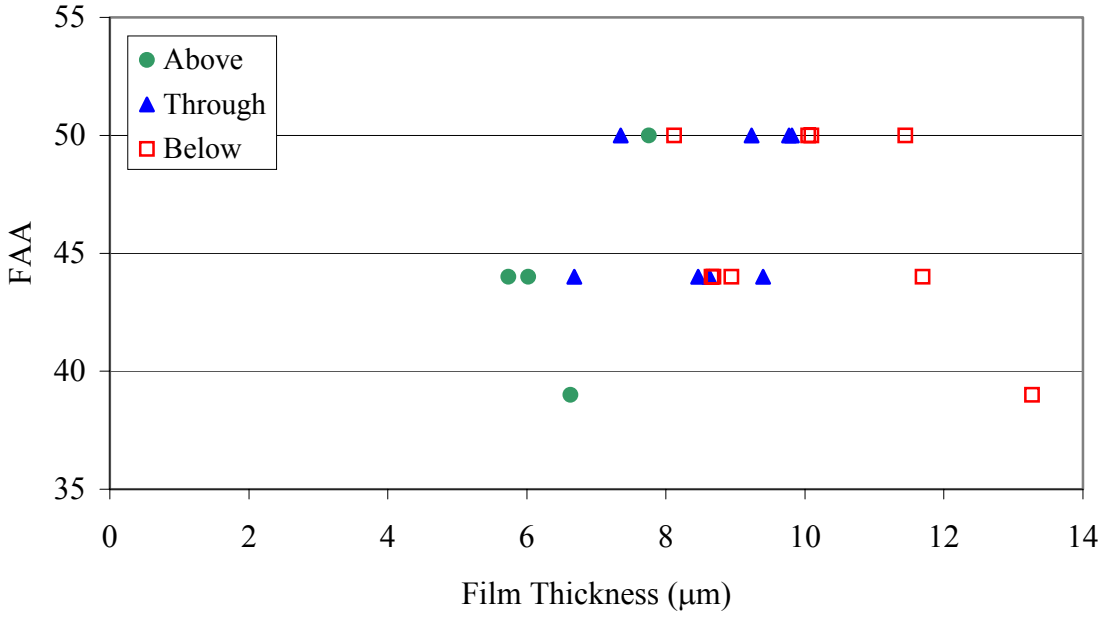

Figure 3.9 FAA and Film Thickness Relationship.

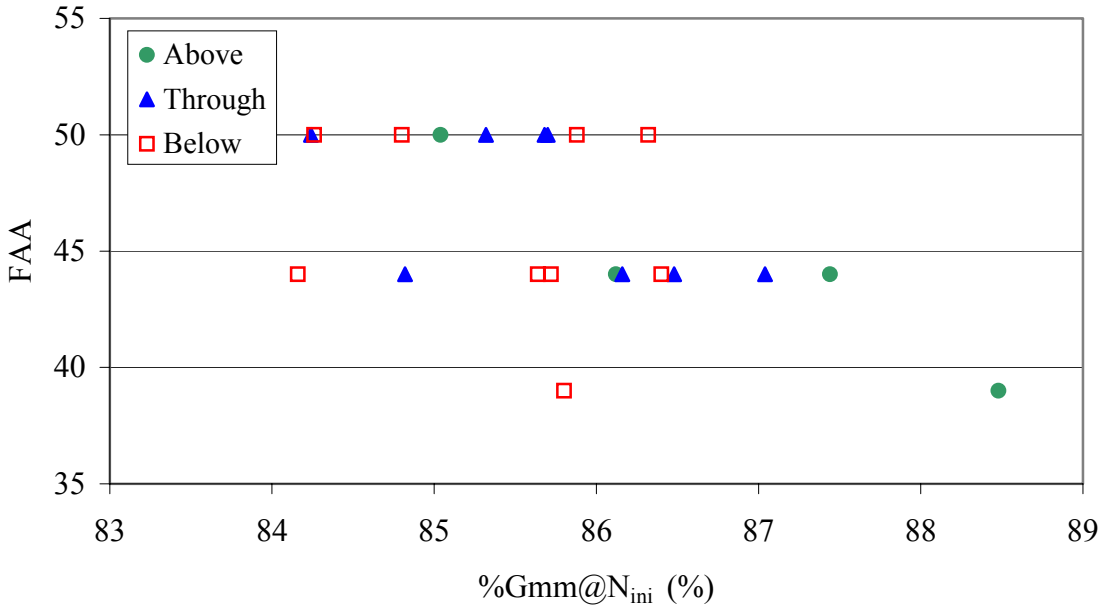

Figure 3.10 FAA and Percent Gmm at $N_{initial}$ Relationship.

4 ACCELERATED PAVEMENT TESTS

4.1. Description of INDOT/PURDUE APT Facility

The prototype scale accelerated pavement testing facility developed by Purdue University for the INDOT was employed for this study. The APT device is shown in Figure 4.1. Prototype scale pavement sections can be installed in a test pit in the facility. The test pit is 6 m (20 ft) wide and 6 m (20 ft) long. There are many miles of concrete pavement with asphalt overlays in Indiana. As a result, tests in previous studies using the APT facility were initiated with asphalt overlays constructed on concrete slabs. A heating system was developed that uses hot water pumped through hoses embedded in the concrete slabs. Temperature sensors embedded at the mid-height of slabs are used in the feedback control loop for the in slab heating system. The concrete slabs on which the asphalt is laid are 1.5 m (5 ft) wide and 6 m (20 ft) long. Each slab can be heated separately. Air heating is also utilized to minimize air/ pavement temperature differential, so that the testing temperature can be maintained reliably even when the outside air temperature is below freezing. The APT structural layout is shown in Figure 4.2.

The APT loading system has the capability of applying moving wheel loads to pavement test sections installed in the facility. The APT is designed to apply up to an 89 kN (40 kips) load on a half axle assembly with standard dual tires or a super single tire. The load carriage travels at 8.3 km/h (5.2 mph). Traffic can be applied repeatedly with or without wander. With wander the wheel path is randomly selected to achieve a normal distribution over a total width of 260 mm (10.2 in.). Traffic can be applied in one or two directions. During application of one-directional traffic the wheel is repositioned while off the pavement and is being returned to the start position for the next load cycle.

Typically, two paving lanes (each lane is 3 m (10 ft) wide) are constructed in the APT facility. Each paving lane includes two test lanes 1.5 m (5 ft) wide. With multiple

test lanes various factors related to mixture performance can be studied. Examples are high and low density (quality of construction), high and low tire pressure, and high and low temperature. Aggregates for the four mixtures were delivered by truck to a local contractor's asphalt plant. Enough total aggregate was ordered to provide 73 Mg (80.5 tons) for calibrating the plant and to produce the desired amount of each mixture. An additional 18 Mg (19.8 tons) of each aggregate was ordered as a stockpile base. Prior to construction of a new test section previously tested mixtures were removed. To facilitate removal, the slab heating system was turned on the afternoon before, heating the old test sections to 50^0C. Under this condition the majority of the mixture can be removed with a backhoe. Laborers remove any remaining material with shovels. The in slab heating system was also utilized in the same manner for test section construction. Heating in combination with construction being inside the APT facility insures good construction conditions.

A light asphalt tack coat was applied to the base concrete slab prior to mixture placement. During the construction process mixtures are delivered by truck and loaded into the asphalt laydown machine hopper outside of the APT facility. The laydown machine with the mixture loaded in the hopper is backed into the facility. Paving proceeds as the laydown machine is driven out of the APT facility. Each paving lane is 3 m (10 ft) wide. After exiting the facility, the laydown machine hopper is refilled and a second 3 m (10 ft) lane is laid. Conventional rollers are then used to achieve desired compaction.

4.1.1. Test Section Construction

Ten mixtures were selected and tested in APT; six 19mm nominal maximum size and four 9.5mm nominal maximum size. The selected mixtures are identified in Tables 4.2 and 4.3. The 19mm mixtures were constructed in one lift 102 mm (4 in.) thick. The 9.5mm mixtures were constructed in 2 lifts. The surface layers were the 9.5mm mixtures and were placed 32 mm (1.5 in.) thick. Depending on the lane position, the binder layer

could be a 12.5mm or a 9.5mm mixture. Typical test section structural cross sections of 19mm and 9.5mm mixtures are shown in Figure 4.3.

4.1.2. Construction of High Density and Low Density Lanes

Mixture sensitivity to in-place density was investigated by constructing high and low density lanes. Another purpose of having different densities was to have a broader range of VMA such that critical VMA could be identified. The mixtures that were constructed in high and low density lanes are identified in Table 4.3. LD and HD indicate low and high density, respectively. High and low density lanes were constructed for a range of 19mm nominal maximum size mixtures. The compaction process involved using static steel wheel, pneumatic tire, and a dual drum vibratory rollers to achieve high density in one paving lane. A nuclear gauge was utilized to monitor density throughout the compaction process. Compaction was terminated when change in density became minimal. This represented the high density lane. Subsequently, the second paving lane was compacted to a density approximately 64 kg/m^3 lower than the high density lane.

4.1.3. Construction of High AC and Low AC Lanes

Mixture sensitivity to asphalt binder content was investigated by constructing two lanes with different AC levels. Another purpose of having different AC levels was to have a broader range of VMA such that critical VMA can be identified. The mixtures that were selected are identified in Tables 4.2 and 4.3. LAC and HAC indicate low and high AC, respectively. The target difference in AC was plus or minus 0.7 percent from the design AC for a given mixture. All high and low AC lanes were compacted until the change in density become minimal.

4.2. Test Parameters

The APT tests were conducted with a 40 kN (9 kips) load on a set of standard dual tires. This load corresponds to an 80 kN (18 kips) standard single axle load. A tire inflation pressure of 620 kPa (90 psi) was used. Gross contact pressure was computed based on wheel load and measured gross tire print area (Huang and White, 1996). The gross tire contact pressure was determined to approximately equal to the tire pressure. The load carriage traveled at 8.3 km/h (5.2 mph). One-directional traffic was applied. All mixtures were tested without transverse wheel wander or in other words, single wheel path loading. Additionally, six of the mixtures were tested employing transverse wheel wander of 260 mm (10.2 in.). This provided the necessary information to assess the effect of transverse wander on the performance of the mixtures. Table 4.4 provides a summary of the mixtures tested with and without wander. A test temperature of 50^0 C (122^0 F) was used to test all mixtures.

4.3. Results

4.3.1. Data Acquisition and Reduction

Prior to the application of traffic, nine transverse cross-sections were laid out at 0.6 m (2 ft.) intervals in the longitudinal direction on each lane. A profilometer is attached to fixed beams of the APT. It can be positioned at a desired cross-section location by rolling along the fixed beams. This configuration provides a fixed height above the pavement surface and a vertical reference for the transverse profile measurements.

Transverse profile measurement is achieved by lowering a small bogey wheel of the profiler to the pavement surface and rolling it across the test lane. When the profilometer wheel rolls, vertical and horizontal position is obtained automatically with cable-based transducers. Rutting was measured after various numbers of load repetitions.

Measurements were more frequent at low repetitions because the change in rutting was more pronounced early in the loading process.

Profile data was recorded on a PC-based system. Software was written to automatically reduce, calculate, and store the transverse profile rutting data in a spreadsheet (Stiady, White, and Reck, 1998). An initial profile was recorded prior to traffic application. This initial profile served as the "zero" reference for determining rutting from subsequent profiles. Subsequent profiles were determined by subtracting the reference from the current transverse profile. This technique allows the downward and uplift components to be accurately determined. A typical reference profile and profile after several thousand wheel passes is shown in Figure 4.4.

4.3.2. Rutting Components after 20000 Wheel Passes

Based on experience, loading is typically terminated in the APT after the application of 20000 wheel passes or when a rut depth of 20 mm (0.8 in) is observed. Accelerated pavement testing traffic can be applied with or without wander. Observed rutting profiles for the two traffic cases are different. Figures 4.5 and 4.6 show typical no wander and wander rutting profiles, respectively. Because loading was applied with dual tires, no wander traffic produces significant uplift between and outside of the tires. When wander is employed, the effect of wander is to substantially compress the upheave between the tires. Rutting component definitions that are applicable and comparable for both cases are required.

The no wander rutting components are defined in Figure 4.5. Imaginary straight edges are drawn from the peak upheave in between tires to the top of the upheave outside the tire edges. Total rut is defined as the vertical distance from the lowest point of the tire path deformation to the straight edge. Rut depth is defined as the vertical distance from the lowest point of the tire path deformation to the original surface. Rise height is defined as the difference between total rut and rut depth. Because there were two tire paths and

sometimes their profiles were slightly unsymmetrical, the reported rutting components were the average of those associated with each tire path.

The with wander wheel path rutting components are defined in Figure 4.6. When wander is used an imaginary straight edge is drawn across the upheave peaks occurring outside the tire edges. Total rut is defined as the vertical distance from the lowest point of the tire path deformation to the straight edge. Rut depth is defined as the vertical distance from the lowest point of the tire path deformation to the original surface. Rise height is defined as the difference between total rut and rut depth. Because there were two tire paths and sometimes their profiles were slightly unsymmetrical, the reported rutting components were the average of same as above.

As previously stated, transverse profiles were recorded at nine cross-sections on each lane. However, three consecutive sections nearest the center of the test section were averaged and used as a single result for mixture evaluation purposes. Figures 4.7 and 4.8 show typical no wander and wander wheel path rutting components for same mixture as a function of number of wheel passes, respectively. In order to compare the performance of different mixtures, rutting after a specified number of wheel passes was used. A decision was made to use rutting components at 20000 wheel passes, because it was believed that the change in rutting was approximately linear at this point. In situations where tests were terminated prior to the application of 20000 wheel passes due to total rut exceeding 20mm (0.8 in.), extrapolation was used to predict rutting components at 20000 wheel passes.

4.4. Discussion on APT Results

All APT data are summarized in Appendix C. The data consists of APT mixture properties prior to traffic loading, APT rutting components at 20000 wheel passes, in-wheel-path APT mixture properties after loading, asphalt extraction, washed sieve analyses, and plots of rutting components as a function of wheel passes for all mixtures.

4.4.1. Rut Resistance Rating

A subjective rut resistance rating scheme was developed for mixture evaluation. The rating is based on no wander rutting components at 20000 wheel passes, because no wander loading was applied to all mixtures. The observed rut depth, rise height, and total rut values for all mixtures tested without wander were sorted and plotted as depicted in Figure 4.9. Based on the total rut component, four categories of rut resistance were established subjectively. Divisions were established at total rut of 10, 15, and 20 mm to form four categories of rut resistance as shown in Figure 4.9 and defined in Table 4.5. The other corresponding rutting components were categorized also. Figure 4.9 indicates that poor rut resistance mixtures tend to have more rise height than rut depth. In other words, severe shear failure is associated with poor rut resistance.

As previously stated, the mixtures tested in APT were constructed either into high and low density or high and low AC. Rutting performance comparison of the mixtures was conducted by selecting mixtures compacted at 6 to 9 percent air voids or mixtures produced at design AC. The selected mixtures are summarized in Table 4.6. It was clear that mixture with FAA of 39 (natural sand) did not perform well. Unlike the typical rutting and number of wheel passes plot, the rise height component of the 19mm limestone with FAA of 39 and gradation plotting below the restricted zone crossed the rut depth component as shown in Figure 4.10. The rise height was greater than the rut depth component at 20000 wheel passes. It is a well recognized that HMA produced with poor quality of natural sand does not provide good shear resistance. This observation for the 19mm limestone with FAA of 39 mixtures suggests that the uplift rutting component dominated the deformation for the poor shear resistant mixture. However, poor rut resistance mixtures do not necessarily exhibit this behavior. Review of the rutting components for the 19mm limestone with FAA of 50 and gradation plotting above the restricted zone mixture shows that the rise height component was smaller than the rut depth component, although the rut resistance rating was poor as shown in Figure 4.11. This shows that the behavior of a poor rut resistance mixture may be dominated by either rise height (uplift) or rut depth (downward) components.

Simply increasing FAA above 44 will not necessarily improve rutting performance. This is clearly observed by comparing the performance of the 19mm limestone with gradation plotting above the restricted zone and the 9.5mm granite with gradation below the restricted zone mixtures. With FAA of 44 and gradation plotting below the restricted zone, the 19mm granite performed better than the 19mm limestone mixtures. The performance of 9.5 and 19mm of granite mixtures with FAA of 44 and gradations plotting below the restricted zone were approximately the same as shown by the rating and the ranking. Both were rated as very good and they ranked number 1 and 2. For the19mm limestone mixtures with FAA of 44, the mixture with a gradation plotting above the restricted zone provided better rut resistance than the mixture with a gradation plotting below the restricted zone. Further specific analysis on gradation was not feasible because other factors were always confounded.

4.4.2. Relationship Among Total Rut, Rut Depth, and Rise Height

The relationship between total rut and rut depth is presented in Figure 4.12. Details of the regression analysis are summarized in Appendix C. A linear relationship was observed. The linear relationship indicates that rut depth contributed to a fixed proportion of total rut; in this case the contribution was approximately 54 percent. It should be noted that most of the total rut observations were less than 30 mm.

The relationship between total rut and rise height is presented in Figure 4.13. The regression analysis details are summarized in Appendix C. Regression through origin was chosen because the origin represents the actual physical condition prior to loading. The relationship appeared to be quadratic with a negative second order parameter. The parameter estimates indicate that rise height was more dominant when total rut was greater than 33 mm. Initially, this estimation contradicted with the observation for the total rut and rut depth relationship. However, this contradiction may be explained by the fact that most of total rut data were less than 30 mm and within this range the relationship between total rut and rise height was approximately linear.

The relationship between rise height and rut depth is shown in Figure 4.14. Details of the regression analysis are summarized in Appendix C. A linear relationship was observed, although the r^2 value was small. It should be noted that most of rut depth data were less than 15mm. The small value of r^2 suggests that the rut depth was not generated proportionally with the rise height.

In summary, the relationships among total rut, rut depth, and rise height based on the APT test results are complex. Rut depth dominated the rutting of good mixtures (total rut < 15 mm) and rise height dominated the rutting of very poor performing mixtures (total rut > 33 mm). This observation does not mean that rut depth dominates the early rutting process followed by rise height. The reason is because, as shown in Figures 4.7 and 4.8, in general rut depth does not intersect rise height as the number of wheel passes increases. Low shear resistance mixtures would exhibit more rise height than rut depth, but low rut resistance mixtures do not always exhibit more rise height than rut depth.

4.4.3. Material Property Effects on APT Total Rut

The significance of nominal maximum aggregate size, coarse aggregate type, fine aggregate angularity, and gradation to rutting components were analyzed using analysis of variance (ANOVA). The ANOVA of total rut is summarized in Table 4.7 and the details of it may be found in Appendix C. The following model was assumed in the analysis.

$$\text{Total rut}_{ijkl} = \mu + N_i + C_j + F_k + G_l + NC_{ij} + NF_{ik} + NG_{il} + CF_{jk} + CG_{jl} + FG_{kl} + \varepsilon_{ijkl} \quad \ldots(4.1)$$

Where:

Total rut = dependent variable
μ = overall mean
N_i = nominal maximum size, i=1, 2
C_j = coarse aggregate type, j= 1, 2
F_k = fine aggregate angularity, k = 1, 2, 3
G_l = gradation, l = 1, 2, 3
NC_{ij} = interaction of nominal maximum size and coarse aggregate type
NF_{ik} = interaction of nominal maximum size and fine aggregate angularity

NG_{il} = interaction of nominal maximum size and gradation
CF_{jk} = interaction of coarse aggregate type and fine aggregate angularity
CG_{jl} = interaction of coarse aggregate type and gradation
FG_{kl} = interaction of fine aggregate angularity and gradation
ε_{ijkl} = error term

Results show that coarse aggregate type and gradation impacted APT total rut significantly at five percent significant level. Because there were many empty cells in the experiment design (Table 4.1), it was not possible to evaluate material property interactions.

4.4.4. Effect of Binder Layer on 9.5mm Mixture APT Total Rut

The effect of different binder layer materials (9.5 vs. 12.5mm) on the performance of 9.5mm mixtures is shown in Figure 4.15. Review of the figure reveals that only two of eight mixtures showed more than a 5 mm difference in total rut. The difference in total rut ranged from –2.3 to 7.3 mm, the difference in rut depth from –2.8 to 3.5 mm, and the difference in rise height from –1.6 to 5.2 mm. A total rut difference greater than 5 mm was observed in 9.5 mm limestone with FAA of 50 and gradation through the restricted zone mixture only.

Due to the limited number of observations, statistical analysis of the effects of the binder course on 9.5 mm mixture performance was not feasible. The combination effects of main factors (coarse aggregate type, FAA, and gradation) and binder layer may influence the rutting components. However, the available data suggests that the effect of binder course materials on 9.5mm mixture rutting was nominal.

4.4.5. Mixture Sensitivity to In-Place Density

As previously mentioned in section 4.1.2. the sensitivity of mixtures to in-place density was evaluated by constructing and loading low and high density lanes. The effect

of initial in-place density on rutting performance is presented in Figure 4.16. Review of the 19mm limestone with FAA of 39 and gradation plotting below the restricted zone and the 19mm limestone with FAA of 50 and gradation plotting above the restricted zone mixtures confirms the common knowledge that over compaction is detrimental to performance. The initial in-place air voids of these mixtures were 2.8 and 4.1 percent, respectively in the high density lanes. The low density lanes had initial air voids of 6.6 and 6.3 percent, respectively. In both cases the high density lanes experienced significantly more rutting; approximately 12mm in each case. The high density 19mm limestone with FAA of 39 and gradation plotting below the restricted zone mixture was compacted to 101% of design Gmb (2.8% air voids). The high density 19mm limestone with FAA of 50 and gradation plotting above the restricted zone was compacted to 99.9% of design Gmb (4.1% air voids). These calculations of density with respect to design Gmb clearly show that field compaction equal to or greater than the design Gmb would lead to poor performance. This technique of evaluating field compaction relative to design Gmb has historically been used in HMA process control for many years. For the 19mm limestone mixtures with gradations plotting above the restricted zone, the mixture with FAA of 50 did not perform better than the mixture with FAA of 44, based on the comparison made at their optimum densities. In general, better performance was observed when mixtures were compacted to optimum (6 to 8% air voids) rather than maximum density.

4.4.6. Mixture Sensitivity to Deviation from Design AC

The sensitivity of mixture behavior to deviation from design AC was evaluated by constructing low and high AC lanes. The effect of deviations from the design AC on rutting performance is presented in Figure 4.17. In all cases increasing AC lead to increased rutting, regardless of the design AC. However, some mixtures were more sensitive to deviations from the design AC than others. The 9.5 mm granite with FAA of 50 and gradation plotting below the restricted zone mixture was the least sensitive. The

most sensitive mixture was the 9.5mm limestone with FAA of 44 and gradation plotting through the restricted zone. However based on the performance of all the mixtures, sensitivity does not appear to be related to FAA or nominal maximum aggregate size.

4.4.7. Relationship Between Rutting Performance and VMA

Gradation, angularity of coarse and fine aggregate, aggregate type, asphalt content, and degree of compaction influence VMA (Roberts, et al. 1991). The effects of gradation, angularity, and aggregate type on VMA were discussed in Chapter 3. A scatter plot of APT total rut and in-place VMA for all mixtures tested in the APT is presented in Figure 4.18. The plot suggests that when VMA resulted from AC deviation, mixture production, and degree of compaction, VMA could not be correlated with APT total rut.

Because the relationship between rutting performance and in-place VMA could not be observed when the in-place VMA resulted from AC deviation and degree of compaction, an attempt to develop a relationship between rutting performance and selected in-place VMA was made. The selected in-place VMA resulted from the mixtures that were compacted at 6 to 9 percent air voids or produced at the design AC. A scatter plot of selected in-place VMA and design VMA values are presented in Figure 4.19. The purpose of the plot is to select mixtures having in-place VMA within 5 percent of the design VMA. The selected mixtures were utilized to develop the relationship between rutting performance and in-place VMA in APT.

The scatter plot between rutting performance and selected in-place VMA is presented in Figure 4.20. The data were categorized based on nominal maximum aggregate size because the VMA requirement for each nominal maximum aggregate size is different. Positive linear relationships were observed for both nominal maximum aggregate sizes. Linear regression analysis was conducted and the results are summarized in Appendix C. The relationships suggest that the rutting performance of 19mm mixtures were more sensitive to VMA change than that of 9.5mm mixtures in APT. Because positive relationships between rutting performance and in-place VMA were observed, the

effort to identify minimum VMA requirement in APT was unsuccessful. On the contrary, the positive relationships suggest the upper limit of VMA be established. The upper limit of VMA for rutting performance is also suggested from fine aggregate angularity study (Lee, 1998).

One of the 19 mm mixtures incorporated natural sand (FAA of 39) as a fine aggregate. This mixture had 25 mm of total rut (poor rating) although it satisfied the minimum VMA requirement during design and construction. On the other hand, the 9.5 mm granite with FAA of 44 and gradation plotting below the restricted zone as well as the 19 mm limestone with FAA of 44 and gradation plotting above the restricted zone mixtures did not meet the minimum VMA requirement during mixture design process (3.4.2). After construction, the mixtures satisfied the minimum VMA requirements. The former mixture exhibited approximately 8 mm total rut (very good rating) and the later about 9.5 mm (very good rating).

In summary, the effort to identify the minimum VMA requirement was unsuccessful. The effort and observations suggested that although VMA describes mixture structure, contribution of many factors to in-place VMA made the relationship between rutting performance and VMA in APT unclear. Positive relationships were observed between rutting performance and selected in-place VMA. The positive relationships suggest that an upper limit of VMA is needed for rutting performance. It should be noted that the number of observations were limited and the range of design VMA was narrow. Additionally, deviations from target design AC and gradations as well as the difference in laboratory and field compaction methods complicated to analysis.

4.4.8. Relationship Between Rutting Performance and VFA

The scatter plot of rutting performance and in-place VFA for all mixtures is presented in Figure 4.21. The 19mm mixtures data suggests that as in-place VFA increases total rut increases. However, the 9.5mm mixtures did not show the same trend.

Because the relationship between rutting performance and in-place VFA could not be observed when the in-place VFA resulted from AC deviation and degree of compaction, an attempt to develop a relationship between rutting performance and selected in-place VFA was made. The selected in-place VFA resulted from the mixtures that were compacted at 6 to 9 percent air voids or produced at the design AC. A scatter plot between selected in-place VFA and design VFA is presented in Figure 4.22. The purpose of the plot is to select mixtures having in-place VFA within 10 percent of the design VFA. The selected mixtures were utilized to develop the relationship between rutting performance and in-place VFA in APT.

A scatter plot of rutting performance and selected in-place VFA is presented in Figure 4.23. There is no clear relationship between rutting performance and selected in-place VFA. Accordingly, the effect of upper limit of VFA allowed for traffic less than 3 x 10^6 ESALs (traffic level for mixture design) on rutting performance could not be evaluated.

In summary, the relationship between rutting performance and VFA in APT was unclear. The effort to evaluate the effect of upper limit of VFA on rutting performance in APT was unsuccessful.

4.4.9. Relationship Between Rutting Performance and Dust Proportion

The relationship between rutting performance and dust proportion (DP) is presented in Figure 4.24. A poor quadratic relationship with a positive second order parameter was observed. This relationship suggests that a good rating of rut resistance corresponded to a range of DP. This observation was consistent with the purpose of dust proportion range requirement. Using the parameter estimates, 0.6 and 0.8 DP corresponded to APT total rut of 19.73 and 15.47 mm, respectively (poor rut resistance). Unfortunately, the upper limit of total rut and DP relationship could not be assessed.

A scatter plot between in-place and design DP is presented in Figure 4.25. This plot could be used to identify good quality of in-place DP. Mixtures having a DP within 0.3 of the design DP were selected. Five mixtures and their corresponding total rut were selected. Two of five well-produced mixtures had 9.5 mm nominal maximum size.

The relationship between APT total rut and selected in-place DP is presented in Figure 4.26. A quadratic relationship with a positive second order parameter was observed. This relationship was consistent with the previous one. Further, the relationship suggests that when the DP was smaller than approximately 0.8, the total rut was greater than 20 mm (poor rating). DP value of 0.8 is consistent with the recently recommended lower DP criterion (Brown, et al., 1999 and AASHTO, 1999). Unfortunately, the upper limit of total rut and DP relationship could not be evaluated because there was no selected in-place DP greater than 1.6.

In summary, design DP could indicate mixture rutting performance. However, when DP were the result of deviation from design AC and target amount of materials passing #200 sieve, it is doubtful that DP would indicate rutting performance.

4.4.10. Relationship Between Rutting Performance and Film Thickness

The relationship between rutting performance and film thickness for all mixtures tested in the APT is presented in Figure 4.27. It should be noted that the observed range of film thickness for 9.5mm mixtures was narrower than that of the 19mm mixtures. This implies that the developed relationship was dominated by the19mm mixtures. The slope of the relationship between total rut and in-place film thickness for all mixtures and the slope of the relationship between total rut and film thickness for 19mm mixtures are approximately the same.

The positive linear relationship between total rut and in-place film thickness shows that total rut increases with film thickness. Further analysis of the relationship revealed that when the film thickness of 7.3 micron corresponded to APT total rut of 10

mm. The ability to develop the relationship between total rut and film thickness considering all mixtures suggests that film thickness is a robust enough parameter to reflect its effect on rutting performance, regardless of deficiencies in mixture production and placement.

4.4.11. Compaction of 19 mm and 9.5 mm Mixtures

As discussed in Chapter 3, the 19 mm mixtures were easier to compact than the 9.5 mm mixtures. This observation was based on percent of Gmm at $N_{initial}$ during mixture design. However, this observation may not apply for field mixtures because of differences in compaction equipment, material production, and environment. Although APT mixtures were not true field mixtures, the mixtures were produced, laid, and compacted using the full scale conventional equipment. Therefore, it is assumed that APT mixtures are equivalent to field mixtures. With this assumption, the hypothesis on compaction of the 19 and 9.5 mm mixtures could be validated with APT mixtures.

The compaction of 19 mm and 9.5 mm mixtures were evaluated based on initial air void comparison. As previously stated, the mixtures tested in APT were constructed either into high and low density or high and low AC. Air void comparison was conducted by selecting mixtures compacted at 6 to 9 percent air voids or mixtures produced at design AC.

The selected in-place mixtures were sorted based on initial in-place air voids and their air voids were plotted as shown in Figure 4.28. The plot shows that the initial in-place air voids of 9.5mm mixtures were higher than those of 19 mm mixtures. The number of observations is obviously limited and the effects of coarse aggregate type, FAA, and gradation are confounded in the plot. This observation could also be explained by the fact that the 19 mm mixtures were constructed 102 mm (4 in) thick while the 9.5mm mixtures were constructed 38 mm (1.5 in) thick. The ratios of lift thickness to nominal maximum aggregate size were 5.4 and 4.0 for the 19 and 9.5mm mixtures, respectively. This explanation is also consistent with SHRP-A-408 finding that air voids

are obtained easily when the pavement is thick (7 to 8 cm), but are extremely difficult to obtain in the case of thin courses (30 to 40 mm) (Cominsky, 1994). Therefore, it is concluded that the 19 mm mixtures were easier to compact than the 9.5 mm mixtures in APT. However, it could not be determined whether this observation was due solely to nominal maximum aggregate size, thickness of the mixtures, or both.

4.4.12. Air Void Reduction Due to Traffic Loading

It is common knowledge that in-place air voids decrease with traffic loading. This phenomenon was observed in this study by comparing the air voids of in-wheel path (after loading) and out-of-wheel path cores. The out-of-wheel path air voids represent the prior to traffic loading condition and the in-wheel path air voids represent the after loading condition. The difference between those two air voids represents the air void reduction due to traffic loading. The air voids were measured on 100 mm (4 in) in diameter cores. The core diameter was smaller than the tire width.

The effect of initial in-place mixture density on air void reduction is presented in Figure 4.29. The plot shows that the air void reduction of the high density mixtures was less than that of low density mixtures. This observation was consistent with the common knowledge that high density mixtures will experience smaller air void reductions after traffic loading. However, smaller air void reductions did not always correspond with better rutting performance. The relationship between air void reduction and rut resistance rating is presented in Figure 4.30. The relationship shows that a poor rut resistance rating (total rut greater than 20 mm) could be obtained with small air void reductions. On the other hand, similar ranges of air void reduction were observed for the mixtures with rating from very good to poor. This observation also suggests that the air void difference between out-of wheel path and in-wheel path mixtures was not a good indicator of rutting performance, especially when the rutting was excessive.

4.4.13. In-Place AC And Gradation Analysis

The asphalt mixtures that were produced and compacted in APT were sampled in accordance with ASTM D 979 "Sampling Bituminous Paving Mixtures." The samples were used to determine theoretical maximum specific gravity (TMD) (ASTM D 2041), asphalt binder content (ASTM D 2172), and gradation (ASTM D 546 and D 1140). The samples used for the TMD determinations were different than those used for asphalt extraction and gradation analysis.

The extraction data are presented in Appendix C and the results are summarized in Table 4.8. As previously stated, some of the mixtures were intentionally produced at AC level than deviated from the design AC in order to construct high and low AC lanes. After extractions, washed sieve analyses were performed on the same samples in accordance to ASTM D 546 and ASTM D 1140. The sieve analyses data are presented in Appendix C and the results are summarized in Tables 4.9 to 4.16. The data show that it was difficult to produce mixtures with gradations close to the design gradations. The primary reason for this was that the volume of mixture produced was too small for the asphalt plant to achieve uniformity.

4.4.14. Comparison of No Wander and Wander Rutting Components

As previously discussed in section 4.4.2, observed transverse profiles are different significantly when wheel wander is used in the loading process. Comparison of the profiles of the same mixture tested with and without wander was made to evaluate the difference. The effect of wander wheel on APT total rut is shown in Figure 4.31. The plot shows that when the total rut was small (good mixtures), both loading conditions result in gave similar results because there were limited deformations. When the total rut was large (poor performing mixtures), results due to the different loading conditions were very different. However, the total rut parameter categorizes the mixtures similarly based on the rut resistance criteria presented in Table 4.5. Based on the available data, it was not conclusive which wheel loading condition was more destructive.

Further analysis on other rutting components was conducted. The effect of wheel wander on APT rut depth parameter is shown in Figure 4.32. The plot suggests that APT rut depth was less sensitive to different wheel loading conditions. The effect of wheel wander on rise height parameter is shown in Figure 4.33. The plot shows that rise height was quite sensitive to the effect of wander, especially when the corresponding total rut was large (poor rut resistance mixture). In general, comparison of no wander and wander rutting components suggests that the selected definitions of rutting components were adequate to evaluate the mixtures consistently.

Table 4.1 HMA Mixtures Tested in INDOT/Purdue Accelerated Pavement Testing Facility.

FAA	Gradation	9.5 mm Nominal Max. Size		19 mm Nominal Max. Size	
		Limestone	Granite	Limestone	Granite
39	Above				
	Below			X	
44	Above			X	
	Through	X			
	Below		X	X	X
50	Above			X	
	Through	X			X
	Below		X		

Table 4.2 Lanes Constructed to Investigate the Effect of Density and Deviation from Design AC Using the APT (9.5mm Mixtures).

FAA	Gradation	9.5 mm Nominal Max. Size							
		Limestone				Granite			
		1	2	3	4	1	2	3	4
39	Above								
	Below								
44	Above								
	Through	HAC	LAC	LAC	HAC				
	Below					LAC	LAC	LAC	LAC
50	Above								
	Through	LAC	HAC	HAC	LAC				
	Below					LAC	HAC	HAC	LAC

Note: 1, 2, 3, 4 = lane number;
LAC =low AC lane; HAC = high AC lane.

Table 4.3 Lanes Constructed to Investigate the Effect of Density and Deviation from Design AC Using the APT (19mm Mixtures).

FAA	Gradation	19 mm Nominal Max. Size							
		Limestone				Granite			
		1	2	3	4	1	2	3	4
39	Above								
	Below	LD			HD				
44	Above		LD	HD					
	Through								
	Below	LD	LD	HD	HD	LAC	LAC	HAC	HAC
50	Above		LD		HD				
	Through					LAC	LAC	HAC	HAC
	Below								

Note: 1, 2, 3, 4 = lane number; LD = low density lane, HD = high density lane
LAC =low AC lane; HAC = high AC lane.

Table 4.4 Layout of APT Tests for Wheel Wander Effects.

FAA	Gradation	9.5 mm Nominal Max. Size								19 mm Nominal Max. Size							
		Limestone				Granite				Limestone				Granite			
		1	2	3	4	1	2	3	4	1	2	3	4	1	2	3	4
39	Above																
	Below									S			S				
44	Above										S	S					
	Through	S	S	S	S												
	Below					S	S	S	S	S	W	W	S	W	S	S	W
50	Above										S		S				
	Through	S	S	S	S									S	W	W	S
	Below					S	S	S	S								

Note: 1, 2, 3, 4 = lane number; S = single wheel path (no wander) effect; W = transverse wander effect

Table 4.5 Subjective Identification of Rut Resistance Using the APT.

Rut Resistance	Total Rut at 20000 wheel passes (mm)	Rut Depth at 20000 wheel passes (mm)	Rise Height at 20000 wheel passes (mm)
Very Good	< 10.0	< 7.0	< 3.0
Good	10.0 – 15.0	7.0 – 10.0	3.0 – 5.0
Fair	15.0 – 20.0	10.0 –12.0	5.0 – 8.0
Poor	> 20.0	> 12.0	> 8.0

Table 4.6 Rutting Performance of HMA Mixtures in The APT.

FAA	Gradation	Rutting Resistance	9.5 mm Nominal Max. Size		19 mm Nominal Max. Size	
			Limestone	Granite	Limestone	Granite
39	Above	Rating				
		Total Rut				
	Below	Rating			Poor	
		Total Rut			25.3 (10)	
44	Above	Rating			Good	
		Total Rut			9.54 (3)	
	Through	Rating	Fair			
		Total Rut	18.1 (8)			
	Below	Rating		Excellent	Fair	Excellent
		Total Rut		8.0 (1)	19.1 (9)	9.5 (2)
50	Above	Rating			Fair	
		Total Rut			15.1 (6)	
	Through	Rating	Fair			Good
		Total Rut	15.5 (7)			12.2 (5)
	Below	Rating		Good		
		Total Rut		11.0 (4)		

Note: Total Rut unit is mm. The number in the bracket () is the rank of the mixture.

Table 4.7 Summary of ANOVA for Factor Effects on APT Total Rut.

Variable	Significance	p value
Nominal Maximum Size	No	0.1844
Coarse Aggregate Type	Yes	0.0411
Fine Aggregate Angularity	No	0.0539
Gradation with Respect to The Restricted Zone	Yes	0.0134

note: p values are based on Type III Sum of Squares

Table 4.8 In-Place AC of HMA Mixtures in APT.

Nom. Max. Size (mm)	Coarse Ag. Type	FAA	Gradation	Design AC (%)	Asphalt Extraction	
					Average (%)	Difference (%)
19	Limestone	39	Below	5.5	5.7	0.2
19	Limestone	44	Above	4.6	4.7	0.1
19	Limestone	44	Below	4.6	4.9	0.3
19	Limestone	50	Above	5.9	5.8	-0.1
19	Granite	44	Below	4.4	4.5	0.1
19	Granite	44	Below	4.4	5.6	1.2
19	Granite	50	Through	5.3	4.5	-0.8
19	Granite	50	Through	5.3	5.4	0.1
9.5	Limestone	44	Through	6.2	5.6	-0.6
9.5	Limestone	44	Through	6.2	6.3	0.1
9.5	Limestone	50	Through	6.6	6	-0.6
9.5	Limestone	50	Through	6.6	6.8	0.2
9.5	Granite	44	Below	5.2	5.2	0
9.5	Granite	44	Below	5.2	5.3	0.1
9.5	Granite	50	Below	5.6	5.5	-0.1
9.5	Granite	50	Below	5.6	6.2	0.6
12.5					5.2	

Table 4.9 In-Place Gradation Analysis of 19LS39B and 19LS44A.

Mixture ID:	19LS39B			19LS44A		
Nom.Max.:	19mm			19mm		
Coarse Agg:	Limestone			Limestone		
FAA:	39			44		
Gradation	Below The Restricted Zone			Above the restricted zone		
AC:	5.7% (+0.1% Design AC)			4.7% (+0.1% Design AC)		
Sieve Size (mm)	Design Gradation (%)	Washed Sieve		Design Gradation (%)	Washed Sieve	
		Average (%)	Difference (%)		Average (%)	Difference (%)
25	100.0	100.0	0.0	100.0	100.0	0.0
19	97.1	97.2	0.1	95.5	97.2	1.7
12.5	87.8	91.1	3.3	80.7	86.5	5.8
9.5	81.5	86.5	5.0	73.1	79.0	5.9
4.75	52.7	60.9	8.2	64.6	68.6	4.0
2.36	29.7	33.4	3.7	48.9	51.5	2.6
1.18	22.0	21.5	-0.5	30.5	30.8	0.3
0.6	15.0	14.7	-0.3	20.8	19.4	-1.4
0.3	8.1	7.4	-0.7	14.4	11.7	-2.7
0.15	4.5	4.1	-0.4	9.0	5.9	-3.1
0.075	3.1	3.1	0.0	5.9	3.3	2.6

Table 4.10 In-Place Gradation Analysis of 19GR44B.

Mixture ID:	19GR44B			19GR44B		
Nom.Max.:	19mm			19mm		
Coarse Agg:	Granite			Granite		
FAA:	44			44		
Gradation	Below The Restricted Zone			Below The Restricted Zone		
AC:	4.5% (+0.1% Design AC)			5.6% (+1.2% Design AC)		
Sieve Size (mm)	Design Gradation (%)	Washed Sieve		Design Gradation (%)	Washed Sieve	
		Average (%)	Difference (%)		Average (%)	Difference (%)
25	100.0	100.0	0.0	100.0	100.0	0.0
19	98.9	99.2	0.3	98.9	98.6	-0.2
12.5	77.7	76.7	-1.0	77.7	80.2	2.6
9.5	58.5	58.0	-0.5	58.5	62.4	3.9
4.75	38.2	36.4	-1.8	38.2	39.9	1.7
2.36	28.3	24.8	-3.5	28.3	28.1	-0.2
1.18	17.6	15.6	-2.0	17.6	18.0	0.4
0.6	12.8	11.1	-1.7	12.8	13.2	0.4
0.3	9.5	8.0	-1.5	9.5	10.2	0.7
0.15	6.5	5.6	-0.9	6.5	8.0	1.5
0.075	4.2	4.1	-0.1	4.2	6.4	2.1

Table 4.11 In-Place Gradation Analysis of 19GR50T.

Mixture ID:	19GR50T			19GR50T		
Nom.Max.:	19mm			19mm		
Coarse Agg:	Granite			Granite		
FAA:	50			50		
Gradation	Through The Restricted Zone			Through The Restricted Zone		
AC:	4.5% (-0.8% Design AC)			5.4% (+0.1% Design AC)		
Sieve Size (mm)	Design Gradation (%)	Washed Sieve		Design Gradation (%)	Washed Sieve	
		Average (%)	Difference (%)		Average (%)	Difference (%)
25	100.0	100.0	0.0	100.0	100.0	0.0
19	99.6	99.2	-0.4	99.6	99.4	-0.2
12.5	92.6	89.7	-2.9	92.6	91.1	-1.5
9.5	83.2	79.6	-3.6	83.2	83.9	0.7
4.75	51.7	42.0	-9.6	51.7	52.1	0.4
2.36	36.8	25.9	-10.9	36.8	33.6	-3.2
1.18	23.9	18.9	-5.1	23.9	23.6	-0.3
0.6	16.8	14.6	-2.2	16.8	17.2	0.4
0.3	11.3	10.9	-0.4	11.3	12.4	1.1
0.15	8.0	7.5	-0.5	8.0	8.6	0.6
0.075	5.5	5.1	-0.4	5.5	5.8	0.4

Table 4.12 In-Place Gradation Analysis of 9.5LS44T.

Mixture ID:	9.5LS44T			9.5LS44T		
Nom.Max.:	9.5mm			9.5mm		
Coarse Agg:	Limestone			Limestone		
FAA:	44			44		
Gradation	Through The Restricted Zone			Through The Restricted Zone		
AC:	5.6% (-0.6% Design AC)			6.3% (+0.1% Design AC)		
Sieve Size (mm)	Design Gradation (%)	Washed Sieve		Design Gradation (%)	Washed Sieve	
		Average (%)	Difference (%)		Average (%)	Difference (%)
12.5	100.0	100.0	0.0	100.0	100.0	0.0
9.5	99.0	99.8	0.8	99.0	99.7	0.7
4.75	83.0	85.0	2.0	83.0	84.1	1.1
2.36	55.8	58.1	2.3	55.8	55.3	-0.5
1.18	33.3	34.9	1.6	33.3	32.0	-1.3
0.6	21.6	21.8	0.2	21.6	20.2	-1.5
0.3	14.2	11.1	-3.1	14.2	12.2	-2.0
0.15	8.4	4.9	-3.5	8.4	7.5	-0.9
0.075	5.3	3.1	-2.2	5.3	5.6	0.3

Table 4.13 In-Place Gradation Analysis of 9.5LS50T.

Mixture ID:	9.5LS50T			9.5LS50T		
Nom.Max.:	9.5mm			9.5mm		
Coarse Agg:	Limestone			Limestone		
FAA:	50			50		
Gradation	Through The Restricted Zone			Through The Restricted Zone		
AC:	6.0% (-0.6% Design AC)			6.8% (+0.2% Design AC)		
Sieve Size (mm)	Design Gradation (%)	Washed Sieve		Design Gradation (%)	Washed Sieve	
		Average (%)	Difference (%)		Average (%)	Difference (%)
12.5	100.0	100.0	0.0	100.0	100.0	0.0
9.5	98.6	99.9	1.4	98.6	100.0	1.4
4.75	75.5	84.7	9.2	75.5	82.4	6.9
2.36	48.3	55.5	7.2	48.3	52.0	3.7
1.18	31.8	38.1	6.3	31.8	36.0	4.2
0.6	21.7	26.7	5.0	21.7	25.6	3.9
0.3	14.6	16.2	1.7	14.6	16.2	1.6
0.15	10.3	10.6	0.3	10.3	11.0	0.7
0.075	7.0	7.8	0.7	7.0	8.4	1.4

Table 4.14 In-Place Gradation Analysis of 9.5GR44B.

Mixture ID:	9.5GR44B			9.5GR44B		
Nom.Max.:	9.5mm			9.5mm		
Coarse Agg:	Granite			Granite		
FAA:	44			44		
Gradation	Below The Restricted Zone			Below The Restricted Zone		
AC:	5.2% (Design AC)			5.3% (+0.1%Design AC)		
Sieve Size (mm)	Design Gradation (%)	Washed Sieve		Design Gradation (%)	Washed Sieve	
		Average (%)	Difference (%)		Average (%)	Difference (%)
12.5	100.0	100.0	0.0	100.0	100.0	0.0
9.5	95.0	97.2	2.2	95.0	96.0	0.1
4.75	61.5	66.6	5.1	61.5	63.0	1.5
2.36	41.9	48.3	6.4	41.9	43.6	1.7
1.18	24.9	30.6	5.7	24.9	25.8	0.8
0.6	17.0	19.8	2.8	17.0	15.5	-1.5
0.3	11.7	10.5	-1.2	11.7	7.8	-3.9
0.15	7.3	4.8	-2.5	7.3	3.7	-3.6
0.075	4.7	3.3	-1.4	4.7	2.6	-2.1

Table 4.15 In-Place Gradation Analysis of 9.5GR50B.

Mixture ID:	9.5GR50B			9.5GR50B		
Nom.Max.:	9.5mm			9.5mm		
Coarse Agg:	Granite			Granite		
FAA:	50			50		
Gradation	Below The Restricted Zone			Below The Restricted Zone		
AC:	5.5% (-0.1%Design AC)			6.2% (+0.6%Design AC)		
Sieve Size (mm)	Design Gradation (%)	Washed Sieve		Design Gradation (%)	Washed Sieve	
		Average (%)	Difference (%)		Average (%)	Difference (%)
12.5	100.0	100.0	0.0	100.0	100.0	0.0
9.5	94.7	95.9	1.2	94.7	97.5	2.8
4.75	58.7	56.9	-1.8	58.7	59.9	1.2
2.36	41.1	37.1	-4.0	41.1	38.4	-2.7
1.18	26.8	25.9	-0.9	26.8	27.3	0.5
0.6	18.8	18.5	-0.3	18.8	20.5	1.7
0.3	12.7	12.6	-0.1	12.7	15.7	3.0
0.15	8.9	8.6	-0.3	8.9	11.9	2.9
0.075	6.1	6.1	0.0	6.1	8.5	2.4

Table 4.16 In-Place Gradation Analysis of Binder Layer.

Mixture ID:	Binder Layer		
Nom.Max.:	12.5mm		
Coarse Agg:	Limestone		
FAA:			
Gradation			
AC:	5.2%		
Sieve Size (mm)	Design Gradation (%)	Washed Sieve	
		Average (%)	Difference (%)
19		100.0	
12.5		94.4	
9.5		85.5	
4.75		55.8	
2.36		39.8	
1.18		28.6	
0.6		19.3	
0.3		9.0	
0.15		4.3	
0.075		3.0	

Figure 4.1 INDOT/Purdue University APT.

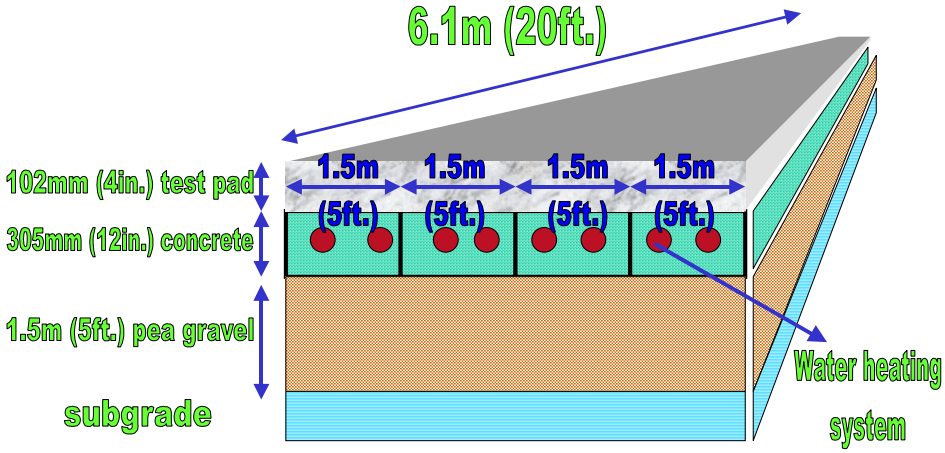

Figure 4.2 APT Structural Layout.

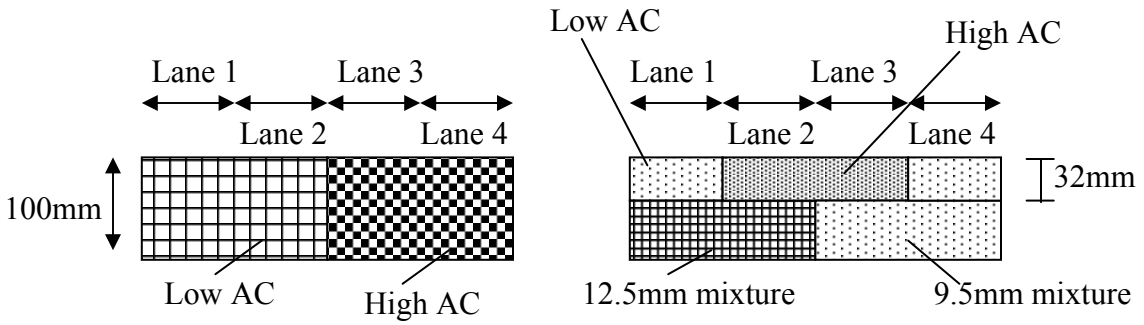

a) 19mm mixture

b) 9.5mm mixture

Figure 4.3 Typical Test Section Construction Layout.

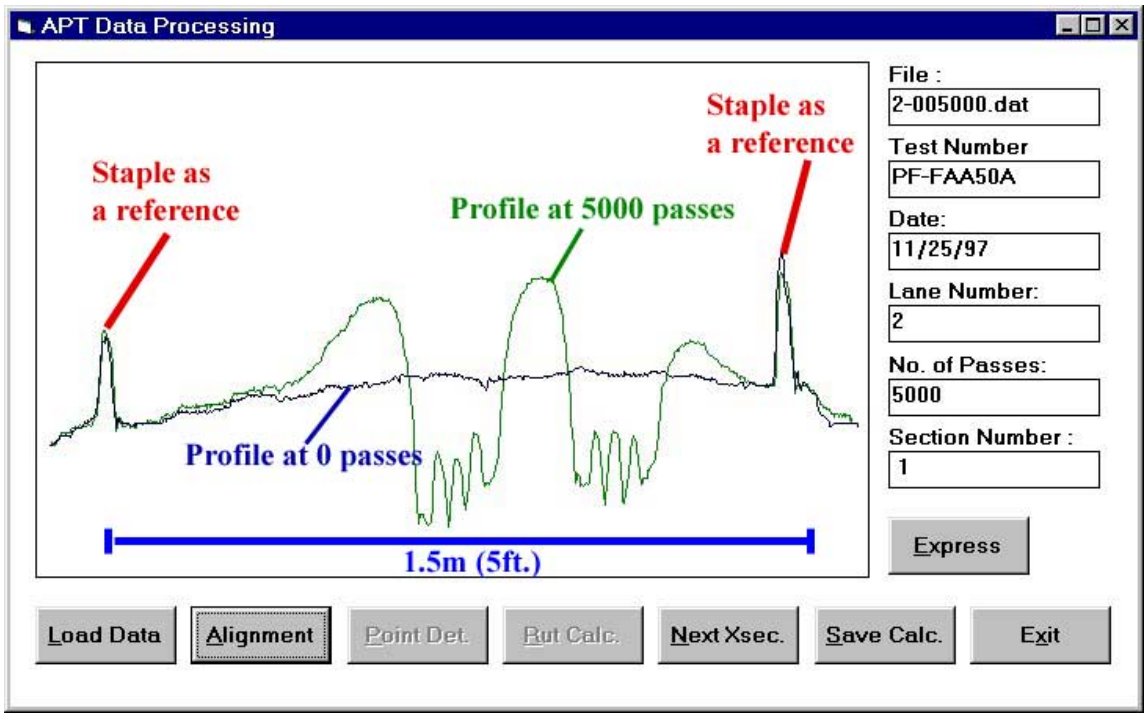

Figure 4.4 Transverse Profile Observed During APT Testing.

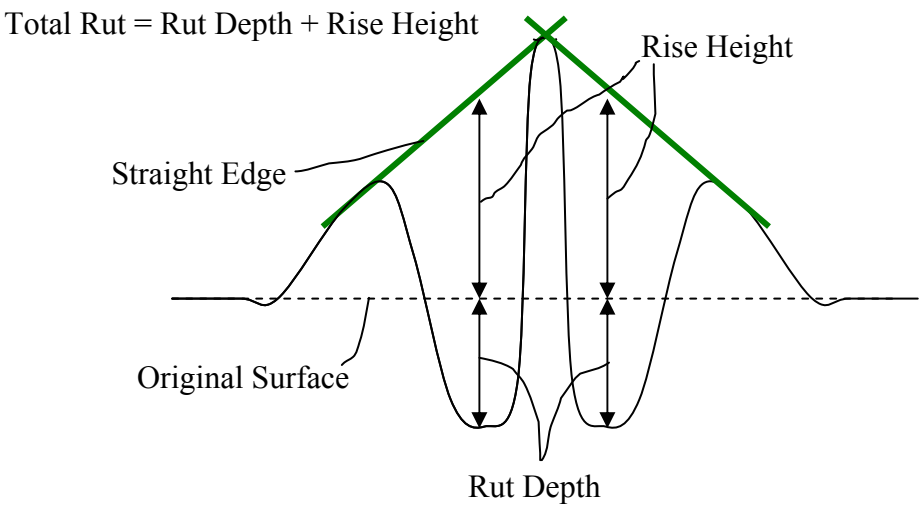

Figure 4.5 Definition of Rutting Components without Wander.

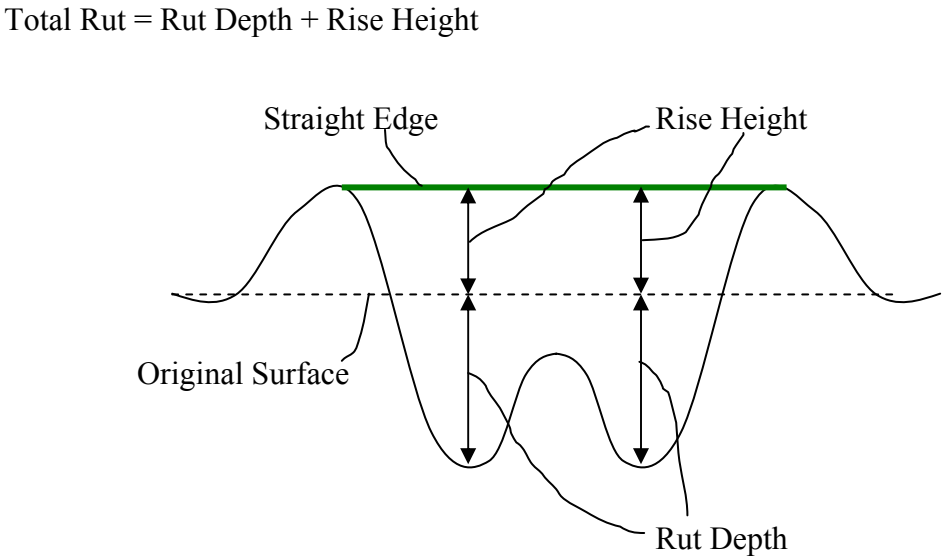

Figure 4.6 Definition of Rutting Components with Wander.

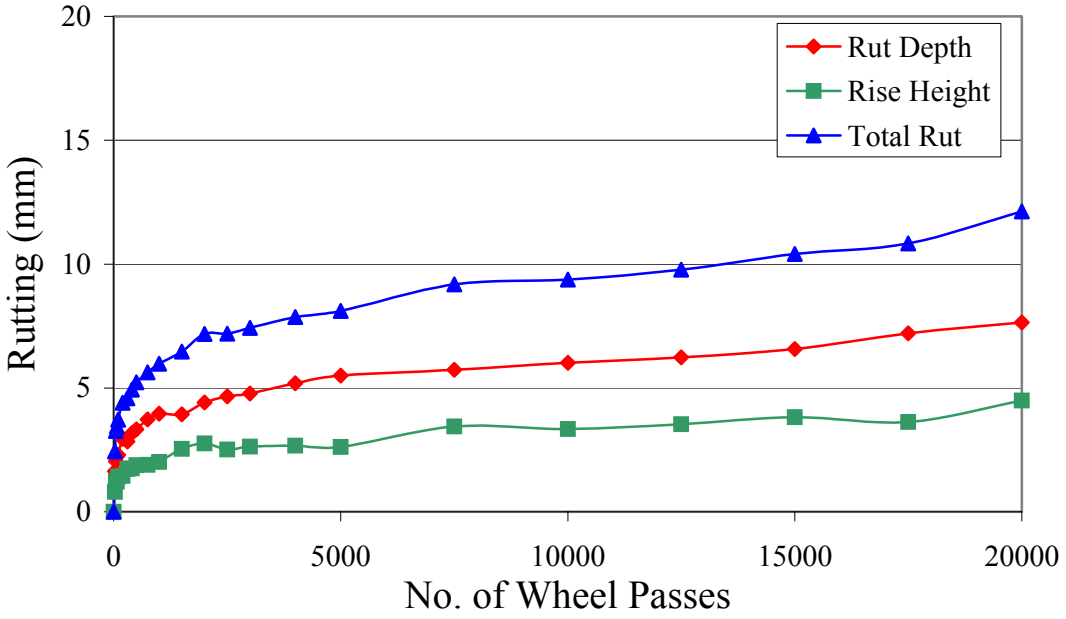

Figure 4.7 Rutting Components without Wander.

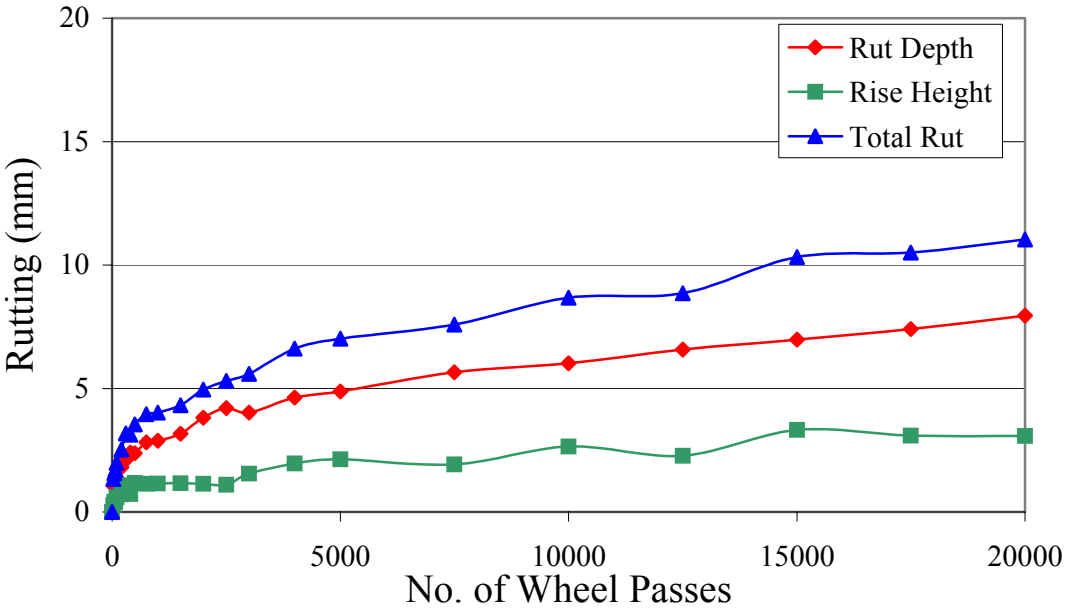

Figure 4.8 Rutting Components with Wander.

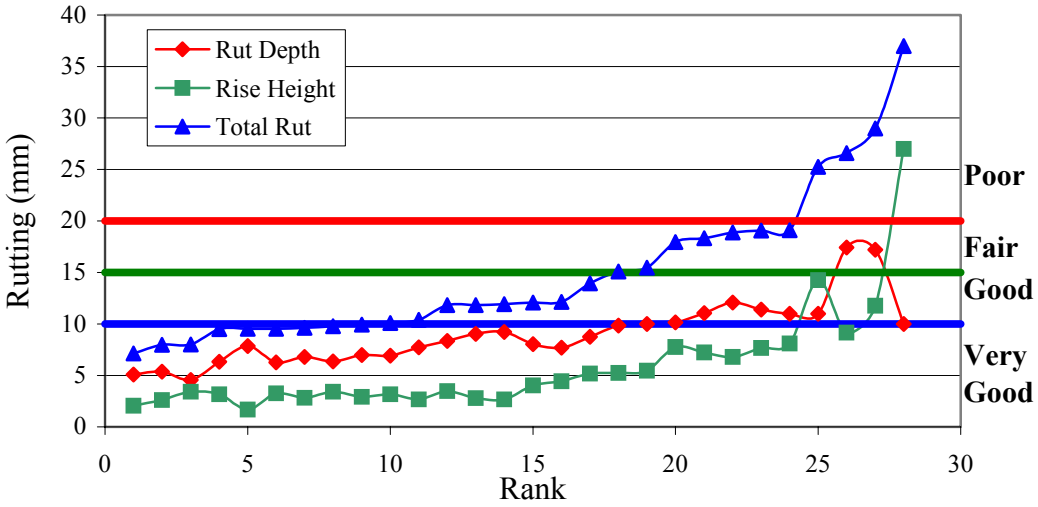

Figure 4.9 Sorted APT Data.

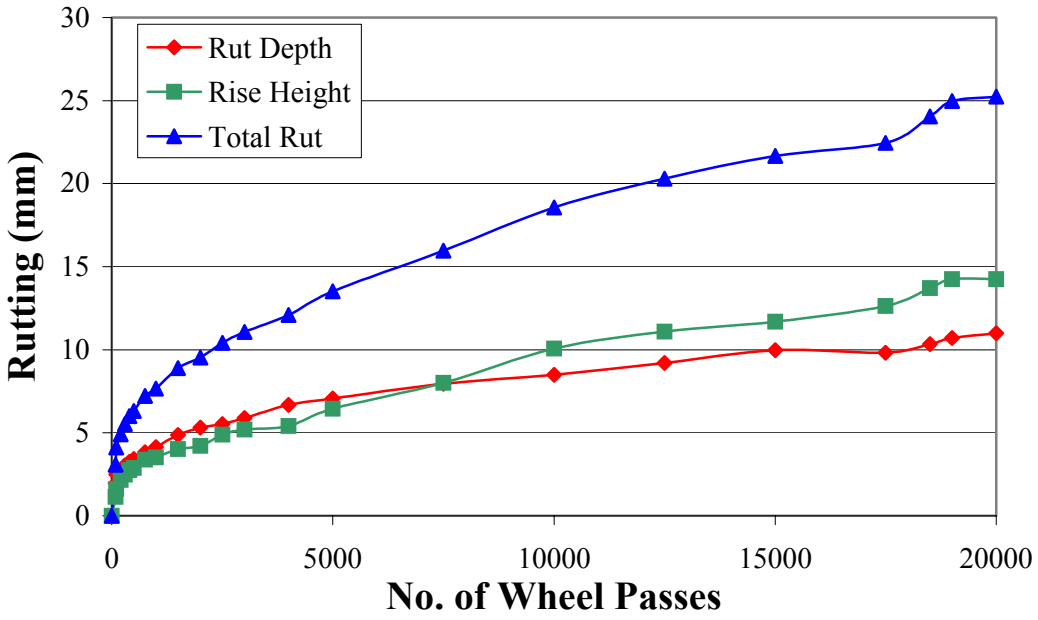

Figure 4.10 No Wander Rutting for 19 mm Limestone with FAA of 39, Gradation Plotting Below The Restricted Zone, Low Density Lane.

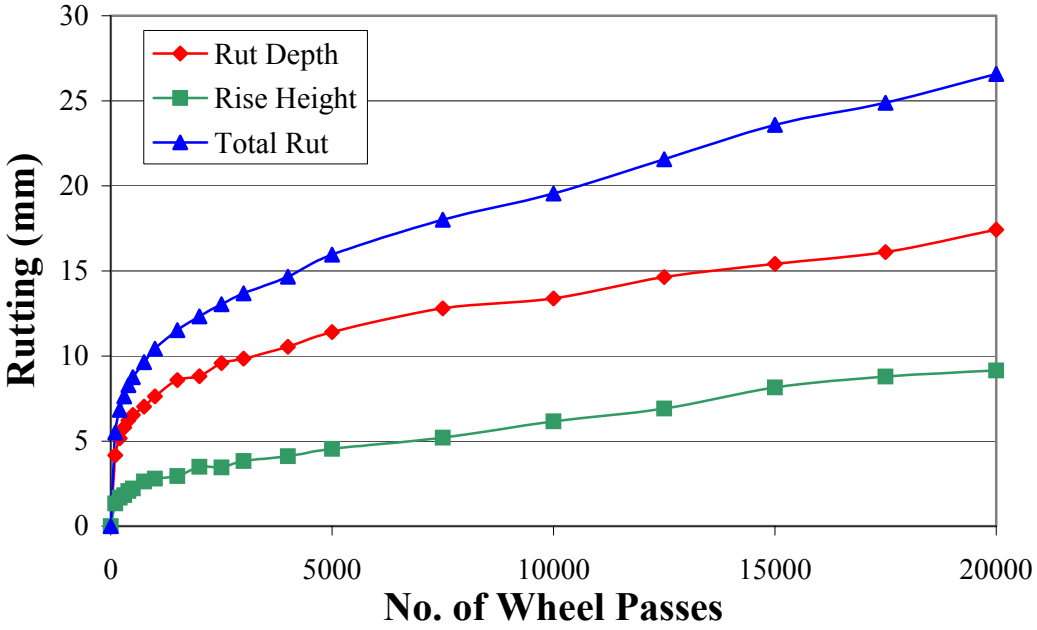

Figure 4.11 No Wander Rutting for 19 mm Limestone with FAA of 50, Gradation Plotting Above The Restricted Zone, High Density Lane.

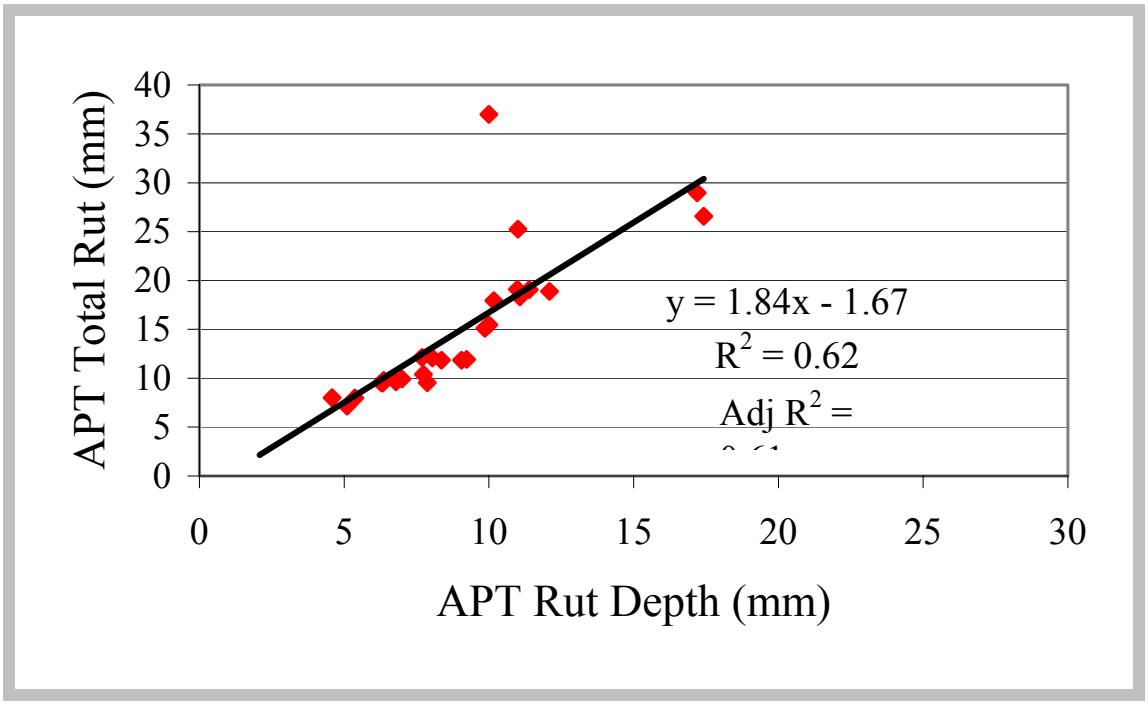

Figure 4.12 Relationship Between Total Rut and Rut Depth in APT.

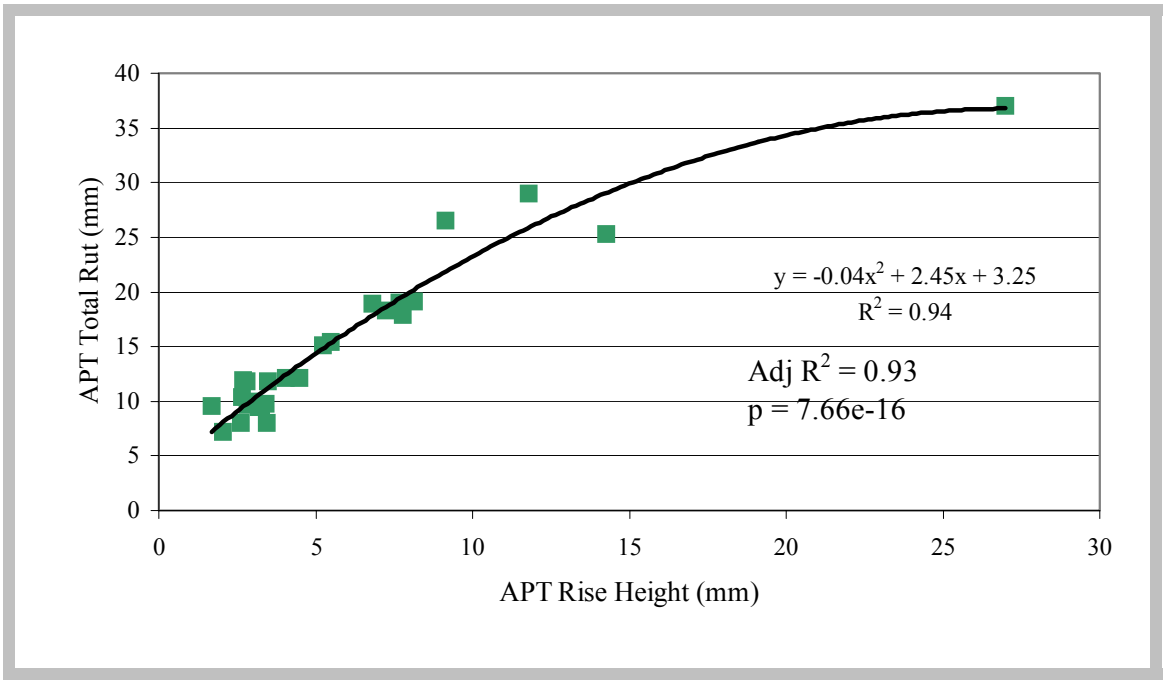

Figure 4.13 Relationship Between Total Rut and Rise Height in APT.

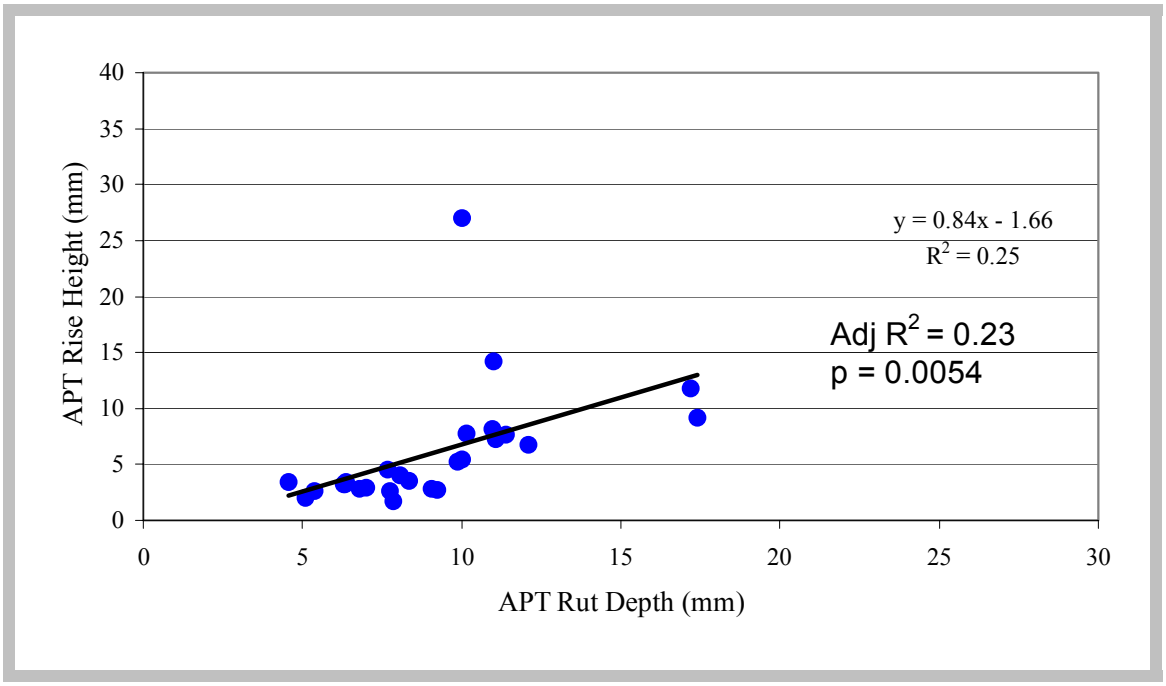

Figure 4.14 Relationship Between Rise Height and Rut Depth in APT.

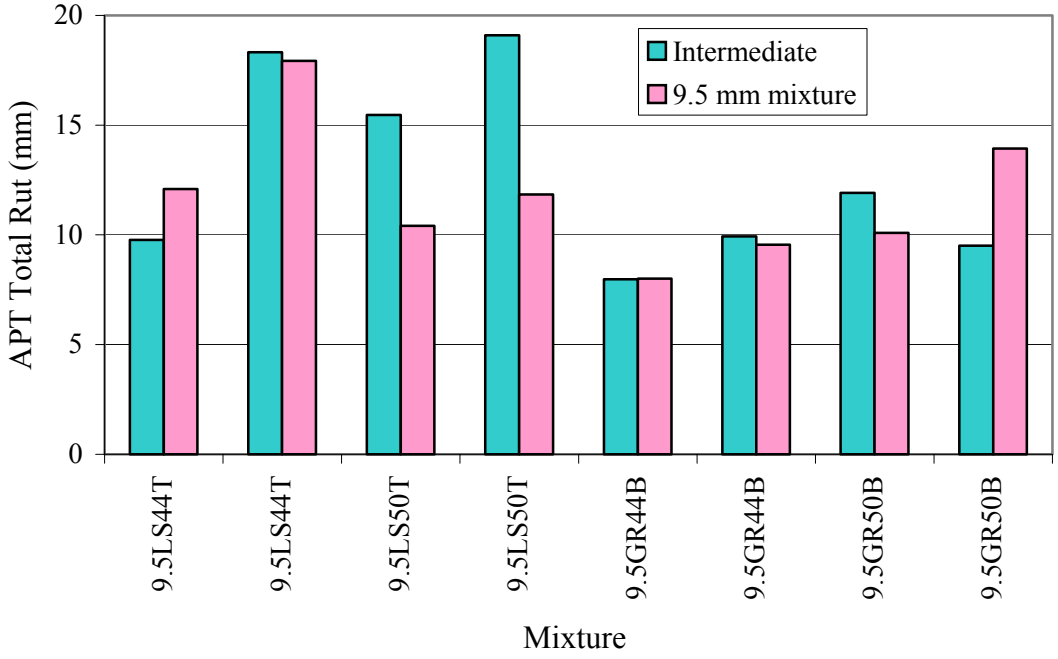

Figure 4.15 Effect of Binder Course on Rutting Performance in the APT.

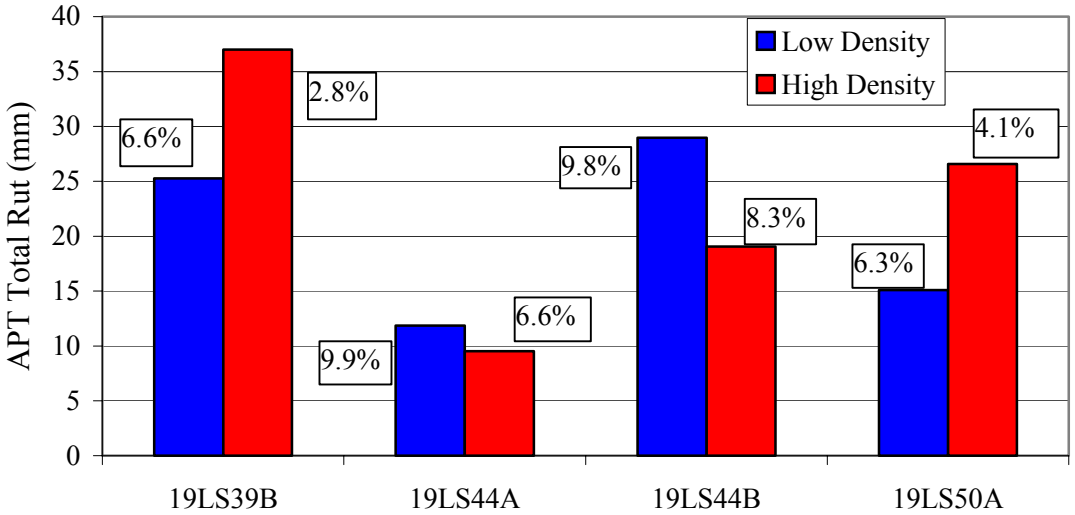

Note: Numbers in the boxes are initial in-place air voids (%).

Figure 4.16 Effect of Initial In-Place Density on Rutting Performance in the APT.

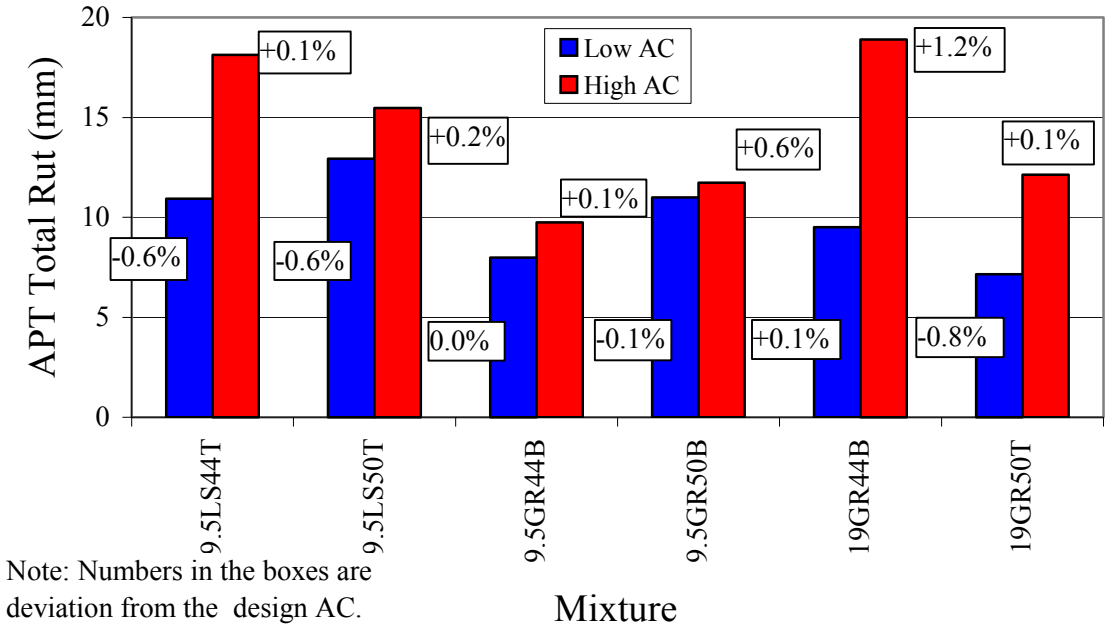

Note: Numbers in the boxes are deviation from the design AC.

Figure 4.17 Effect of Deviation from Design AC on Rutting Performance in the APT.

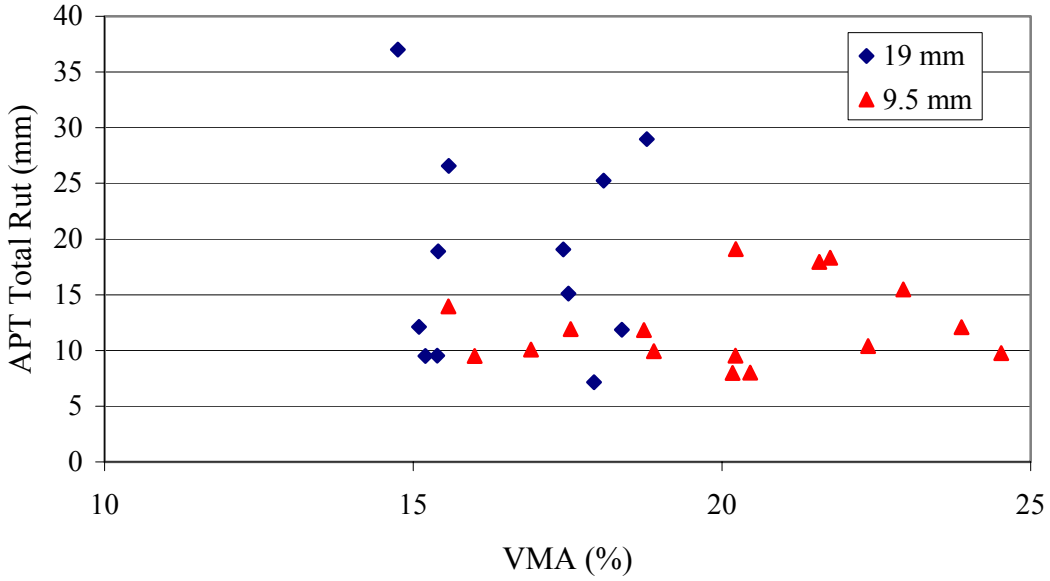

Figure 4.18 Scatter Plot of Total Rut and VMA (All APT Mixtures).

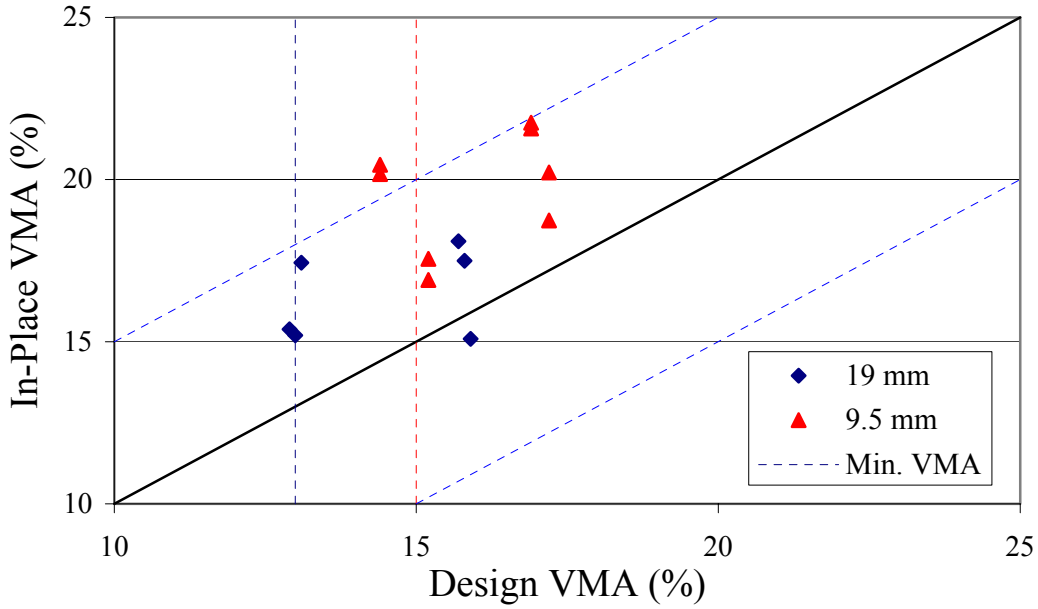

Figure 4.19 Scatter Plot of Selected In-Place and Design VMA.

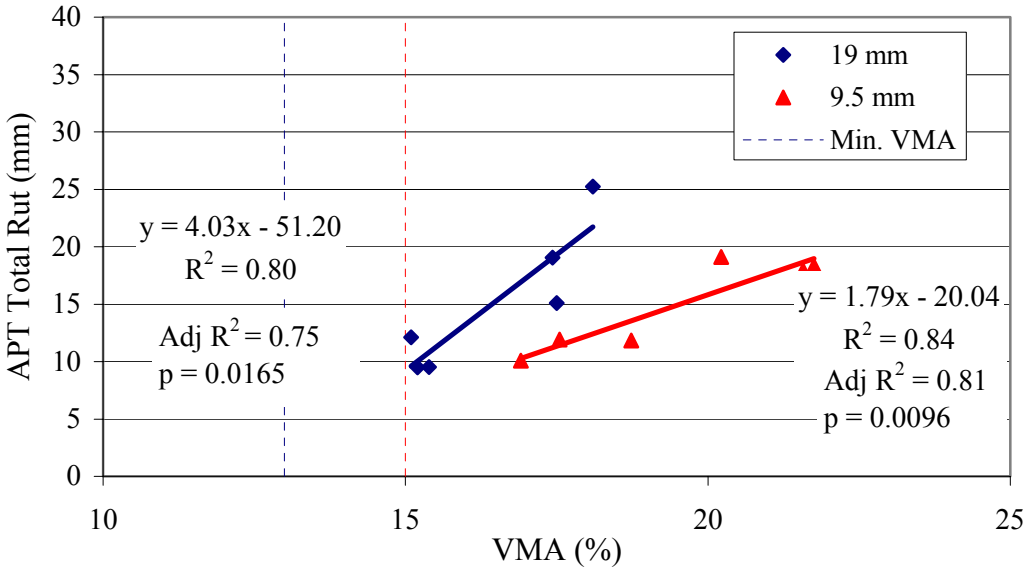

Figure 4.20 Relationship between APT Total Rut and Selected In-Place VMA.

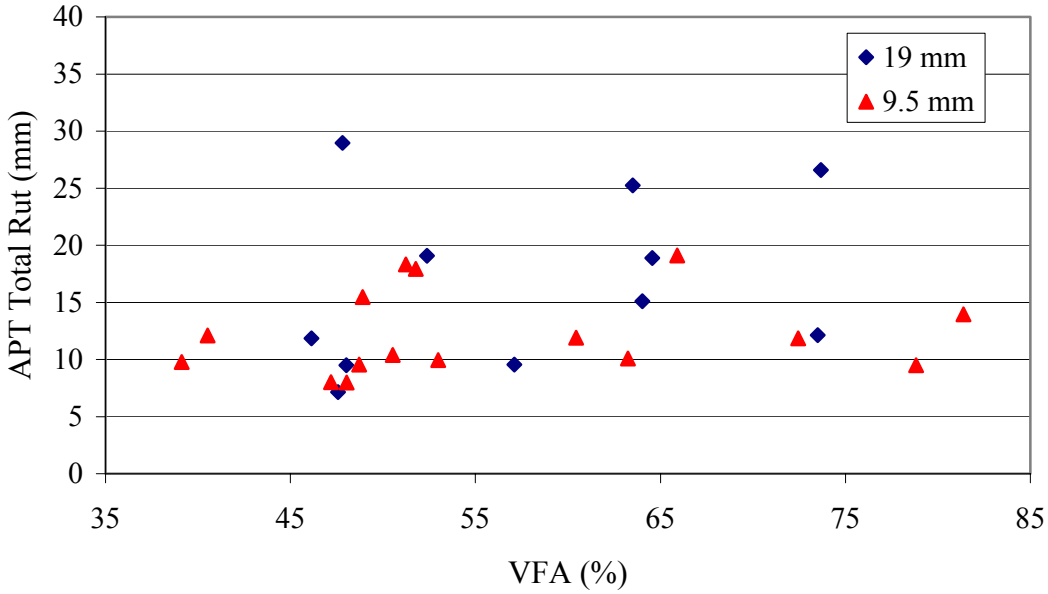

Figure 4.21 Scatter Plot of APT Total Rut and In-Place VFA (All APT Mixtures).

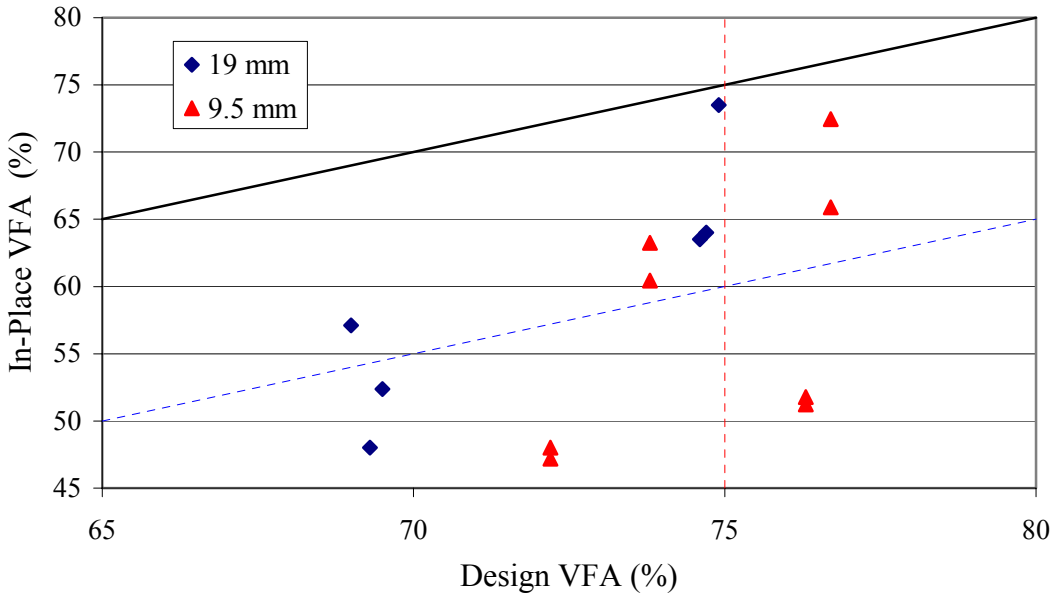

Figure 4.22 Scatter Plot of Selected In-Place VFA and Design VFA.

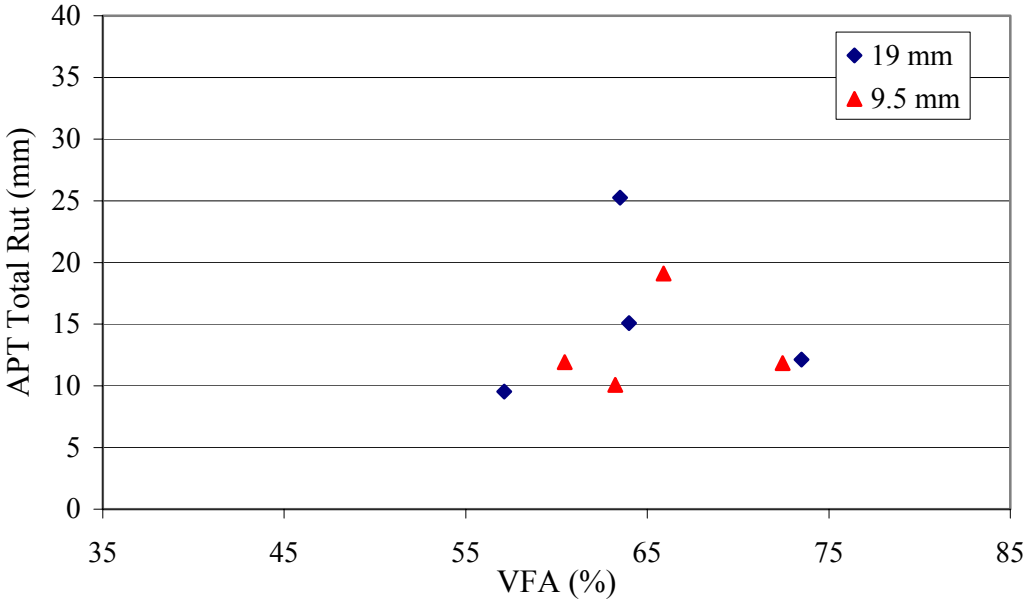

Figure 4.23 Scatter Plot of APT Total Rut and Selected In-Place VFA.

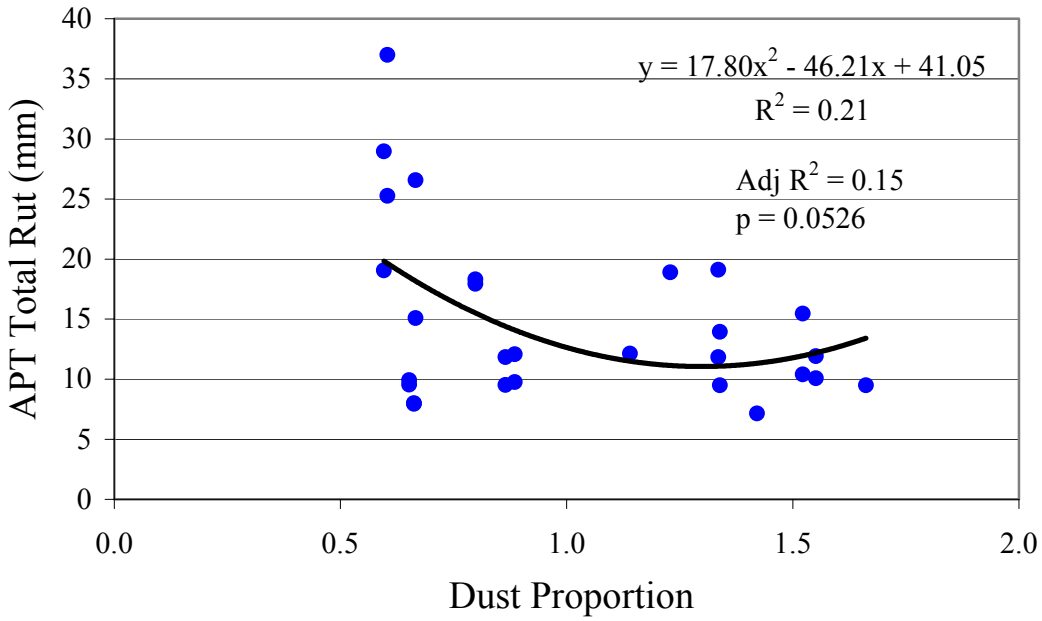

Figure 4.24 Relationship Between APT Total Rut and In-Place Dust Proportion (All APT Mixtures).

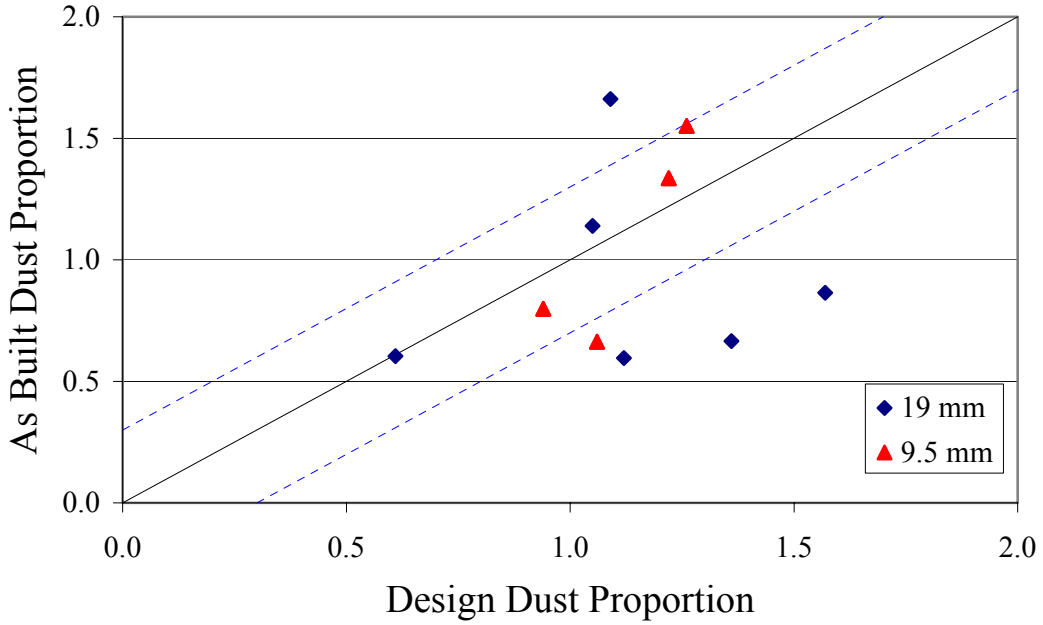

Figure 4.25 Scatter Plot of In-Place Dust Proportion and Design Dust Proportion.

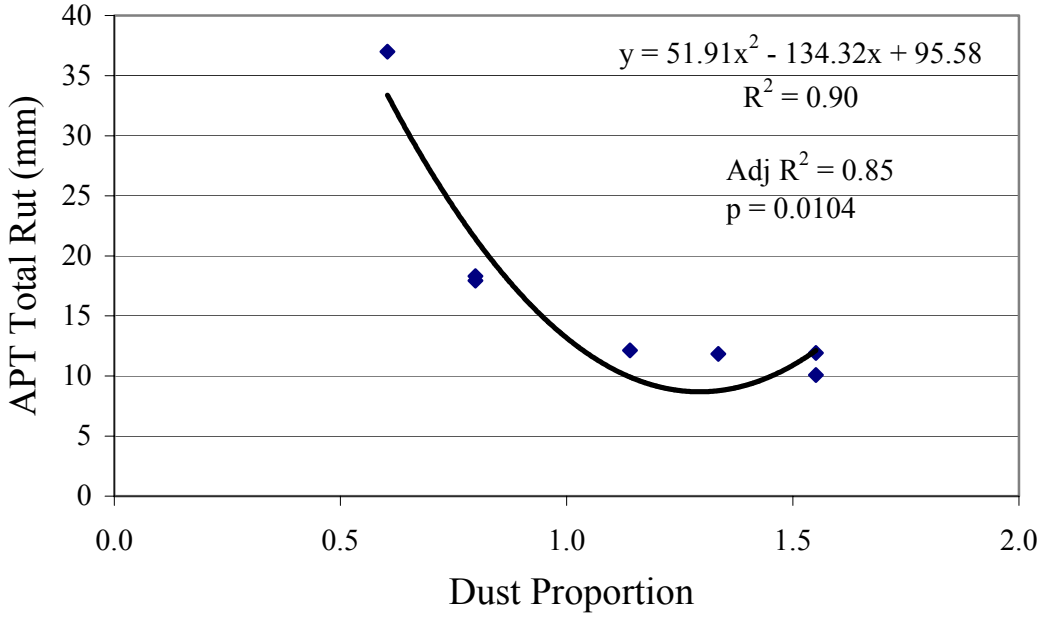

Figure 4.26 Relationship Between APT Total Rut and Selected In-Place Dust Proportion.

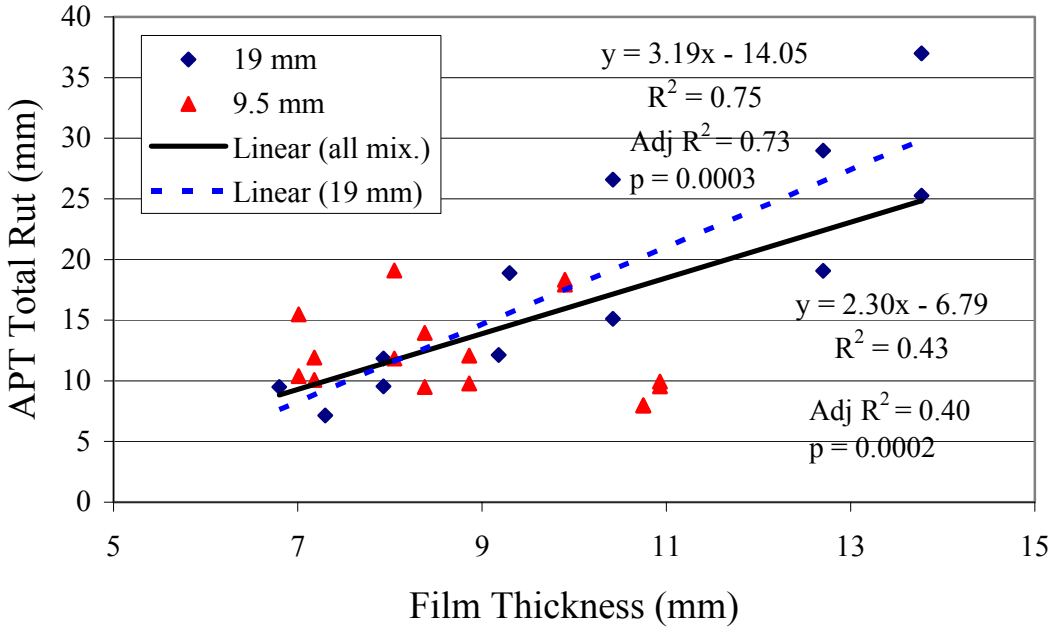

Figure 4.27 Relationship Between APT Total Rut and In-Place Film Thickness.

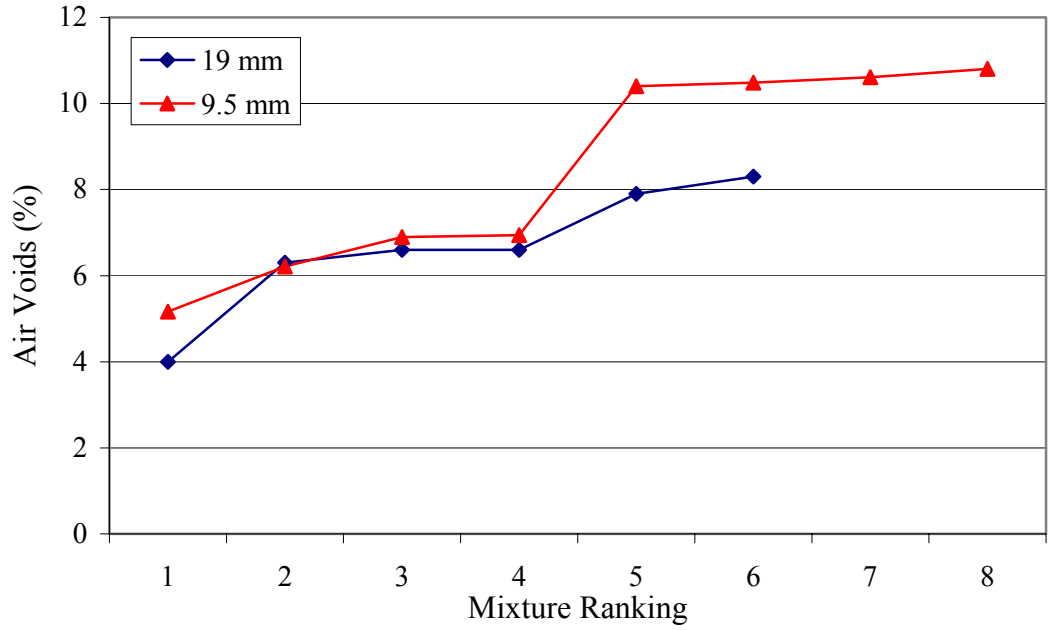

Figure 4.28 Effect of In-Place Air Voids of Mixture Rutting.

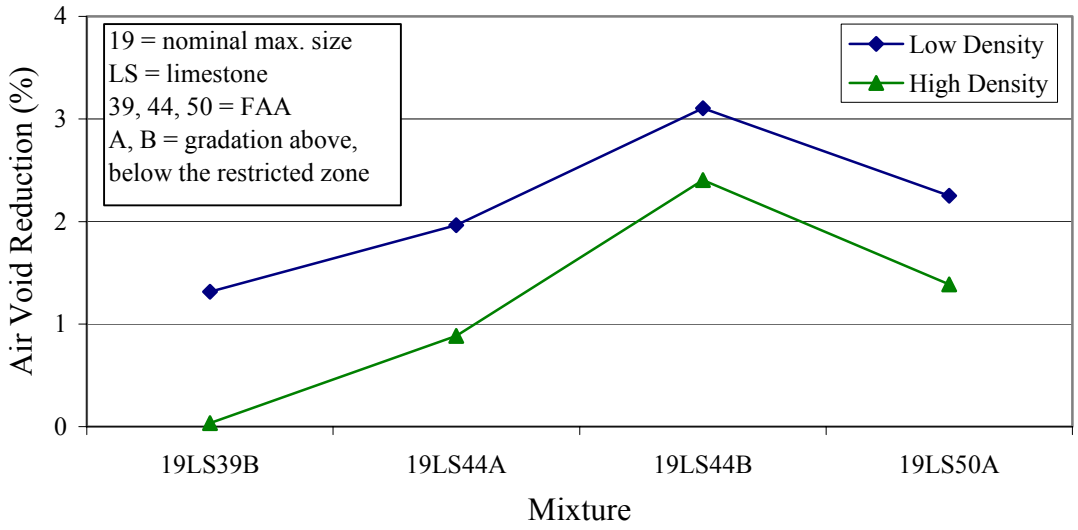

Figure 4.29 Effect of Initial In-Place Density on Reduction in Air Void Due to Loading

Figure 4.30 Scatter Plot of Reduction in Air Void and Rut Resistance Rating

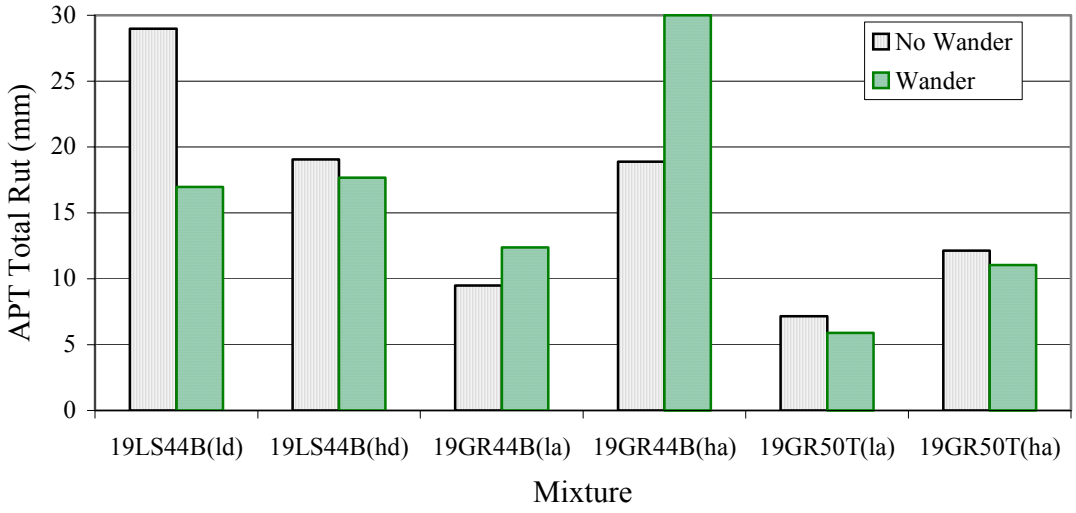

19 = nominal max. size, LS = limestone, GR = Granite; 39, 44, 50 = FAA; A, B, T = gradation above, below , through the restricted zone, ld = low density, hd=high density, la = low AC, ha= high AC

Figure 4.31 Effect of Wander Wheel on APT Total Rut.

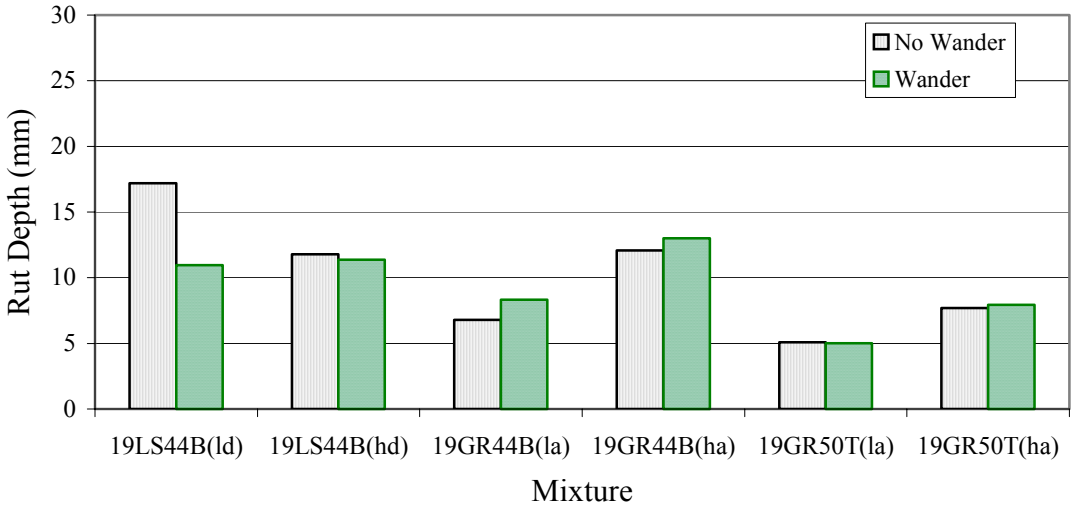

19 = nominal max. size, LS = limestone, GR = Granite; 39, 44, 50 = FAA; A, B, T = gradation above, below , through the restricted zone, ld = low density, hd=high density, la = low AC, ha= high AC

Figure 4.32 Effect of Wander Wheel on APT Rut Depth.

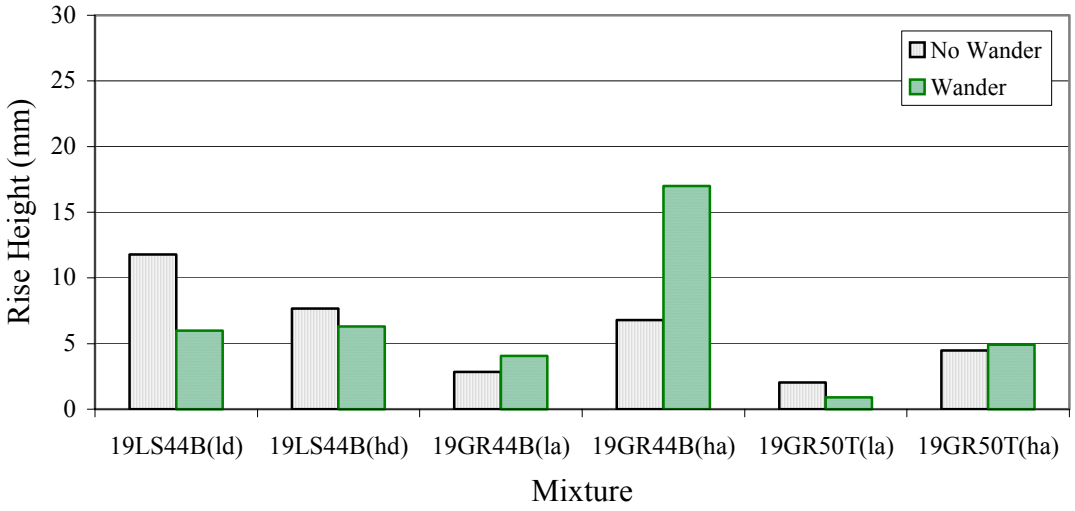

19 = nominal max. size, LS = limestone, GR = Granite; 39, 44, 50 = FAA; A, B, T = gradation above, below , through the restricted zone, ld = low density, hd=high density, la = low AC, ha= high AC

Figure 4.33 Effect of Wander Wheel on APT Rise Height

5 LABORATORY WHEEL TRACK TESTS

5.1. Description of Purdue Laboratory Wheel Track Test Device (PURWheel)

The Purdue laboratory wheel track test device or PURWheel (Figure 5.1) was designed to represent conditions associated with both rutting and stripping (Pan, 1997). These conditions include the presence of moisture, high temperatures, and moving wheel loads. There are currently several laboratory wheel testing devices in addition to the PURWheel being utilized in the United States. These include the French Rut Tester, Georgia Loaded Wheel Tester now referred to as the Asphalt Pavement Analyzer (APA), and the Hamburg steel wheel tracking device. Conceptually, wheel tracking tests simulate the effect of moving wheel loads. After reviewing features of available wheel testing devices, the Hamburg device, which tests compacted slabs immersed in hot water, was considered the most effective device for evaluation effect of stripping on rutting potential.

A number of features were added to the basic Hamburg concept in order to develop the PURWheel. The added features included:

1. Use of two air cylinders to drive the wheels independently as well as achieve a constant speed throughout the stroke;
2. A wheel mounting assembly for different types of wheels (steel, rubber coated, or pneumatic);
3. A transverse mechanism to incorporate wheel wander (Figure 5.2);
4. A larger sample box to minimize boundary effects (Figure 5.3);
5. Ability to measure rutting over the entire length of specimen using movable transducers (Figure 5.4); and

6. The testing chamber was modified so that tests could be conducted in hot/dry as well as hot/wet conditions. The heating system for the hot/dry condition consists of two components. One involves hot water circulated through conduits in sandwiched plates under the specimen. The second component involves an air heating system. The air heating system was added to minimize sample/air temperature differential and ensure uniform temperature through the specimens. The air heating system uses electric resistance heating elements and a blower as shown in Figure 5.5. Thermocouples embedded in dummy samples are used as a feedback component to achieve test temperature set point.

As previously stated, the test environment can be either hot/wet or hot/dry. Typical test temperature ranges from 55^0C to 60^0C, although the test temperature can vary from room temperature to 65^0C. The wheel velocity can be set from 20 cm/sec to 40 cm/sec by adjusting the air cylinder valve controls. Initial tests were conducted with samples 292 mm (11.5 in.) wide by 622 mm (24.5 in.) long. In these tests, the observed rutting appeared to be uniform over the entire sample length. As a result, a decision was made to reduce the length of the sample by one-half. Concrete blocks with the same thickness as that of samples are currently used to fill in on both ends of the new shorter test specimens. Figure 5.6 illustrates typical rutting. Specimen thickness varies depending on nominal maximum aggregate size of the mixture being tested. For example, the typical specimen thickness for a 19mm nominal maximum mixture is 51 mm (2 in.).

Tests can be conducted on laboratory compacted specimens as well as specimens taken from in-service pavements. The Purdue linear compactor was designed and fabricated to produce laboratory compacted specimens for PURWheel testing.

5.2. Description of Purdue Laboratory Linear Compactor

The Purdue laboratory linear compactor is shown in Figure 5.7. It was designed and fabricated as a multi-purpose compactor. Its design concept is based on a similar device developed for Koch asphalt in preparing samples for the Hamburg wheel tester

(Haberman, 1994). The modifications included the ability to compact larger slabs. Maximum length and width of slabs that can be prepared are 622 mm (24.5 in.) by 292 mm (11.5 in.), respectively. These dimensions were selected as part of the design parameters for the PURWheel testing device to minimize end and side boundary effects. The maximum slab thickness that can be prepared is 102 mm (5 in.). Essential features of the linear compactor include a 292 mm (11.5 in.) wide by 622 mm (24.5 in.) long by 368 mm (14.5 in.) tall steel mold (Figure 5.8). An air cylinder is attached to the steel mold. When activated the air cylinder moves the mold back and forth through a distance of 630 mm. Compaction load is achieved by a hydraulic ram that applies a downward force through a longitudinal frame spanning the mold. A steel roller is fixed to the frame for compaction. In effect, the roller moves across a series of the ends of vertical steel plates 12.7 mm (0.5 in.) thick by 292 mm (11.5 in.) wide resting on top of the asphalt mixture being compacted. The roller contacts the ends of the individual plates as the mold is moved. When loaded, a plate compacts the mix independently of the adjoining plates. The process is taken as being analogous to a steel wheel roller. Slab samples can also be used for tests with moisture/density gauges. In addition, core samples can be obtained for indirect tensile as well as creep tests. Beams can also be sawn for flexural fatigue testing. The linear compactor has proven to be an effective, flexible laboratory compaction device.

For this study, specimens were compacted to a target density. Target density is achieved by compacting the required amount of material into a given volume. The volume is calculated after the thickness of the specimen is determined based on the nominal maximum aggregate size. Once the target density is determined, the required amount of material may be calculated. The compaction procedure is terminated when the target specimen thickness is achieved. Practically, this is observed when the series of vertical steel plates are level with the top of the compaction mold. This procedure ensures a level specimen surface. One limitation of this technique is that compaction energy cannot be determined. Details of compaction procedure are given in Appendix D1.

5.3. Test Specimen Type and Thickness

One goal of the study was to compare PURWheel with INDOT/Purdue Accelerated Pavement Tester (APT) tests. Preliminary results indicated that mixture preparation and compaction methods may result in different mixture behavior (Haddock, et al., 1998). Therefore, the comparison was conducted based on three different specimen types, i.e., field mixed-field compacted (FMFC), field mixed-laboratory compacted (FMLC), and laboratory mixed-laboratory compacted to observed field properties (LMLCF) specimens. Once the comparison is established, effects of mixture properties could be evaluated further using laboratory mixed-laboratory compacted samples at design conditions (LMLCD). Mixtures that were tested in the PURWheel are presented in Table 5.1.

Field mixed-field compacted (FMFC) specimens were obtained by cutting slabs directly from APT test sections prior to traffic loading. They were approximately 305 mm (12 in.) wide, 330 mm (13 in.) long, and 102 mm (4 in.) thick. They were trimmed to 292 mm (11.5 in.) wide, 311 mm (12.3 in.) long, and 76 mm (3 in.) thick in order to fit in PURWheel test device. FMFC specimens were obtained for seven of ten APT mixtures.

Field mixed-laboratory compacted (FMLC) specimens were slabs that were made from loose mix sampled behind the paver and were compacted using the Purdue Linear Compactor. The mixtures were identical to the mixtures that were placed in APT test sections, but the compaction method was different. The mixtures were stored in buckets and were reheated to 140 ± 3^{0}C (compaction temperature) for a period of 90±5 minutes before compaction. The mixtures were compacted to the same density as their corresponding APT density. For example, the 19 mm granite with FAA of 44, gradation plotting below the restricted zone, and +0.1 percent design AC mixture was compacted to an air void level of 7.9 percent in the APT test section. The FMLC specimens of the mixture were also compacted to 7.9 percent air voids. The compaction temperature used was 140 ± 3^{0}C. Two FMLC specimens were produced simultaneously because the steel compaction mold length was twice as long as the required PURWheel specimen length. A

FMLC sample was approximately 292 mm (11.5 in.) wide and 311 mm (12.3 in.) long. FMLC specimens were produced for six of ten APT mixtures.

Laboratory mixed-laboratory compacted at observed field properties (LMLCF) specimens were slabs that were made of laboratory prepared mixtures and were compacted using the Purdue Linear Compactor. The specimens were prepared at the observed asphalt binder content, gradation, and in-place density levels. The mixtures were blended using the washed-sieve gradation results, mixed at the extracted AC results, and compacted to their corresponding APT density. For example, the 19mm granite with FAA of 44, gradation plotting below the restricted zone, and +0.1 percent design AC mixture was compacted to air voids of 7.9 percent in APT test section. The LMLCF specimens of the mixture were blended following the washed-sieve gradation results (Table C.8), mixed at 4.5 percent AC (+0.1% design AC), and compacted to 7.9 percent air voids. The mixing and compaction temperatures used were 155 ± 3^0C and 140 ± 3^0C, respectively. The specimens were subjected to four hours of short-term aging in a forced draft oven maintained at a constant 140 ± 3^0C. Two LMLCF specimens were produced simultaneously because the steel compaction mold length was twice as long as the required PURWheel specimen length. A LMLCF sample was approximately 292 mm (11.5 in.) wide and 311 mm (12.3 in.) long. LMLCF specimens were produced for six of ten APT mixtures.

Laboratory mixed-laboratory compacted at design condition (LMLCD) specimens were slabs that were made of laboratory prepared mixtures and were compacted using the Purdue Linear Compactor. The mixtures were blended in accordance with mixture design gradation, mixed at specific AC levels, and compacted to their corresponding design densities. For example, the 19mm granite with FAA of 44 and gradation plotting below the restricted zone mixture had 4 percent air voids at the design AC. The LMLCD specimens for this mixture were blended following the design gradation (Figure 3.3), mixed at 4.4 percent AC (design AC), and compacted to 4 percent air voids. The mixing and compaction temperatures used were 155 ± 3^0C and 140 ± 3^0C, respectively. The specimens were subjected to four hours of short-term aging in a forced draft oven

maintained at a constant 140±3^{0}C. Two LMLCD specimens were produced simultaneously because the steel compaction mold length was twice as long as the required PURWheel specimen length. A LMLCD sample was approximately 292 mm (11.5 in.) wide and 311 mm (12.3 in.) long. LMLCD specimens were produced for all twenty-one mixtures that were designed in accordance with Superpave volumetric design procedures.

As previously stated, the thickness of laboratory compacted specimens was determined based on nominal maximum aggregate size. The larger the nominal maximum aggregate size the thicker the specimen. The 9.5mm nominal maximum size laboratory compacted specimens were 38 mm (1.5 in.) thick and the 19mm nominal maximum size laboratory compacted specimens were 51 mm (2 in.) thick. The field compacted specimens were trimmed using a wet mansory saw to 76 mm (3 in.) thick for practical reasons. Details of specimen thicknesses are presented in Table 5.2.

5.4. Test Parameters

5.4.1. Tire Contact Pressure and Wheel Velocity

To simplify the attempt to compare PURWheel with INDOT/Purdue APT test results, the tire contact pressure of the PURWheel needed to be set to that of the APT. The PURWheel tire has a 2-ply construction. Typically, as tire pressure increases, contact area decreases because the tire "stiffens" with added pressure. However, the PURWheel tire stiffens up to a point and then begins to "balloon" with added pressure, which increases the contact area. In order to achieve the 620 kPa (90 psi) contact pressure with the PURWheel tire, a 1.7 kN (385 lb.) load is applied to each wheel at a tire inflation pressure of 793 kPa (115 psi). Because of the lever mechanism of the wheel configuration, the actual vertical force needs to be measured. The vertical force was measured with a balance and it was 1.5 kN (334.1 lb.). The contact area was determined from a physical measurement of the tire print. The gross contact area was 2394 mm^2

(3.712 in^2) and resulted in a gross contact pressure of 620 kPa (90 psi). However, when only the treads were accounted for, the actual contact area was 1800 mm^2 (2.79 in^2) and resulted in actual contact pressure of 824.8 kPa (120 psi). The wheel velocity was set to 330±20 mm/sec (0.74 mph).

5.4.2. Test Condition and Temperature

The testing condition was hot/dry for all specimens. For comparison with APT tests, the FMFC, FMLC, and LMLCF specimens were tested at 50^0 C (122^0 F). The LMLCD specimens were tested at 57.5^0 or 60^0 C (135.5^0 or 140^0 F) in order to magnify the rutting. Details of the test temperatures employed are given in Table 5.3.

5.5. PURWheel Test Results

5.5.1. Rut Depth at 20000 Wheel Passes

As previously stated, rutting was measured with electric transducers. The transducers are attached in such a way that they can measure vertical deformation as the wheels move back and forth across a specimen. The advantages of this technique are the deformation can be measured at any location on the sample and it can be recorded at any wheel pass interval automatically. The disadvantage is that the vertical deformation is measured from the original surface downward. The downward vertical deformation is termed as rut depth and is illustrated in Figure 5.9. The other component of rutting, the uplift, has to be measured manually.

A typical plot of rut depth versus number of wheel passes is presented in Figure 5.10. The plot shows the results for two identical FMFC specimens tested simultaneously in the PURWheel at 50^0 C. The specimens were cut from the same APT lane. This insured that the specimens were the same mixture, at the same compaction energy, and

same densities. The plots show also the sensitivity of the PURWheel transducers. In order to evaluate performance of different mixtures, rutting after a specific number of wheel passes was used. A decision was made to use observed rut depths at 20000 wheel passes. There were two reasons for this decision. The first was that it is believed that the change in rutting is linear at this point. The second was from a practical point of view; it takes approximately eight hours to accomplish 20000 wheel passes.

5.5.2. Accuracy of PURWheel Measurement

The PURWheel transducers are Linear Variable Differential Transformers (LVDT). This electronic device is subject to electrical noise. The noise affects the accuracy of measurement. Measurements indicated that the transducer is sensitive to three bits of noise corresponding to 0.03 mm (0.001 in.). Therefore the accuracy of measured rut depths was ± 0.03 mm (0.001 in.).

5.5.3. Sensitivity to Air Voids

Test results show that the PURWheel is very sensitive to air voids (Pan, 1997). This characteristic is good because field pavement rutting is also very sensitive to air voids (Roberts, et al., 1991). Although two PURWheel samples could be produced simultaneously in one compaction process, as previously discussed, it was very unlikely that both samples would have exactly the same air voids. In most cases, the target air void level was in between the resulting air voids for a pair of specimens. By employing interpolation, the rutting performance at the target air voids could be evaluated. A procedure for evaluating mixtures at the target air void level is described in the following paragraph.

The evaluation procedure is illustrated in Figure 5.11. Four 292 mm (11.5 in.) wide and 311 mm (12.3 in.) long samples of the same mixture were tested in the

PURWheel. The density of each sample was measured before the test. The air void level for each specimen was calculated and wheel track rutting at 20000 wheel passes was recorded. A relationship between wheel track rutting at 20000 wheel passes and air voids is established. Because the air void difference among the samples is typically small (± 2%), the relationship is linear. Using the established relationship, the rut depth at 20000 wheel passes at the target air void level could be determined. In the example shown in Figure 5.11, the target air void level was 6.9 percent. Using the linear relationship, the rut depth at 6.9 percent air void level was determined to be 2.14 mm.

5.6. Discussion of PURWheel Test Results

5.6.1. Correlation Between Rut Depth and Total Rut in PURWheel

The rutting component measured automatically in PURWheel tests is the downward rutting (rut depth). The overall rutting (total rut) needs to be measured manually using a straight edge and a micrometer at the end of a test. Therefore, only total rut at 20000 wheel passes was measured. This series of data was used to develop a relationship between total rut and rut depth.

The relationship between total rut and rut depth is presented in Figure 5.12. A positive linear relationship was observed. This relationship is consistent with the relationship between total rut and rut depth developed for INDOT/Purdue APT (Chapter 4). Regression analysis was conducted and the results are presented in Appendix D3. The linear relationship indicates that rut depth contributed to a fixed proportion of total rut; in this case the contribution was approximately 53 percent. It should be noted that most of the rut depth observations were less than 3 mm.

5.6.2. Correlation Between APT and PURWheel

Figure 5.6 illustrates the fact that the transverse surface profile of HMA tested in PURWheel exhibits similar characteristics to profiles observed in actual rutted field pavements. Note that both consolidation in the wheel path as well as upheave, due to shear failure, is observed at the edges of the tire. This observation lends credence to using the PURWheel to evaluate field pavement rutting performance. However, the profile alone is not adequate because there are other factors that may impact the evaluation, such as mixture properties, compaction methods, and mixture preparation techniques. Therefore, it is necessary to determine whether PURWheel test results evaluate consistently field pavement rutting performance. The correlation between APT and PURWheel test results would be the initial step of field pavement rutting performance evaluation because the traffic loading and compaction method in the APT is essentially identical to field conditions. The correlation between the two tests is reliable because the environment conditions, such as temperature, contact pressure, wheel velocity can be controlled consistently. A comparison between load and geometry parameters of PURWheel and APT test conditions is presented in Figure 5.13.

Previous results suggested that mixture preparation and compaction methods impact the correlation between APT and PURWheel tests (Haddock, et al. 1998). Similar findings were also observed at Westrack (Hand, 1998). Therefore, the correlation was developed by taking into account the effects of mixture preparation and compaction methods. The correlation between APT total rut and PURWheel rut depth is presented in Figure 5.l4. The correlation was found to be weak, but the scatter plot suggests that two groups of data were obvious. The data were separated into two groups based on the nominal maximum aggregate size of the mixtures, i.e., 19mm and 9.5mm. The correlation for the 19mm mixtures is presented in Figure 5.15 and that for 9.5mm mixtures in Figure 5.16. The detailed regression analysis is presented in Appendix D3. The r^2 values increased substantially when the data were separated by nominal maximum aggregate size. This suggests that the nominal maximum aggregate size of mixtures affected the correlation between APT and PURWheel tests. However, the correlation for the mixtures having less than 10 mm total rut in APT (very good rutting resistance) would be

independent of the nominal maximum aggregate size. This is shown from back calculation using the regression equations for both 19 and 9.5mm mixtures. As the APT total rut increased, the correlation slopes of the 19mm mixtures became steeper than those of the 9.5 mm mixtures. This suggests that the 19mm mixtures were more difficult to deform in the PURWheel and thus the PURWheel would evaluate the 9.5mm mixtures better. The interactions among PURWheel tire size, tire contact pressure, sample boundary conditions, sample dimension, and the mixture nominal maximum aggregate size appeared to become more significant as the rut depth increases.

Mixture preparation and compaction methods also affected rutting performance in the PURWheel. The correlation between APT total rut and PURWheel rut depth using FMFC specimens appeared to be the strongest. This suggests that the rutting mechanism of APT and PURWheel tests were similar and scalable. The correlation between APT total rut and PURWheel rut depth using FMLC specimens indicates that the linear compactor and storing field mixtures resulted in stronger (more rut resistant) mixtures. The aggregate structures produced by linear compactor and field compactor appeared to be different and the linear compactor produced stronger aggregate structures. The correlation between APT total rut and PURWheel rut depth using LMLCF specimens indicates that laboratory and field (asphalt plant) prepared mixtures exhibited differences in rutting resistance also.

The correlations between the rut depth in APT and PURWheel tests are presented in Figures 5.16 and 5.17 for the 19 and 9.5mm mixtures, respectively. Most of the PURWheel rutting components were dominated by rut depth because the rut depths were less than 11.4 mm (Section 5.6.1). Most of the APT rutting components was also dominated by rut depth because the total ruts were less than 20 mm (Section 4.5.2). However, the r^2 values from APT rut depth and PURWheel rut depth correlations were lower than those from APT total rut and PURWheel rut depth correlations. This suggests that the proportions of rutting components generated in APT and PURWheel were not the same. It is hypothesized that the boundary conditions, sample dimension, tire size, and tire contact pressure impacted the proportions of rutting components generated.

Because the relationship between PURWheel total rut and rut depth is linear, the correlation between APT and PURWheel total rut would appear to be a linear transformation of the correlation between APT total rut and PURWheel rut depth. Thus because most of PURWheel rutting components were dominated by rut depth measurements, it was more practical and reliable to use PURWheel rut depth measurement results directly.

5.6.3. Correlation Among PURWheel Tests on FMFC, FMLC, and LMLCF Specimens

The correlation among FMLC and LMLCF to FMFC in PURWheel tests is presented in Figure 5.19. Details of the regression analysis are presented in Appendix D3. Correlation between FMFC and FMLC specimens in PURWheel tests confirms the previous discussed observation that the mixtures compacted by the laboratory linear compactor were more rut resistant than those compacted in the field using conventional compaction equipment. It should be noted that the mixtures were stored in the bucket and reheated before the compaction. It is well documented that storing and reheating process lead to stiffer mixtures. This supports the fact that the linear compactor produced stronger mixtures at the same level of density. It is hypothesized that the compaction mold provided greater confinement and resulted in better aggregate structures. Correlation between FMFC and LMLCF specimens in PURWheel tests suggests that the specimens produced with the combination of laboratory preparation and linear compaction were stronger than those produced with the combination of field (asphalt plant) production and field compaction.

Correlation between FMLC and LMLCF specimens in PURWheel tests is presented in Figure 5.20 and details of the regression analysis are presented in Appendix D3. The correlation suggests that the laboratory prepared mixtures were stronger than the field mixtures at the same gradation, AC level, and density. This confirms the general knowledge that storing and reheating processes result in stiffer mixtures. It was almost

impossible to produce specimens using field mixtures in the laboratory at the field density without reheating. Therefore, it was not conclusive whether the field mixtures were different than the laboratory prepared mixtures.

5.6.4. Correlation Between PURWheel Tests on LMLCF and LMLCD Specimens

Correlation between LMLCF and LMLCD specimens in PURWheel tests involved the effects of differences in gradation, density, and test temperature. As previously discussed, the PURWheel is highly sensitive to air voids (Section 5.5.3.). A scatter plot of LMLCF and LMLCD air voids is presented in Figure 5.21. Based on air void differences and the number of observations, it was decided that the maximum tolerance of air void difference was four percent. The specimens within this range were selected and correlation between PURWheel tests on LMLCF and LMCD specimens was developed. The correlation is presented in Figure 5.22. Details of the regression analysis are presented in Appendix D3. The correlation was weak as shown by the r^2 value of 0.28. It is unfortunate that the range of PURWheel rut depth observations was narrow. However, the existing correlation suggests that the PURWheel was sensitive to deviation in gradation and test temperature differences.

The developed correlation also suggests that LMLCF specimens exhibited smaller rut depths than LMLCD specimens. The test temperature used for LMLCD specimens was 10^0C higher than that of LMLCF specimens. The LMLCF specimens also had higher air voids than the LMLCD specimens because they were compacted to match the field (APT) air voids. The LMLCD specimens were compacted to four percent air voids to match the mixture design conditions. With respect to design bulk specific gravity (Gmb), the LMLCD specimens were compacted to 100 percent design Gmb while the LMLCF specimens were compacted to approximately 96 percent of design Gmb. The combination of lower test temperature, lower percentage of design Gmb, and gradation deviations resulted in smaller observed rut depths for LMLCF specimens.

5.6.5. Correlation Between APT Total Rut and PURWheel LMLCD Rut Depth

Correlation between APT total rut and PURWheel LMLCD rut depth is presented in Figure 5.23. Details of the regression analysis are presented in Appendix D3. It is important to note that the LMLCD specimens were tested at a temperature 10^0C higher than the APT tests were conducted (Table 5.3). In addition to temperature difference, the effects of gradation and air void deviations were incorporated in the correlation.

The correlations between APT total rut and PURWheel LMLCD rut depth and those between APT total rut and PURWheel LMLCF rut depth appeared to be similar. Therefore, it hypothesized that similar observations from PURWheel LMLCD and APT tests would be expected. The hypothesis is important because conducting testing using PURWheel LMLCD specimens is very practical. The reason is that this is what would actually be done in the mixture design process to access the rutting potential of a mixture.

5.6.6. Material Property Effects on PURWheel Rut Depth

Subjective identification of rut resistance criteria for PURWheel tests was developed based on the correlation between APT total rut and PURWheel rut depth. Because the correlations between APT and PURWheel tests were affected by the nominal maximum aggregate size, mixture preparation, and compaction methods criteria were developed by incorporating these factors. The criteria are presented in Tables 5.4 and 5.5 for 19 and 9.5mm mixtures, respectively.

The rutting performance of twenty-one LMLCD mixtures were evaluated and categorized using the rut resistance criteria presented in Tables 5.4 and 5.5. The results are presented in Table 5.6. The criteria suggest that all 9.5mm mixtures and most of the 19mm mixtures exhibited good or very good rutting resistance. This indicates that the rut resistance of 9.5 and 19mm mixtures was approximately equal. The rut resistance of limestone and granite mixtures was approximately the same also. The rut resistance of the mixtures with FAA of 39 (natural sand) was fair or poor. This supports the common

knowledge that mixtures incorporating poor quality natural sand do not provide good rutting resistance. The rut resistance of the mixtures with FAA of 44 appeared to be better than that of the mixtures with FAA of 50. This indicates that incorporating very high FAA into the mixtures will not necessarily improve rutting resistance. Similar observations of FAA effects on rutting performance were reported by Lee in a recent fine aggregate angularity study (Lee, 1998). There is no clear indication that the rutting resistance of mixtures with gradations plotting above, through, or below the restricted zone was different. The effects of nominal maximum aggregate size, coarse aggregate type, fine aggregate angularity, and gradation type on PURWheel rut depth are similar to their effects on APT total rut (Chapter 4).

Review of the complete rut resistance criteria (Tables 5.4 and 5.5) reveals that the major difference among the criteria resulted from the compaction method. For the purpose of identifying rutting potential in the mixture design process, it is more practical to use laboratory compacted specimens. Therefore, the complete criteria could be simplified by eliminating the effects of mixture preparation methods and nominal maximum aggregate size. The simplified rut resistance criteria are presented in Table 5.7. A comparison between the complete and simplified rut resistance criteria were conducted on the mixtures tested in the PURWheel and the results are summarized in Table 5.8. Review on the comparison reveals that there was no major difference in categorizing the mixtures. It should be noted that most the mixtures was categorized as good or very good.

The effects of nominal maximum aggregate size, coarse aggregate type, fine aggregate angularity, and gradation on rut depth were assessed using paired t-tests. Results are summarized in Table 5.9. The test results on the effect of fine aggregate angularity confirm the general observations previously discussed.

The significance of nominal maximum aggregate size, coarse aggregate type, fine aggregate angularity, and gradation type to PURWheel rut depth was analyzed using analysis of variance (ANOVA). The ANOVA of PURWheel rut depths is summarized in Table 5.10 and the details are presented in Appendix D3. The following model was assumed in the analysis.

$$\text{Rut depth}_{ijkl} = \mu + N_i + C_j + F_k + G_l + NC_{ij} + NF_{ik} + NG_{il} + CF_{jk} + CG_{jl} + FG_{kl} + \varepsilon_{ijkl} \quad \ldots(5.1)$$

Where:
Rut depth = dependent variable
μ = overall mean
N_i = nominal maximum size, i=1, 2
C_j = coarse aggregate type, j= 1, 2
F_k = fine aggregate angularity, k = 1, 2, 3
G_l = gradation, l = 1, 2, 3
NC_{ij} = interaction of nominal maximum size and coarse aggregate type
NF_{ik} = interaction of nominal maximum size and fine aggregate angularity
NG_{il} = interaction of nominal maximum size and gradation
CF_{jk} = interaction of coarse aggregate type and fine aggregate angularity
CG_{jl} = interaction of coarse aggregate type and gradation
FG_{kl} = interaction of fine aggregate angularity and gradation
ε_{ijkl} = error term

The results show that fine aggregate angularity and the interaction between fine aggregate angularity and gradation impact PURWheel rut depths significantly at the five percent significant level. The ANOVA results are consistent with the general observations and paired t-tests.

5.6.7. Sensitivity of PURWheel Rut Depth to AC Level

Sensitivity of PURWheel rut depth to AC level was evaluated from test on LMLCD specimens compacted at five different AC levels. The AC levels were the Superpave design AC, design AC ±0.5 percent, and design AC ±1.0 percent. During the mixture design process, samples at different AC levels were compacted under the same compaction energy. In order to be similar to the mixture design process, the specimens prepared at all five different AC levels needed to be compacted at the same compaction energy. Unfortunately, it was not possible to control the compaction energy in the linear compactor. This limitation was overcome by relating the linear compactor with the Superpave Gyratory Compactor (SGC) specimens. Initially, four SGC specimens were

compacted at a specific AC to the N_{design} number of gyrations. The average density was used as the target density for the specimens prepared using the linear compactor. Therefore, it is reasonable to assume that all LMLCD specimens received compaction energy that was equivalent to the N_{design} energy. From a practical standpoint, this assumption was verified by observing that the aggregate weights required for different AC levels for the LMLCD PURWheel specimens of the same mixture were approximately equal.

The sensitivity of sixteen of the twenty-one Superpave mixtures to AC level in the PURWheel was evaluated. The sensitivity of the 19mm mixtures with FAA of 44 and 50 is presented in Figures 5.25 and 5.26, respectively. The sensitivity of the 9.5mm mixtures with FAA of 44 and 50 is presented in Figures 5.27 and 5.28, respectively. The fact that nine of sixteen mixtures showed U-shaped relationships between rut depth and AC level suggested that there is an AC level corresponding to minimum rut depth. Four of nine mixtures indicated that the AC level corresponding to minimum rut depth was 0.5 percent lower than the Superpave design AC. Comparing the 19 and 9.5mm plots indicates that the 9.5mm mixtures were more sensitive to AC level changes. However, because different correlations with APT tests exist based on the nominal maximum aggregate size, the rutting resistance of 9.5mm mixtures is not necessary more sensitive to AC level in the field (APT).

The sensitivity of limestone and granite mixtures to AC level was approximately the same. The sensitivity of mixtures with FAA of 44 and 50 to AC level was approximately the same. The sensitivity of mixtures to AC level with gradations plotting through the restricted zone was higher than that of mixtures with gradations plotting below the restricted zone. As discussed in Chapter 3, mixtures with FAA of 44 and gradations plotting below the restricted zone had lower VMA than mixtures with FAA of 50 and gradations plotting through the restricted zone, respectively. Observations on the effects of FAA and gradation with respect to the restricted zone on mixture sensitivity to AC level suggest that lower VMA mixtures were not always more sensitive to AC level changes. It is generally believed that low VMA mixtures are more sensitive to AC level changes (Roberts, et al., 1991). However, lower VMA mixtures require smaller amount

of asphalt to reduce air voids to four percent under a given level of compaction. Therefore, some lower VMA mixtures were less sensitive to AC level changes.

Because PURWheel rut depths were sensitive to AC level, an effort was made to assess the difference in PURWHeel and Superpave indicated optimum AC levels for rutting resistance. The AC corresponding to the minimum PURWheel rut depth was used to identify the state at which the HMA mixture transformed from the stable to unstable condition. AC level corresponding to minimum PURWheel rut depth was identified with respect to the design AC for all mixtures tested. The results are summarized in Table 5.11. For eight of sixteen mixtures the AC level corresponding to the peak shear strength was approximately 0.5 or more percent lower than the Superpave design AC.

VMA values corresponding to the state at which the HMA mixture transforms from the stable to unstable condition could be defined as critical VMA. The VMA value for each mixture is summarized in Table 5.12. Statistical analysis was conducted on the data and the results are summarized in Table 5.16. The analysis showed that the average critical VMA was 14.6 percent for 19mm mixtures and 16.3 percent for 9.5mm mixtures. These values are slightly higher than the Superpave minimum VMA requirements.

VFA values corresponding to the state at which the HMA mixture transformed from the stable to unstable condition for each mixture were also identified. The results are summarized in Table 5.13. Statistical analysis was conducted on the data and the results are summarized in Table 5.16. The analysis showed that the average VFA values corresponding to the state at which the HMA mixture transformed from the stable to unstable condition were 69.4 percent for 19mm mixtures and 66.4 percent for 9.5mm mixtures. These values are within the range of 65 to 75 percent, which is the Superpave lower and upper limit of VFA allowed for traffic less than 1×10^7 ESALs (traffic level for mixture design).

Dust proportion values corresponding to the state at which the HMA mixture transformed from the stable to unstable condition for each mixture were identified. The results are summarized in Table 5.14. Statistical analysis was conducted on the data and the results are summarized in Table 5.16. The analysis showed that the average dust

proportion value corresponding to the state at which the HMA mixture transformed from the stable to unstable condition was 1.1, the minimum value was 0.9, and the maximum value was 1.2 for 19mm mixtures. For 9.5mm mixtures, the average dust proportion value corresponding to the state at which the HMA mixture transformed from the stable to unstable condition was 1.3, the minimum value was 1.0, and the maximum value was 2.2. All the values, except the maximum value for the 9.5mm mixtures, satisfy the recently recommended dust proportion criteria (Brown et. al, 1999 and AASHTO, 1999).

Film thickness values corresponding to the state at which the HMA mixture transformed from the stable to unstable condition for each mixture were identified. The results are summarized in Table 5.15. Statistical analysis was conducted on the data and the results are summarized in Table 5.16. Analysis showed that the average film thickness corresponding to the state at which the HMA mixture transformed from the stable to unstable condition was 9.1 micron for the 19mm mixtures and 7.7 micron for the 9.5mm mixtures. These film thickness values are very close to the recently recommended 8 micron film thickness by Kandhal based on the NCAT Report 98-1 targeted at reviewing of VMA requirements in Superpave (Kandhal et al., 1998).

5.6.8. Relationship Between PURWheel Rut Depth and VMA

A scatter plot of observed PURWheel rut depths and corresponding VMA values is presented in Figure 5.28. The plot includes all the LMLCD data. The VMA shown includes the effects of different AC levels. The plot suggests that no clear relationship between PURWheel rut depth and VMA. This plot is similar to the scatter plot of APT total rut and VMA for all tested mixtures presented in Chapter 4.

The scatter plot between PURWheel rut depth and design VMA is shown in Figure 5.29. Design VMA represents the VMA at Superpave design AC and design air voids. This VMA was obtained by selecting the LMLCD data at design AC and interpolating the rut depth at design air voids. A poor quadratic relationship with positive second order parameter was observed for the 19mm mixtures. Details of the regression

analysis are presented in Appendix D3. The quadratic relationship suggests that at the low VMA levels, as VMA decreased, rut depth increased. On the other hand, the quadratic relationship suggests that as VMA increased at the high VMA levels, rut depth increased. For a given mixture with a typical U-shaped VMA curve, the stability is typically observed as VMA decreases to a minimum (dry side) and then beyond the minimum (wet side) stability typically diminishes. It was discussed in Chapter 3 that as VMA increases the amount of asphalt required to reduce air voids to four percent under a given level of compaction increases. This would result in higher rut depth. There was no relationship observed for the 9.5mm mixtures.

5.6.9. Relationship Between PURWheel Rut Depth and VFA

The relationship between observed PURWheel rut depths and corresponding VFA values is presented in Figure 5.30. A linear relationship was observed regardless of the nominal maximum aggregate size. Details of the regression analysis are presented in Appendix D3. Although the r^2 value is small (0.23), the positive slope is clearly observed. This suggests that as VFA increased rut depth increased. The 65% to 75% Superpave VFA criteria for traffic less than 1 x 10^7 ESALs (design traffic level) would correspond to PURWheel rut depth of 2.32 to 2.72 mm, respectively.

5.6.10. Relationship Between PURWheel Rut Depth and Dust Proportion

The relationship between observed PURWheel rut depth and corresponding dust proportion (DP) values is presented in Figure 5.31. Details of the regression analysis are presented in Appendix D3. A quadratic relationship with a positive second order parameter was observed, although the r^2 value of was very small (0.15). A similar relationship was observed using APT data (Chapter 4). Using the relationship, the 0.6 to

1.2 Superpave dust proportion criteria would correspond to 3.53 to 2.02mm rut depths, respectively.

The relationship between observed PURWheel rut depth and corresponding design DP values is presented in Figure 5.32. Details of the regression analysis are presented in Appendix D3. Design DP represents the DP at design AC and air voids. This DP was obtained by selecting the LMLCD data at design AC and interpolating the corresponding rut depth at design air voids. A quadratic relationship with a positive second order parameter was observed. The r^2 value was small (0.32), but double the r^2 of PURWheel rut depth and DP relationship presented in Figure 5.31. Using the relationship, the 0.6 to 1.2 Superpave dust proportion criteria would correspond to 3.50 to 1.74mm PURWheel rut depths, respectively. The increase in r^2 suggests that when DP resulted from AC deviation, the relationship between PURWheel rut depth and DP got weaker.

5.6.11. Relationship Between PURWheel Rut Depth and Film Thickness

The relationship between observed PURWheel rut depths and corresponding film thickness (FT) values is presented in Figure 5.33. Details of the regression analysis are presented in Appendix D3. A quadratic relationship with a positive second order parameter was observed, although the r^2 value was small (0.29). Using the relationship, FT of 7.3 micron corresponded to 2.00 mm PURWheel rut depth. The value of 7.3 micron corresponded to APT total rut of 10 mm. Therefore, the FT value provides an alternative method to correlate APT and PURWheel data.

The relationship between PURWheel rut depth and design FT is presented in Figure 5.34. Details of the regression analysis are presented in Appendix D3. A quadratic relationship with a positive second order parameter was observed. The r^2 value of the PURWheel rut depth and design FT relationship was much higher than that of PURWheel rut depths and all FT values (Figure 5.33). Using the relationship, FT of 7.3 micron corresponds to 2.06 mm PURWheel rut depth. This suggests that the relationships

between PURWheel rut depth and all FT and between PURWheel rut depth and design FT were essentially the same.

5.6.12. Characterizing Mixture Gradation for PURWheel Rutting Performance

As previously discussed in Section 5.6.6. , there is no clear indication that the rutting resistance of mixtures with gradations plotting above, through, or below the restricted zone was different. This suggests that the restricted zone alone was not adequate to distinguish consistently the observed PURWheel rutting resistance. It was hypothesized that the restricted zone size was too small to influence the aggregate structures.

It is common knowledge that sufficient air void space must be available in the mixture to avoid rutting (Roberts, et al., 1991). An attempt to characterize mixture gradations by measuring the vertical distance for a given gradation to the maximum density line at different levels of percent passing was made. The vertical distances were measured at 25, 50, and 75 percent passing as presented in Figure 5.35. The unit of the measured vertical distance was percent. The vertical distances of twelve 19mm mixtures were measured and the results are presented in Figure 5.36. The results show that the restricted zone consistently controlled the vertical distances at 25 percent passing within each gradation type. However, the restricted zone appeared to have less influence on the vertical distances at 50 and 75 percent passing. The vertical distances of nine 9.5mm mixtures were measured and the results are presented in Figure 5.37. The results show that the restricted zone controlled the vertical distances at 25 and 50 percent passing consistently within each gradation type. However, the restricted zone appeared to have less influence on the vertical distances at 75 percent passing. These observations would further support that there is no clear indication that the rutting resistance of mixtures with gradations plotting above, through, or below the restricted zone were different.

Table 5.1 Summary of Mixtures Tested in PURWheel.

FAA	Gradation	9.5 mm Nominal Max. Size								19 mm Nominal Max. Size							
		Limestone				Granite				Limestone				Granite			
		1	2	3	4	1	2	3	4	1	2	3	4	1	2	3	4
39	Above												X				
	Below												X				
44	Above				X								X				
	Through	X	X	X	X				X				X				X
	Below				X	X	X	X	X	X			X	X	X	X	X
50	Above												X				
	Through	X	X	X	X				X				X	X	X	X	X
	Below				X	X	X	X	X				X				X

Note: 1 = field mixed-field compacted specimen (FMFC)

2 = field mixed-laboratory compacted specimen (FMLC)

3 = laboratory mixed-laboratory compacted specimen at observer field properties (LMLCF)

4 = laboratory mixed-laboratory compacted specimen at design condition (LMLCD)

Table 5.2 PURWheel Specimen Thicknesses in millimeters.

FAA	Gradation	9.5 mm Nominal Max. Size								19 mm Nominal Max. Size							
		Limestone				Granite				Limestone				Granite			
		1	2	3	4	1	2	3	4	1	2	3	4	1	2	3	4
39	Above												51				
	Below												51				
44	Above				38								51				
	Through	76	38	38	38				38				51				51
	Below				38	76	38	38	38	76			51	76	51	51	51
50	Above												51				
	Through	76	38	38	38				38				51	76	51	51	51
	Below				38	76	38	38	38				51				51

Note: 1 = field mixed-field compacted specimen (FMFC)

2 = field mixed-laboratory compacted specimen (FMLC)

3 = laboratory mixed-laboratory compacted specimen at observer field properties (LMLCF)

4 = laboratory mixed-laboratory compacted specimen at design condition (LMLCD)

Table 5.3 PURWheel Specimen Testing Temperatures in Degree Centigrade.

FAA	Gradation	9.5 mm Nominal Max. Size								19 mm Nominal Max. Size							
		Limestone				Granite				Limestone				Granite			
		1	2	3	4	1	2	3	4	1	2	3	4	1	2	3	4
39	Above												57.5				
	Below												57.5				
44	Above				60								57.5				
	Through	50	50	50	60				60				60				60
	Below				60	50	50	50	60	50			57.5	50	50	50	60
50	Above												57.5				
	Through	50	50	50	60				60				60	50	50	50	60
	Below				60	50	50	50	60				60				60

Note: 1 = field mixed-field compacted specimen (FMFC)

2 = field mixed-laboratory compacted specimen (FMLC)

3 = laboratory mixed-laboratory compacted specimen at observer field properties (LMLCF)

4 = laboratory mixed-laboratory compacted specimen at design condition (LMLCD)

Table 5.4 Subjective Identification of 19 mm Mixture Rut Resistance Using The PURWheel

Specimen Type	FMFC	FMLC	LMLCF	LMLCD
Rut Resistance	Rut Depth at 20000 wheel passes (mm)	Rut Depth at 20000 wheel passes (mm)	Rut Depth at 20000 wheel passes (mm)	Rut Depth at 20000 wheel passes (mm)
Very Good	< 4.3	< 1.7	<1.8	< 1.3
Good	4.3 – 5.3	1.7 – 2.2	1.8 – 2.4	1.3 – 2.2
Fair	5.3 – 6.3	2.2 – 2.6	2.4 – 3.0	2.2 – 3.0
Poor	> 6.3	> 2.6	>3.0	> 3.0

Table 5.5 Subjective Identification of 9.5 mm Mixture Rut Resistance Using The PURWheel

Specimen Type	FMFC	FMLC	LMLCF	LMLCD
Rut Resistance	Rut Depth at 20000 wheel passes (mm)	Rut Depth at 20000 wheel passes (mm)	Rut Depth at 20000 wheel passes (mm)	Rut Depth at 20000 wheel passes (mm)
Very Good	<5.5	<2.5	<1.5	<1.3
Good	5.5 – 11.4	2.5 – 6.1	1.5 – 3.1	1.3 – 3.8
Fair	11.4 – 17.4	6.1 – 9.6	3.1 – 4.7	3.8 – 6.2
Poor	>17.4	>9.6	>4.7	>6.2

Table 5.6 Rutting Performance of LMLCD Specimens in PURWheel.

FAA	Gradation	Rutting Resistance	9.5 mm Nominal Max. Size		19 mm Nominal Max. Size	
			Limestone	Granite	Limestone	Granite
39	Above	Rating			Fair	
		Rut Depth			2.71	
	Below	Rating			Poor	
		Rut Depth			4.47	
44	Above	Rating	Good		Good	
		Rut Depth	2.12		2.14	
	Through	Rating	Good	Good	Good	Very Good
		Rut Depth	1.56	1.61	1.42	1.23
	Below	Rating	Good	Very Good	Good	Good
		Rut Depth	1.71	1.24	2.01	1.54
50	Above	Rating			Fair	
		Rut Depth			2.68	
	Through	Rating	Good	Good	Fair	Good
		Rut Depth	1.80	2.28	3.00	1.72
	Below	Rating	Good	Good	Good	Good
		Rut Depth	1.65	1.97	1.95	1.81

Table 5.7 Simplified Subjective Identification of Mixture Rut Resistance Using the Laboratory Compacted Specimens in PURWheel

Specimen Type	Laboratory Compacted
Rut Resistance	Rut Depth at 20000 wheel passes (mm)
Very Good	<1.8
Good	1.8 – 2.4
Fair	2.4 – 3.0
Poor	> 3.0

Table 5.8 Comparison Between Complete and Simplified Rutting Performance Rating in PURWheel.

FAA	Gradation	Rutting Resistance Rating	9.5 mm Nominal Max. Size		19 mm Nominal Max. Size	
			Limestone	Granite	Limestone	Granite
39	Above	Complete			Fair	
		Simplified			Fair	
	Below	Complete			Poor	
		Simplified			Poor	
44	Above	Complete	Good		Good	
		Simplified	Good		Good	
	Through	Complete	Good	Good	Good	Very Good
		Simplified	Very Good	Very Good	Very Good	Very Good
	Below	Complete	Good	Very Good	Good	Good
		Simplified	Very Good	Very Good	Good	Good
50	Above	Complete			Fair	
		Simplified			Fair	
	Through	Complete	Good	Good	Fair	Good
		Simplified	Good	Good	Poor	Very Good
	Below	Complete	Good	Good	Good	Good
		Simplified	Good	Good	Good	Good

Table 5.9 Summary of Statistical Analysis of Experimental Variable Effects on Rutting Performance of LMLCD Specimens in PURWheel.

Comparison	Significance	p value
RD of 19 mm mixtures > RD of 9.5 mm mixtures	No	0.5851
RD of limestone mixtures > RD of granite mixtures	No	0.3099
RD of FAA of 44 mixtures < RD of FAA of 50 mixtures	Yes	0.0188
RD of above gradation mixtures > RD of through gradation mixtures	No	0.4266
RD of above gradation mixtures > RD of below gradation mixtures	No	0.8407
RD of through gradation mixtures > RD of below gradation mixtures	No	0.6184

Table 5.10 Summary of ANOVA for Factor Effects on PURWheel Rut Depth.

Variable	Significance	p value
Nominal Maximum Size	No	0.8651
Coarse Aggregate Type	No	0.6239
Fine Aggregate Angularity	Yes	0.0053
Gradation with Respect to The Restricted Zone	No	0.0909
Nominal Max. Size * Coarse Aggregate Type	No	0.1135
Nominal Max. Size * Fine Aggregate Angularity	No	0.8518
Nominal Max. Size * Gradation	No	0.1390
Coarse Agg. Type * Fine Aggregate Angularity	No	0.4424
Coarse Agg. Type * Gradation	No	0.9597
Fine Aggregate Angularity * Gradation	Yes	0.0099

note: p values are based on Type III Sum of Squares

Table 5.11 Location of AC Corresponding to Minimum PURWheel Rut Depth.

FAA	Gradation	9.5 mm Nominal Max. Size		19 mm Nominal Max. Size	
		Limestone	Granite	Limestone	Granite
39	Above				
	Below				
44	Above	-1.0			
	Through	-0.5	-1.0	+0.0	+0.0
	Below	+0.0	+0.0		+0.0
50	Above				
	Through	+0.0	-1.0	-0.5	+0.0
	Below	+0.0	-0.5	-0.5	-0.5

Note: the location of AC is relative to the design AC.

Table 5.12 VMA Values Corresponding to Minimum PURWheel Rut Depth.

FAA	Gradation	9.5 mm Nominal Max. Size		19 mm Nominal Max. Size	
		Limestone	Granite	Limestone	Granite
39	Above				
	Below				
44	Above	17.1			
	Through	15.3	18.2	14.0	15.1
	Below	14.4	15.8		13.9
50	Above				
	Through	16.4	17.6	15.6	15.0
	Below	16.7	15.0	13.6	15.1

Table 5.13 VFA Values Corresponding to Minimum PURWheel Rut Depth.

FAA	Gradation	9.5 mm Nominal Max. Size		19 mm Nominal Max. Size	
		Limestone	Granite	Limestone	Granite
39	Above				
	Below				
44	Above	50.2			
	Through	78.3	42.8	77.6	61.7
	Below	70.8	63.5		65.7
50	Above				
	Through	81.6	61.9	76.0	71.9
	Below	80.8	67.9	72.4	60.5

Table 5.14 Dust Proportion Values Corresponding to Minimum PURWheel Rut Depth.

FAA	Gradation	9.5 mm Nominal Max. Size		19 mm Nominal Max. Size	
		Limestone	Granite	Limestone	Granite
39	Above				
	Below				
44	Above	2.15			
	Through	1.03	1.76	0.89	1.02
	Below	0.96	1.08		1.07
50	Above				
	Through	1.21	1.52	1.10	1.18
	Below	1.04	1.39	1.03	1.15

Table 5.15 Film Thickness Values Corresponding to Minimum PURWheel Rut Depth.

FAA	Gradation	9.5 mm Nominal Max. Size		19 mm Nominal Max. Size	
		Limestone	Granite	Limestone	Granite
39	Above				
	Below				
44	Above	4.53			
	Through	8.55	5.16	9.65	8.36
	Below	9.24	8.49		8.84
50	Above				
	Through	9.84	6.86	9.39	8.70
	Below	9.92	7.34	10.04	8.53

Table 5.16 Summary of Material Properties Corresponding to Minimum PURWheel Rut Depth.

Nominal Maximum Size (mm)	Mixture Property	Average	Standard Deviation	COV (%)	Min.	Max.
19	VMA (%)	14.6	0.8	5.2	13.6	15.6
	VFA (%)	69.4	6.8	9.8	60.5	77.6
	Dust Proportion	1.1	0.1	9.1	0.9	1.2
	Film Thickness (μm)	9.1	0.6	6.9	8.4	10.0
9.5	VMA (%)	16.3	1.3	7.7	14.4	18.2
	VFA (%)	66.4	13.5	20.3	42.8	81.6
	Dust Proportion	1.3	0.4	29.7	1.0	2.2
	Film Thickness (μm)	7.7	1.8	24.1	4.5	9.9

Figure 5.1 Purdue Laboratory Wheel Track Test Device.

Figure 5.2 Wheel Wander Feature.

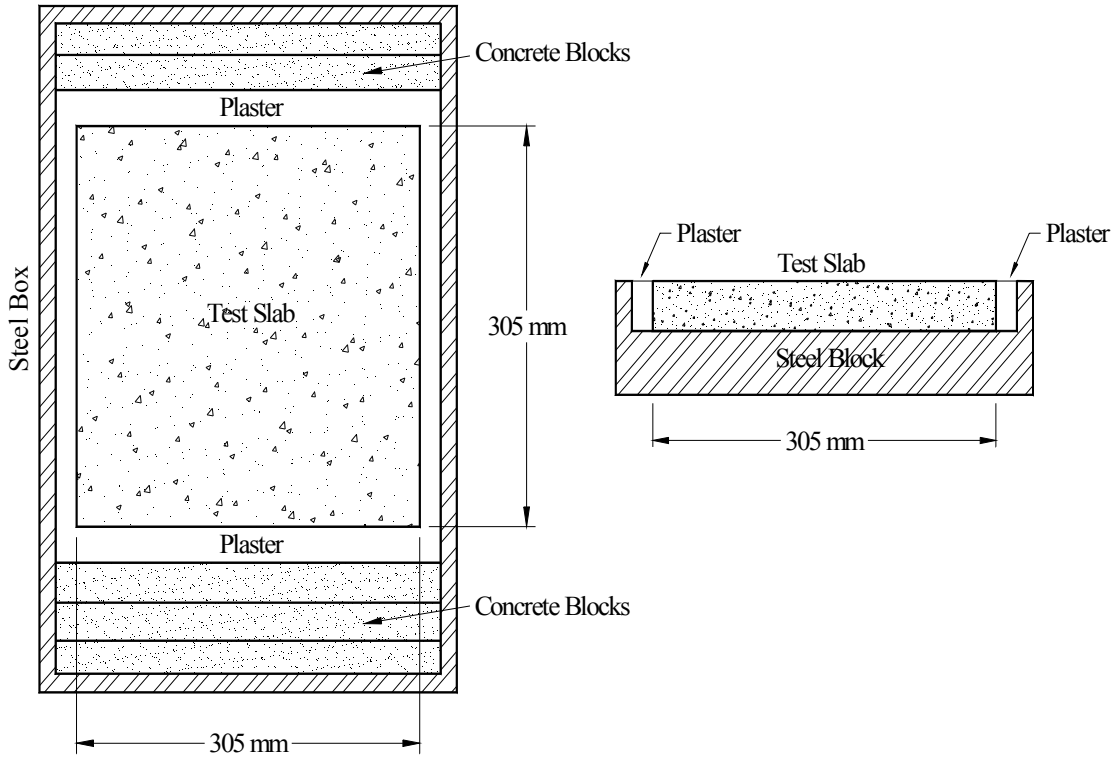

Figure 5.3 Schematic of Sample Mounting Box.

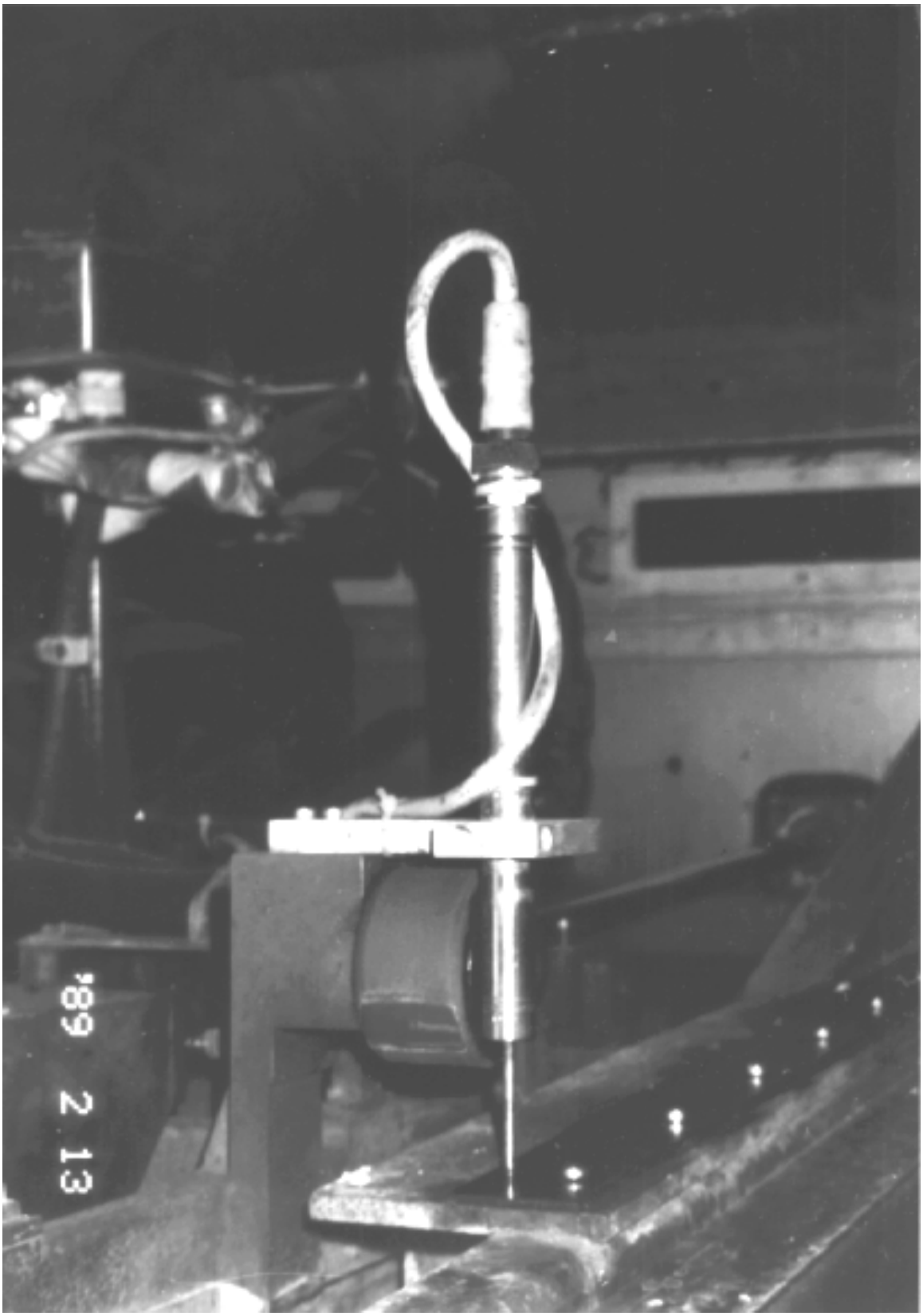

Figure 5.4 PURWheel Transducer.

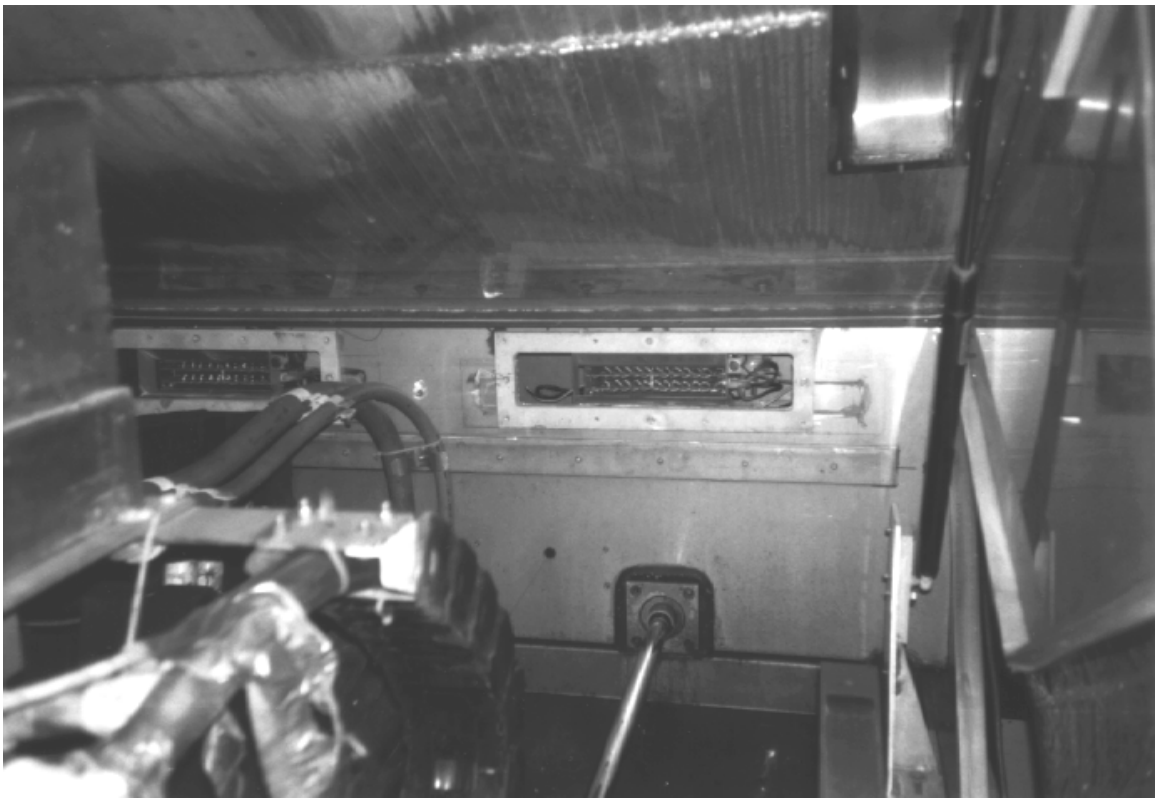

Figure 5.5 PURWheel Air Heater.

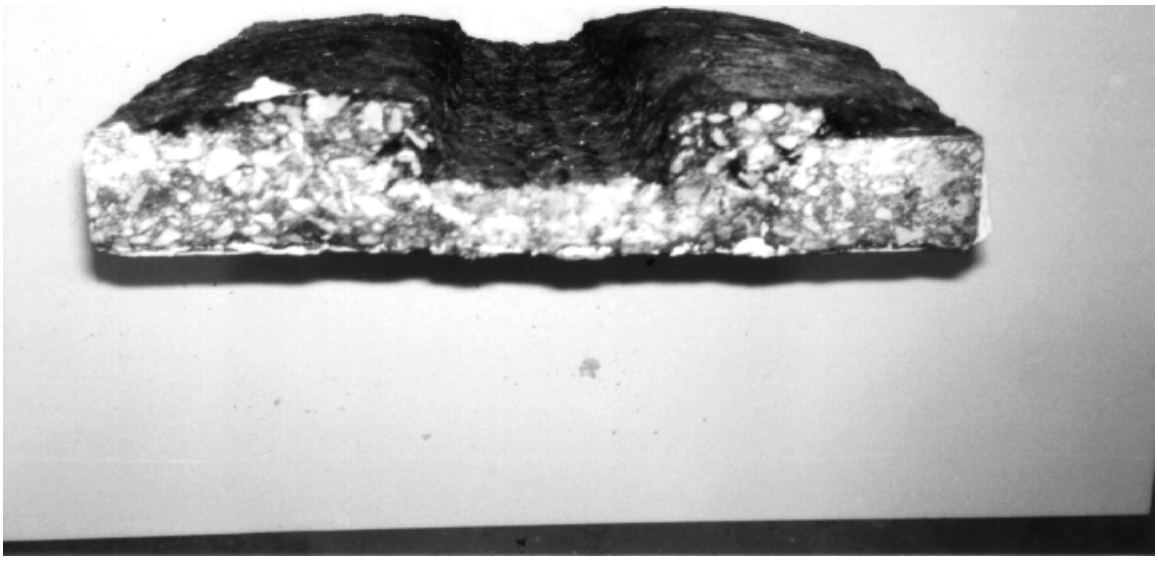

Figure 5.6 Typical PURWheel Slab Section Deformation.

Figure 5.7 Purdue Linear Compactor.

Figure 5.8 Linear Compactor Steel Mold.

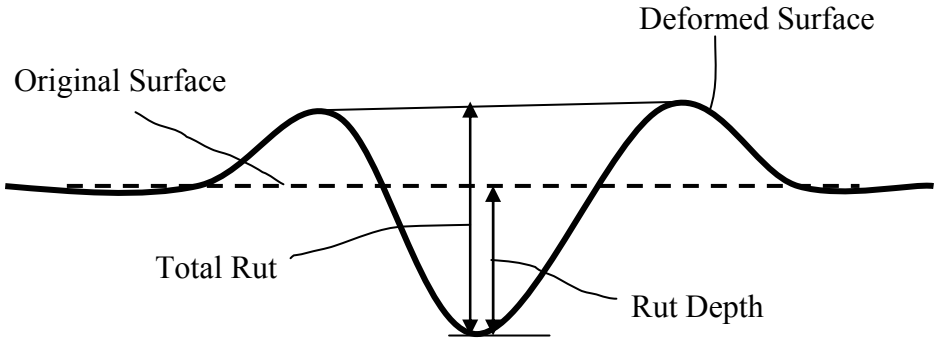

Figure 5.9 Rut Depth Definition.

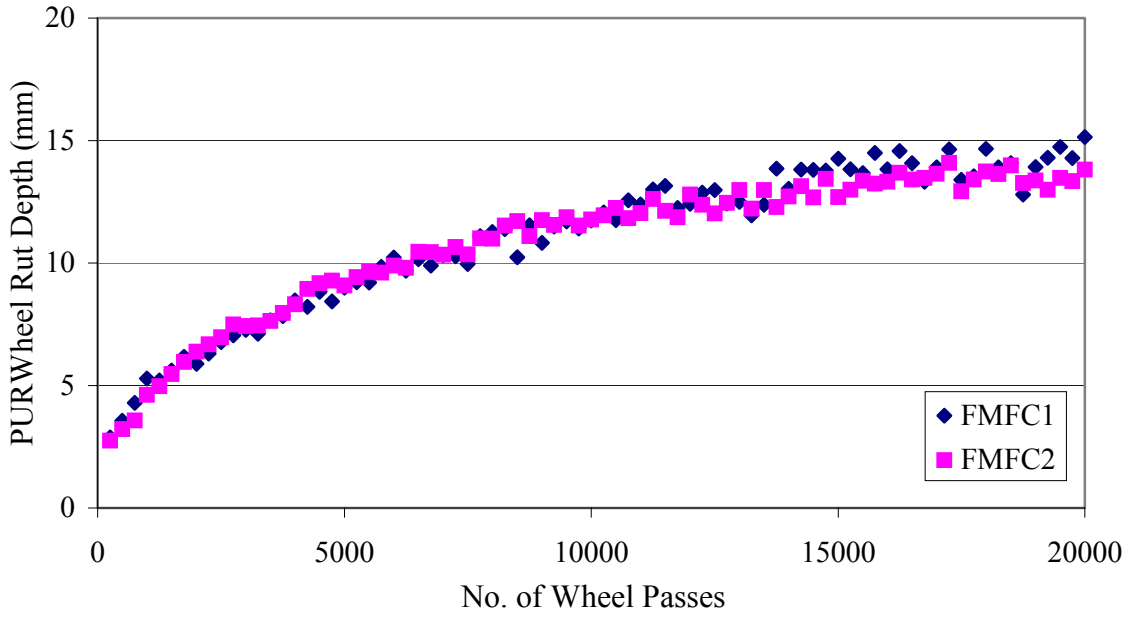

Figure 5.10 Typical Plot of Rut Depth and Wheel Passes.

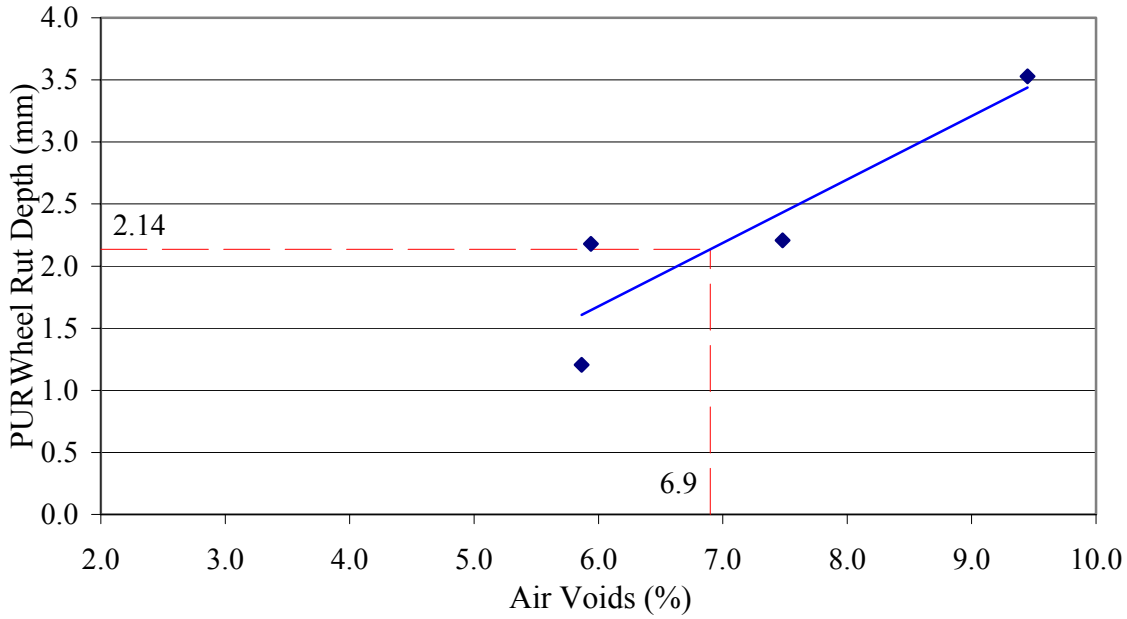

Figure 5.11 Interpolation Procedure.

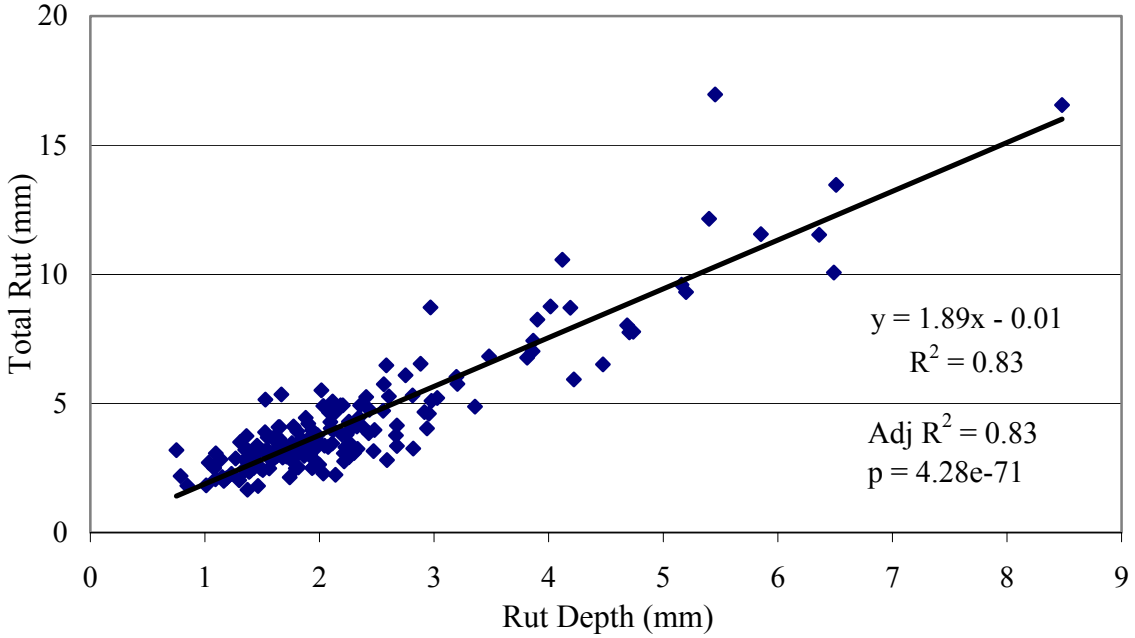

Figure 5.12 Relationship Between PURWheel Total Rut and Rut Depth.

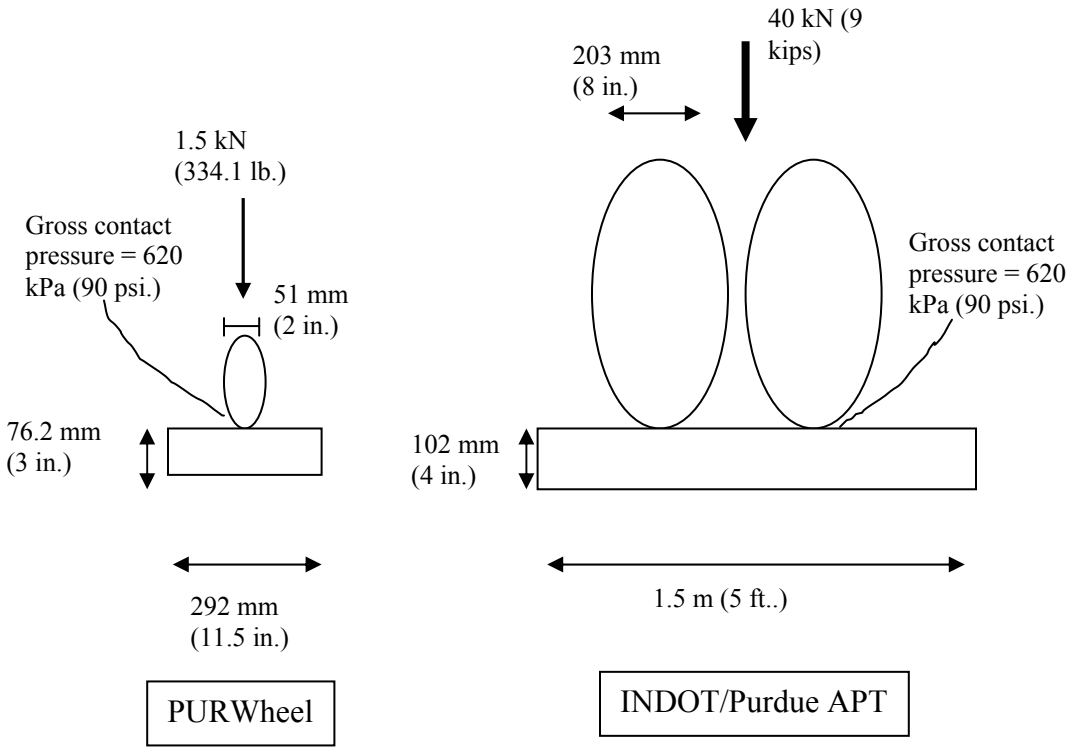

Figure 5.13 Comparison Between Load and Geometry Parameters of PURWheel and APT.

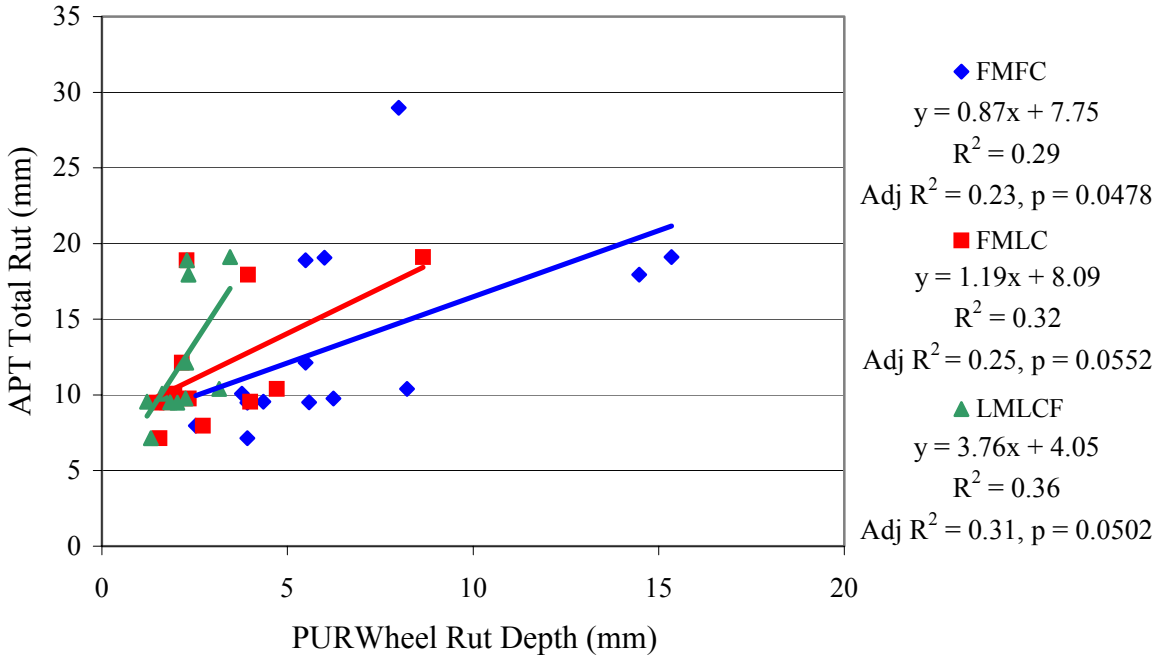

Figure 5.14 Relationship Between APT Total Rut and PURWheel Rut Depth (All mixtures).

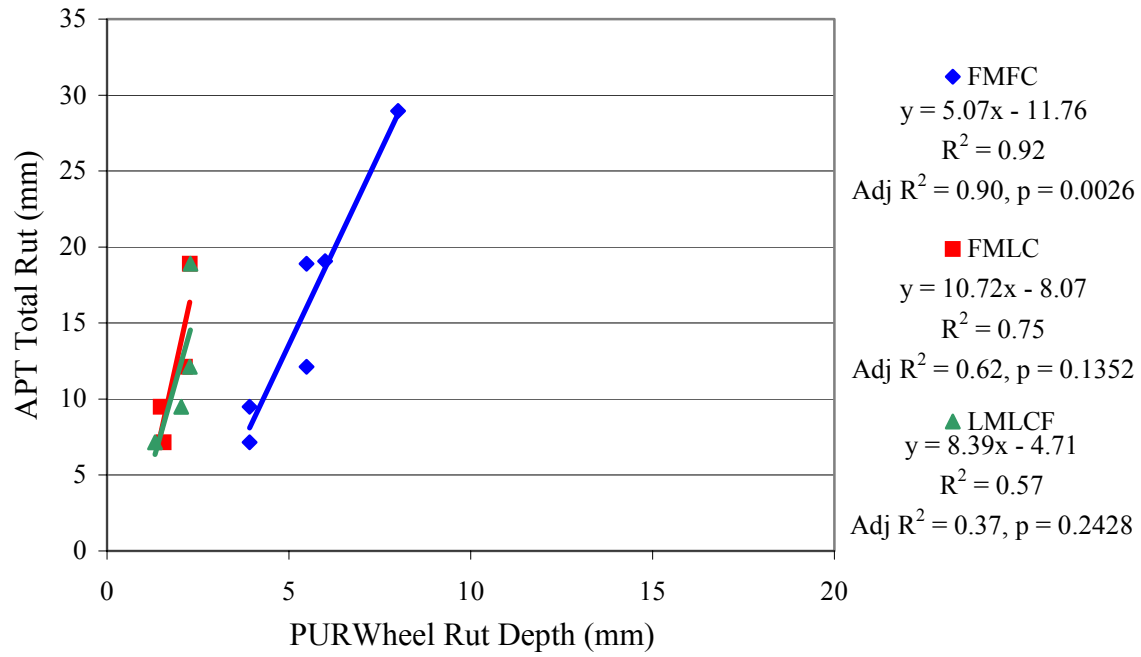

Figure 5.15 Relationship Between APT Total Rut and PURWheel Rut Depth (19 mm mixtures).

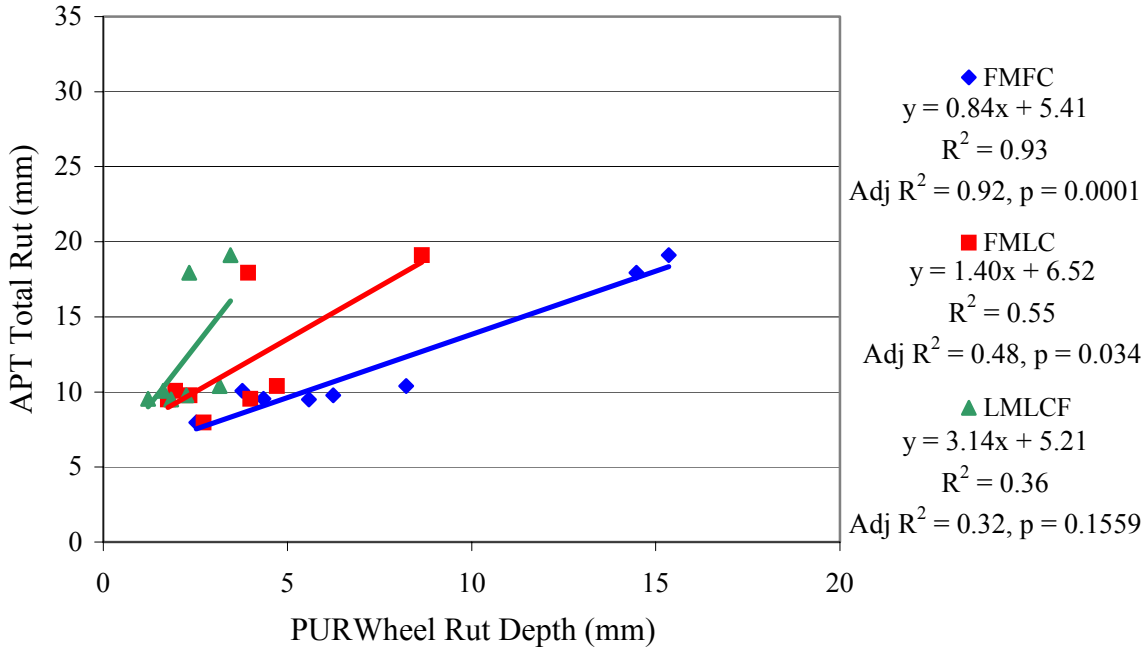

Figure 5.16 Relationship Between APT Total Rut and PURWheel Rut Depth (9.5 mm mixtures).

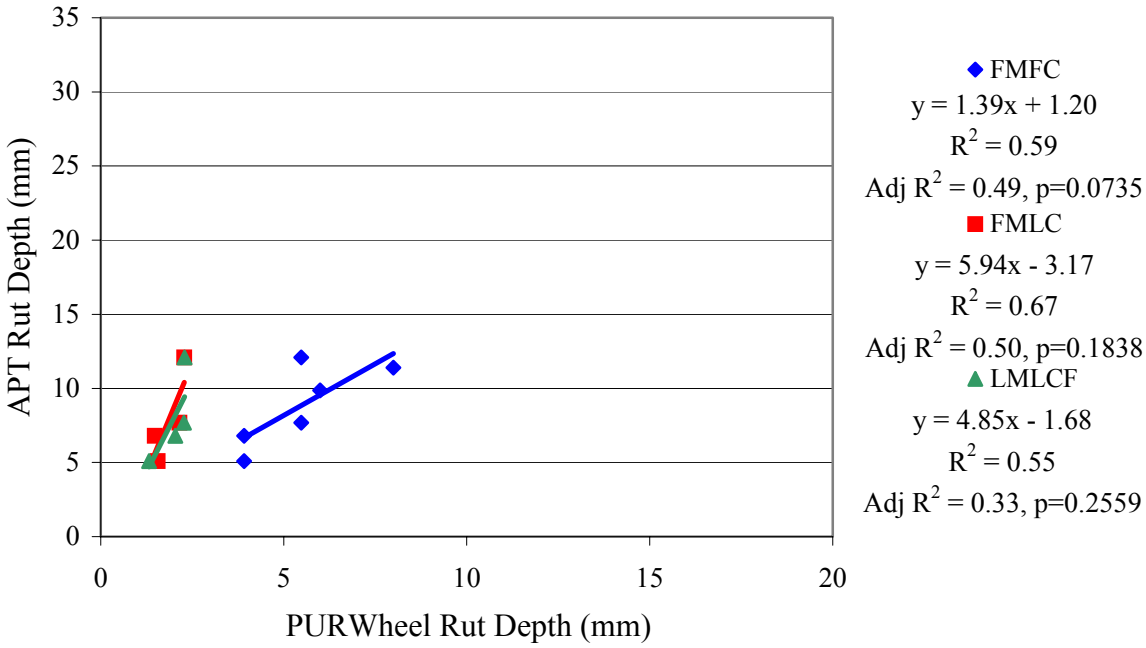

Figure 5.17 Relationship Between APT Rut Depth and PURWheel Rut Depth (19 mm mixtures).

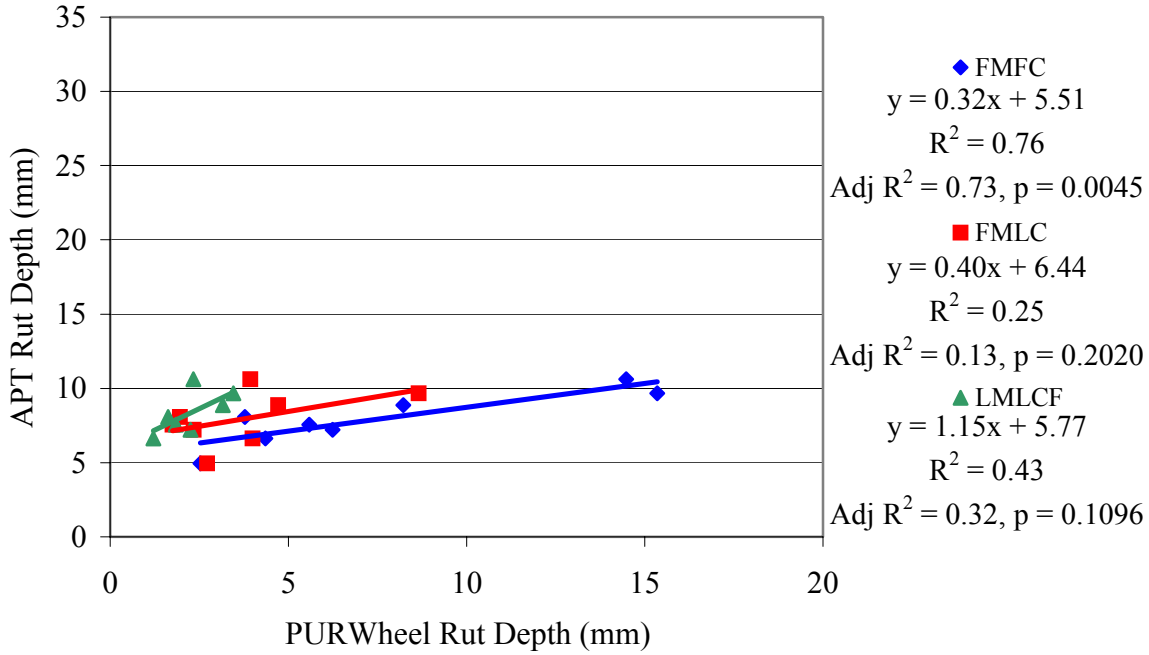

Figure 5.18 Relationship Between APT Rut Depth and PURWheel Rut Depth (9.5 mm mixtures).

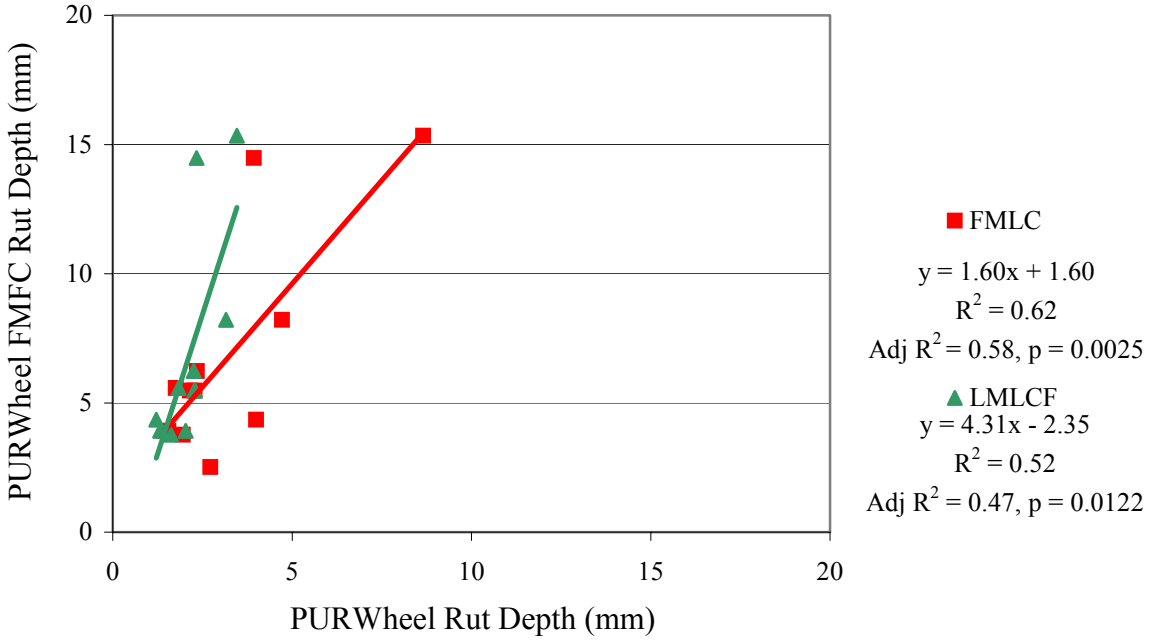

Figure 5.19 Relationship Among FMFC, FMLC, and LMLCF in PURWheel.

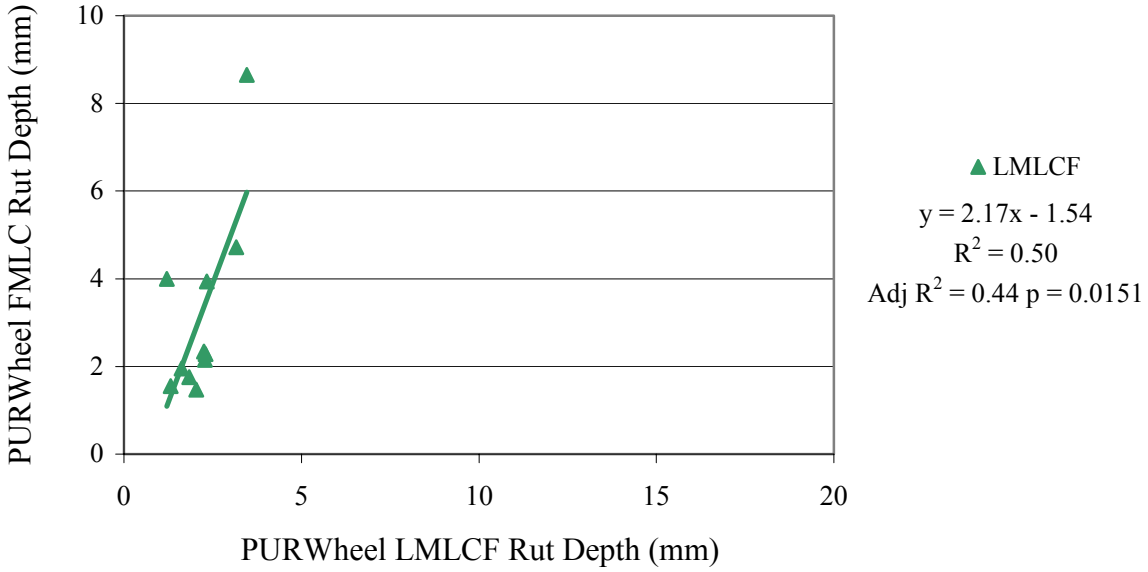

Figure 5.20 Relationship Between FMLC and LMLCF in PURWheel.

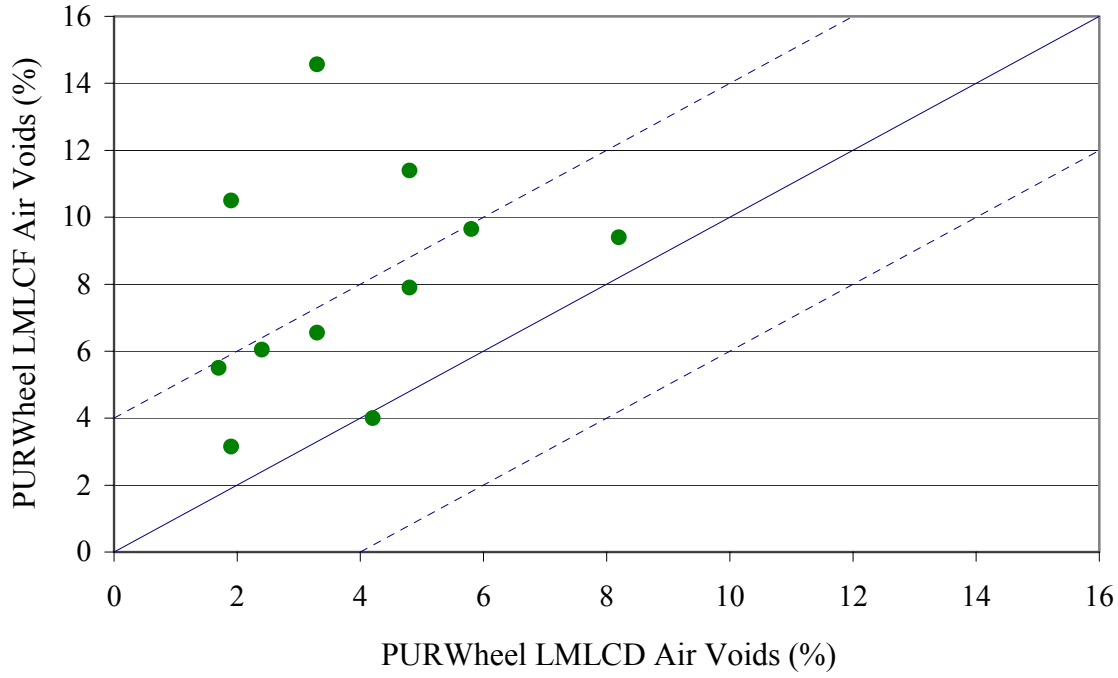

Figure 5.21 Scatter Plot of LMLCF and LMLCD Air Voids.

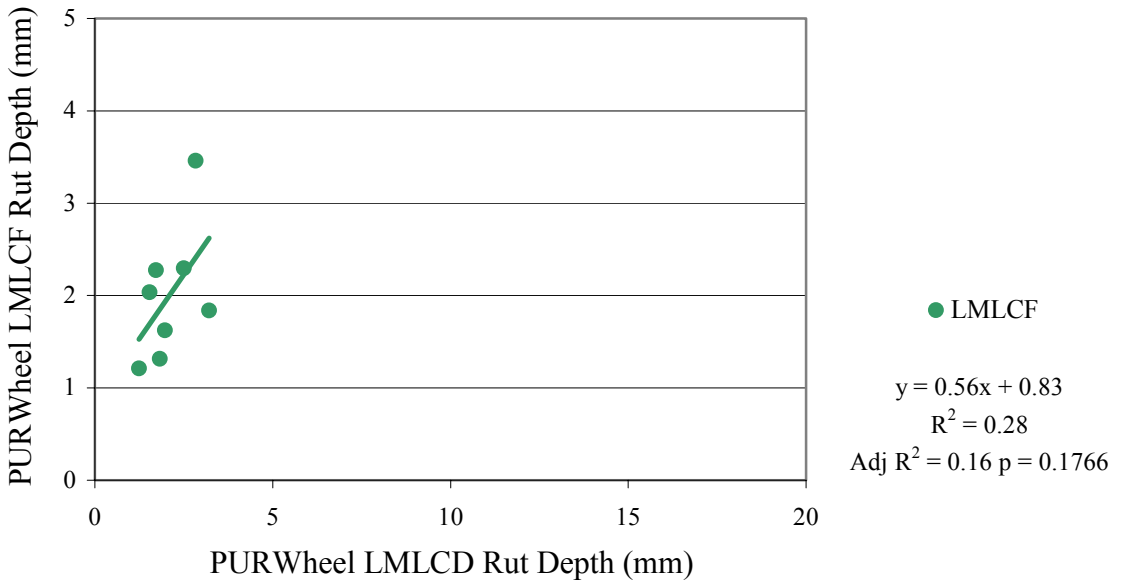

Figure 5.22 Relationship Between LMLCF and LMLCD in PURWheel.

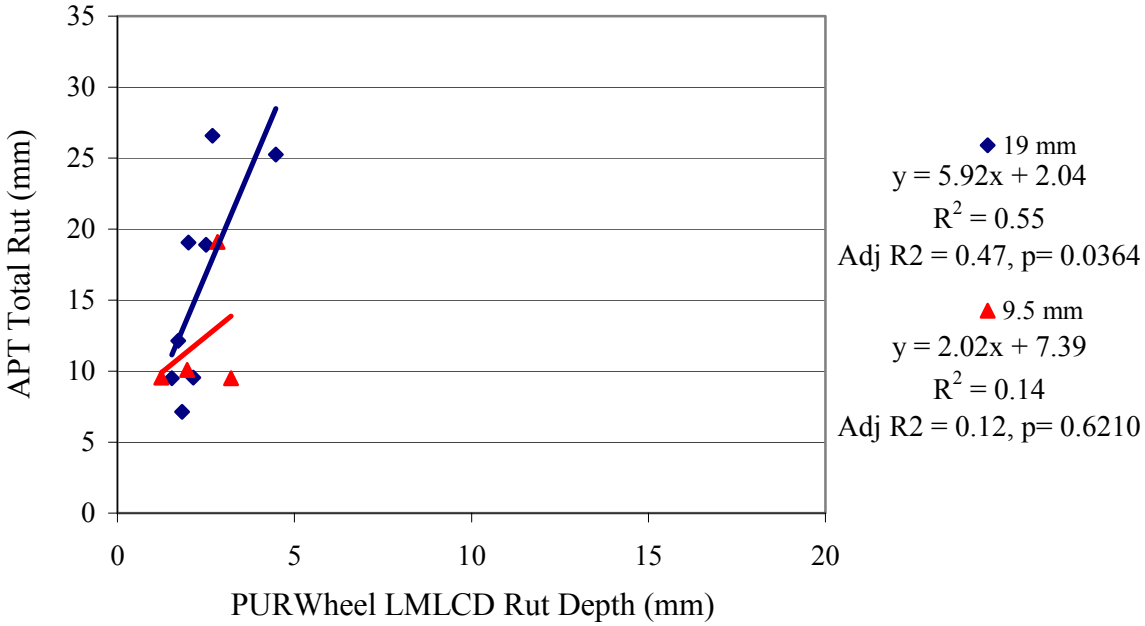

Figure 5.23 Relationship Between APT Total Rut and PURWheel LMLCD Rut Depth.

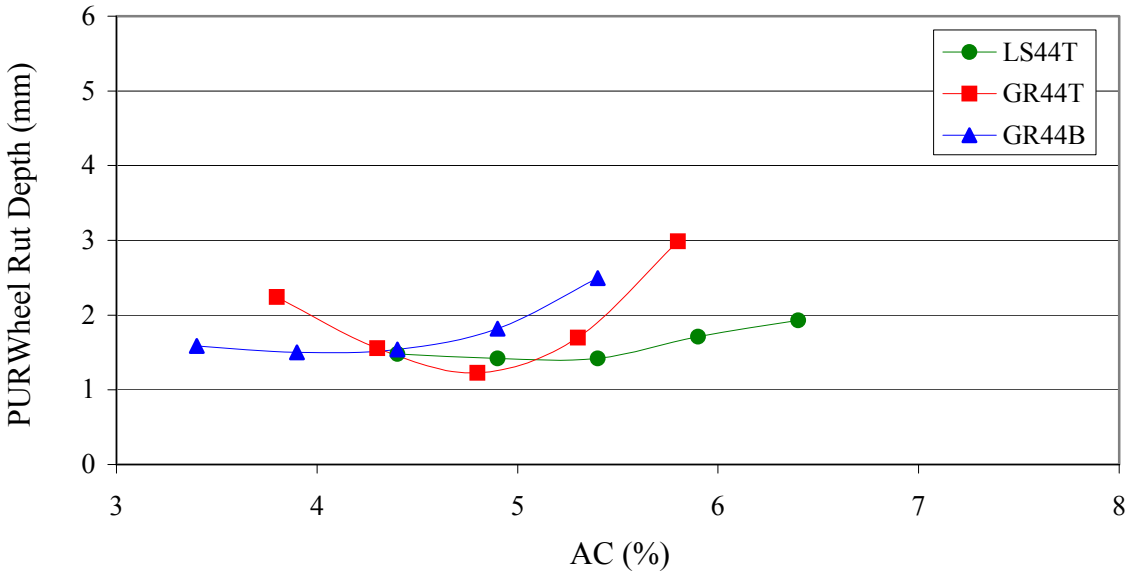

Note: LS = limestone, GR = granite; 44 = fine aggregate angularity
T, B = gradation plotting through and below the restricted zone

Figure 5.24 Sensitivity of 19mm Mixtures with FAA of 44 to AC Level.

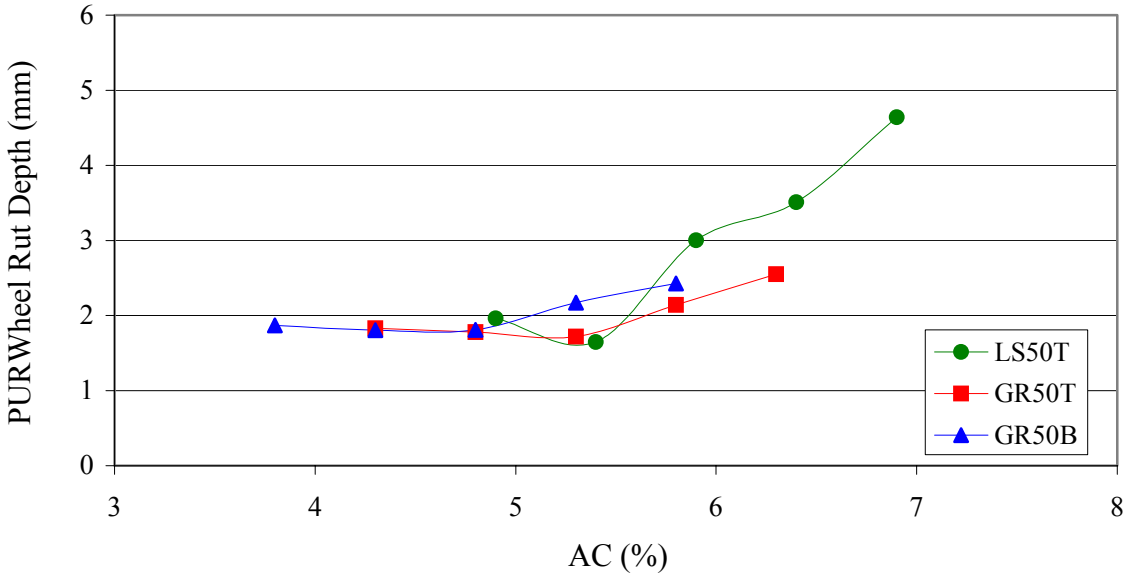

Note: LS = limestone, GR = granite; 50 = fine aggregate angularity
T, B = gradation plotting through and below the restricted zone

Figure 5.25 Sensitivity of 19mm Mixtures with FAA of 50 to AC Level.

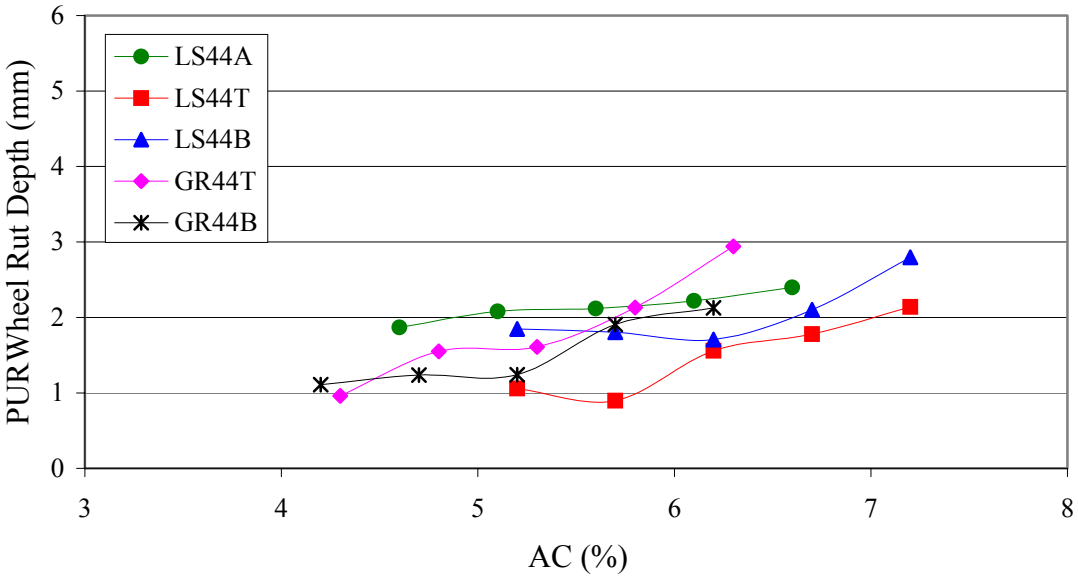

Note: LS = limestone, GR = granite; 44 = fine aggregate angularity
A, T, B = gradation plotting above, through, and below the restricted zone

Figure 5.26 Sensitivity of 9.5mm Mixtures with FAA of 44 to AC Level.

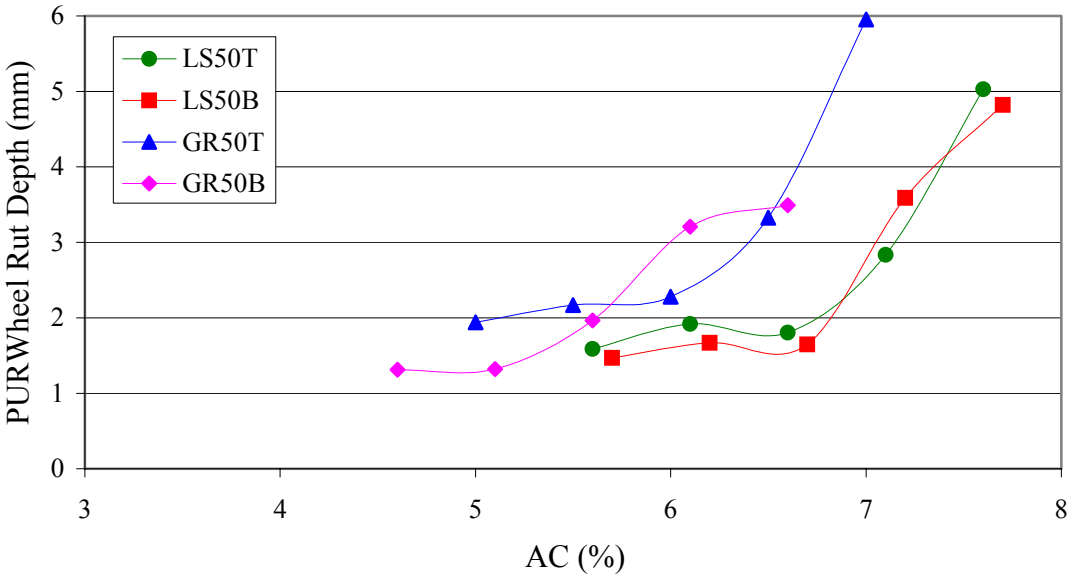

Note: LS = limestone, GR = granite; 50 = fine aggregate angularity
T, B = gradation plotting through and below the restricted zone

Figure 5.27 Sensitivity of 9.5mm Mixtures with FAA of 50 to AC Level.

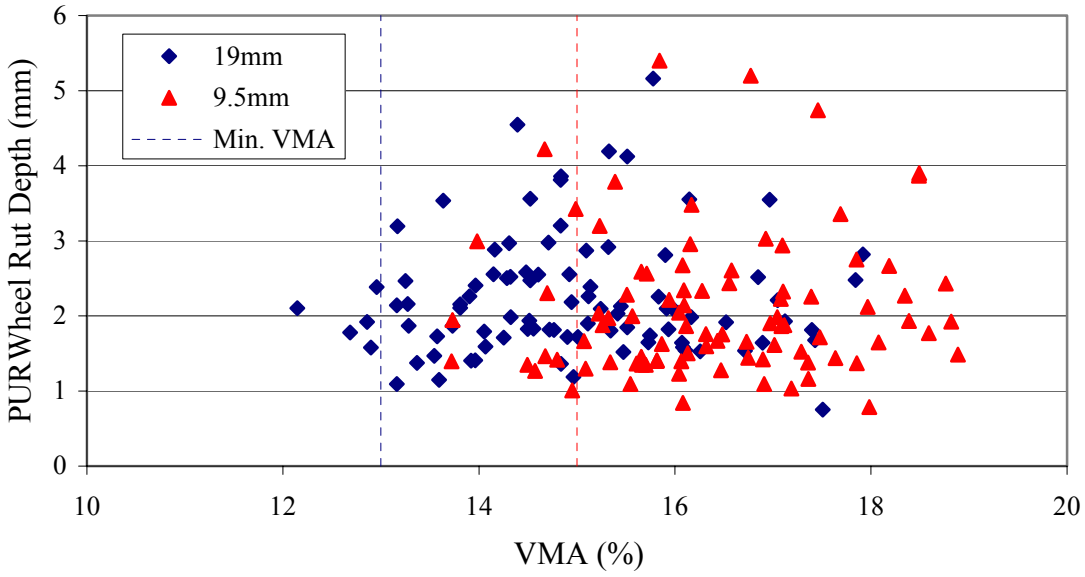

Figure 5.28 Scatter Plot of PURWheel Rut Depth and VMA (LMLCD).

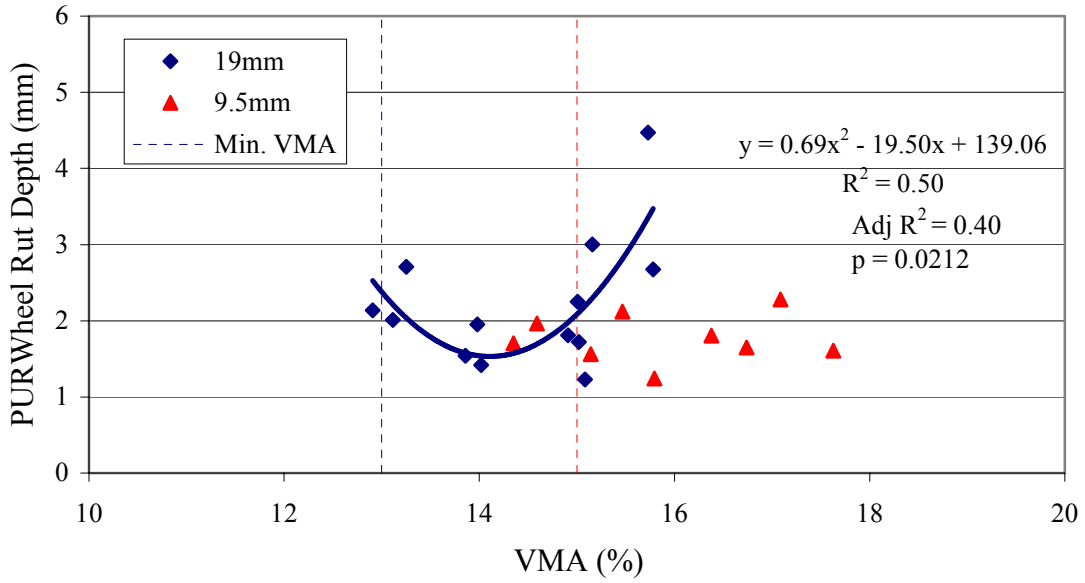

Figure 5.29 Scatter Plot of PURWheel Rut Depth and Design VMA (LMLCD).

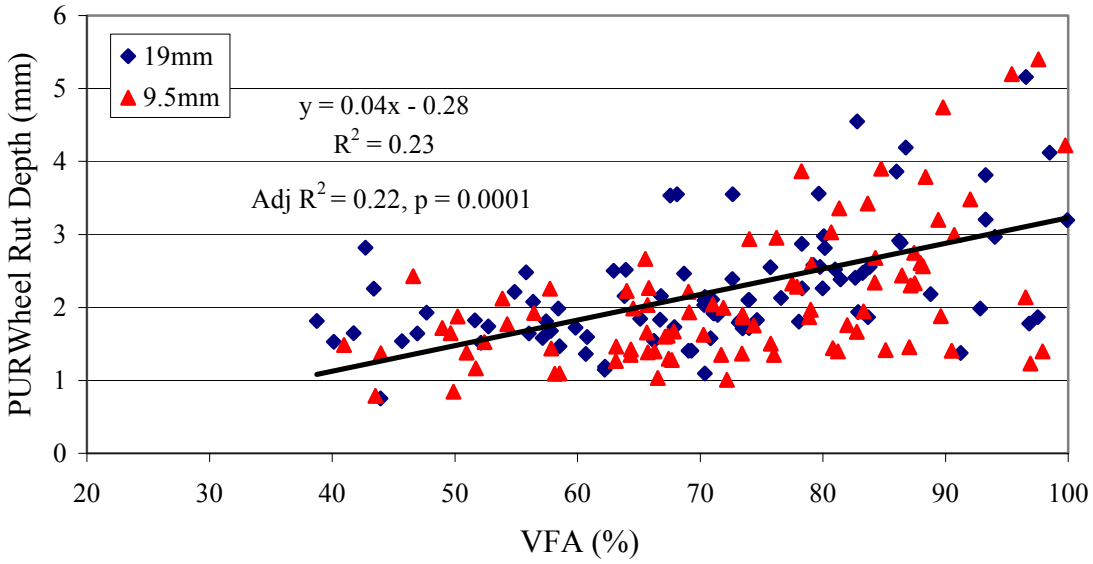

Figure 5.30 Relationship Between PURWheel Rut Depth and VFA (LMLCD).

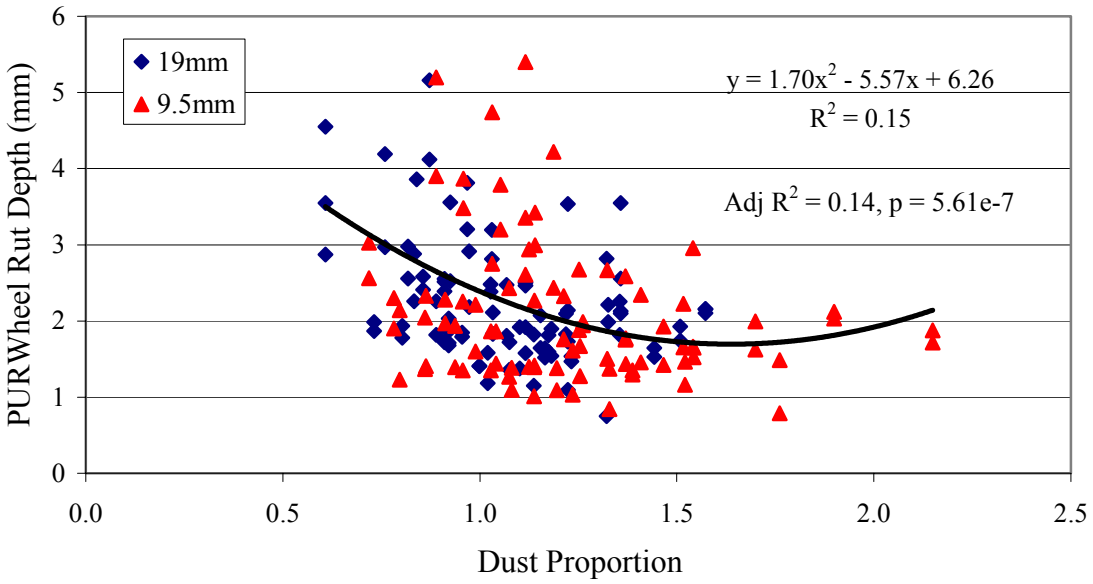

Figure 5.31 Relationship Between PURWheel Rut Depth and Dust Proportion (LMLCD).

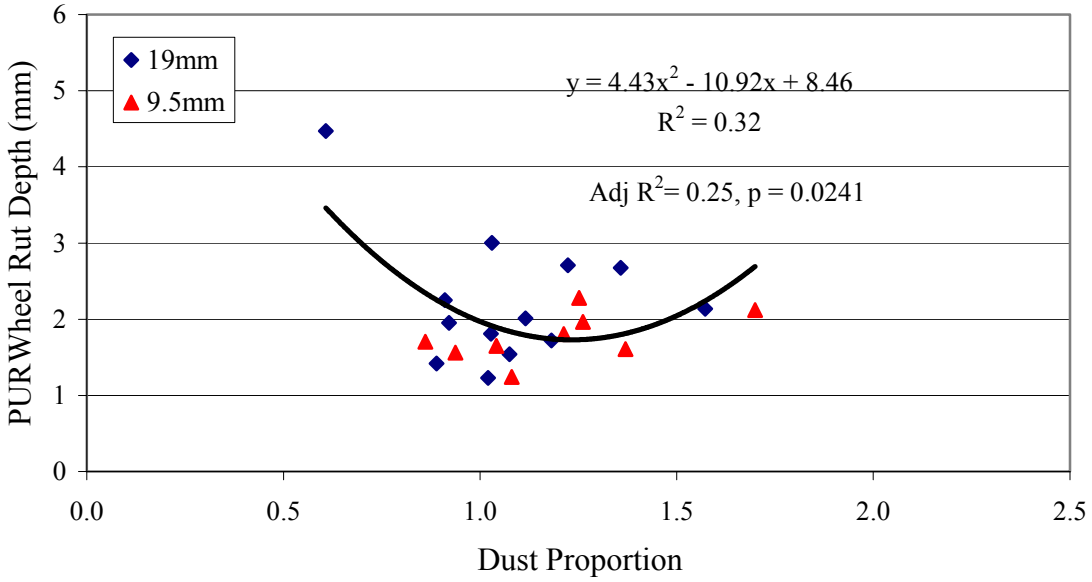

Figure 5.32 Relationship Between PURWheel Rut Depth and Design Dust Proportion (LMLCD).

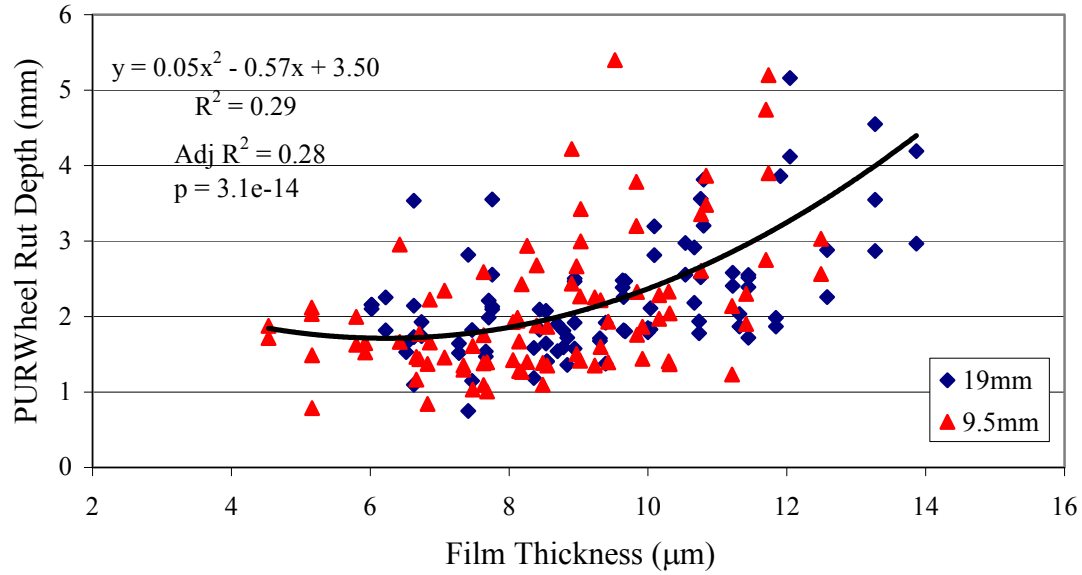

Figure 5.33 Relationship Between PURWheel Rut Depth and Film Thickness (LMLCD).

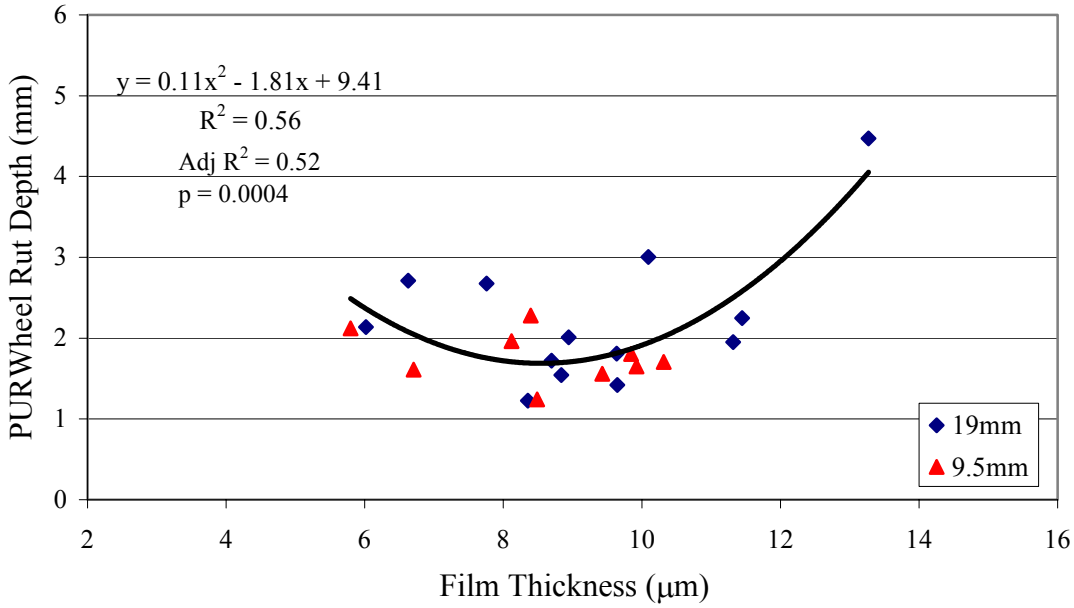

Figure 5.34 Relationship Between PURWheel Rut Depth and Design Film Thickness (LMLCD).

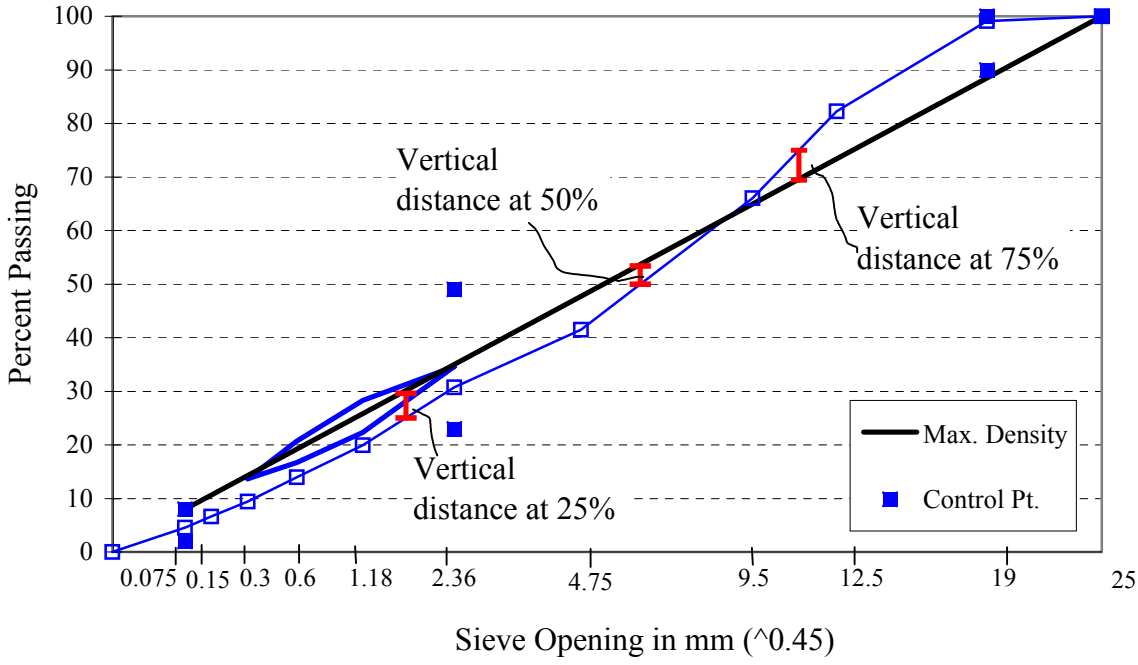

Figure 5.35 Measurement of Vertical Distance to the Maximum Density Line.

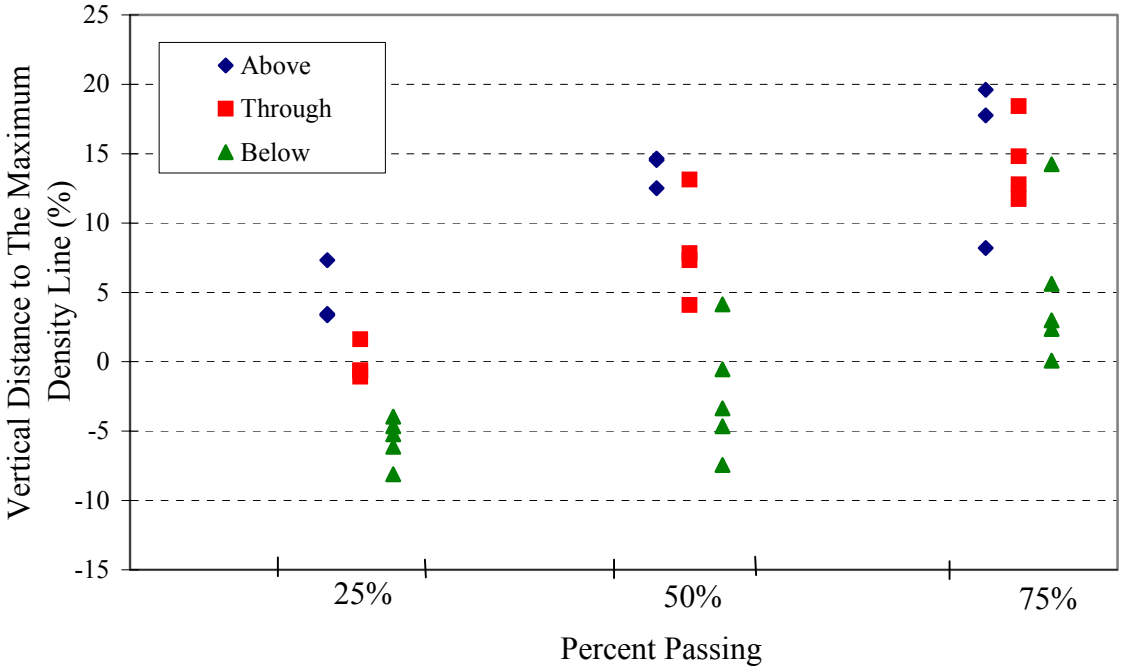

Figure 5.36 Vertical Distance to The Maximum Density Line of 19mm Mixtures.

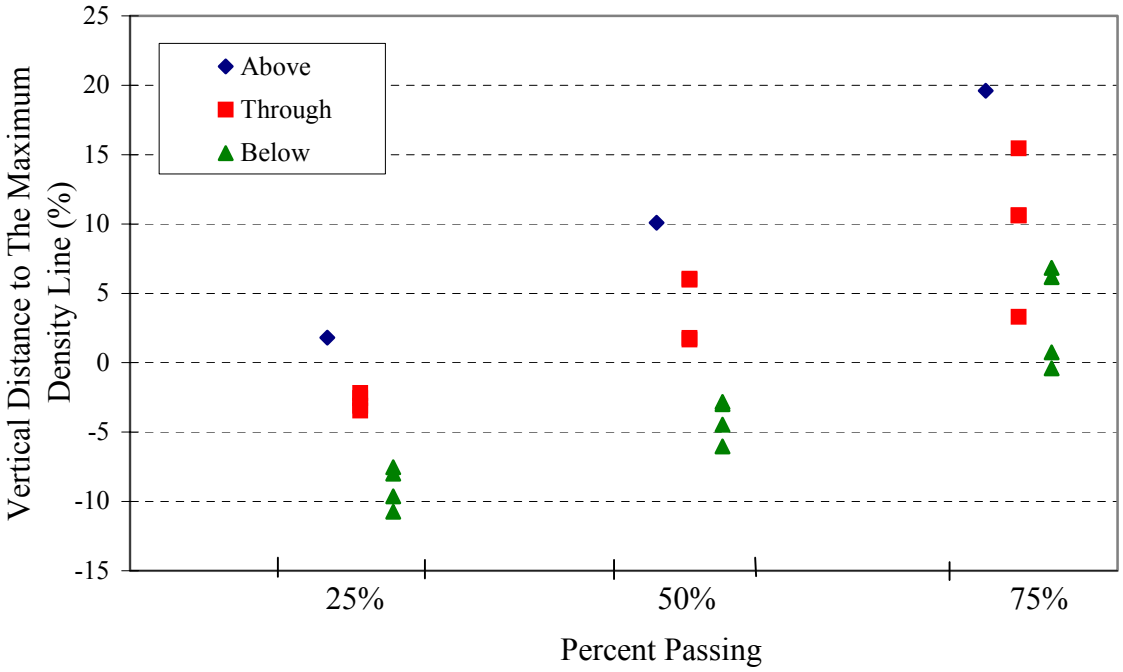

Figure 5.37 Vertical Distance to The Maximum Density Line of 9.5mm Mixtures.

6 TRIAXIAL TESTS

6.1. Description of Triaxial Test

The triaxial test method is widely used in geotechnical engineering. The volumetric components of field asphalt mixtures are aggregate, asphalt binder, water, and air. Volume occupied by air may also be occupied by water. These components are analogous to soils, which are composed of soil particles, water, and air. Because of the similarities, the triaxial test has been applied to asphalt mixtures. A number of studies using the triaxial test on asphalt mixtures were conducted in the 1940s and 1950s.

In 1956, Monismith and Vallerga conducted triaxial tests on HMA mixtures. Test specimens were prepared with a kneading compactor using three different compactive efforts and over a range of asphalt binder contents. The specimens were tested at a temperature of 60^0C and with a confining pressure of 138±1 kPa (20±0.1 psi). Testing involved loading the specimen at a rate of 1.25 mm/min (0.05 in/min) until failure. Shear stress at 1 percent strain and its corresponding bulk specific gravity are shown in Figure 6.1. These data indicate that above a specific AC level shear strength decreases. The AC corresponding to peak shear strength is considered to identify the state at which the HMA mixture transforms from the stable to unstable condition. This phenomenon is analogous with triaxial testing of soils when tested over a range of moisture contents.

There was a strong desire to use specimens prepared with the SGC for triaxial testing. The reasons for this were because it would allow for evaluation of mixtures under the same conditions (aggregate structure, volumetric state, and compaction energy) that are used to select the design AC in the Superpave mixture design method. However, a typical SGC sample height is approximately 112.5 mm (4.4 in) when compacted to the design number of gyration (N_{design}). Using a single SGC sample would result in a specimen height to diameter ratio of 0.75. ASTM requires height to diameter ratios of 2.0

to 2.5, and even 3.0 (ASTM D 4767, D5202, D2664, D 4341) for triaxial specimen. Von Quintus, et al. recommended a height to diameter ratio of one for uniaxial tests in the NCHRP Asphalt-Aggregate Mixture Analysis System (AAMAS) study provided that there is no friction between the test specimen ends and loading platens and that the deformations are measured over the entire test specimen (Von Quintus, et al., 1991). As part of the on going Superpave models evaluation a study on specimen geometry of uniaxial tests for use in permanent deformation predictions indicates a minimum height to diameter ratio of 1.5 is acceptable regardless of nominal maximum aggregate size of the mixtures (Witczak, et al., 2000). This is illustrated in Figure 6.2.

The issue of height to diameter ratio could be addressed by stacking SGC samples. Stacking samples creates a horizontal discontinuity plane in the test specimen. The effect of discontinuity plane orientation is a classic issue in rock mechanics. The discontinuity plane influences the measurement of intact specimen properties when the angle of the plane is within the range of 5 to 45 degree from the vertical as shown in Figure 6.3 (Goodman, 1976). Therefore, the horizontal discontinuity, which resulted from stacking SGC samples, should not affect the measurement of intact specimen properties. Witczak has also investigated the effect of stacking SGC specimens as part of the Superpave models evaluation (Witczak, et al., 2000). The study conducted specifically to determine the most appropriate stacking arrangement concluded that stacked and monolith specimens exhibited the same material properties in complex modulus and permanent deformation tests.

The triaxial test was proposed for the study as a means of identifying when a HMA mixture transformed from a stable to an unstable condition with increasing asphalt content. The mixtures tested are identified in Table 6.1.

6.2. Test Specimen Preparation

Initially, 150 mm (6 in.) in diameter by 300 mm (12 in.) tall samples were to be prepared using a modified kneading compactor. However, identifying the compaction

effort for the equipment to achieve densities equivalent to those of the Superpave gyratory compactor (SGC) became very involved. Essentially, determining the compactive effort for each mixture became a mini-study. Consequently, a decision was made to use samples prepared with the SGC. Because of the exploratory nature of the triaxial tests, a decision was also made to stack two SGC samples as shown in Figure 6.4. This resulted in a triaxial test specimen 150 mm (6 in.) in diameter and approximately 225 mm (9 in.) tall and thus a height to diameter ratio of 1.5. Each of the individual SGC samples was blended, mixed and cured carefully in accordance with Superpave volumetric design procedures as specified in AASHTO PP28-97, "Practice for Superpave Volumetric Design for Hot Mix Asphalt (HMA)" (AASHTO, June 1997). Details of the specimen preparation are presented in Appendix E1.

Initially, testing was conducted on specimens prepared at three compaction levels. They were 76, 96 (N_{design}), and 152 ($N_{maximum}$) gyrations in the SGC. These compaction levels were selected to capture effects of compaction on the triaxial test results. It was hypothesized that the aggregate interlock (aggregate structure) was not well developed at the 76 gyration compaction level (Haddock, et al, 1998). The basis for the hypothesis was that the shear strength at 1 percent axial strain of specimens compacted to 76 gyrations did not show any sensitivity as AC level changes. Accordingly, it was decided to evaluate the effect of two compaction levels, i.e. 96 and 152 gyrations only.

For each compaction level mixtures were prepared at five AC levels, Superpave design AC, design AC ± 0.5 percent, and design AC ± 1.0 percent. Duplicate specimens were prepared and tested for each AC level. As previously discussed, a triaxial specimen consisted of two stacked SGC samples. Accordingly, four SGC samples would be required to make two triaxial specimens. The bulk specific gravity (Gmb) of individual SGC samples was measure in accordance with ASTM D2726. Pairs of SGC samples with the closest Gmb values were selected and stacked in order to make triaxial specimens.

6.3. Test Parameters

The air-dry triaxial test was selected because pavement rutting generally occurs under the air-dry condition. This test type is not commonly conducted in soils. During testing, no water was utilized and the drainage line was open to free air. Accordingly, no pore water pressure was generated. This would make the total stresses close to the effective stresses. Taking an analogy to the traditional triaxial test types in soils, the air-dry triaxial test is similar to the consolidated drained (CD) test. However, the volume change during testing could not be measured.

It is important that the strain rate be selected such that no excess pore pressure is generated. A strain rate of 1.25 mm/min (0.05 in/min) was selected following Monismith and Valerga's work in 1956. During testing, although the drainage line was kept open to free air, the pore pressure transducer was attached to monitor the pore pressure. The absolute value of pore pressure measurements was not an accurate indication of pore pressure because the device was not designed to measure air pressure and the drainage line was in contact with free air. However, the value of pore pressure measurement could indicate when significant pore pressure was generated during testing. Pore pressure monitoring indicated that the strain rate was acceptable because no significant pore pressure was generated during the tests. Another advantage of attaching the pore pressure transducer to the drainage line is to detect membrane leakage.

The confining pressure was selected at 138±1 kPa (20 psi) following Monismith and Valerga's work also. From a practical standpoint, the maximum confining pressure depends on the maximum axial load that the machine can apply. The minimum confining pressure should be selected such that the effect of membrane tension is negligible and the stress-strain curve could be well observed. Test results indicated that the selected confining pressure was appropriate such that the machine capacity was not exceeded and stress-strain curves were well observed.

A test temperature of 60^0 C (140^0 F) was selected following Monismith and Valerga's work in 1956. The test temperature needs to be selected such that the maximum load capacity of the machine is not exceeded. It is useful to test at a

temperature that is representative of a temperature at which rutting would occur in HMA under actual field conditions. It is also important to consider the binder grade used in the mixtures to ensure that the test temperature does not significantly exceed expected HMA pavement temperatures that would be observed in environments where that grade could be used. Based on balancing test machine capacity, binder grade (PG64-22), and other considerations the 60^0 C (140^0 F) test temperature was appropriate. Before the test, specimens were placed in a 60^0 C oven overnight to achieve a uniform temperature. During the test, the temperature inside the environment chamber was automatically controlled at 60^0 C.

A seating load of 0.6 kN (132 lb.) was applied prior to testing. This load corresponded to 33.9 kPa (4.9 psi) axial stress. In general, the applied seating load was less than 5 percent of the compressive strength of the specimens as required by ASTM D2850. The purpose of the seating load is to ensure proper specimen seating and proper contact between the specimen and the cap.

Gas or air was utilized as the confining pressure. All the testing was conducted using an INDOT MTS triaxial test device. The device was designed to use air as the confining media because electronic sensors are used inside the pressure chamber. There is a concern that air penetrates the membrane. The air penetration would result in a condition of partial saturation and inaccuracy of pore water pressure measurement. However, the air-dry triaxial test does not require saturation nor pore pressure measurement. Therefore, it is reasonable to assume that air penetration would not impact the test results. Double rubber membranes were utilized to minimize the potential for air penetration effect. Details of the procedure used to conduct the air-dry triaxial tests are presented in Appendix E1.

6.4. Triaxial Test Results

6.4.1. Data Acquisition

The INDOT MTS triaxial test device was utilized in this study. The strain rate and testing temperature are electronically controlled. The confining pressure was applied manually and the actual confining pressure was measured electronically. The axial load, axial displacement, and time data were recorded automatically (MTS, 1994). The time and displacement data were used to verify the strain rate. The initial height of the specimen was equal to the total height of the individual SGC samples stacked together. From these data, axial strain and deviator stress were calculated. The formula utilized for calculation is presented in Appendix E1. An example plot of deviator stress and axial strain is presented in Figure 6.6.

6.4.2. Triaxial Shear Strength

In order to evaluate different mixtures consistently, a single value of shear strength was utilized. A decision was made to utilize the shear strength at 1 percent axial strain as shown in Figure 6.6. Vallerga and Monismith used shear strength at 0.5, 1, and 2 percent axial strains to evaluate the HMA mixtures (Vallerga and Monismith, 1956). Triaxial test results indicated that at 0.5 percent axial strain, the shear strength has not been positively mobilized and at 2 percent axial strain, some mixtures were very close to the peak strength. The peak strength was not selected to evaluate mixtures because generally the tire contact pressure is less than the peak shear strength of the mixtures. For example, the tire contact pressure in the INDOT/Purdue APT was approximately equal to the tire inflation pressure of 620 kPa (90 psi) and typical observed triaxial peak shear strengths were approximately 1800 kPa (261 psi) at approximately 3 percent axial strain.

Occasionally, a correction procedure was required in obtaining shear strength at 1 percent axial strain. The correction procedure amounts to shifting the origin such that a linear stress strain relationship would be observed at the low level of strain as shown in

Figure 6.6. This correction procedure is similar to the one commonly employed for CBR tests (ASTM D1883). It is hypothesized that the non-linearity at the low level of strain was due to the misalignment of the load piston and sample cap, the improper seating of the specimen and sample cap, and/or the discontinuity plane between the surfaces of the two stacked SGC samples.

6.5. Discussion on Triaxial Test Results

6.5.1. Failure Plane after Triaxial Testing

The observed failure planes of several HMA specimens after triaxial testing are presented in Figure 6.7. Four specimen configurations with different height to diameter ratio were tested as shown. The tallest specimen consisted of 3 stacked SGC specimens with parallel cut faces. The second tallest consisted of 2 stacked SGC specimens without parallel cut faces. The third tallest specimen consisted of 2 stacked SGC specimens with parallel cut faces. The shortest specimen was a SGC specimen with parallel cut faces. The cut faces were produced by trimming the samples using a mansory saw. Observations on the specimens after testing revealed that a shear failure plane was well observed on all the specimens except on the one consisting of a single SGC specimen with parallel cut faces. This suggested that when the height to diameter ratio of a specimen was to small, the shear failure plane could not develop.

The shear failure plane is a necessary condition for further interpretation because the failure plane would confirm the state of stresses that actually lead to specimen failure. It appeared that the stacking of two SGC samples did not influence significantly the shear failure plane. The observed shear failure plane was similar to the failure plane that typically occurs in soil testing.

6.5.2. Effect of Height to Diameter Ratio

Stacking two SGC samples introduced al horizontal discontinuity plane and resulted in a height to diameter ratio of 1.5. The SGC sample ends surface smoothness is dependent on nominal maximum aggregate size of the mixture. As previously stated, the effect of a horizontal discontinuity plane on the triaxial strength of the intact specimen is minimal.

Height to diameter ratio and sample surface smoothness cause significant end effects and influence the strength measured in triaxial tests. As previously discussed (Section 6.5.1.), four specimens with two different nominal maximum aggregate sizes and different height to diameter ratios, and surface smoothness were tested. The effect of height to diameter ratio on 19mm granite with FAA of 44 and gradations plotting below the restricted zone in triaxial tests is presented in Figure 6.8. The effect of height to diameter ratio on 9.5mm granite with FAA of 44 and gradations plotting below the restricted zone mixtures in triaxial tests is presented in Figure 6.9. The plots suggested that smaller height to diameter ratios resulted in greater peak shear strength, larger axial strain corresponding to peak shear strength, and lower shear strength at 1 percent axial strain. A plot of shear strength at 1 percent axial strain and height to diameter ratio is presented in Figure 6.10. The plot suggests that nominal maximum aggregate size did not significantly influence shear strength at 1 percent axial strain. Further, this observation suggested that although the surface smoothness of the 19 and 9.5mm mixtures was different, the shear strength at 1 percent axial strain was not influenced. This observation contradicts with observations on the effects of surface roughness on triaxial tests of sands, triaxial tests of rocks, and compressive strength tests of concrete. It is common knowledge that the surface roughness would affect the test results, because the roughness creates additional friction between the specimen and the sample caps. The additional friction increases the confining pressure at the ends of the specimen. There are several methods to minimize the surface roughness, for example capping (ASTM C 617). It is hypothesized that the surface roughness does not influence the triaxial test results significantly because HMA mixtures are more plastic at high temperatures than sands, rocks, or concrete.

ASTM D2850 specifies a height to diameter ratio for triaxial test specimens between 2 and 2.5. The stacking of two SGC samples resulted in a height to diameter ratio of approximately 1.5. The relationship between shear strength at 1 percent axial strain and height to diameter ratio (Figure 6.10) indicated that the difference between shear strength at 1 percent axial strain for a height to diameter ratio 1.5 and that for a height to diameter ratio 2 was approximately 10 percent.

Stacking three SGC samples would result in a total height of approximately 338 mm. The height to diameter ratio of this specimen would be approximately 2.3. However, the INDOT MTS triaxial test device is only capable of testing 300 mm tall specimens. Trimming three SGC samples to satisfy height to diameter ratio of 2.0 was not practical because a total of 420 triaxial specimens were to be tested.

Unconfined and confined creep tests have been conducted on stacked HMA specimens also. Unconfined static creep tests have been conducted with three stacked laboratory prepared specimens (Regan, et al., 1987). Confined creep tests have been conducted on two stacked field cores (Parker, et al., 1990). In the latter study, a cement grout was used to seat and bond the two cores.

In summary, the triaxial test results using two stacked SGC samples were mainly affected by the height to diameter ratio, not by the discontinuity plane between the two SGC samples. Additionally, the stacking study suggested that a maximum difference in strength of 10 percent may have been observed due to height to diameter ratio of 1.5 although other recent research suggests it could be even less (Witczak, et al., 2000).

6.5.3. Variability of Triaxial Test Results

The variability of triaxial test results was assessed by evaluating observed coefficient of variability for shear strength at 1 percent axial strain. The coefficient of variations from 220 test results were categorized, counted, and plotted in Figure 6.11. The plot indicates that approximately 45 percent of the triaxial tests had coefficients of

variation less than 5 percent and 42 percent of the tests had coefficients of variation between 5 to 15 percent. Therefore, the bulk of the triaxial test results had associated coefficients of variation of less than 10 percent, which is considered good.

6.5.4. Correlation Between PURWheel and Triaxial Test

Although the triaxial test was used to measure the shear strength of HMA mixtures, the state of stress while rutting is occurring in a HMA pavement is more complicated than the state of stress during a triaxial test. The Purdue Laboratory Wheel Track Test Device (PURWheel) was designed specifically to simulate conditions associated with rutting (Pan, 1997). Therefore, triaxial test results could be assessed relative to and by correlating with PURWheel test results.

The correlation between triaxial and PURWheel tests was made by conducting both tests at 60^0C. The PURWheel specimens were compacted to the density of SGC samples (density at N_{design} = 96). A series of plots of triaxial and PURWheel test results are presented in Figures 6.12 through 6.27. The plots reveal that the AC corresponding to maximum shear strength and minimum PURWheel rut depth is essentially equal for most mixtures. This suggests that either test could be used to refine design AC obtained from the volumetric mix design process to optimize rutting performance. The summary plot of triaxial shear strength and PURWheel rut depth is presented in Figure 6.28. Details of regression analysis are presented in Appendix E3. Although the r^2 value is small (0.32), there is a clear indication that as shear strength decreases PURWheel rut depth increases.

6.5.5. Material Property Effects on Triaxial Test Results

The effects of nominal maximum aggregate size, coarse aggregate type, fine aggregate angularity, gradation type, number of gyrations, and AC level on triaxial test results were analyzed using analysis of variance (ANOVA). In order to conduct a

balanced analysis, the experimental data was arranged as shown in Table 6.2. The ANOVA of PURWheel rut depth is summarized in Figure 6.3. Details of the analysis can be found in Appendix E3. The following model was assumed in the analysis.

$$Strength_{ijkl} = \mu + N_i + C_j + F_k + G_l + R_m + A_n + NC_{ij} + NF_{ik} + NG_{il} + NR_{im} + NA_{in} + CF_{jk} + CG_{jl} + CR_{jm} + CA_{jn} + FG_{kl} + FR_{km} + FA_{kn} + GR_{lm} + GA_{ln} + RA_{mn} + \varepsilon_{ijklmn} \quad \ldots(6.1)$$

Where:
Strength = dependent variable
μ = overall mean
N_i = nominal maximum size, i=1, 2
C_j = coarse aggregate type, j= 1, 2
F_k = fine aggregate angularity, k = 1, 2, 3
G_l = gradation, l = 1, 2, 3
R_m = number of gyrations = 1, 2
A_n = AC level = 1, 2, 3, 4, 5
NC_{ij} = interaction of nominal maximum size and coarse aggregate type
NF_{ik} = interaction of nominal maximum size and fine aggregate angularity
NG_{il} = interaction of nominal maximum size and gradation
NR_{im} = interaction of nominal maximum size and number of gyrations
NA_{in} = interaction of nominal maximum size and AC level
CF_{jk} = interaction of coarse aggregate type and fine aggregate angularity
CG_{jl} = interaction of coarse aggregate type and gradation
CR_{jm} = interaction of coarse aggregate type and number of gyrations
CA_{jn} = interaction of coarse aggregate type and AC level
FG_{kl} = interaction of fine aggregate angularity and gradation
FR_{km} = interaction of fine aggregate angularity and number of gyrations
FA_{kn} = interaction of fine aggregate angularity and AC level
GR_{lm} = interaction of gradation and number of gyrations
GA_{ln} = interaction of gradation and AC level
RA_{mn} = interaction of number of gyrations and AC level
ε_{ijklmn} = error term

Results show that coarse aggregate type, fine aggregate angularity, gradation type, number of gyrations, AC level, interaction between nominal maximum aggregate size and coarse aggregate type, interaction between nominal maximum aggregate size and fine aggregate angularity, interaction between nominal maximum aggregate size and number of gyrations, interaction between coarse aggregate type and fine aggregate angularity, interaction between coarse aggregate type and AC level, and interaction between number

of gyrations and AC level all impacted triaxial shear strength significantly at the five percent significant level.

Factor level comparison was conducted on coarse aggregate type, fine aggregate angularity, gradation type, number of gyrations, and AC level using the Student Newman Keuls (SNK) method. The results are summarized in Table 6.4 and details are presented in Appendix E3. Results show that the limestone mixtures exhibited greater strength than the granite mixtures, mixtures with FAA of 44 exhibited greater strength than those with FAA of 50, mixtures with gradations plotting through the restricted zone exhibited greater strength than those with gradations plotting below the restricted zone, mixtures compacted to 152 gyrations ($N_{maximum}$) exhibited greater strength than those compacted to 96 gyrations (N_{design}), and mixtures with AC level 0.5 percent less than the design AC exhibited greater strength than those at the design AC.

Review of Chapter 3 (Superpave mixture design) reveals that the major difference between limestone and granite mixtures compacted in the SGC was the percent Gmm at $N_{initial}$. The percent Gmm at $N_{initial}$ of limestone mixtures was lower than that of granite mixtures. This indicates that the limestone mixtures were more difficult to compact than the granite mixtures and as a result the VMA of limestone mixtures was higher than that of granite mixtures. These facts provide an explanation for the limestone mixtures exhibiting greater strength than the granite mixtures.

The fact that mixtures with FAA of 44 exhibited greater strength than those with FAA of 50 suggests that mixtures incorporating very high FAA did not provide better strength. This also emphasizes that FAA has an important role in characterizing the shear strength of HMA mixtures as would be expected. Again the high FAA (50) mixtures were harsher, thus resulting in higher VMA and Superpave design AC levels ultimately leading to lower triaxial strengths and higher rut depths in PURWheel and APT tests as would be expected with the over-asphalting of the mixtures.

The mixture design data reveal that the major difference between mixtures with gradations plotting through the restricted zone and those with gradations plotting below the restricted zone was VMA. The VMA of mixtures with gradations plotting through the

restricted zone was higher than that of mixtures with gradations plotting below the restricted zone. This fact could provide an explanation for the strength of mixtures with gradations plotting through the restricted zone being higher than that of mixtures with gradations plotting below the restricted zone. It is more likely due to the fact that the contact stresses between particles would be lower in the more densely graded mixtures that plotted through the restricted zone because of the increased quantity of particle-to-particle contacts.

Although factor level comparison indicates that mixtures compacted to 152 gyrations exhibited greater strength than those compacted to 96 gyrations, review of the relationship between triaxial shear strength and AC level (Appendix E2) shows that the strength of mixtures compacted to 152 gyrations declined after a given AC level. The decline in strength was very drastic such that the strength of mixtures compacted to 152 gyrations crossed that of mixtures compacted to 96 gyrations for some mixtures. The AC level where both strengths crossed was identified and measured with respect to the Superpave design AC. The results are summarized in Table 6.5. For ten of nineteen mixtures, the strength after 152 gyrations crossed that of mixtures compacted to 96 gyrations. Preliminary results showed that mixtures compacted to 76 gyrations exhibited lower strengths than those compacted to 96 gyrations (Haddock, et al., 1998). In addition, the strength of mixtures compacted to 76 gyrations did not show sensitivity with AC level changes. These findings suggest that 76 gyrations were inadequate to develop the optimum aggregate structure for the mixtures evaluated. They also suggest that for over half of the mixtures (ten of nineteen) the design level of compaction (N_{design} = 96 gyrations) was inadequate to develop an optimum aggregate structure in terms of shear strength. Of course a balance between durability and shear strength must always be achieved in the mixture design process, so these findings are reasonable. However, they do suggest that the recently adopted new N_{design} table which dictates 50 and 75 (N_{design} and $N_{maximum}$, respectively) for low traffic volumes may be inappropriate for these low volume applications if any of the expected traffic is heavy (trucks) (Brown, et al., 1999 and AASHTO, 1999).

6.5.6. Mixture Properties at Peak Shear Strength (Ndesign)

As previously discussed, mixture shear strength changes over a range of AC. The AC corresponding to peak shear strength is considered to identify the state at which the HMA mixture transforms from the stable to unstable condition. AC level corresponding to peak shear strength was identified with respect to the design AC for all mixtures tested. The results are summarized in Table 6.6. For twelve of nineteen mixtures (65%), the AC level corresponding to the peak shear strength was approximately 0.5 percent less than the Superpave design AC.

VMA values corresponding to the state at which the HMA mixture transforms from the stable to unstable condition could be defined as critical VMA. The VMA levels corresponding to the peak shear strength for mixtures tested in triaxial tests are summarized in Table 6.7. Statistical analysis was conducted on the data and the results are summarized in Table 6.11. The analysis shows that the average VMA corresponding to peak shear strength was 14.5 percent for 19mm mixtures and 16.2 percent for 9.5mm mixtures. These values are slightly higher than the Superpave minimum VMA requirements.

VFA values corresponding to the peak shear strength for mixtures tested in triaxial tests were also identified. The results are summarized in Table 6.8. Statistical analysis was conducted on the data and the results are summarized in Table 6.11. The analysis shows that the average VFA values corresponding to peak shear strength were 66.6 percent for 19mm mixtures and 69.9 percent for 9.5mm mixtures. These values are lower than 75 percent, which is the Superpave upper limit of VFA allowed for traffic less than 1×10^7 ESALs (traffic level for mixture design).

Dust proportion values corresponding to the peak shear strengths for the mixtures were also identified. The results are summarized in Table 6.9. Statistical analysis was conducted on the data and the results are summarized in Table 6.11. The analysis shows that the average dust proportion value corresponding to peak shear strength was 1.2, the minimum value was 1.0, and the maximum value was 1.6 for 19mm mixtures. For 9.5mm mixtures, the average dust proportion value corresponding to peak shear strength was 1.3,

the minimum value was 0.8, and the maximum value was 1.9. All of the values, except the maximum value corresponding to peak shear strength for the 9.5mm mixtures, satisfy the recently recommended dust proportion criteria (Brown et. al, 1999 and AASHTO, 1999).

Film thickness values corresponding to the peak shear strengths are summarized in Table 6.10. Statistical analysis was conducted on the data and the results are summarized in Table 6.11. The analysis shows that the average film thickness corresponding to peak shear strength was 8.1 micron for the 19mm mixtures and 8.2 micron for the 9.5mm mixtures. As previously mentioned, an 8 micron film thickness was also recently recommended by Kandhal (Kandhal et al., 1998).

6.5.7. Relationship Between Triaxial Test Results and VMA

A scatter plot of all triaxial shear strength at 1 percent axial strain and VMA is presented in Figure 6.29. There is clearly no relationship between shear strength and VMA. An effort to select specific limited sets of triaxial test results and their corresponding VMA was made. A first selection was to include the results corresponding to the mixture design AC. This selection procedure is similar to the selection procedure conducted on APT and PURWheel test results. A second selection was to include the results corresponding to peak strengths. However, neither selection procedure resulted in a relationship between triaxial test results and VMA.

Review of the scatter plot reveals that VMA of the 9.5mm mixtures was higher than that of the 19mm mixtures. This observation is consistent with the analysis of VMA and nominal maximum aggregate size relationship in Chapter 3.

6.5.8. Relationship Between Triaxial Test Results and VFA

The relationship between triaxial shear strength at 1 percent axial strain and VFA is presented in Figure 6.30. Regression analysis revealed a very poor relationship between triaxial test results and VFA. It is quadratic with a negative second order parameter. Details of the regression analysis are presented in Appendix E3. The r^2 value is very small due (0.18) to the scattered data. The basic trend is reasonable however because triaxial shear strength decreased as VFA increased. The parameter estimates indicate that the triaxial shear strength corresponding to VFA of 75 percent was approximately 1210 kPa (175 psi). The VFA value of 75 is corresponding to the upper limit of VFA for the design traffic (less than 10 million ESALs).

6.5.9. Relationship Between Triaxial Test Results and Dust Proportion

A scatter plot of triaxial test results and dust proportion is presented in Figure 6.31. Although the data were scattered, there is an indication that the triaxial shear strength increased as the dust proportion increased. An attempt to select specific limited triaxial test results and their corresponding dust proportions was made. A first selection was to include the results corresponding to the mixture design AC. This selection procedure is similar to the selection procedure conducted on APT and PURWheel test results. A second selection was to include the results corresponding to peak strengths. However, neither selection procedures revealed a better relationship between triaxial test results and dust proportion.

6.5.10. Relationship Between Triaxial Test Results and Film Thickness

The relationship between triaxial test results and film thickness is presented in Figure 6.32. Regression analysis revealed a weak relationship between triaxial test results and film thickness that is quadratic with a positive second order parameter. Details of regression analysis are presented in Appendix E3. The r^2 value is low (0.35) due to the scattered data, but the basic trend is reasonable because the triaxial shear strength

decreased as film thickness increased. The parameter estimates indicate that the triaxial shear strength corresponding to a film thickness of 8 microns was approximately 1170 kPa (170 psi). This shear strength value is very close to the shear strength value established by the VFA value of 75 percent. The film thickness value of 8 micron is the value corresponding to the peak shear strength as was discussed in Section 6.5.6.

6.5.11. Effect of Gradation Type on Triaxial Test Results

The effect of gradation type on triaxial test results is depicted by a plot of selected triaxial shear strengths and gradations with respect to the restricted zone as shown in Figure 6.33. As previously stated, the triaxial tests were conducted over 5 levels of AC and 3 levels of compaction (numbers of gyration). The triaxial shear strength used to evaluate the effect of gradation type was the peak shear strength and it was selected for mixtures compacted to 96 gyrations (N_{design}). The purpose of the selection was to minimize the effects of AC level and number of gyrations on the analysis. Preliminary study indicates that the mixtures with gradations plotting above the restricted zone exhibited greatest shear strength than those with gradations plotting through or below the restricted zone (Haddock, et al., 1998). Analysis in Section 6.5.5 indicated that the mixtures with gradations plotting through the restricted zone exhibited greater shear strengths than those with gradations plotting below the restricted zone. Review of Figure 6.33 reveals that the peak strength of mixtures compacted to N_{design} gyrations was scattered when it was plotted with respect to the restricted zone. This suggests that the restricted zone alone may not be adequate to characterize mixture gradation in triaxial tests.

Table 6.1 Mixtures Tested in Triaxial (5 AC level).

FAA	Gradation	No. of Gyration	9.5 mm Nominal Max. Size		19 mm Nominal Max. Size	
			Limestone	Granite	Limestone	Granite
39	Above					
	Below					
44	Above	76	XXXXX		XXXXX	
		96	XXXXX		XXXXX	
		152	XXXXX		XXXXX	
	Through	76	XXXXX		XXXXX	
		96	XXXXX	XXXXX	XXXXX	XXXXX
		152	XXXXX	XXXXX	XXXXX	XXXXX
	Below	76	XXXXX		XXXXX	
		96	XXXXX	XXXXX	XXXXX	XXXXX
		152	XXXXX	XXXXX	XXXXX	XXXXX
50	Above	96			XXXXX	
		152			XXXXX	
	Through	96	XXXXX	XXXXX	XXXXX	XXXXX
		152	XXXXX	XXXXX	XXXXX	XXXXX
	Below	96	XXXXX	XXXXX	XXXXX	XXXXX
		152	XXXXX	XXXXX	XXXXX	XXXXX

Note: one X represents two samples tested at one AC level.

Table 6.2 Triaxial Experiment Layout for ANOVA.

FAA	Gradation	Gyration	Replicates	9.5 mm Nominal Max. Size										19 mm Nominal Max. Size									
				Limestone					Granite					Limestone					Granite				
				AC level					AC level					AC level					AC level				
				1	2	3	4	5	1	2	3	4	5	1	2	3	4	5	1	2	3	4	5
44	Through	96	1	X	X	X	X	X	X	X	X	X	X	X	X	X	X	X	X	X	X	X	X
			2	X	X	X	X	X	X	X	X	X	X	X	X	X	X	X	X	X	X	X	X
		152	1	X	X	X	X	X	X	X	X	X	X	X	X	X	X	X	X	X	X	X	X
			2	X	X	X	X	X	X	X	X	X	X	X	X	X	X	X	X	X	X	X	X
	Below	96	1	X	X	X	X	X	X	X	X	X	X	X	X	X	X	X	X	X	X	X	X
			2	X	X	X	X	X	X	X	X	X	X	X	X	X	X	X	X	X	X	X	X
		152	1	X	X	X	X	X	X	X	X	X	X	X	X	X	X	X	X	X	X	X	X
			2	X	X	X	X	X	X	X	X	X	X	X	X	X	X	X	X	X	X	X	X
50	Through	96	1	X	X	X	X	X	X	X	X	X	X	X	X	X	X	X	X	X	X	X	X
			2	X	X	X	X	X	X	X	X	X	X	X	X	X	X	X	X	X	X	X	X
		152	1	X	X	X	X	X	X	X	X	X	X	X	X	X	X	X	X	X	X	X	X
			2	X	X	X	X	X	X	X	X	X	X	X	X	X	X	X	X	X	X	X	X
	Below	96	1	X	X	X	X	X	X	X	X	X	X	X	X	X	X	X	X	X	X	X	X
			2	X	X	X	X	X	X	X	X	X	X	X	X	X	X	X	X	X	X	X	X
		152	1	X	X	X	X	X	X	X	X	X	X	X	X	X	X	X	X	X	X	X	X
			2	X	X	X	X	X	X	X	X	X	X	X	X	X	X	X	X	X	X	X	X

Table 6.3 Summary of ANOVA for Factor Effects on Triaxial Test Results.

Variable	Significance	p value
Nominal Maximum Size	No	0.1693
Coarse Aggregate Type	Yes	0.0001
Fine Aggregate Angularity	Yes	0.0001
Gradation with Respect to The Restricted Zone	Yes	0.0001
Number of Gyrations	Yes	0.0001
AC level	Yes	0.0001
Nominal Max. Size * Coarse Aggregate Type	Yes	0.0074
Nominal Max. Size * Fine Aggregate Angularity	Yes	0.0001
Nominal Max. Size * Gradation	No	0.3139
Nominal Max. Size * Gyrations	Yes	0.0376
Nominal Max. Size * AC level	No	0.2922
Coarse Agg. Type * Fine Aggregate Angularity	Yes	0.0001
Coarse Agg. Type * Gradation	No	0.5835
Coarse Agg. Type * Gyrations	No	0.8594
Coarse Agg. Type * AC level	Yes	0.0001
Fine Aggregate Angularity * Gradation	No	0.0705
Fine Aggregate Angularity * Gyrations	No	0.1475
Fine Aggregate Angularity * AC level	No	0.0665
Gradation * Gyrations	No	0.4308
Gradation * AC level	No	0.6986
Gyration * AC level	Yes	0.0001

note: p values are based on Type III Sum of Squares

Table 6.4 Summary of SNK for Main Factor Means of Triaxial Test Results.

Variable	Results
Nominal Maximum Size	19mm = 9.5mm
Coarse Aggregate Type	Limestone > Granite
Fine Aggregate Angularity	44 > 50
Gradation	Through > Below
No. of Gyrations	152 > 96
AC Level	1=2>3>4>5

Table 6.5 Location of AC Corresponding to Crossing of $N_{maximum}$ and N_{design} Triaxial Peak Strengths.

FAA	Gradation	9.5 mm Nominal Max. Size		19 mm Nominal Max. Size	
		Limestone	Granite	Limestone	Granite
39	Above				
	Below				
44	Above	+0.7		+0.7	
	Through	+0.5	+0.7	+0.0	-1.0
	Below	-0.5	N/A	N/A	-0.5
50	Above			N/A	
	Through	N/A	N/A	-0.1	N/A
	Below	+1.0	N/A	N/A	N/A

Note: the location of AC is relative to the design AC. N/A means the $N_{maximum}$ and N_{design} Triaxial Peak Strength did not cross the other.

Table 6.6 Location of AC Corresponding to Triaxial Peak Strengths at N_{design}

FAA	Gradation	9.5 mm Nominal Max. Size		19 mm Nominal Max. Size	
		Limestone	Granite	Limestone	Granite
39	Above				
	Below				
44	Above	-0.5		+0.0	
	Through	-0.5	-0.5	+0.0	-0.5
	Below	+0.0	+0.0	-0.5	+0.0
50	Above			-0.5	
	Through	-0.5	-0.5	+0.0	-0.5
	Below	+0.0	-0.5	-0.5	-0.5

Note: the location of AC is relative to the design AC.

Table 6.7 VMA Values Corresponding to Triaxial Peak Strengths.

FAA	Gradation	9.5 mm Nominal Max. Size		19 mm Nominal Max. Size	
		Limestone	Granite	Limestone	Granite
39	Above				
	Below				
44	Above	16.7		14.25	
	Through	15.3	18.3	14.0	16.0
	Below	15.6	15.8	12.2	13.9
50	Above			14.8	
	Through	16.8	15.4	15.3	16.0
	Below	16.7	15.0	13.5	15.0

Table 6.8 VFA Values Corresponding to Triaxial Peak Strengths.

FAA	Gradation	9.5 mm Nominal Max. Size		19 mm Nominal Max. Size	
		Limestone	Granite	Limestone	Granite
39	Above				
	Below				
44	Above	58.7		61.0	
	Through	78.4	54.1	77.8	50.5
	Below	83.0	63.5	63.0	65.0
50	Above			72.0	
	Through	72.0	70.5	85.0	59.0
	Below	81.0	68.0	72.5	60.6

Table 6.9 Dust Proportion Values Corresponding to Triaxial Peak Strengths.

FAA	Gradation	9.5 mm Nominal Max. Size		19 mm Nominal Max. Size	
		Limestone	Granite	Limestone	Granite
39	Above				
	Below				
44	Above	1.90		1.61	
	Through	1.02	1.42	1.00	1.16
	Below	0.75	1.08	1.34	1.07
50	Above			1.52	
	Through	1.32	1.58	1.04	1.33
	Below	1.04	1.39	1.03	1.15

Table 6.10 Film Thickness Values Corresponding to Triaxial Peak Strengths.

FAA	Gradation	9.5 mm Nominal Max. Size		19 mm Nominal Max. Size	
		Limestone	Granite	Limestone	Granite
39	Above				
	Below				
44	Above	5.16		5.88	
	Through	8.61	6.50	8.62	7.28
	Below	11.85	8.49	7.40	8.84
50	Above			6.91	
	Through	8.97	6.61	10.12	7.71
	Below	9.92	7.34	10.04	8.53

Table 6.11 Summary of Material Properties Corresponding to Peak Triaxial Shear Strengths.

Nominal Maximum Size (mm)	Mixture Property	Average	Standard Deviation	COV (%)	Min.	Max.
19	VMA (%)	14.5	1.2	8.1	12.2	16.0
	VFA (%)	66.6	10.2	15.2	50.5	85.0
	Dust Proportion	1.2	0.2	17.6	1.0	1.6
	Film Thickness (μm)	8.1	1.4	16.6	5.9	10.1
9.5	VMA (%)	16.2	1.0	6.4	15.0	18.3
	VFA (%)	69.9	9.9	14.2	54.1	83.0
	Dust Proportion	1.3	0.3	27.0	0.8	1.9
	Film Thickness (μm)	8.2	2.0	24.7	5.2	11.9

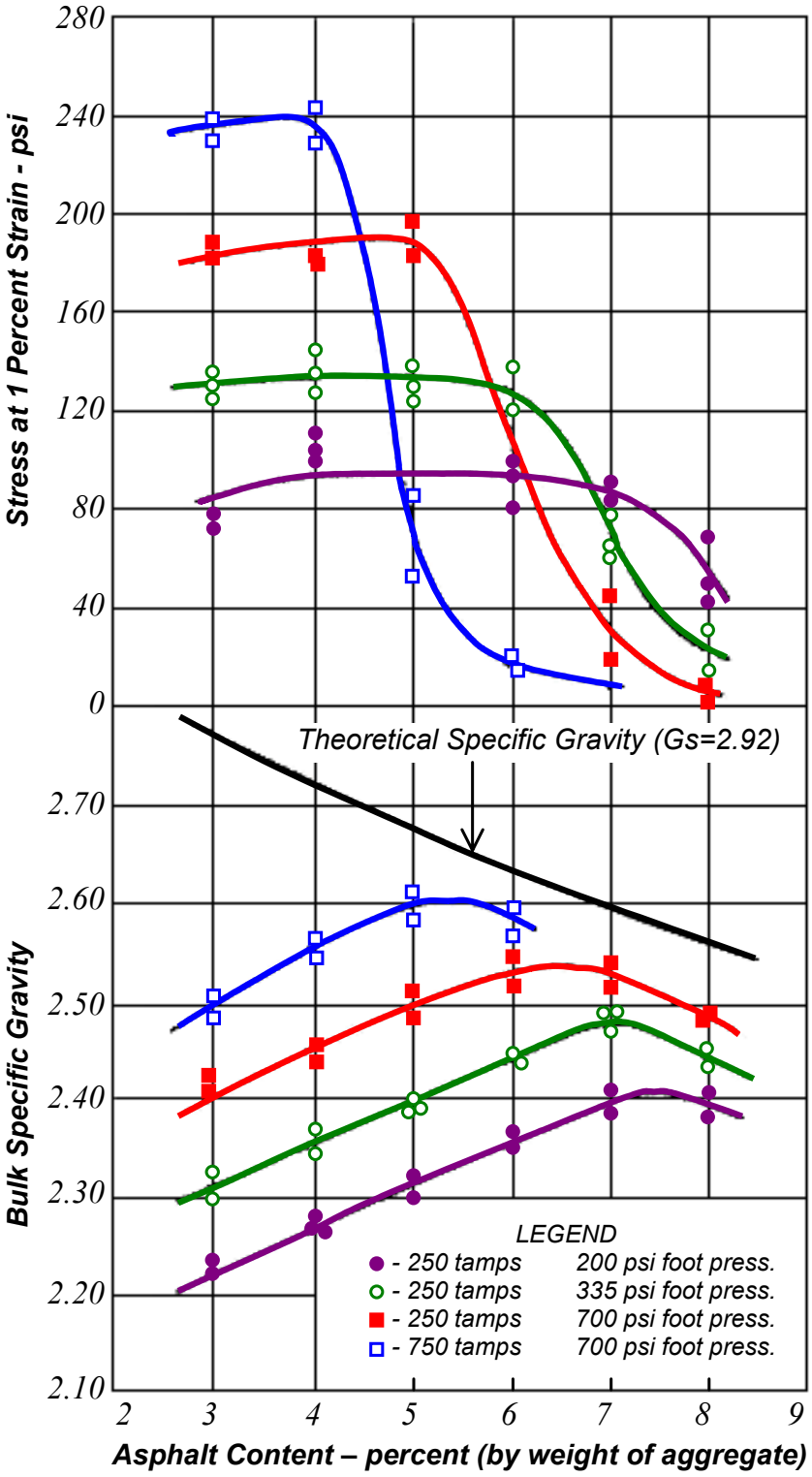

Figure 6.1 Monismith and Vallerga Triaxial Test Results (1956).

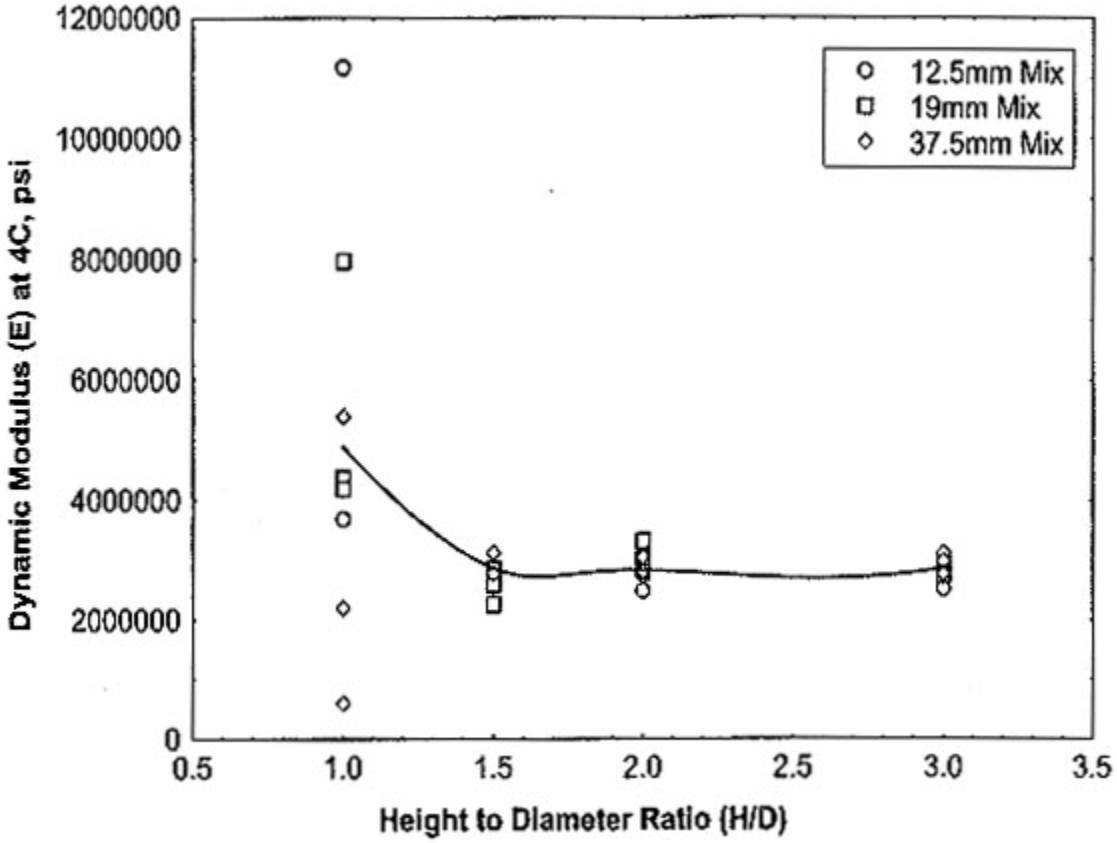

Figure 6.2 Effect of Height to Diameter Ratio (Witczak, et al., 2000).

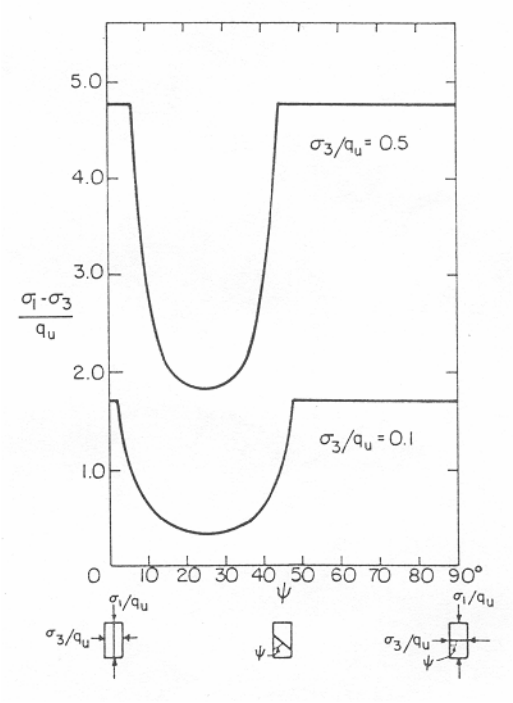

Figure 6.3 Effect of Discontinuity Plane Orientation on Strength Measurements (Goodman, 1976).

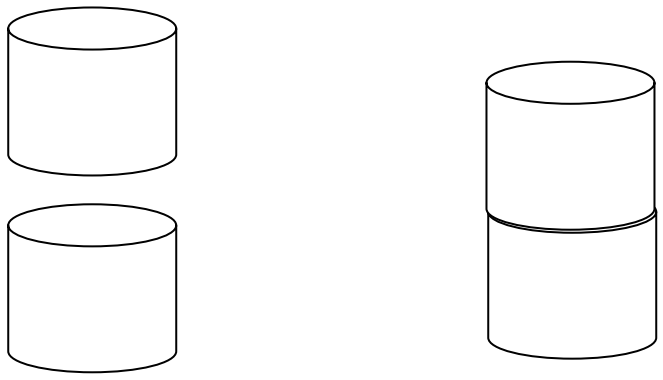

Figure 6.4 Stacking of Two SGC Samples.

Figure 6.5 Triaxial Test Specimen.

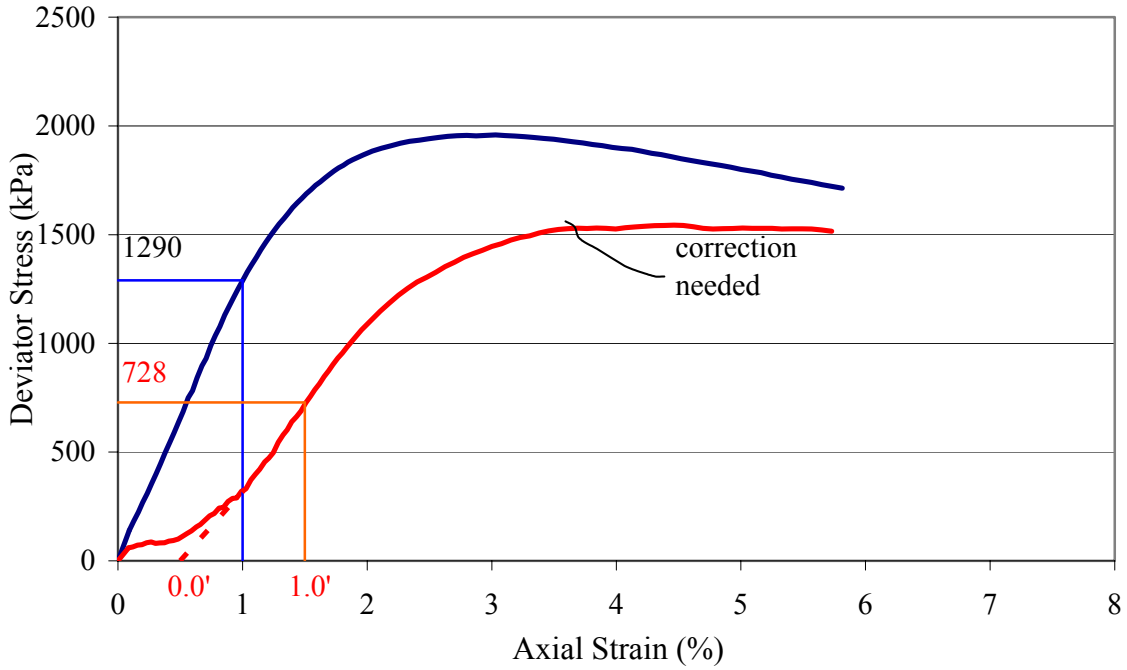

Figure 6.6 Typical Triaxial Test Result.

Figure 6.7 Observed Failure Planes for Different Height to Diameter Ratios.

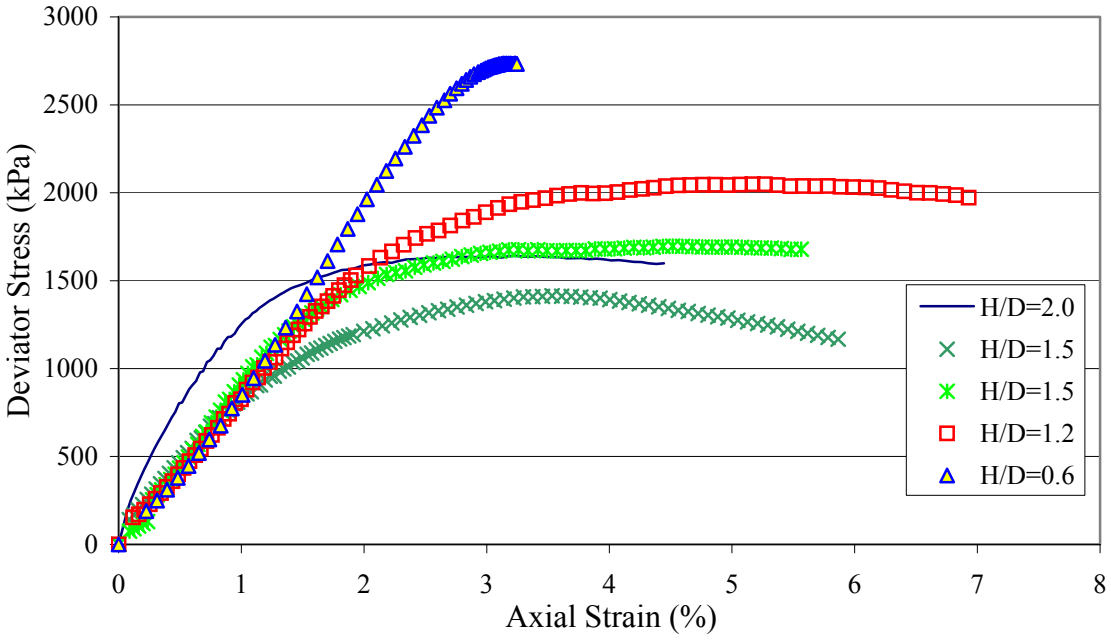

Figure 6.8 Effect of Height to Diameter Ratio on 19mm Granite with FAA of 44 and Gradations Plotting Below the Restricted Zone Mixtures.

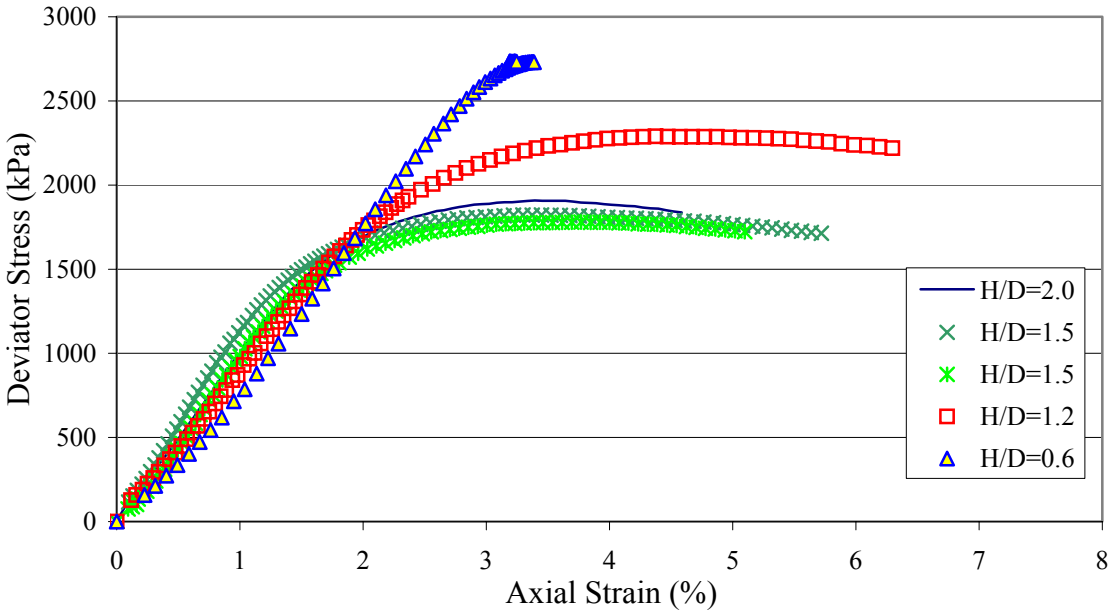

Figure 6.9 Effect of Height to Diameter Ratio on 9.5mm Granite with FAA of 44 and Gradations Plotting Below the Restricted Zone Mixtures.

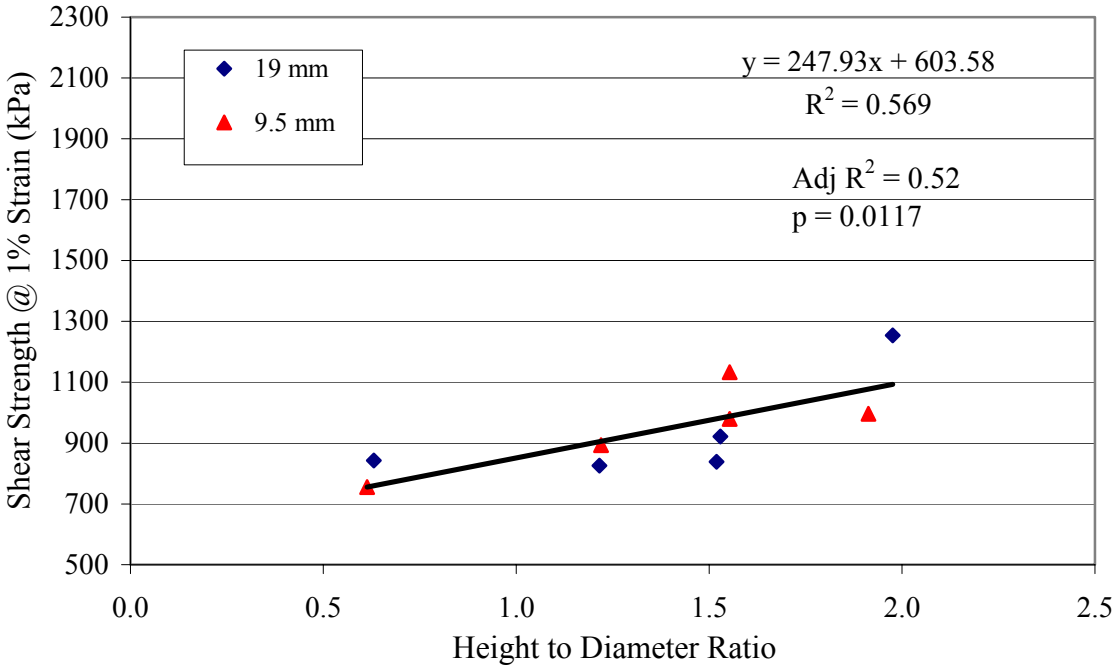

Figure 6.10 Effect of Height to Diameter Ratio on Triaxial Shear Strength.

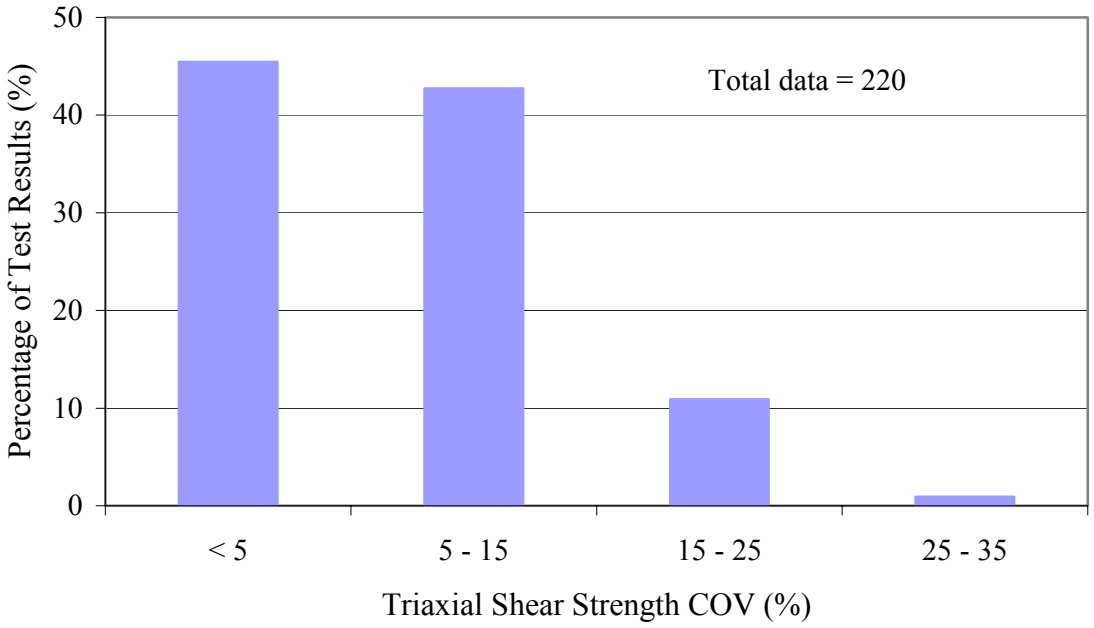

Figure 6.11 Variability Associated with Triaxial Test Results.

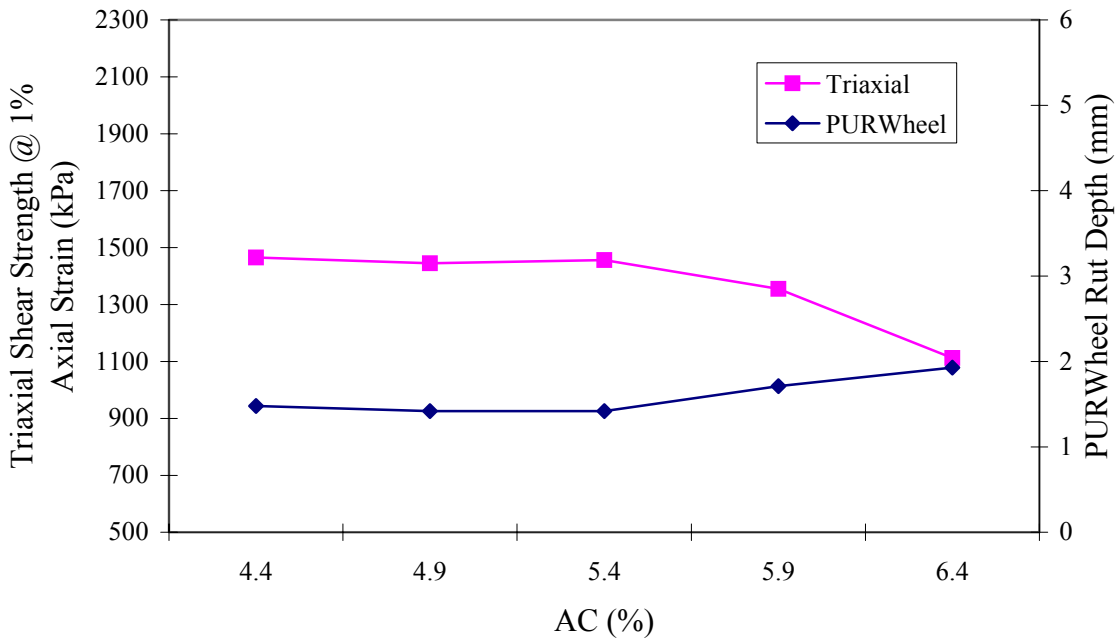

Figure 6.12 Triaxial Shear Strength and PURWheel Rut Depth of 19mm Limestone with FAA of 44 and Gradation Plotting Through the Restricted Zone Mixture.

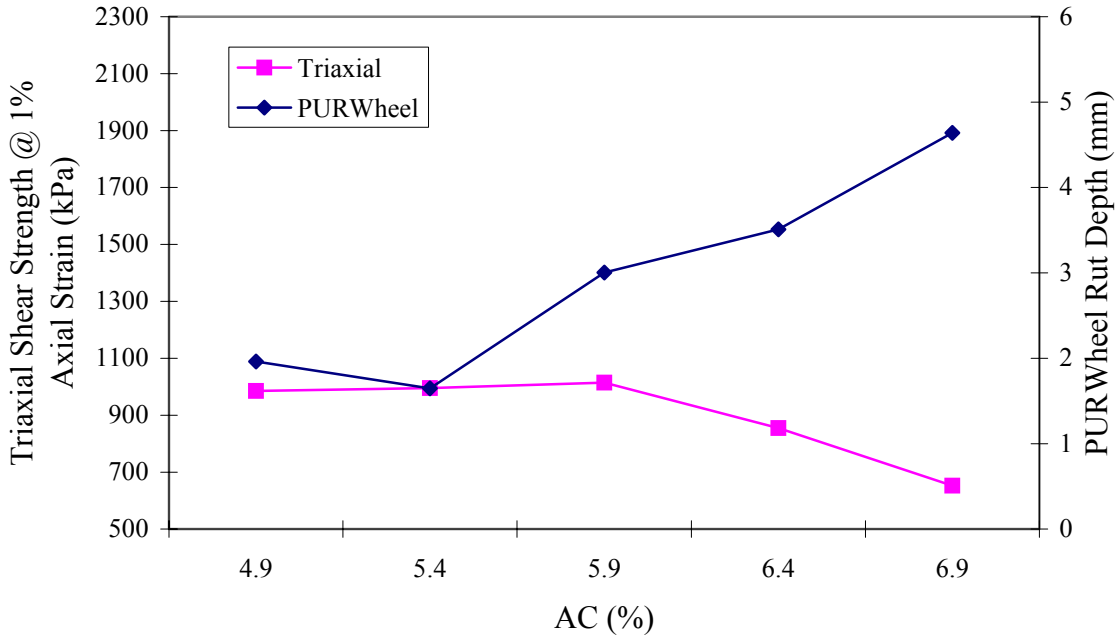

Figure 6.13 Triaxial Shear Strength and PURWheel Rut Depth of 19mm Limestone with FAA of 50 and Gradation Plotting Through the Restricted Zone Mixture.

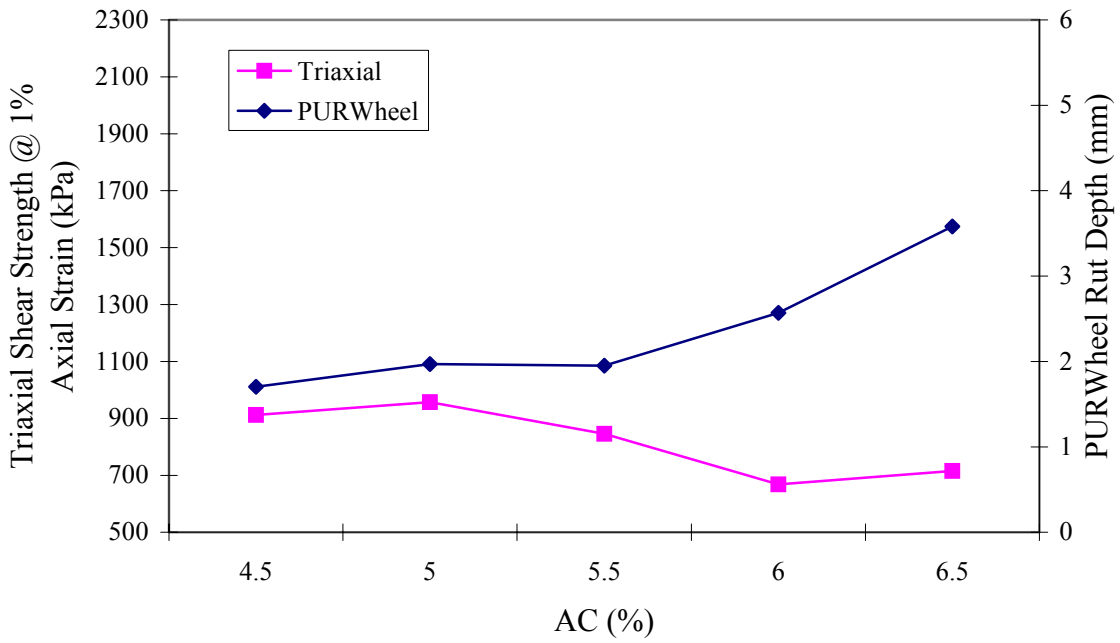

Figure 6.14 Triaxial Shear Strength and PURWheel Rut Depth of 19mm Limestone with FAA of 50 and Gradation Plotting Below the Restricted Zone Mixture.

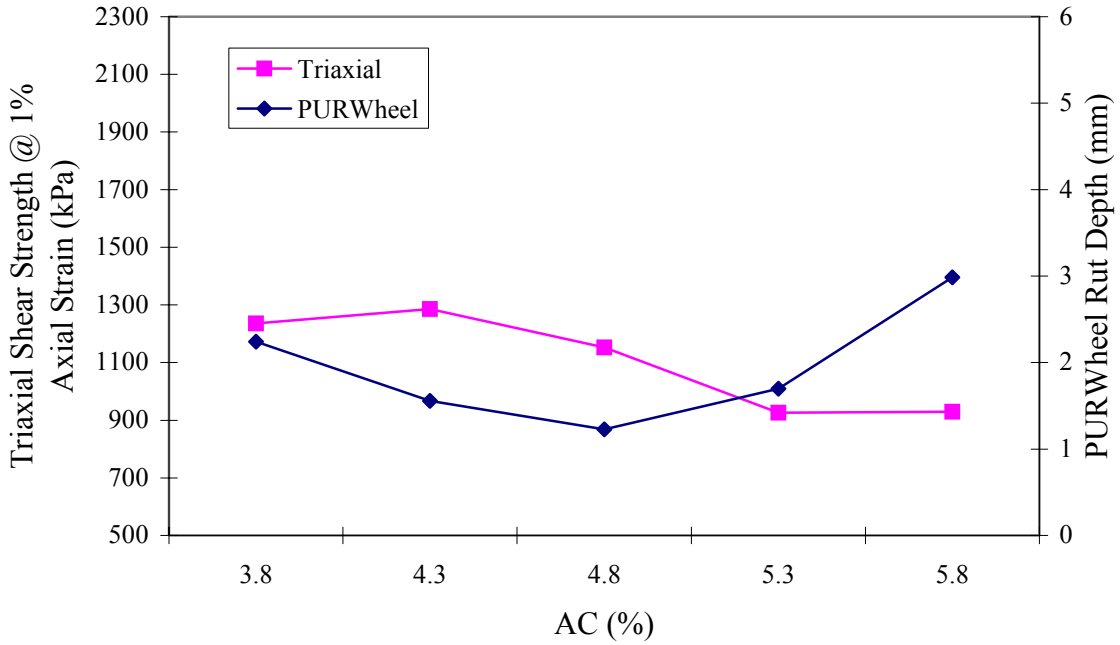

Figure 6.15 Triaxial Shear Strength and PURWheel Rut Depth of 19mm Granite with FAA of 44 and Gradation Plotting Through the Restricted Zone Mixture.

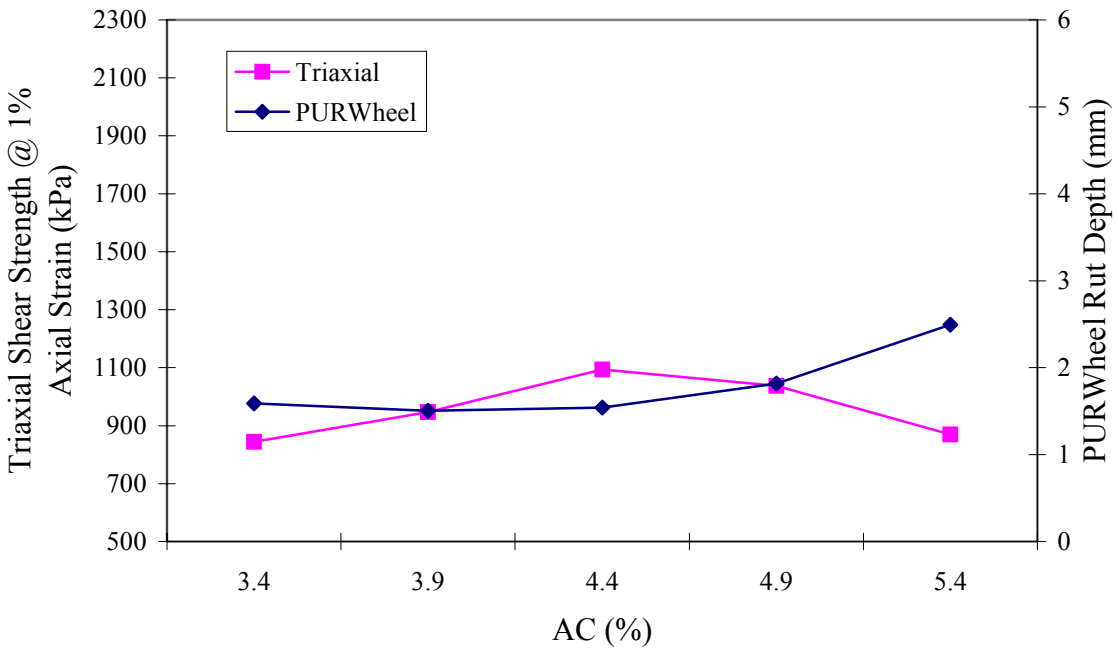

Figure 6.16 Triaxial Shear Strength and PURWheel Rut Depth of 19mm Granite with FAA of 44 and Gradation Plotting Below the Restricted Zone Mixture.

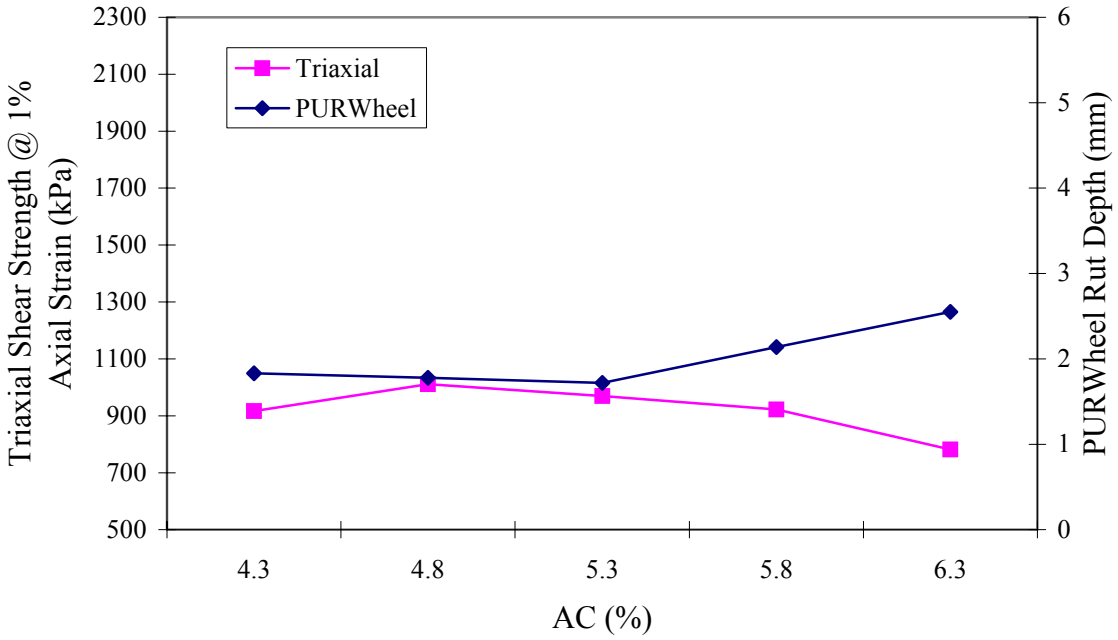

Figure 6.17 Triaxial Shear Strength and PURWheel Rut Depth of 19mm Granite with FAA of 50 and Gradation Plotting Through the Restricted Zone Mixture.

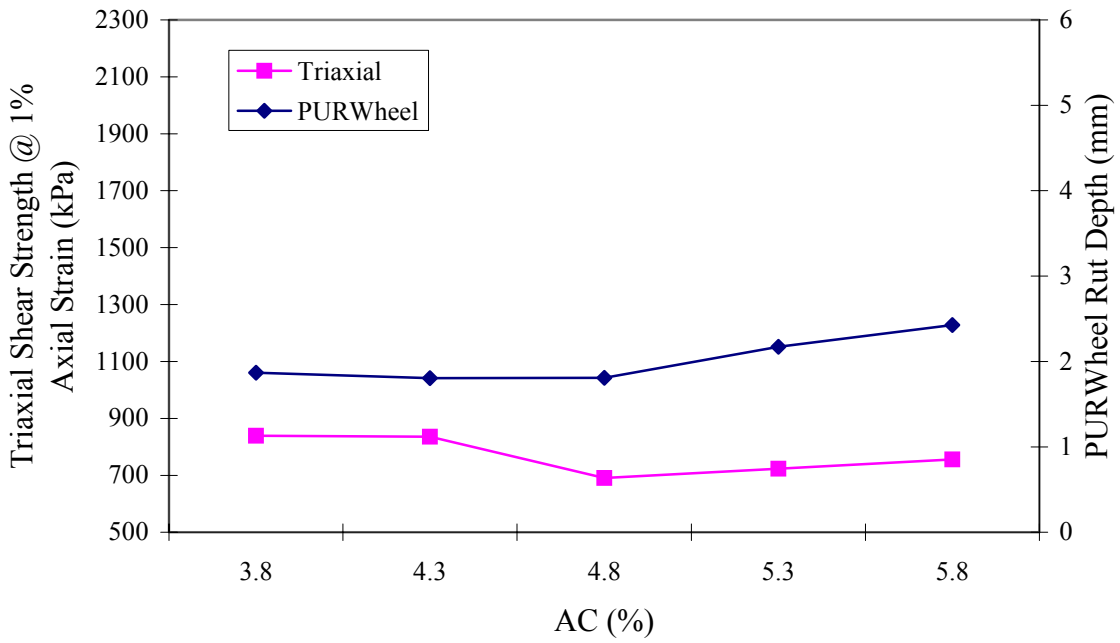

Figure 6.18 Triaxial Shear Strength and PURWheel Rut Depth of 19mm Granite with FAA of 50 and Gradation Plotting Below the Restricted Zone Mixture.

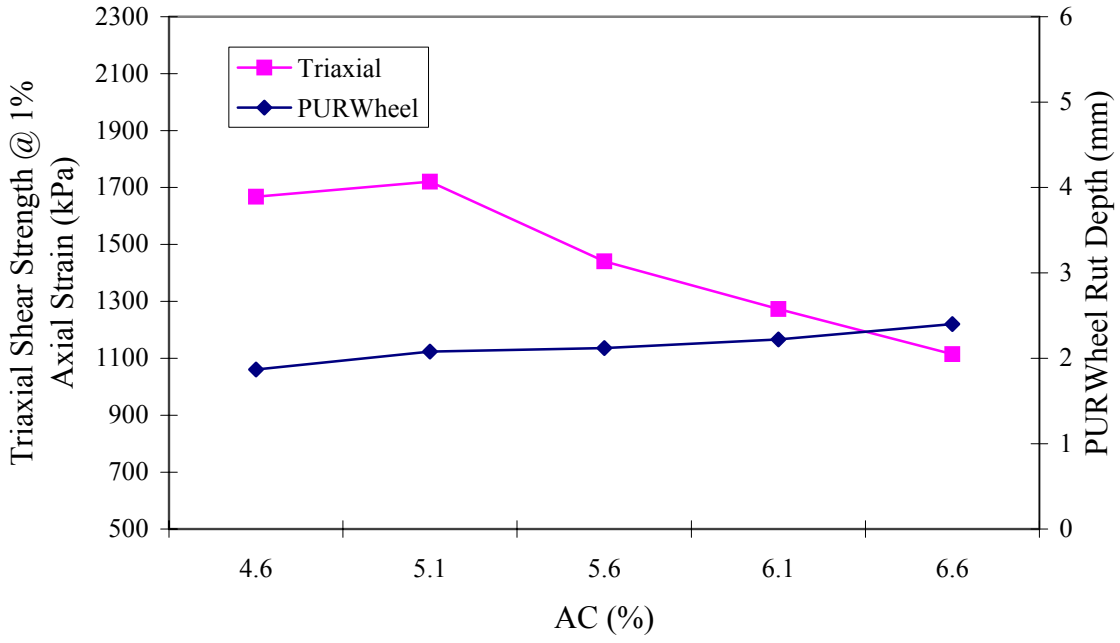

Figure 6.19 Triaxial Shear Strength and PURWheel Rut Depth of 9.5mm Limestone with FAA of 44 and Gradation Plotting Above the Restricted Zone Mixture.

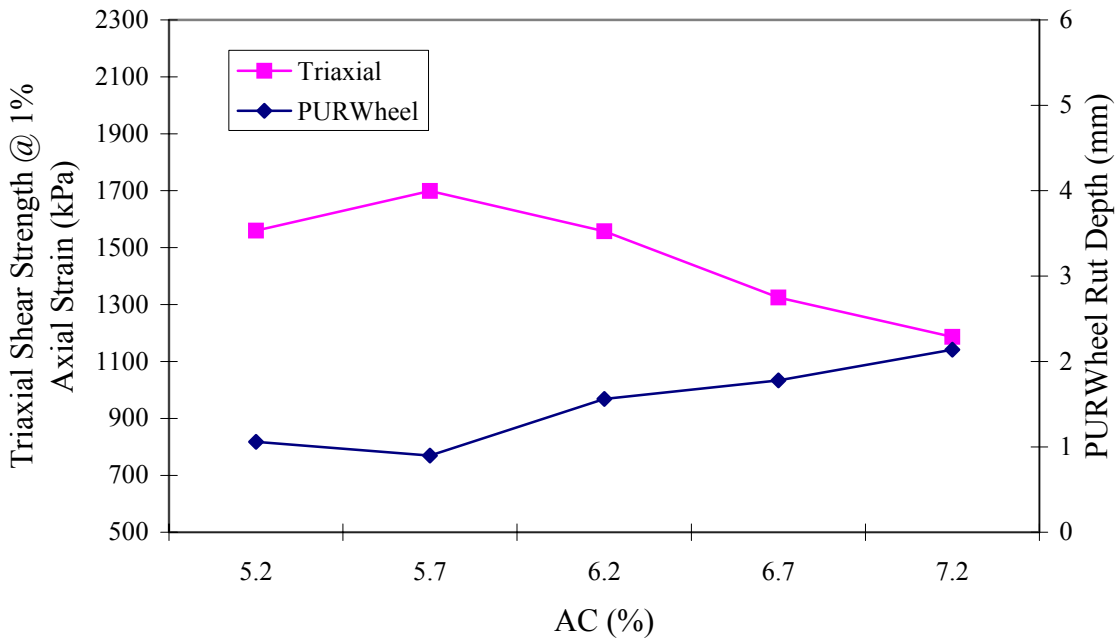

Figure 6.20 Triaxial Shear Strength and PURWheel Rut Depth of 9.5mm Limestone with FAA of 44 and Gradation Plotting Through the Restricted Zone Mixture.

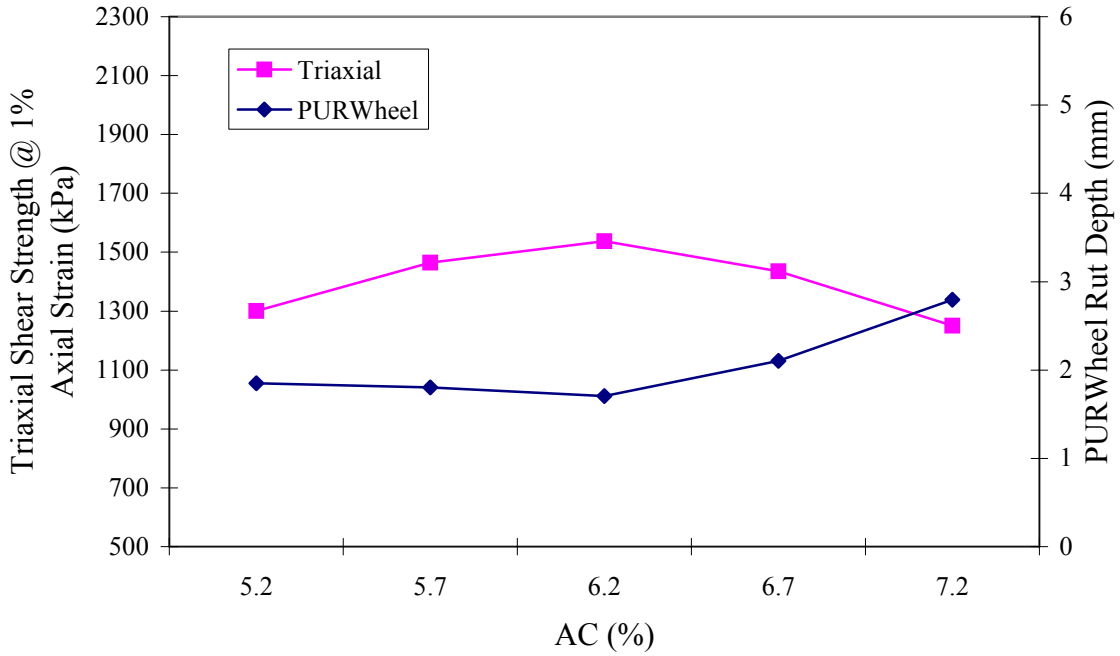

Figure 6.21 Triaxial Shear Strength and PURWheel Rut Depth of 9.5mm Limestone with FAA of 44 and Gradation Plotting Below the Restricted Zone Mixture.

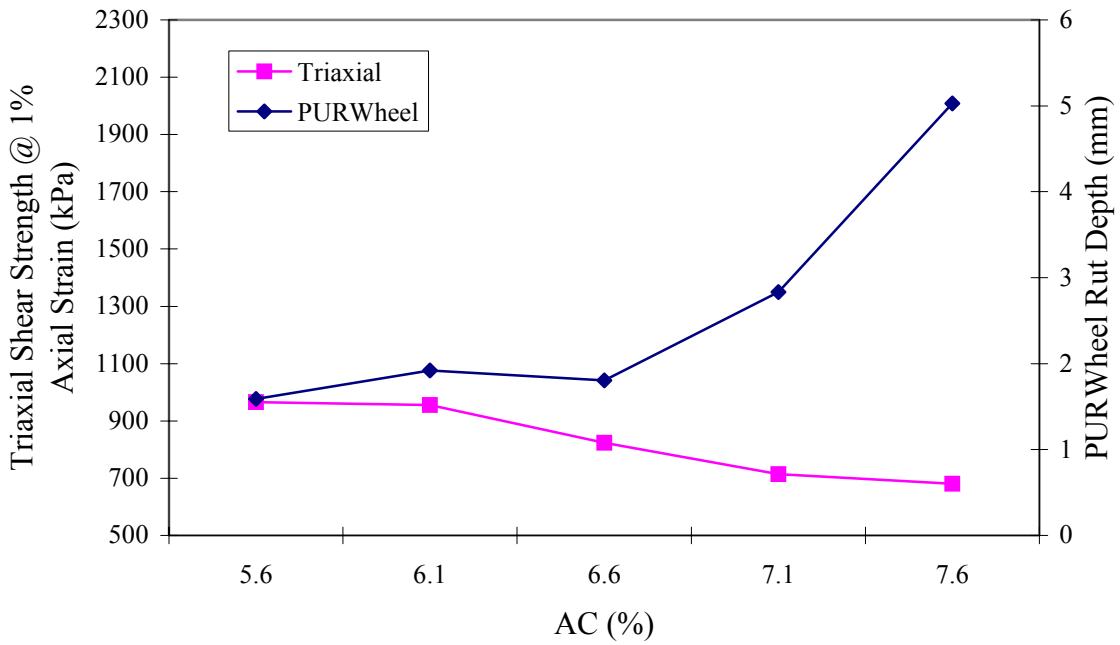

Figure 6.22 Triaxial Shear Strength and PURWheel Rut Depth of 9.5mm Limestone with FAA of 50 and Gradation Plotting Through the Restricted Zone Mixture.

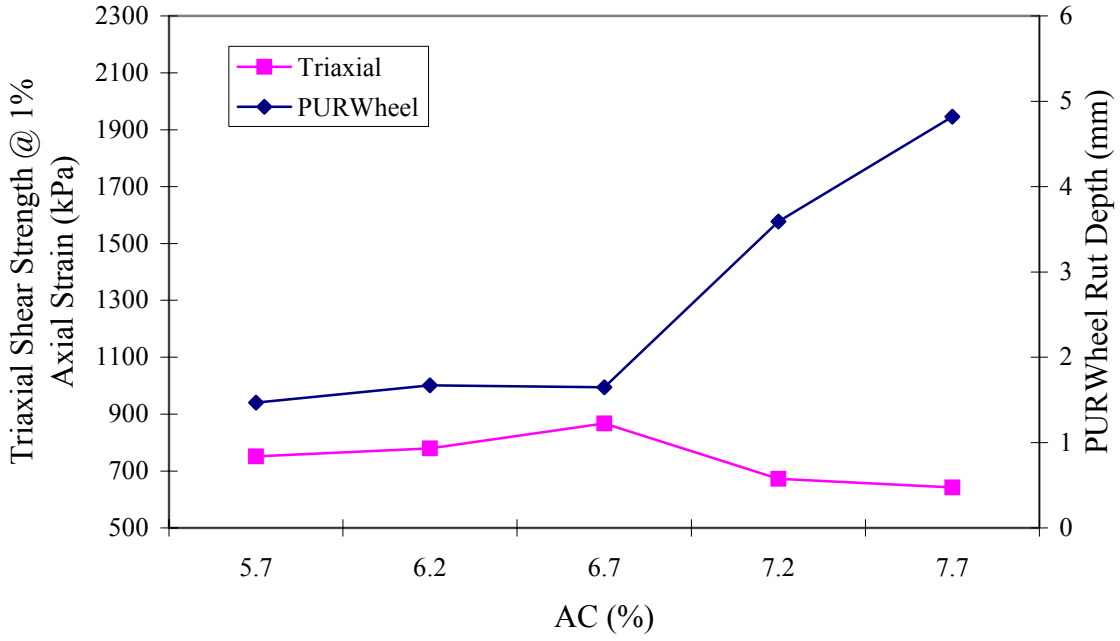

Figure 6.23 Triaxial Shear Strength and PURWheel Rut Depth of 9.5mm Limestone with FAA of 50 and Gradation Plotting Below the Restricted Zone Mixture.

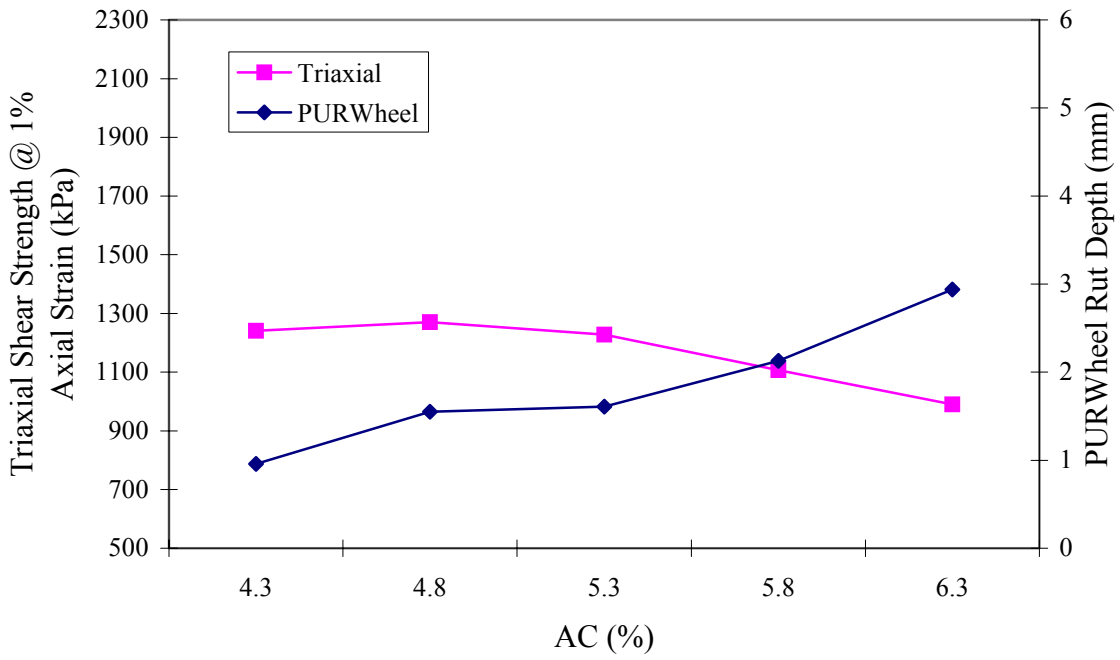

Figure 6.24 Triaxial Shear Strength and PURWheel Rut Depth of 9.5mm Granite with FAA of 44 and Gradation Plotting Through the Restricted Zone Mixture.

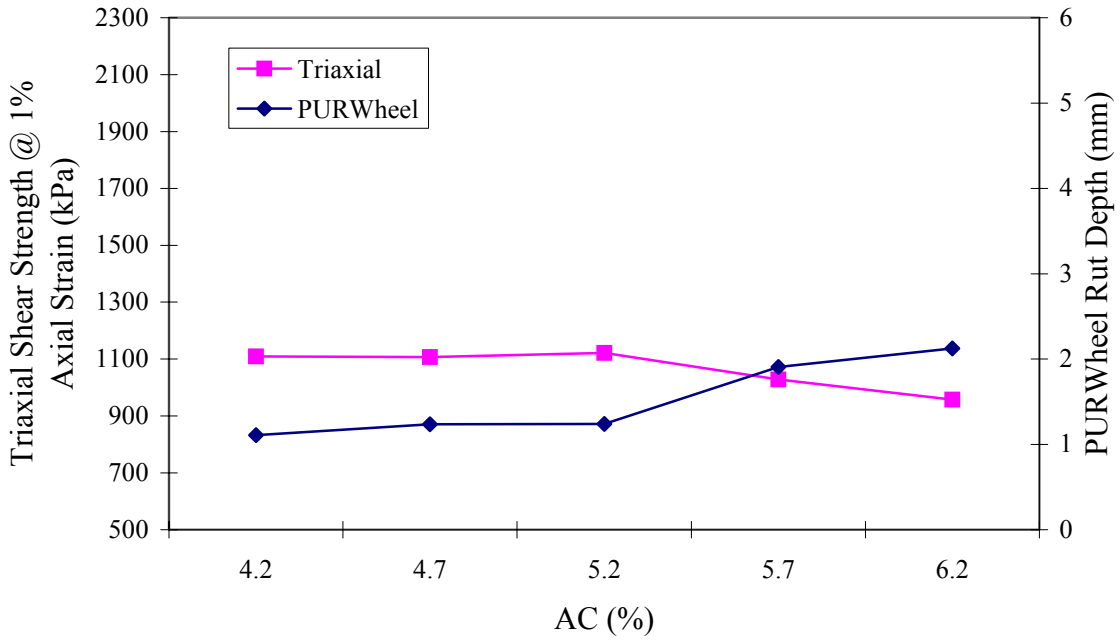

Figure 6.25 Triaxial Shear Strength and PURWheel Rut Depth of 9.5mm Granite with FAA of 44 and Gradation Plotting Below the Restricted Zone Mixture.

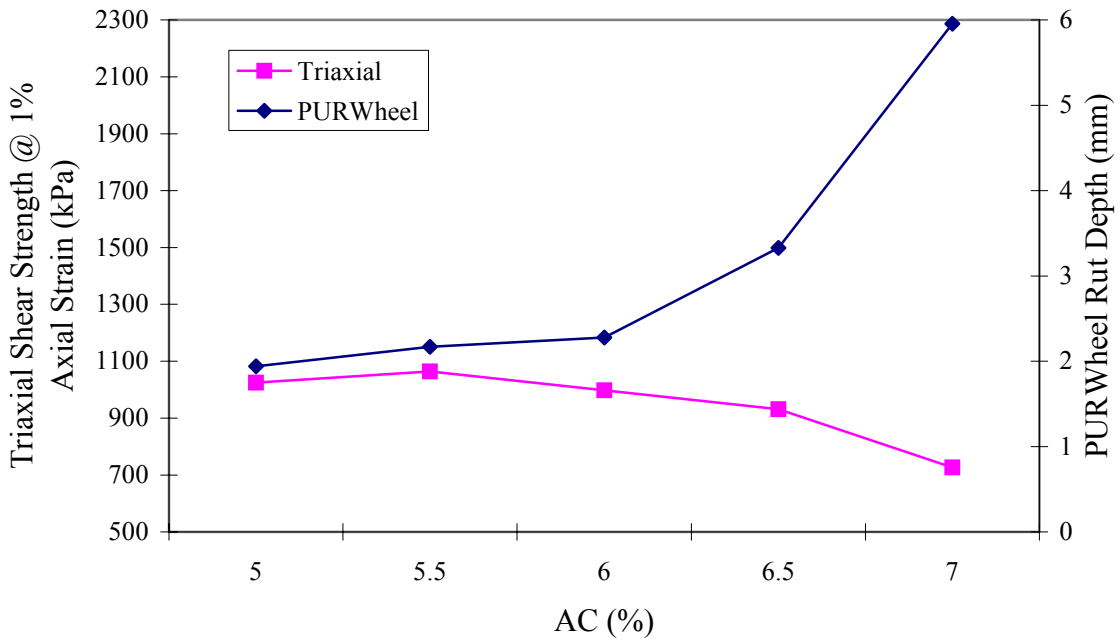

Figure 6.26 Triaxial Shear Strength and PURWheel Rut Depth of 9.5mm Granite with FAA of 50 and Gradation Plotting Through the Restricted Zone Mixture.

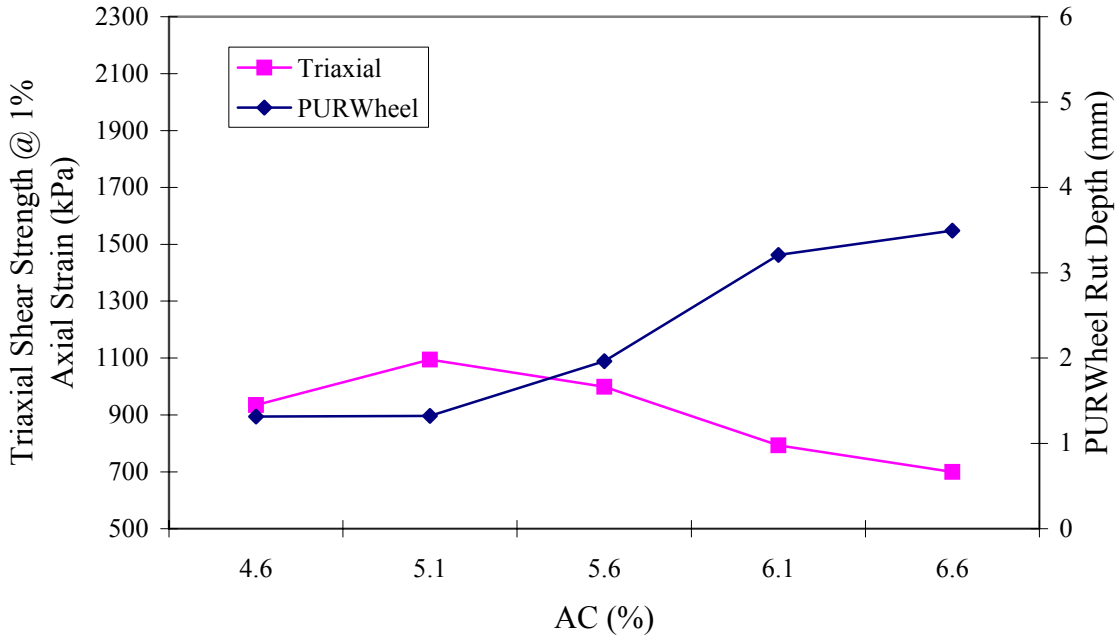

Figure 6.27 Triaxial Shear Strength and PURWheel Rut Depth of 9.5mm Granite with FAA of 50 and Gradation Plotting Below the Restricted Zone Mixture.

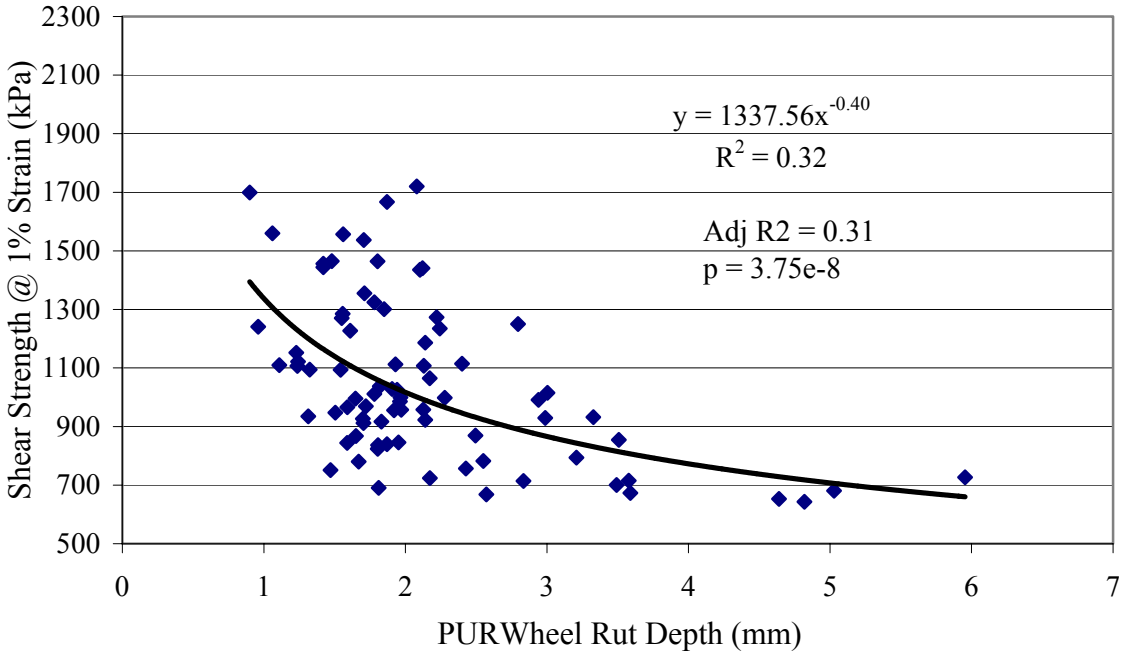

Figure 6.28 Correlation Between Triaxial Shear Strength and PURWheel Rut Depth.

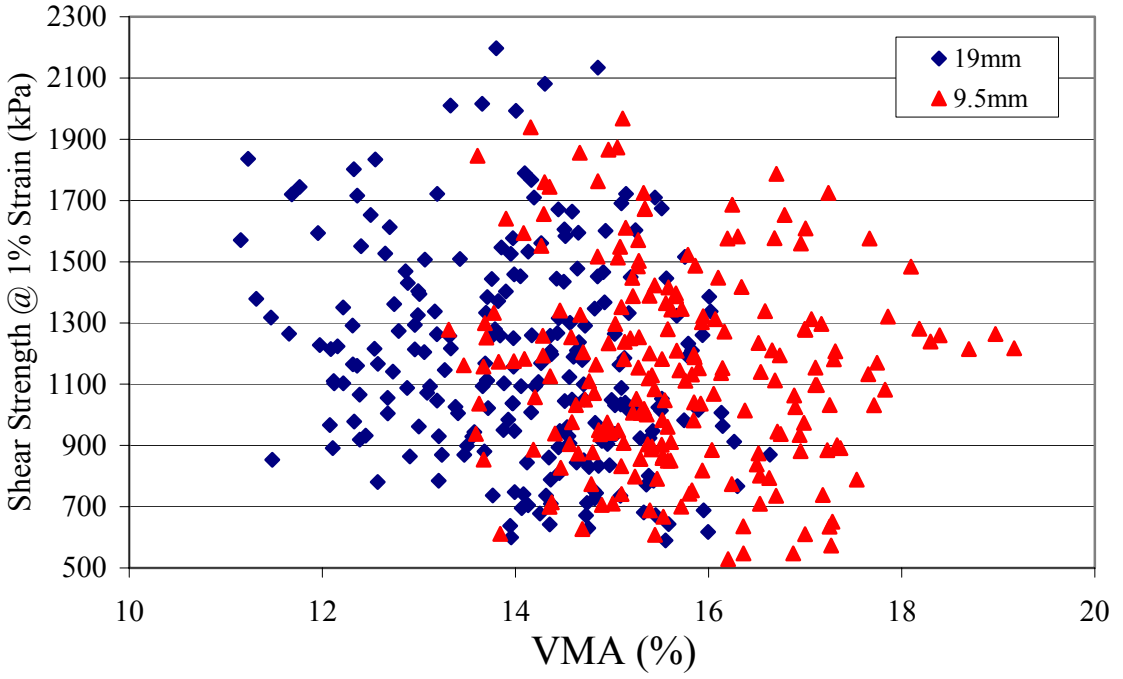

Figure 6.29 Scatter Plot of Triaxial Test Results and VMA.

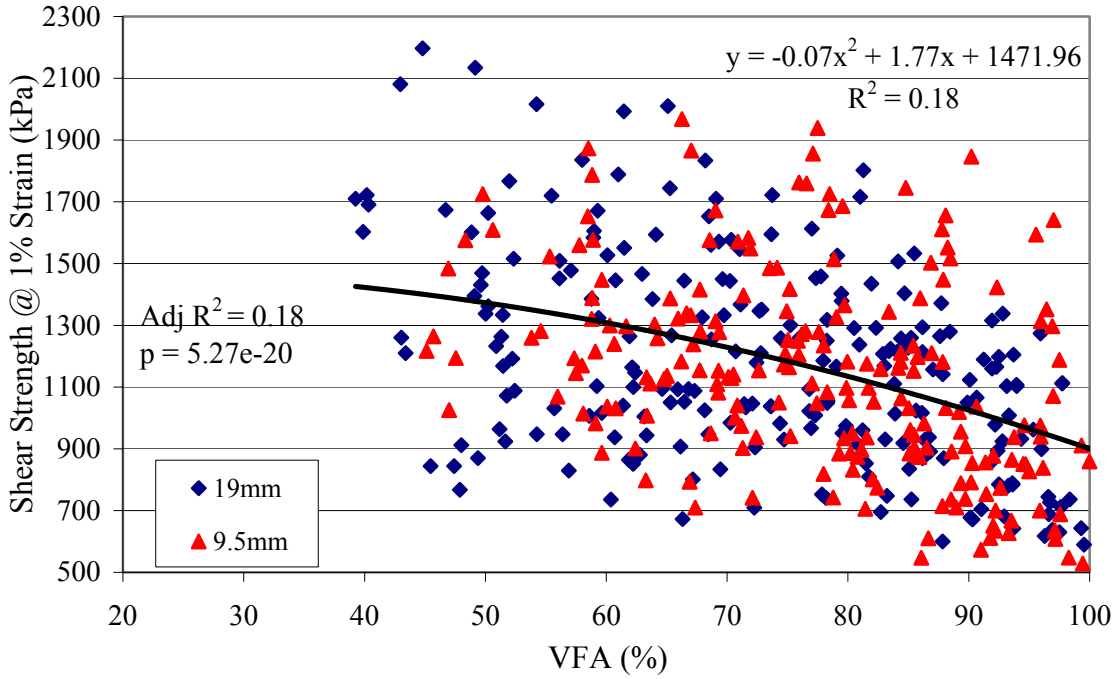

Figure 6.30 Scatter Plot of Triaxial Test Results and VFA.

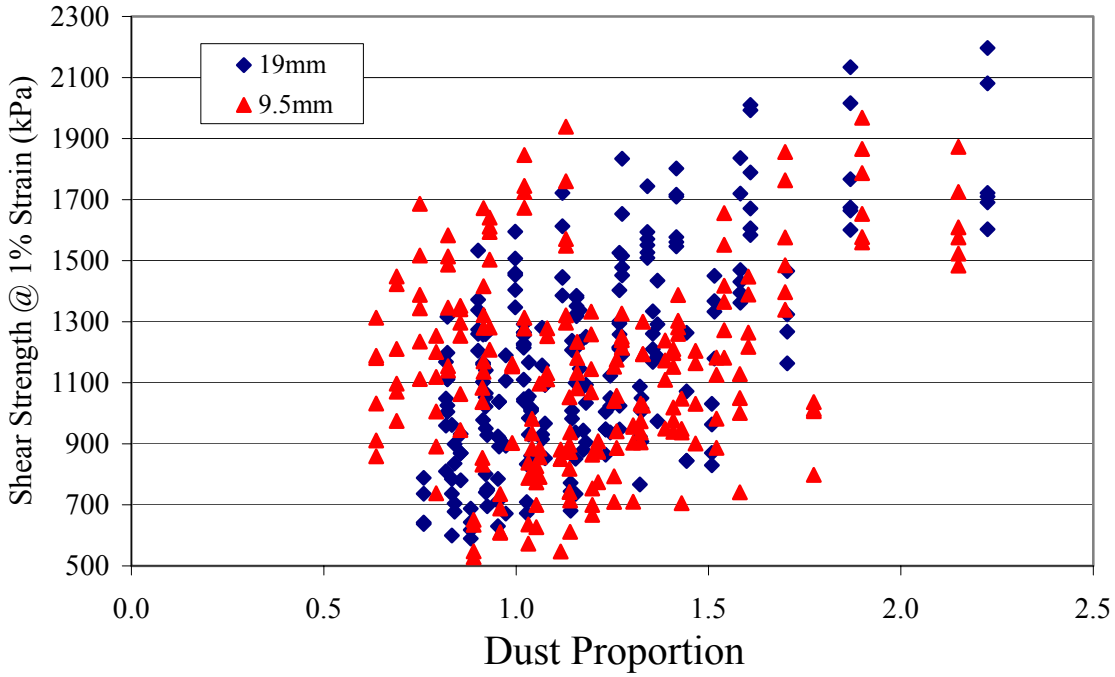

Figure 6.31 Scatter Plot of Triaxial Test Results and Dust Proportion.

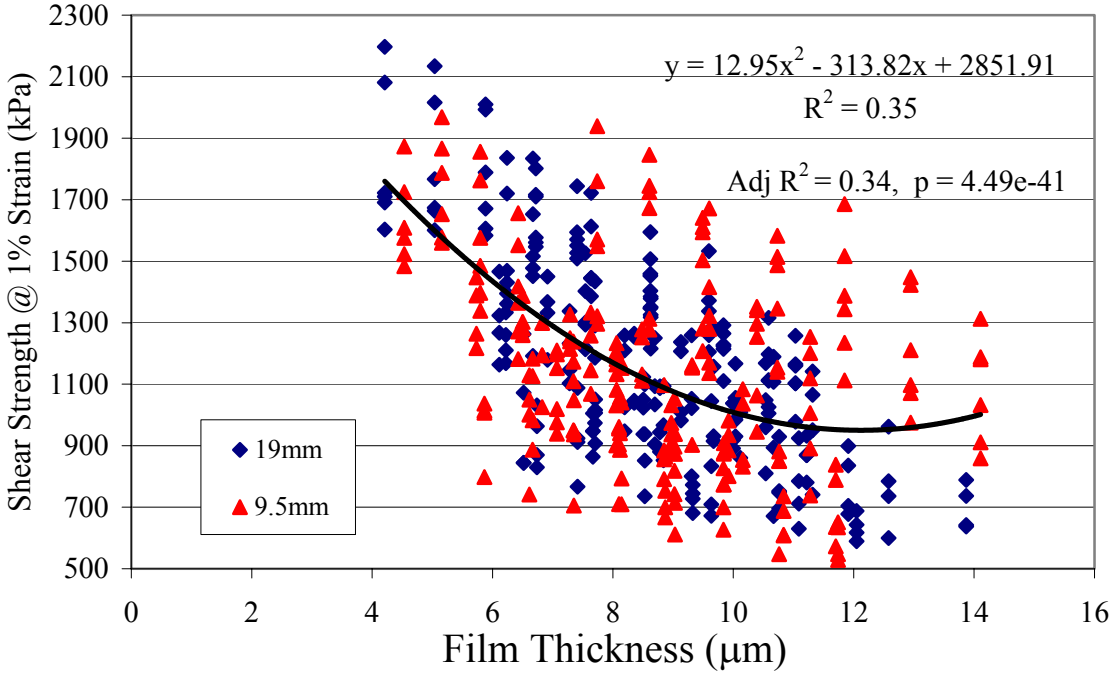

Figure 6.32 Relationship Between Triaxial Test Results and Film Thickness.

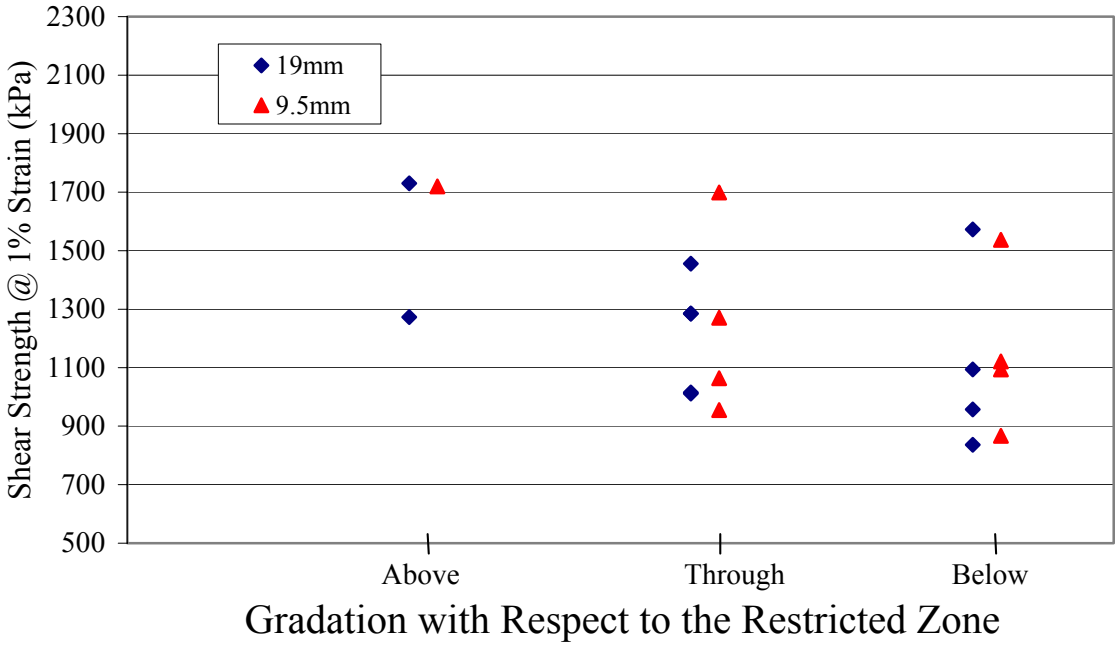

Figure 6.33 Relationship Between Selected Triaxial Test Results and Gradations.

7 SUPERPAVE SHEAR TESTER

7.1. Introduction

As originally developed, the Superpave mixture design and analysis system incorporated performance tests for situations involving moderate to high traffic (Cominsky, et al., 1994). The two performance test devices incorporated into the system were the Superpave Shear Tester (SST) and the Indirect Tensile Tester (IDT). The SST was to be used for rutting and fatigue analysis and the IDT was to be used for fatigue and thermal cracking analyses. This study focuses on rutting performance, so only the SST will be further discussed. The Superpave protocol included six SST test modes:

- Volumetric test;
- Uniaxial strain test;
- Repeated shear test at constant height (RSCH);
- Repeated shear test at constant stress ratio (RSCS);
- Simple shear test at constant height (SSCH); and
- Frequency sweep test at constant height (FSCH).

The volumetric and uniaxial strain tests were recommended for what was termed the Superpave Level Three Mixture Design. The repeated shear test at constant height (RSCH) test was not a part of the Superpave mixture design and analysis system. Level Two (also part of the original Superpave terminology) and Level Three designs relied on repeated shear at constant stress ratio, simple shear at constant height, and frequency sweep at constant height tests (FSCH). In this study, the frequency sweep test at constant height (FSCH) and repeated shear test at constant height (RSCH) tests were employed.

7.2. Test Specimen Preparation

The HMA mixtures that were planned for testing in the SST are summarized in Table 7.1. There were four types of specimen. The first was field mixed-field compacted (FMFC) specimens or cores that were obtained from APT test sections prior to traffic loading. The second was field mixed-laboratory compacted (FMLC) specimens that were made from loose mix sampled behind the paver and were compacted to their corresponding APT in-place densities using the SGC. The third was laboratory mixed-laboratory compacted to observed field properties (LMLCF) specimens. The specimens were prepared in accordance with the observed gradation, mixed at the observed asphalt binder content, and compacted to their corresponding APT in-place densities using the SGC. The fourth was laboratory mixed-laboratory compacted at design condition (LMLCD) specimens. The specimens were prepared in accordance with mixture design gradations, mixed at specific AC levels, and compacted to their corresponding design densities using the SGC. All types of specimens were made and prepared for testing.

A summary of the HMA mixtures that were tested with the SST is presented in Table 7.2. Two types of specimen were employed. The first type is laboratory mixed laboratory compacted specimens at standard design conditions (LMLCS). These specimens were prepared in accordance with SHRP Method of Test M-003 (Harrigan et al. 1994) using the Superpave Gyratory Compactor (SGC). The numbers of gyrations were controlled such that samples were produced with 7±1 percent air voids. The second specimen type is field mixed field compacted (FMFC) specimen. These specimens were 150 mm (6 in.) diameter cores that were taken from APT test sections. The cores were trimmed such that they satisfied the height requirement of 50 mm (1.97 in.).

7.3. Test Parameters

Two test modes were employed: the frequency sweep test at constant height (FSCH) and repeated shear test at constant height (RSCH). The test temperature used for

LMLCS specimens was the design test temperature (39^0 C) and for FMFC specimens the test temperature used in the APT testing (50^0 C) was employed.

7.4. Superpave Shear Tester (SST) Results

7.4.1. Frequency Sweep Test at Constant Height (FSCH)

The plot between complex shear modulus and frequency for the LMLCS specimens is presented in Figure 7.1. The complex shear modulus at 10 Hz for each specimen was plotted as shown in Figure 7.2. Review of the plot suggests that FAA significantly impacted complex shear modulus. The complex shear modulus increased as the FAA value increased from 39 to 44. However, when FAA increased from 44 to 50, the complex shear modulus decreased. This suggests that mixtures incorporating very high FAA values would not perform better than those incorporating typical FAA values. Figure 7.2 further suggests that mixtures with gradations plotting above the restricted zone would perform slightly better than those with gradations plotting below the restricted zone.

Plots of complex shear modulus versus frequency for FMFC specimens are presented in Figures 7.3 to 7.9. Unfortunately an SST control computer hard drive failure resulted in the loss of several test results. The series of plots also provides an indication of the repeatability of the FSCH test. Recall that this testing was conducted at 50^oC. As stated in Section 4.2, several of the APT mixtures were constructed at either high and low density and/or high and low AC constant. Accordingly, the effect of in-place density and asphalt binder content on FSCH test results could be evaluated. For example, the effect of in-place density on FSCH test results is demonstrated in Figure 7.10. As in-place density increased complex shear modulus at 10 Hz increased. However, APT test results (Section 4.5.5) indicated that higher in-place density mixtures do not necessary perform better especially when the in-place density is equal to or greater than the design density. In other words, when the in-place air voids are very low. The effect of deviation from

design AC on FSCH results is presented in Figure 7.11. The plot suggests that some mixtures showed higher complex shear modulus as AC level increased. This observation contradicts with APT test results (Figure 4.17). A plot of complex shear modulus at 10 Hz for selected mixtures is presented in Figure 7.12. The mixtures selected were those that were compacted at 6 to 9 percent in-place air voids or produced at the design AC level only. The plots show that FAA and nominal maximum aggregate size had minimal impact on the complex shear modulus of those mixtures considered.

7.4.2. Repeated Shear Test at Constant Height (RSCH)

Figure 7.13 is a plot of shear strain and number of cycles for the LMLCS specimens tested at 39^{o}C. The shear strain at 5000 cycles data are summarized in Figure 7.14. This plot shows that FAA significantly impacted the observed shear strains. For mixtures incorporating gradations plotting above the restricted zone, the shear strain at 5000 cycles decreased as the FAA value increased. For mixtures incorporating gradations plotting below the restricted zone, the shear strain decreased as FAA values increased from 39 to 44. However, when FAA increased from 44 to 50, the shear strains increased. Test results for mixtures incorporating gradations plotting below the restricted zone were consistent with test results from FSCH, APT, PURWheel, and triaxial tests. Figure 7.14 further suggests that the effect of gradation with respect to the restricted zone on shear strain at 5000 cycles was not completely clear. However, at all FAA levels the above the restricted zone mixtures provided equal or better performance than the below the restricted zone mixtures.

Plots of shear strain and number of cycles for FMFC specimens are presented in Figures 7.15 to 7.19. This series of plots provides an indication of the repeatability of RSCH tests. The repeatability ranged from good to poor. Some not tested until 5000 cycles because they experienced large ($\geq$ 0.05) shear strains before reaching 5000 cycles. In order to evaluate all mixtures consistently, after 5000 cycles a natural logarithmic interpolation was applied for test result on mixtures that failed prior to the application of 5000 load cycles. The effect of in-place density and asphalt binder content on RSCH test

results could also be evaluated. The effect of in-place density on RSCH test results is demonstrated in Figure 7.20. The plot suggests that as the in-place density increased the shear strain after 5000 cycles decreased. However, APT test results (Section 4.5.5) indicated that higher in-place density mixtures do not necessary perform better especially when the in-place density is equal to or greater than the design (96% of ???) density. The effect of deviation from design AC on RSCH results is presented in Figure 7.21. As expected, shear strain after 5000 cycles increased as AC level increased. This observation is consistent with APT test results (Figure 4.17). A plot of shear strain at 5000 cycles for selected mixtures is presented in Figure 7.22. The mixtures selected were those that were compacted at 6 to 9 percent air voids or produced at the design AC. The effect of FAA, gradation, and nominal maximum aggregate size are not clear, but this is likely due to the limited available data.

7.5. Discussion of SST Test Results

7.5.1. Relationship Between SST Test Results and VMA

The relationship between complex shear modulus and VMA for LMLCS specimens is presented in Figure 7.23. A quadratic relationship with a positive second order parameter was observed. It should be noted that all LMLCS specimens were 19mm limestone mixtures. Parameter estimates indicate that the VMA corresponding to optimum complex shear modulus was 17.6 percent. This VMA value was approximately 4.6 percent greater than the minimum VMA requirement for 19mm mixtures.

A scatter plot of complex shear modulus and in-place VMA for FMFC specimens is presented in Figure 7.24. As VMA increased the complex shear modulus increased for 19mm mixtures. However, for 9.5mm mixtures complex shear modulus was essentially constant over a range of VMA.

A scatter plot of shear strain at 5000 cycles and VMA for LMLCS specimens is presented in Figure 7.25. No relationship was observed. Recall that all LMLCS

specimens were the 19mm limestone mixtures. A scatter plot of shear strain after 5000 cycles and VMA for FMFC specimens is presented in Figure 7.26. No relationship was observed for the 19mm mixtures. There was a trend that as VMA increased shear strain after 5000 cycles increased for the 9.5mm mixtures. However, only four data points were available for the 9.5mm mixtures.

7.5.2. Relationship Between SST Test Results and VFA

The relationship between complex shear modulus and VFA for LMLCS specimens is presented in Figure 7.27. A negative linear relationship was observed. All LMLCS specimens were the 19mm limestone mixtures. A scatter plot of complex shear modulus and in-place VFA for FMFC specimens is presented in Figure 7.28. No relationship was observed for either the 19 nor 9.5mm mixtures.

A scatter plot of shear strain at 5000 cycles and VFA for the 19mm limestone LMLCS specimens is presented in Figure 7.29. No relationship was observed. A scatter plot of shear strain at 5000 cycles and in-place VFA for FMFC specimens is presented in Figure 7.30. Again, no relationship was observed for either 19 nor 9.5mm mixtures.

7.5.3. Relationship Between SST Test Results and Dust Proportion

The relationship between complex shear modulus and dust proportion for the 19mm limestone LMLCS specimens is presented in Figure 7.31. A very weak quadratic relationship with a positive second order parameter was observed. This relationship suggests that as dust proportion increased complex shear modulus increased for LMLCS specimen.

The relationship between complex shear modulus and dust proportion for FMFC specimens is presented in Figure 7.32. Again, a weak quadratic relationship was observed. This relationship would suggest that there was a dust proportion level

corresponding to minimum complex shear modulus. However, the relationship is meaningless due to the scatter in the data.

The scatter plot of shear strain after 5000 cycles and dust proportion for the 19mm limestone LMLCS specimens is presented in Figure 7.33. No relationship was observed.

The relationship between shear strain after 5000 cycles and dust proportion for FMFC specimens is presented in Figure 7.34. A quadratic relationship with a negative second order parameter was observed. The relationship suggests that there was a dust proportion level of approximately 1.0 percent corresponding to maximum shear strain after 5000 cycles. This observation is consistent with that based on complex shear modulus.

7.5.4. Relationship Between SST Results and Film Thickness

The relationship between complex shear modulus and film thickness for the 19mm limestone LMLCS specimens is presented in Figure 7.35. This relationship suggests that as film thickness increased complex shear modulus decreased for LMLCS specimen.

A scatter plot of complex shear modulus and film thickness for FMFC specimens is presented in Figure 7.36. No clear trend is observed, but the moduli of the 19mm mixtures with high film thicknesses are much greater than all others.

The very weak relationship between shear strain at 5000 cycles and film thickness for the 19mm limestone LMLCS specimens is presented in Figure 7.37. A positive linear relationship was observed. Although weak, this relationship suggests that as film thickness increased the shear strain increased.

A scatter plot of shear strain after 5000 cycles and film thickness for FMFC specimens is presented in Figure 7.38. No clear trend is observed and in fact a few data points show a reduction in shear strain with high film thickness.

7.5.5. Relationship between SST and APT Tests

The relationship between FSCH for LMLCS specimens and APT test results is presented in Figure 7.39. A very weak relationship was observed, but it shows that as complex shear modulus decreased the APT total rut increased. Although the relationship was reasonable, it should be noted that the mixture preparation method, test temperature, and compaction method between the two tests were different.

A scatter plot of FSCH for FMFC specimens and APT test results is presented in Figure 7.40. No relationship was observed although the mixture preparation method, test temperature, and compaction method between the two tests were identical. This observation suggests that sample geometry of SST samples impacted FSCH test results. It was difficult to trim some of the cores taken from APT test lanes to satisfy SST sample geometry requirements. As a result, some samples exhibited geometry imperfections such as less than parallel surfaces and thicknesses less than 50mm which may have impacted the test results.

The relationship between RSCH for LMLCS specimens and APT test results is presented in Figure 7.41. This relationship suggests that as the shear strain at 5000 cycles increased the APT total rut increased. Although the relationship was reasonable, it should be noted that the mixture preparation method, test temperature, and compaction method between the two tests were different (LMLC versus FMFC).

A scatter plot of RSCH for FMFC specimens and APT test results is presented in Figure 7.42. There is a weak general trend suggesting that as APT total rut increased the shear strain after 5000 cycles increased. Although the trend was weak, it was reasonable.

7.5.6. Relationship Between SST and PURWheel Tests

The relationship between the limited FSCH for LMLCS specimens and PURWheel test results is presented in Figure 7.43. As complex shear modulus decreased the PURWheel rut depth increased. Although the relationship was reasonable, it should

be noted that the mixture preparation method, test temperature, and compaction method between the two tests were different and is based on limited data.

A scatter plot of FSCH for FMFC and PURWheel test results is presented in Figure 7.44. No relationship was observed although the mixture preparation method, test temperature, and compaction method between the two tests was the same.

A scatter plot of RSCH for LMLCS specimens and PURWheel test results is presented in Figure 7.45. There is no clear trend in the data.

Figure 7.46 shows the relationship between RSCH for FMFC specimens and PURWheel test results. A positive linear relationship was observed. This relationship shows that as PURWheel rut depths increased the shear strain after 5000 cycles increased. Although the relationship was weak, it is reasonable.

7.5.7. Relationship Between SST and Triaxial Tests

The relationship between FSCH tests on LMLCS and triaxial test results is presented in Figure 7.47. It shows that as complex shear modulus increased, triaxial shear strength increased. Although the relationship is reasonable, it should be noted that the density and test temperature of the two test specimen types were different.

The relationship between RSCH on LMLCS and triaxial test results is presented in Figure 7.48. This relationship suggests that as shear strain at 5000 cycles decreased the triaxial shear strength increased. Although the relationship is reasonable, it should be noted that the density and test temperature of the two test specimen types were different.

7.5.8. Relationship Between RSCH and FSCH Tests

A scatter plot of RSCH and FSCH test results for LMLCS specimens is presented in Figure 7.49. Although no strong relationship is observed, there was a slight trend that

as the shear strain at 5000 cycles decreased the complex modulus increased. This trend was reasonable because both tests indicated the performance of the mixtures consistently.

A scatter plot of RSCH and FSCH test results for FMFC specimen is presented in Figure 7.50. Again no relationship was observed, but there is a trend that as the shear strain at 5000 cycles decreased the complex modulus increased. This trend is reasonable because both tests indicated the performance of the mixtures consistently.

7.5.9. Comparison Between LMLCS and FMFC Test Results

The major differences between LMLCS and FMFC test results were the mixture preparation method, test temperature, compaction method, and sample geometry. FMFC specimens tended to exhibit geometry imperfections, particularly those at low density, because the specimens were trimmed from cores taken from APT test lanes.

The FSCH test results on LMLCS specimens exhibited approximately 1.5 to 15 times higher moduli than those for FMFC specimens. This suggests that FSCH test results were very sensitive to mixture preparation method, test temperature, and compaction method. On the other hand, the RSCH test results on LMLCS specimens exhibited a maximum of 2 times lower shear strain than those of the FMFC specimens. The 11^{o}C difference in test temperature is likely the primary reason for the differences.

Based on LMLCS specimens, both FSCH and RSCH tests exhibited reasonable comparisons with APT, PURWheel, and Triaxial test results.

Based on FMFC specimens, RSCH test results exhibited slightly better correlations with both APT and PURWheel test results than did FSCH test results. However, the variability associated with FMFC tests was greater and the available data were limited.

Table 7.1 Test Plan for Superpave Shear Tests.

FAA	Gradation	9.5 mm Nominal Max. Size								19 mm Nominal Max. Size							
		Limestone				Granite				Limestone				Granite			
		1	2	3	4	1	2	3	4	1	2	3	4	1	2	3	4
39	Above												X				
	Below												X				
44	Above				X								X				
	Through	X	X	X	X				X				X				X
	Below				X	X	X	X	X	X			X	X	X	X	X
50	Above												X				
	Through	X	X	X	X				X				X	X	X	X	X
	Below				X	X	X	X	X				X				X

Note: 1 = field mixed-field compacted specimen (FMFC)
2 = field mixed-laboratory compacted specimen (FMLC)
3 = laboratory mixed-laboratory compacted specimen at observer field properties (LMLCF)
4 = laboratory mixed-laboratory compacted specimen at design condition (LMLCD) or at standard condition (LMLCS).

Table 7.2 Mixtures Tested with the Superpave Shear Tester.

FAA	Gradation	9.5 mm Nominal Max. Size								19 mm Nominal Max. Size							
		Limestone				Granite				Limestone				Granite			
		1	2	3	4	1	2	3	4	1	2	3	4	1	2	3	4
39	Above									X		X					
	Below									X		X					
44	Above									X		X					
	Through		X														
	Below						X			X	X	X					
50	Above									X		X					
	Through		X												X		
	Below						X			X		X					

Note: 1 = Frequency sweep test at constant height (FSCH) using laboratory mixed laboratory compacted specimen at standard design condition (LMLCS) at 39^0C

2 = Frequency sweep test at constant height (FSCH) using field mixed field compacted specimen (FMFC) at 50^0C

3 = Repeated shear test at constant height (RSCH) using laboratory mixed laboratory compacted specimen at standard design condition (LMLCS) at 39^0C

4 = Repeated shear test at constant height (RSCH) using field mixed field compacted specimen (FMFC) at 50^0C

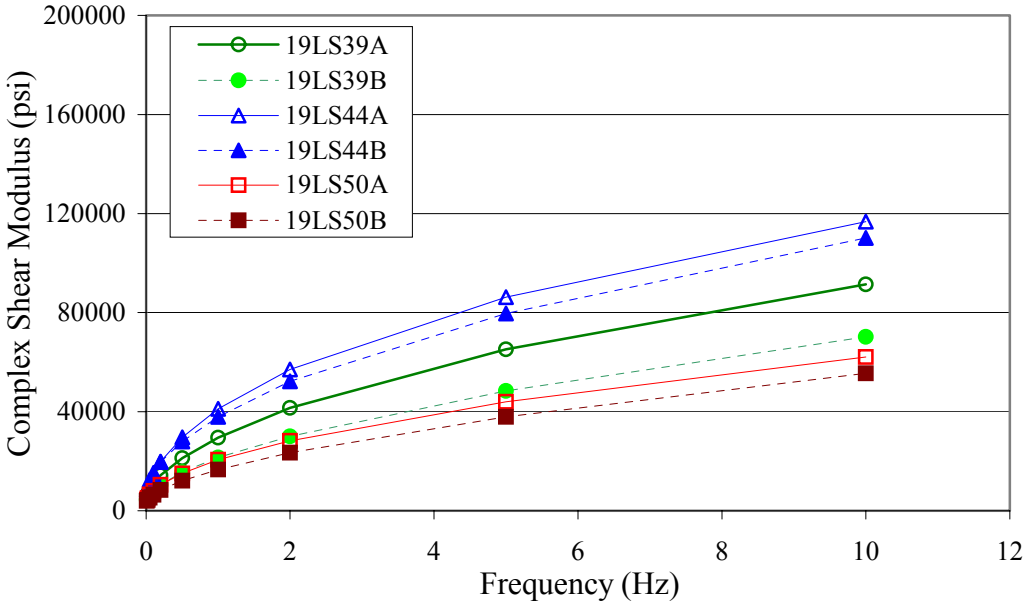

Note: 19 = nominal max. size; LS = limestone; 39, 44, 50 = FAA; A, B, T = gradation above, below, through the restricted zone.

Figure 7.1 Frequency Sweep Test at Constant Height Result for LMLCS Specimens (39^0C).

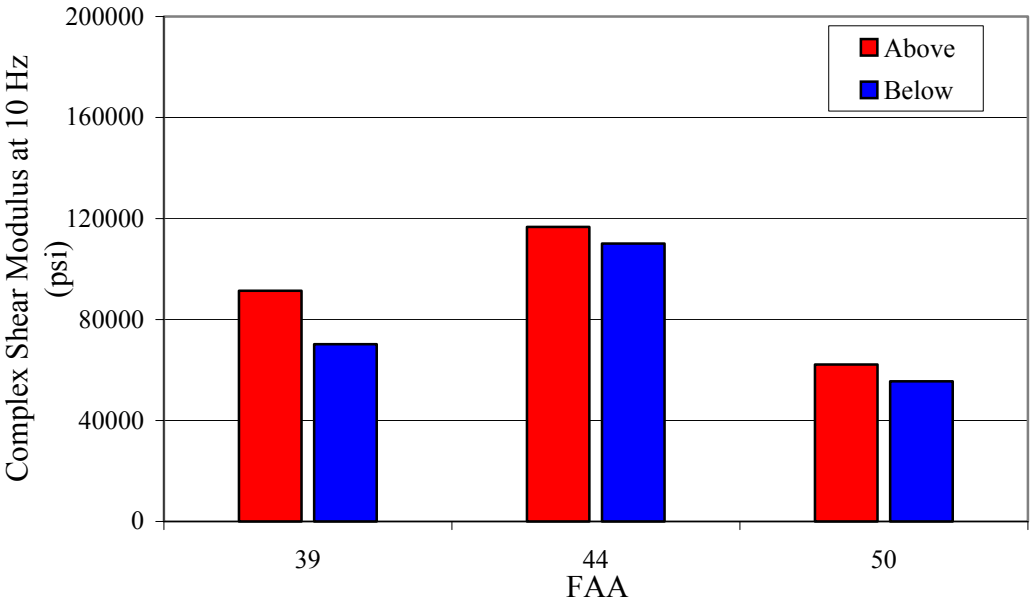

Figure 7.2 Effect of FAA and Gradation with Respect to The Restricted Zone on Complex Shear Modulus of 19mm Limestone Mixtures (LMLCS Specimens, 39^0C).

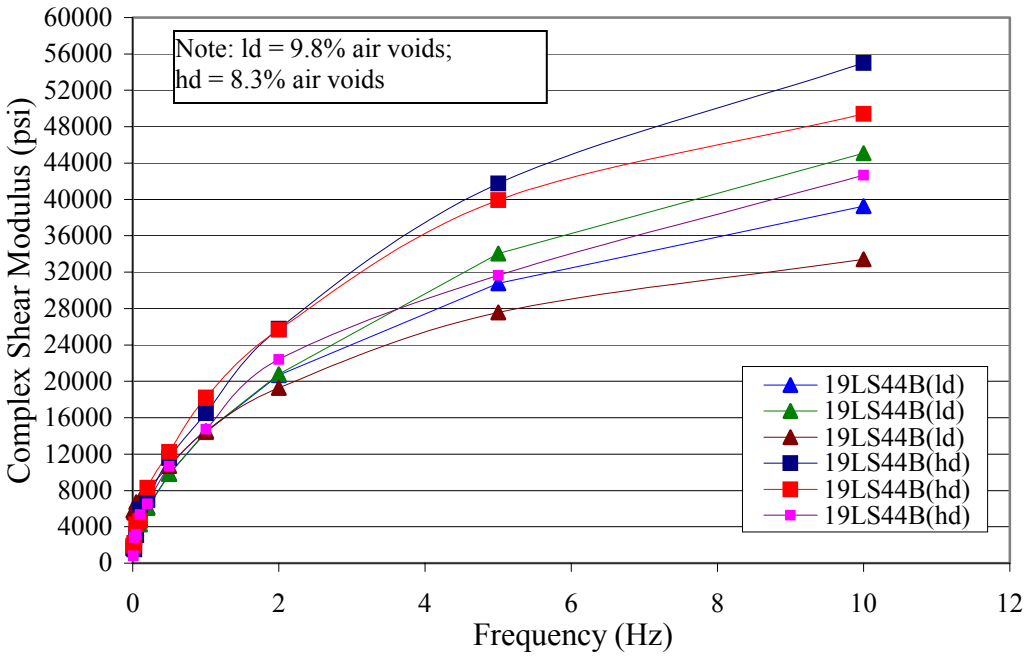

Figure 7.3 Frequency Sweep Test at Constant Height Result for 19mm Limestone with FAA of 44, Gradations Plotting Below The Restricted Zone FMFC Specimens (50^0C).

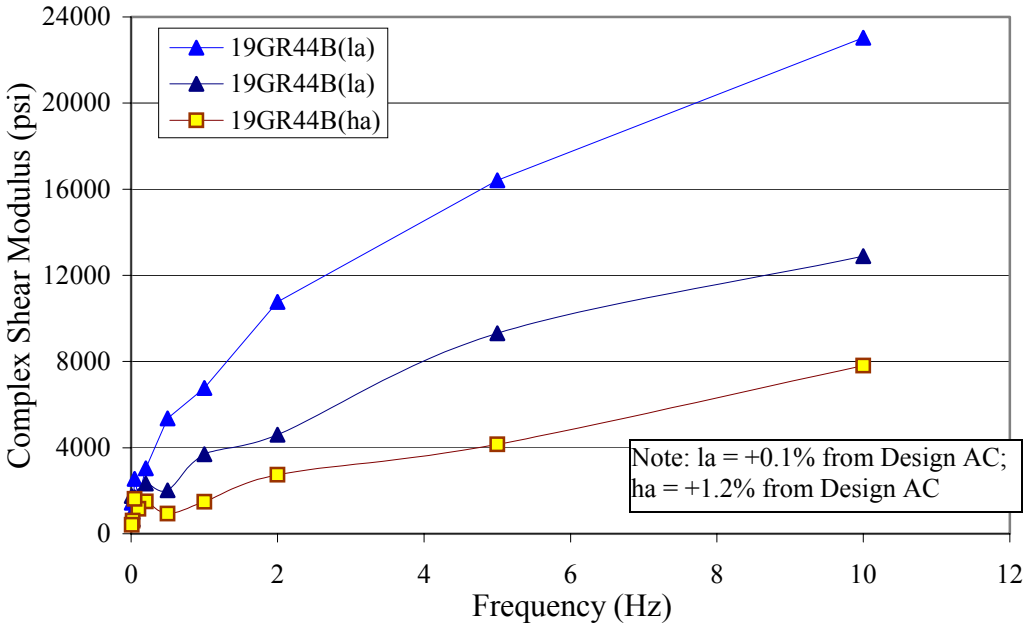

Figure 7.4 Frequency Sweep Test at Constant Height Result for 19mm Granite with FAA of 44, Gradations Plotting Below The Restricted Zone FMFC Specimens (50^0C).

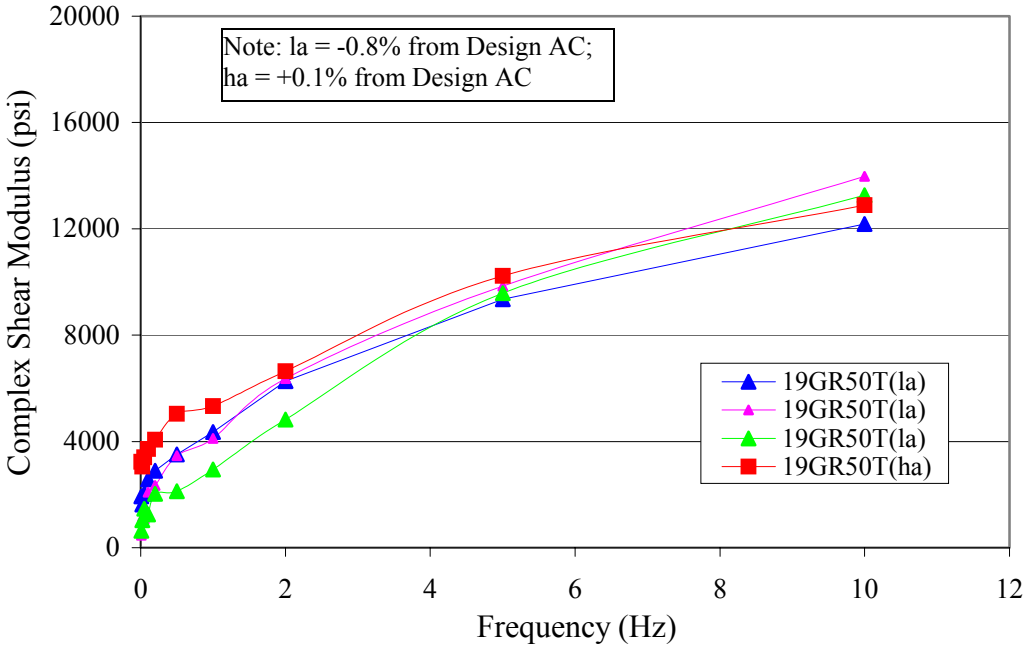

Figure 7.5 Frequency Sweep Test at Constant Height Result for 19mm Granite with FAA of 50, Gradations Plotting Through The Restricted Zone FMFC Specimens (50^0C).

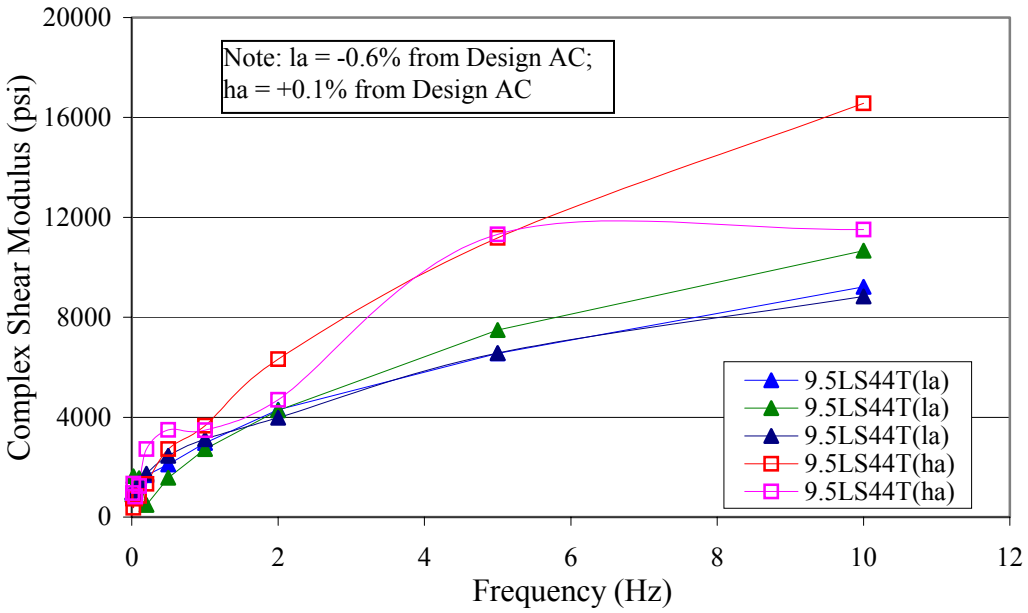

Figure 7.6 Frequency Sweep Test at Constant Height Result for 9.5mm Limestone with FAA of 44, Gradations Plotting Through The Restricted Zone, and at –0.6% from Design AC FMFC Specimens (50^0C).

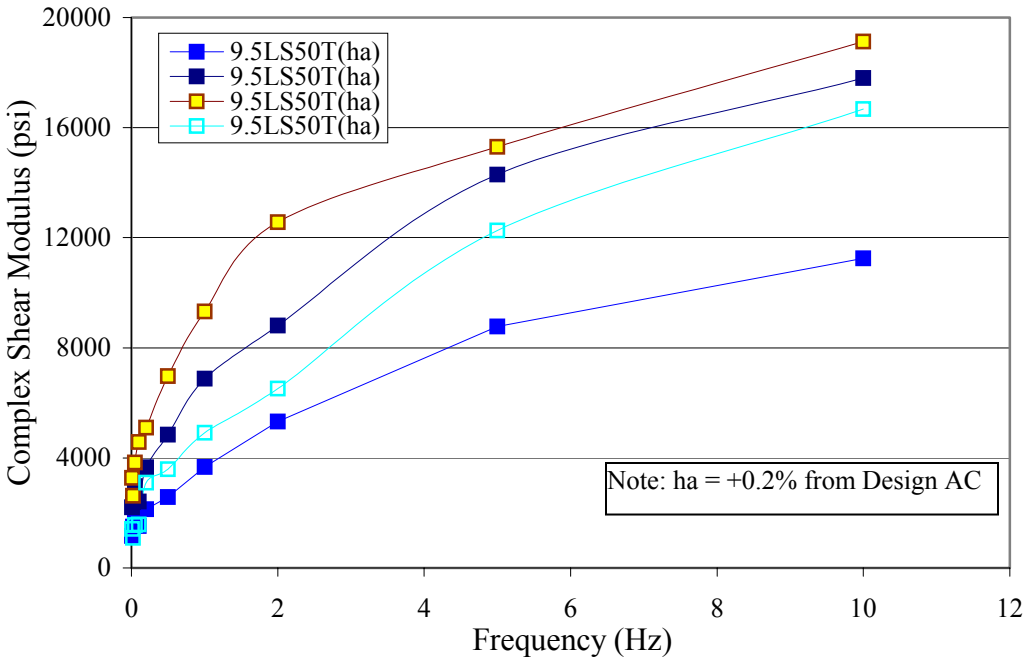

Figure 7.7 Frequency Sweep Test at Constant Height Result for 9.5mm Limestone with FAA of 50, Gradations Plotting Through The Restricted Zone FMFC Specimens (50^0C).

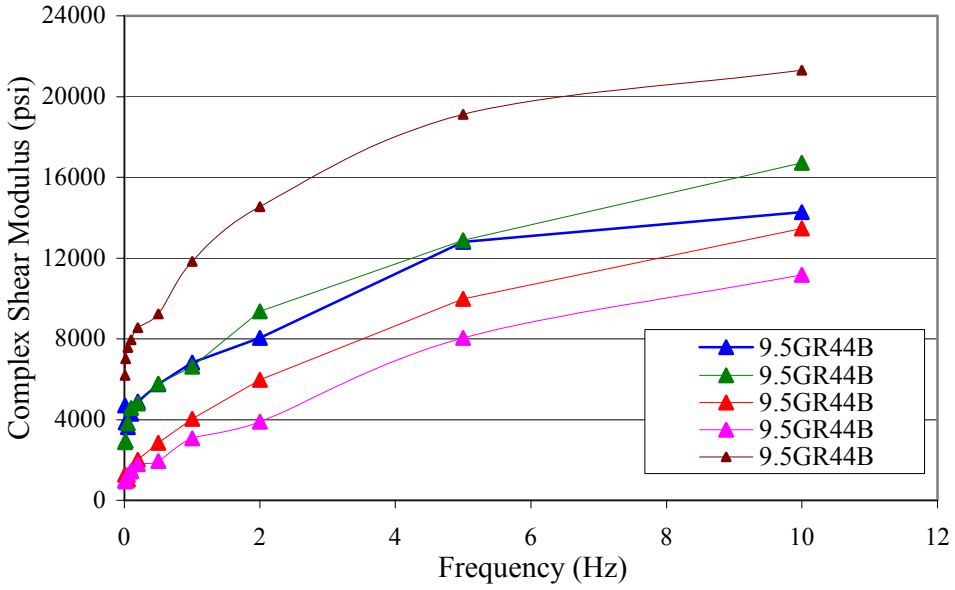

Figure 7.8 Frequency Sweep Test at Constant Height Result for 9.5mm Granite with FAA of 44, Gradations Plotting Below The Restricted Zone, and at Design AC FMFC Specimens (50^0C).

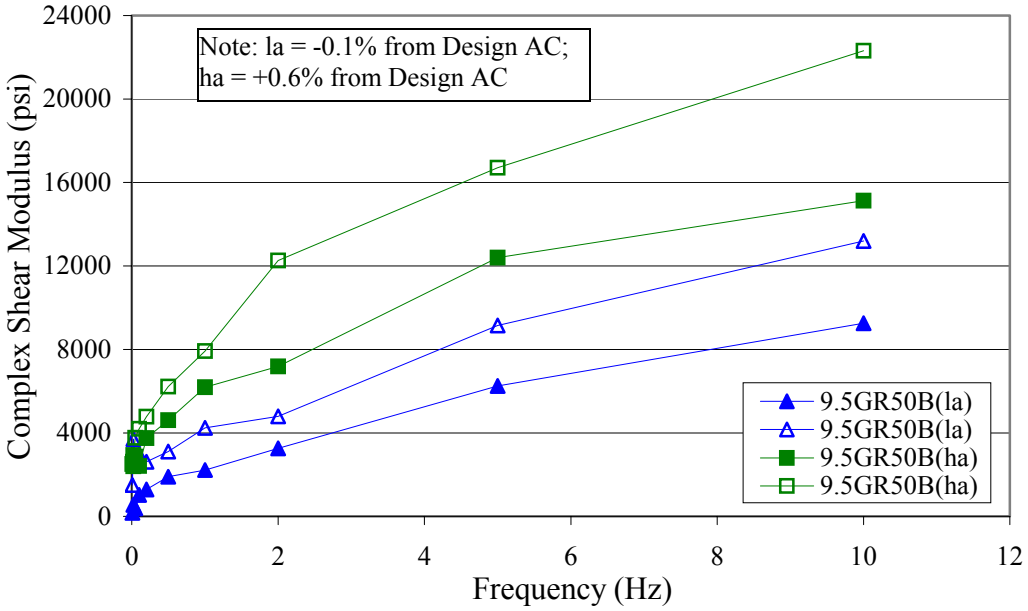

Figure 7.9 Frequency Sweep Test at Constant Height Result for 9.5mm Granite with FAA of 50 and Gradations Plotting Below The Restricted Zone FMFC Specimens (50^0C).

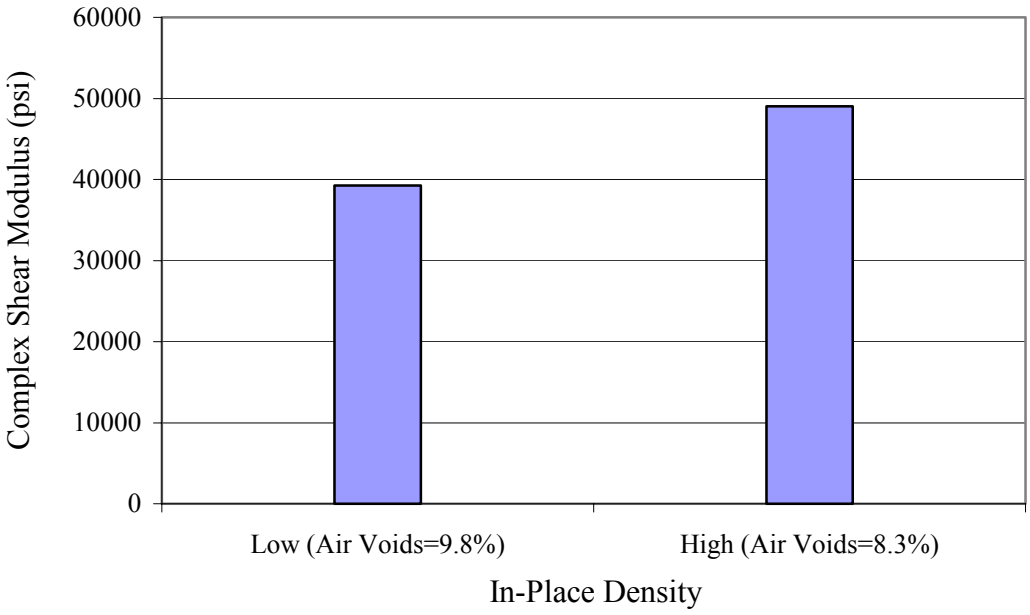

Figure 7.10 Effect of Initial In-Place Density on Complex Shear Modulus for 19mm Limestone with FAA of 44 and Gradation Plotting Below The Restricted Zone (FMFC specimen, 50^0C).

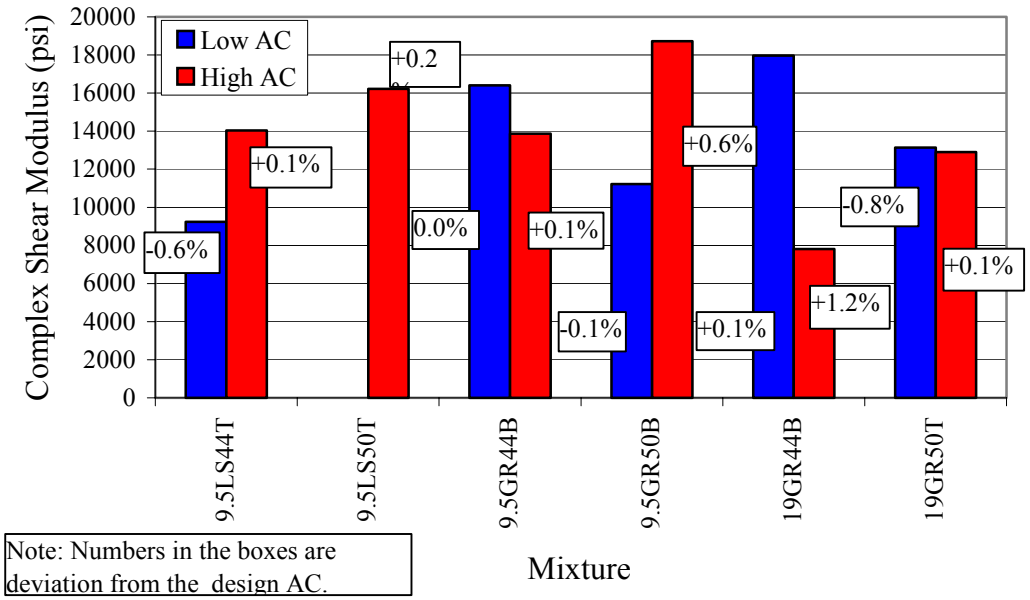

Figure 7.11 Effect of Deviation from Design AC on Complex Shear Modulus for FMFC Specimens (50^0C).

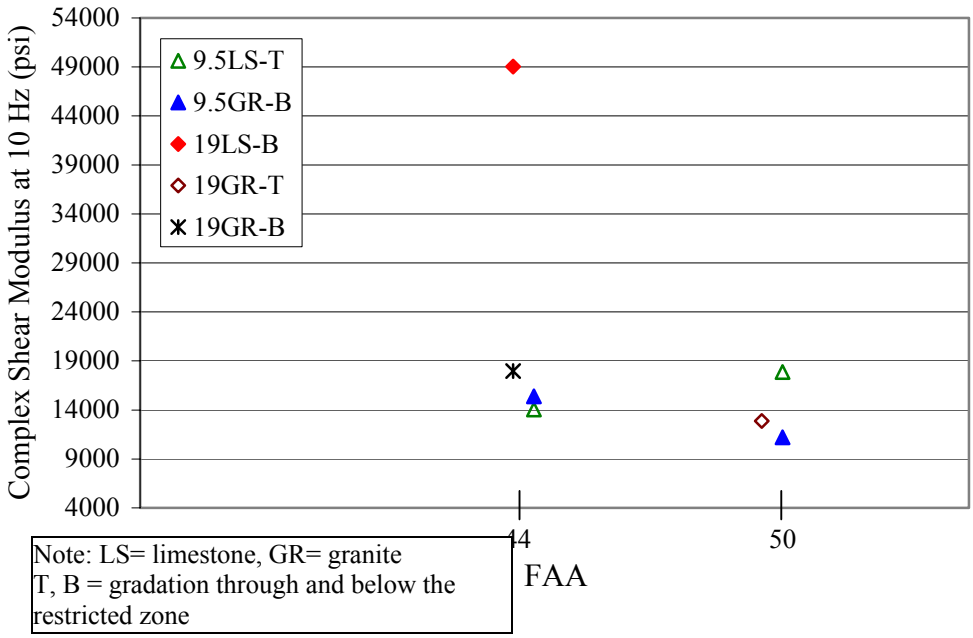

Figure 7.12 Effect of FAA and Gradation with Respect to The Restricted Zone on Complex Shear Modulus (FMFC Specimens, 50^0C).

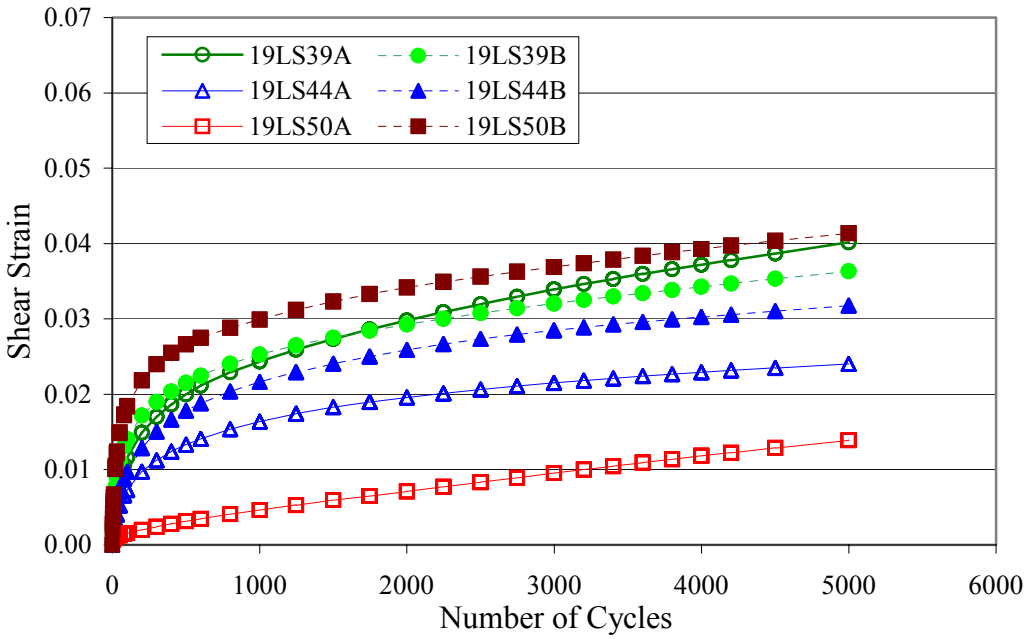

Figure 7.13 Repeated Shear Test at Constant Height Result for LMLCS Specimens (39^0C).

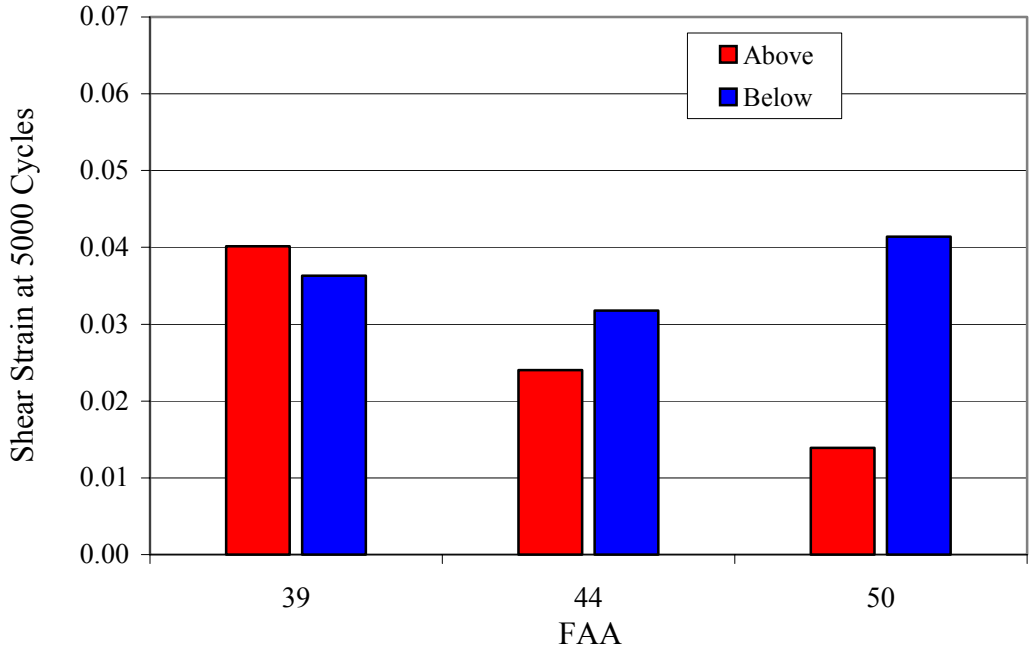

Figure 7.14 Effect of FAA and Gradation with Respect to The Restricted Zone on Shear Strain at 5000 Cycles for 19mm Limestone Mixtures (LMLCS Specimens, 39^0C).

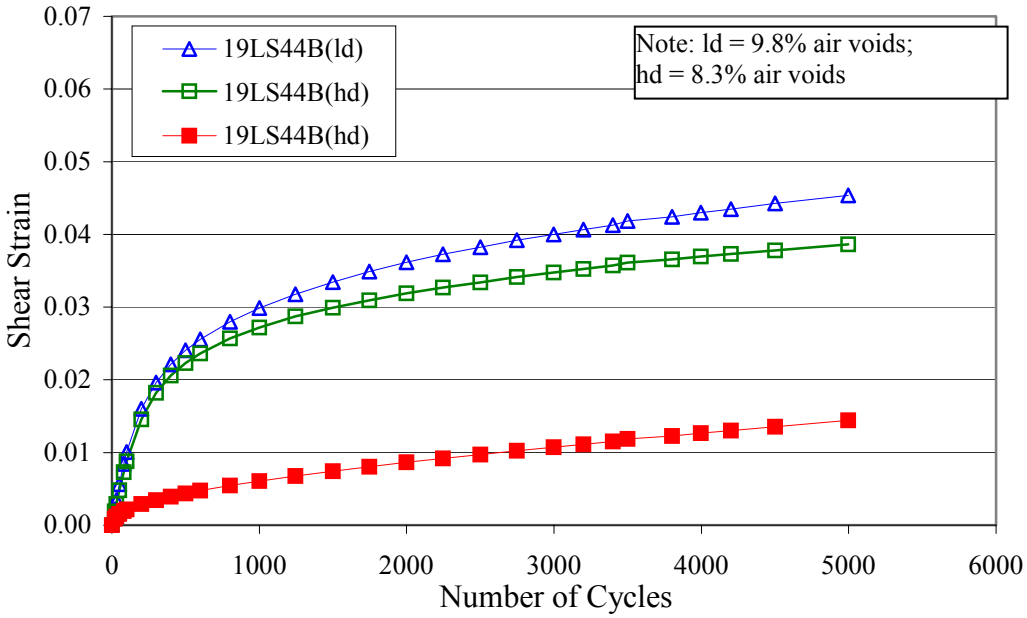

Figure 7.15 Repeated Shear Test at Constant Height Result for 19mm Limestone with FAA of 44, Gradations Plotting Below The Restricted Zone FMFC Specimens (50^0C).

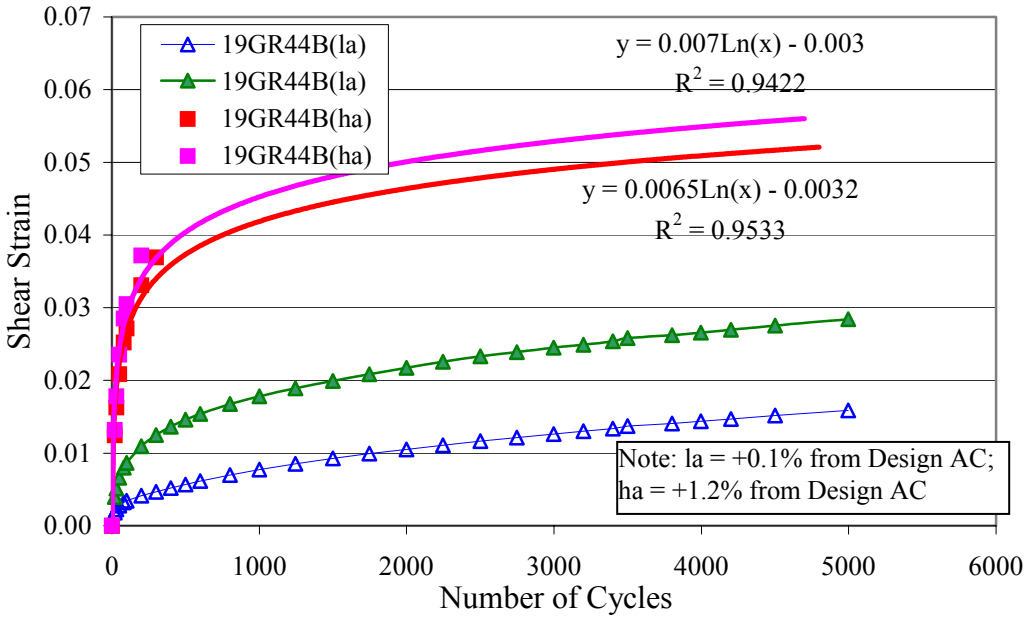

Figure 7.16 Repeated Shear Test at Constant Height Result for 19mm Granite with FAA of 44, Gradations Plotting Below The Restricted Zone FMFC Specimens (50^0C).

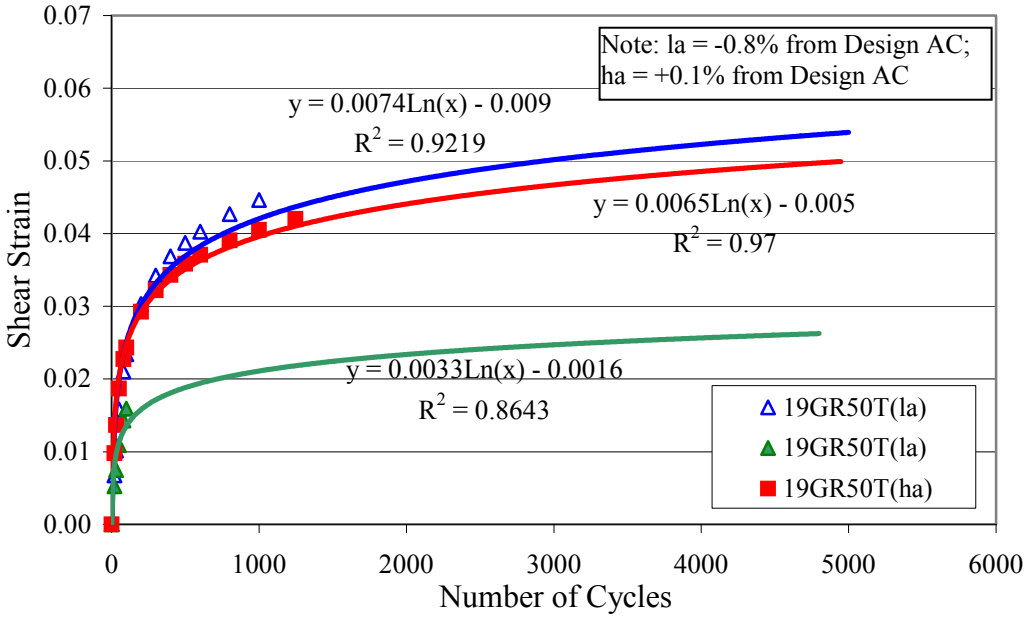

Figure 7.17 Repeated Shear Test at Constant Height Result for 19mm Granite with FAA of 50, Gradations Plotting Through The Restricted Zone FMFC Specimens (50^0C).

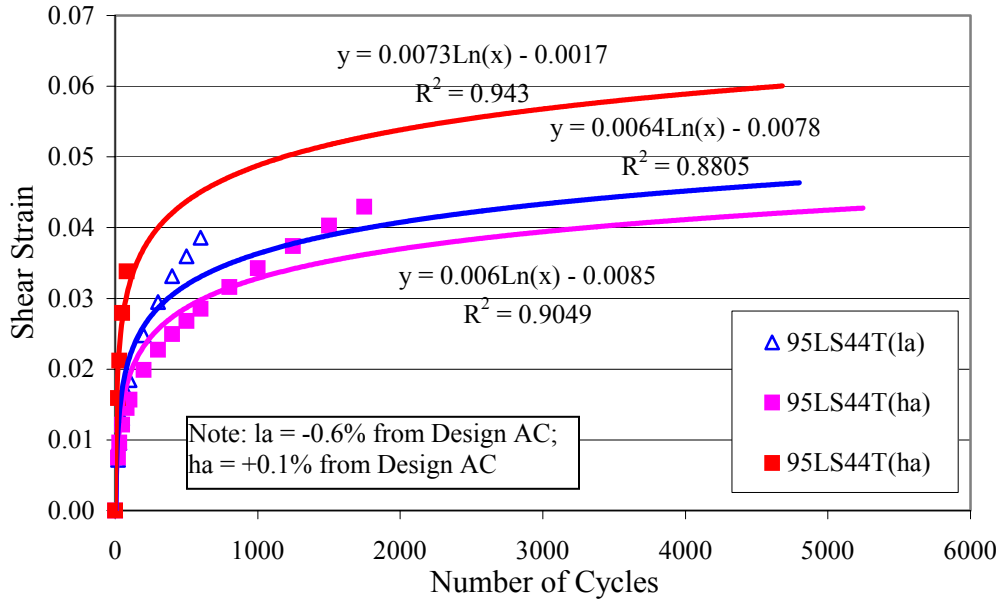

Figure 7.18 Repeated Shear Test at Constant Height Result for 9.5mm Limestone with FAA of 44, Gradations Plotting Through The Restricted Zone, and at –0.6% from Design AC FMFC Specimens (50^0C).

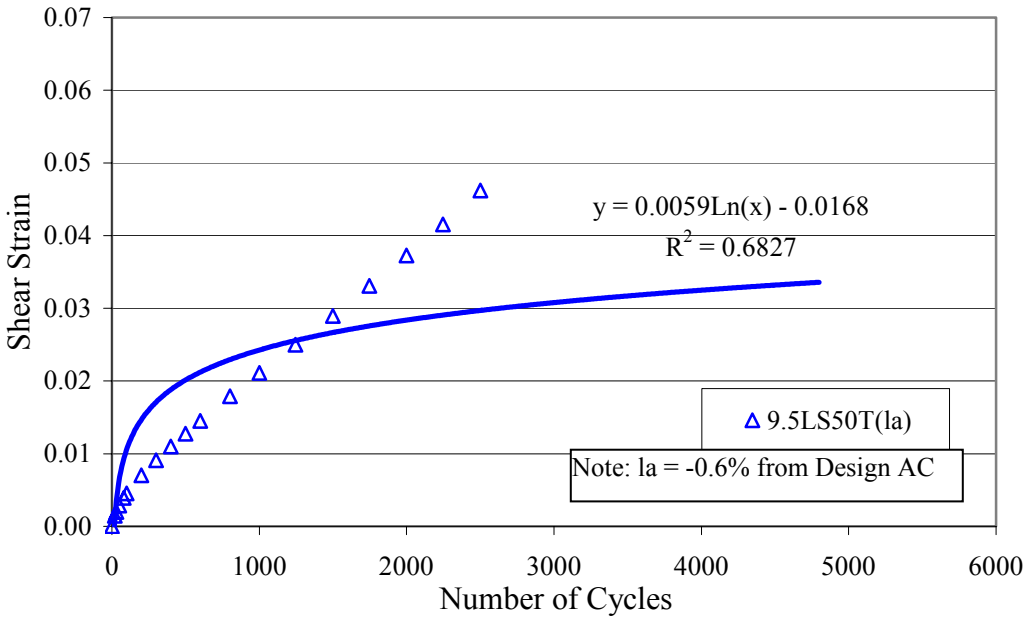

Figure 7.19 Repeated Shear Test at Constant Height Result for 9.5mm Limestone with FAA of 50, Gradations Plotting Through The Restricted Zone FMFC Specimens (50^0C).

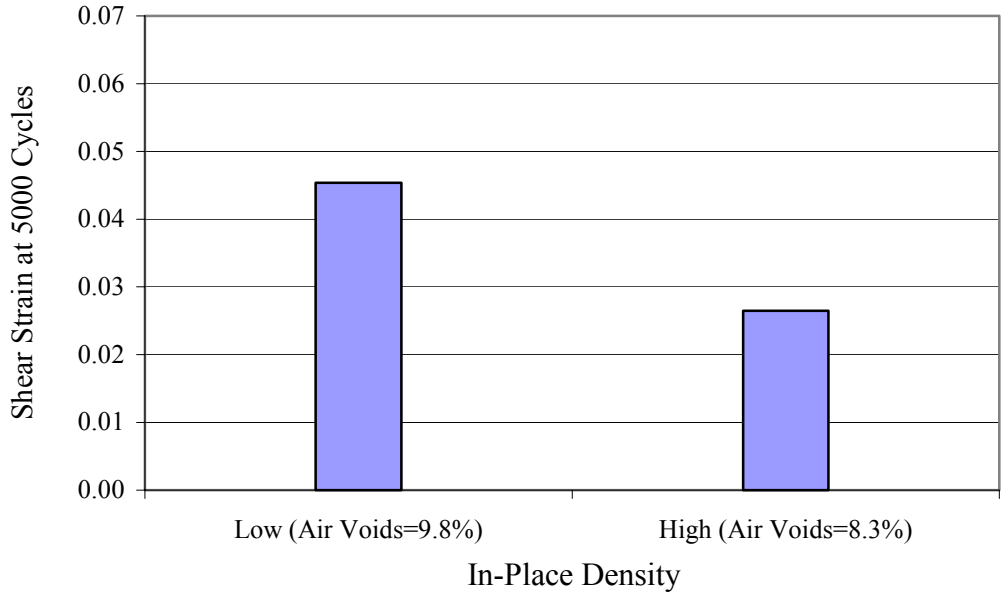

Figure 7.20 Effect of Initial In-Place Density on Shear Strain at 5000 Cycles for 19mm Limestone with FAA of 44 and Gradation Plotting Below The Restricted Zone (FMFC specimen, 50^0C).

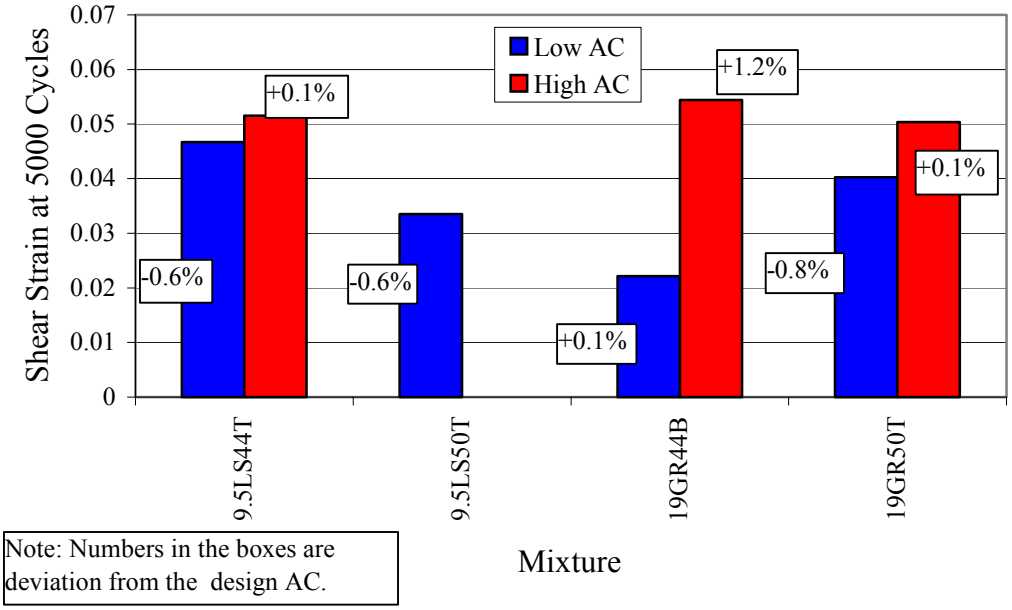

Figure 7.21 Effect of Deviation from Design AC on Shear Strain at 5000 Cycles for FMFC Specimens (50^0C).

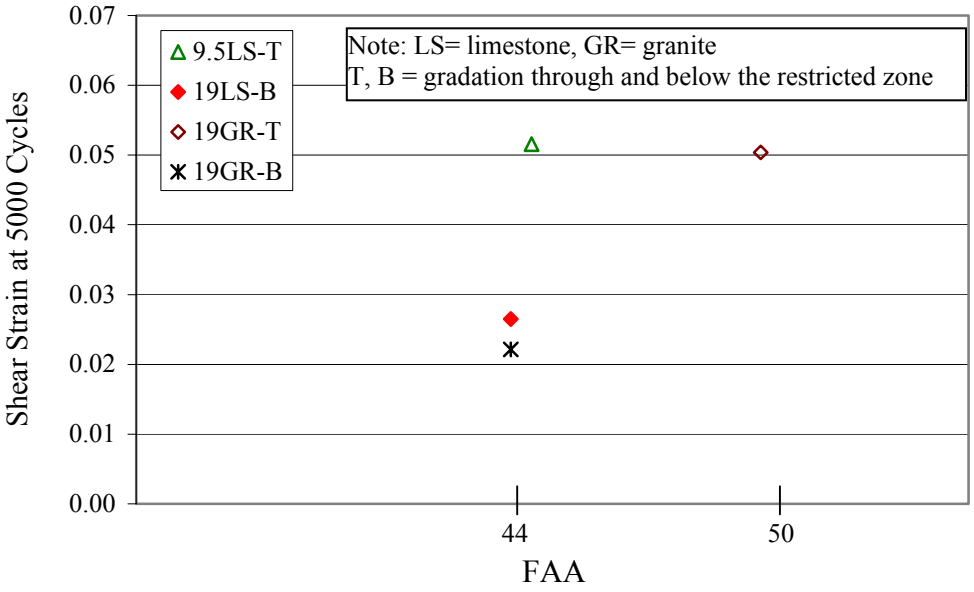

Figure 7.22 Effect of FAA and Gradation with Respect to The Restricted Zone on Shear Strain (FMFC Specimens, 50^0C).

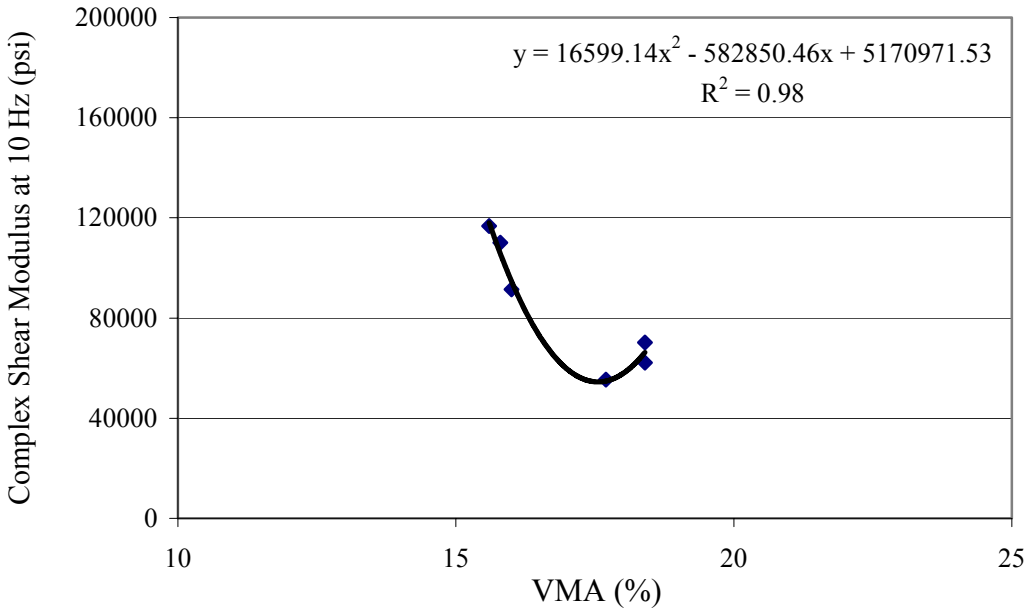

Figure 7.23 Relationship Between Complex Shear Modulus and VMA for LMLCS Specimens (39^0C).

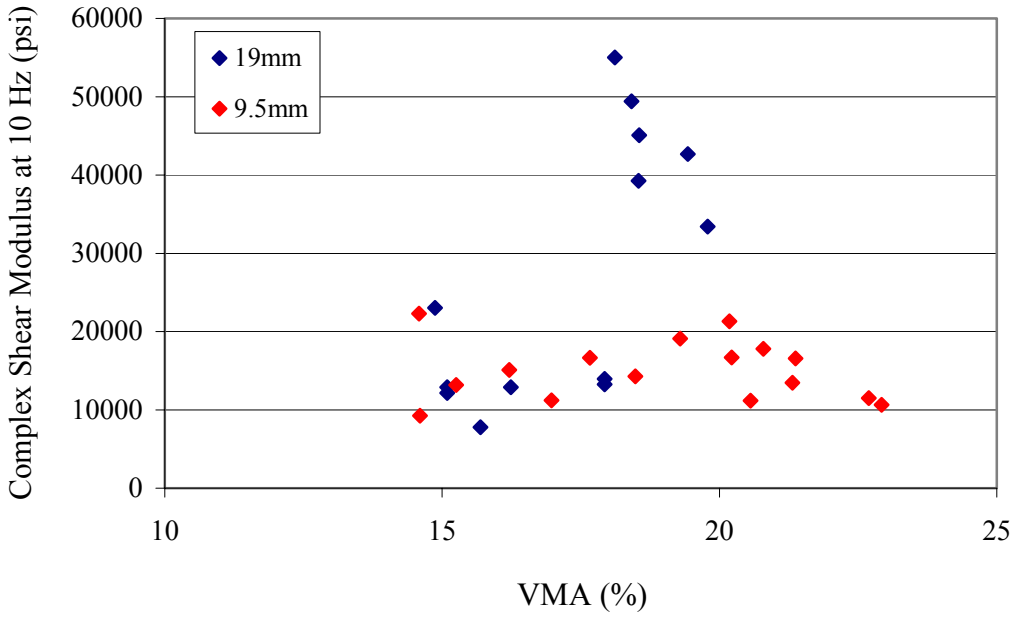

Figure 7.24 Scatter Plot of Complex Shear Modulus and VMA for FMFC Specimens (50^0C).

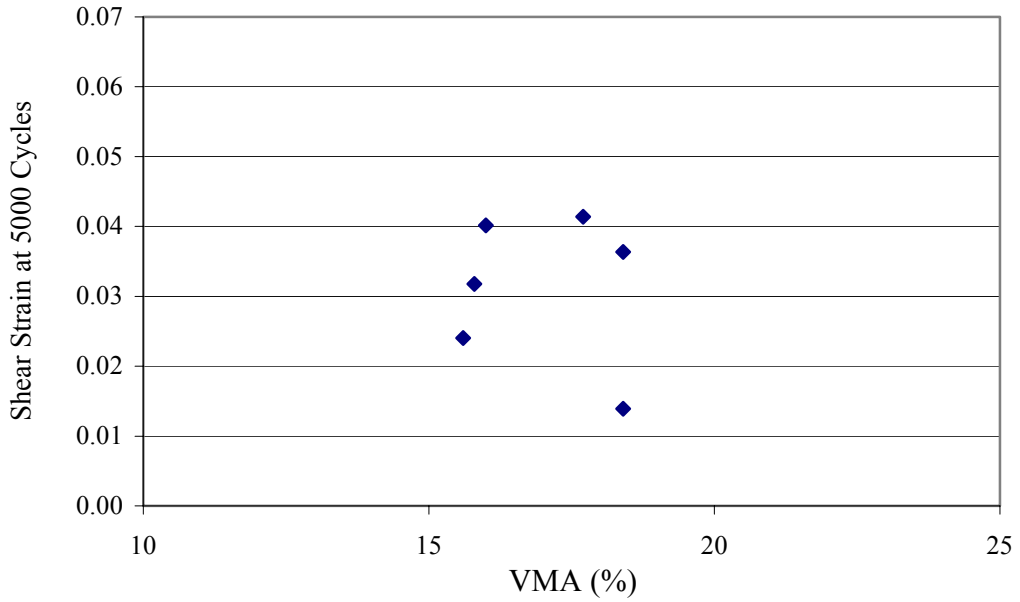

Figure 7.25 Scatter Plot of Shear Strain and VMA for LMLCS Specimens (39^0C).

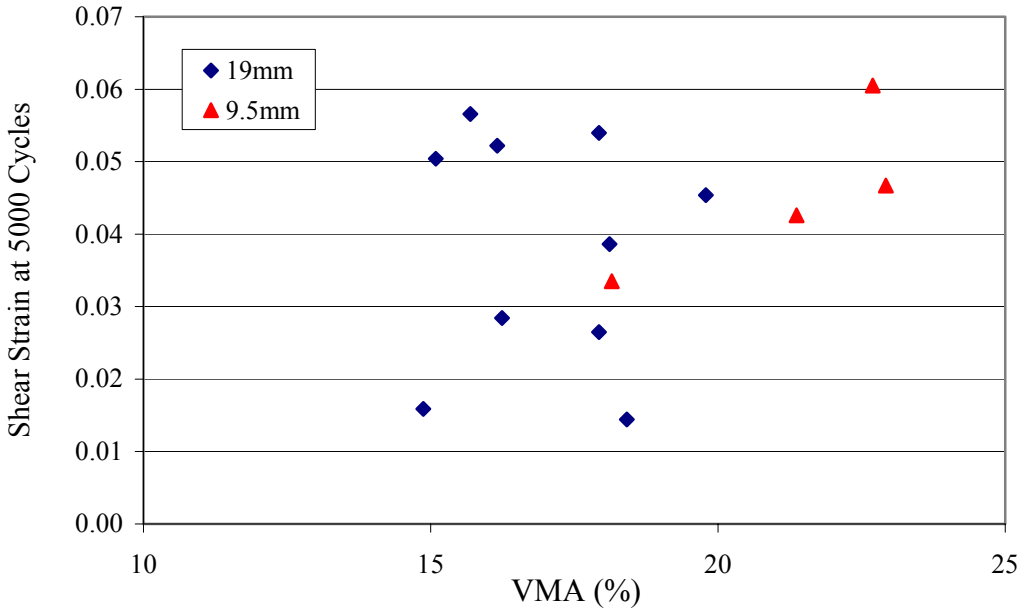

Figure 7.26 Scatter Plot of Shear Strain and VMA for FMFC Specimens (50^0C).

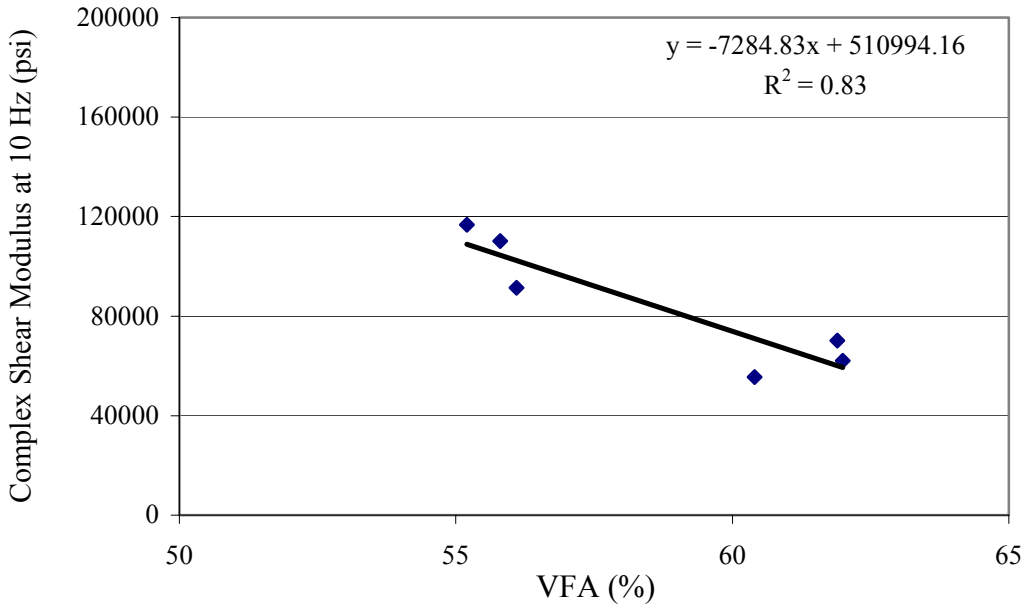

Figure 7.27 Relationship Between Complex Shear Modulus and VFA for LMLCS Specimens (39^0C).

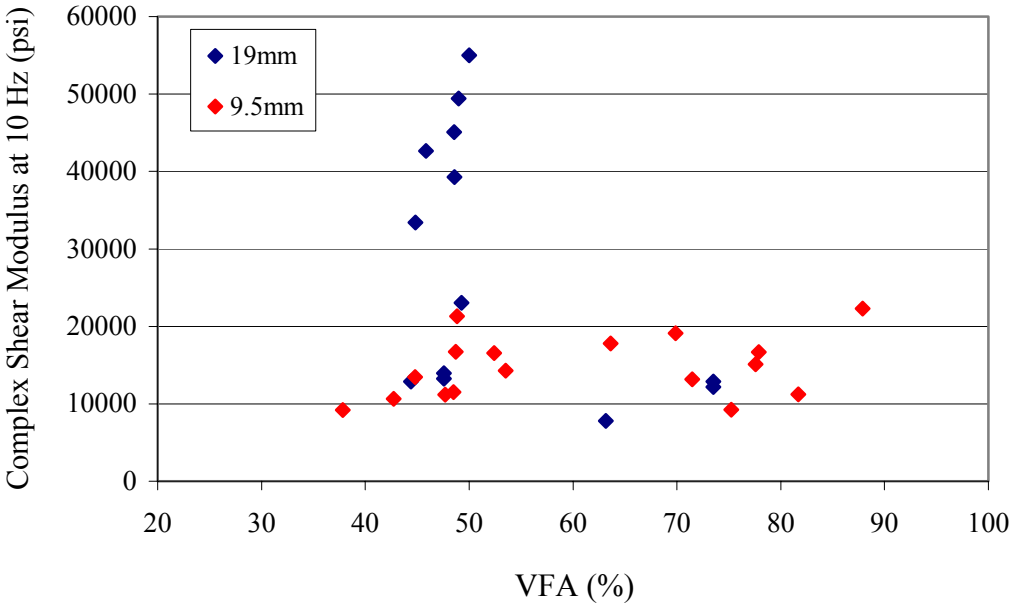

Figure 7.28 Scatter Plot of Complex Shear Modulus and VFA for FMFC Specimens (50^0C).

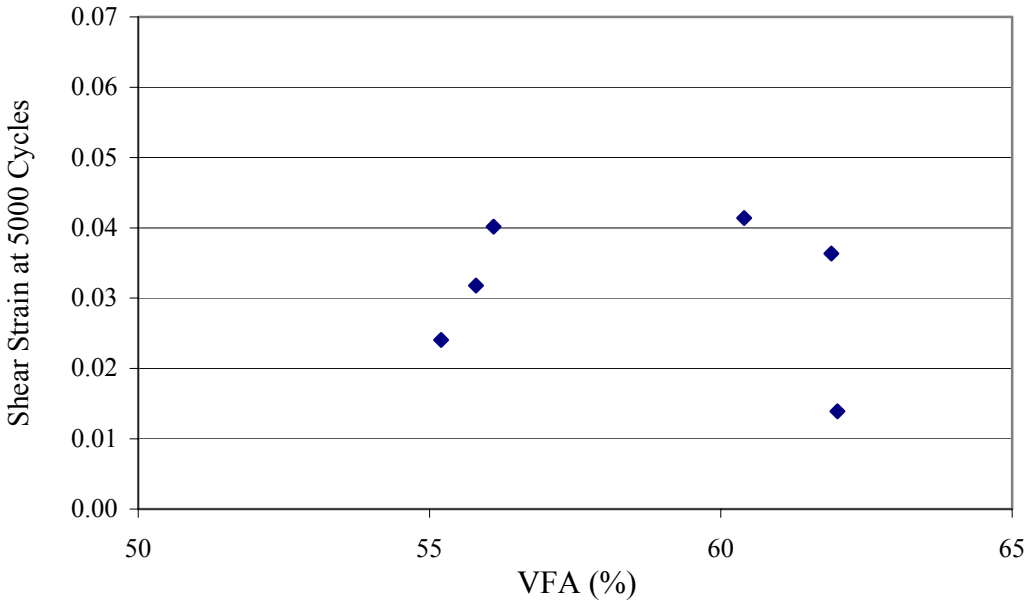

Figure 7.29 Scatter Plot of Shear Strain and VFA for LMLCS Specimens (39^0C).

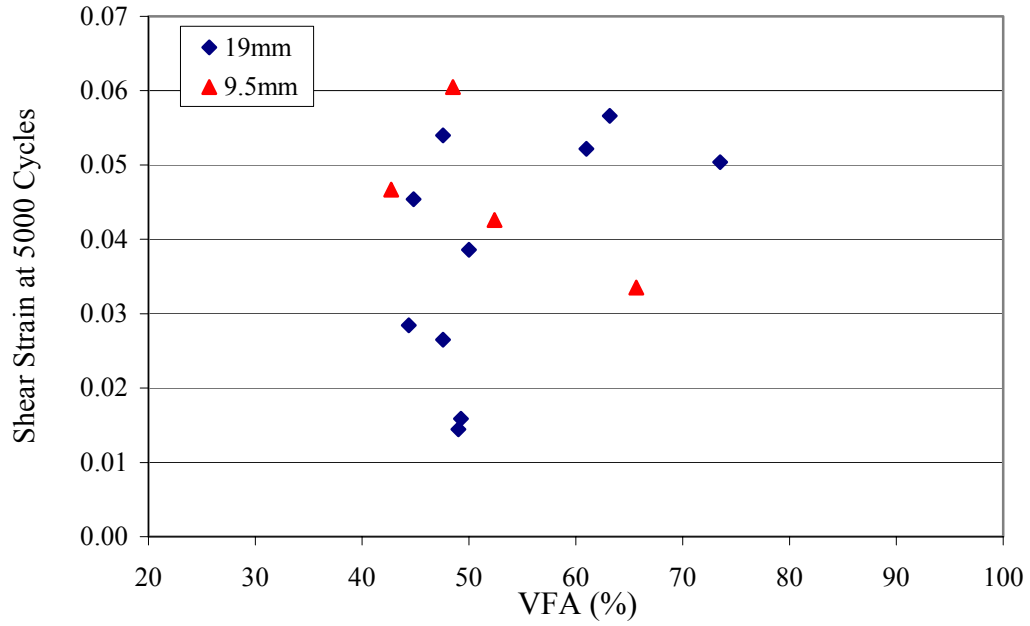

Figure 7.30 Scatter Plot of Shear Strain and VFA for FMFC Specimens (50^0C).

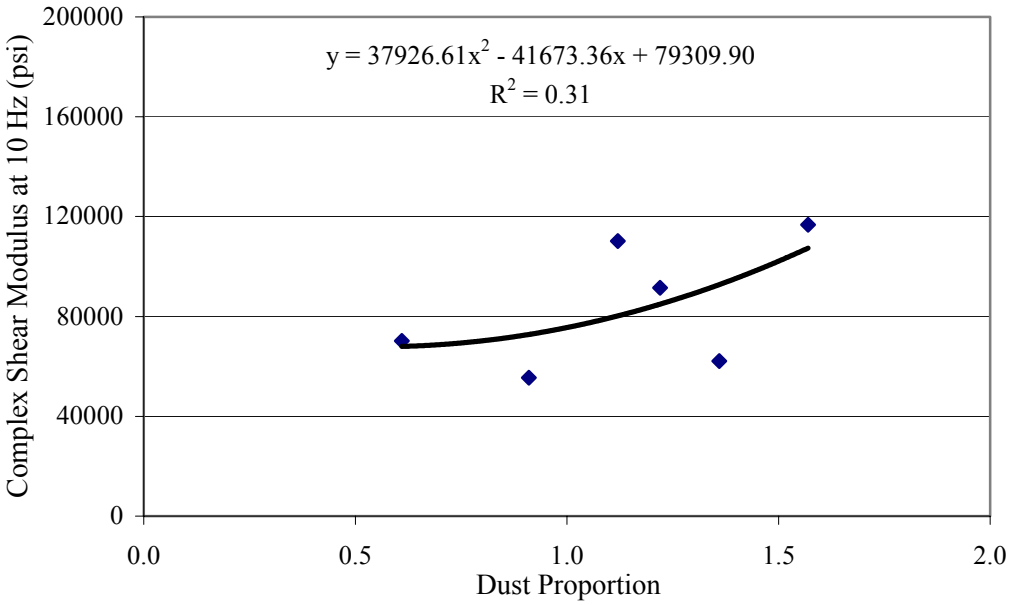

Figure 7.31 Relationship Between Complex Shear Modulus and Dust Proportion for LMLCS Specimens (39^0C).

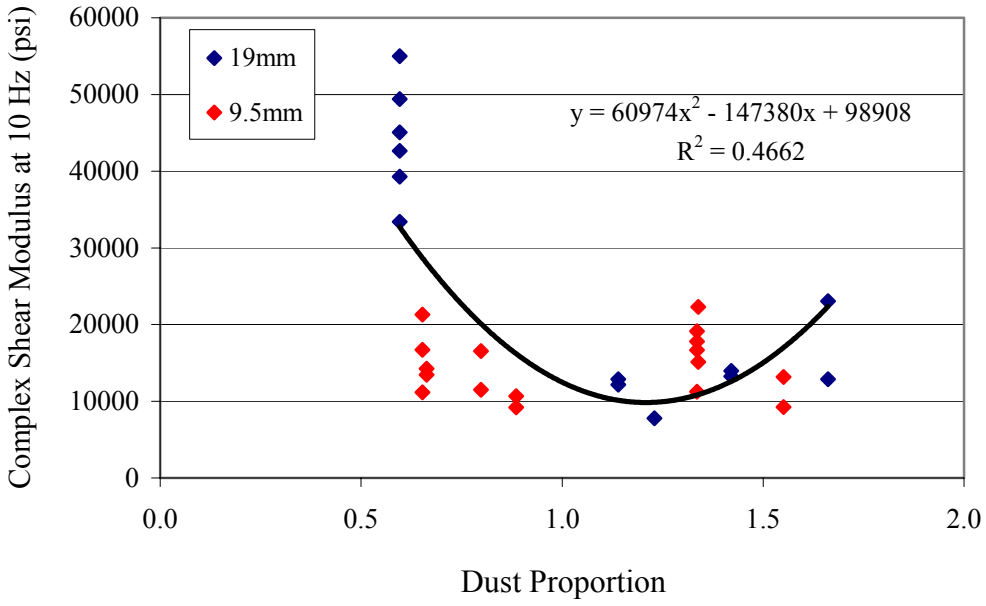

Figure 7.32 Relationship Between Complex Shear Modulus and Dust Proportion for FMFC Specimens (50^0C).

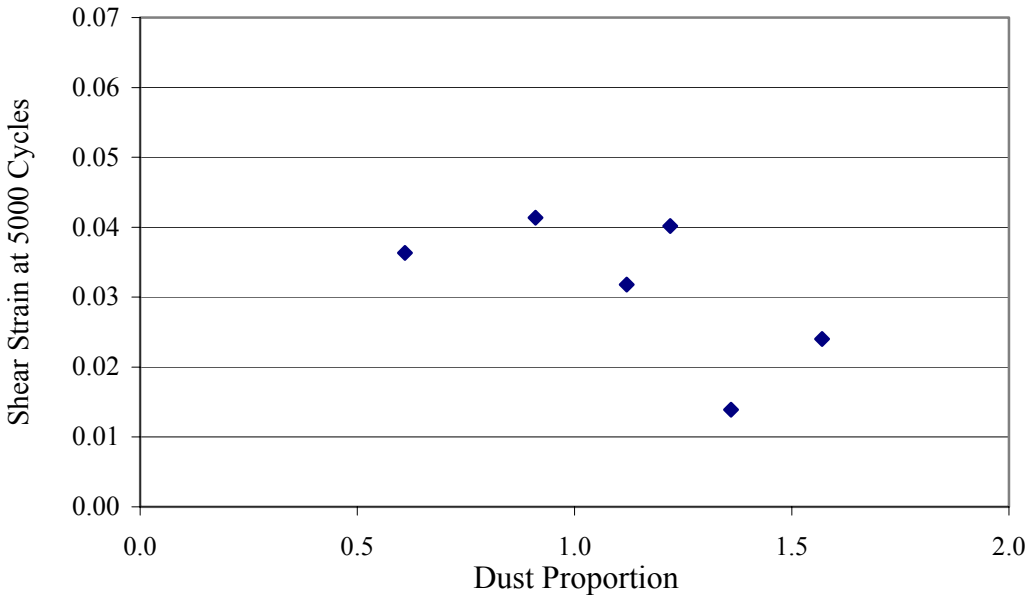

Figure 7.33 Scatter Plot of Shear Strain and Dust Proportion for LMLCS Specimens (39^0C).

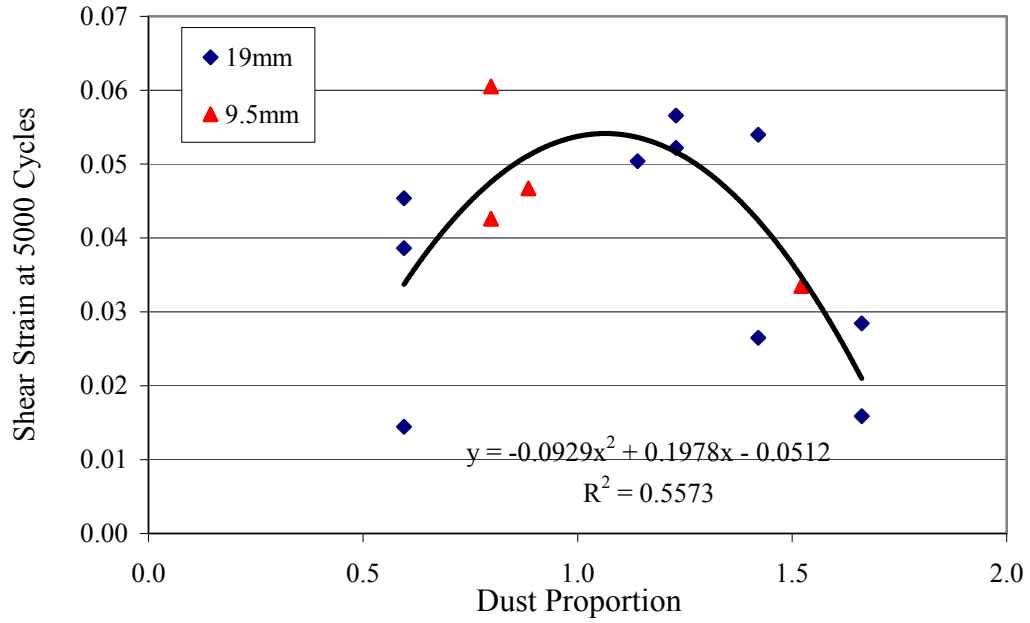

Figure 7.34 Relationship Between Shear Strain and Dust Proportion for FMFC Specimens (50^0C).

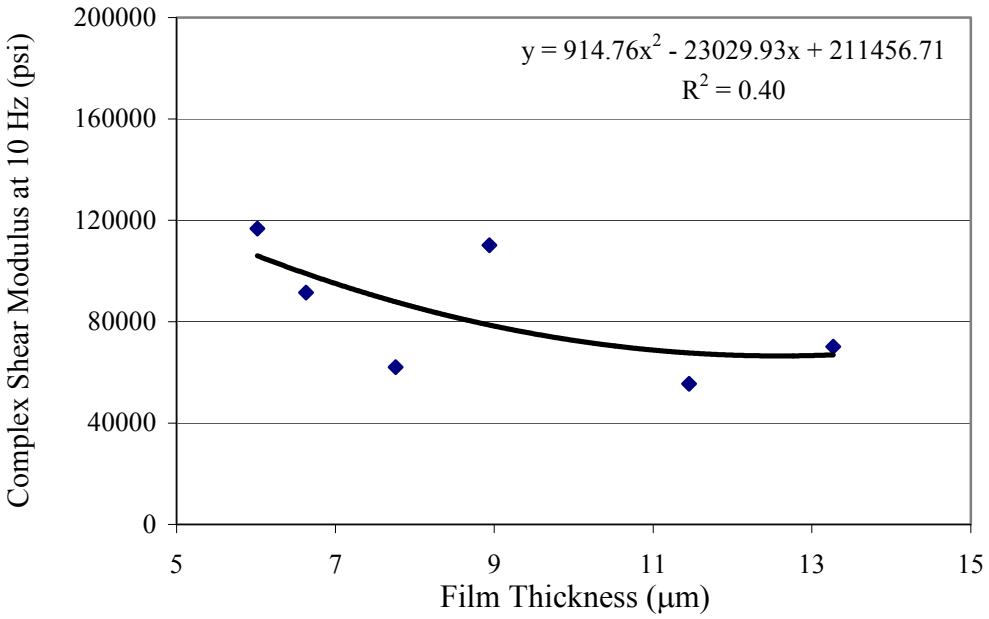

Figure 7.35 Relationship Between Complex Shear Modulus and Film Thickness for LMLCS Specimens (39^0C).

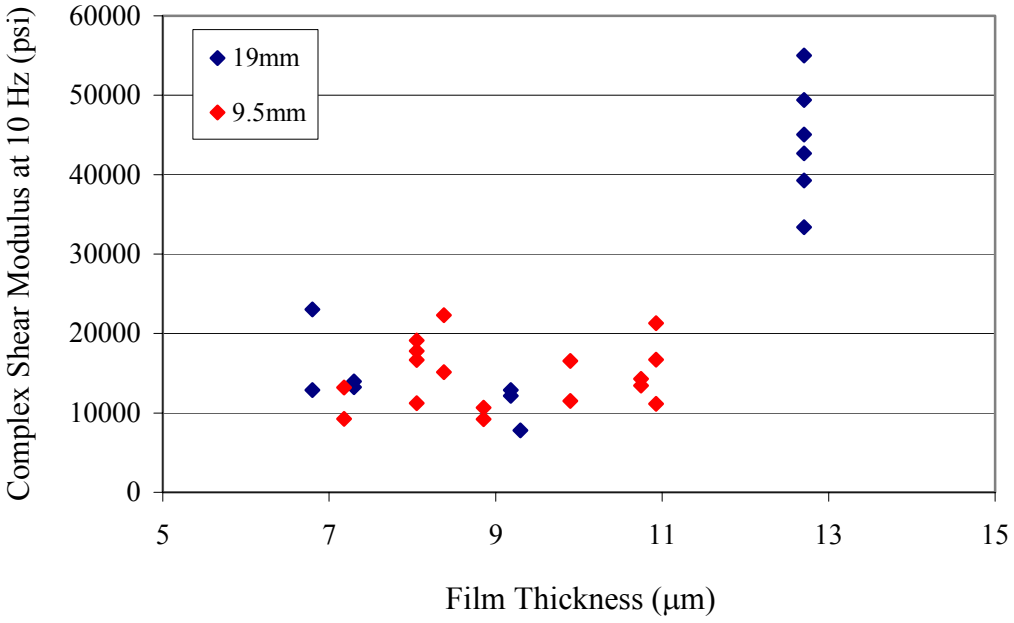

Figure 7.36 Relationship Between Complex Shear Modulus and Film Thickness for FMFC Specimens (50^0C).

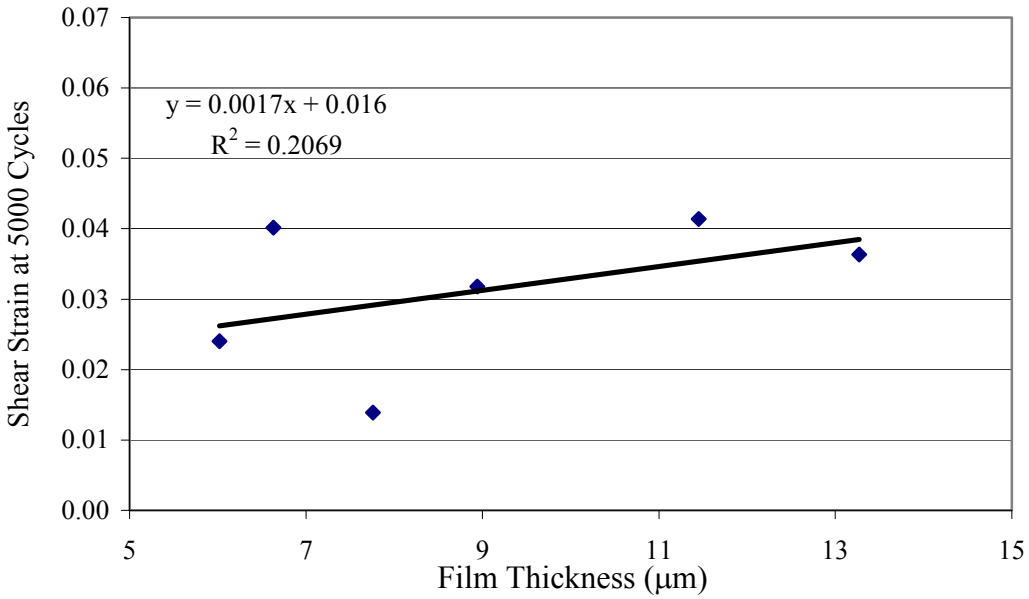

Figure 7.37 Relationship Between Shear Strain and Film Thickness for LMLCS Specimens (39^0C).

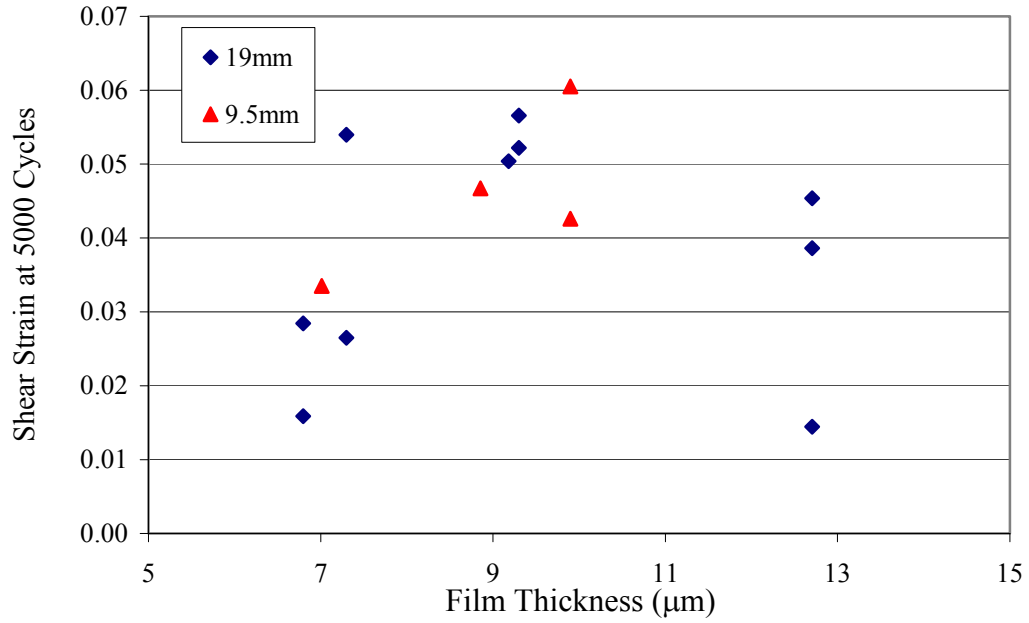

Figure 7.38 Relationship Between Shear Strain and Film Thickness for FMFC Specimens (50^0C).

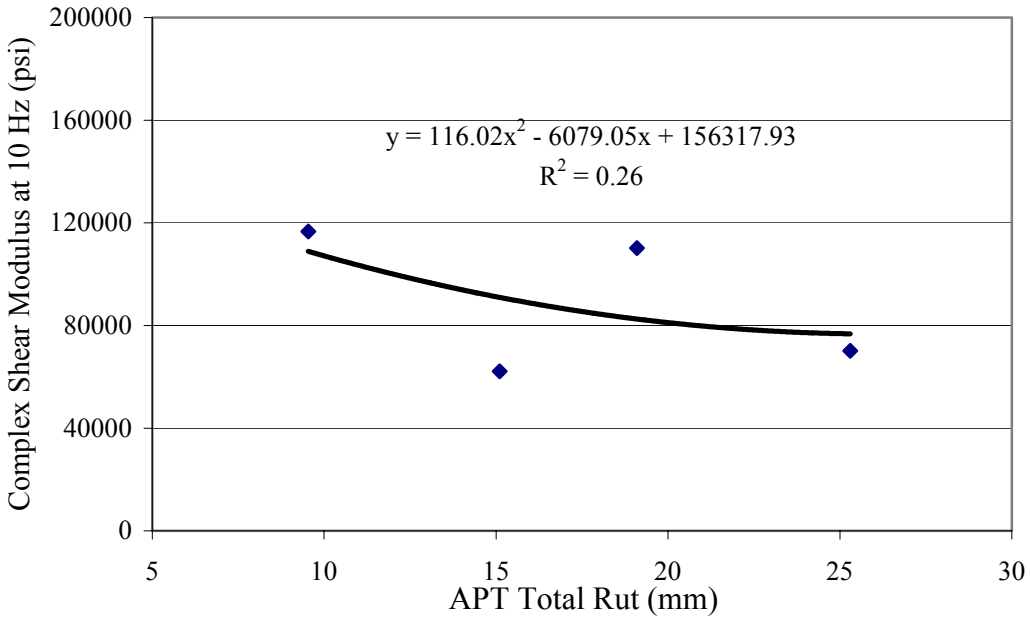

Figure 7.39 Relationship Between Complex Shear Modulus (LMLCS, 39^{0}C) and APT Total Rut (50^{0}C).

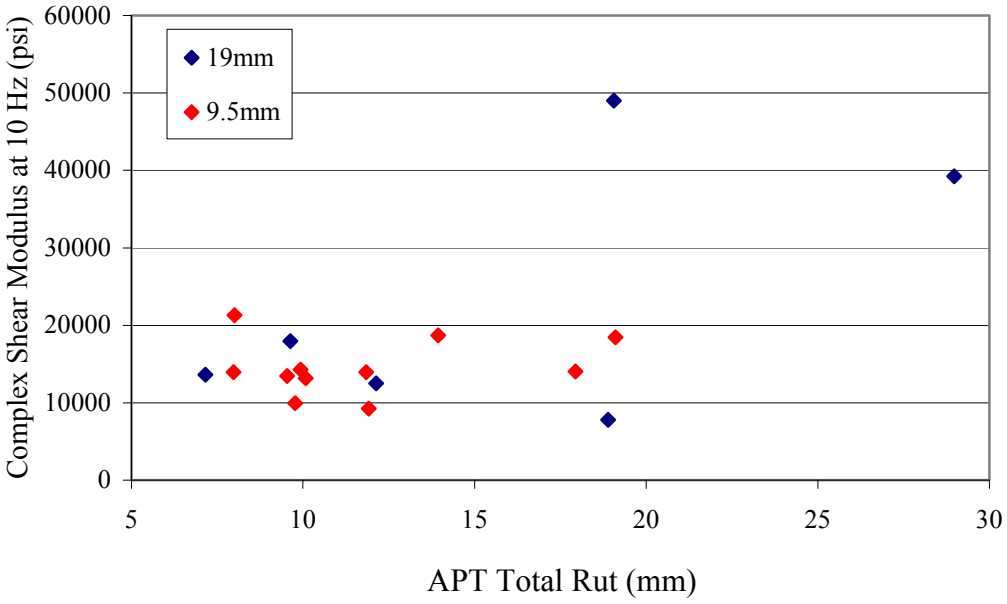

Figure 7.40 Scatter Plot of Complex Shear Modulus (FMFC, 50^{0}C) and APT Total Rut (50^{0}C).

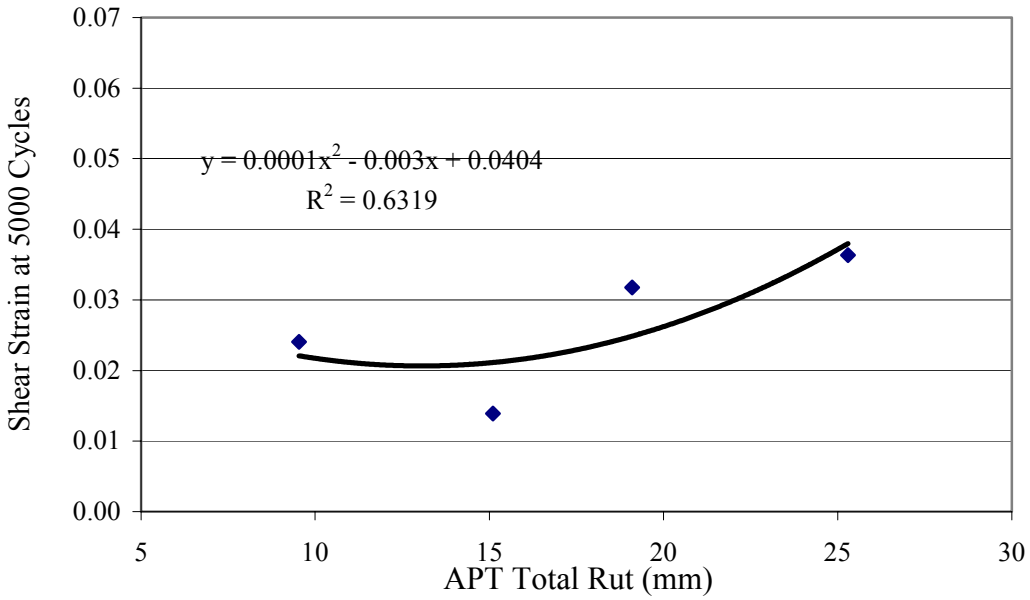

Figure 7.41 Relationship Between Shear Strain (LMLCS, 39^{0}C) and APT Total Rut (50^{0}C).

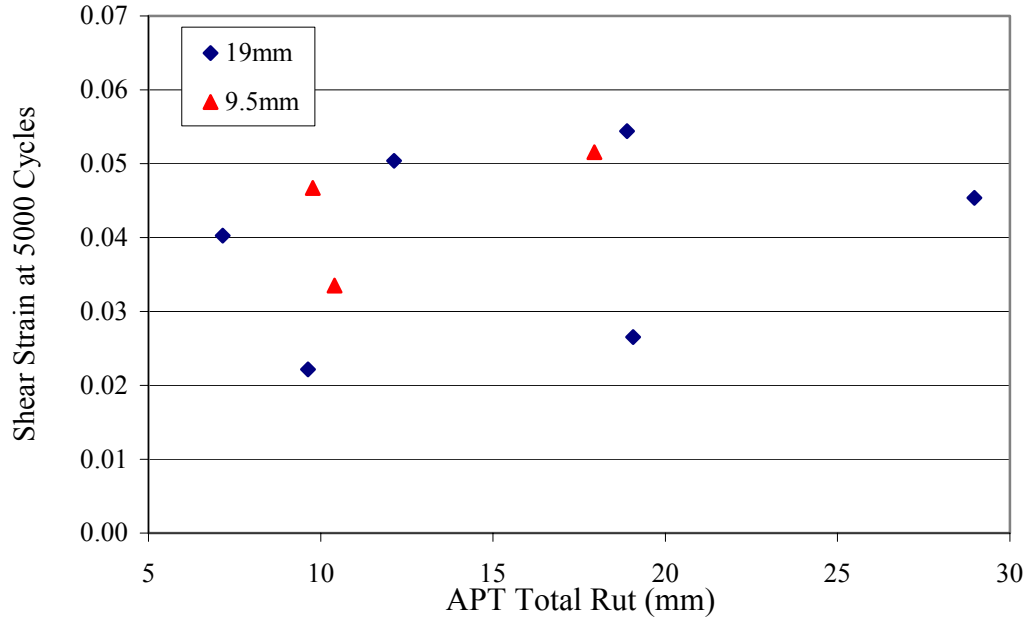

Figure 7.42 Scatter Plot of Shear Strain (FMFC, 50^{0}C) and APT Total Rut (50^{0}C).

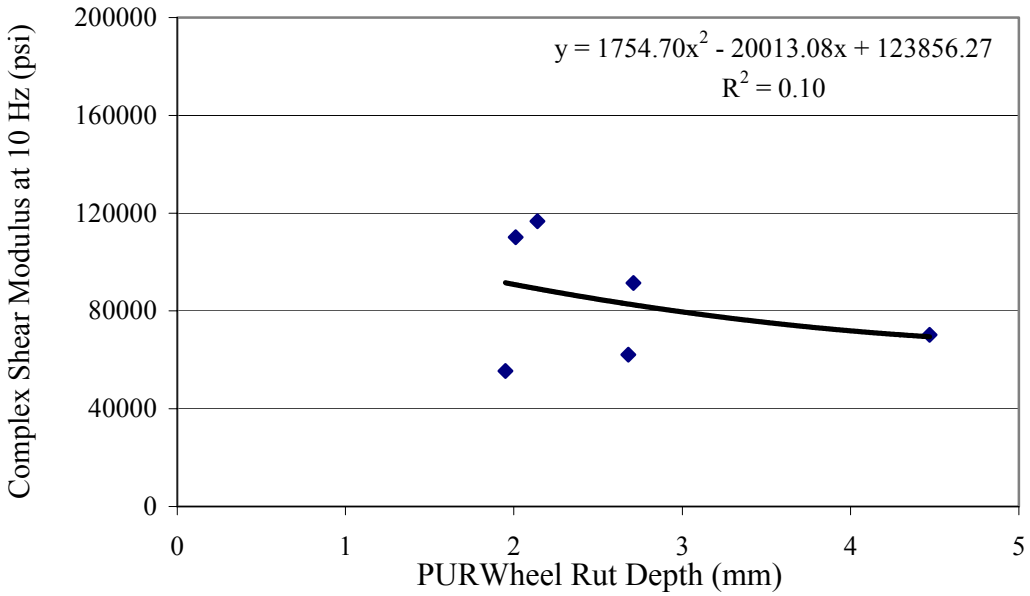

Figure 7.43 Relationship Between Complex Shear Modulus (LMLCS, 39^{0}C) and PURWheel Rut Depth (LMLCD, 60^{0}C).

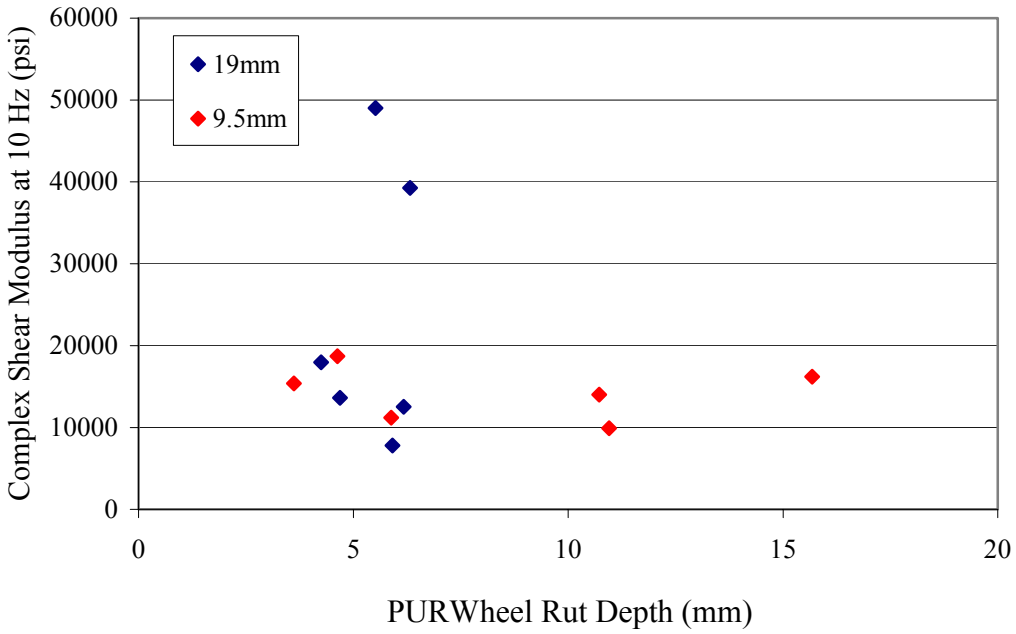

Figure 7.44 Relationship Between Complex Shear Modulus (FMFC, 50^{0}C) and PURWheel Rut Depth (FMFC, 50^{0}C).

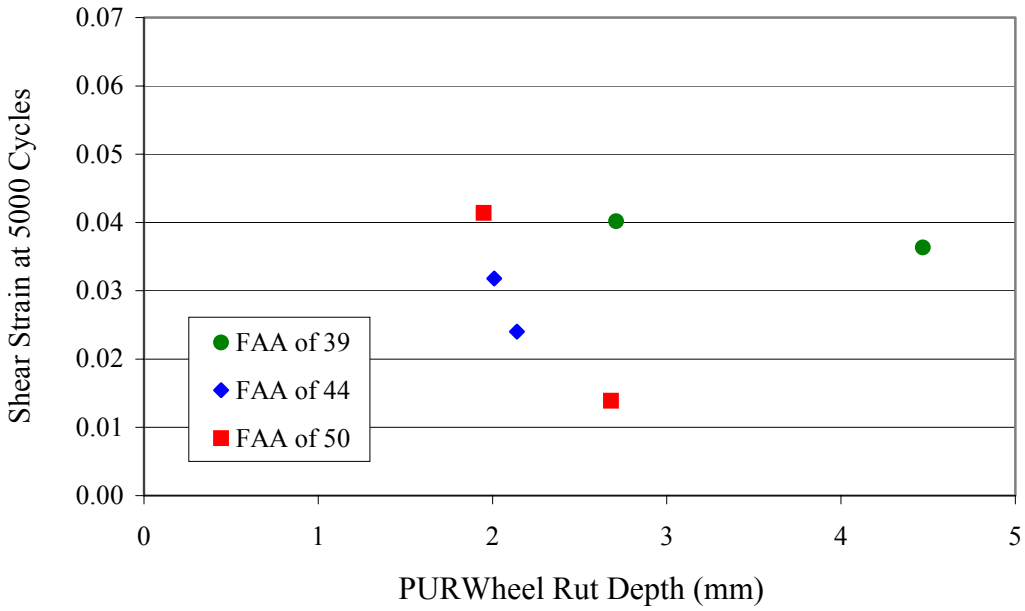

Figure 7.45 Scatter Plot of Shear Strain (LMLCS, 39^{0}C) and PURWheel Rut Depth (LMLCD, 60^{0}C).

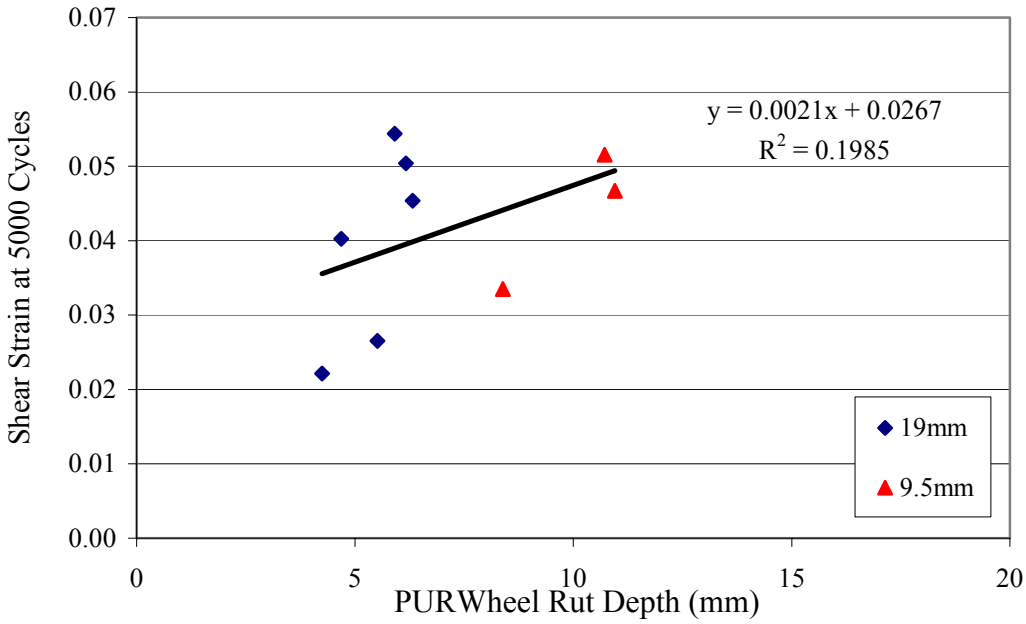

Figure 7.46 Relationship Between Shear Strain (FMFC, 50^{0}C) and PURWheel Rut Depth (FMFC, 50^{0}C).

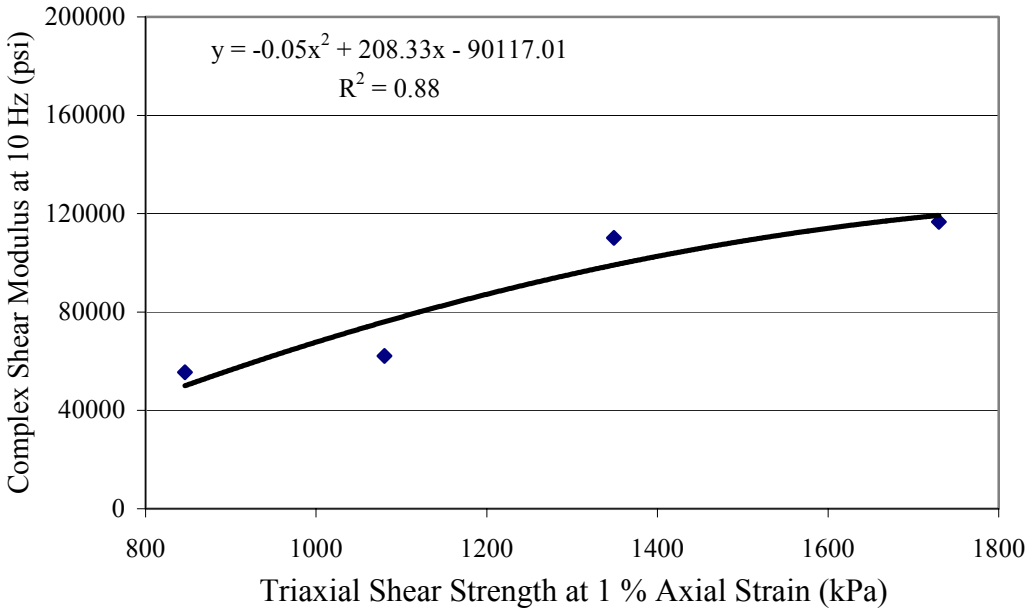

Figure 7.47 Relationship Between Complex Shear Modulus (LMLCS, 39^0C) and Triaxial Shear Strength (LMLCD, 60^0C).

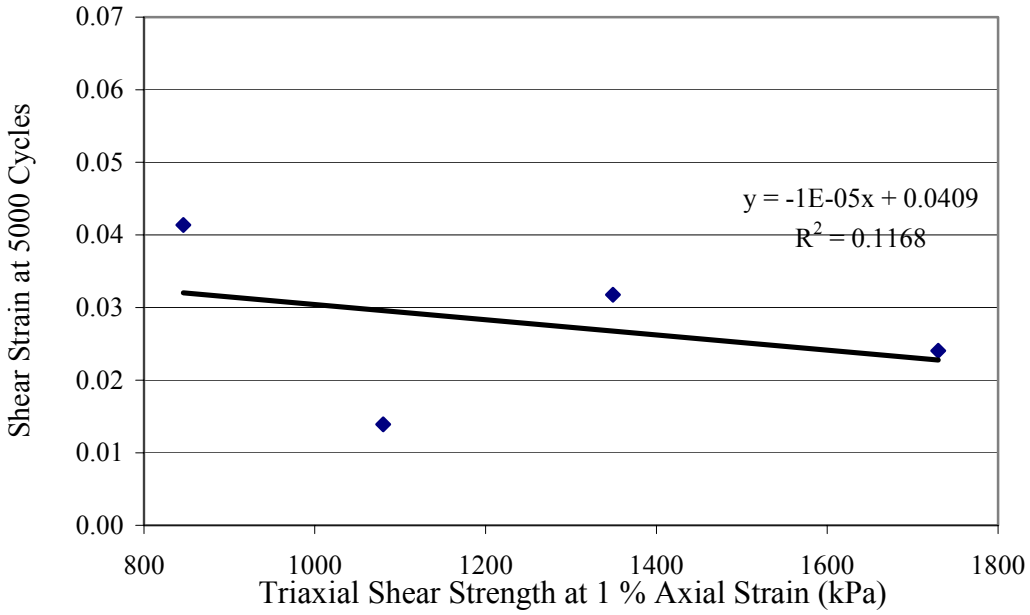

Figure 7.48 Relationship Between Shear Strain (LMLCS, 39^0C) and Triaxial Shear Strength (LMLCD, 60^0C).

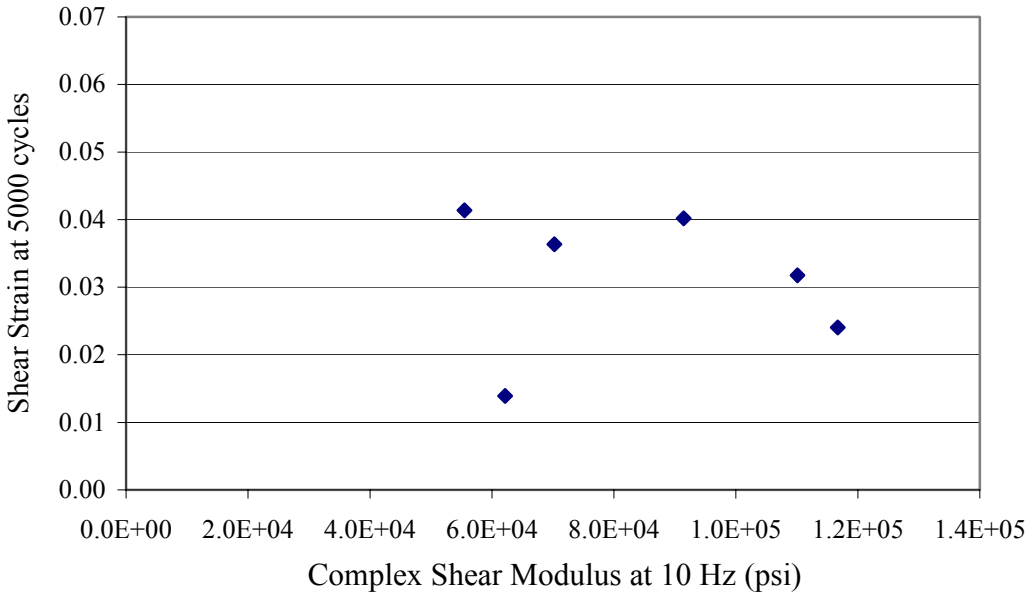

Figure 7.49 Scatter Plot of RSCH and FSCH Test Results for LMLCS Specimens (39^0C).

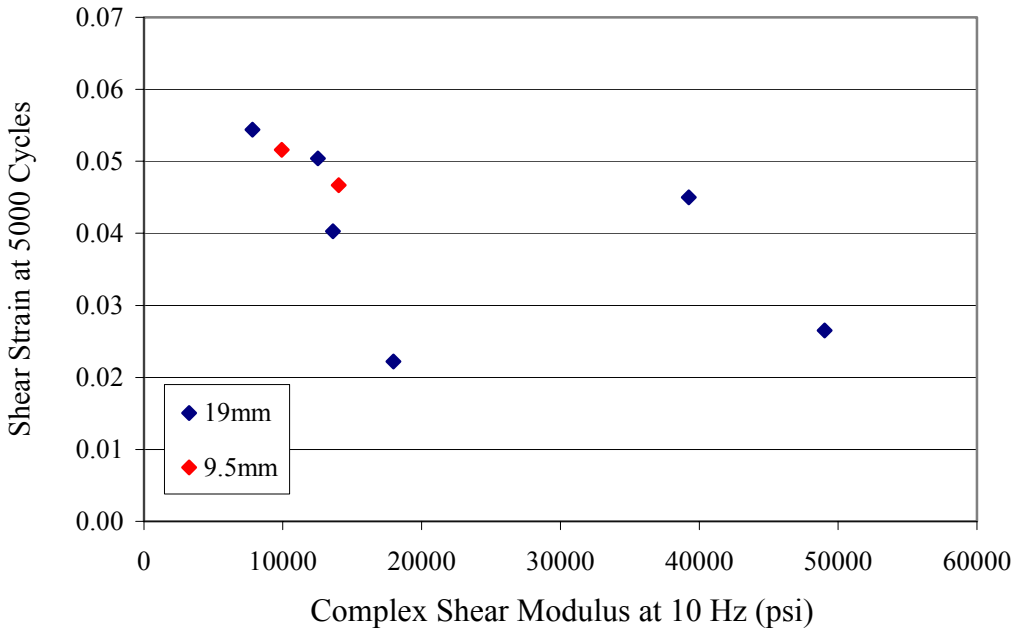

Figure 7.50 Scatter Plot of RSCH and FSCH Test Results for FMFC Specimens (50^0C).

8 FINITE ELEMENT ANALYSIS

8.1. Advantage of Finite Element Analysis

APT and PURWheel test results are highly dependent on testing conditions, such as test temperature, tire pressure, load magnitude, wheel speed, size and thickness of the test slabs, boundary conditions and wheel path position. Because of these variations, the usefulness of accelerated pavement testing would be greatly enhanced through rational analysis of the time dependent material properties, loading methods, real geometries, boundary conditions, tire pressures, wheel load magnitudes and wheel path positions. Such a detailed analysis would not only make possible comparison and extrapolation of the test results but also make it possible to compare test results across different testing devices or facilities. In addition, this systematical analysis would make the prediction of in service pavement performance possible in a rational way instead of using empirical methods.

There were two purposes for employing finite element analysis in this study:

1. The first purpose was to develop simple and reliable models to study the main factors in the APT and PURWheel tests that significantly impacted measured rutting performance. Modeling and analyzing of these factors would enhance understanding of the testing mechanism and allow extrapolation of the test results.
2. The second purpose was to back-calculate the basic time dependent material properties (creep model parameters) of the HMA mixtures tested. The back-calculated parameters were then used to compare APT and PURWheel test methods.

8.2. Material Model

HMA mixture is a time, temperature, and stress dependent material. HMA mixture subjected to repeated loading exhibits the elastic, plastic, visco-elastic, and visco-plastic responses [Perl, et al, 1983]. The elastic properties do not contribute to permanent deformation and can be modeled by modulus of elasticity and Poisson's Ratio. The time dependent plastic properties contribute to the permanent deformation that is cumulative under repeated loading. A creep model was utilized to characterize the time dependent material properties for finite element analysis.

The creep model used in the analysis is formulated as follows:

$$\dot{\varepsilon} = A\sigma^n t^m \quad \text{.....(8.1)}$$

where: $\dot{\varepsilon}$ = creep strain rate
σ = stress level
t = time
A, m, and n = constants

Equation 8.1 is termed the Bailey-Norton law [Kraus, 1980]. A, m, and n are dependent on temperature and HMA properties.

When rutting and total loading time (number of wheel passes) are plotted on a log-log scale, the creep parameter A impacts the intercept between rut depth and initial time. The effect of parameter A on the intercept is presented in Figure 8.1. The plot indicates that the predicted maximum rut depth increased in a parallel manner as the A value increased while other factors were kept constant.

The creep parameter m ranges from –1 to 0. When rutting and total loading time (number of wheel passes) are plotted on a log-log scale, the creep parameter m impacts both the slope and the intercept of rut depth versus time curve. The effect of parameter m on the curve slope and intercept is presented in Figure 8.2. The plot suggests that as the

m value decreased (closer to –1.0) the curve slope decreased and the curve intercept increased.

The creep parameter *n* is dependent on the contact tire pressure. The contact tire pressure in APT and PURWheel was kept constant at 620 kPa (90 psi). Accordingly, the parameter *n* was fixed at 0.8, following a previous finite element study using the INDOT APT facility (Huang, 1995).

8.3. Load Application Method

The main idea of loading application method is to convert the actual wheel loading mechanism into a time variable (equation 8.1). This technique allows the wheel speed, number of wheel passes, and transverse wander wheel be considered in the model. An ideal method to simulate the actual wheel loading is the application of a repeated step load function. This method involved tremendous computing times. Therefore, a single step load function was adopted in order to simplify the loading condition without sacrificing accuracy.

A single step load function for the entire wheel path was first successfully adopted by Huang (1995) and subsequently by Pan (1997). In this method, the loading time representing a single wheel pass on an element was cumulatively added to form a total loading time for that element during the whole testing duration. This total cumulative loading time was the same for every element under the wheel path and was applied over the wheel path elements simultaneously. The schematic diagram of using total cumulative time in a single step is presented in Figure 8.3.

8.4. INDOT/Purdue APT Modeling

8.4.1. Model Geometry

Initially, a three-dimensional finite element model was developed to simulate APT testing. In the middle of the mesh, the predicted rutting was uniformly distributed along the longitudinal (traffic) direction. There was almost no horizontal deformation in the longitudinal direction except at the very end of the test lane. This resulted from symmetry of the loading configuration and the mesh geometry in the transverse direction and similarity along the longitudinal direction. Accordingly, the three dimensional model could be reduced to a two-dimensional plane-stain model without significant difference in results. The computing time was reduced significantly by using the two dimensional model.

A plane strain element type CPE4 in the ABAQUS two-dimensional solid element library was utilized REF. The element is presented in Figure 8.4. The active degrees of freedom associated with each node are two translational degrees of freedoms, u_x, and u_y. The developed two-dimensional finite element mesh is presented in Figure 8.5. The mesh dimension was 1524 mm (60 in.) long and 76.2 mm (3 in) thick. There were 900 elements and 1,057 nodes in the mesh. The model has six element layers in the vertical direction in order to maintain a good aspect ratio (length to height ratio of 0.8). Symmetry was not applied in the model in order to accommodate transverse wheel wander analysis.

8.4.2. Boundary Conditions

Boundary conditions significantly influence model response. Two different boundary conditions were assigned to the bottom and edge of the HMA layer. The contact between the bottom of HMA layer and the underlying concrete slab was modeled as a bonded contact. The translations of the node on the bottom of the asphalt layer were constrained in order to prevent separation from and sliding along the element surface.

The edge of HMA layer was modeled as an elastic foundation because the HMA layer would move laterally under repeated vertical load.

8.4.3. Tire Pressure Distribution Model

As previously stated in Section 4.3, a 40 kN (9 kips) load was applied to dual tires with 620 kPa (90 psi) inflation pressure in APT. The tire print is presented in Figure 8.6. Review of transverse profiles indicated that the tire treads influenced the deformed profile. This observation suggests that the pressure distribution among the tire treads was non-uniform. The 3D non-uniform tire pressure distribution has been studied with the Vehicle-Road Surface Pressure Transducer Array (VRSPTA) system (De Beer, et al., 1997). The VRSPTA test results were interpolated for determination of non-uniform tire pressure distribution for the APT loading model. The calculated tire pressure distribution is presented in Figure 8.7. Figure 1.8 is a comparison of predicted and observed profiles for an APT test. Review of the figure indicates that the rutting profile resulting from the application of non-uniform tire pressure distribution was more similar to the observed rutting profile in APT tests than would be observed with the use of a uniform contact stress.

8.5. PURWheel Modeling

8.5.1. Model Geometry

A three-dimensional finite element model was developed to simulate PURWheel tests. Based on successful application in previous pavement analyses, an eight-node, linear brick element with reduced integration (C3D8R) in the ABAQUS element library was used (Zaghloul and White, 1993, 1994, Huang, 1995, Pan, 1997). The element is presented in Figure 8.9. The active degrees of freedom associated with each node were three translational degrees of freedoms, u_x, u_y, and u_z.

Because of symmetry in the transverse and longitudinal directions of the slab geometry and the loading configuration, a quarter of the slab was modeled. The three dimensional PURWheel finite element mesh is presented in Figure 8.10. The mesh consisted of 3,500 elements and 4,536 nodes. A typical example of the deformed shape of the mesh is presented in Figure 8.11.

8.5.2. Boundary Conditions

Two different boundary conditions were assigned to the bottom and edge of PURWheel test slab. Because there was no gap between the bottom of slab and its mounting steel box and the slab could not slide over the steel box during the test, the nodes at the bottom of the slab were fixed and no relative movements in all directions were allowed. Because the gap between the slab perimeter and the box was filled with plaster and no permanent deformation of plaster was observed during and after tests, the nodes at the slab perimeter were fixed and no relative movements in all directions were allowed.

8.5.3. Tire Pressure Distribution Model

As previously stated in Section 5.4, a 1.7 kN (385 lb.) load was applied to a tire with 793 kPa (115 psi) inflation pressure in PURWheel. The actual vertical force was measured with a balance and it was 1.5 kN (334.1 lb.). The contact area was determined from the measured tire print presented in Figure 8.12. The gross contact area was 2394 mm^2 (3.712 in^2) and resulted in a gross contact pressure of 620 kPa (90 psi). However, when only the treads was accounted for, the actual contact area was 1800 mm^2 (2.793 in^2) and resulted in actual contact pressure of 824.8 kPa (120 psi).

The actual tire print was modeled with five rectangular strips as shown in Figure 8.13. The actual contact pressure between the tire and slab may not be uniformly

distributed. The contact pressure distribution depends on tire inflation pressure, tire dimensions, tire load, and the deformed shape of the test slab. It was extremely difficult, if not impossible, to measure the actual tire contact pressure due to the scale and its irregular pattern of the tire used in PURWheel. Accordingly, it was assumed that the contact pressure was uniformly distributed over the contact area. Considering the small size of the tire, this assumption is reasonable and would not significantly impact the predicted rutting response. For example, rutting profile resulting from the tire pressure distribution model is presented in Figure 8.14. Review of the plot shows that the rutting profile resulting from the application of a uniform tire pressure distribution with five strips was similar to the observed rutting profile in PURWheel tests.

8.6. Model Application

8.6.1. Modeling Wheel Wander for APT Tests

There are several factors that impact transverse wheel path distribution (wander) in field pavements. They include: roadway geometry, lateral clearance, traffic condition, roadway characteristics, weather conditions, and vehicle type. In the APT, wheel wander was randomly applied in a normal distribution fashion. The maximum total wander distance was 260 mm (10.2 in.). As previously discussed in Section 4.4.2, the transverse rutting profiles for no wander and wheel wander cases were different as presented in Figure 8.15.

In modeling the wheel wander feature for APT tests, the actual transverse load distribution was converted into a loading time distribution in the transverse direction. Because the loads were applied by a series of tire treads, the total loading time for any point across the testing lane was the sum of the loading times on the tire treads. Each tread had the same normal distribution across the transverse direction of the slab with different mean position (centerline) but equal standard deviation. The total loading time

distribution in the transverse direction used for the APT test modeling is presented in Figure 8.16.

Review of Figure 8.16 reveals that the total loading time under the original tire print position (no wander) significantly reduced with increasing wander distance. On the contrary, the loading time between the tires gradually increased from zero with wander distance. In addition, the loading time was widely distributed in the transverse direction with increased wander distance. The effect of individual tire treads disappeared when the wander distance was greater than 76.2 mm (3 in.). When the wander distance was approximately equal to the centerline distance between dual tires, the loading time distribution was similar to that for a single large tire without wander.

An example of the effect of loading time distribution on deformed surface profiles is presented in Figure 8.17. Review of the plots shows that as the wander distance increased the uplift between the dual tires significantly decreased. The maximum rut depth and the total rut decreased as the wander distance increased. It is noted that the shape of the deformed surface profile was similar to the loading time distribution profile. A comparison between observed and predicted rutting profiles for a wander distance of 260mm is presented in Figure 8.18. The comparison indicates that the predicted profile is very similar to the observed profile.

8.6.2. Modeling Wheel Speed Effect for APT and PURWheel Tests

It is common knowledge that loading speed impacts rutting because of the visco elastic properties of HMA. As loading speed increases the load becomes less destructive. This phenomenon could be conveniently modeled by converting the loading speed to loading time.

The loading time for one wheel pass was dependent on the length of the tire print and wheel speed. Consequently, loading time varied with wheel speed given that other conditions were kept constant. As the wheel speed increased, the loading time for a given

element decreased. As the loading time decreased, the predicted rutting decreased according to equation 8.1. Using this loading time concept, the rutting results from a given wheel speed could be extrapolated to other test speeds.

The effect of wheel speed on the predicted maximum rut depths corresponding to 5,000 wheel passes for a given mixture is presented in Figure 8.19 and 8.20 for APT and PURWheel tests, respectively. Because of reduced loading time, the rut depth decreased dramatically with increasing speed as expected.

8.6.3. Modeling Tire Inflation Pressure Effect for APT and PURWheel Tests

Actual tire pavement contact pressure impacts rutting. As contact pressure increases rutting increases. The contact pressure is dependent on tire inflation pressure and wheel load. Variation of tire inflation pressure impacts the contact area and the tire/pavement contact pressure.

The effect of tire inflation pressure was modeled by converting the tire inflation pressure to loading time and stress level variables. Because it was difficult to measure the real tire/pavement contact pressure, the gross contact pressure was used in this analysis. In addition, the width of the tire print and the wheel load magnitude were kept constant. Variation of tire inflation pressure resulted in variation of gross contact area. Because the tire print width was kept constant, variation of gross contact area resulted in variation in tire print length. The tire print length impacted loading time. Therefore, variation of tire inflation pressure resulted in variation of stress level and loading time.

The effect of tire inflation pressure on predicted rut depth corresponding to 5,000 wheel passes for a given mixture is presented in Figures 8.21 and 8.22 for APT and PURWheel, respectively. Review of the plots reveals that the predicted rut depths increased as the tire inflation pressure increased as expected.

8.6.4. Modeling Wheel Load Effect for APT and PURWheel Tests

Wheel load magnitude impacts rutting because wheel load impacts the gross tire/pavement contact pressure. The effect of wheel load magnitude was modeled by converting the wheel load to loading time and stress level variables. The width of the tire print was kept constant. Variation of wheel load magnitude resulted in variation of gross contact area. Because the tire print width was kept constant, variation of gross contact area resulted in variation of tire print length. The tire print length impacted loading time. Therefore, variation of wheel load magnitude resulted in variation of stress level and loading time.

The effect of wheel load magnitude on predicted rut depth corresponding to 5,000 wheel passes for a given mixture is presented in Figures 8.23 and 8.24 for APT and PURWheel, respectively. Review of the plots reveals that the predicted rut depth increased as the wheel load magnitude increased as expected.

8.6.5. Modeling Specimen Thickness Effect for APT and PURWheel Tests

Pavement thickness significantly impacts rut depth magnitude. The effect of specimen thickness was modeled by changing the mesh thickness while other parameters were kept constant. The effect of specimen thickness on predicted rut depth corresponding to 5,000 wheel passes for a given mixture is presented in Figures 8.25 and 8.26 for APT and PURWheel, respectively. The plots show that predicted rut depth increased as the specimen thickness increased. This observation suggests that as the mesh thickness decreased the bonded boundary condition at the mesh bottom resulted in less rut depth. This explanation is reasonable because the translation in each direction were constrained at the mesh bottom.

Thickness of the APT test lanes varied from 76 mm to 125 mm for 19mm limestone mixtures. The test results were compared using a common thickness of 76mm. The conversion to a common thickness was conducted by back-calculating the creep

parameters from the actual test results with their corresponding actual thicknesses. After the creep parameters were acquired, they were used as input creep parameters to a model with a standard thickness of 76 mm (3 in). The observed rutting data for the 19mm limestone mixtures are presented in Figure 8.27. The predicted rutting based on a common thickness of 76 mm for 19mm limestone mixtures are presented in Figure 8.28. Review of the plots reveals that there was a change of performance order between the 44b4 and 50a2 mixtures. Comparison between the predicted and the observed rut depths is presented in Figure 8.29. A positive linear relationship was observed with a high r^2 value (0.83). This relationship suggests that the predicted rut depths based on a common thickness of 76mm (3 in.) were slightly less than the observed rut depths.

8.6.6. Correlation between APT and PURWheel Tests

A correlation between APT and PURWheel tests was developed by correlating the material properties that were back calculated from APT and PURWheel test results. Basically, the back calculation procedure was used to adjust the creep parameters (*A* and *m*) such that the predicted rut depths fit well with the observed data. The creep parameters back calculated from APT test results are summarized in Table 8.1 and those back calculated from PURWheel FMFC test results in Table 8.2.

The PURWheel field mixed field compacted (FMFC) specimens were slabs that were cut from APT test sections prior to traffic loading. The correlation between the back-calculated creep parameter *m* for PURWheel and APT tests is presented in Figure 8.30. A good correlation was observed. The correlation suggests that the creep parameter *m* back calculated from PURWheel test results was smaller than that back calculated from APT test results. The parameter *m* correlation and review of the plot in Figure 8.2 indicate that the creep slope for PURWheel test was less steep than that observed for APT tests given the same mixture. The correlation between PURWheel and APT based on the back-calculated creep parameter *A* is presented in Figure 8.31. The correlation is poor. Review of the plot in Figure 8.1 reveals that the parameter *A* represents the

intercept between rut depth and initial time. Therefore, the rut resistance of material was mainly influenced by parameter *m* while parameter *A* only impacted the initial behavior. The initial behavior is impacted by initial air voids. Because the initial air voids of mixtures tested in the APT were intentionally not uniform, the observed correlation is both reasonable and logical. Unlike the correlation developed in Section 5.6.2, the correlation between PURWheel and APT tests using finite element model was independent of the nominal maximum aggregate size of the mixtures. This clearly shows the ability of finite element analysis in eliminating the effect of nominal maximum aggregate size in PURWheel and APT correlations.

Table 8.1 Back Calculated Creep Parameters from APT Test Results.

Nom. Max. Size (mm)	Coarse Aggregate	FAA	Gradation	Feature	Creep parameters ($\dot{\varepsilon} = A\sigma^n t^m$)		
					A (10^{-4})	m	n
19	Limestone	39	Below	Low Density	3.5	-0.74	0.8
19	Limestone	39	Below	High Density	5.0	-0.77	0.8
19	Limestone	44	Above	Low Density	3.1	-0.83	0.8
19	Limestone	44	Above	High Density	2.9	-0.84	0.8
19	Limestone	44	Below	Low Density	4.6	-0.73	0.8
19	Limestone	44	Below	High Density	3.1	-0.81	0.8
19	Limestone	50	Above	Low Density	3.2	-0.74	0.8
19	Limestone	50	Above	High Density	5.0	-0.76	0.8
19	Granite	44	Below	Low AC	3.9	-0.90	0.8
19	Granite	44	Below	High AC	4.5	-0.79	0.8
19	Granite	50	Through	Low AC	2.8	-0.85	0.8
19	Granite	50	Through	High AC	3.0	-0.83	0.8
9.5	Limestone	44	Through	Low AC	4.1	-0.84	0.8
9.5	Limestone	44	Through	High AC	5.6	-0.79	0.8
9.5	Limestone	50	Through	Low AC	4.1	-0.74	0.8
9.5	Limestone	50	Through	High AC	4.3	-0.77	0.8
9.5	Granite	44	Below	Low AC	2.7	-0.82	0.8
9.5	Granite	44	Below	High AC	3.6	-0.80	0.8
9.5	Granite	50	Below	Low AC	4.5	-0.81	0.8
9.5	Granite	50	Below	High AC	3.7	-0.77	0.8
Range					2.7-5.6	-0.73--0.9	

Table 8.2 Back Calculated Creep Parameters from PURWheel Test Results.

Nom. Max. Size (mm)	Coarse Aggregate	FAA	Gradation	Feature	Creep parameters ($\dot{\varepsilon} = A\sigma^n t^m$)		
					A (10^{-4})	m	n
19	Limestone	44	Below	Low Density	4.1	-0.79	0.8
19	Limestone	44	Below	High Density	3.7	-0.79	0.8
19	Granite	44	Below	Low AC	3.0	-0.80	0.8
19	Granite	44	Below	High AC	3.0	-0.71	0.8
19	Granite	50	Through	Low AC	2.9	-0.75	0.8
19	Granite	50	Through	High AC	4.0	-0.78	0.8
9.5	Limestone	44	Through	Low AC	3.9	-0.72	0.8
9.5	Limestone	44	Through	High AC	4.2	-0.64	0.8
9.5	Limestone	50	Through	Low AC	2.4	-0.58	0.8
9.5	Limestone	50	Through	High AC	2.7	-0.57	0.8
9.5	Granite	44	Below	Low AC	1.5	-0.73	0.8
9.5	Granite	44	Below	High AC	1.8	-0.65	0.8
9.5	Granite	50	Below	Low AC	2.3	-0.71	0.8
9.5	Granite	50	Below	High AC	2.8	-0.68	0.8
Range					1.5-4.2	-0.57—0.8	

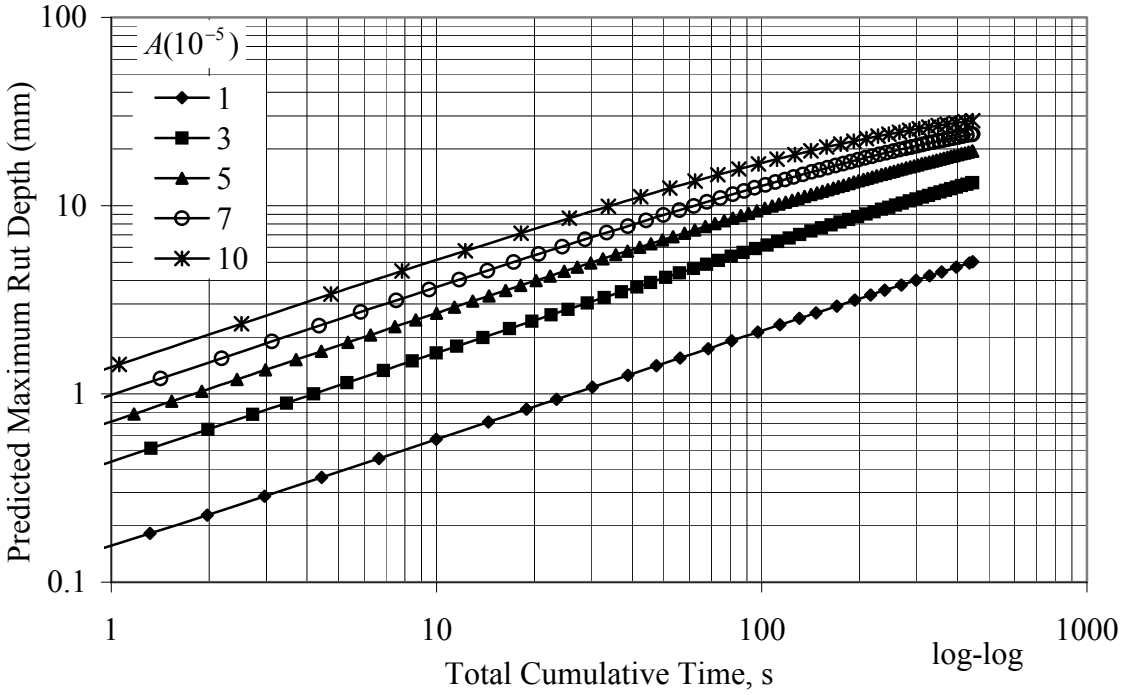

Figure 8.1 Effect of Creep Parameter *A* on Rutting Curve Intercept (APT Model).

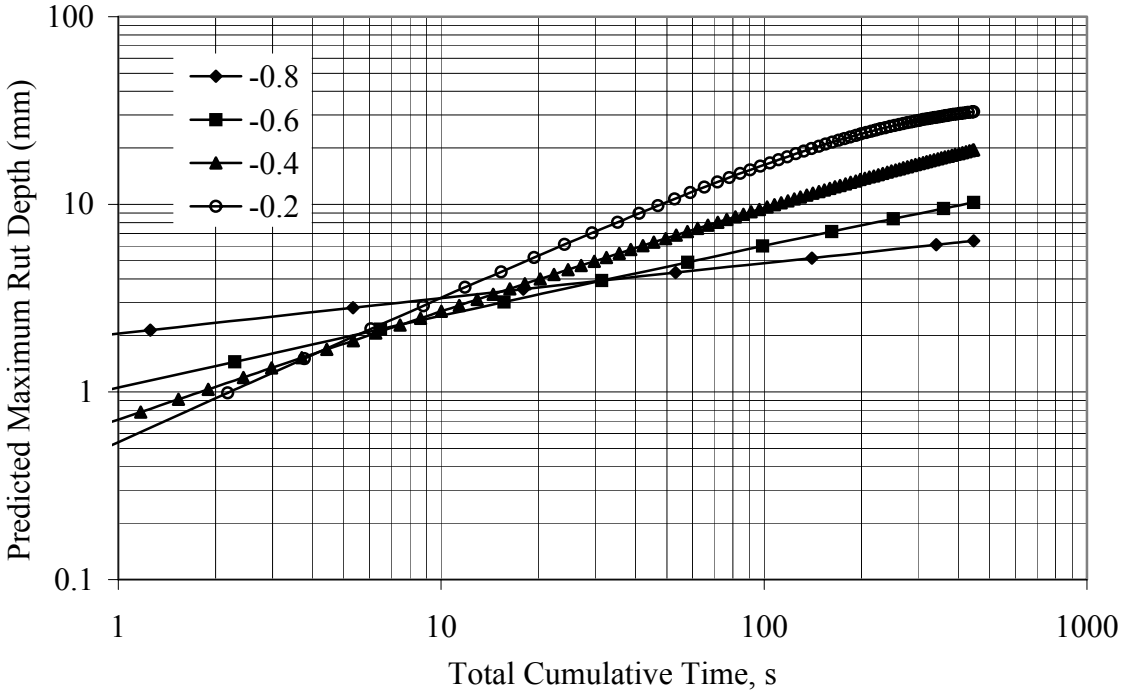

Figure 8.2 Effect of Creep Parameter *m* on Rutting Curve Slope and Intercept (APT Model).

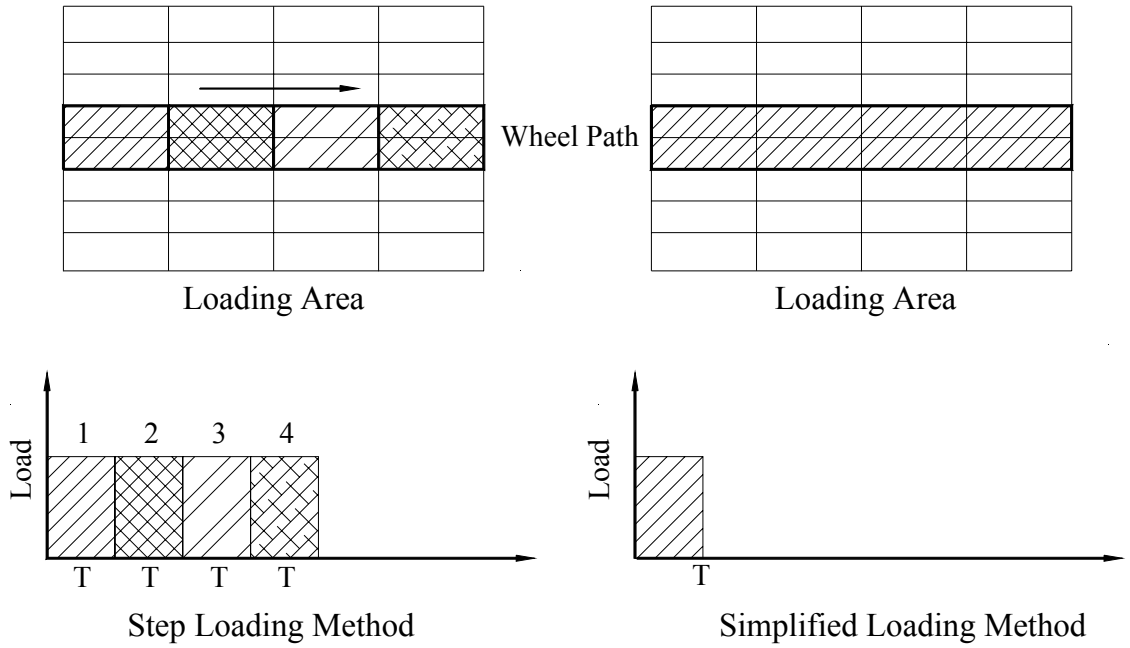

Figure 8.3 Comparison of Step and Loading Time for Repeated Step Loading and Single Step Loading.

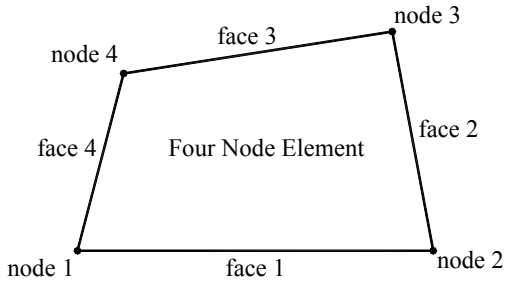

Figure 8.4 Four-node Bilinear Two-Dimensional Finite Element for APT Model.

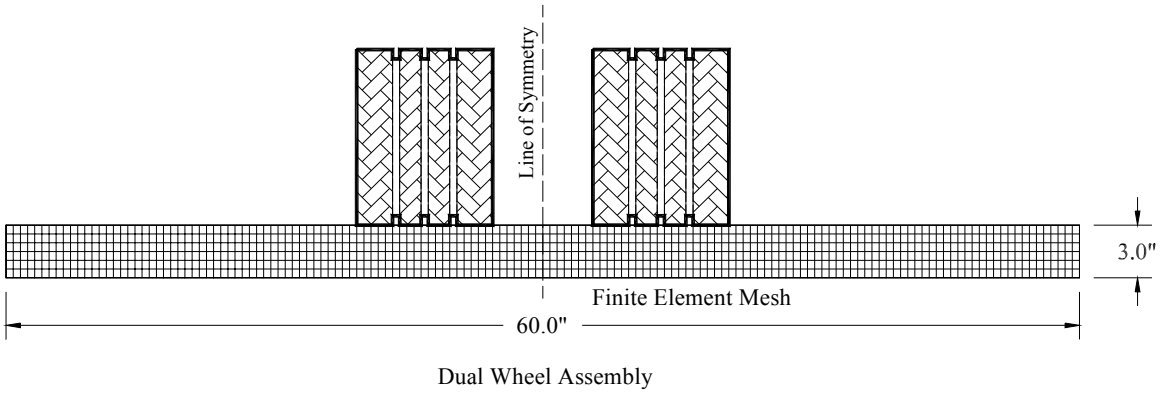

Figure 8.5 Two-Dimensional Finite Element Mesh for APT Model.

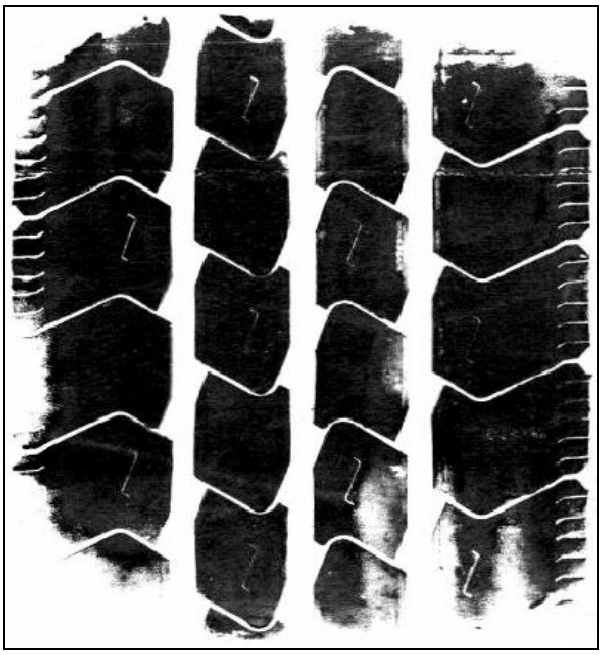

Figure 8.6 Tire Print of Tire Used in the APT.

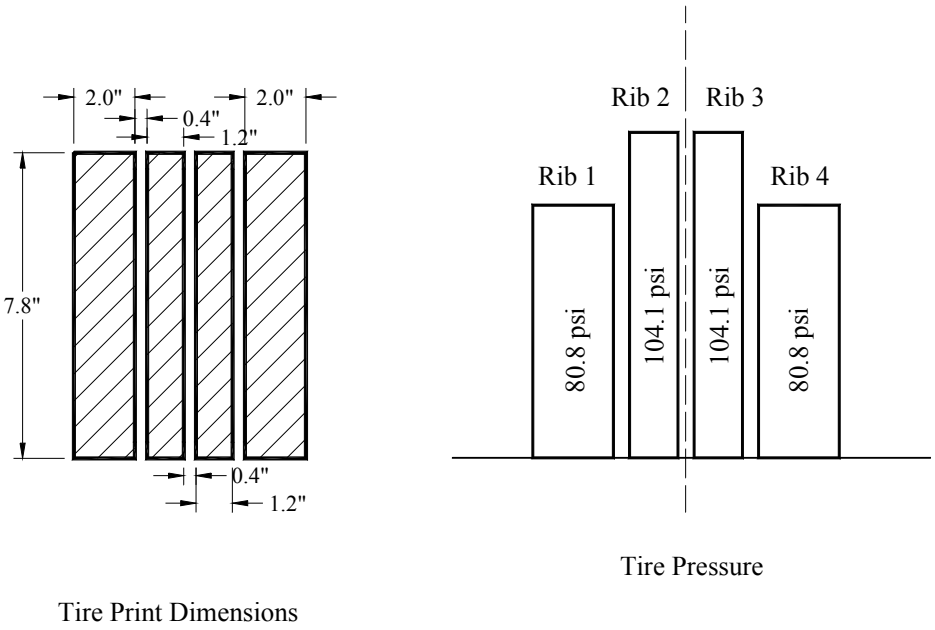

Figure 8.7 Tire Pressure Distribution for APT Loading Model.

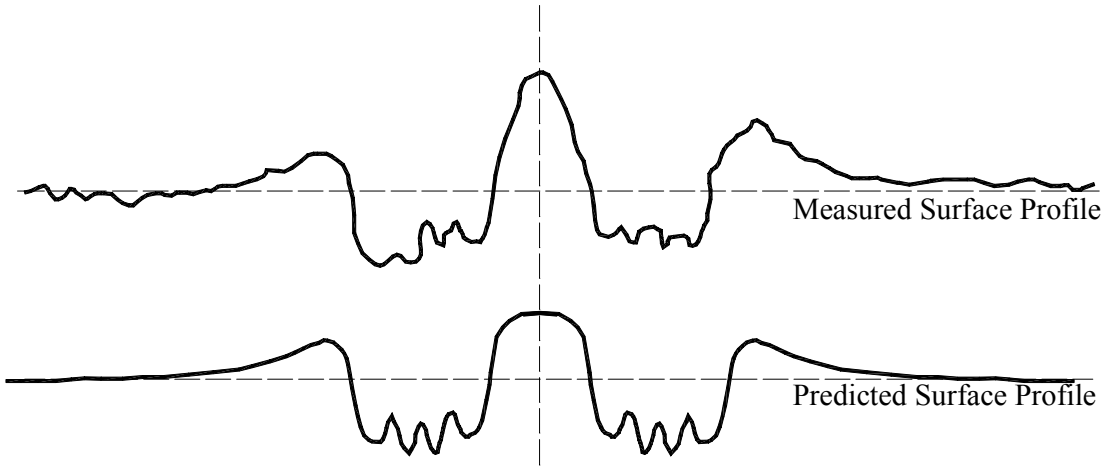

Figure 8.8 Comparison of the Rutting Profile with Non-uniform Tire Pressure Distribution for APT Test.

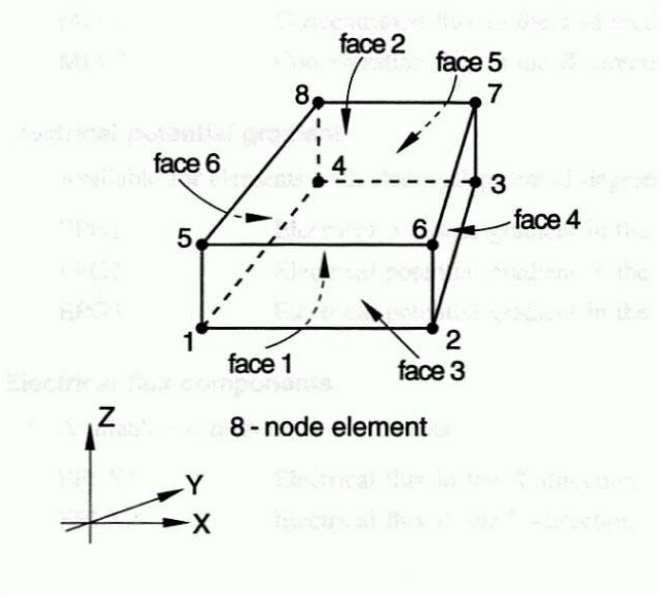

Figure 8.9 Eight-node Linear Brick Element, C3D8R for PURWheel Model.

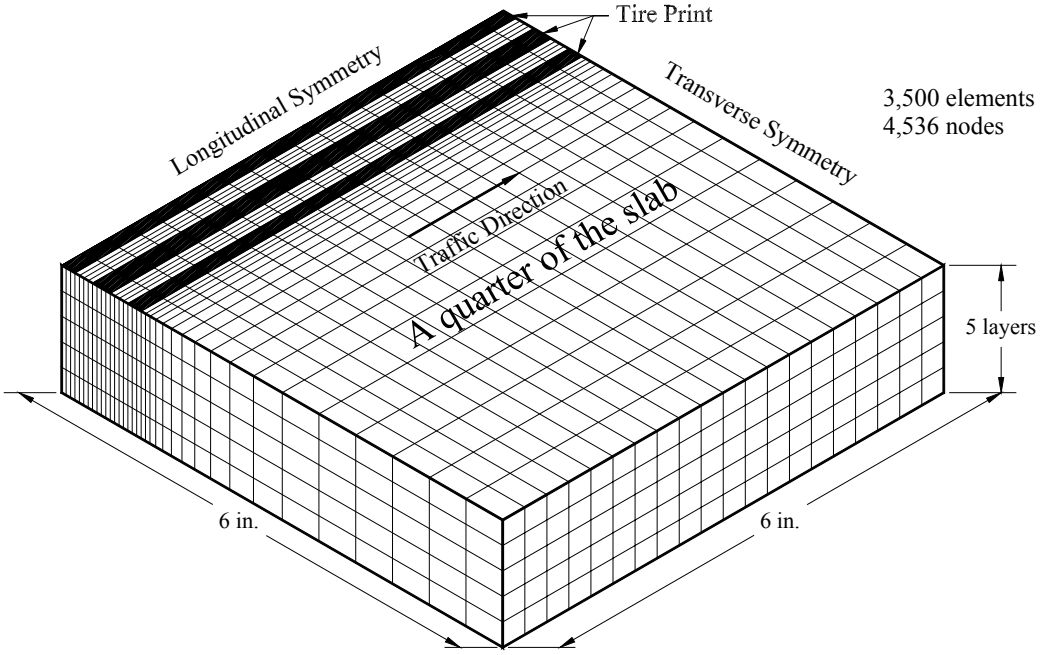

Figure 8.10 Three-dimensional Finite Element Mesh of PURWheel Test Slab.

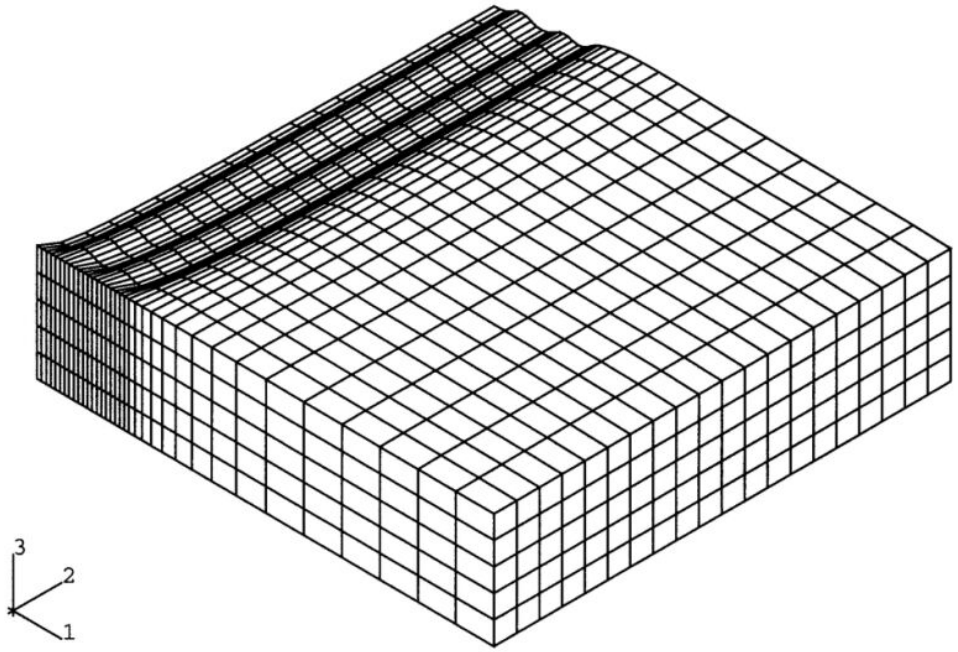

Figure 8.11 Deformed Shape of the PURWheel Finite Element Mesh.

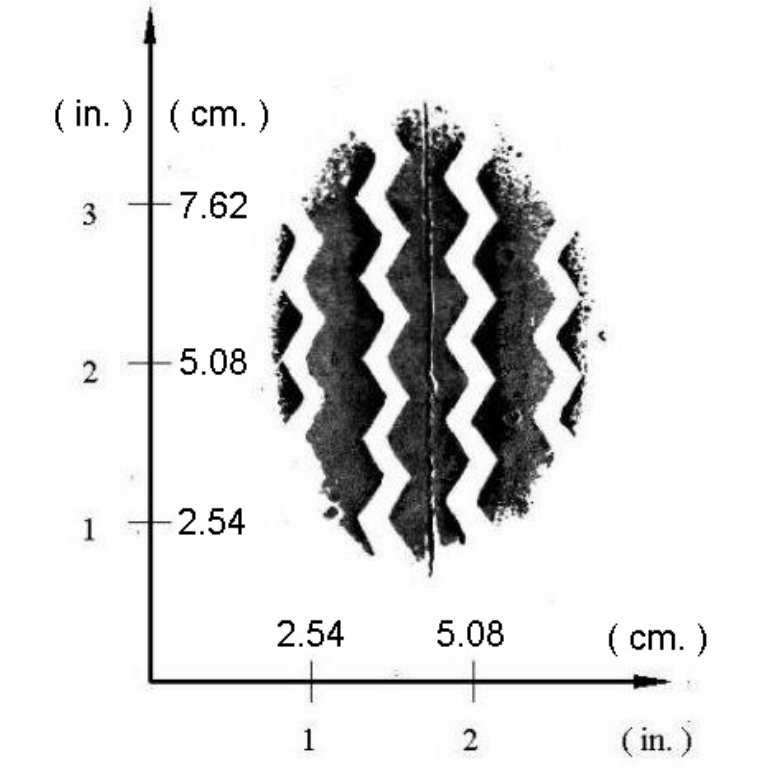

Figure 8.12 PURWheel Tire Print.

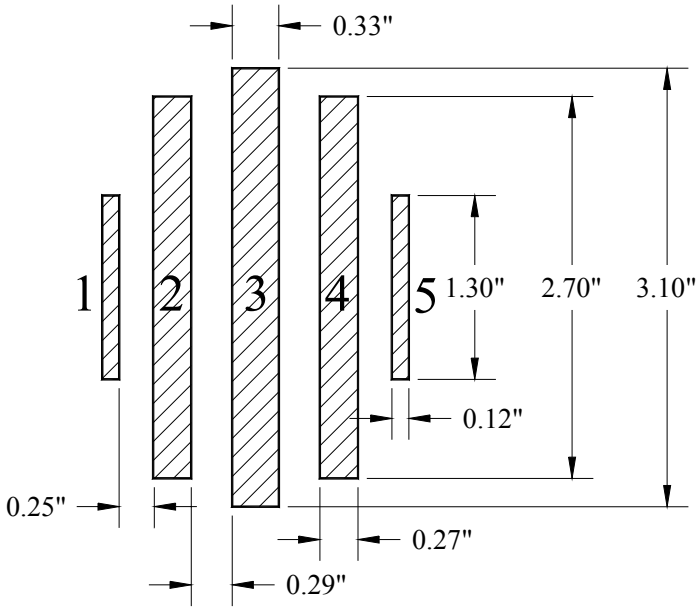

Figure 8.13 Tire Loading Geometry for PURWheel Model.

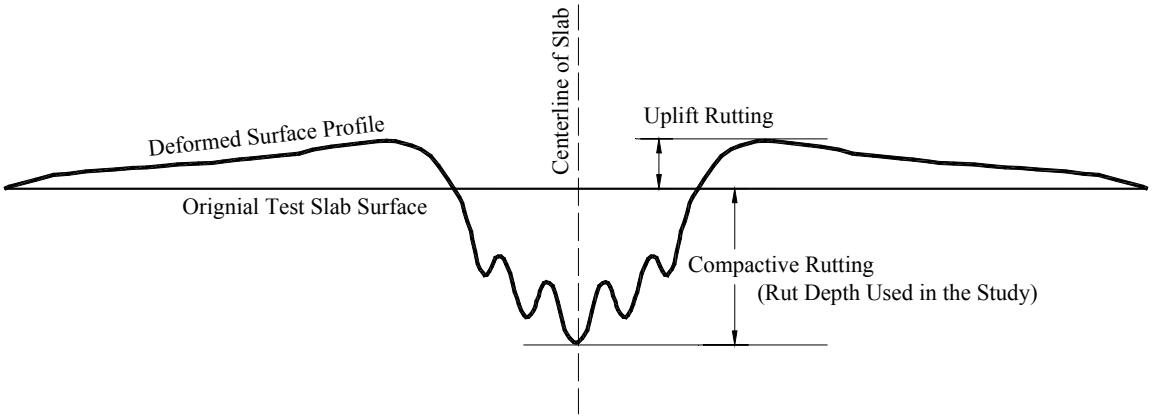

Figure 8.14 Predicted Rutting Profile for PURWheel Test.

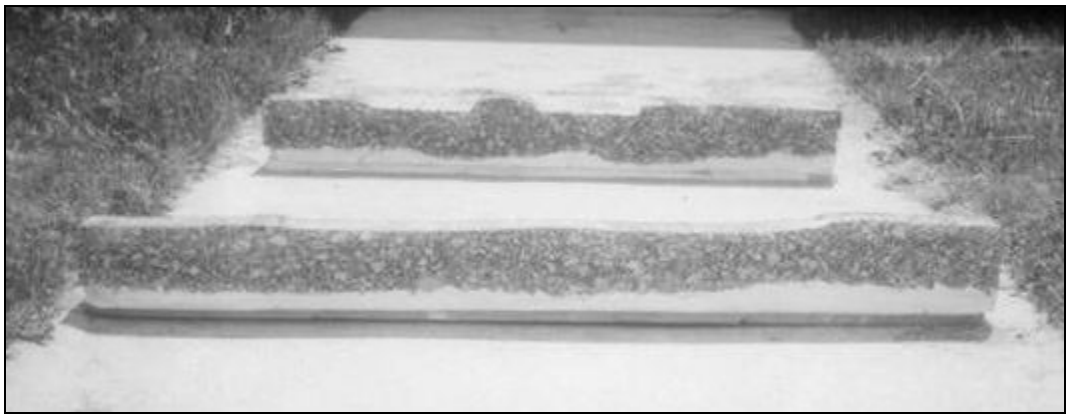

Figure 8.15 Transverse Rutting Profiles for No Wander and Wander Traffic in APT.

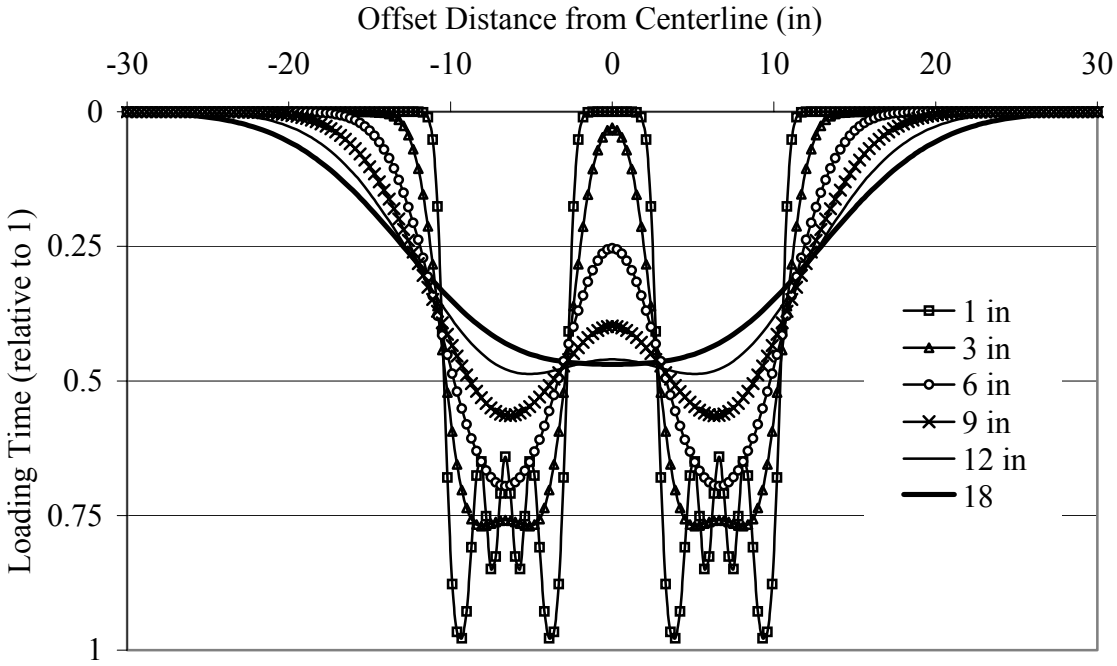

note: numbers in the legend are the wander distances.

Figure 8.16 Loading Time Distribution for Wander Wheel Modeling in APT.

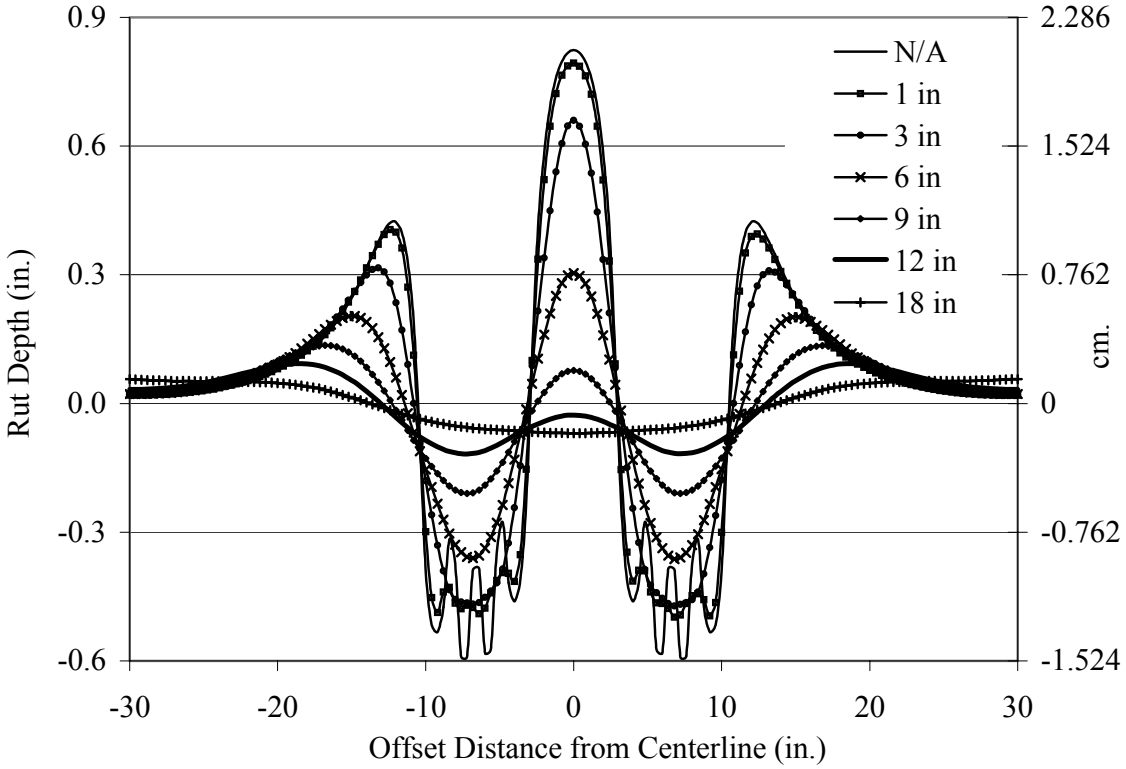

Figure 8.17 Effect of Wander Wheel Distance on The Deformed Surface Profile in APT Model.

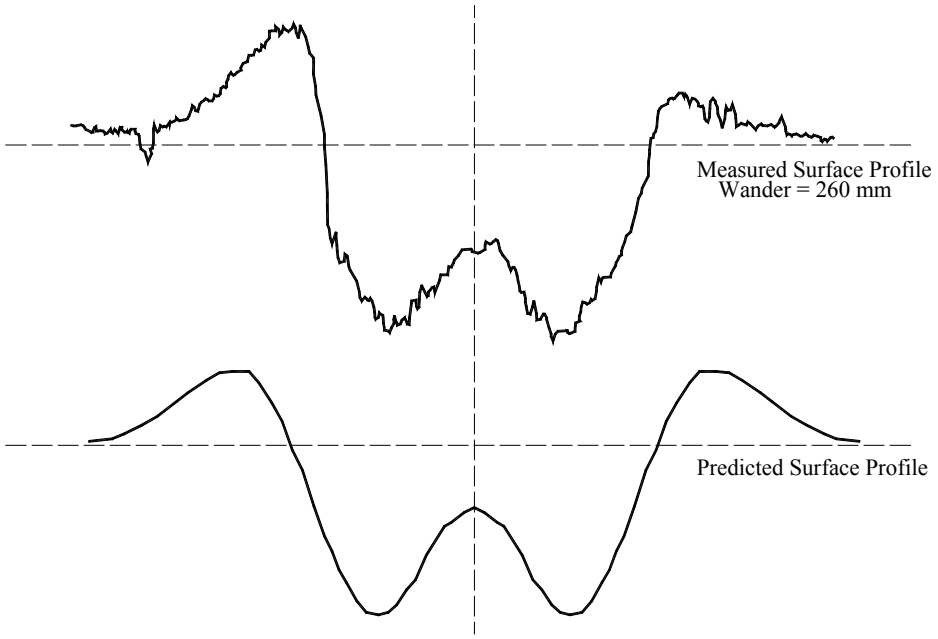

Figure 8.18 Comparison of the Observed and Predicted Rutting Profiles for Wander Distance of 260 mm in APT (5,000 Wheel Passes).

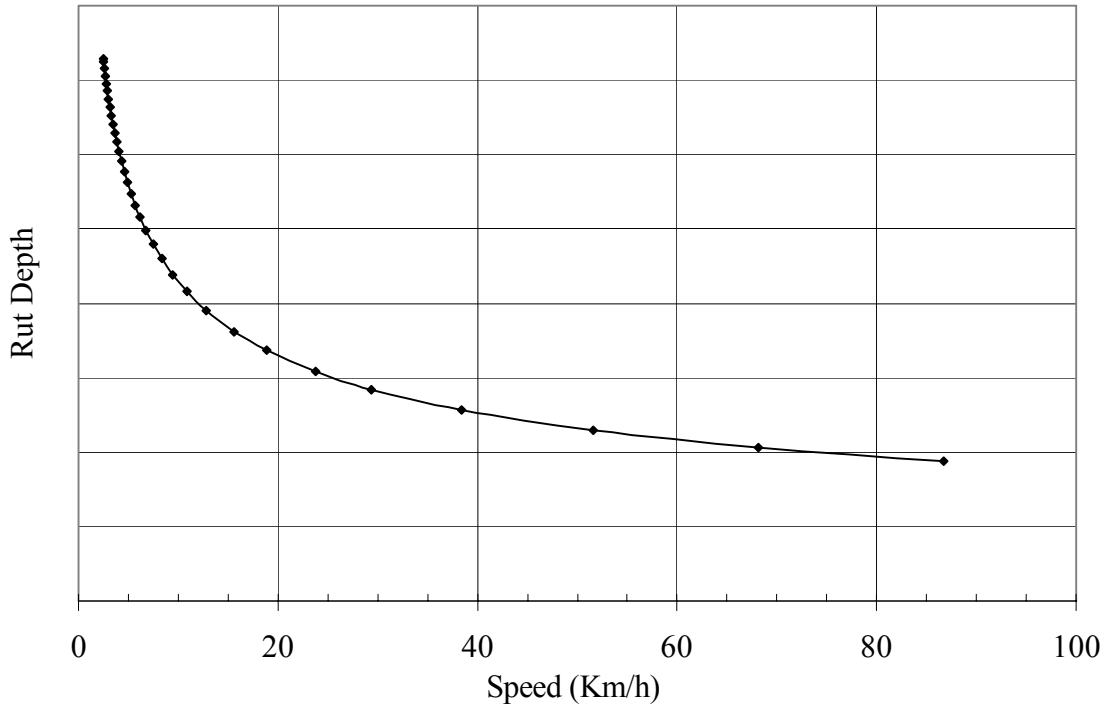

Figure 8.19 Modeling Wheel Speed Effect for APT Tests.

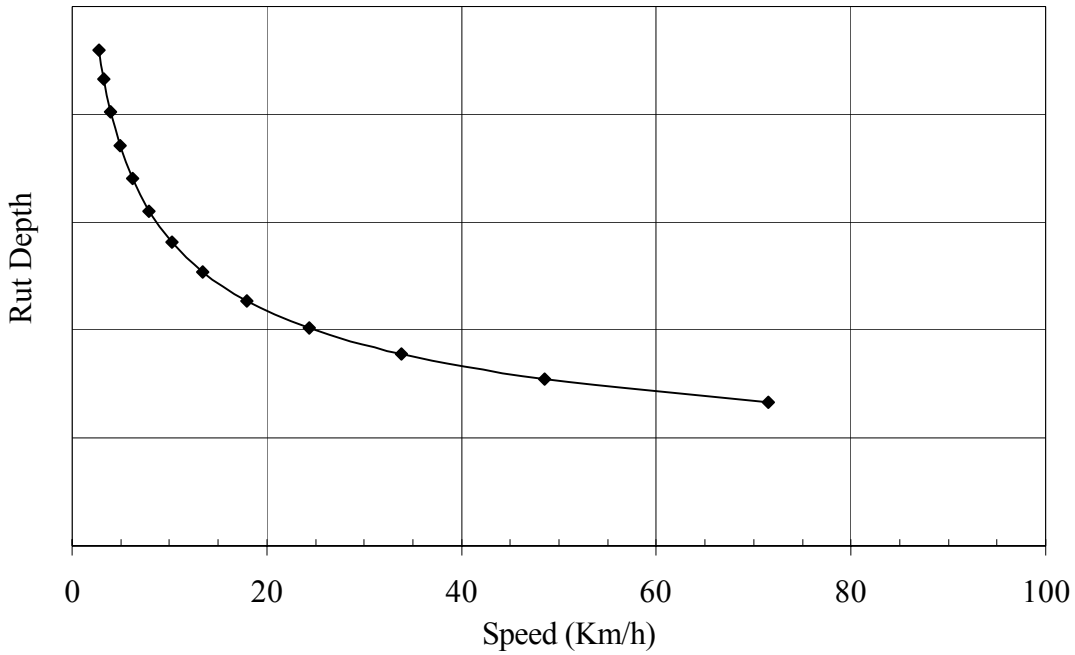

Figure 8.20 Modeling Wheel Speed Effect for PURWheel Tests.

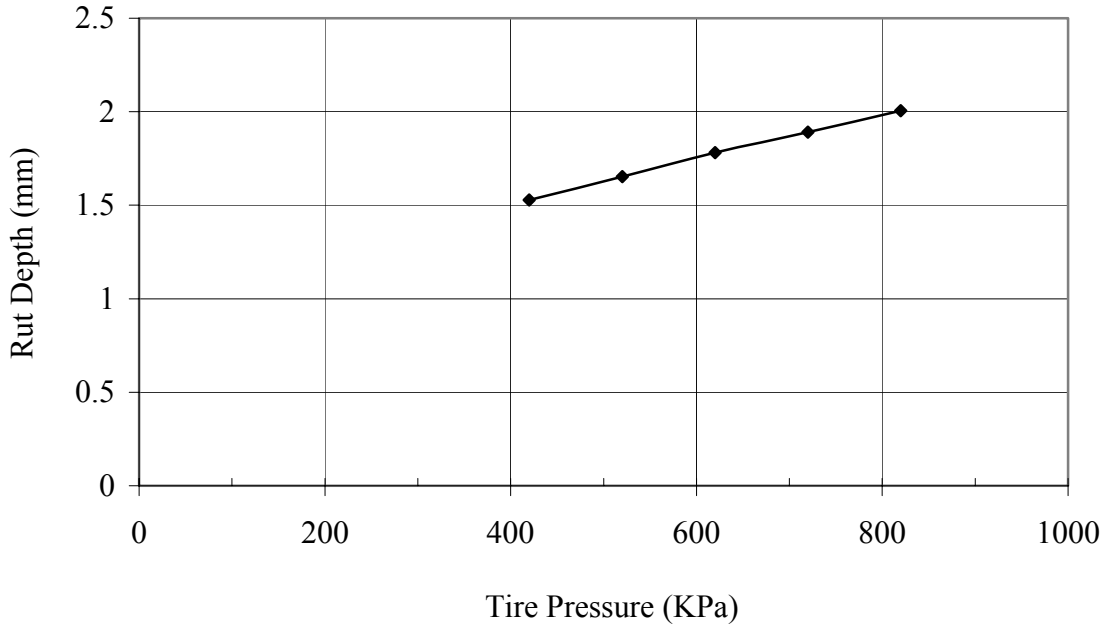

Figure 8.21 Modeling Tire Inflation Pressure Effect for APT Tests.

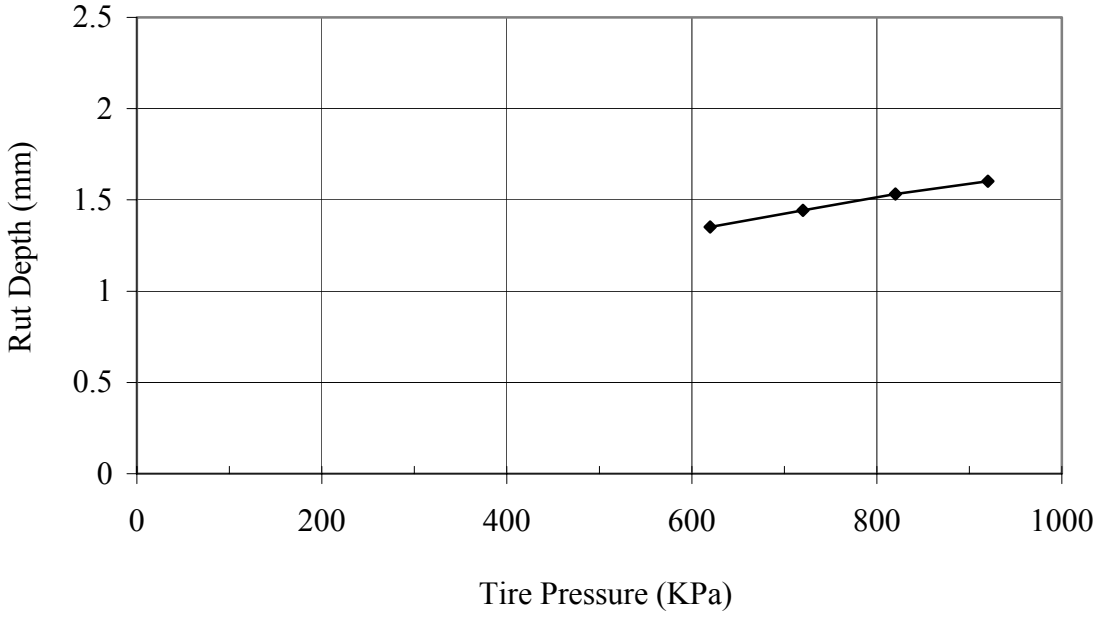

Figure 8.22 Modeling Tire Inflation Pressure Effect for PURWheel Tests.

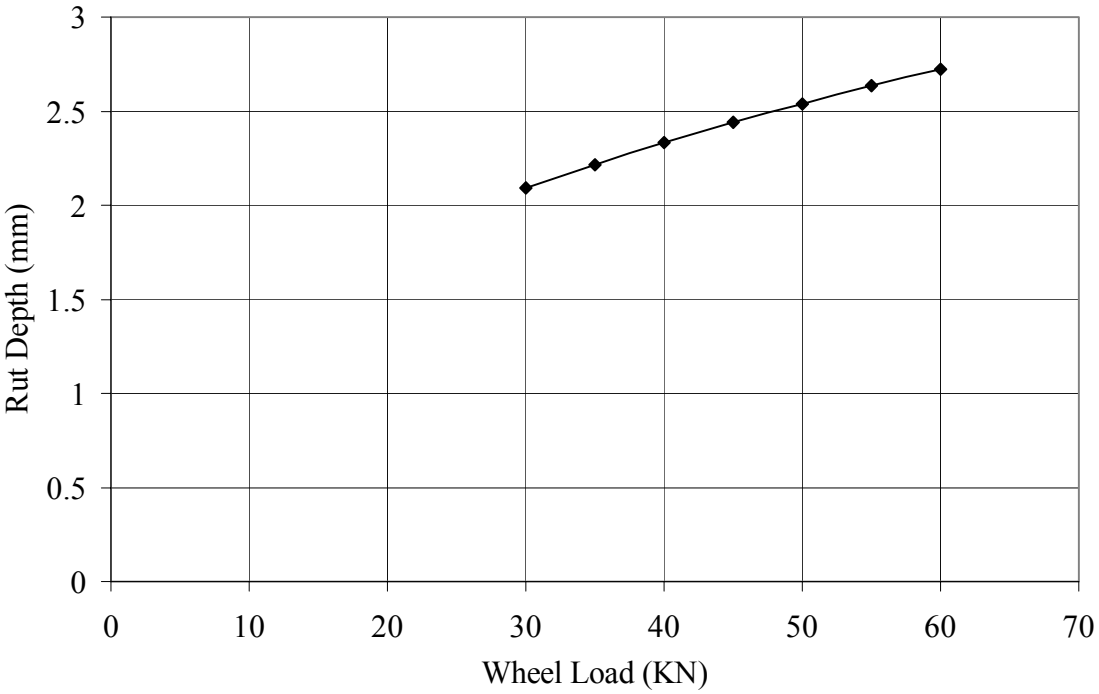

Figure 8.23 Modeling Wheel Load Effect for APT Tests.

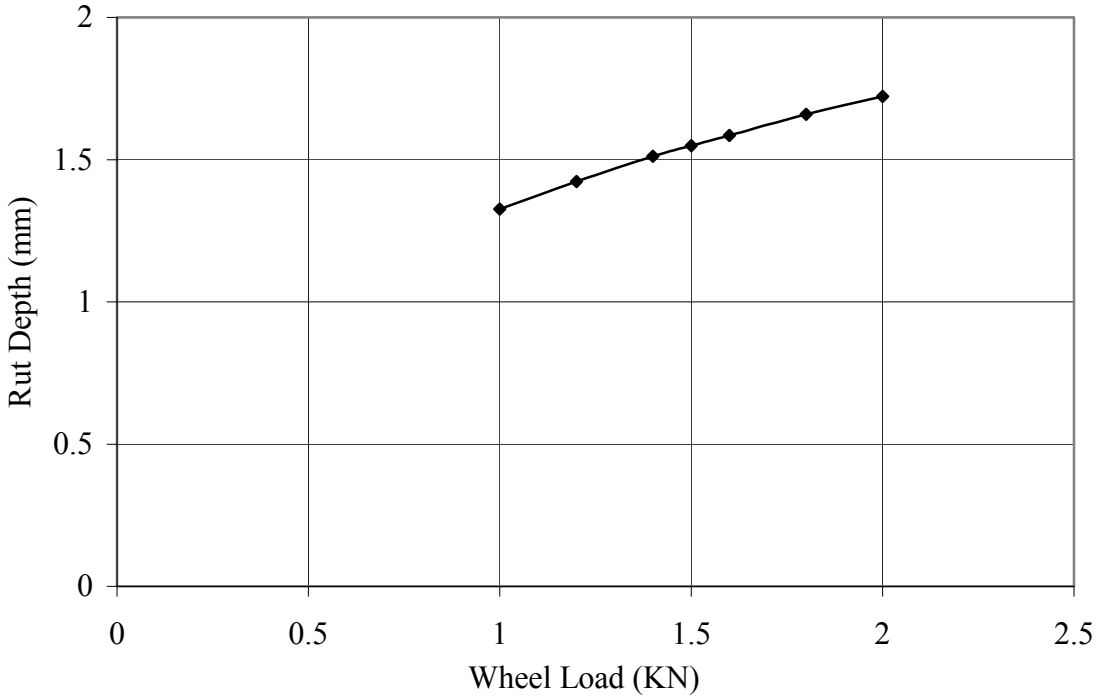

Figure 8.24 Modeling Wheel Load Effect for PURWheel Tests.

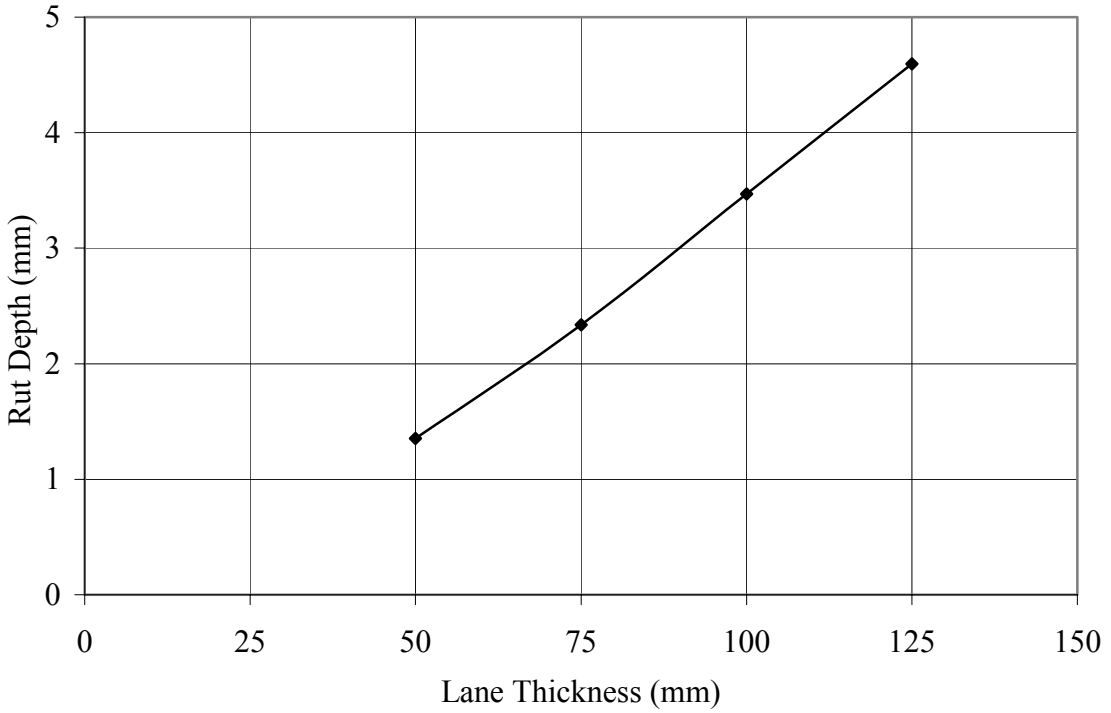

Figure 8.25 Modeling Pavement Thickness Effect for APT Tests.

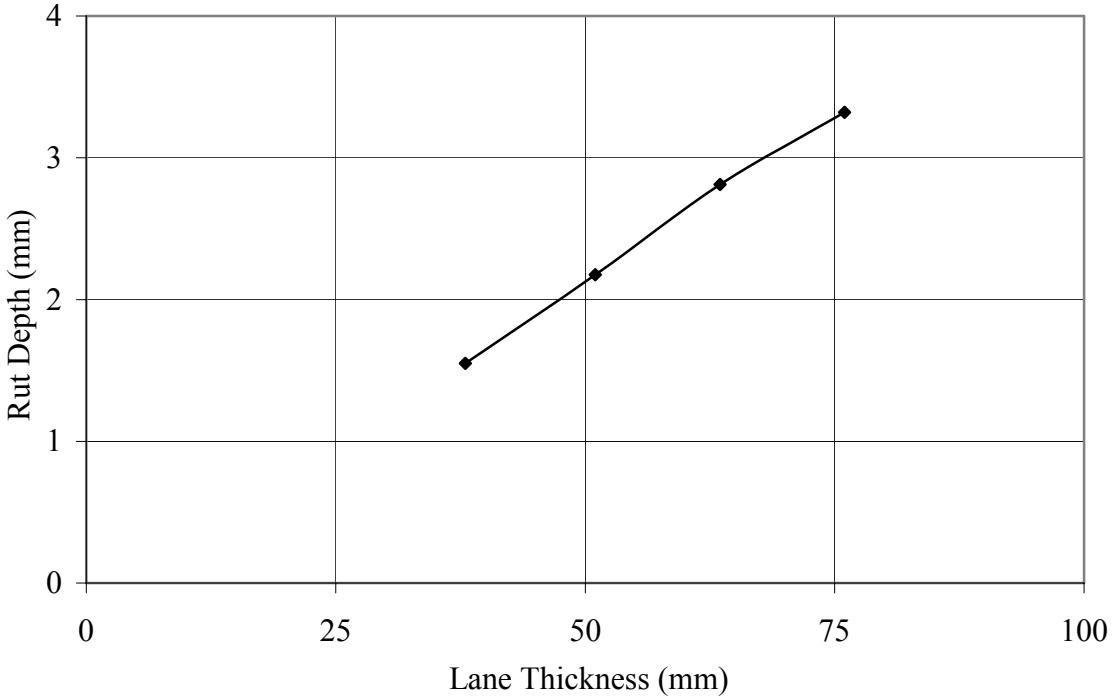

Figure 8.26 Modeling Specimen Thickness Effect for PURWheel Tests.

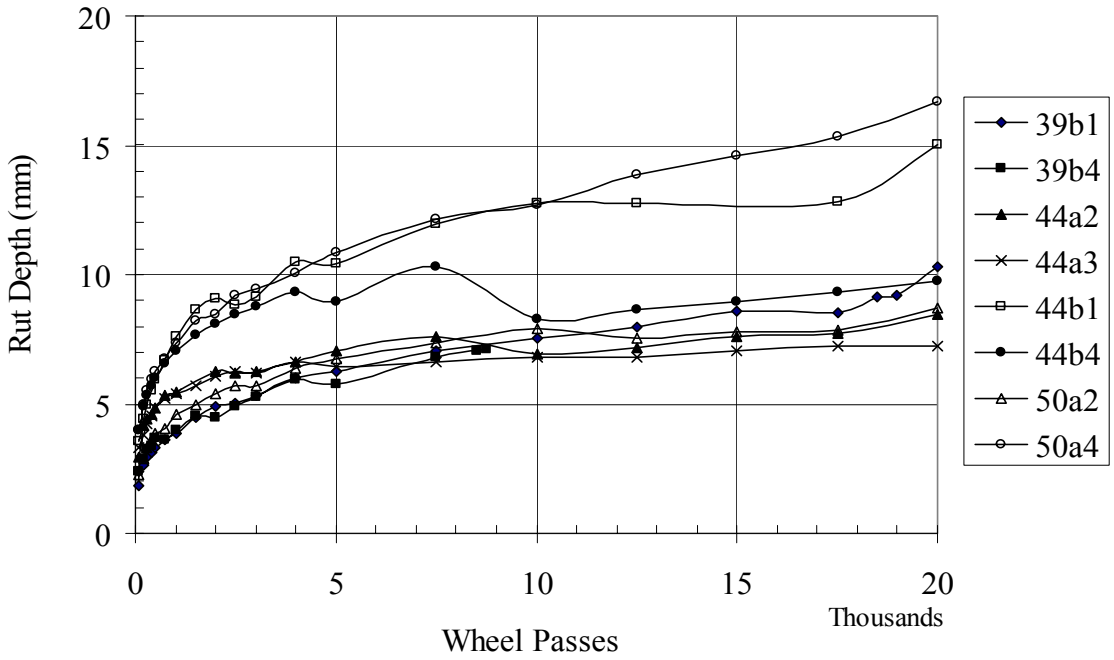

Figure 8.27 Observed Rutting for 19mm Limestone Mixtures in APT Test.

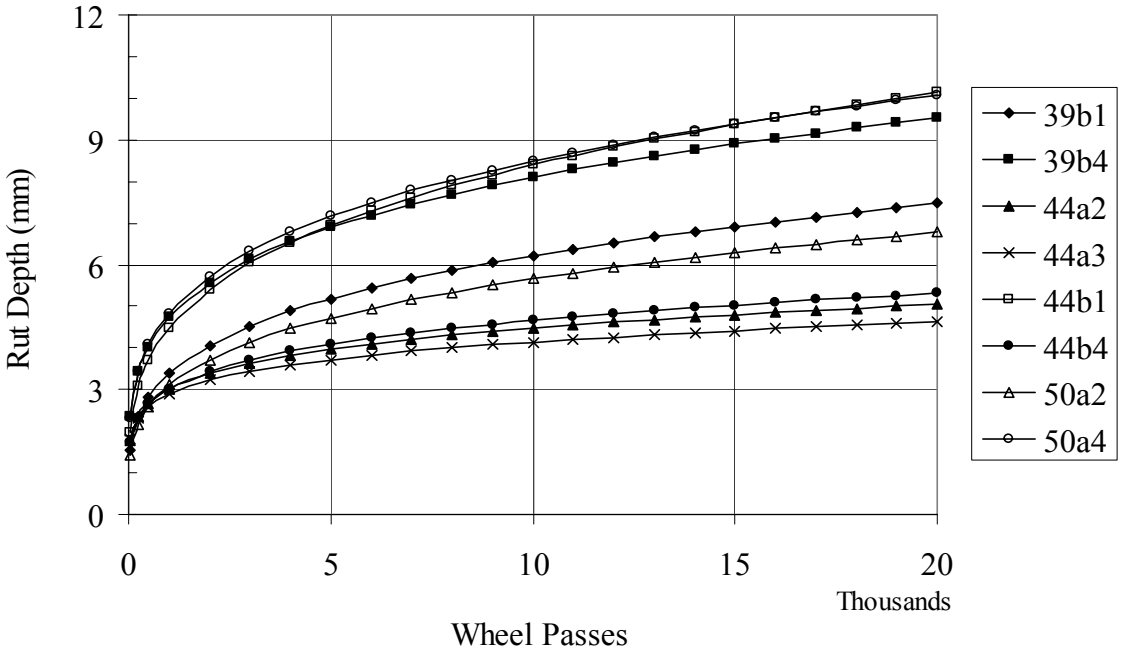

Figure 8.28 Predicted Rutting Based on Common Thickness of 76 mm for 19mm Limestone Mixtures in APT Test.

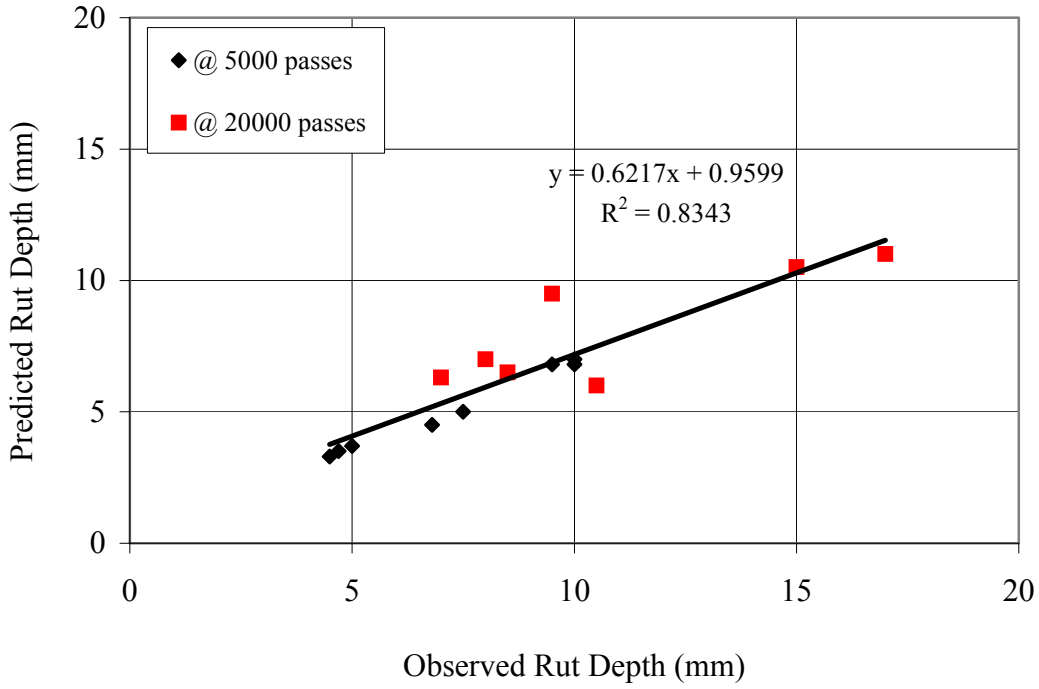

Figure 8.29 Comparison Between Predicted and Observed Rut Depth for 19mm Limestone Mixtures in APT Test

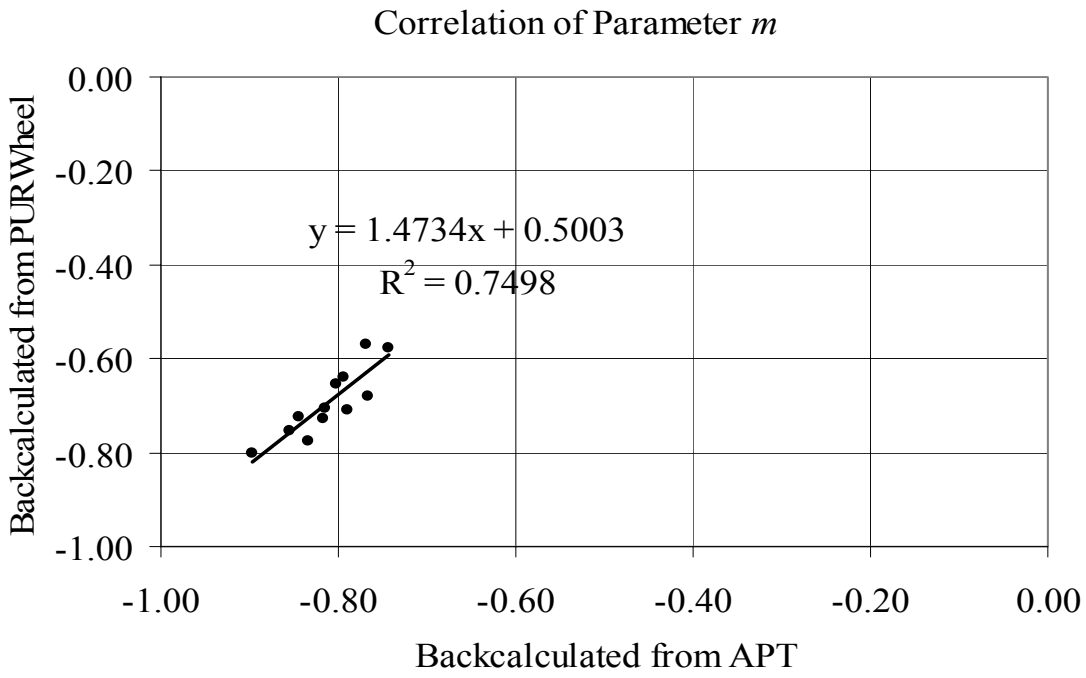

Figure 8.30 Correlation Between PURWheel and APT Tests Based on Creep Parameter *m*.

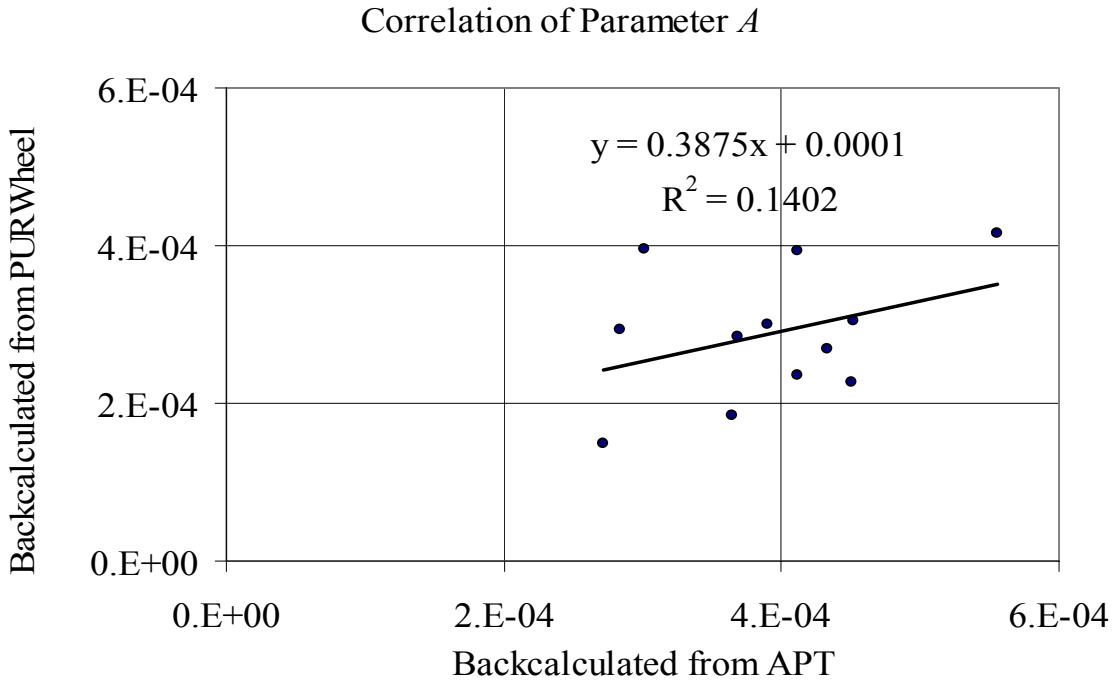

Figure 8.31 Correlation Between PURWheel and APT Tests Based on Creep Parameter *A*.

9 SUMMARY

9.1. Effect of Nominal Maximum Size

The effect of nominal maximum aggregate size on design VMA is depicted in Figure 9.1. Review of the plot reveals that VMA of 9.5mm mixtures was greater than that of 19mm mixtures. The effect of nominal maximum size on the location of design AC on VMA vs. AC curves at 96 N_{design} gyrations is depicted in Figure 9.2. The plot suggests that the percentage of mixtures with the position of design AC located on the "dry" sideof the VMA curve decreased as the nominal maximum size increased. The effect of nominal maximum size on design VFA is depicted in Figure 9.3. The VFA of 9.5mm mixtures was greater than that of 19mm mixtures as expected. The effect of nominal maximum size on design dust proportion is depicted in Figure 9.4. The plot suggests that nominal maximum size did not impact design dust proportion. The effect of nominal maximum size on design film thickness is depicted in Figure 9.5. The plot suggests that nominal maximum size did not impact design film thickness. The effect of nominal maximum size on percent Gmm at $N_{initial}$ is depicted in Figure 9.6. The plot suggests that the percent Gmm at $N_{initial}$ for 19mm mixtures was slightly greater than that for 9.5mm mixtures. This indicates that the 19mm mixtures were less resistant to compact than the 9.5mm mixtures. The effect of nominal maximum size on percent Gmm at $N_{maximum}$ is depicted in Figure 9.7. The plot indicates that nominal maximum size did not impact the percent Gmm at $N_{maximum}$.

The effect of nominal maximum size on rutting performance in the APT is presented in Figure 9.8. The plot suggests that nominal maximum size had a limited impact on rutting performance in APT tests. The effect of nominal maximum size on rutting performance in PURWheel tests is presented in Figure 9.9. The plot indicates that nominal maximum size did not impact rutting performance in PURWheel tests. The

effect of nominal maximum size on triaxial test results is presented in Figure 9.10. The plot shows that nominal maximum size did not impact the triaxial test results.

9.2. Effect of Coarse Aggregate Type

The effect of coarse aggregate type on design VMA is depicted in Figure 9.11. The plot suggests that design VMA of limestone mixtures was greater than that of granite mixtures. The effect of nominal maximum size on the location of design AC on VMA vs. AC curves at N_{design} gyrations is depicted in Figure 9.12. The plot suggests that the percentage of granite mixtures with the position of design AC located on the "dry" side of the VMA curve was greater than that of limestone mixtures. The effect of coarse aggregate type on design VFA is depicted in Figure 9.13. The plot suggests that design VFA of limestone mixtures was greater than that of granite mixtures. The effect of coarse aggregate type on design dust proportion is depicted in Figure 9.14. The plot indicates that coarse aggregate type did not impact design dust proportion. The effect of coarse aggregate type on design film thickness is depicted in Figure 9.15. The plot suggests that design film thickness of limestone mixtures was greater than that of granite mixtures. The effect of coarse aggregate type on percent Gmm at $N_{initial}$ is depicted in Figure 9.16. The plot suggests that percent Gmm at $N_{initial}$ for granite mixtures was greater than that limestone mixtures. This indicates that the granite mixtures were less resistant to compact than the limestone mixtures. The effect of coarse aggregate type on percent Gmm at $N_{maximum}$ is depicted in Figure 9.17. The plot indicates that coarse aggregate type did not impact the percent Gmm at $N_{maximum}$.

The effect of coarse aggregate type on rutting performance in APT tests is presented in Figure 9.18. The plot suggests that the rutting performance of granite mixtures was slightly better than that of limestone mixtures in APT tests. The effect of coarse aggregate type on rutting performance in PURWheel tests is presented in Figure 9.19. The plot indicates that the rutting performance of granite mixtures was slightly better than that of limestone mixtures in PURWheel tests. The effect of coarse aggregate

type on triaxial test results is presented in Figure 9.20. The plot indicates that the triaxial test results of limestone mixtures were slightly better than that of granite mixtures.

9.3. Effect of Fine Aggregate Angularity

The effect of fine aggregate angularity on design VMA is depicted in Figure 9.21. The plot suggests that as the FAA value increased the design VMA increased. The effect of fine aggregate angularity on the location of design AC on VMA vs. AC curves at N_{design} gyrations is depicted in Figure 9.22. The plot suggests that incorporating very high FAA reduced the percentage of mixtures with the position of design AC located on the "dry" side of the VMA curve. The effect of fine aggregate angularity on design VFA is depicted in Figure 9.23. The plot suggests that as the FAA value increased the design VFA increased. The effect of fine aggregate angularity on design dust proportion is depicted in Figure 9.24. The plot suggests that fine aggregate angularity had a limited impact on design dust proportion. The effect of fine aggregate angularity on design film thickness is depicted in Figure 9.25. The plot suggests that fine aggregate angularity had a limited impact on design film thickness. The effect of fine aggregate angularity on percent Gmm at $N_{initial}$ is depicted in Figure 9.26. The plot suggests that as the FAA value increased the percent Gmm at $N_{initial}$ decreased. This indicates that as the FAA value increased, the mixtures were more resistant to compact. The effect of fine aggregate angularity on percent Gmm at $N_{maximum}$ is depicted in Figure 9.27. The plot indicates that fine aggregate angularity did not impact the percent Gmm at $N_{maximum}$.

The effect of fine aggregate angularity on rutting performance in APT tests is presented in Figure 9.28. The plot suggests that fine aggregate angularity significantly impacted the rutting performance in APT tests. However, mixtures incorporating very high FAA values (50) did not perform better than those incorporating typical FAA values (44). The effect of fine aggregate angularity on rutting performance in PURWheel tests is presented in Figure 9.29. The data clearly shows that fine aggregate angularity significantly impacted the rutting performance in PURWheel tests. However, mixtures

incorporating very high FAA values (50) did not perform better than those incorporating typical FAA values (44). The effect of fine aggregate angularity on triaxial test results is presented in Figure 9.30. The data shows that the shear strength of mixtures incorporating very high FAA value (50) was not greater than that of mixtures incorporating typical FAA values (44). The effect of fine aggregate angularity on FSCH results is presented in Figure 9.31. The data shows that the complex shear modulus of mixtures incorporating very high FAA value (50) was not greater than that of mixtures incorporating typical FAA values (44). The effect of fine aggregate angularity on FSCH results is presented in Figure 9.32. The data suggests that the shear strain at 5000 cycles of mixtures incorporating very high FAA value (50) was greater than that of mixtures incorporating typical FAA values (44).

9.4. Effect of Gradation

The effect of gradation on design VMA is depicted in Figure 9.33. The plot suggests that gradation with respect to the restricted zone had a limited impact on design VMA. The effect of gradation on the location of design AC on VMA vs. AC curves at N_{design} gyrations is depicted in Figure 9.34. The plot suggests that as gradation type moves from above to below the restricted zone the percentage of mixtures with the position of design AC located on the “dry” side of the VMA curve decreased.The effect of gradation on design VFA is depicted in Figure 9.35. The plot suggests that gradation with respect to the restricted zone had a limited impact on design VFA. The effect of gradation on design dust proportion is depicted in Figure 9.36. The plot indicates that as gradation type moves from below to above the restricted zone dust proportion increased. The effect of gradation on design film thickness is depicted in Figure 9.37. The plot indicates that as gradation type moves from above to below the restricted zone film thickness increased. The effect of gradation on percent Gmm at $N_{initial}$ is depicted in Figure 9.38. The plot suggests that as gradation type moves from above to below the restricted zone the percent Gmm at $N_{initial}$ decreased. This indicates that the mixtures with gradations plotting above the

restricted zone were less resistant to compact. The effect of gradation on percent Gmm at $N_{maximum}$ is depicted in Figure 9.39. The plot indicates that gradation with respect to the restricted zone did not impact the percent Gmm at $N_{maximum}$.

The effect of gradation on rutting performance in APT tests is presented in Figure 9.40. The plot suggests that the effects of gradation with respect to the restricted zone on rutting performance in APT tests was unclear. The effect of gradation on rutting performance in PURWheel tests is presented in Figure 9.41. The plot indicates that the rutting performance of mixtures with gradations plotting through the restricted zone was better than that of mixtures with gradations plotting above or below the restricted zone in PURWheel. The effect of gradation on triaxial test results is presented in Figure 9.42. The plot indicates that the triaxial test results of mixtures with gradations plotting above the restricted zone were slightly better than those of mixtures with gradations plotting through or below the restricted zone. Review on the plots in Figures 7.40 to 7.42 reveals that the data were scattered. This suggests that the restricted zone was not adequate to characterize gradations to ensure adequate rutting performance. Measurements of the difference in the percent passing between the maximum density line and each given gradations (above, through, and below) for all mixtures at 25, 50, and 75 percent passing gradations are presented in Figures 7.43 and 7.44. The measurements indicated that the restricted zone consistently categorized the difference at 25 percent passing only. The effect of gradation types on FSCH results is presented in figure 9.31. The data shows that the complex shear modulus of mixtures incorporating gradations plotting above the restricted zone was greater than that of mixtures incorporating gradations plotting below the restricted zone. The effect of gradation types on FSCH results is presented in Figure 9.32. The data suggests that the shear strain at 5000 cycles of incorporating gradations plotting above the restricted zone was greater than that of mixtures incorporating gradations plotting below the restricted zone

9.5. Effect of VMA

The effect of VMA on rutting performance in APT tests is presented in Figure 9.45. The plot indicates that the relationship between VMA and rutting performance is dependent on nominal maximum aggregate size of the mixtures. The positive linear relationship suggests that an upper limit of VMA be established. The effect of location of design AC on VMA vs. AC curves at N_{design} gyrations on rutting performance in APT is presented in Figure 9.46. The plot suggests that mixtures with design AC located on the dry side of the VMA curve performed slightly better in APT tests.

The effect of VMA on rutting performance in PURWheel tests is presented in Figure 9.47. A quadratic relationship was observed for the 19mm mixtures and no relationship was observed for the 9.5mm mixtures. The quadratic relationship with a positive second order parameter indicates that the VMA corresponding to the minimum measured rut depth in PURWheel tests was 14.1 percent. The effect of location of design AC on VMA vs. AC curves at N_{design} gyrations on rutting performance in PURWheel tests is presented in Figure 9.48. The plot suggests that mixtures with design AC located on the dry side of the VMA curve performed slightly better in PURWheel tests.

The effect of VMA on triaxial test results in presented in Figure 9.49. No relationship between triaxial test results and VMA was observed. The effect of location of design AC on VMA vs. AC curve at N_{design} gyrations on triaxial test results is presented in Figure 9.50. The plot suggests that mixtures with design AC located on the dry side of the VMA curve had slightly greater shear strength.

The effect of VMA on FSCH results in presented in Figure 9.51. A quadratic relationship with positive second order parameter was observed. Parameter estimates indicate that the VMA corresponding to optimum complex shear modulus was 17.6 percent. The effect of VMA on RSCH results in presented in . No relationship between RSCH results and VMA was observed.

The measured critical VMA for optimum rutting performance is presented in Figure 9.53. The critical VMA for rutting performance in APT tests is defined as the VMA corresponding to a 10 mm total rut. Using the relationships in Figure 9.45, the

measured critical VMA for rutting performance in APT tests was 15.1 percent for the 19mm mixtures and 16.1 percent for the 9.5mm mixtures. The critical VMA for rutting performance in PURWheel tests is defined as the VMA corresponding to minimum PURWheel rut depths for the LMLCD mixture tested at five different AC levels. The measured critical VMA for rutting performance in PURWheel was 14.6 percent for the 19mm mixtures and 16.3 percent for the 9.5mm mixtures. The critical VMA for triaxial test results is defined as the VMA corresponding to peak shear strength of the mixture tested at five different AC levels. The measured critical VMA for triaxial test results was 14.5 percent for 19mm mixtures and 16.2 percent for 9.5mm mixtures. A pooled average coefficient of variation (COV) was 6.7 and 7 percent for 19 and 9.5mm mixtures, respectively.

9.6. Effect of VFA

The effect of VFA on rutting performance in APT tests is presented in Figure 9.54. The plot suggests that the relationship between VFA and rutting performance in APT tests was unclear. The effect of VFA on rutting performance in PURWheel tests is presented in Figure 9.55. A positive linear relationship was observed, regardless the nominal maximum size. The parameter estimates indicate that VFA of 75 percent (upper limit for the design traffic level) corresponds to PURWheel rut depths of 2.72 mm. The effect of VFA on triaxial test results is presented in Figure 9.56. A quadratic relationship with a negative second order parameter was observed. The parameter estimates indicate that VFA of 75 percent corresponds to shear strength of 1210 kPa. The effect of VFA on FSCH results is presented in Figure 9.57. A negative linear relationship was observed. The effect of VFA on RSCH results is presented in Figure 9.58. No relationship was observed.

The measured critical VFA for optimum rutting performance is presented in Figure 9.59. The critical VFA for rutting performance in APT tests is undefined because the relationship between VFA and rutting performance in APT tests was unclear. The

critical VFA for rutting performance in PURWheel tests is defined as the VFA corresponding to the minimum PURWheel rut depth for the LMLCD mixture tested at five different AC levels. The measured critical VFA for rutting performance in PURWheel tests was 69.4 percent for the 19mm mixtures and 66.4 percent for the 9.5mm mixtures. The critical VFA for triaxial test results is defined as the VFA corresponding to peak shear strength of the mixture tested at five different AC levels. The measured critical VFA for triaxial test results was 66.6 percent for the 19mm mixtures and 69.9 percent for the 9.5mm mixtures. A pooled average coefficient of variation (COV) was 12.5 and 17 percent for 19 and 9.5mm mixtures, respectively.

9.7. Effect of Dust Proportion

The effect of dust proportion on rutting performance in APT tests is presented in Figure 9.60. A quadratic relationship with a positive second order parameter was observed. Parameter estimates indicate that a dust proportion of 1.3 corresponded to the minimum measured total rut in APT tests. The effect of dust proportion on rutting performance in PURWheel tests is presented in Figure 9.61. A quadratic relationship with a positive second order parameter was observed. Parameter estimates indicate that a dust proportion of 1.2 corresponded to minimum measured rut depth in PURWheel tests. The effect of dust proportion on triaxial test results in presented in Figure 9.62. The plot suggests that shear strength increased as dust proportion increased. The effect of dust proportion on FSCH results is presented in Figure 9.63. A quadratic relationship with positive second order parameter was observed. The effect of dust proportion on RSCH results is presented in Figure 9.64. No relationship was observed.

The measured critical dust proportion for optimum rutting performance is presented in Figure 9.65. The critical dust proportion for rutting performance in APT tests is defined as the dust proportion corresponding to the minimum measured total rut in APT tests. Using the relationship in Figure 9.60, the measured critical dust proportion was 1.3 for 19 and 9.5mm mixtures. The critical dust proportion for rutting performance

in PURWheel tests is defined as the dust proportion corresponding to minimum PURWheel rut depth for the LMLCD mixture tested at five different AC levels. The measured critical dust proportion for rutting performance in PURWheel tests was 1.1 for the 19mm mixtures and 1.3 for the 9.5mm mixtures. The critical dust proportion for triaxial test results is defined as the dust proportion corresponding to peak shear strength of the mixture tested at five different AC levels. The measured critical dust proportion for triaxial test results was 1.2 for the 19mm mixtures and 1.3 for the 9.5mm mixtures. A pooled average coefficient of variation (COV) was 14 and 28 percent for 19 and 9.5mm mixtures, respectively.

9.8. Effect of Film Thickness

The effect of film thickness on rutting performance in APT tests is presented in Figure 9.66. A positive linear relationship was observed. Parameter estimates indicate that film thickness of 7.3 micron corresponded to the 10 mm total rut in APT tests. The effect of film thickness on rutting performance in PURWheel tests is presented in Figure 9.67. A quadratic relationship with a positive second order parameter was observed. Parameter estimates indicate that a film thickness of 8.2 micron corresponded to minimum measured rut depth in PURWheel tests. The effect of film thickness on triaxial test results in presented in Figure 9.68. The plot suggests that film thickness of 12.1 micron corresponded to minimum measured triaxial shear strength. The effect of film thickness on FSCH results is presented in Figure 9.69. A quadratic relationship with positive second order parameter was observed. The effect of film thickness on FSCH results is presented in Figure 9.70. A positive linear relationship was observed.

The measured critical film thickness for optimum rutting performance is presented in Figure 9.71. The critical film thickness for rutting performance in APT tests is defined as the film thickness corresponding to the 10 mm total rut in APT tests. Using the relationship in Figure 9.66, the measured critical film thickness was 7.3 micron for 19 and 9.5mm mixtures. The critical film thickness for rutting performance in PURWheel

tests is defined as the film thickness corresponding to minimum PURWheel rut depth for the LMLCD mixture tested at five different AC levels. The measured critical film thickness for rutting performance in PURWheel tests was 9.1 micron for the 19mm mixtures and 7.7 micron for the 9.5mm mixtures. The critical film thickness for triaxial test results is defined as the film thickness corresponding to peak shear strength of the mixture tested at five different AC levels. The measured critical film thickness for triaxial test results was 8.1 micron for the 19mm mixtures and 8.2 micron for the 9.5mm mixtures. A pooled average coefficient of variation (COV) was 12 and 24 percent for 19 and 9.5mm mixtures, respectively.

The combined effects of the individual experimental parameters discussed in the previous chapters are summarized in the conclusions presented in the following chapter.

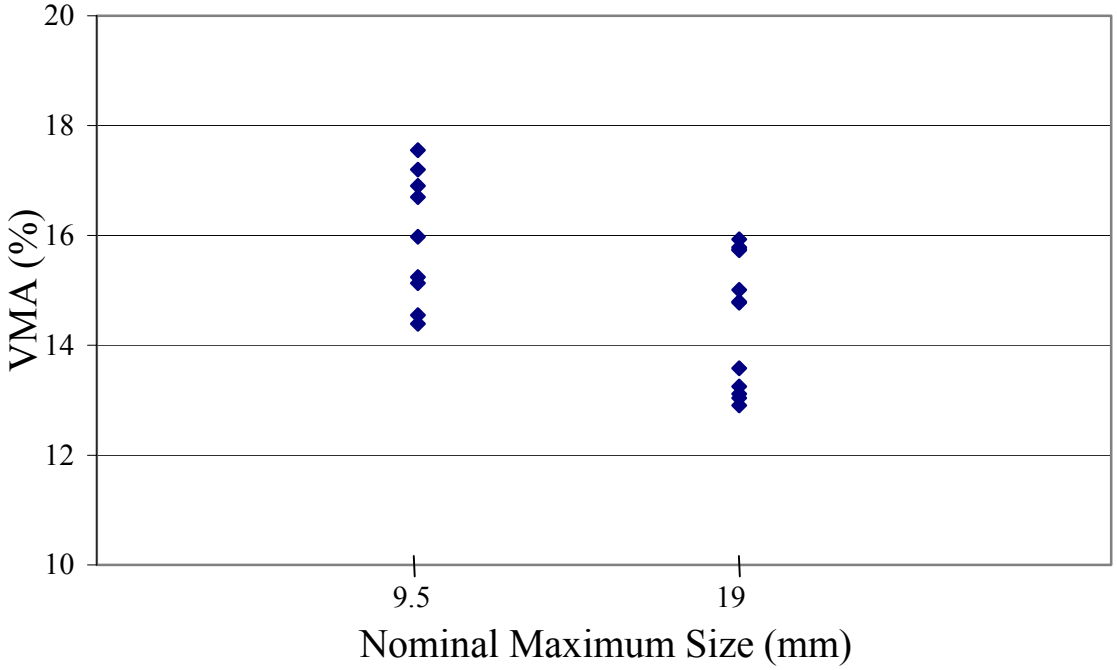

Figure 9.1 Effect of Nominal Maximum Size on Design VMA.

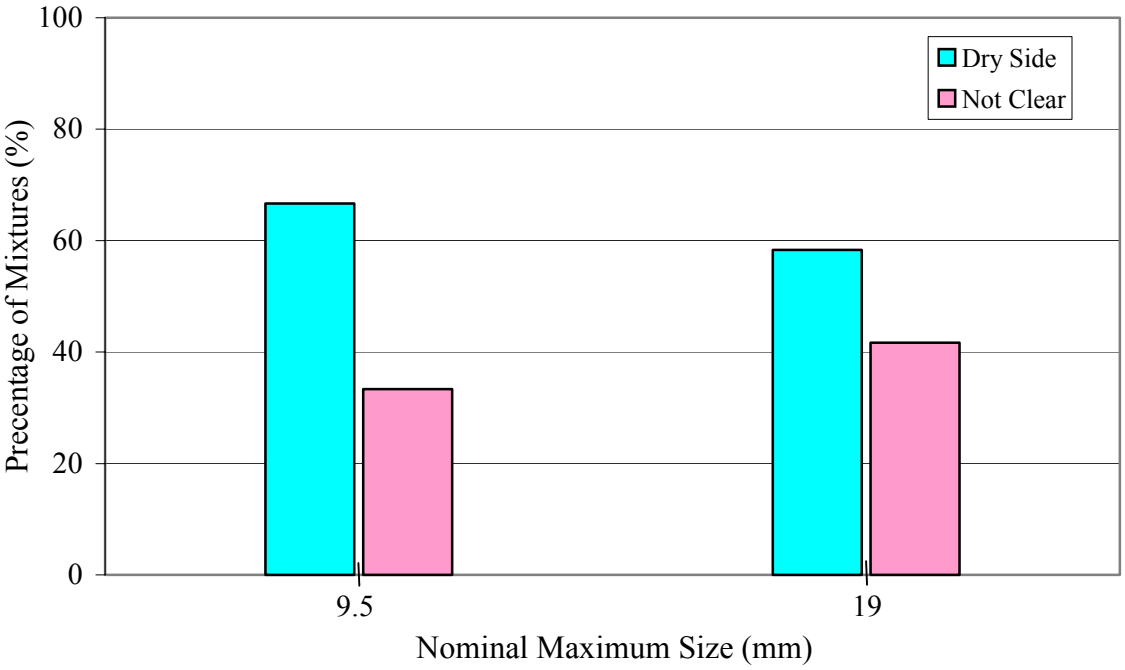

Figure 9.2 Effect of Nominal Maximum Size on Location of Design AC on VMA Curve at N_{design} Gyrations.

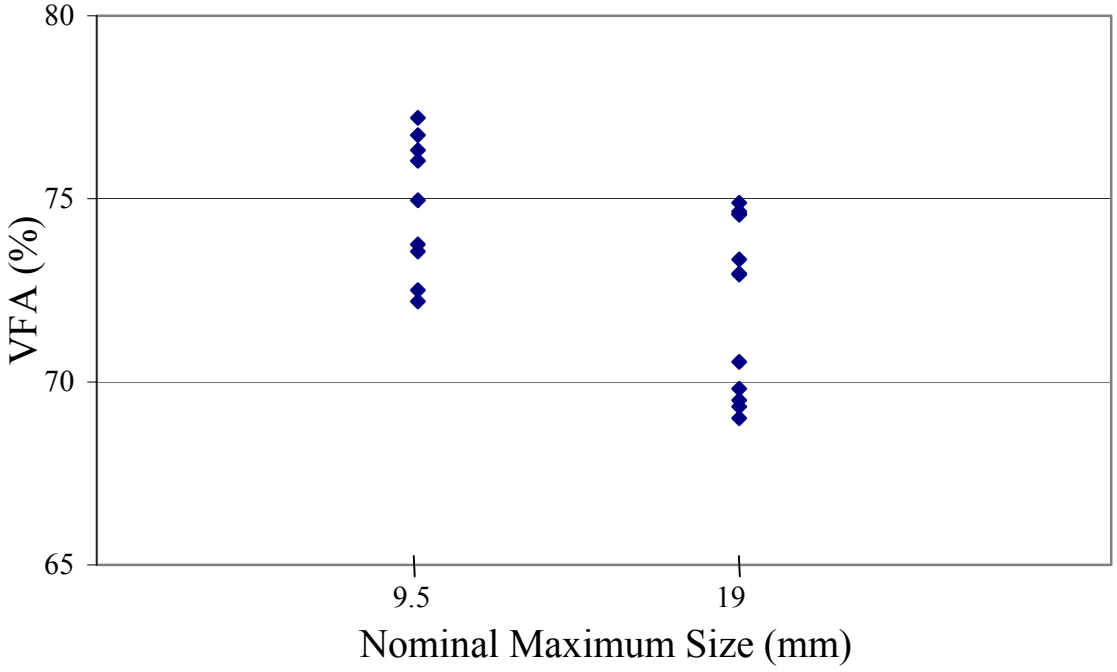

Figure 9.3 Effect of Nominal Maximum Size on Design VFA.

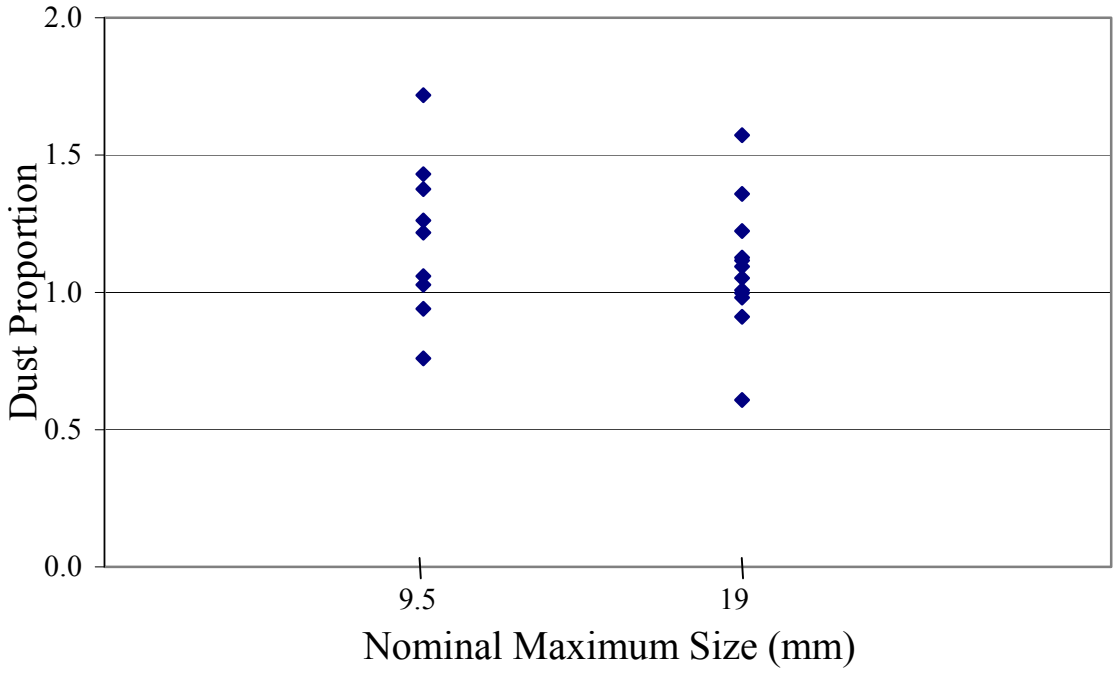

Figure 9.4 Effect of Nominal Maximum Size on Design Dust Proportion.

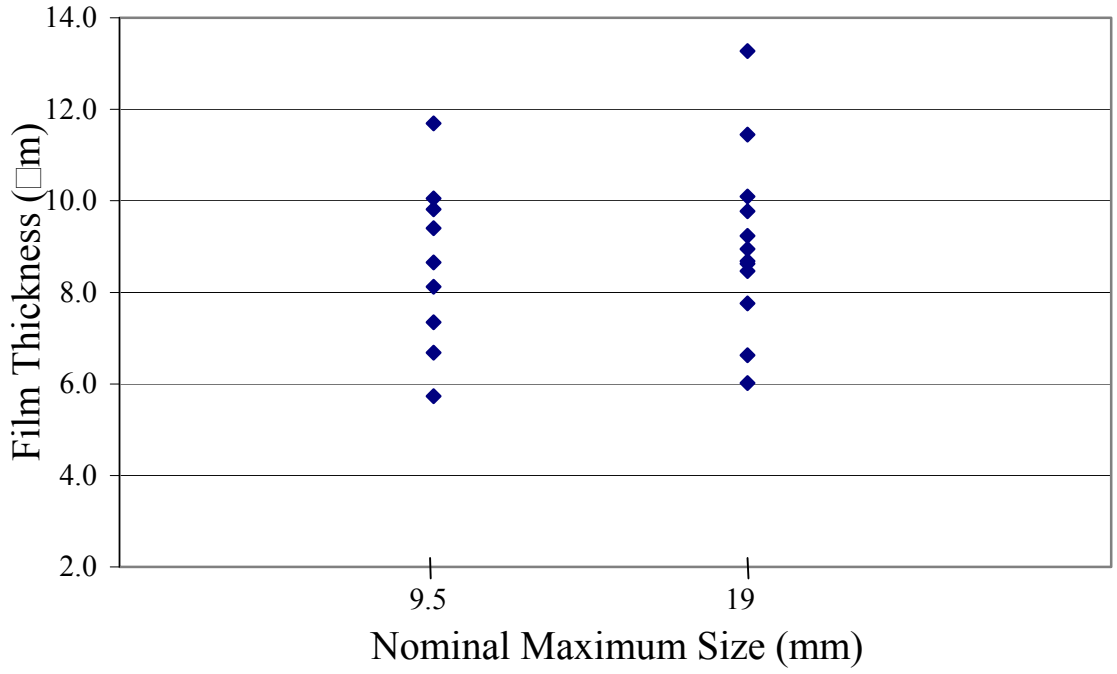

Figure 9.5 Effect of Nominal Maximum Size on Design Film Thickness.

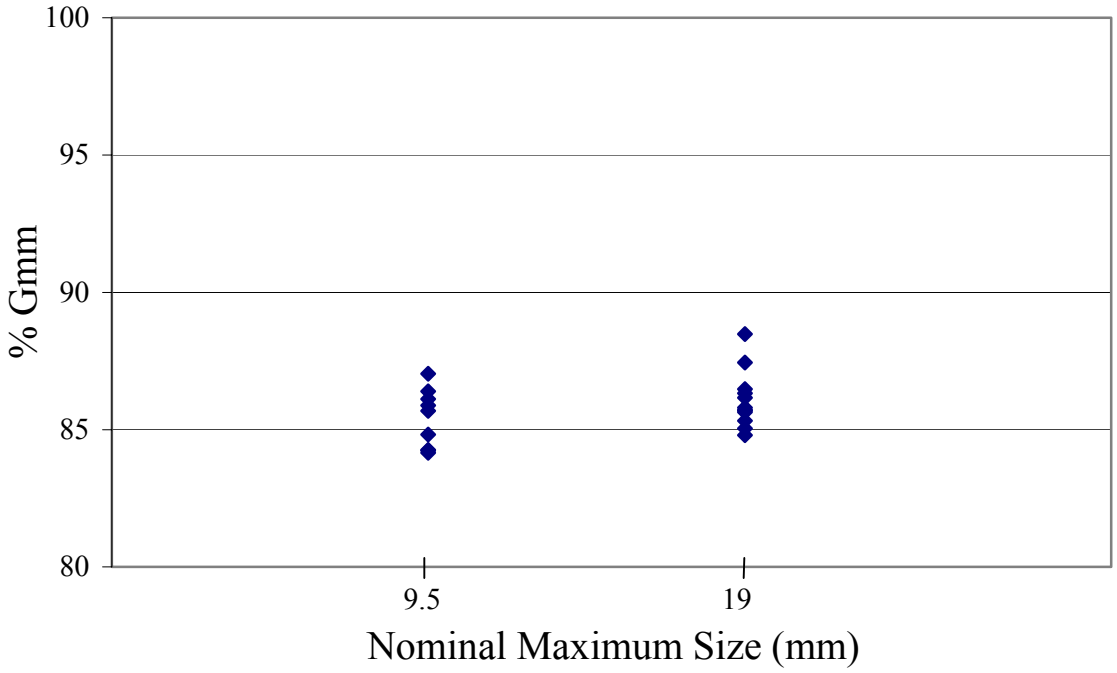

Figure 9.6 Effect of Nominal Maximum Size on Percent Gmm at $N_{initial}$.

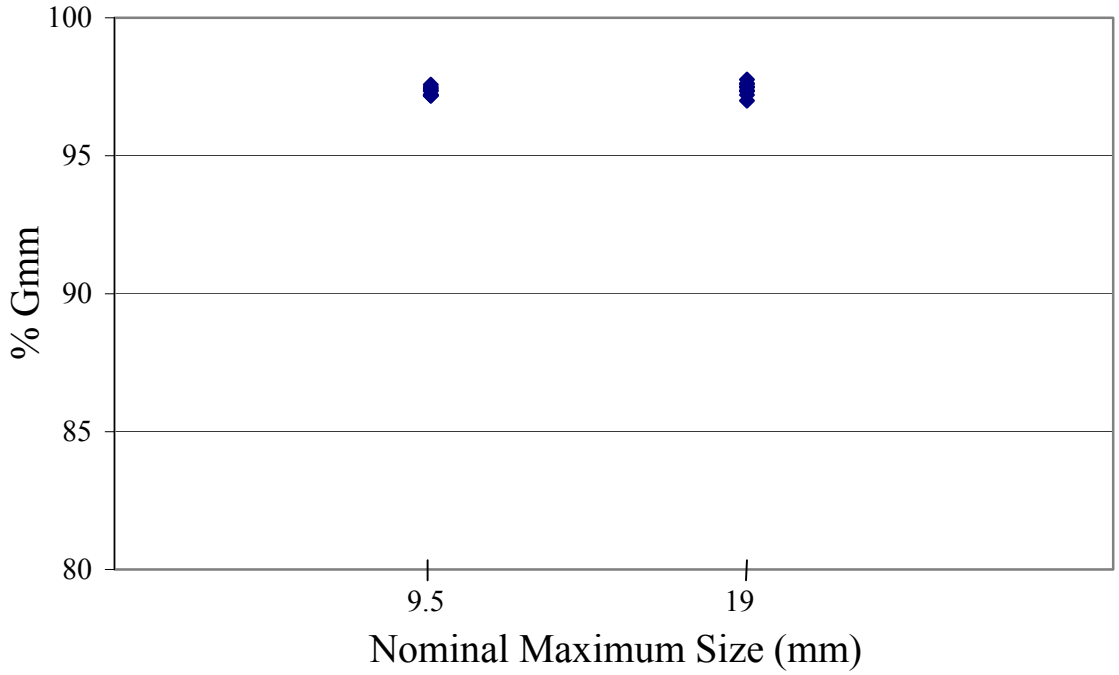

Figure 9.7 Effect of Nominal Maximum Size on Percent Gmm at $N_{maximum}$.

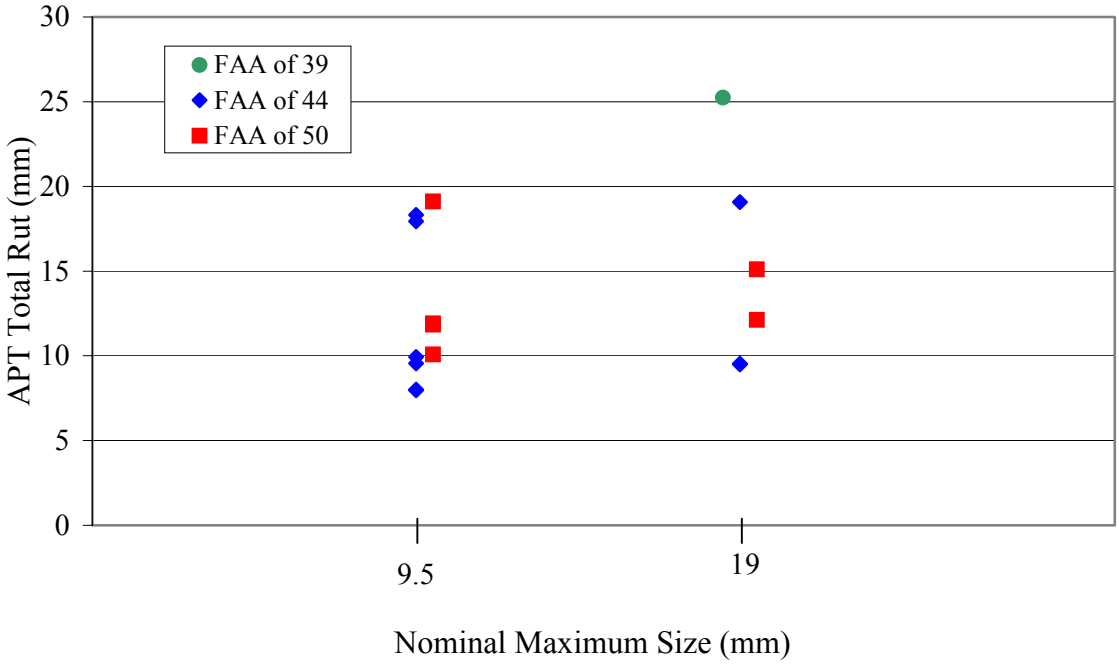

Figure 9.8 Effect of Nominal Maximum Size on Rutting Performance in APT.

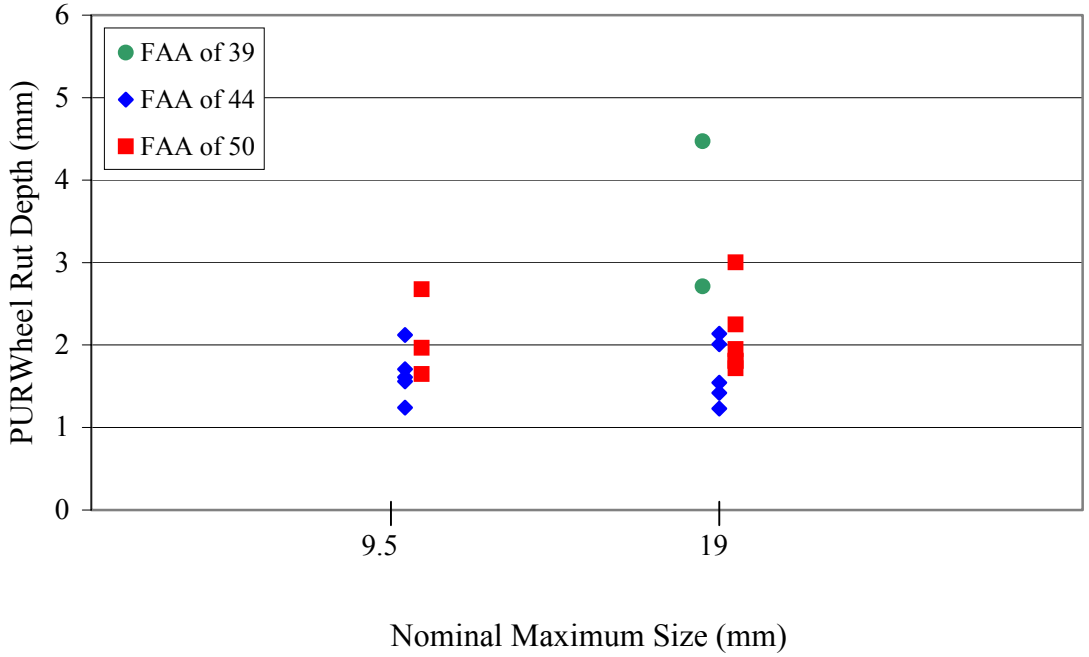

Figure 9.9 Effect of Nominal Maximum Size on Rutting Performance in PURWheel (LMLCD).

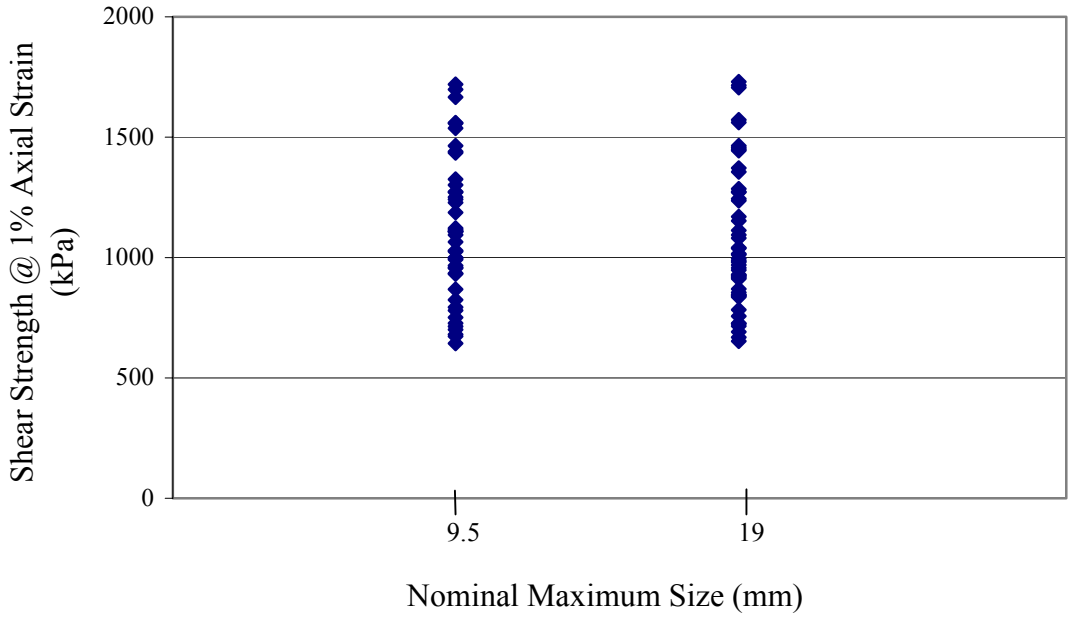

Figure 9.10 Effect of Nominal Maximum Size on Triaxial Test Results.

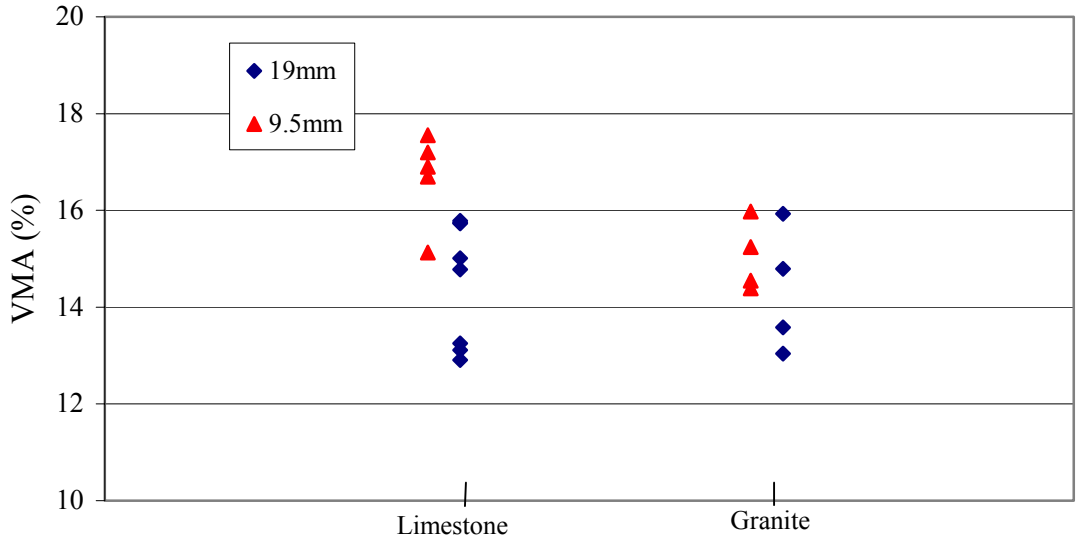

Figure 9.11 Effect of Coarse Aggregate Type on Design VMA.

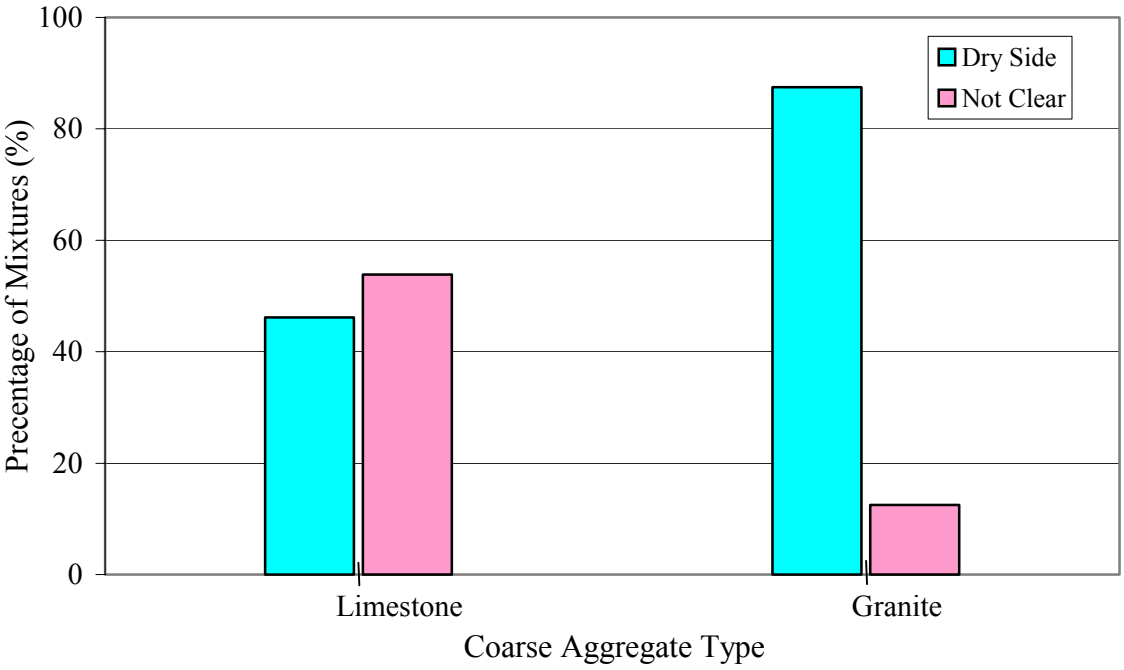

Figure 9.12 Effect of Coarse Aggregate Type on Location of Design AC on VMA Curve at N_{design} Gyrations.

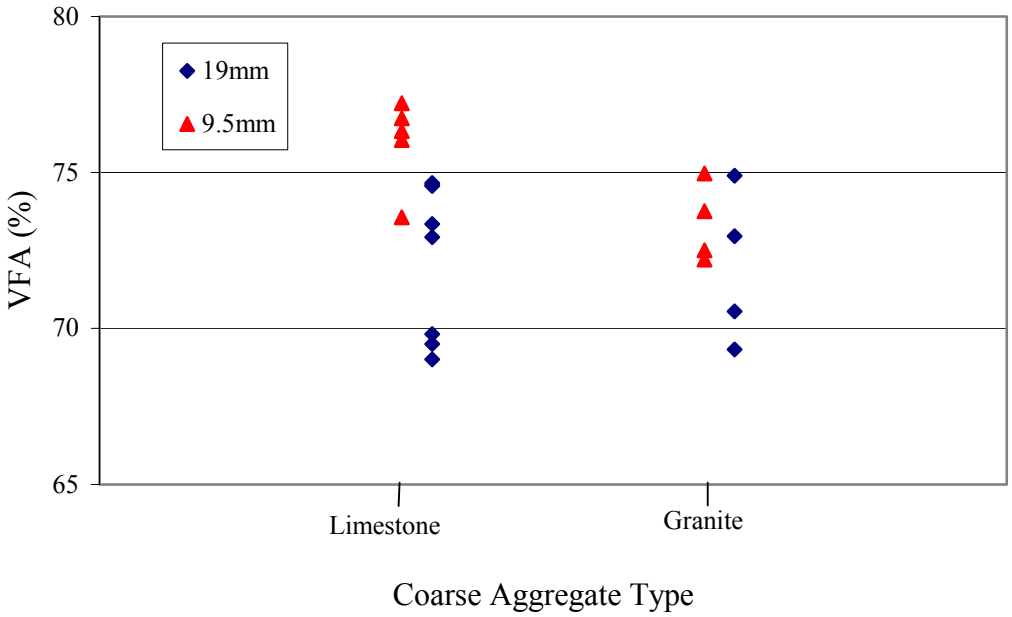

Figure 9.13 Effect of Coarse Aggregate Type on Design VFA.

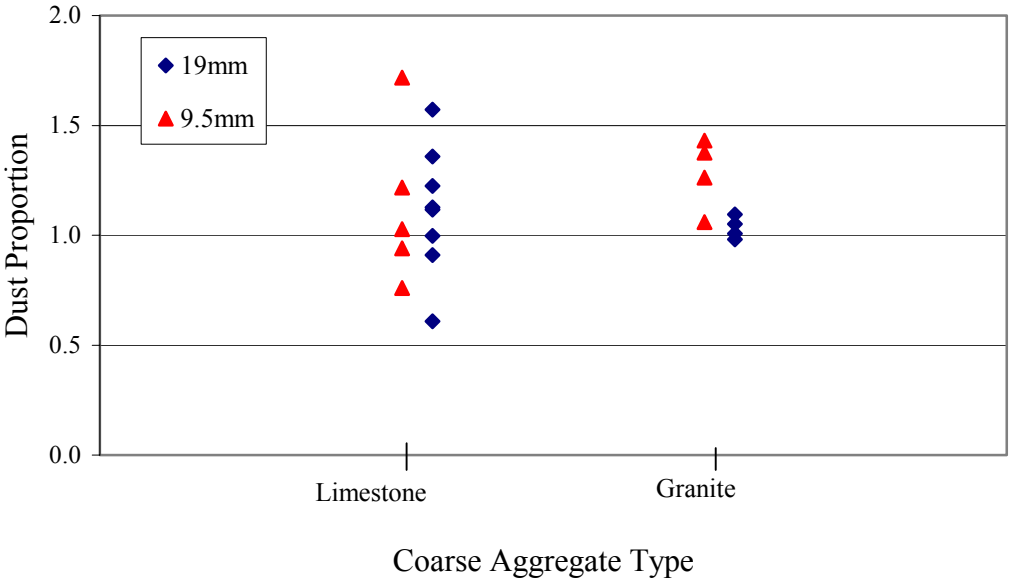

Figure 9.14 Effect of Coarse Aggregate Type on Design Dust Proportion.

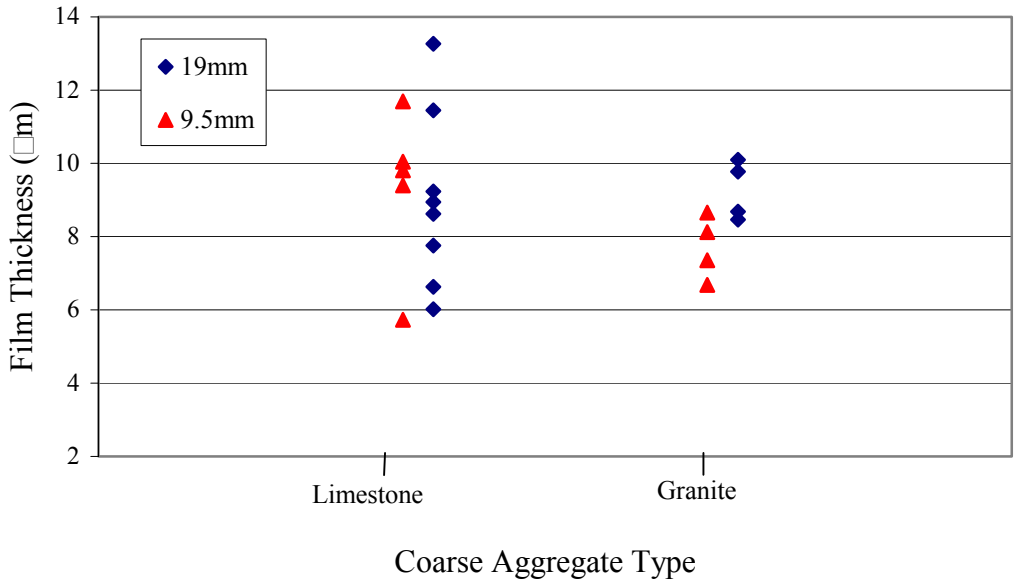

Figure 9.15 Effect of Coarse Aggregate Type on Design Film Thickness.

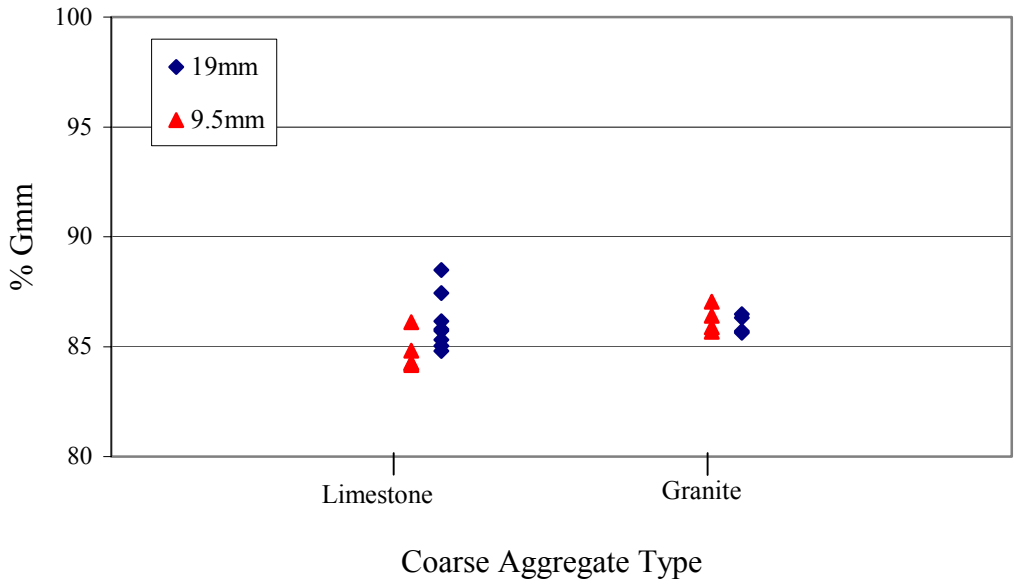

Figure 9.16 Effect of Coarse Aggregate Type on Percent Gmm at $N_{initial}$.

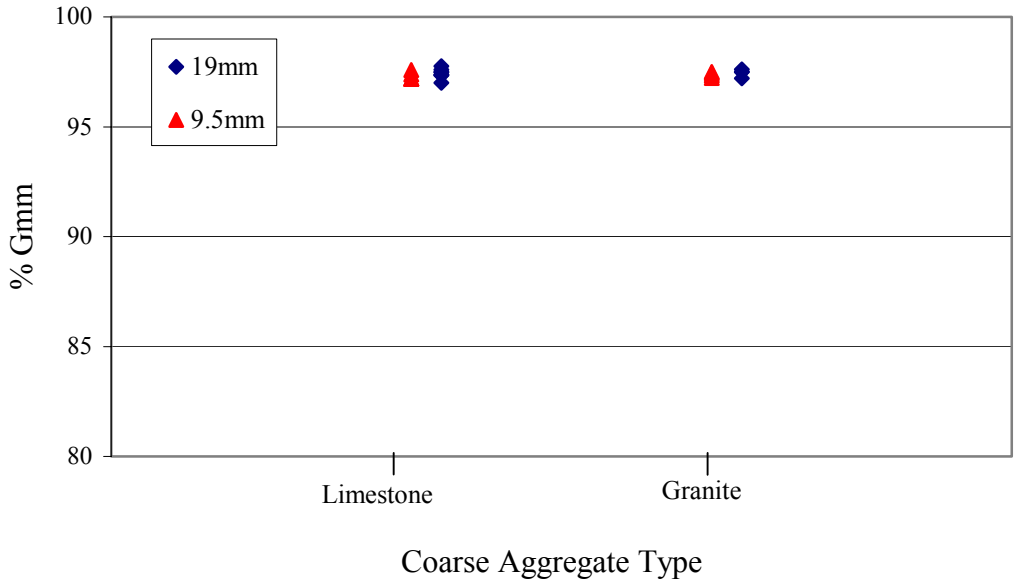

Figure 9.17 Effect of Coarse Aggregate Type on Percent Gmm at $N_{maximum}$.

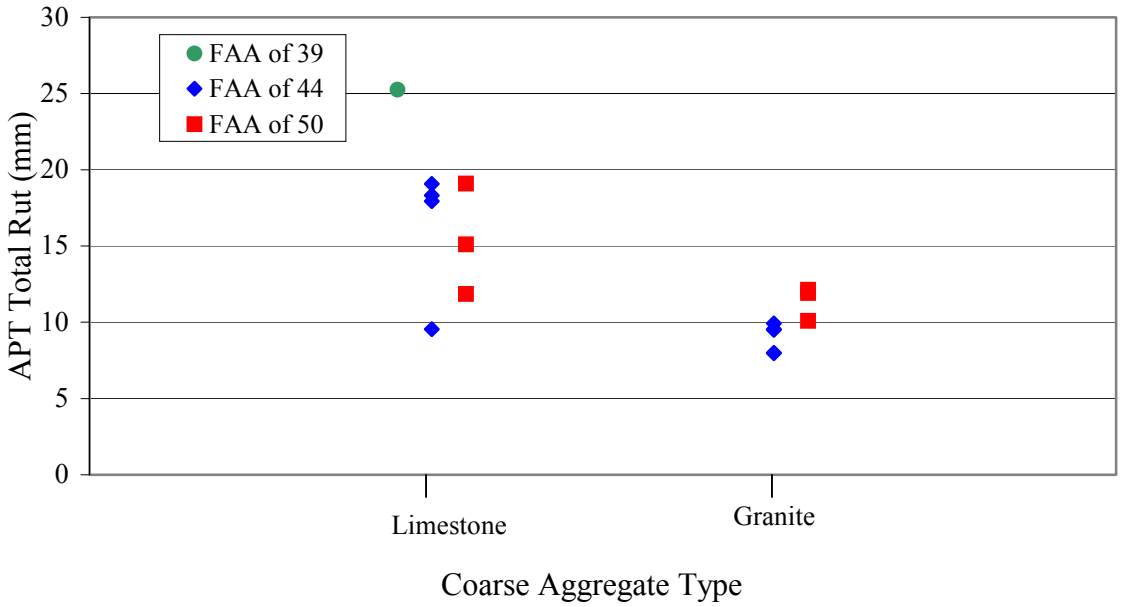

Figure 9.18 Effect of Coarse Aggregate Type on Rutting Performance in APT.

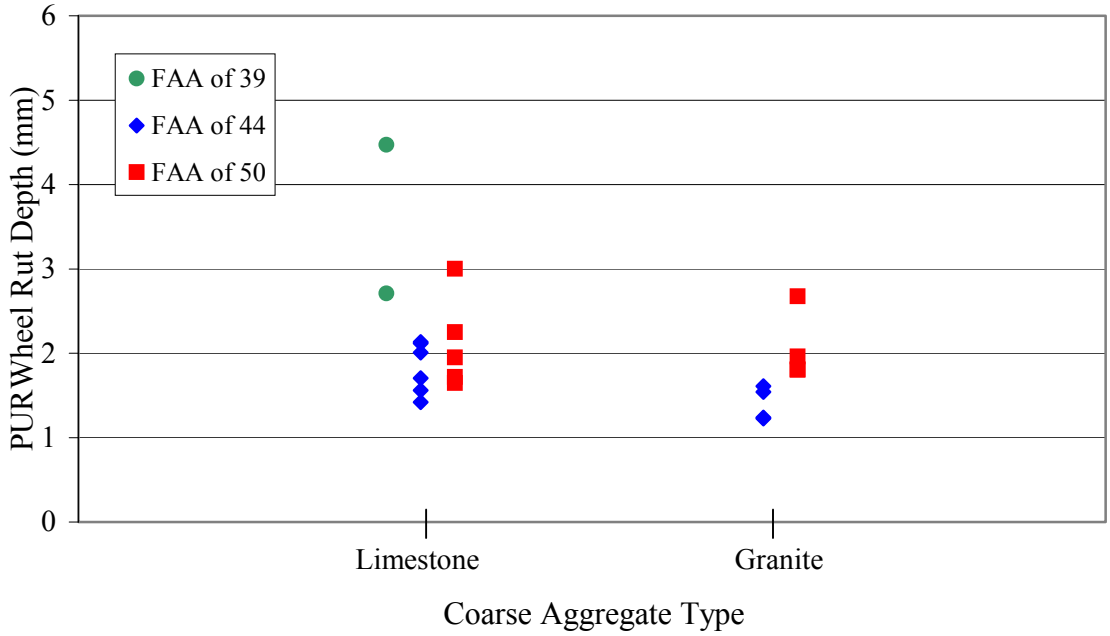

Figure 9.19 Effect of Coarse Aggregate Type on Rutting Performance in PURWheel (LMLCD).

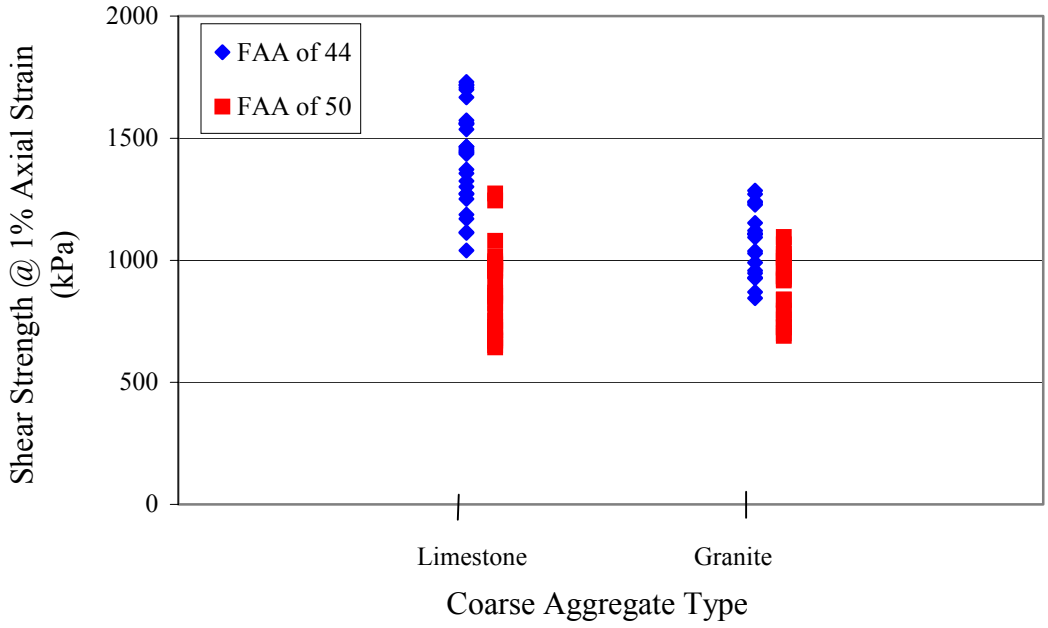

Figure 9.20 Effect of Coarse Aggregate Type on Triaxial Test Results.

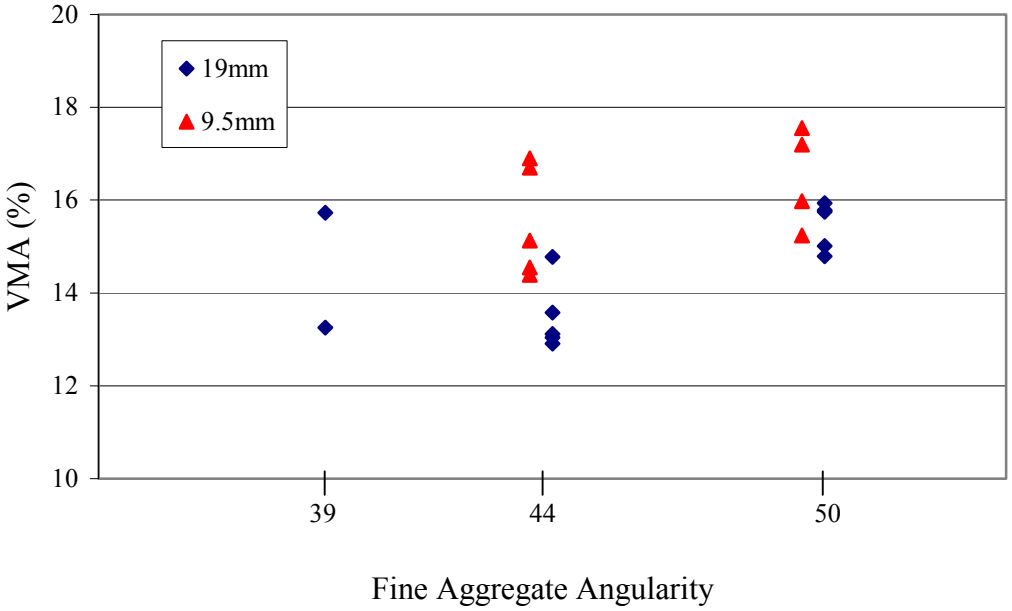

Figure 9.21 Effect of Fine Aggregate Angularity on Design VMA.

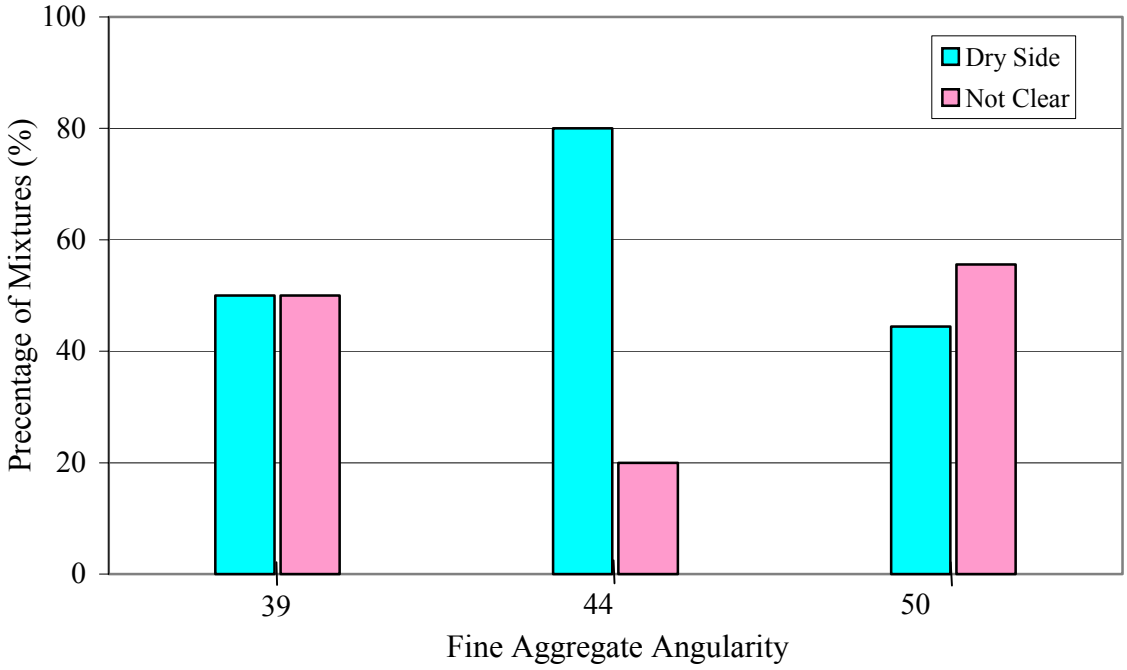

Figure 9.22 Effect of Fine Aggregate Angularity on Location of Design AC on VMA Curve at N_{design} Gyrations.

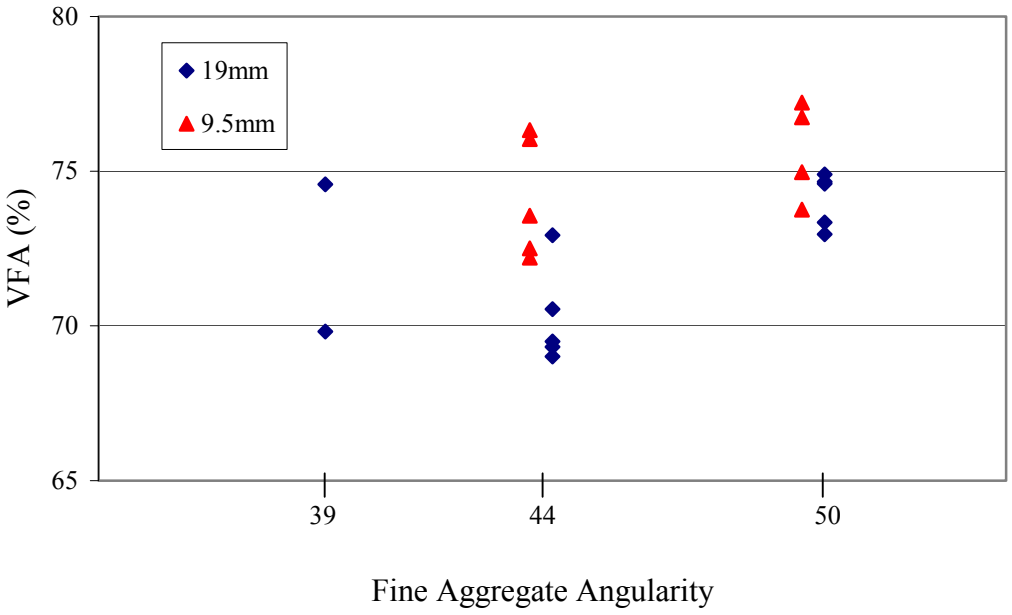

Figure 9.23 Effect of Fine Aggregate Angularity on Design VFA.

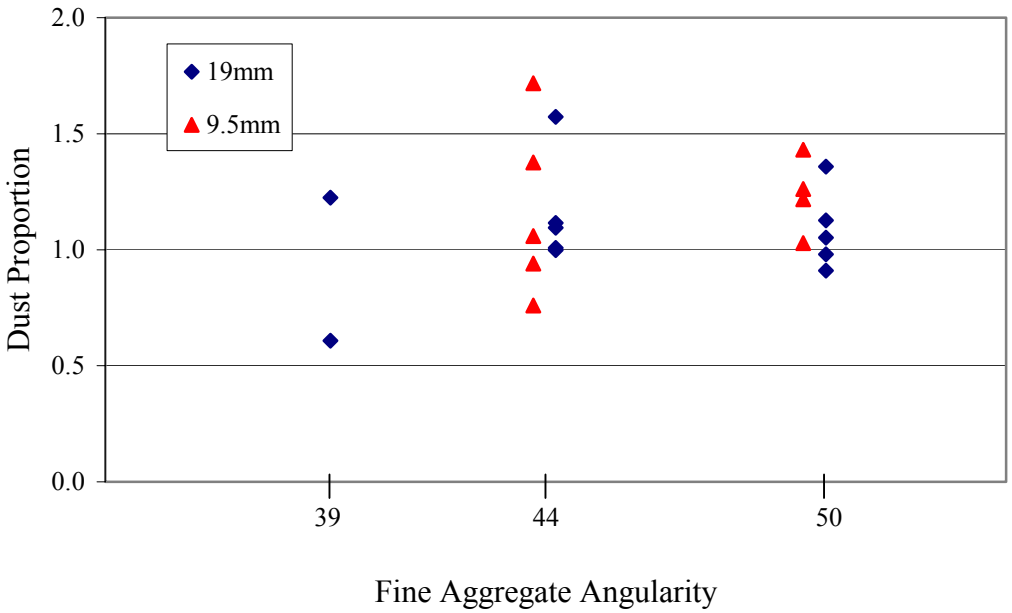

Figure 9.24 Effect of Fine Aggregate Angularity on Design Dust Proportion.

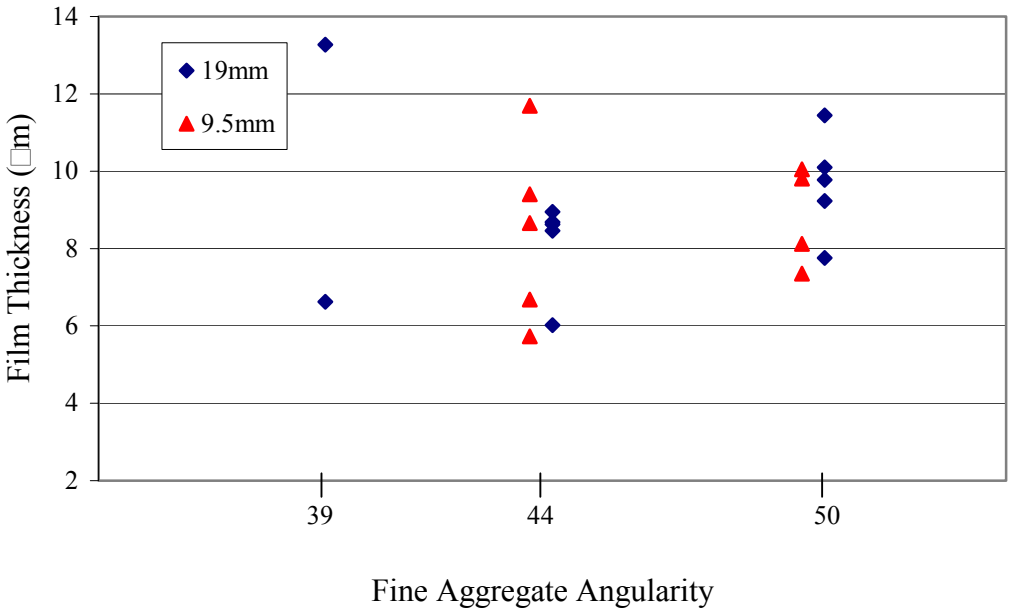

Figure 9.25 Effect of Fine Aggregate Angularity on Design Film Thickness.

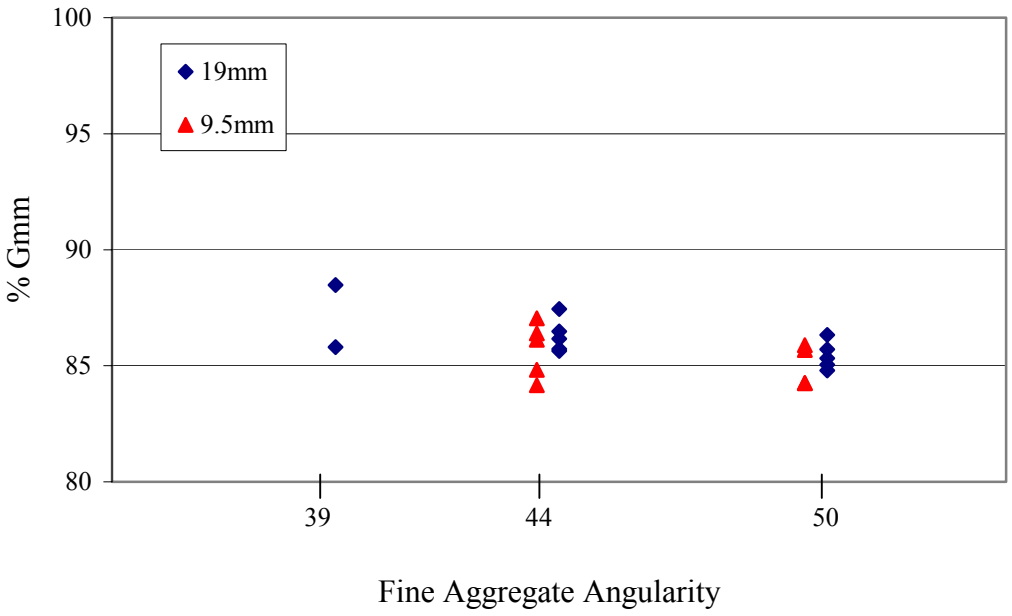

Figure 9.26 Effect of Fine Aggregate Angularity on Percent Gmm at $N_{initial}$.

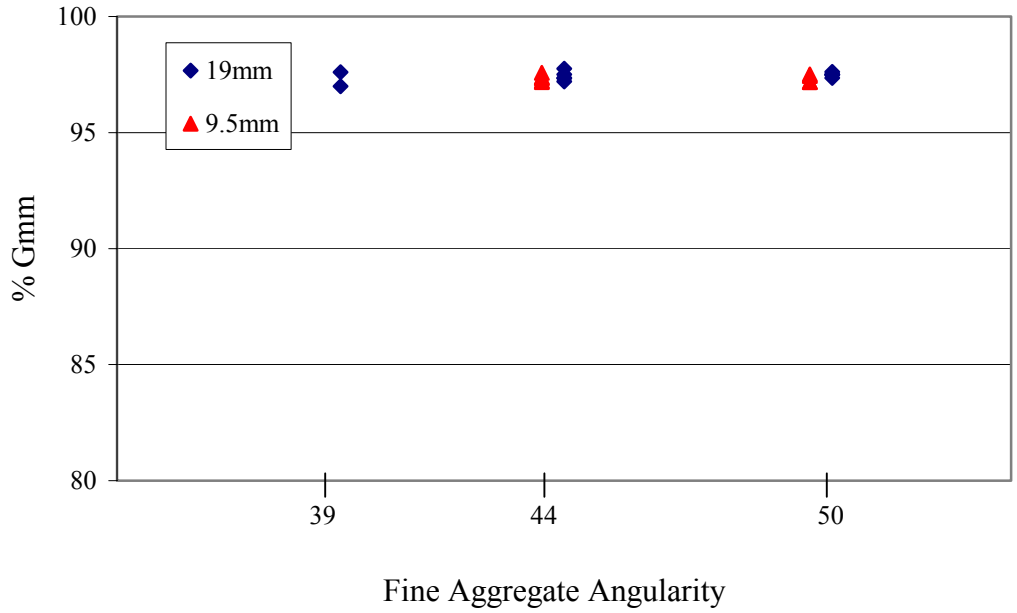

Figure 9.27 Effect of Fine Aggregate Angularity on Percent Gmm at $N_{maximum}$.

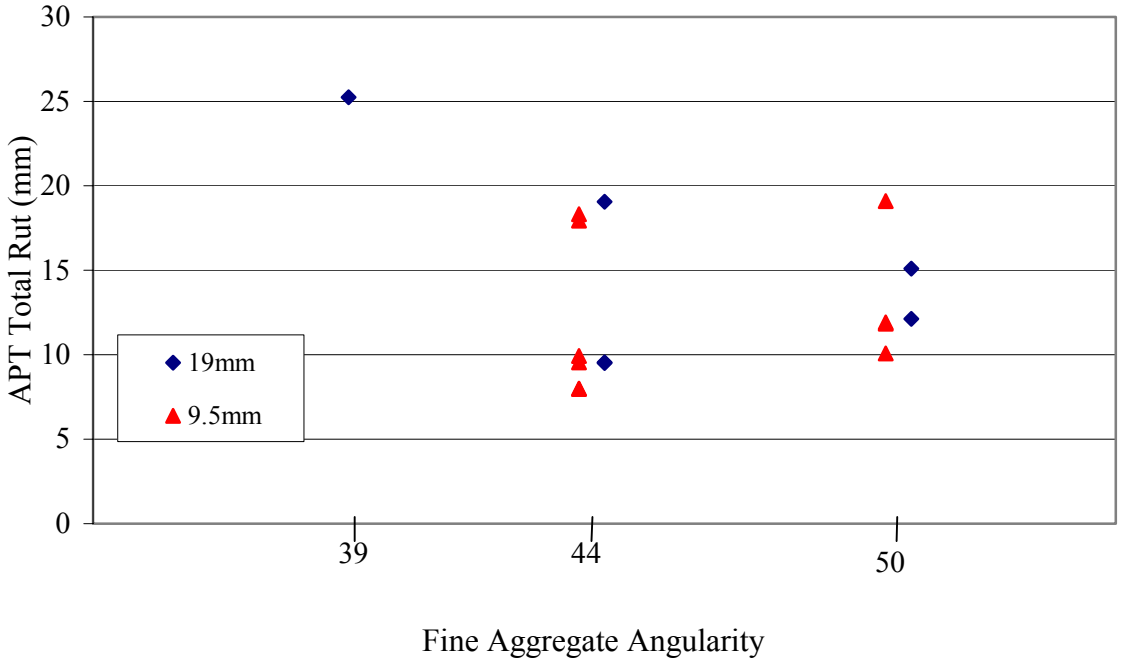

Figure 9.28 Effect of Fine Aggregate Angularity on Rutting Performance in APT.

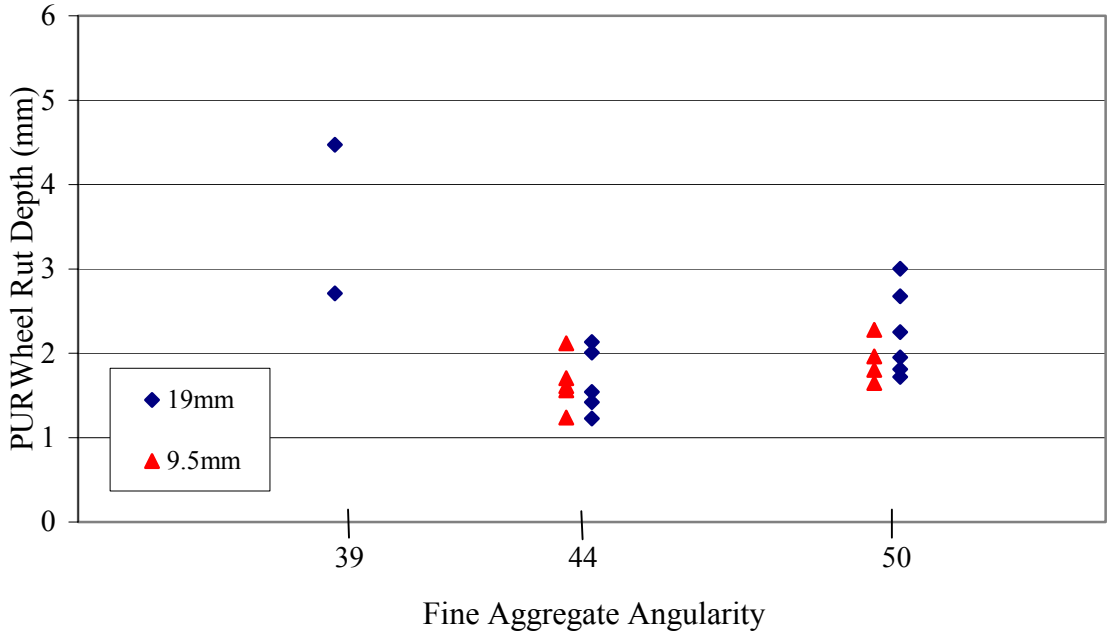

Figure 9.29 Effect of Fine Aggregate Angularity on Rutting Performance in PURWheel (LMLCD).

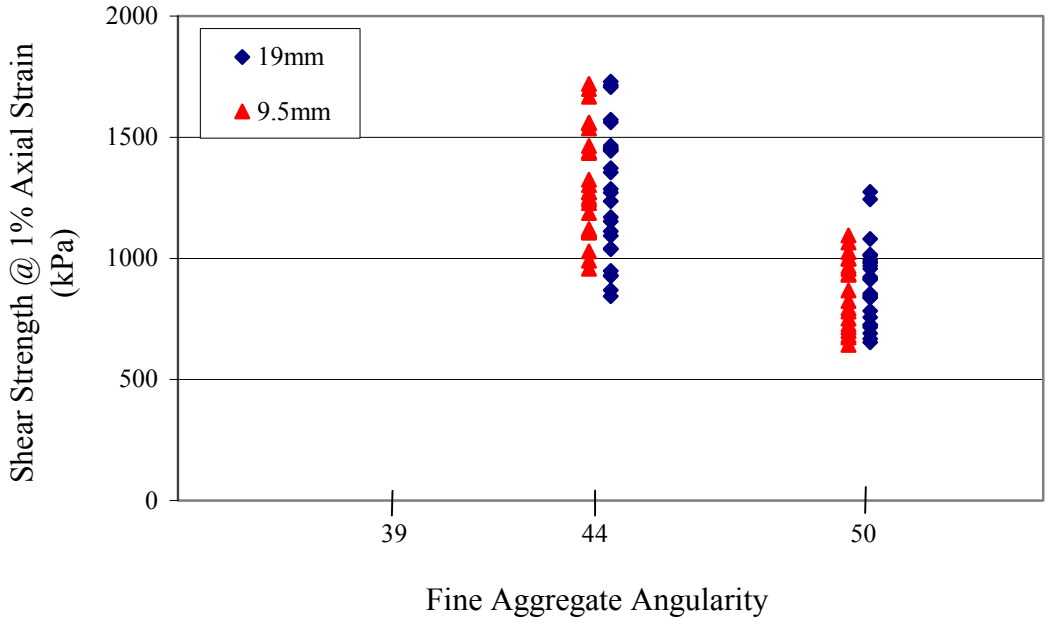

Figure 9.30 Effect of Fine Aggregate Angularity on Triaxial Test Results.

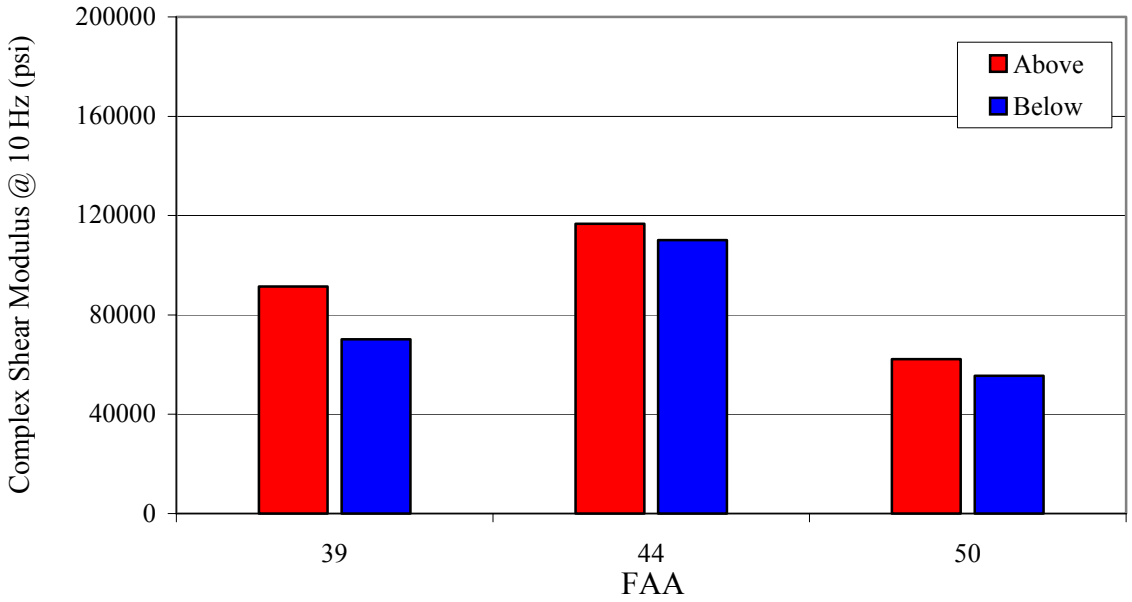

Figure 9.31 Effect of FAA and Gradation with Respect to The Restricted Zone on Complex Shear Modulus of 19mm Limestone Mixtures (LMLCS Specimens).

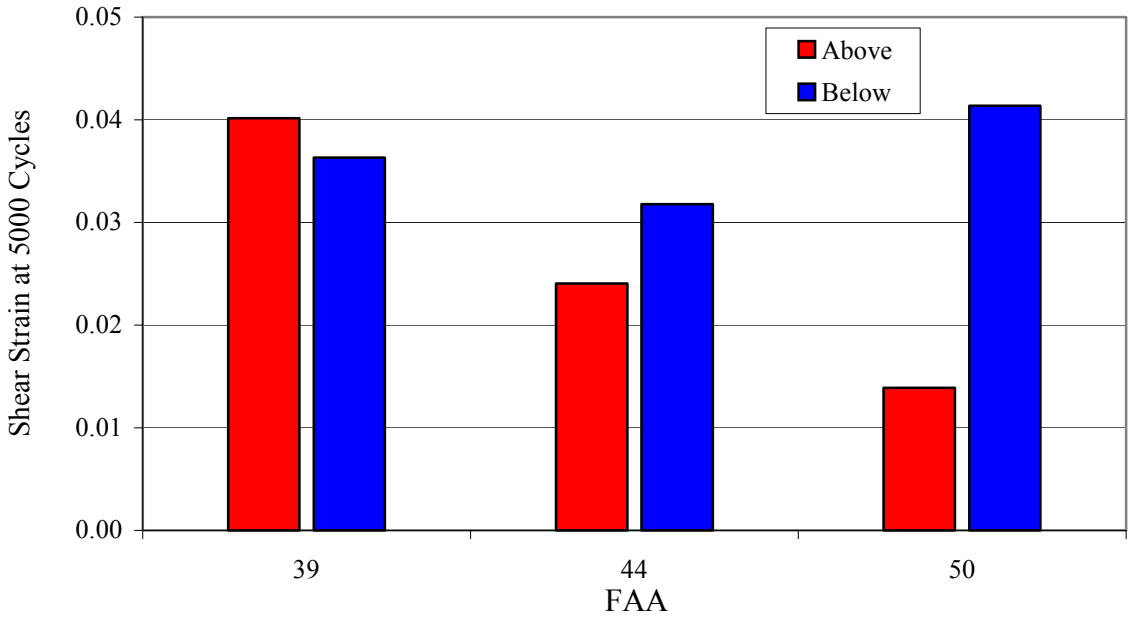

Figure 9.32 Effect of FAA and Gradation with Respect to The Restricted Zone on Shear Strain at 5000 Cycles of 19mm Limestone Mixtures (LMLCS Specimens).

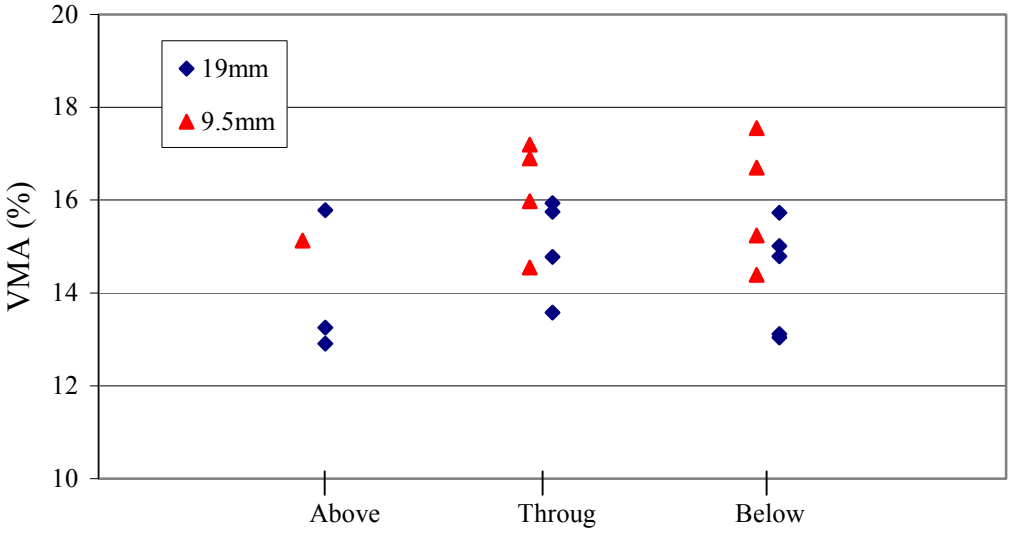

Figure 9.33 Effect of Gradation on Design VMA.

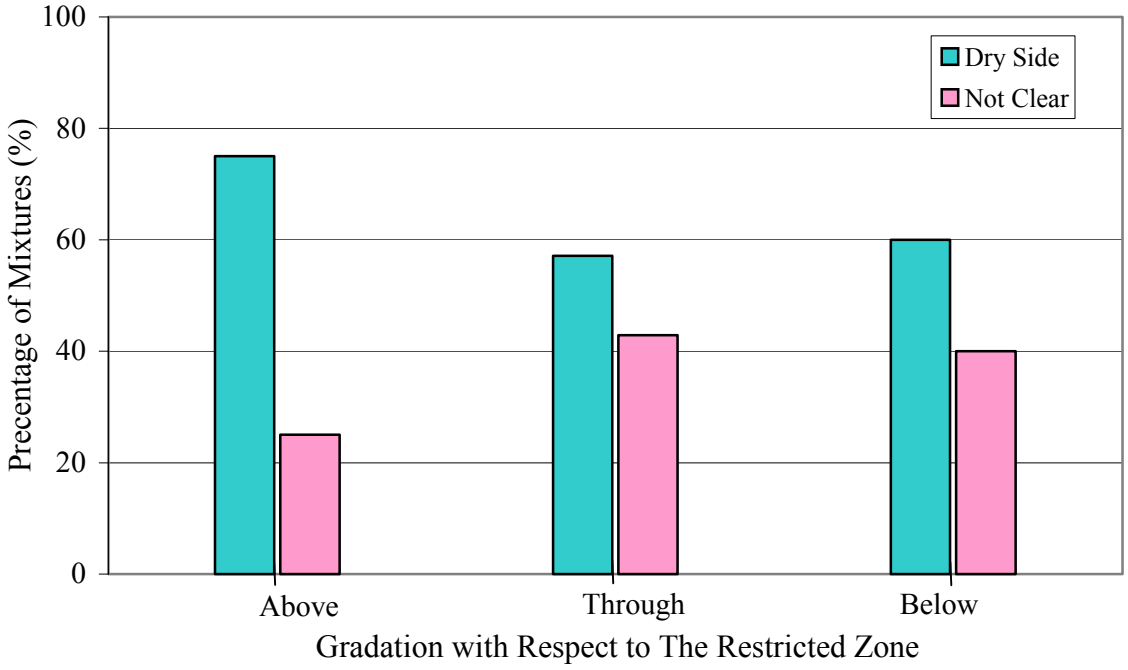

Figure 9.34 Effect of Gradation on Location of Design AC on VMA Curve at N_{design} Gyrations.

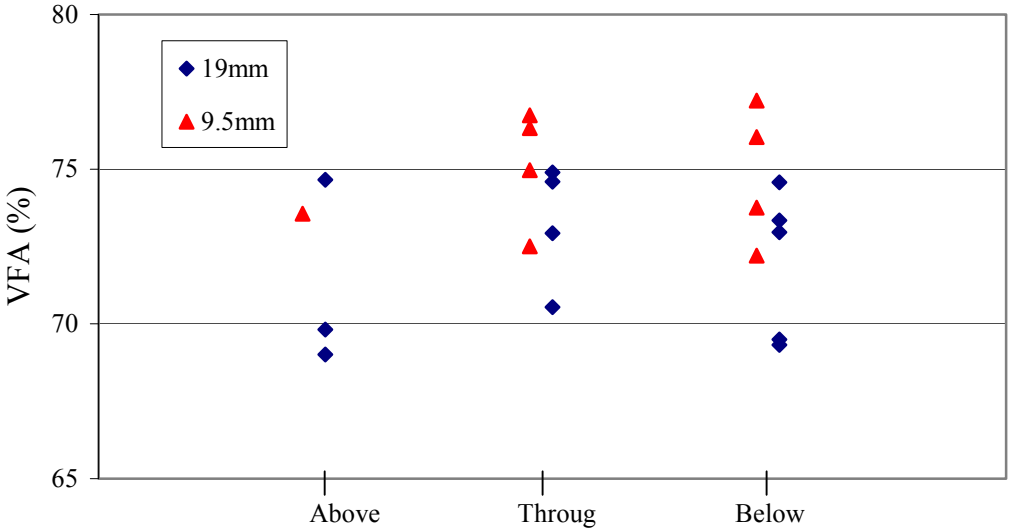

Gradation with Respect to the Restricted Zone

Figure 9.35 Effect of Gradation on Design VFA.

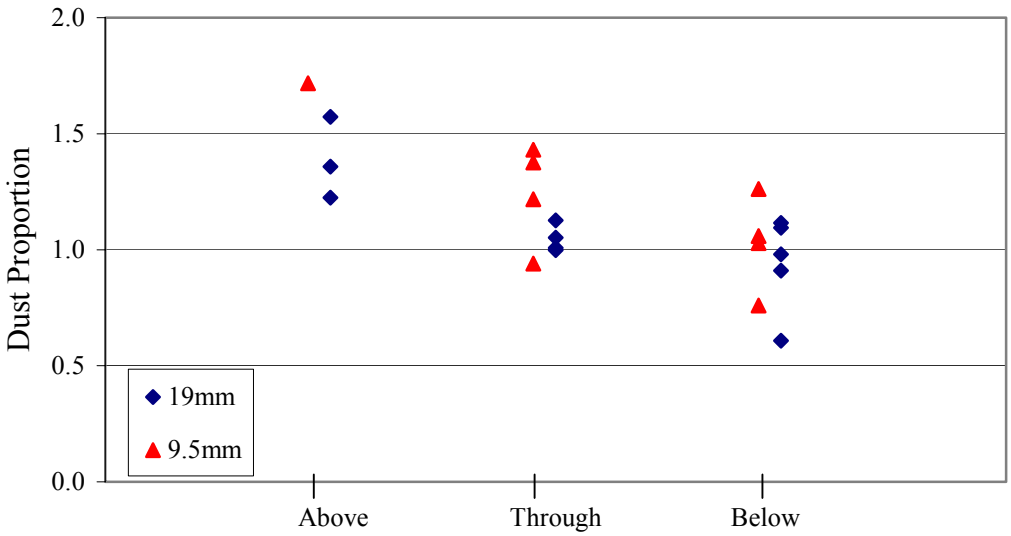

Gradation with Respect to the Restricted Zone

Figure 9.36 Effect of Gradation on Design Dust Proportion.

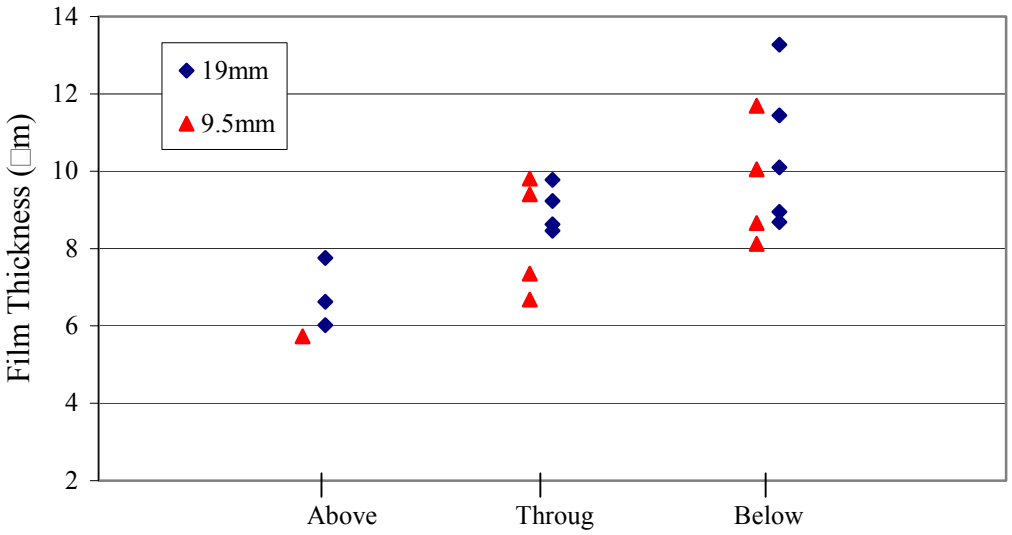

Gradation with Respect to the Restricted Zone

Figure 9.37 Effect of Gradation on Design Film Thickness.

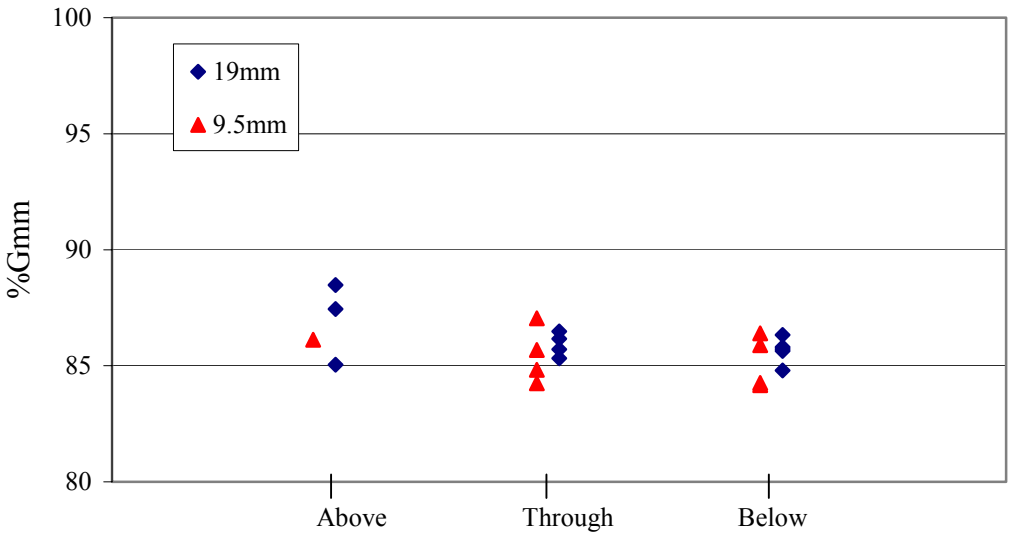

Gradation with Respect to the Restricted Zone

Figure 9.38 Effect of Gradation on Percent Gmm at $N_{initial}$.

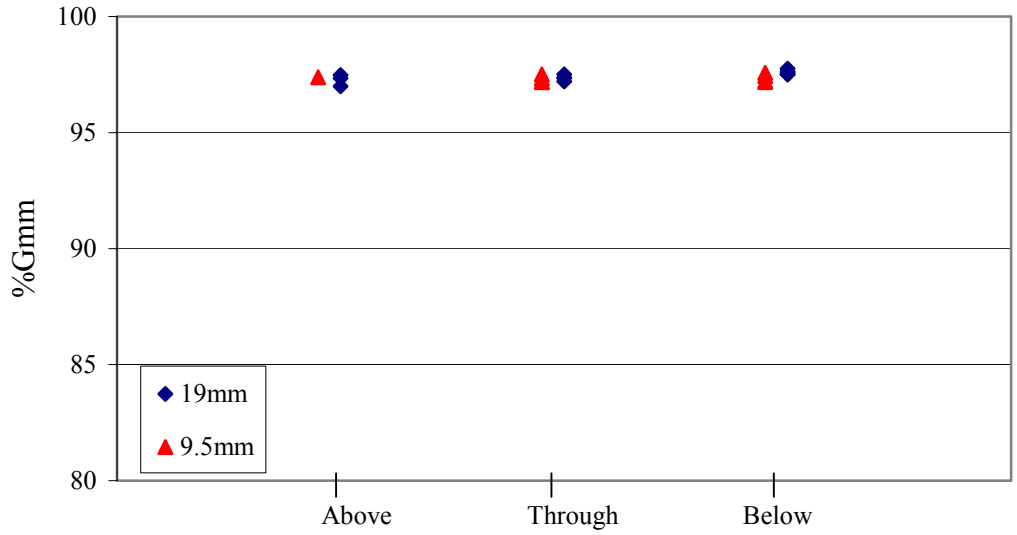

Figure 9.39 Effect of Gradation on Percent Gmm at $N_{maximum}$.

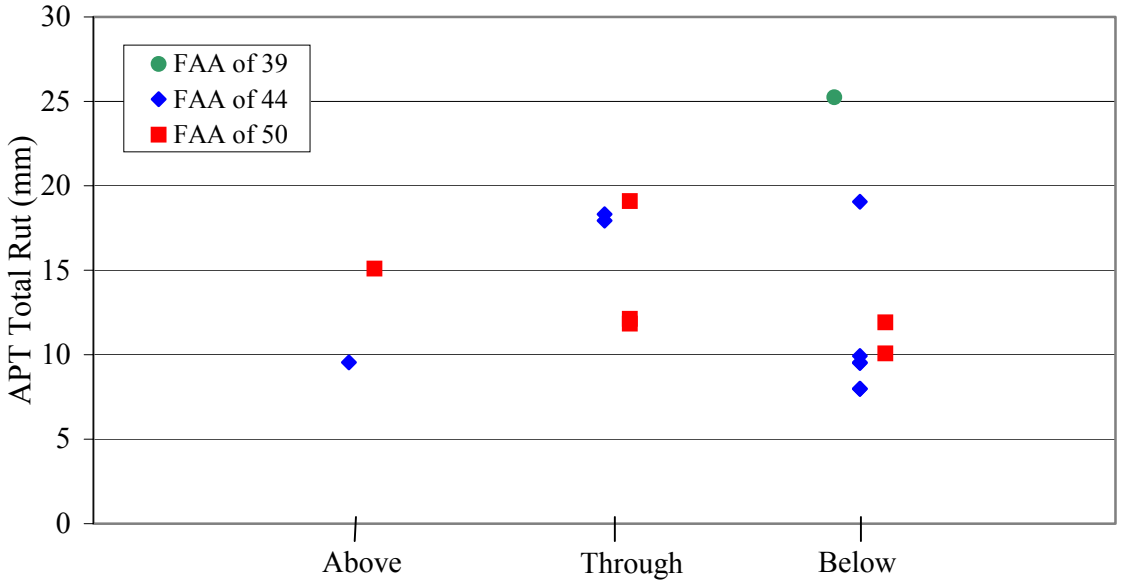

Figure 9.40 Effect of Gradation on Rutting Performance in APT.

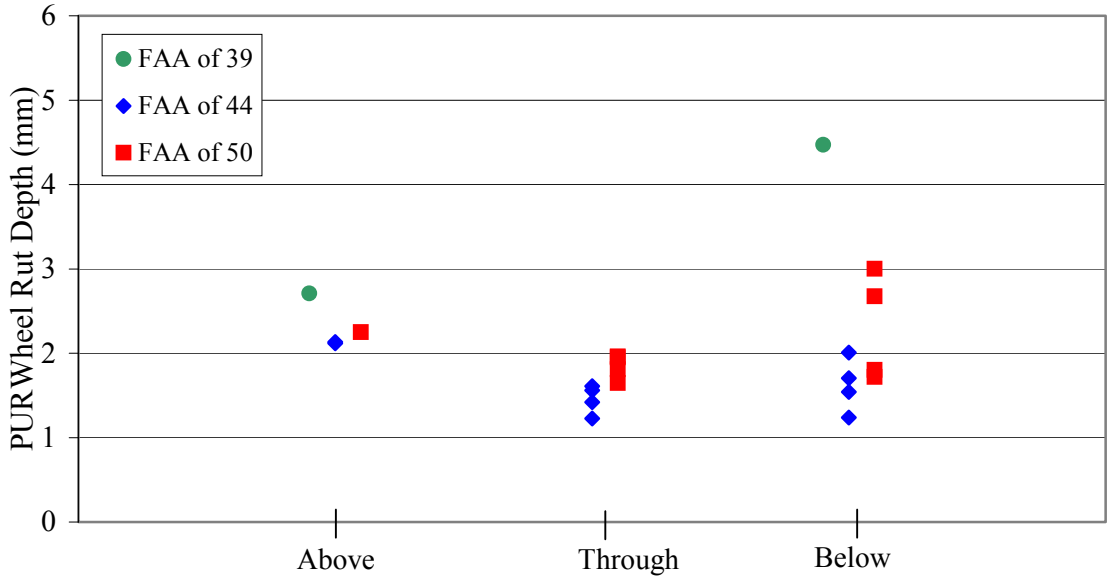

Figure 9.41 Effect of Gradation on Rutting Performance in PURWheel (LMLCD).

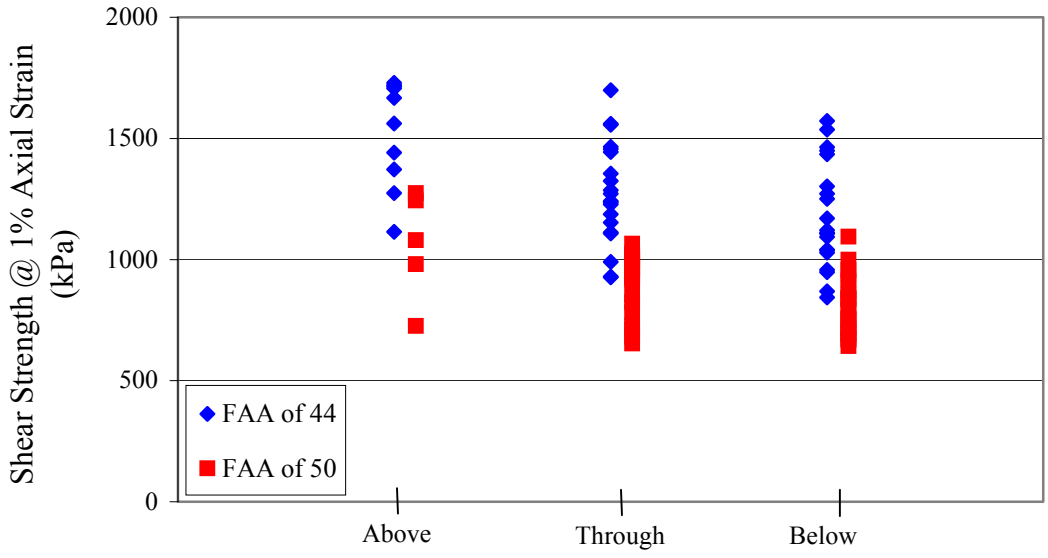

Figure 9.42 Effect of Gradation on Triaxial Test Results.

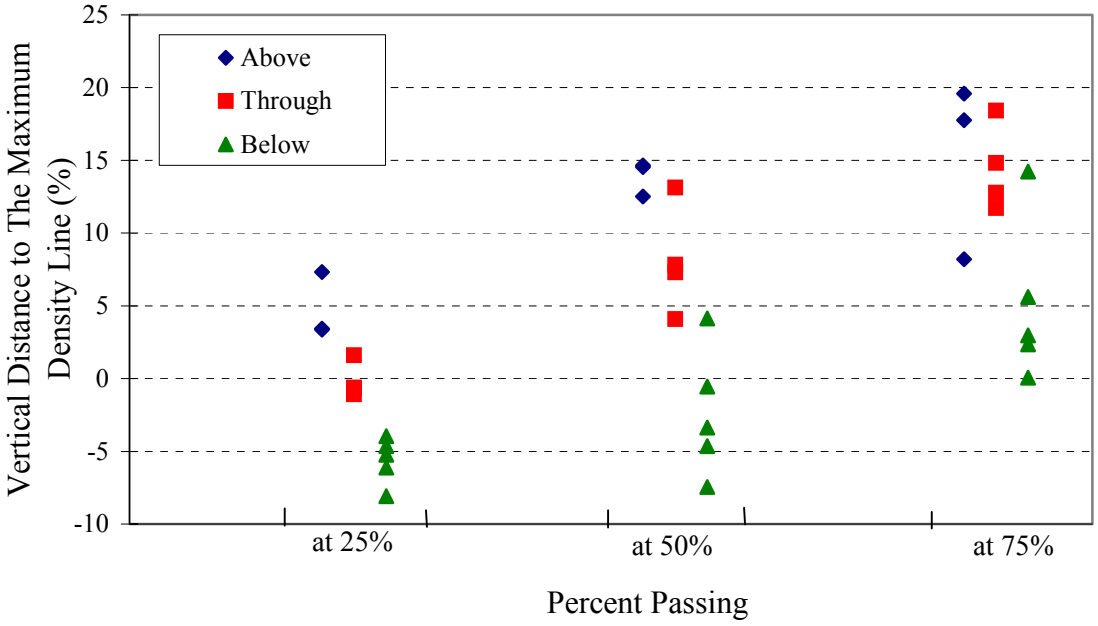

Figure 9.43 Vertical Distance to The Maximum Density Line for 19mm Mixtures.

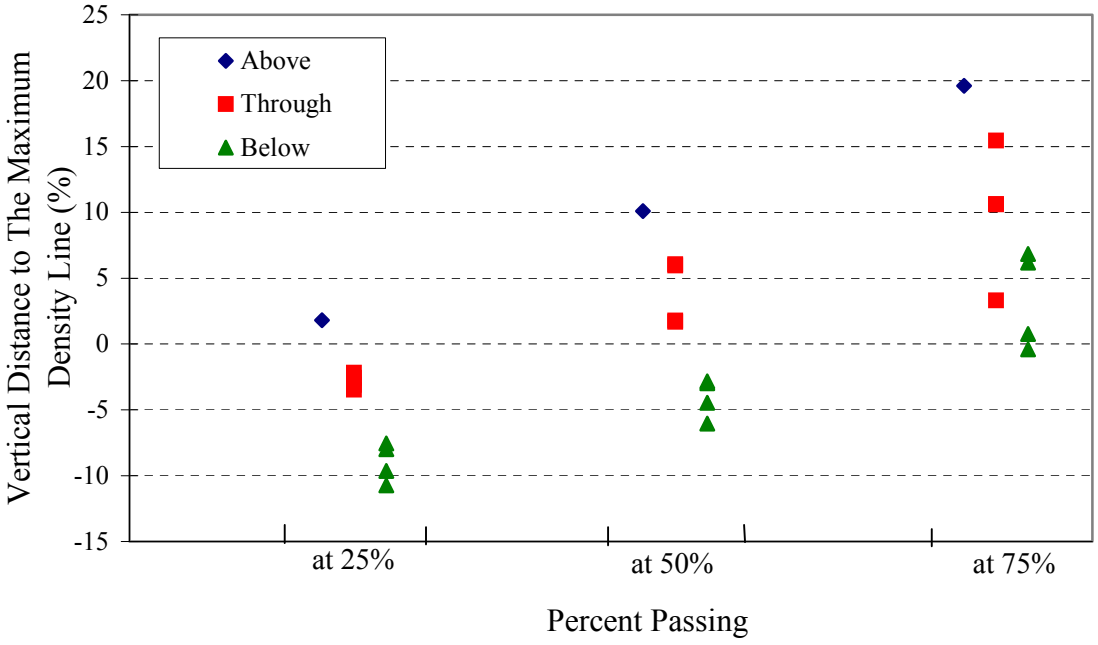

Figure 9.44 Vertical Distance to The Maximum Density Line for 9.5mm Mixtures.

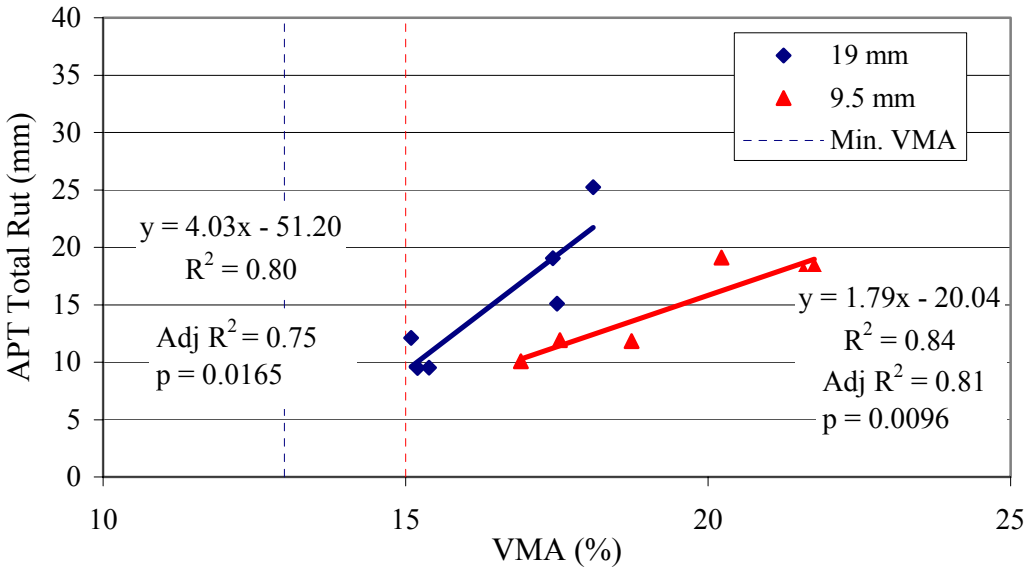

Figure 9.45 Effect of VMA on Rutting Performance in APT.

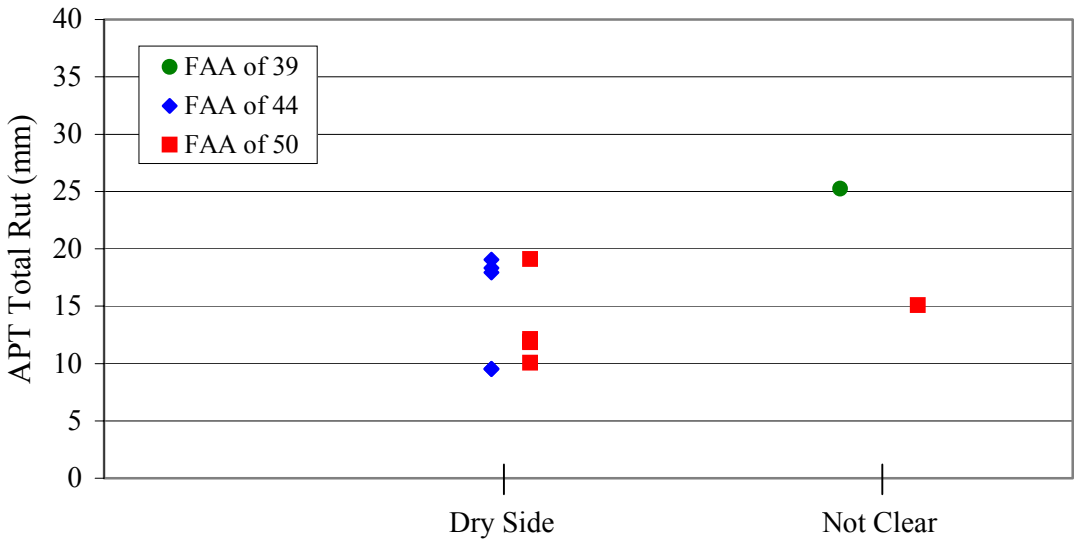

Figure 9.46 Effect of Location of Design AC on VMA Curve at N_{design} Gyrations on Rutting Performance in APT.

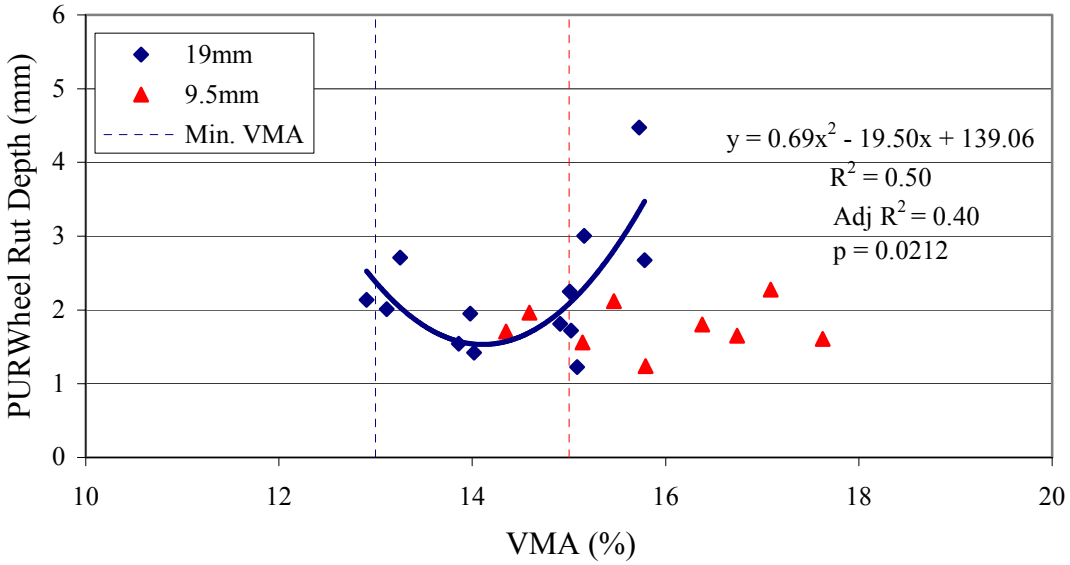

Figure 9.47 Effect of VMA on Rutting Performance in PURWheel.

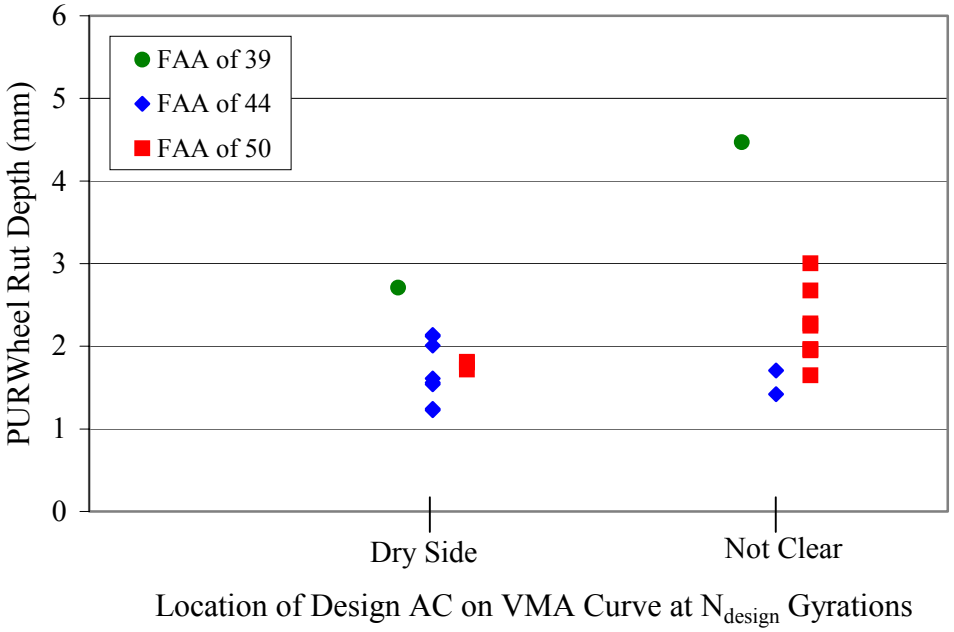

Figure 9.48 Effect of Location of Design AC on VMA Curve at N_{design} Gyrations on Rutting Performance in PURWheel.

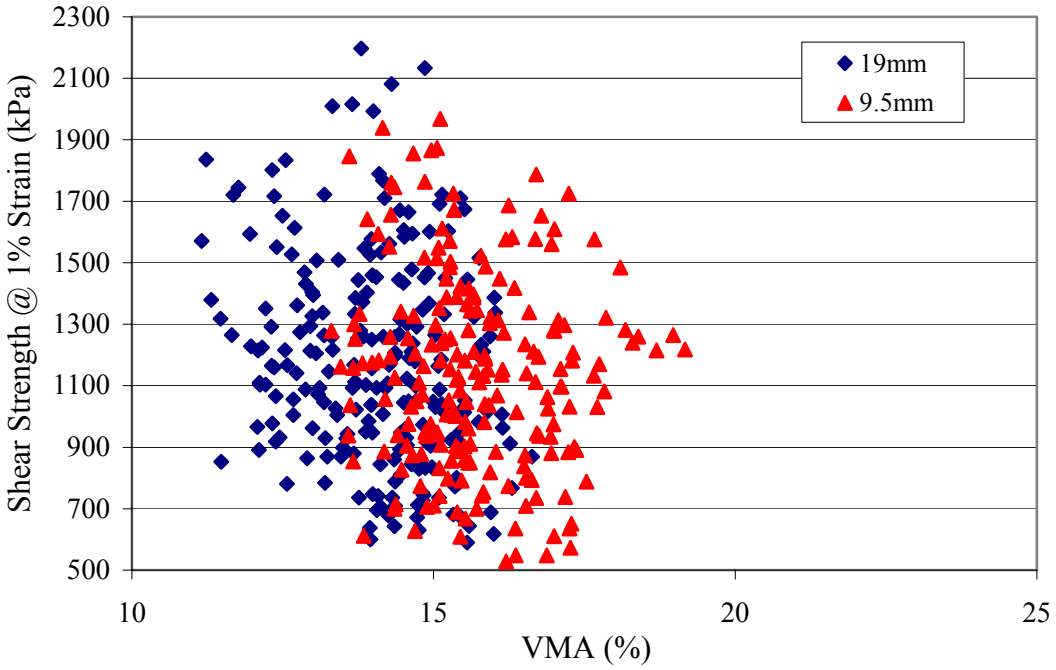

Figure 9.49 Effect of VMA on Triaxial Test Results.

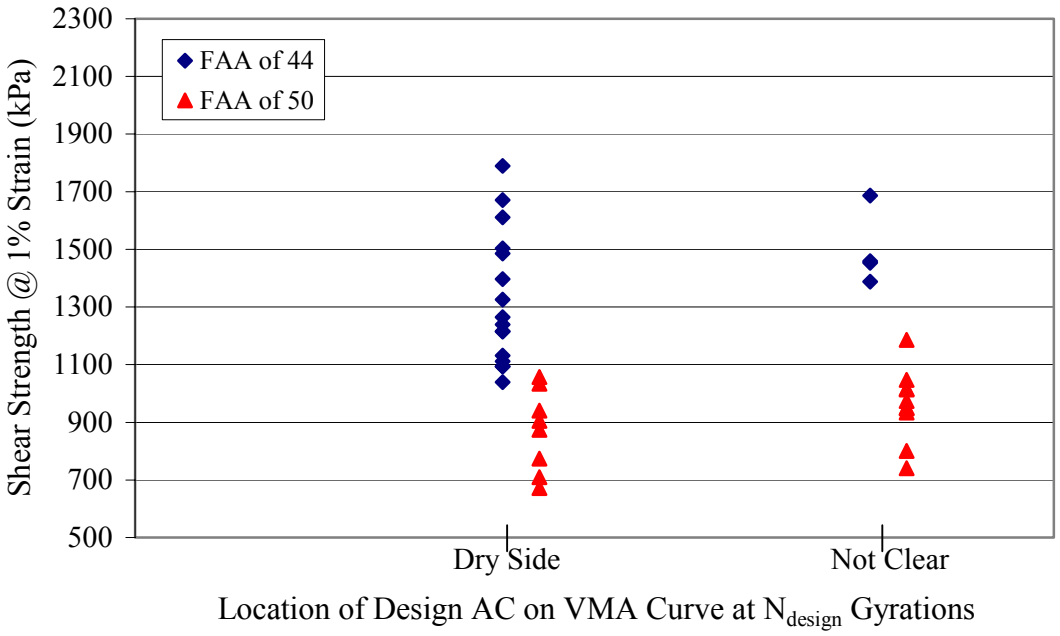

Figure 9.50 Effect of Location of Design AC on VMA Curve at N_{design} Gyrations on Triaxial Test Results.

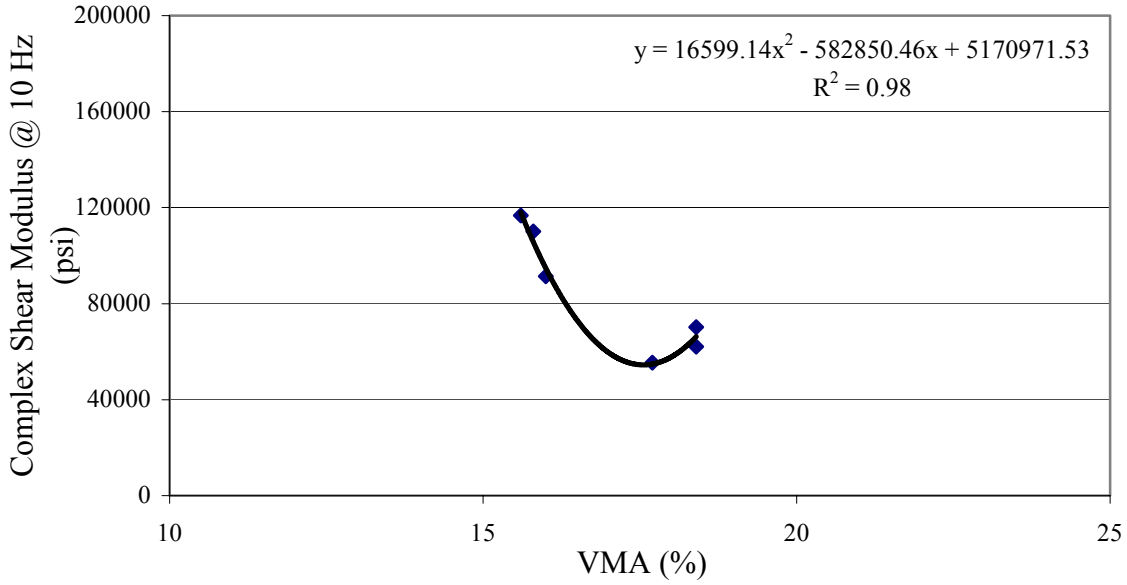

Figure 9.51 Effect of VMA on FSCH Results for LMLCS Specimens.

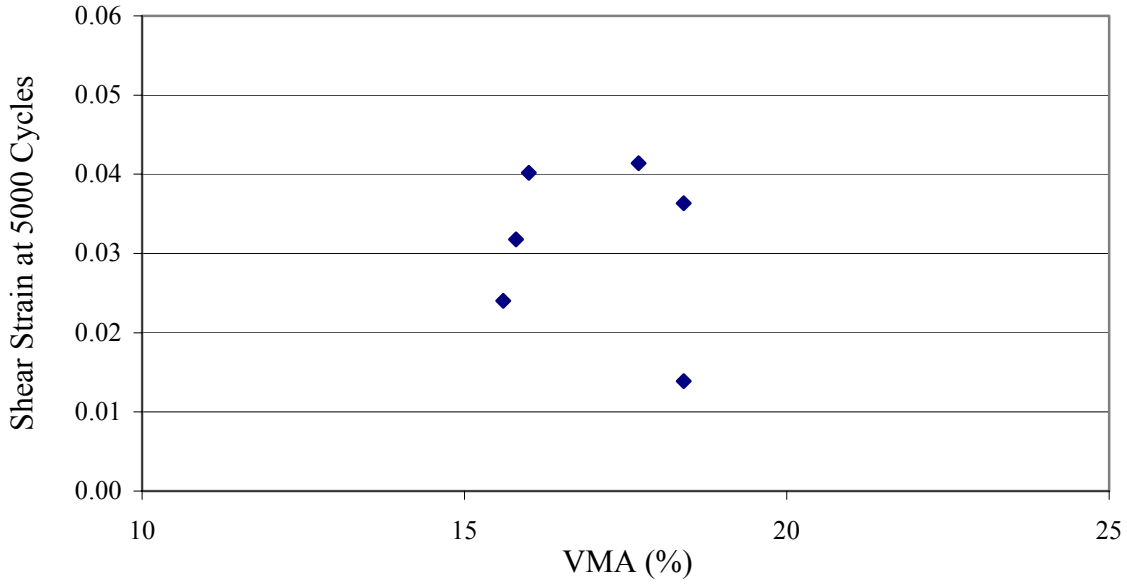

Figure 9.52 Effect of VMA on RSCH Results for LMLCS Specimens.

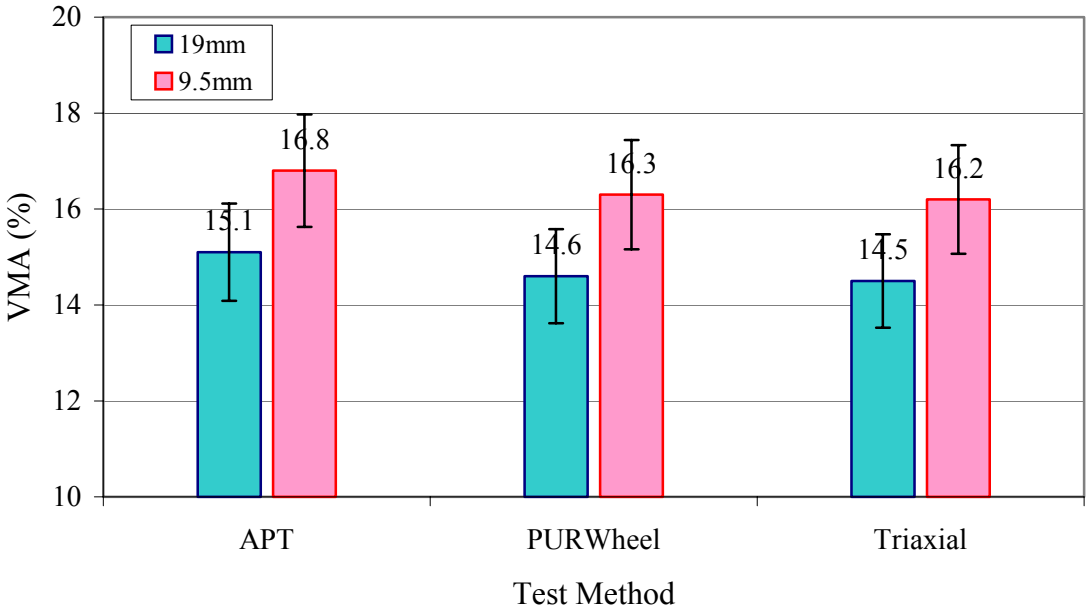

Figure 9.53 Measured Critical VMA.

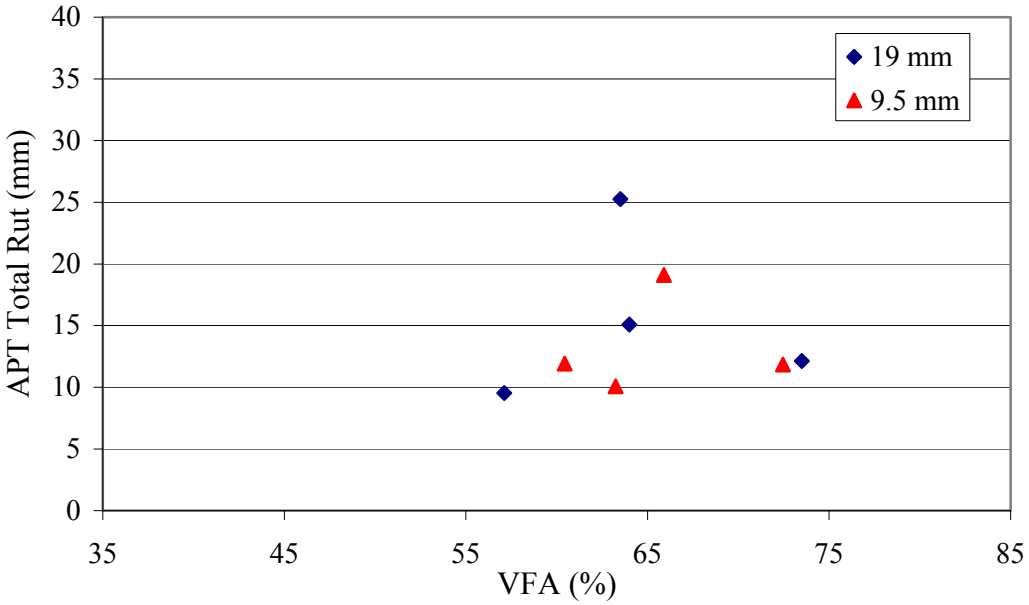

Figure 9.54 Effect of VFA on Rutting Performance in APT.

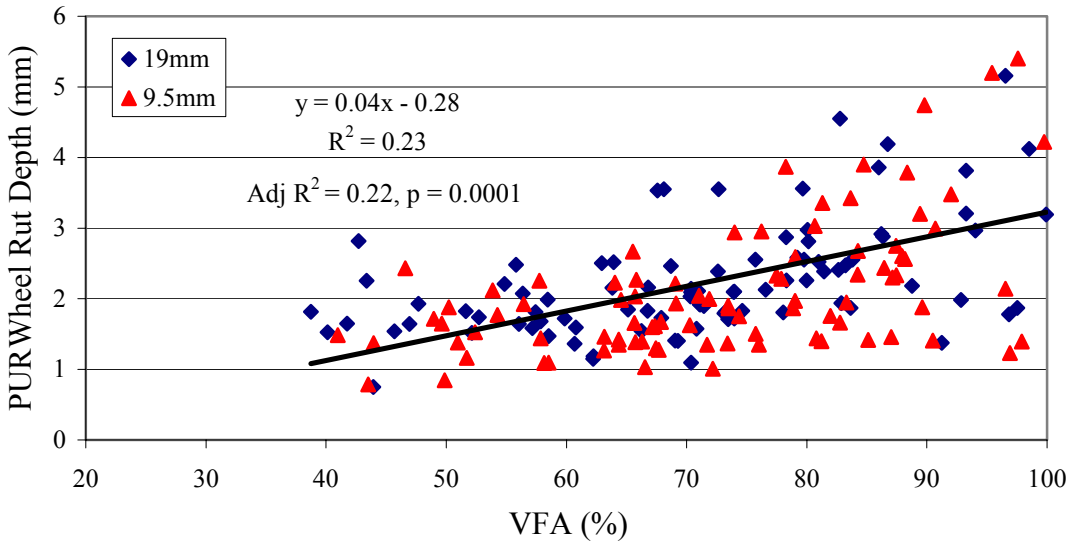

Figure 9.55 Effect of VFA on Rutting Performance in PURWheel.

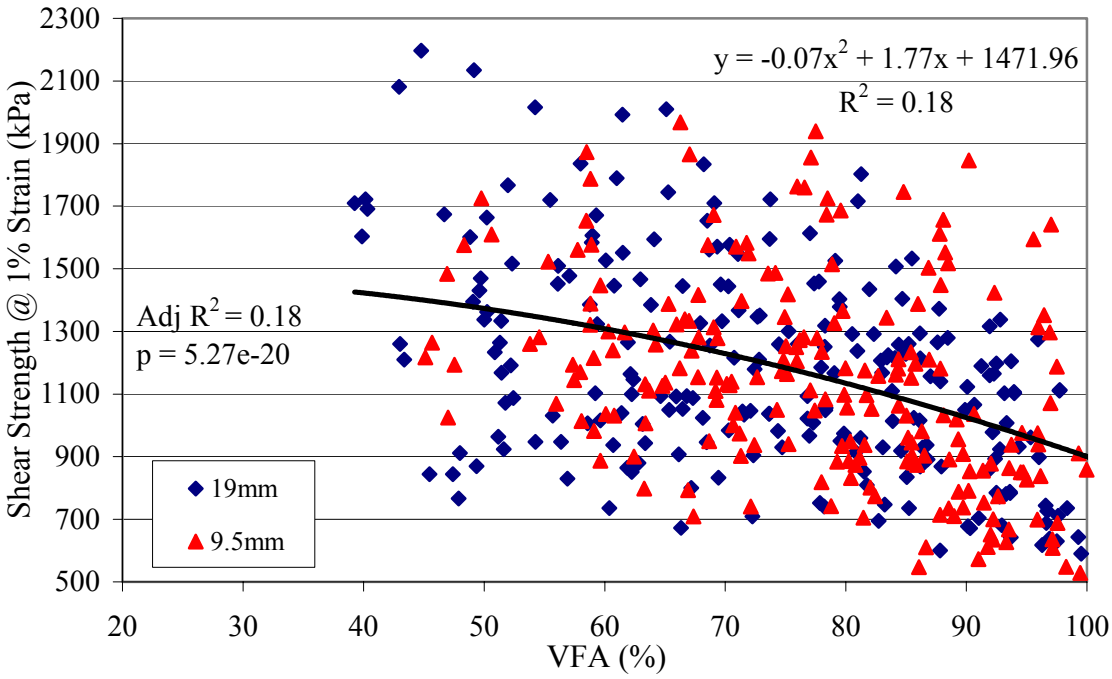

Figure 9.56 Effect of VFA on Triaxial Test Results.

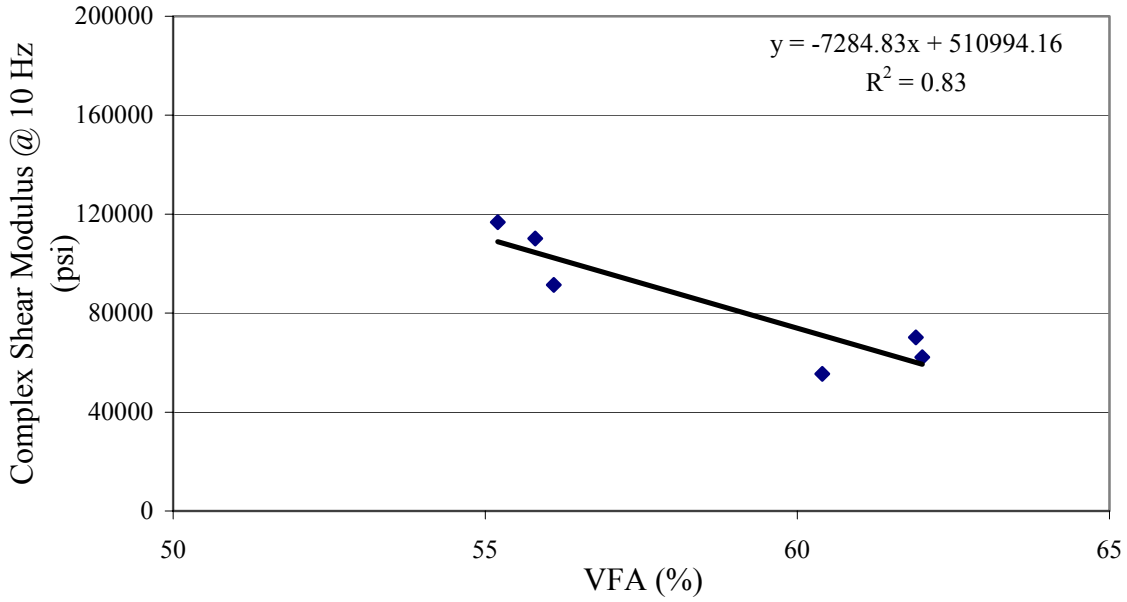

Figure 9.57 Effect of VFA on FSCH Results for LMLCS Specimens.

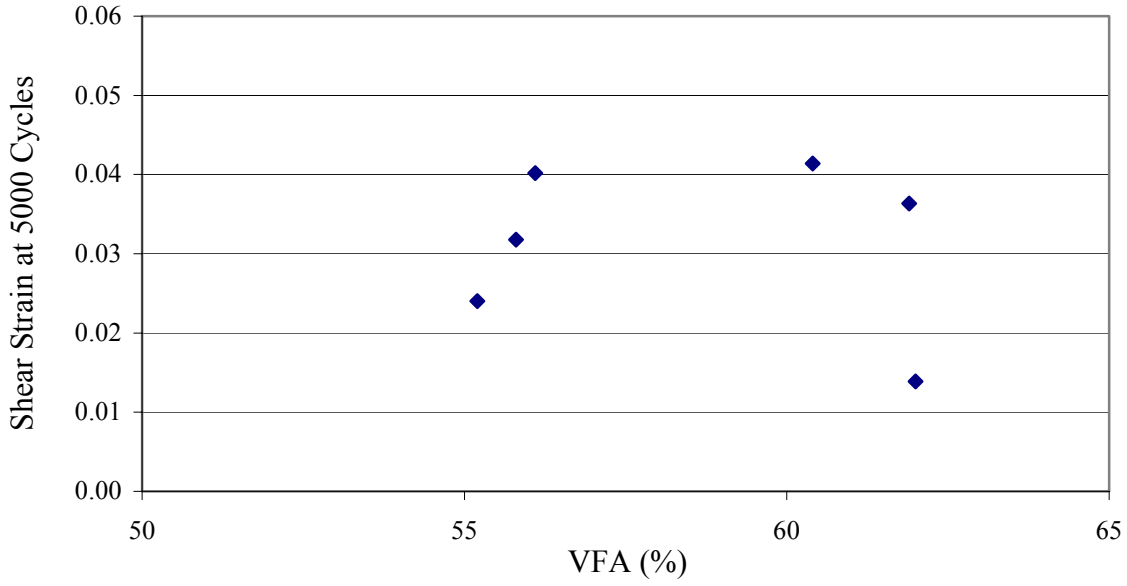

Figure 9.58 Effect of VFA on RSCH Results for LMLCS Specimens.

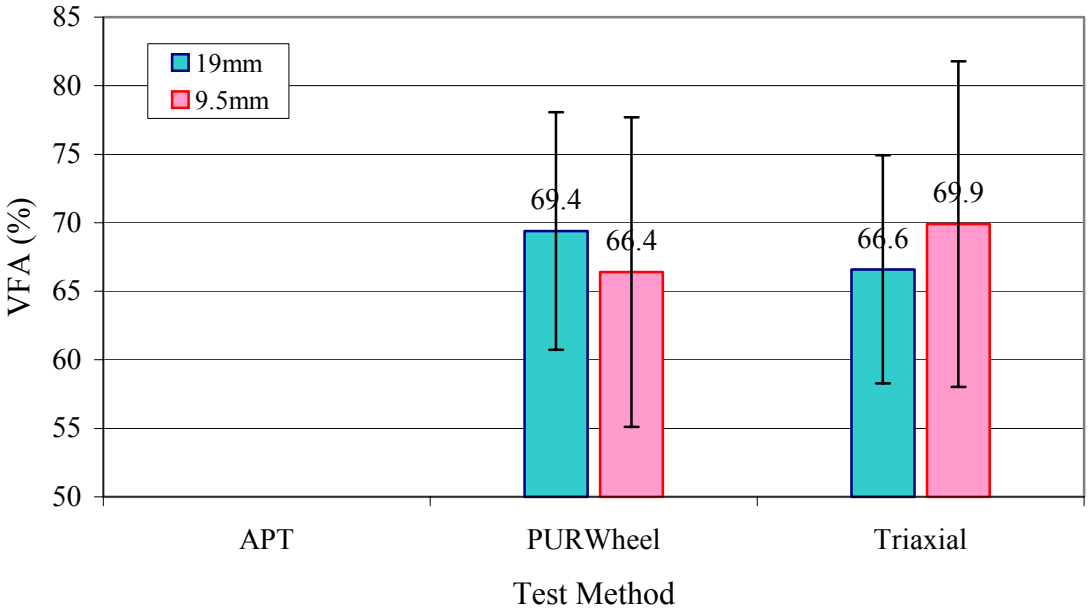

Figure 9.59 Measured Critical VFA.

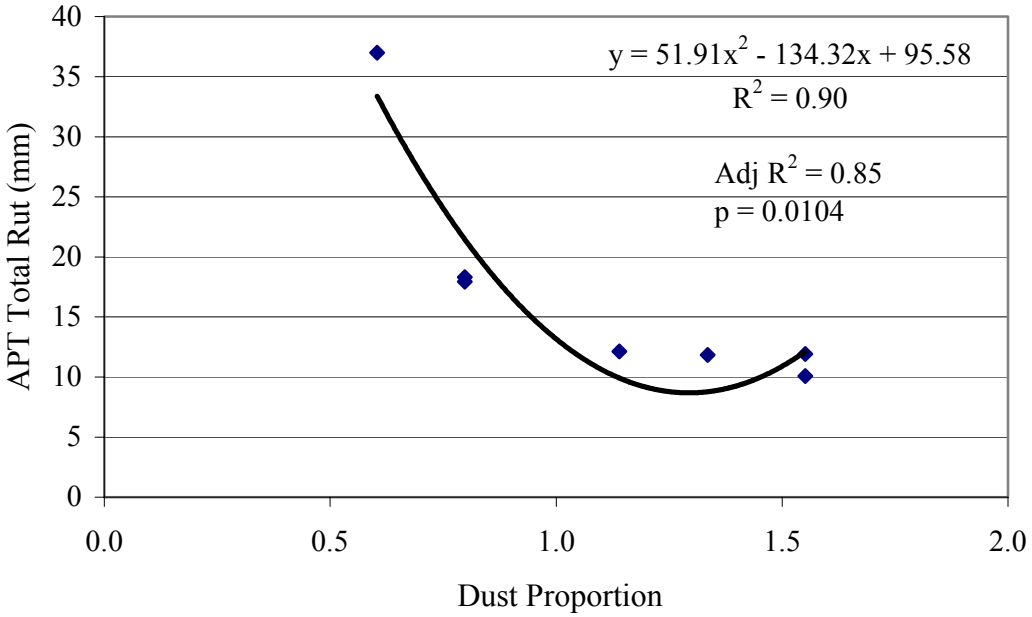

Figure 9.60 Effect of Dust Proportion on Rutting Performance in APT.

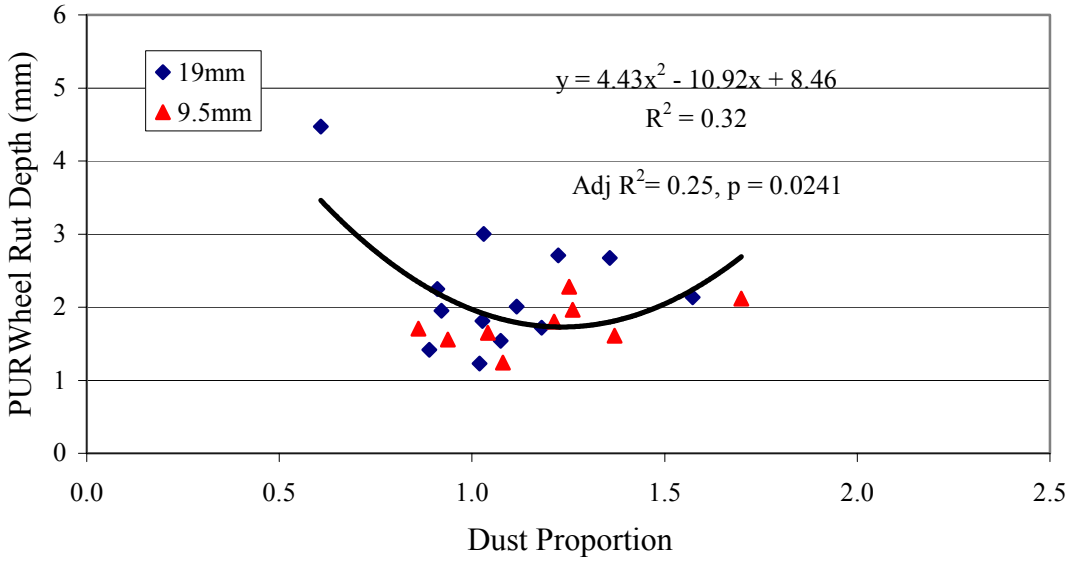

Figure 9.61 Effect of Dust Proportion on Rutting Performance in PURWheel.

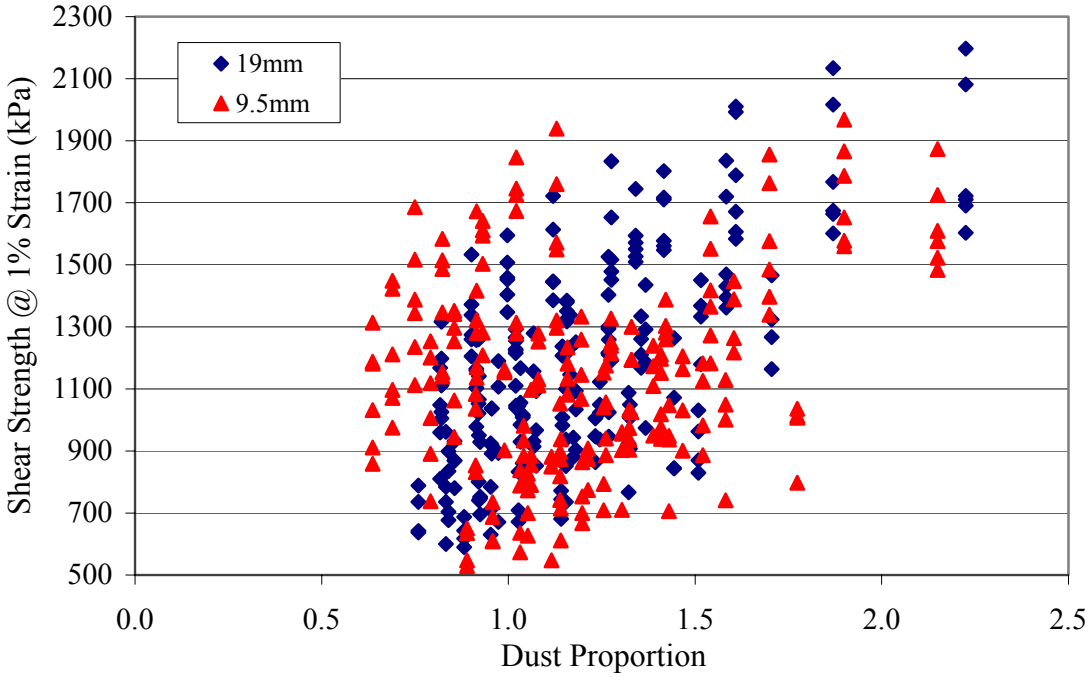

Figure 9.62 Effect of Dust Proportion on Triaxial Test Results.

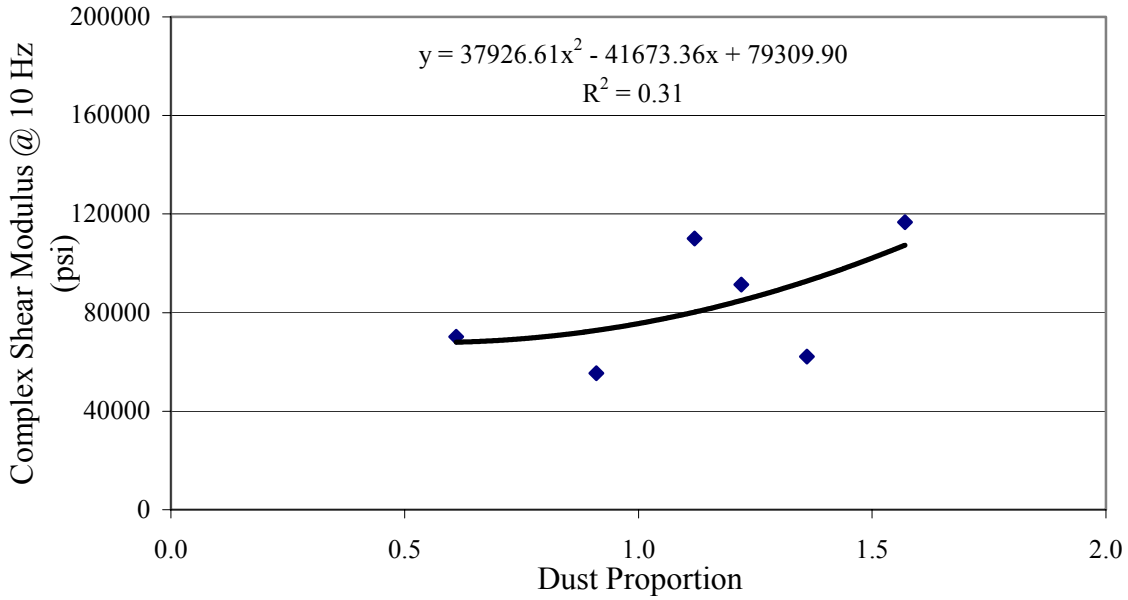

Figure 9.63 Effect of Dust Proportion on FSCH Results for LMLCS Specimens.

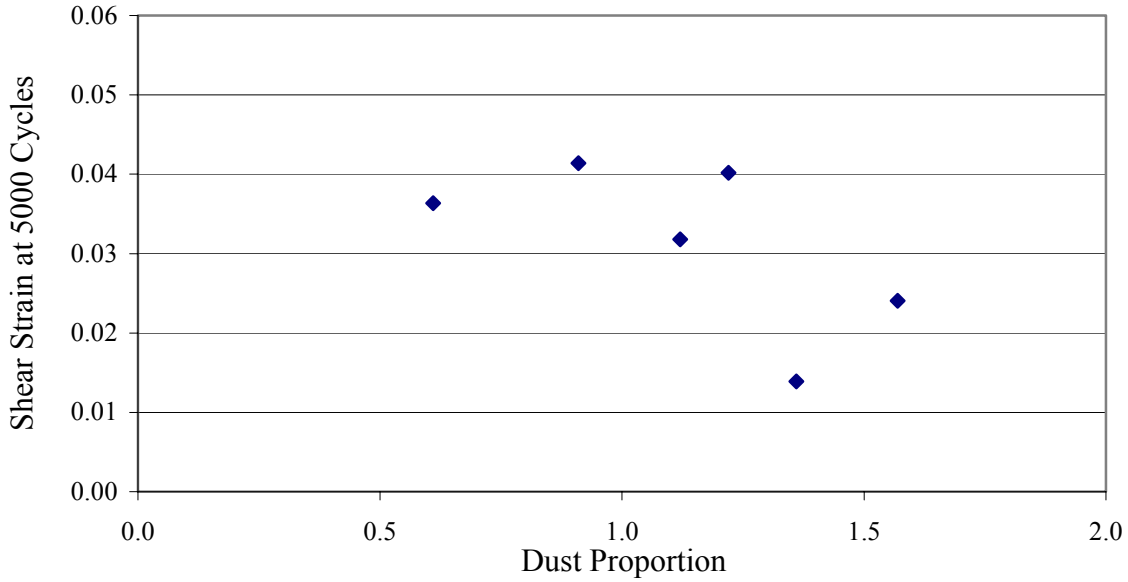

Figure 9.64 Effect of Dust Proportion on RSCH Results for LMLCS Specimens.

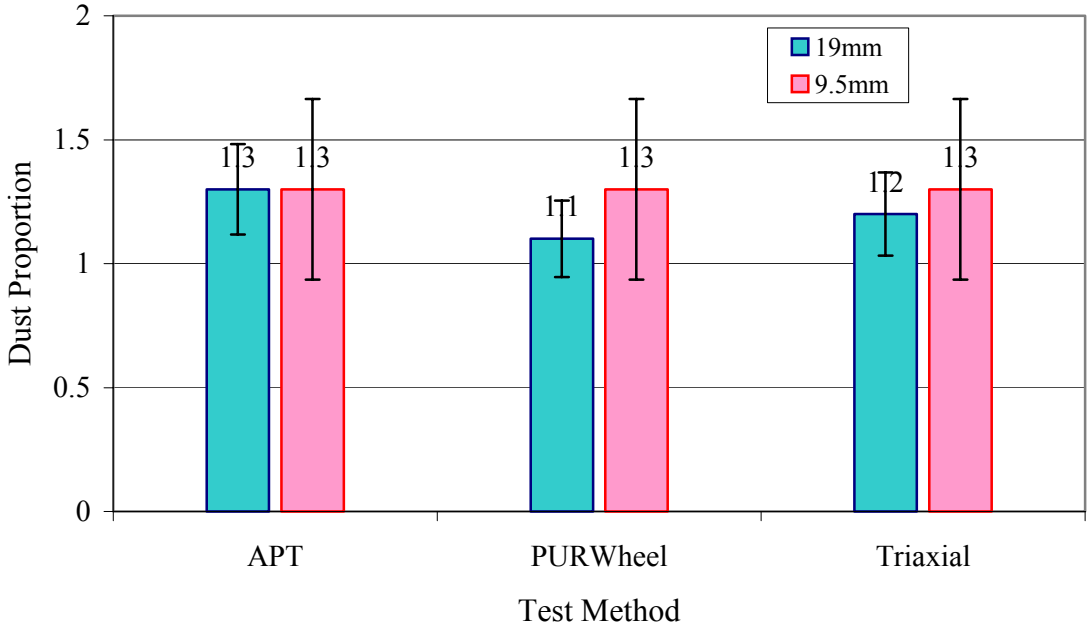

Figure 9.65 Measured Critical Dust Proportion.

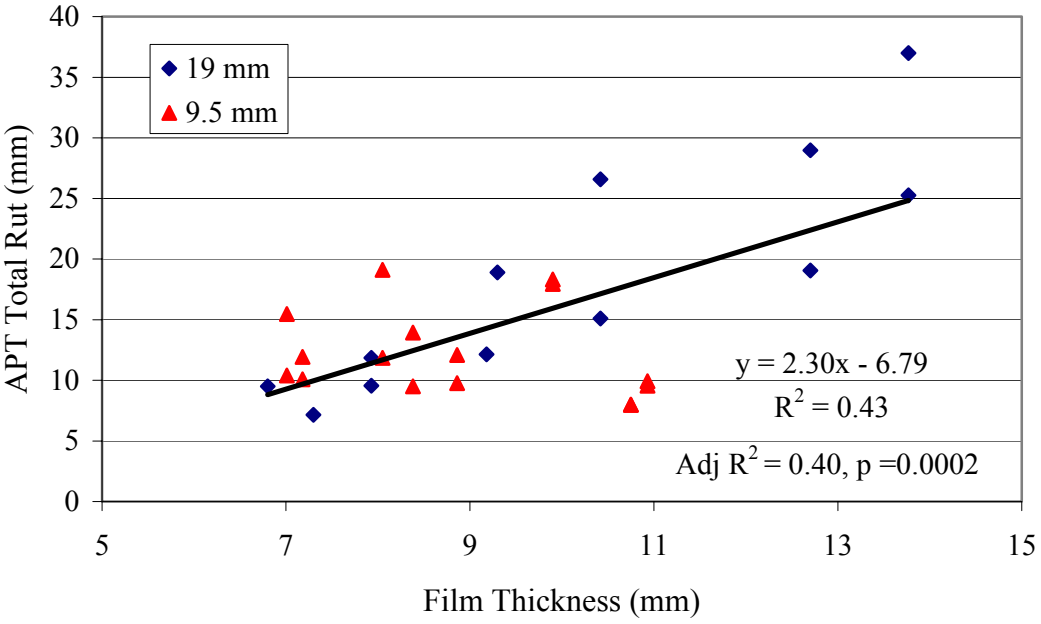

Figure 9.66 Effect of Film Thickness on Rutting Performance in APT.

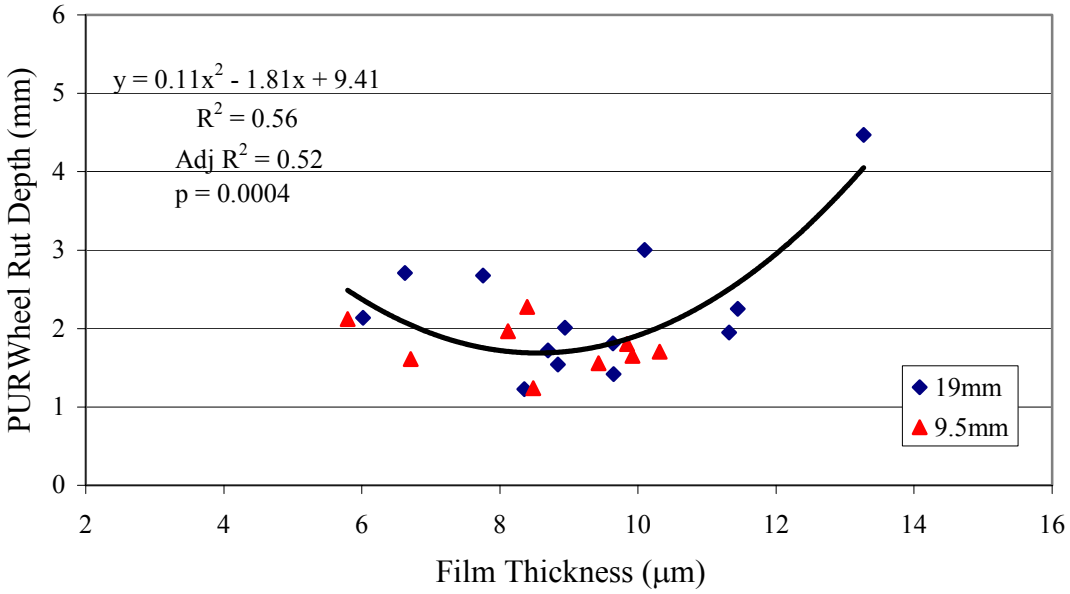

Figure 9.67 Effect of Film Thickness on Rutting Performance in PURWheel.

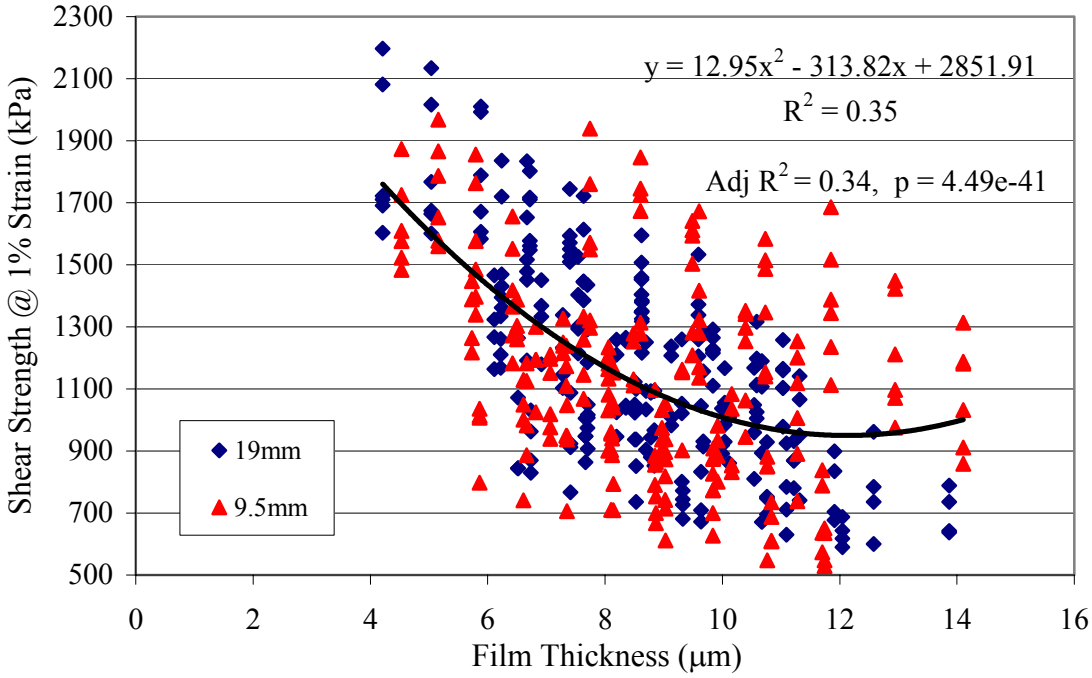

Figure 9.68 Effect of Film Thickness on Triaxial Test Results.

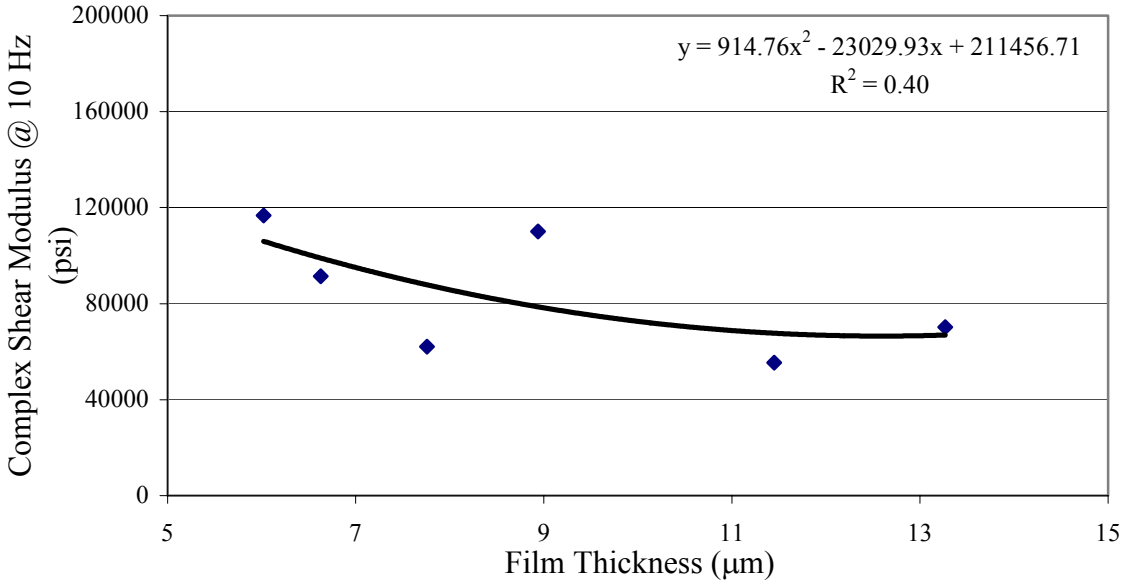

Figure 9.69 Effect of Film Thickness on FSCH Results for LMLCS Specimens.

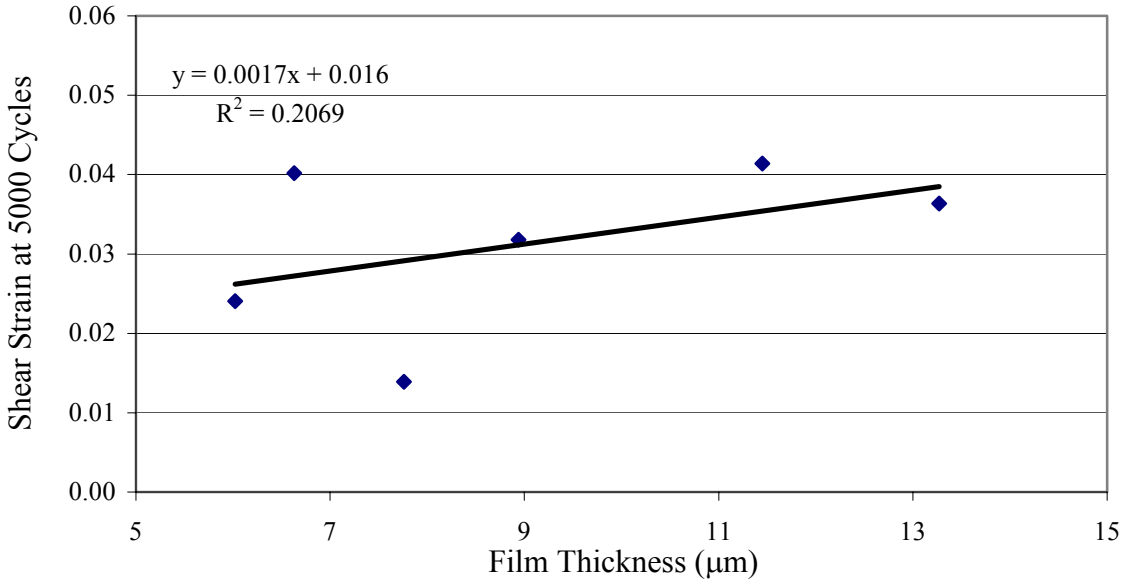

Figure 9.70 Effect of Film Thickness on RSCH Results for LMLCS Specimens.

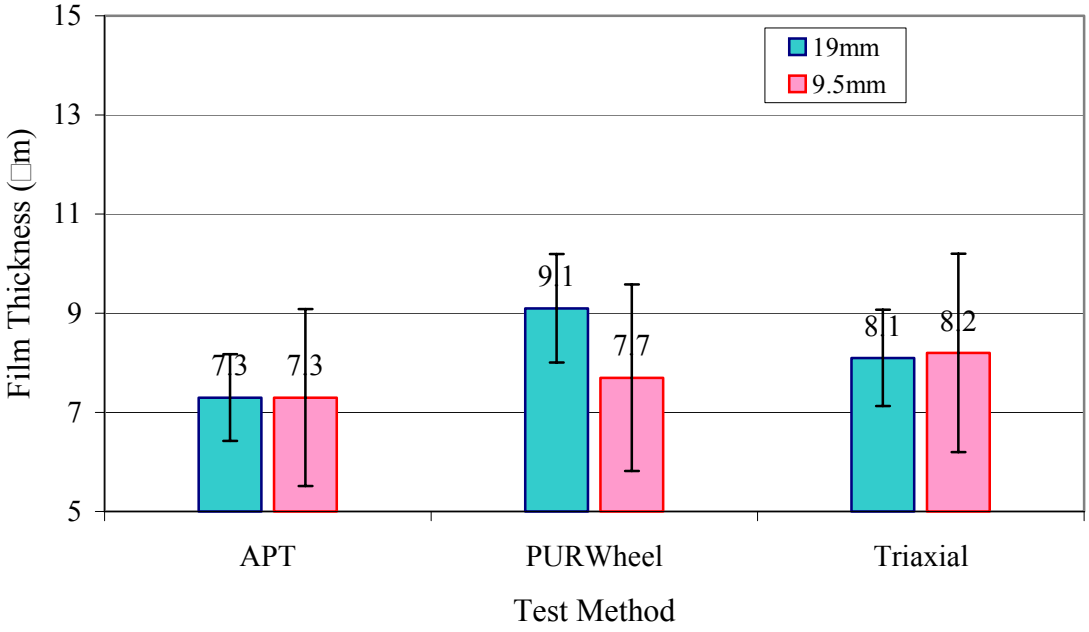

Figure 9.71 Critical Film Thickness.

10 CONCLUSIONS AND RECOMMENDATIONS

10.1. Conclusions

The main objective of the study presented herein is to validate various HMA aggregate specifications and volumetric relationships established in the Superpave. Effects of voids in mineral aggregate (VMA), fine aggregate angularity (FAA), and HMA mixture gradation on permanent deformation (rutting) performance of mixtures designed using the Superpave volumetric design procedure (N-design of 96) are investigated. Full scale APT, Laboratory scale APT (PURWheel), triaxial tests and Superpave Shear tests (SST) are used as performance indicators.

The research study is designed to provide answers to the following specific questions:

- Does the Superpave minimum VMA vs. nominal maximum aggregate size relationship adequately define the threshold between stable and unstable mixtures?
- Is the Superpave minimum VMA vs. nominal maximum aggregate size relationship independent of fine aggregate angularity (FAA)?
- Is the Superpave minimum VMA vs. nominal maximum aggregate size relationship independent of the shape of gradation?
- What effect does fine aggregate angularity have on the performance of otherwise identical mixtures?
- What effect does gradation (above, through, and below the restricted zone) have on the performance of similar mixtures?

Based on test results and analyses, the answers to these specific questions are addressed as follows:

- **Does the Superpave minimum VMA vs. nominal maximum aggregate size relationship adequately define the threshold between stable and unstable mixtures?** No, it is concluded that the Superpave minimum VMA requirements

alone are not adequate to define the threshold between stable and unstable mixtures. Study results did not dispute or support the current Superpave VMA criteria. However, the importance of VMA for durability considerations and in describing aggregate structure can not be disputed.

- **Is the Superpave minimum VMA vs. nominal maximum aggregate size relationship independent of fine aggregate angularity (FAA)?** No, it is concluded that mixtures incorporating fine aggregates with higher values of FAA resulted in greater value of VMA, regardless of the nominal maximum size of the mixtures. Therefore, the VMA for mixtures with higher FAA values would be greater than that for mixtures with lower FAA values. However, the current Superpave FAA requirements can not be disputed or supported based on the results of this study. In addition, it is concluded that the performance of mixtures incorporating very high FAA values (50) was not necessarily better than that of mixtures incorporating typical FAA values (44). In other words, increasing VMA through the use of fine aggregates with very high FAA may actually be detrimental to mixture performance in some cases under the Superpave volumetric mixture design system. Especially when the mixtures are difficult to compact due to the high FAA, which can ultimately lead to over asphalting of a mixture.

- **Is the Superpave minimum VMA vs. nominal maximum aggregate size relationship independent of the shape of gradation?** No, however, it is concluded that the effect of gradation with respect to the restricted zone (above or below) on the critical VMA is minimal. Results indicate that it is reasonable to have a VMA specification that is a function of nominal maximum aggregate size regardless of gradation shape.

- **What effect does FAA have on the performance of similar mixtures?** Increase in FAA was found to improve performance (resistance to permanent deformation); however mixtures produced with very high fine aggregate angularity (50) did not necessarily perform better than those incorporating typical

levels of fine aggregate angularity. This trend was consistently observed with APT, PURWheel, and triaxial tests.

- **What effect does gradation (above, through, and below the restricted zone); have on the performance of similar mixtures?** The effect of gradation with respect to the restricted zone on performance (resistance to permanent deformation or rutting) was not significant for some performance indicators and significant for others. The effect of gradation shape with respect to the restricted zone on performance was investigated employing APT, PURWheel, and triaxial tests. The effect of gradation with respect to the restricted zone on performance (resistance to permanent deformation or rutting) was not significant in the full scale APT. However, mixtures with gradations plotting through the restricted zone were more rut resistant than those with gradations plotting above or below the restricted zone in PURWheel tests. The triaxial shear strength of mixtures with gradations plotting above the restricted zone was higher than that of mixtures with gradations plotting through or below the restricted zone. These observations suggest that the restricted zone alone may not be an adequate characterization for gradations to optimize rutting performance. Results also suggest that equally adequate rutting performance can be achieved with gradations plotting above, through, and below the restricted zone.

The following conclusions are drawn based on evaluation of relationships between mixture properties and rutting performance indicators:

- Asphalt film thickness was identified as a robust parameter that reflects performance. A film thickness range for optimum rutting performance of 7 to 9 microns (calculated employing effective volume of asphalt and surface area of aggregate) was identified from APT, PURWheel, and triaxial test results. It is recommended that asphalt film thickness should be considered as one of the parameters in the volumetric mixture design.
- The observed critical VFA value (or limit of acceptable performance) associated with PURWheel and triaxial test results was 66% to 70%, i.e., within the current

Superpave limits of VFA for the design traffic level considered (3 – 10 millions ESALs).

- The measured range of critical dust proportion (or limits of acceptable performance) associated with APT, PURWheel, and triaxial test results were approximately 0.9 to 1.7.

The following conclusions are drawn based on analysis of relationship among material properties, Superpave designs, and rutting performance indicators:

- APT, PURWheel and triaxial test results indicated that the AC corresponding to minimum rut depth or maximum shear strength was approximately 0.5 percent lower than the Superpave design AC for most mixtures (N-design of 96). This indicates that volumetric properties alone are inadequate to ensure good rutting performance and that performance test(s) must be incorporated into the Superpave volumetric mixture design system.
- APT test results indicated that mixtures that exhibited greater design VMA did not provide better rutting performance. Design VMA increased with design AC (the amount of asphalt required to reduce air voids to four percent under a given level of compaction).
- APT, PURWheel, and triaxial test results indicated that mixtures incorporating very high FAA values (50) did not necessarily perform better than mixtures incorporating typical FAA values (44). Review of mixture design results indicates that mixtures incorporating very high FAA exhibited greater VMA and resulted in greater design AC using Superpave criterion. Therefore, mixtures incorporating very high FAA values did not perform better than those incorporating typical values of FAA because the design AC of very high FAA mixtures was also greater than that of typical FAA value mixtures.

Based on APT test results, the following conclusions are drawn:

- A subjective criterion were established that may be used in the mixture design process to rank the expected rutting performance of HMA assuming that

performance in the APT correlates to field performance. The same technique could be used to establish similar criteria for other laboratory wheel track testers.

- Higher in-place mixture density did not always result in better rutting performance. The reason is that higher density could be achieved as a result of over-compaction and/or higher AC. The detrimental effect of over-compaction was well observed in APT tests. The detrimental effect of AC above the design level was well observed in APT, PURWheel, and triaxial test results.
- Better rutting performance in APT tests was observed when mixtures were compacted to optimum (6 to 8 percent air voids) rather than very high densities. It was also observed that when in-place density approached the design density (at the design AC), in other words when in-place Gmb approach 100 percent of the design Gmb, performance rapidly decreased.

Based on PURWheel test results, the following conclusions are drawn:

- The PURWheel was shown to be sensitive to changes in mixture properties. It was effectively used to identify the transition from the stable to unstable condition when mixtures were tested over a range of asphalt binder contents. Thus the device could be used to compliment volumetric mixture design procedures to optimize rutting performance.
- A good correlation was observed between PURWheel and Triaxial test results and both indicate that in order to optimize rutting performance design AC levels should be less than or equal to those obtained through the Superpave volumetric design procedure.
- The correlation between APT and PURWheel test results is influenced by nominal maximum aggregate size, compaction technique, and mixture preparation method. The relationship between APT and PURWheel test results was more sensitive for the 19mm mixtures, laboratory compacted specimens, and laboratory prepared specimens.

- Rutting performance in the PURWheel is very sensitive to density. Similarly, field performance of HMA is also very sensitive to in-place density. It does demand that close attention be given to density in the preparation and analysis of PURWheel test results.

Based on triaxial test results, the following conclusions are drawn:

- The triaxial test was shown to be sensitive to changes in mixture properties. It was effectively used to identify the transition from the stable to unstable condition when mixtures were tested over a range of asphalt binder contents. Thus the device could be used to compliment volumetric mixture design procedures to optimize rutting performance.
- The triaxial test results using two stacked SGC samples were nominally influenced by height to diameter ratio, but do not appear to have been influenced by the discontinuity plane between the two SGC samples. The stacking of two SGC samples resulted in a height to diameter ratio of 1.5. The shear strength observed for a height to diameter ratio of 1.5 was approximately 10 percent less than that observed for a height to diameter ratio of 2.0.
- A good correlation between triaxial and PURWheel test results was observed based on the AC corresponding to the peak shear strength in triaxial tests and that of minimum PURWheel rut depths. The relationship between triaxial and PURWheel test results showed that as the triaxial shear strength decreased PURWheel rut depth increased. This suggests that either test could be used to supplement the existing Superpave volumetric mixture design method for optimizing rutting performance. Both the triaxial and PURWheel tests indicated that to optimize rutting performance an AC level equal to or less than the Superpave design AC by up to 0.5 percent would be required.

Based on SST results, the following conclusions are drawn:

- The SST was shown to be sensitive to changes in mixture properties. It is also very sensitive to changes in temperature, mixture preparation method, and compaction technique.
- Reasonable relationships between SST and APT tests, SST and PURWheel tests, and SST and triaxial tests were observed. However, it should be noted that there were effects of test temperature, mixture preparation method, and compaction technique in developing the relationships. Further study maybe required to evaluate these effects in the relationships.

Based on finite element analysis results, the following conclusions are drawn:

- Finite element analysis is a powerful tool for comparing test results across different testing devices or facilities. In addition, this systematical analysis would allow the prediction of the in service pavements performance possible in a rational way instead of using an empirical method.
- Finite element analysis is capable of modeling the effects of transverse wheel wander, speed, tire inflation pressure, wheel load, and specimen thickness on rutting performance. However, validation of the predicted rutting performance is needed.
- The correlation between APT and PURWheel tests developed by finite element analysis was independent of nominal maximum aggregate size. This correlation suggests that finite element analysis may be used as a tool for comparing test results of different accelerated pavement test devices.

10.2. Recommendations

- **Main recommendation** is that the Superpave volumetric mixture design process should be supplemented with performance tests conducted over a range of AC

levels to identify the AC corresponding to optimum pavement performance. This study has shown that INDOT/Purdue full scale APT, PURWheel, and triaxial tests are sensitive to mixture property changes including AC level, aggregate properties and gradation, and mixture density and hence are recommended as performance indicators for HMA.

- It is recommended that the use of a typical value of FAA is suggested for acceptable rutting performance, rather than very high FAA values because the high values may lead to over asphalting of mixtures and ultimately poor rutting performance. High FAA fine aggregates can be used, but optimum performance may be observed when they are blended with limited percentages of natural sand.
- Despite the importance of gradation in building aggregate structure, the rigorous specification of gradation with respect to the restricted zone (above, through, and below) as a requirement for performance is not recommended.
- Asphalt film thickness was identified as a robust parameter that reflects performance. A film thickness range for optimum rutting performance of 7 to 9 microns was identified from APT, PURWheel, and triaxial test results. It is recommended that asphalt film thickness should be considered as one of the parameters in the volumetric mixture design.
- Further studies may be required to validate the relationship between VFA and other design traffic levels.
- The measured range of critical dust proportion associated with APT, PURWheel, and triaxial test results was approximately 0.9 to 1.7. This range is recommended for future designs although it exceeds the upper limit of the current Superpave dust proportion criteria (0.6 to 1.2). However, it is very close to the recently recommended dust proportion range of 0.8 to 1.6. These values, however, should be considered in lieu of their impact on durability.

REFERENCES

AASHTO Provisional Standards, Interim Edition, May 1999.

AASHTO PP6-97, "Practice for Grading or Verifying the Performance Grade of an Asphalt Binder", AASHTO, 1997

AASHTO PP28-97, "Practice for Superpave Volumetric Design for Hot Mix Asphalt (HMA)", AASHTO, June 1997.

Al-Abdul, Wahhab, H.I., Fatani, M.N., Noureldin, A.S., Bubshait, A., and I.A., Al-Dubabe, "National Study of Asphalt Pavement Rutting in Saudi Arabia", Transportation Research Record, TRR 1473, Transportation Research Board, National Research Council, Washington, D.C., 1995.

Anderson, R. M. and Bahia, H. U., "Evaluation and Selection of Aggregate Gradations for Asphalt Mixtures Using Superpave." Transportation Research Record, TRR 1583, Transportation Research Board, National Research Council, Washington, D.C., 1997.

ASTM D1073-94, "Standard Specification for Fine Aggregate for Bituminous Paving Mixtures", Annual Book of ASTM Standards, Vol. 04.03: Road and Paving Materials; Vehicle-Pavement Systems, 1998.

ASTM D2850-87, "Standard Test Method for Unconsolidated, Undrained Compressive Strength of Cohesive Soils in Triaxial Compression", Annual Book of ASTM Standards, Vol. 04.08: Soil and Rock; dimension Stone; Geosynthetics, 1992.

Brown, E. R., and Buchanan, M. S., "Consolidation of the N_{design} Compaction Matrix and Evaluation of Gyratory Compaction Requirements", Proceedings of the Association of Asphalt Paving Technologist, Vol. 68, 1999.

Campen, J. F., Smith, J. R., Erickson, L. G. and Mertz, L. R., "The Relationship between Voids, Surface Area, Film Thickness and Stability in Bituminous Paving Mixtures", Proceeding, AAPT, Vol. 28, 1959.

Cominsky, R. J., "The Superpave Mix Design Manual for New Construction and Overlays", Strategic Highway Research Program-A-407, National Research Council, 1994.

Cominsky, R. J., Leahy, R. B., Harrigan, E. T., "Level One Mix Design: Materials Selection, Compaction, and Conditioning", Strategic Highway Research Program-A-408, National Research Council, 1994.

Coree, B. J. and Hislop, W. P., "Difficult Nature of Minimum Voids in The Mineral Aggregate Historical Perspective", **"**, Paper No. 99-0512, Transportation Research Record, TRR 1681, Transportation Research Board, National Research Council, Washington, D.C., 1999.

De Beer, M., Fisher, C., Jooste, F., J., "Determination of Pneumatic Tire/Pavement Interface Contact Stresses Under Moving Loads and Some Effects on Pavements with Thin Asphalt Surfacing Layers", Division of Roads and Transport Technology, CSIR, 1997.

Fee, F. "Report on Lab Rut Tester Study", unpublished report, Transportation Research Board Committee A2D05, April 1997.

Goodman, R. E., "Methods of Geological Engineering in Discontinuous Rocks", West Publishing Co., 1976.

Haberman, J. A., "Design Features and a Preliminary Study of Purdue Linear Compactor and the PURWheel Tracking Device", M.S. Thesis, Purdue University, 1994.

Haddock, J., Pan, C., Feng, A., Galal, K., and White, T. D., "National Pooled Fund Study No. 176: Validation of SHRP Asphalt Mixture Specifications Using Accelerated Testing", Interim Report, T. E. Nantung and A. S. Noureldin, editor, Indiana Department of Transportation, Research Division, December 1998.

Hand, A. J. T., "Relationships Between Laboratory Measured HMA Material and Mixture Properties and Pavement Performance at Westrack", Dissertation, University of Nevada – Reno, August 1998.

Hinrichsen, J. A. and Heggen, J., "Minimum Voids in Mineral Aggregate in Hot-Mix Asphalt Based on Gradation and Volumetric Properties", Transportation Research Record, TRR 1545, Transportation Research Board, National Research Council, Washington, D.C., 1996.

Huang, H.M., "Analysis of Accelerated Pavement Tests and Finite Element Modeling of Rutting Phenomenon", A Thesis Submitted to the Faculty of Purdue University, August 1995.

Huang, H., and White, T.D., "Minimum Crushed Aggregate Requirements in Asphalt Mixtures", Joint Highway Research Project Draft Final Report, Purdue University, November 1996.

Huber, G. A., and Shuler, T. S., "Providing Sufficient Void Space for Asphalt Cement: Relationship of Mineral Aggregate Voids and Aggregate Gradation", Effects of Aggregates and Mineral Fillers on Asphalt Mixture Performance, ASTM STP 1147, Richard C. Meininger, editor, American Society for Testing and Materials, Philadelphia, 1992.

Huber, G. A., and Schrocman, J. A., "Superpave and Westrack: Did They Perform as Expected?", Canadian Technical Asphalt Association, 1999.

Kandhal, P.S., Foo, K. Y., and Mallick, R. B., "A Critical Review of VMA Requirements in Superpave", Preprint for the Transportation Research Board 77th Annual Meeting, Washington D.C., January 1998.

Kallas, B.F., "Gyratory testing Machine Procedures for Selecting the Design Asphalt Content of Paving Mixtures", Proceedings of the Association of Asphalt Paving Technologists, Vol. 33, 1964.

Kennedy, T.W., Huber, G. A., Harrigan, E. T., Cominsky, R. J., Hughes, C. S., Von Quintus, H. L., and Moulthrop, J. S., "Superior Performing Asphalt Pavements (Superpave): The Product of the SHRP Asphalt Research Program", Strategic Highway Research Program, SHRP-A-410, 1994.

Kraus, Harry, "Creep Analysis", A Wiley-Interscience Publication, 1980.

Lee, C. J., "Effects of Fine Aggregate Angularity on Asphalt Mixture Performance", Dissertation, Purdue University, December 1998.

Lefebvre, J., "Recent Investigations of Design of Asphalt Paving Mixtures", Proceedings of the Association of Asphalt Paving Technologists , Vol. 26, 1957.

Lytton, Robert L., "Characterizing Asphalt Pavements for Performance" Preprint of TRB Distinguished Lecture for the Transportation Research Board 79th Annual Meeting, Paper no 00-2878, Washington D.C., January 2000.

McGennis, R.B., Anderson, R.M., Kennedy, T.W., and Solaimanian, M., "Background of SUPERPAVE Asphalt Mixture Design and Analysis", Publication No. FHWA-SA-95-003, Federal Highway Administration, February 1995.

McLeod, N.W., "Void Requirements for Dense-graded Bituminous Paving Mixtures," American Society for Testing and Materials, STP 252, 1959.

Metcalf, J. B., 'Application of Full-Scale Accelerated Pavement Testing", National Cooperative Highway Research Program, Synthesis of Highway Practice 235, Transportation Research Board, Washington D. C., 1996.

Minutes of TAC Meeting Held at the INDOT Division of Research, May 1996.

Monismith, C.L., Vallerga, B.A., "Relationship between Density and Stability of Asphaltic Paving Mixtures," Proceedings of the Association of Asphalt Paving Technologists, Vol. 25, 1956.

MTS, User's Manual, "Pavement Test System Operation", April 1994.

Neter, J., Kutner, M. H., Nachtsheim, C. J., and Wasserman, W. "Applied Linear Statistical Models", 4th ed., Irwin, 1996.

Pan, C.L., "Analysis of Bituminous Mixtures Stripping/Rutting Potential", A Thesis Submitted to the Faculty of Purdue University, August 1997.

Perl, M., Uzan, J., and Sides, A., "Visco-Elasto-Plastic Constitutive Law for a Bituminous Mixture Under Repeated Loading," Transportation Research Record 911, National research Council, Washington, D.C., pp. 21-27, 1983.

Parker, F. and Brown, E. R., "A Study of Rutting of Alabama Asphalt Pavements", Highway Research Center, Auburn University, AL, Project Number ST 2019-9, August 1990.

Regan, G. L., "A Laboratory Study of Asphalt Concrete Mix Designs for High-Contact Pressure Airdraft Traffic", Engineering & Services Laboratory, Air Force Engineering & Services Center, Tyndall Air Force Base, FL, Report ESL-TR-85-86, July 1987

Roberts, F.L., et al., "Hot Mix Asphalt Materials, Mixture Design and Construction," 1st edition, National Center for Asphalt Technology, 1991.

Stiady, J. L., White, T.D., and Reck, C.R., "Rut 3.3 : A Computer Program to Process APT Data.", User's Manual, Purdue University, June 1998 (unpublished).

Von Quintus, H.L., Scherocman, J.A., Hughes, C.S., and Kennedy, T.W., "Asphalt Aggregate Mixture Analysis System", National Cooperative Highway Research Program Report 338, Transportation Research Board, National Research Concil, Washington, D.C., 1991.

Williams, R. C. and Prowell, B. D., "Comparison of Laboratory Wheel-Tracking Test Resutls with WesTrack Performance", Paper No. 99-1456 of Transportation Research Record, TRR 1681, Transportation Research Board, Washington D. C., 1999.

Witczak, M. W., Bonaquist, R., Von Quintus, H., and Kaloush, K., "Specimen Geometry and Aggregate Size Effects in Uniaxial Compression and Constant Height Shear Tests", Preprint of Proceedings of the Association of Asphalt Paving Technologists , Vol. 69, 2000.

Work Plan Proposal, National Pooled Fund Study No. 176, August 1996.

APPENDIX A Superpave Mix Design Results

Mixture Design for 19mm Limestone with FAA of 39 and Gradation Plotting Above The Restricted Zone

Project Name:	NPF	**N Initial:**	8
Workbook Name:		**N Design:**	96
Technician:	CP	**N Max:**	152
Date:		**Nom. Sieve Size:**	19mm
Asphalt Grade:	64-22	**Design Temperature:**	38°C
Compaction Temp:	150°C	**Design ESAL's (millions):**	3-10

Blend	%AC	%Gmm @ N = 8	%Gmm @ N = 96	%Gmm @ N = 152	%Air Voids @ NDesign	%VMA @ NDesign
Blend 1	4.5	88.0	95.4	96.4	4.6	13.5
Blend 2	5.0	89.2	97.0	97.9	3.0	12.6
Blend 3	5.5	90.1	97.9	98.6	2.1	12.7
Blend 4	6.0	90.9	98.4	98.7	1.6	13.1

	Blend 1	Blend 2	Blend 3	Blend 4	Design AC
Agg. Bulk Specific Gravity (Gsb):	2.644	2.644	2.644	2.644	**2.644**
Percent Binder by wt. of mix (Pbi):	4.5	5.0	5.5	6.0	**4.7**
Percent Aggregate (Ps):	95.5	95.0	94.5	94.0	**95.3**
Specific Gravity of Binder (Gb):	1.030	1.030	1.030	1.030	**1.030**
Fines (%Passing 0.075mm Sieve):	4.8	4.8	4.8	4.8	**4.8**
Rice Specific Gravity (Gmm):	2.510	2.508	2.495	2.484	**2.507**
Effective Specific Gravity (Gse):	2.6923	2.7129	2.7202	2.7300	**2.6978**
Effective % Binder (Pbe):	3.8	4.0	4.4	4.8	**3.9**
% Binder Absorption (Pba):	0.7	1.0	1.1	1.2	**0.8**
Dust Proportion (0.6-1.2%):	1.3	1.2	1.1	1.0	**1.2**
Surface Area(m^2/Kg):	5.79	5.79	5.79	5.79	**5.79**
Film Thickness(micron):	6.41	6.80	7.51	8.17	**6.63**

Mixture Design for 19mm Limestone with FAA of 39 and Gradation Plotting Above The Restricted Zone

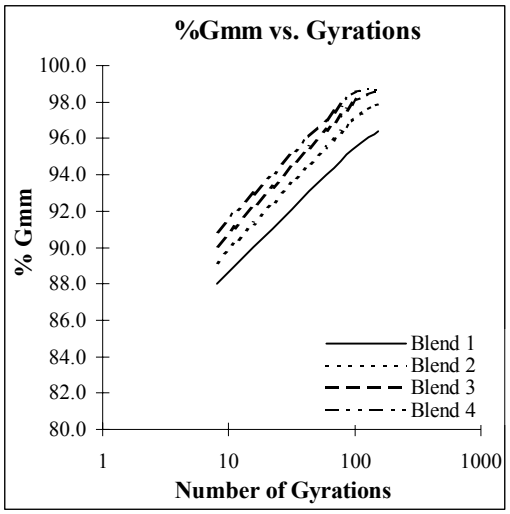

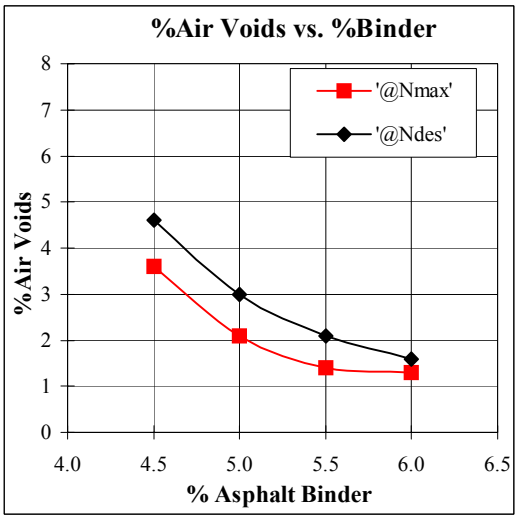

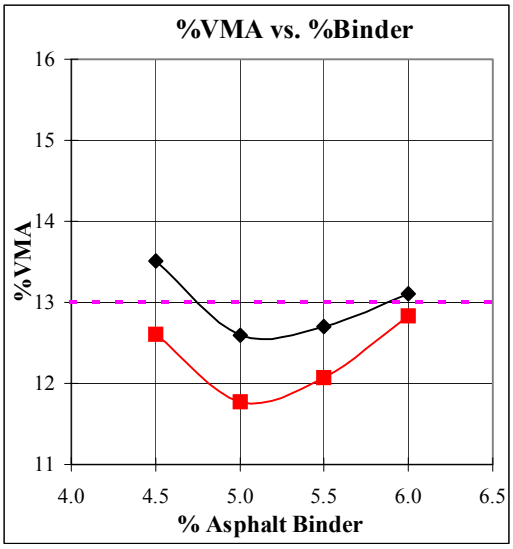

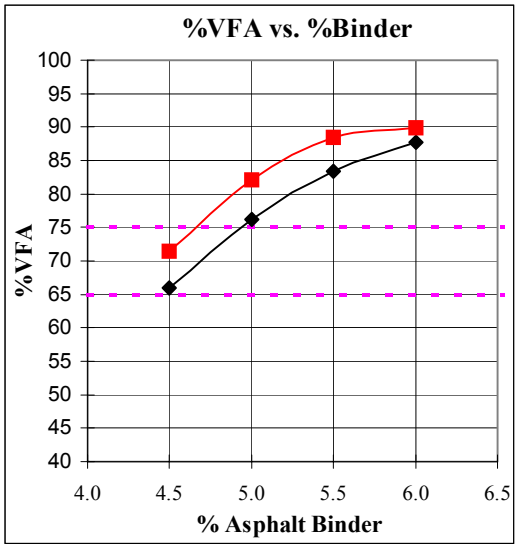

Blend	%AC	Air Voids @ NDesign	%VMA @ NDesign	%VFA @ NDesign	Air Voids @ NMax	%VMA @ Nmax	%VFA @ Nmax
Blend1	4.5	4.6	13.5	66.0	3.6	12.6	71.4
Blend2	5.0	3.0	12.6	76.2	2.1	11.8	82.2
Blend3	5.5	2.1	12.7	83.5	1.4	12.1	88.4
Blend4	6.0	1.6	13.1	87.8	1.3	12.8	89.9

Mixture Design for 19mm Limestone with FAA of 39 and Gradation Plotting Above The Restricted Zone

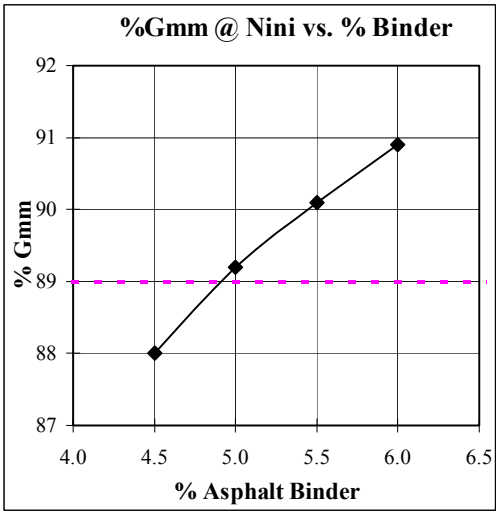

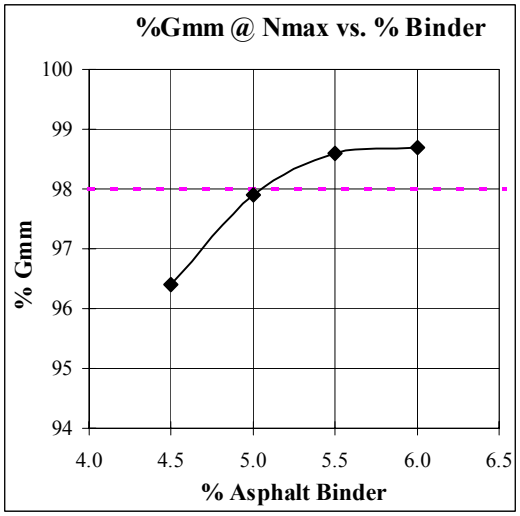

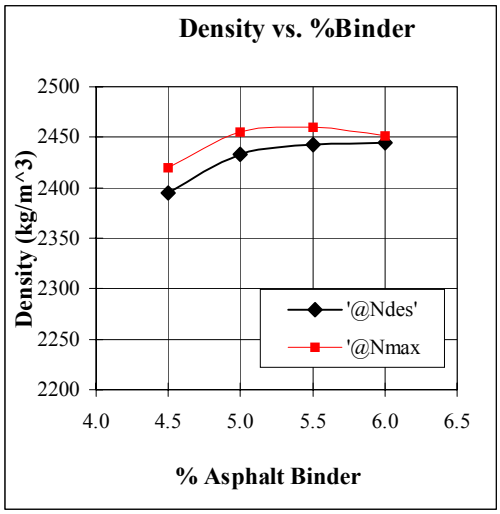

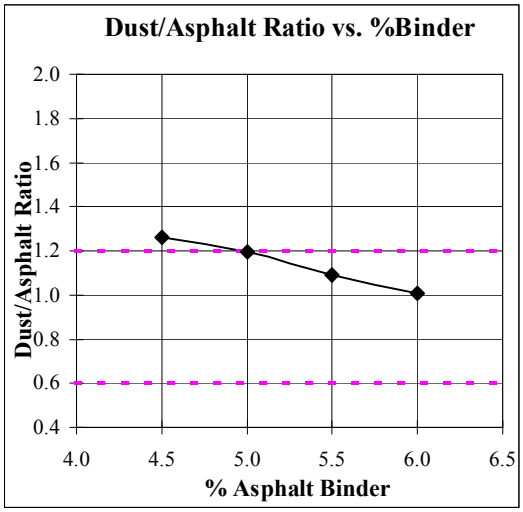

Blend	%AC	%Gmm @ Nini	%Gmm @ Nmax	Density @Ndes (kg/m3)	Density @Nmax (kg/m3)	D/A ratio
Blend1	4.5	88.0	96.4	2394.5	2419.6	1.3
Blend2	5.0	89.2	97.9	2432.8	2455.3	1.2
Blend3	5.5	90.1	98.6	2442.6	2460.1	1.1
Blend4	6.0	90.9	98.7	2444.3	2451.7	1.0

Mixture Design for 19mm Limestone with FAA of 39 and Gradation Plotting Below The Restricted Zone

Project Name:	NPF	**N Initial:**	8
Workbook Name:		**N Design:**	96
Technician:	CP	**N Max:**	152
Date:		**Nom. Sieve Size:**	19mm
Asphalt Grade:	64-22	**Design Temperature:**	38°C
Compaction Temp:	150°C	**Design ESAL's (millions):**	3-10

Blend	%AC	%Gmm @ N = 8	%Gmm @ N = 96	%Gmm @ N = 152	%Air Voids @ NDesign	%VMA @ NDesign
Blend 1	4.5	83.4	93.1	94.6	6.9	15.4
Blend 2	5.0	84.5	94.3	95.8	5.7	15.3
Blend 3	5.5	85.8	96.0	97.6	4.0	14.7
Blend 4	6.0	86.2	96.8	98.5	3.2	14.9

	Blend 1	Blend 2	Blend 3	Blend 4	Design AC
Agg. Bulk Specific Gravity (Gsb):	2.645	2.645	2.645	2.645	**2.645**
Percent Binder by wt. of mix (Pbi):	4.5	5.0	5.5	6.0	**5.5**
Percent Aggregate (Ps):	95.5	95.0	94.5	94.0	**94.5**
Specific Gravity of Binder (Gb):	1.030	1.030	1.030	1.030	**1.030**
Fines (%Passing 0.075mm Sieve):	3.1	3.1	3.1	3.1	**3.1**
Rice Specific Gravity (Gmm):	2.516	2.502	2.488	2.473	**2.488**
Effective Specific Gravity (Gse):	2.6995	2.7055	2.7114	2.7159	**2.7114**
Effective % Binder (Pbe):	3.7	4.1	4.5	5.0	**4.5**
% Binder Absorption (Pba):	0.8	0.9	1.0	1.0	**1.0**
Dust Proportion (0.6-1.2%):	0.8	0.8	0.7	0.6	**0.7**
Surface Area(m^2/Kg):	3.79	3.79	3.79	3.79	**3.79**
Film Thickness(micron):	9.56	10.69	11.83	13.04	**11.83**

Mixture Design for 19mm Limestone with FAA of 39 and Gradation Plotting Below The Restricted Zone

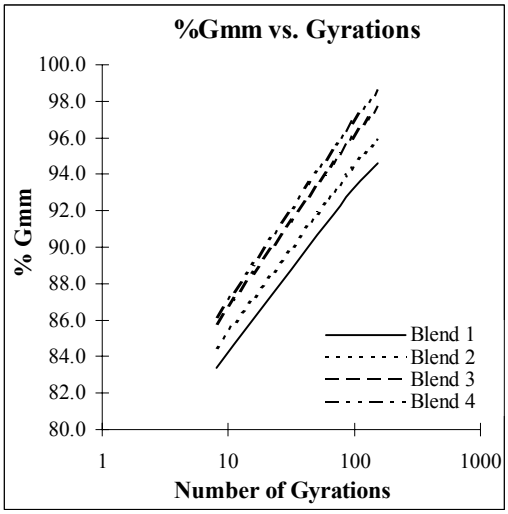

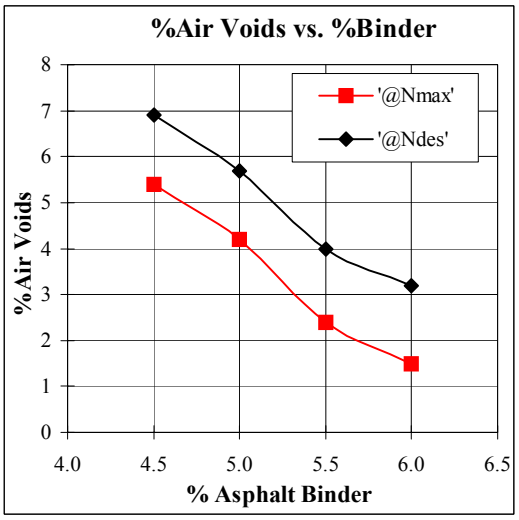

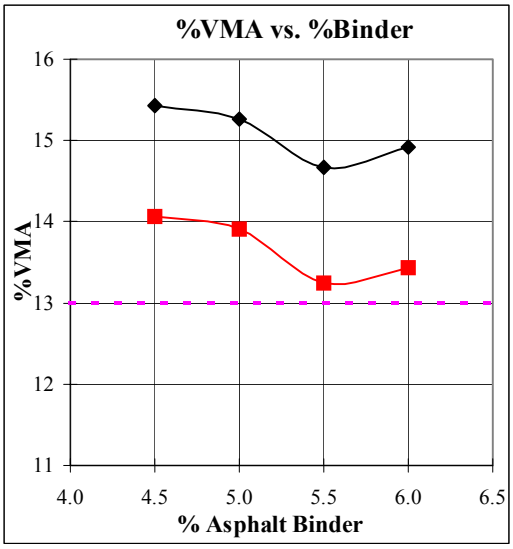

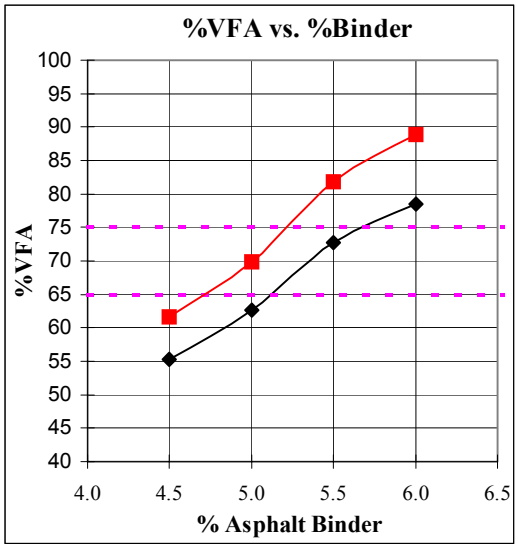

Blend	%AC	Air Voids @ NDesign	%VMA @ NDesign	%VFA @ NDesign	Air Voids @ NMax	%VMA @ Nmax	%VFA @ Nmax
Blend1	4.5	6.9	15.4	55.3	5.4	14.1	61.6
Blend2	5.0	5.7	15.3	62.6	4.2	13.9	69.8
Blend3	5.5	4.0	14.7	72.7	2.4	13.2	81.9
Blend4	6.0	3.2	14.9	78.6	1.5	13.4	88.8

Mixture Design for 19mm Limestone with FAA of 39 and Gradation Plotting Below The Restricted Zone

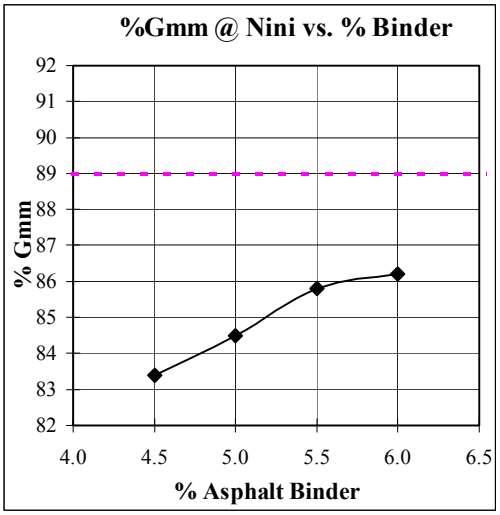

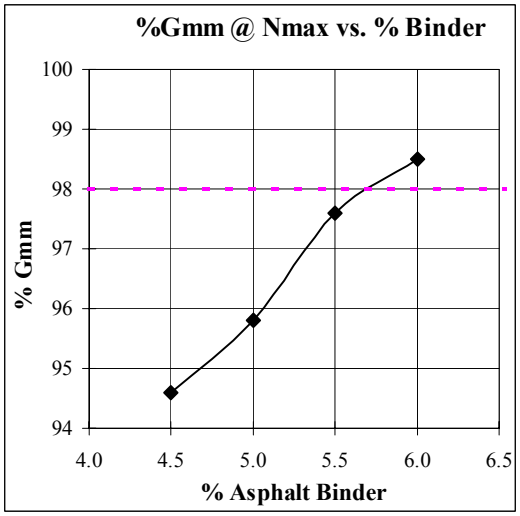

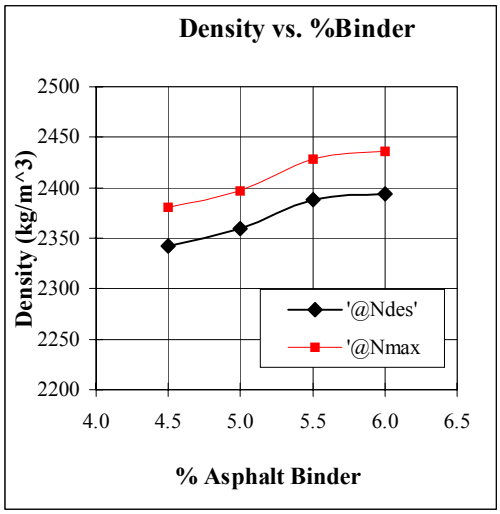

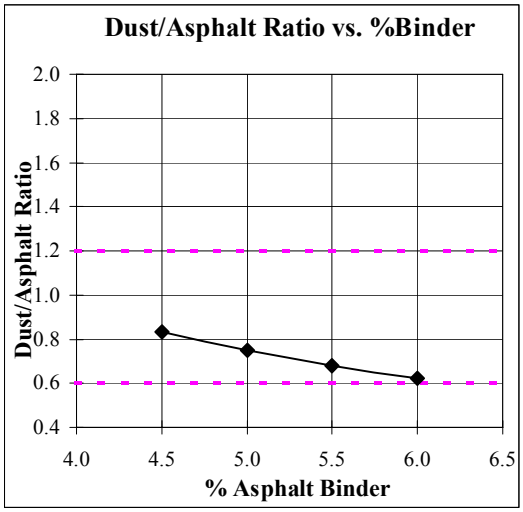

Blend	%AC	%Gmm @ Nini	%Gmm @ Nmax	Density @Ndes (kg/m3)	Density @Nmax (kg/m3)	D/A ratio
Blend1	4.5	83.4	94.6	2342.4	2380.1	0.8
Blend2	5.0	84.5	95.8	2359.4	2396.9	0.8
Blend3	5.5	85.8	97.6	2388.5	2428.3	0.7
Blend4	6.0	86.2	98.5	2393.9	2435.9	0.6

Mixture Design for 19mm Limestone with FAA of 44 and Gradation Plotting Above The Restricted Zone

Project Name:	NPF	**N Initial:**	8
Workbook Name:		**N Design:**	96
Technician:	CP	**N Max:**	152
Date:		**Nom. Sieve Size:**	19mm
Asphalt Grade:	64-22	**Design Temperature:**	38°C
Compaction Temp:	150°C	**Design ESAL's (millions):**	3-10

Blend	%AC	%Gmm @ N = 8	%Gmm @ N = 96	%Gmm @ N = 152	%Air Voids @ NDesign	%VMA @ NDesign
Blend 1	4.5	87.1	95.7	97.0	4.3	13.1
Blend 2	5.0	88.8	97.6	98.7	2.4	12.2
Blend 3	5.5	89.4	99.3	100.0	0.7	11.7
Blend 4	6.0	89.0	99.2	99.8	0.8	12.7

	Blend 1	Blend 2	Blend 3	Blend 4	Design AC
Agg. Bulk Specific Gravity (Gsb):	2.651	2.651	2.651	2.651	**2.651**
Percent Binder by wt. of mix (Pbi):	4.5	5.0	5.5	6.0	**4.6**
Percent Aggregate (Ps):	95.5	95.0	94.5	94.0	**95.4**
Specific Gravity of Binder (Gb):	1.030	1.030	1.030	1.030	**1.030**
Fines (%Passing 0.075mm Sieve):	5.9	5.9	5.9	5.9	**5.9**
Rice Specific Gravity (Gmm):	2.522	2.509	2.495	2.481	**2.519**
Effective Specific Gravity (Gse):	2.7068	2.7141	2.7202	2.7261	**2.7077**
Effective % Binder (Pbe):	3.7	4.1	4.5	4.9	**3.8**
% Binder Absorption (Pba):	0.8	0.9	1.0	1.1	**0.8**
Dust Proportion (0.6-1.2%):	1.6	1.4	1.3	1.2	**1.6**
Surface Area(m^2/Kg):	6.09	6.09	6.09	6.09	**6.09**
Film Thickness(micron):	5.93	6.60	7.31	8.03	**6.07**

Mixture Design for 19mm Limestone with FAA of 44 and Gradation Plotting Above The Restricted Zone

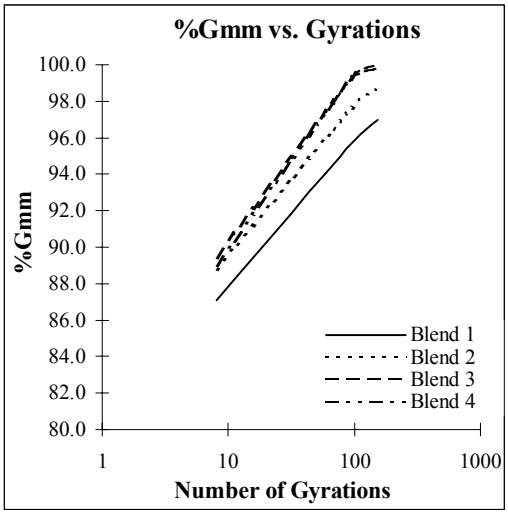

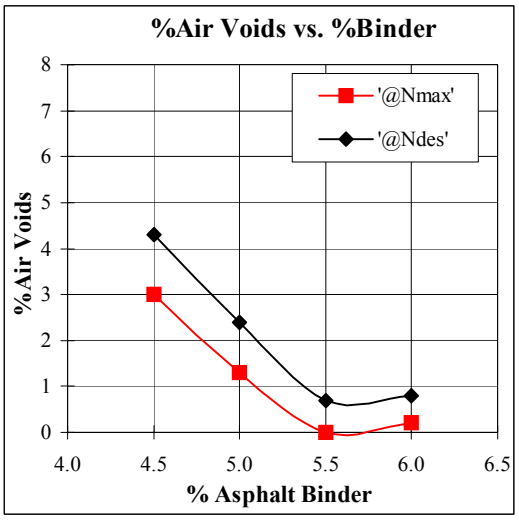

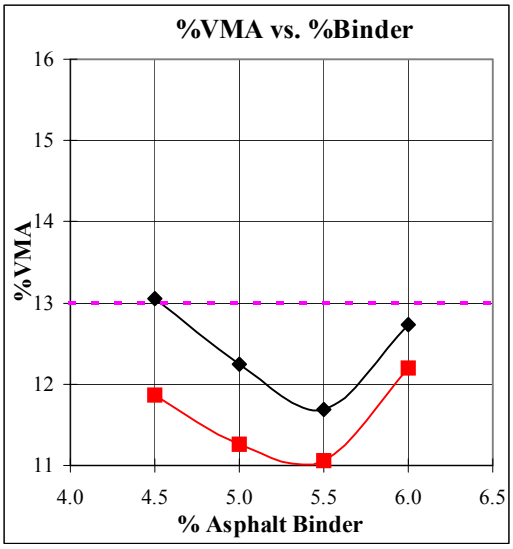

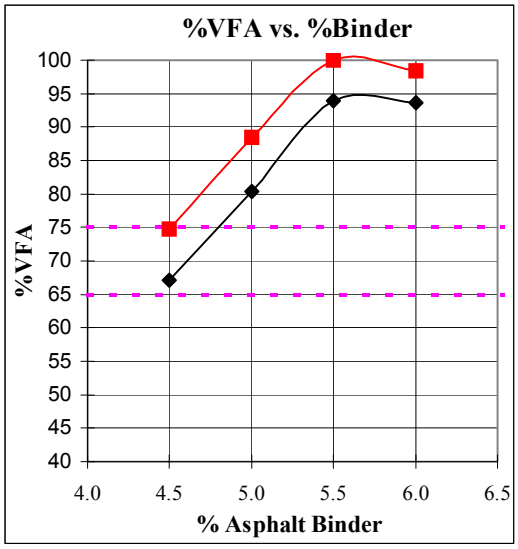

Blend	%AC	Air Voids @ NDesign	%VMA @ NDesign	%VFA @ NDesign	Air Voids @ NMax	%VMA @ Nmax	%VFA @ Nmax
Blend1	4.5	4.3	13.1	67.1	3.0	11.9	74.7
Blend2	5.0	2.4	12.2	80.4	1.3	11.3	88.5
Blend3	5.5	0.7	11.7	94.0	0.0	11.1	100.0
Blend4	6.0	0.8	12.7	93.7	0.2	12.2	98.4

Mixture Design for 19mm Limestone with FAA of 44 and Gradation Plotting Above The Restricted Zone

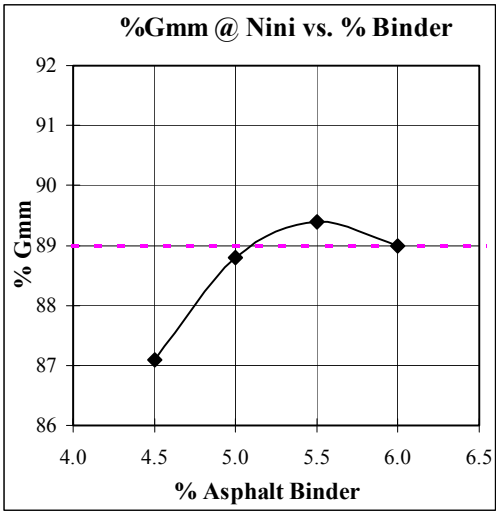

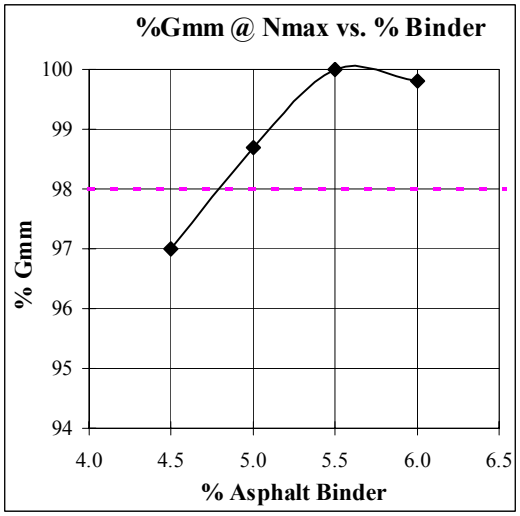

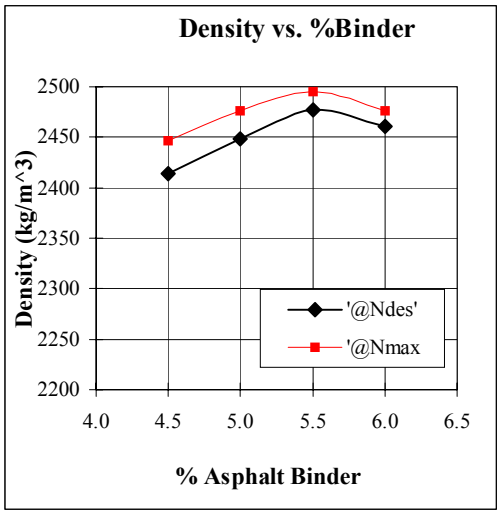

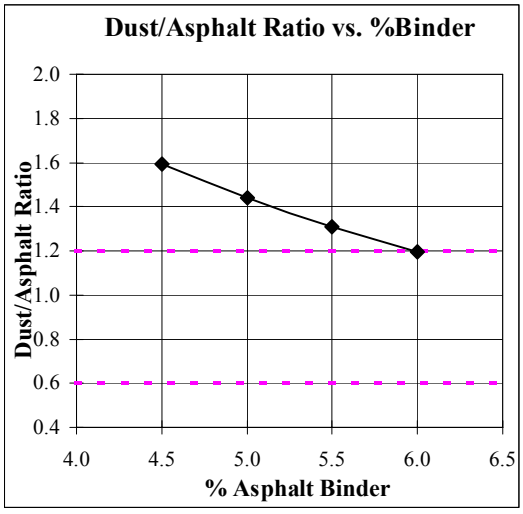

Blend	%AC	%Gmm @ Nini	%Gmm @ Nmax	Density @Ndes (kg/m3)	Density @Nmax (kg/m3)	D/A ratio
Blend1	4.5	87.1	97.0	2413.6	2446.3	1.6
Blend2	5.0	88.8	98.7	2448.8	2476.4	1.4
Blend3	5.5	89.4	100.0	2477.5	2495.0	1.3
Blend4	6.0	89.0	99.8	2461.2	2476.0	1.2

Mixture Design for 19mm Limestone with FAA of 44 and Gradation Plotting Through The Restricted Zone

Project Name:	NPF	**N Initial:**	8
Workbook Name:		**N Design:**	96
Technician:	CP	**N Max:**	152
Date:		**Nom. Sieve Size:**	19mm
Asphalt Grade:	64-22	**Design Temperature:**	38°C
Compaction Temp:	150°C	**Design ESAL's (millions):**	3-10

Blend	%AC	%Gmm @ N = 8	%Gmm @ N = 96	%Gmm @ N = 152	%Air Voids @ NDesign	%VMA @ NDesign
Blend 1	4.5	84.5	93.5	94.9	6.5	15.0
Blend 2	5.0	85.6	94.9	96.4	5.1	14.9
Blend 3	5.5	86.3	96.2	97.6	3.8	14.8
Blend 4	6.0	87.4	97.5	98.9	2.5	14.8

	Blend 1	Blend 2	Blend 3	Blend 4	Design AC
Agg. Bulk Specific Gravity (Gsb):	2.647	2.647	2.647	2.647	**2.647**
Percent Binder by wt. of mix (Pbi):	4.5	5.0	5.5	6.0	**5.4**
Percent Aggregate (Ps):	95.5	95.0	94.5	94.0	**94.6**
Specific Gravity of Binder (Gb):	1.030	1.030	1.030	1.030	**1.030**
Fines (%Passing 0.075mm Sieve):	4.6	4.6	4.6	4.6	**4.6**
Rice Specific Gravity (Gmm):	2.521	2.500	2.480	2.460	**2.484**
Effective Specific Gravity (Gse):	2.7055	2.7030	2.7013	2.6992	**2.7017**
Effective % Binder (Pbe):	3.7	4.2	4.7	5.2	**4.6**
% Binder Absorption (Pba):	0.8	0.8	0.8	0.8	**0.8**
Dust Proportion (0.6-1.2%):	1.3	1.1	1.0	0.9	**1.0**
Surface Area(m^2/Kg):	5.27	5.27	5.27	5.27	**5.27**
Film Thickness(micron):	6.77	7.81	8.83	9.87	**8.62**

Mixture Design for 19mm Limestone with FAA of 44 and Gradation Plotting Through The Restricted Zone

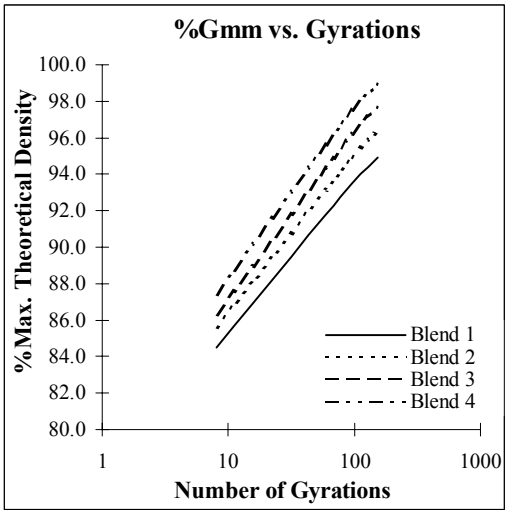

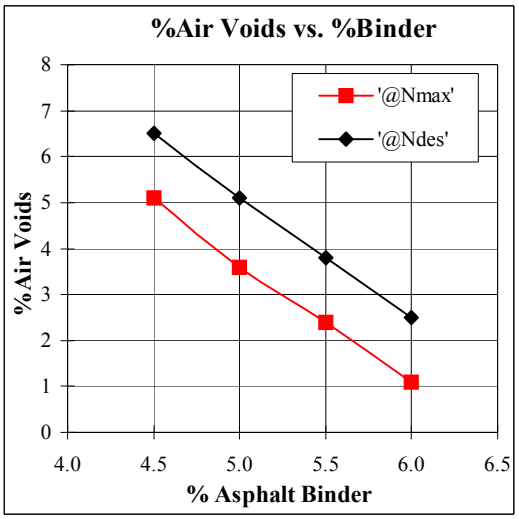

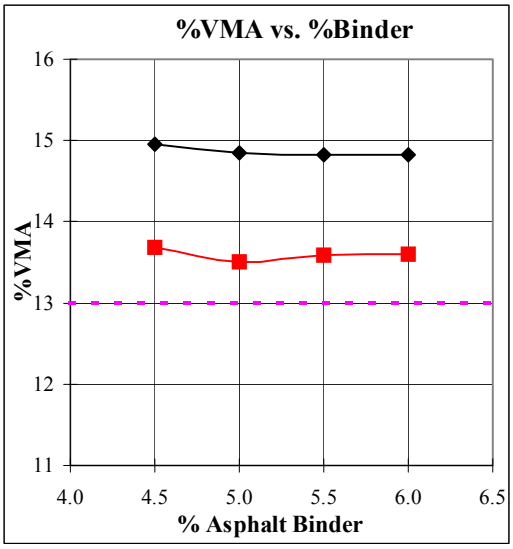

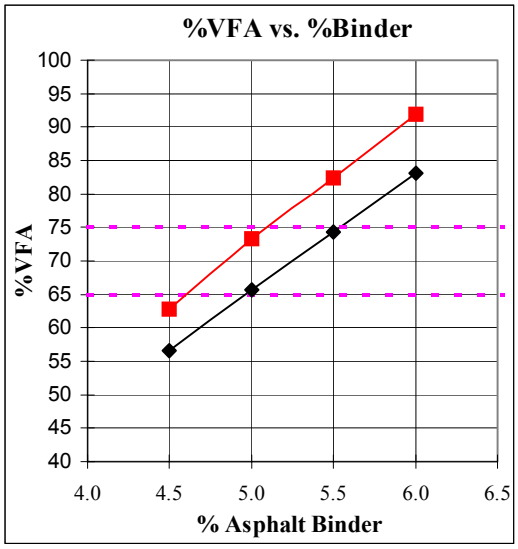

Blend	%AC	Air Voids @ NDesign	%VMA @ NDesign	%VFA @ NDesign	Air Voids @ NMax	%VMA @ Nmax	%VFA @ Nmax
Blend1	4.5	6.5	15.0	56.5	5.1	13.7	62.7
Blend2	5.0	5.1	14.9	65.7	3.6	13.5	73.3
Blend3	5.5	3.8	14.8	74.4	2.4	13.6	82.3
Blend4	6.0	2.5	14.8	83.1	1.1	13.6	91.9

Mixture Design for 19mm Limestone with FAA of 44 and Gradation Plotting Through The Restricted Zone

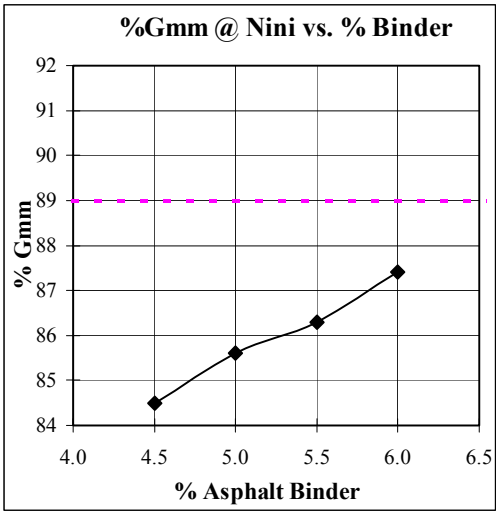

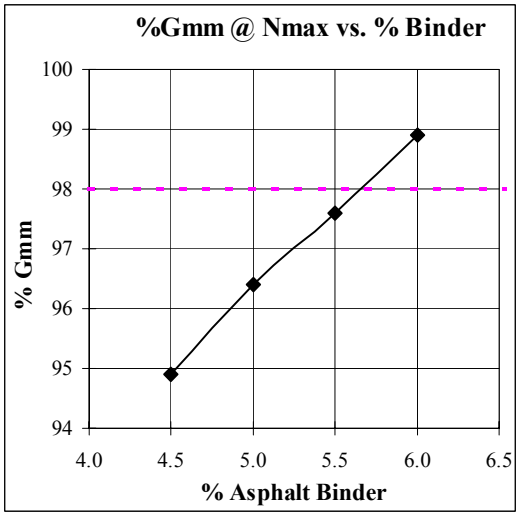

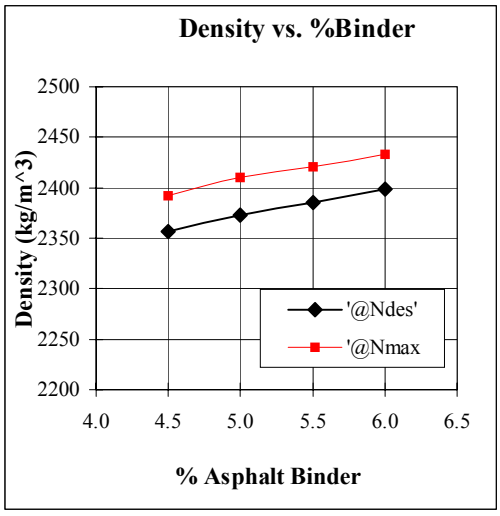

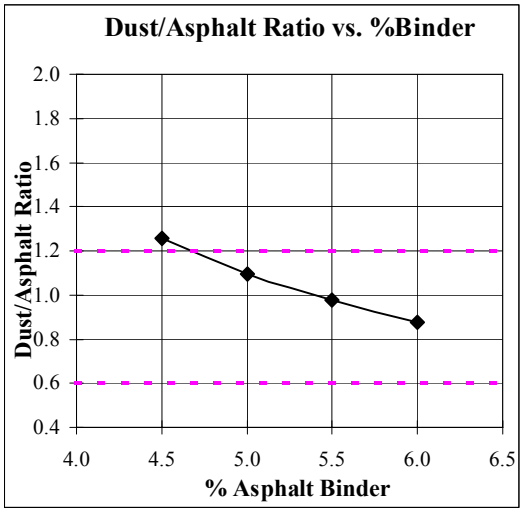

Blend	%AC	%Gmm @ Nini	%Gmm @ Nmax	Density @Ndes (kg/m3)	Density @Nmax (kg/m3)	D/A ratio
Blend1	4.5	84.5	94.9	2357.1	2392.4	1.3
Blend2	5.0	85.6	96.4	2372.5	2410.0	1.1
Blend3	5.5	86.3	97.6	2385.8	2420.5	1.0
Blend4	6.0	87.4	98.9	2398.5	2432.9	0.9

Mixture Design for 19mm Limestone with FAA of 44 and Gradation Plotting Below The Restricted Zone

Project Name:	NPF	**N Initial:**	8
Workbook Name:		**N Design:**	96
Technician:	CP	**N Max:**	152
Date:		**Nom. Sieve Size:**	19mm
Asphalt Grade:	64-22	**Design Temperature:**	38°C
Compaction Temp:	150°C	**Design ESAL's (millions):**	3-10

Blend	%AC	%Gmm @ N = 8	%Gmm @ N = 96	%Gmm @ N = 152	%Air Voids @ NDesign	%VMA @ NDesign
Blend 1	4.5	85.2	95.6	97.3	4.4	13.4
Blend 2	5.0	87.8	98.3	99.6	1.7	11.8
Blend 3	5.5	89.5	99.3	100.0	0.7	11.8
Blend 4	6.0	89.0	99.2	99.8	0.8	12.7

	Blend 1	Blend 2	Blend 3	Blend 4	Design AC
Agg. Bulk Specific Gravity (Gsb):	2.651	2.651	2.651	2.651	**2.651**
Percent Binder by wt. of mix (Pbi):	4.5	5.0	5.5	6.0	**4.6**
Percent Aggregate (Ps):	95.5	95.0	94.5	94.0	**95.4**
Specific Gravity of Binder (Gb):	1.030	1.030	1.030	1.030	**1.030**
Fines (%Passing 0.075mm Sieve):	4.3	4.3	4.3	4.3	**4.3**
Rice Specific Gravity (Gmm):	2.516	2.505	2.493	2.481	**2.515**
Effective Specific Gravity (Gse):	2.6995	2.7092	2.7177	2.7261	**2.7029**
Effective % Binder (Pbe):	3.8	4.2	4.5	4.9	**3.9**
% Binder Absorption (Pba):	0.7	0.8	1.0	1.1	**0.7**
Dust Proportion (0.6-1.2%):	1.1	1.0	0.9	0.9	**1.1**
Surface Area(m^2/Kg):	4.21	4.21	4.21	4.21	**4.21**
Film Thickness(micron):	8.81	9.71	10.65	11.61	**8.94**

Mixture Design for 19mm Limestone with FAA of 44 and Gradation Plotting Below The Restricted Zone

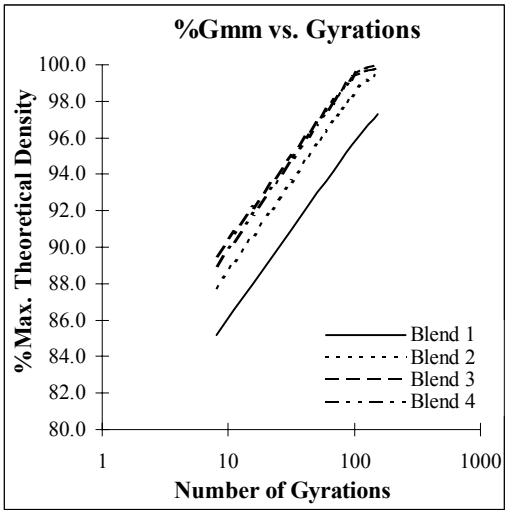

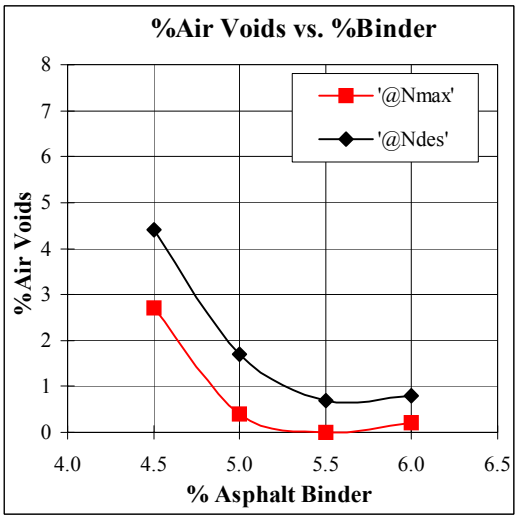

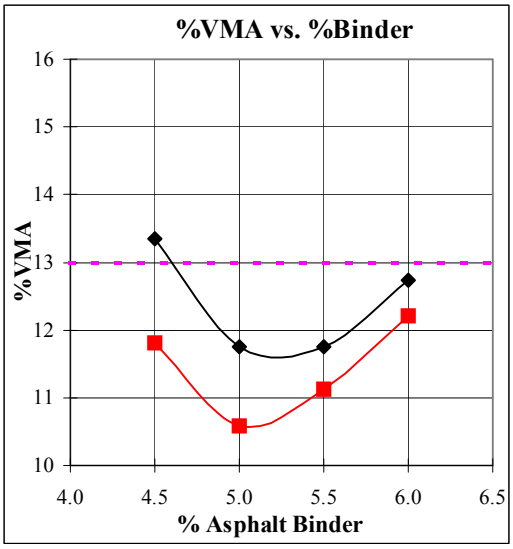

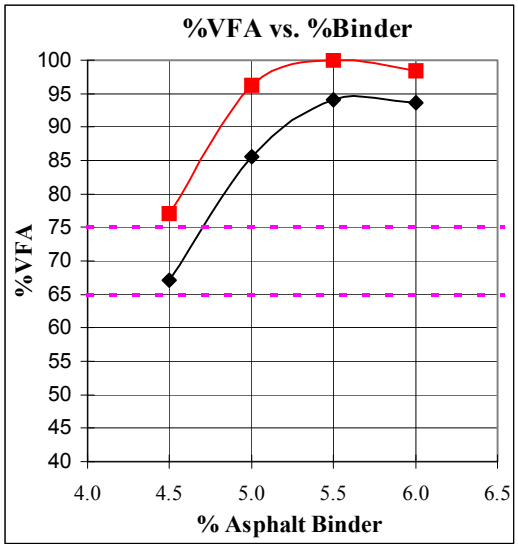

Blend	%AC	Air Voids @ NDesign	%VMA @ NDesign	%VFA @ NDesign	Air Voids @ NMax	%VMA @ Nmax	%VFA @ Nmax
Blend1	4.5	4.4	13.4	67.0	2.7	11.8	77.1
Blend2	5.0	1.7	11.8	85.5	0.4	10.6	96.2
Blend3	5.5	0.7	11.8	94.0	0.0	11.1	100.0
Blend4	6.0	0.8	12.7	93.7	0.2	12.2	98.4

Mixture Design for 19mm Limestone with FAA of 44 and Gradation Plotting Below The Restricted Zone

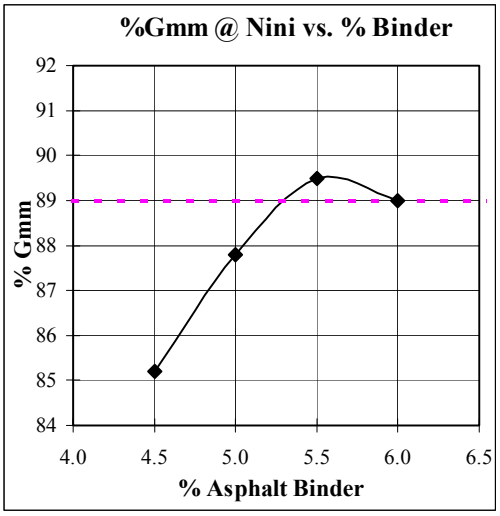

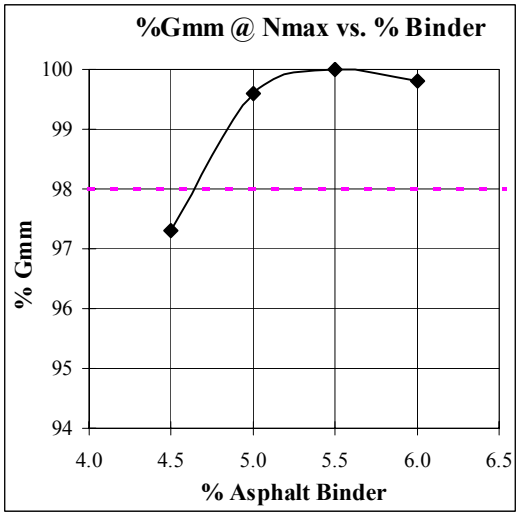

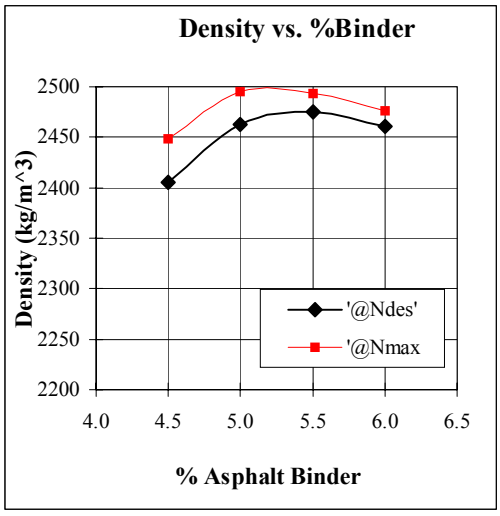

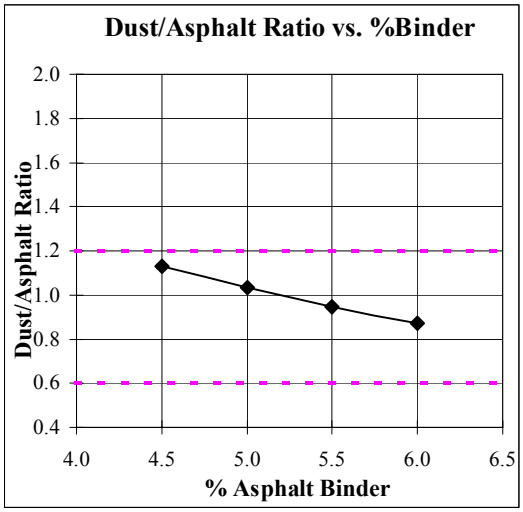

Blend	%AC	%Gmm @ Nini	%Gmm @ Nmax	Density @Ndes (kg/m3)	Density @Nmax (kg/m3)	D/A ratio
Blend1	4.5	85.2	97.3	2405.3	2448.1	1.1
Blend2	5.0	87.8	99.6	2462.4	2495.0	1.0
Blend3	5.5	89.5	100.0	2475.5	2493.0	0.9
Blend4	6.0	89.0	99.8	2461.2	2476.0	0.9

Mixture Design for 19mm Limestone with FAA of 50 and Gradation Plotting Above The Restricted Zone.

Project Name:	NPF	**N Initial:**	8
Workbook Name:		**N Design:**	96
Technician:	CP	**N Max:**	152
Date:		**Nom. Sieve Size:**	19mm
Asphalt Grade:	64-22	**Design Temperature:**	38°C
Compaction Temp:	150°C	**Design ESAL's (millions):**	3-10

Blend	%AC	%Gmm @ N = 8	%Gmm @ N = 96	%Gmm @ N = 152	%Air Voids @ NDesign	%VMA @ NDesign
Blend 1	5.0	83.6	94.1	95.7	5.9	15.1
Blend 2	5.5	84.8	95.3	97.0	4.7	15.3
Blend 3	6.0	85.1	96.1	97.6	3.9	15.7
Blend 4	6.5	87.3	98.0	98.9	2.0	15.4

	Blend 1	Blend 2	Blend 3	Blend 4	Design AC
Agg. Bulk Specific Gravity (Gsb):	2.643	2.643	2.643	2.643	**2.643**
Percent Binder by wt. of mix (Pbi):	5.0	5.5	6.0	6.5	**5.9**
Percent Aggregate (Ps):	95.0	94.5	94.0	93.5	**94.1**
Specific Gravity of Binder (Gb):	1.030	1.030	1.030	1.030	**1.030**
Fines (%Passing 0.075mm Sieve):	6.9	6.9	6.9	6.9	**6.9**
Rice Specific Gravity (Gmm):	2.511	2.487	2.466	2.441	**2.469**
Effective Specific Gravity (Gse):	2.7166	2.7101	2.7069	2.6979	**2.7060**
Effective % Binder (Pbe):	3.9	4.5	5.1	5.7	**5.0**
% Binder Absorption (Pba):	1.1	1.0	0.9	0.8	**0.9**
Dust Proportion (0.6-1.2%):	1.7	1.5	1.4	1.2	**1.4**
Surface Area(m^2/Kg):	6.49	6.49	6.49	6.49	**6.49**
Film Thickness(micron):	5.96	6.89	7.76	8.76	**7.62**

Mixture Design for 19mm Limestone with FAA of 50 and Gradation Plotting Above The Restricted Zone.

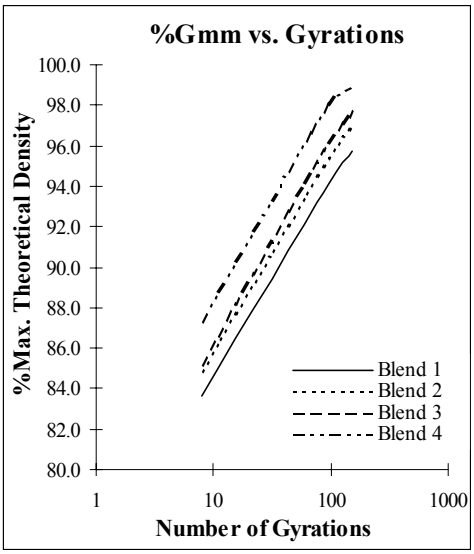

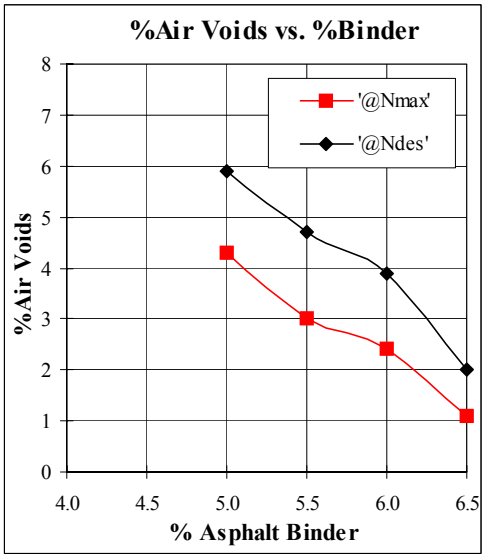

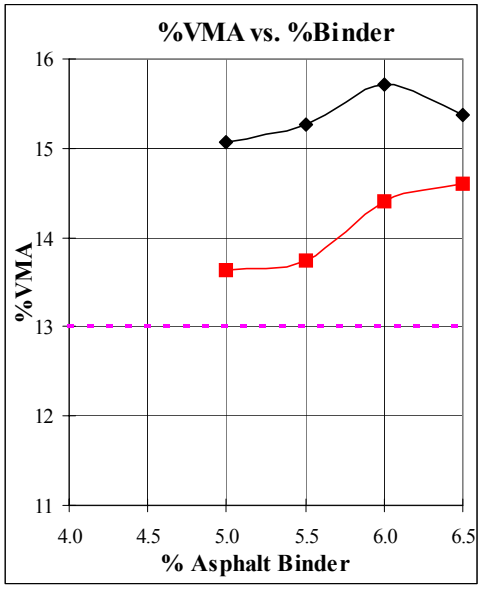

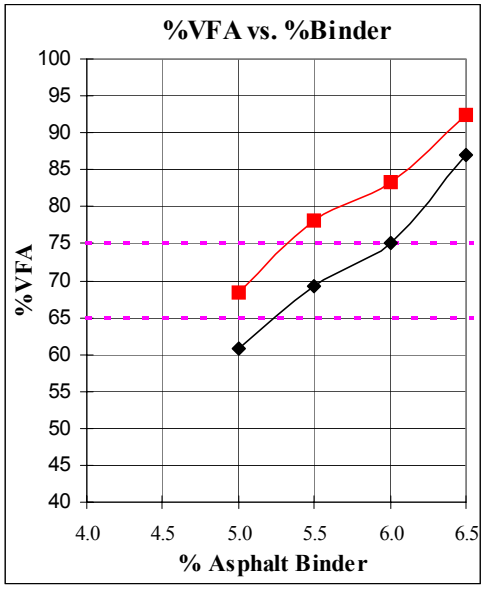

Blend	%AC	Air Voids @ NDesign	%VMA @ NDesign	%VFA @ NDesign	Air Voids @ NMax	%VMA @ Nmax	%VFA @ Nmax
Blend1	5.0	5.9	15.1	60.8	4.3	13.6	68.4
Blend2	5.5	4.7	15.3	69.2	3.0	13.7	78.2
Blend3	6.0	3.9	15.7	75.2	2.4	14.4	83.3
Blend4	6.5	2.0	15.4	87.0	1.1	14.6	92.5

Mixture Design for 19mm Limestone with FAA of 50 and Gradation Plotting Above The Restricted Zone.

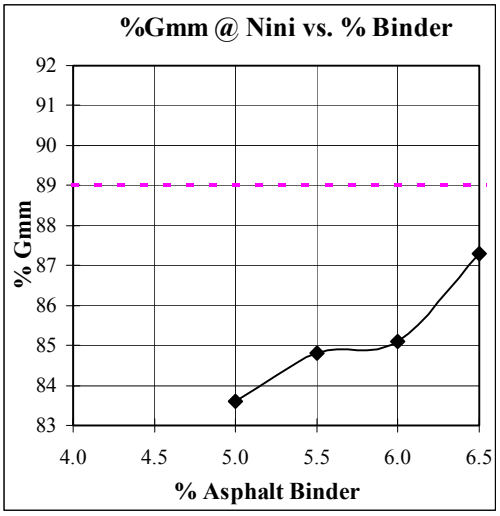

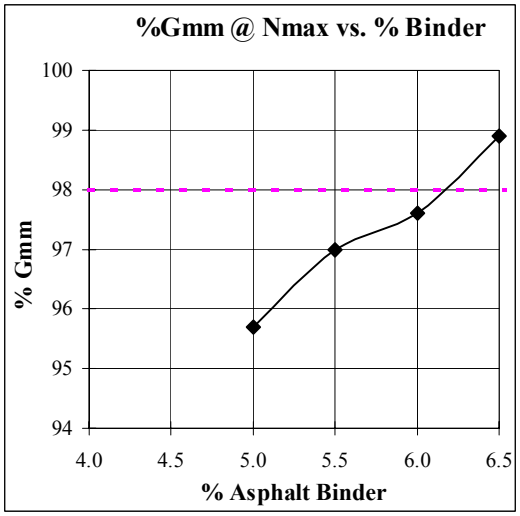

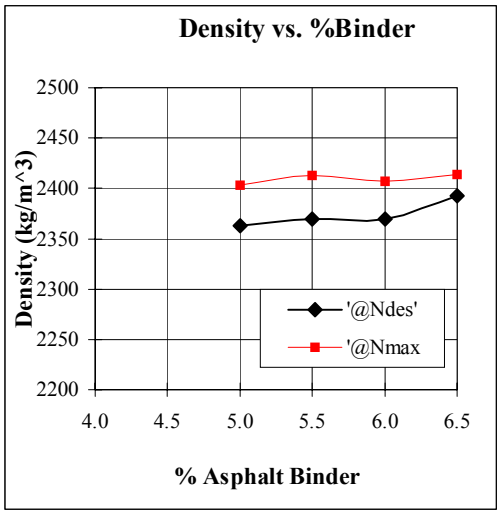

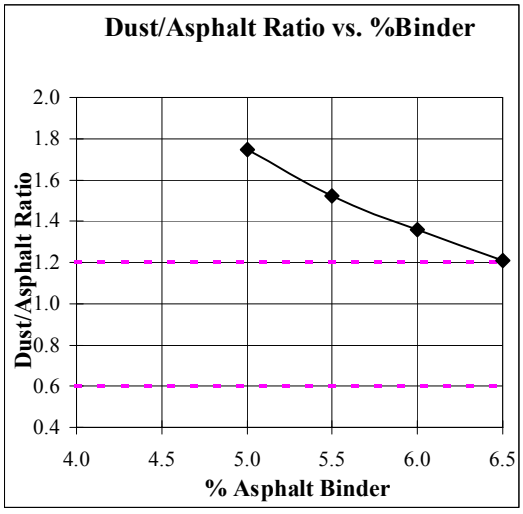

Blend	%AC	%Gmm @ Nini	%Gmm @ Nmax	Density @Ndes (kg/m3)	Density @Nmax (kg/m3)	D/A ratio
Blend1	5.0	83.6	95.7	2362.9	2403.0	1.7
Blend2	5.5	84.8	97.0	2370.1	2412.4	1.5
Blend3	6.0	85.1	97.6	2369.8	2406.8	1.4
Blend4	6.5	87.3	98.9	2392.2	2414.1	1.2

Mixture Design for 19mm Limestone with FAA of 50 and Gradation Plotting Through The Restricted Zone.

Project Name:	NPF	**N Initial:**	8
Workbook Name:		**N Design:**	96
Technician:	CP	**N Max:**	152
Date:		**Nom. Sieve Size:**	19mm
Asphalt Grade:	64-22	**Design Temperature:**	38°C
Compaction Temp:	150°C	**Design ESAL's (millions):**	3-10

Blend	%AC	%Gmm @ N = 8	%Gmm @ N = 96	%Gmm @ N = 152	%Air Voids @ NDesign	%VMA @ NDesign
Blend 1	4.7	82.6	92.8	94.3	7.2	16.2
Blend 2	5.2	83.1	93.5	95.1	6.5	16.5
Blend 3	5.7	84.8	95.3	96.8	4.7	15.9
Blend 4	6.2	86.1	96.8	98.2	3.2	15.6

	Blend 1	Blend 2	Blend 3	Blend 4	Design AC
Agg. Bulk Specific Gravity (Gsb):	2.644	2.644	2.644	2.644	**2.644**
Percent Binder by wt. of mix (Pbi):	4.7	5.2	5.7	6.2	**5.9**
Percent Aggregate (Ps):	95.3	94.8	94.3	93.8	**94.1**
Specific Gravity of Binder (Gb):	1.030	1.030	1.030	1.030	**1.030**
Fines (%Passing 0.075mm Sieve):	5.7	5.7	5.7	5.7	**5.7**
Rice Specific Gravity (Gmm):	2.506	2.490	2.473	2.457	**2.466**
Effective Specific Gravity (Gse):	2.6966	2.6999	2.7018	2.7047	**2.7022**
Effective % Binder (Pbe):	3.9	4.4	4.9	5.3	**5.1**
% Binder Absorption (Pba):	0.8	0.8	0.8	0.9	**0.8**
Dust Proportion (0.6-1.2%):	1.4	1.3	1.2	1.1	**1.1**
Surface Area(m^2/Kg):	5.43	5.43	5.43	5.43	**5.43**
Film Thickness(micron):	7.10	7.95	8.86	9.75	**9.23**

Mixture Design for 19mm Limestone with FAA of 50 and Gradation Plotting Through The Restricted Zone.

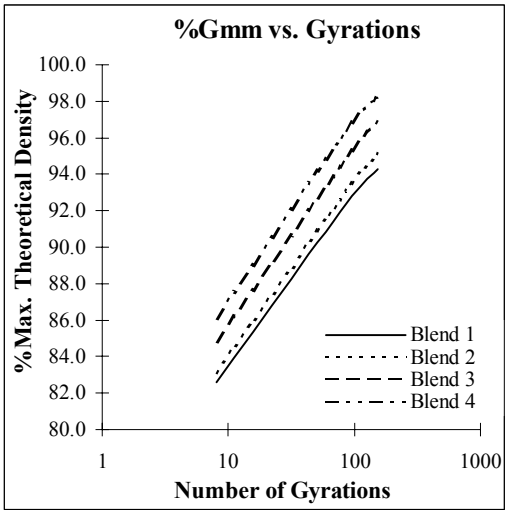

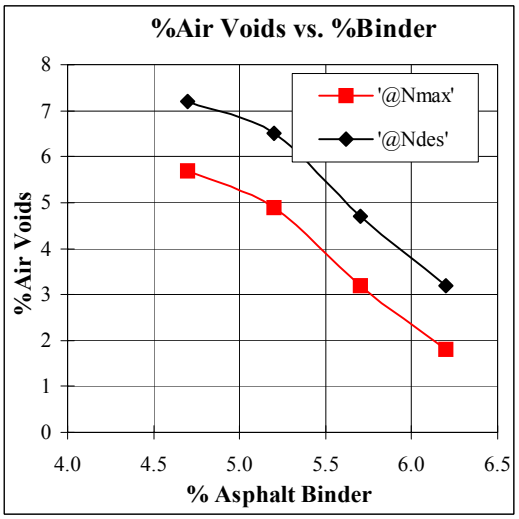

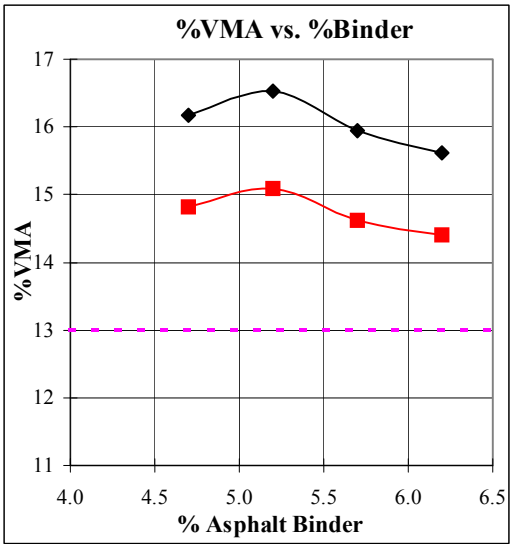

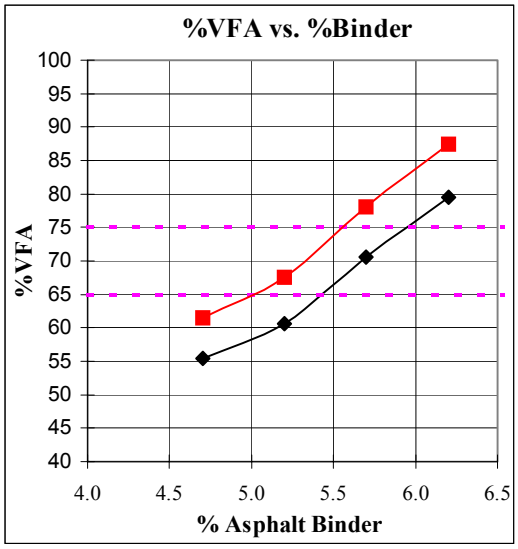

Blend	%AC	Air Voids @ NDesign	%VMA @ NDesign	%VFA @ NDesign	Air Voids @ NMax	%VMA @ Nmax	%VFA @ Nmax
Blend1	4.7	7.2	16.2	55.5	5.7	14.8	61.5
Blend2	5.2	6.5	16.5	60.7	4.9	15.1	67.5
Blend3	5.7	4.7	15.9	70.5	3.2	14.6	78.1
Blend4	6.2	3.2	15.6	79.5	1.8	14.4	87.5

Mixture Design for 19mm Limestone with FAA of 50 and Gradation Plotting Through The Restricted Zone.

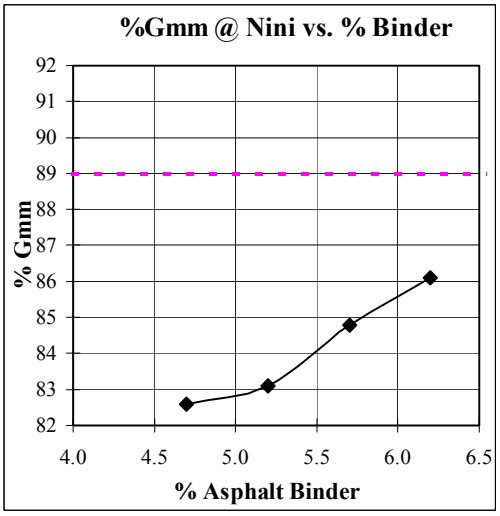

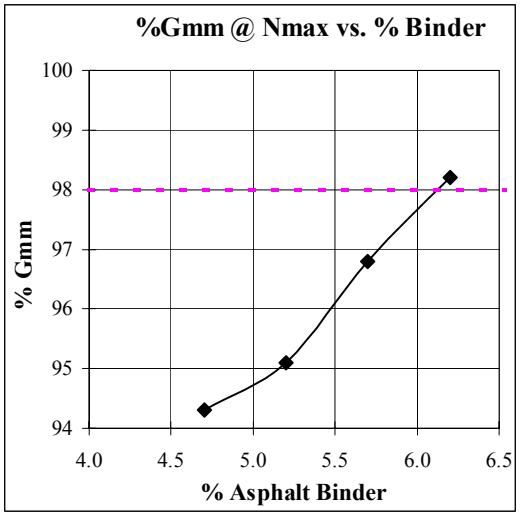

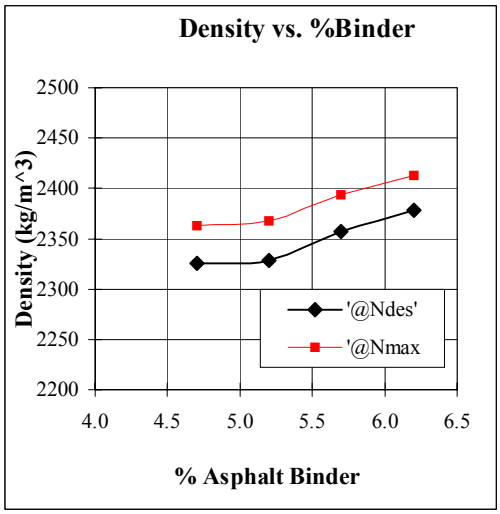

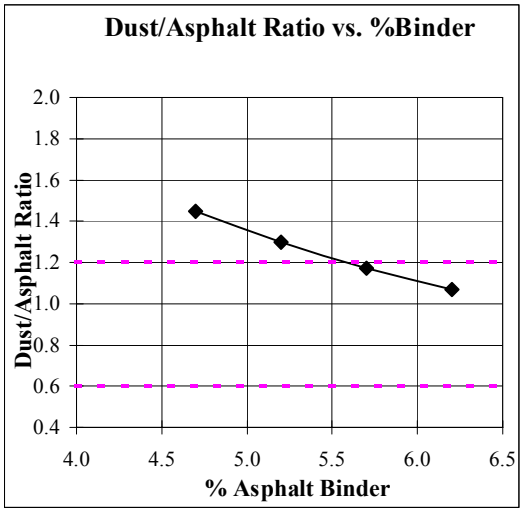

Blend	%AC	%Gmm @ Nini	%Gmm @ Nmax	Density @Ndes (kg/m3)	Density @Nmax (kg/m3)	D/A ratio
Blend1	4.7	82.6	94.3	2325.6	2363.2	1.4
Blend2	5.2	83.1	95.1	2328.2	2368.0	1.3
Blend3	5.7	84.8	96.8	2356.8	2393.9	1.2
Blend4	6.2	86.1	98.2	2378.4	2412.8	1.1

Mixture Design for 19mm Limestone with FAA of 50 and Gradation Plotting Below The Restricted Zone.

Project Name:	NPF	**N Initial:**	8
Workbook Name:		**N Design:**	96
Technician:	CP	**N Max:**	152
Date:		**Nom. Sieve Size:**	19mm
Asphalt Grade:	64-22	**Design Temperature:**	38°C
Compaction Temp:	150°C	**Design ESAL's (millions):**	3-10

Blend	%AC	%Gmm @ N = 8	%Gmm @ N = 96	%Gmm @ N = 152	%Air Voids @ NDesign	%VMA @ NDesign
Blend 1	4.5	83.5	93.9	95.6	6.1	14.4
Blend 2	5.0	83.5	94.1	95.8	5.9	15.4
Blend 3	5.5	84.8	95.9	97.5	4.1	15.1
Blend 4	6.0	85.3	96.7	98.5	3.3	15.6

	Blend 1	Blend 2	Blend 3	Blend 4	Design AC
Agg. Bulk Specific Gravity (Gsb):	2.645	2.645	2.645	2.645	**2.645**
Percent Binder by wt. of mix (Pbi):	4.5	5.0	5.5	6.0	**5.5**
Percent Aggregate (Ps):	95.5	95.0	94.5	94.0	**94.5**
Specific Gravity of Binder (Gb):	1.030	1.030	1.030	1.030	**1.030**
Fines (%Passing 0.075mm Sieve):	4.3	4.3	4.3	4.3	**4.3**
Rice Specific Gravity (Gmm):	2.526	2.502	2.478	2.456	**2.478**
Effective Specific Gravity (Gse):	2.7116	2.7055	2.6988	2.6941	**2.6988**
Effective % Binder (Pbe):	3.5	4.1	4.7	5.3	**4.7**
% Binder Absorption (Pba):	1.0	0.9	0.8	0.7	**0.8**
Dust Proportion (0.6-1.2%):	1.2	1.0	0.9	0.8	**0.9**
Surface Area(m^2/Kg):	4.07	4.07	4.07	4.07	**4.07**
Film Thickness(micron):	8.50	9.95	11.45	12.89	**11.45**

Mixture Design for 19mm Limestone with FAA of 50 and Gradation Plotting Below The Restricted Zone.

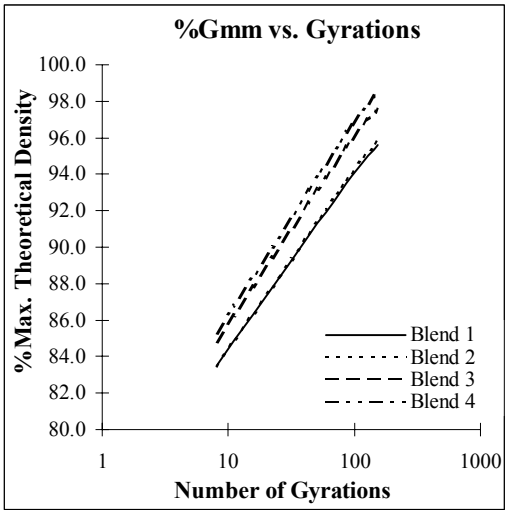

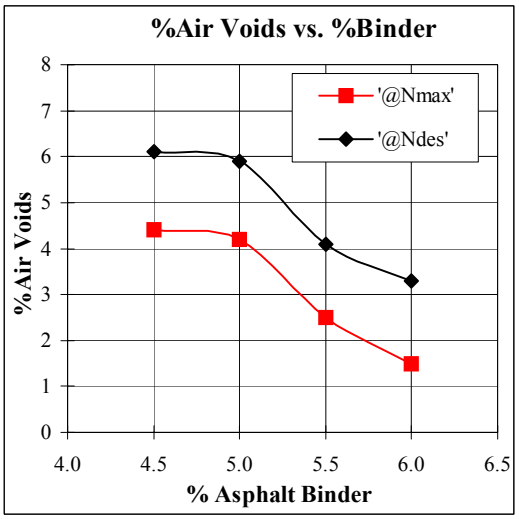

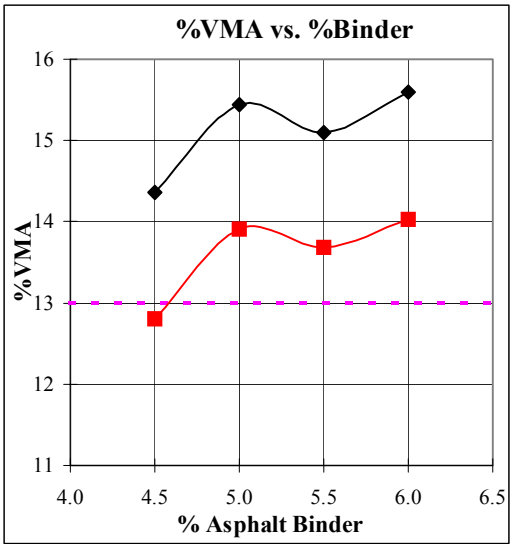

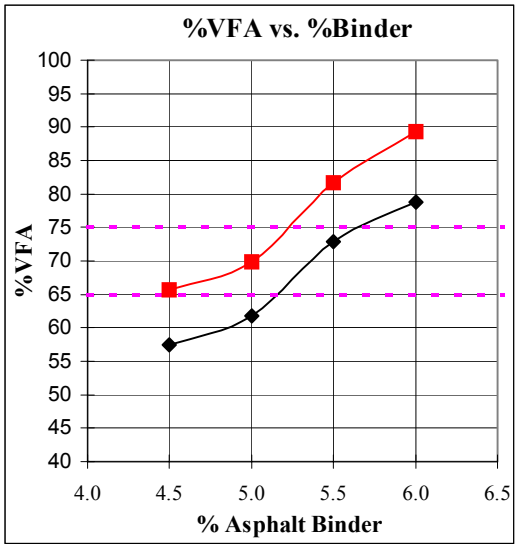

Blend	%AC	Air Voids @ NDesign	%VMA @ NDesign	%VFA @ NDesign	Air Voids @ NMax	%VMA @ Nmax	%VFA @ Nmax
Blend1	4.5	6.1	14.4	57.5	4.4	12.8	65.7
Blend2	5.0	5.9	15.4	61.8	4.2	13.9	69.8
Blend3	5.5	4.1	15.1	72.8	2.5	13.7	81.7
Blend4	6.0	3.3	15.6	78.8	1.5	14.0	89.3

Mixture Design for 19mm Limestone with FAA of 50 and Gradation Plotting Below The Restricted Zone.

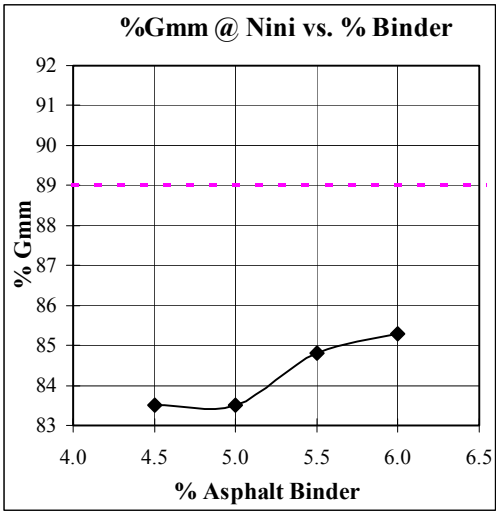

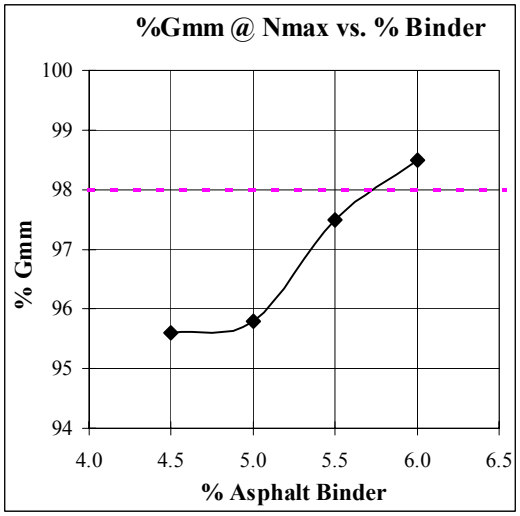

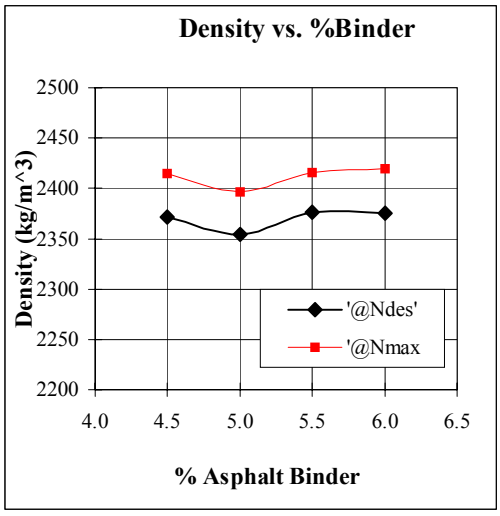

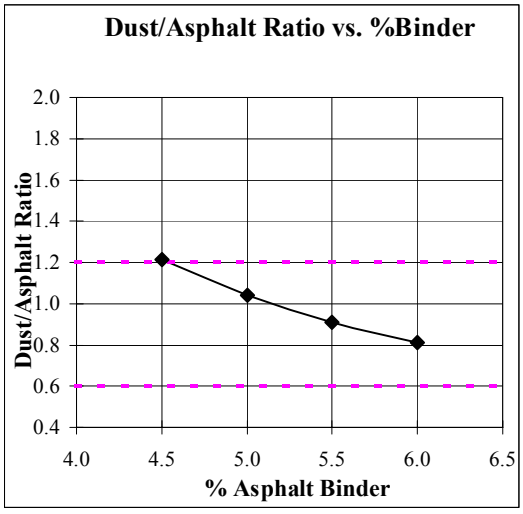

Blend	%AC	%Gmm @ Nini	%Gmm @ Nmax	Density @Ndes (kg/m3)	Density @Nmax (kg/m3)	D/A ratio
Blend1	4.5	83.5	95.6	2371.9	2414.9	1.2
Blend2	5.0	83.5	95.8	2354.4	2396.9	1.0
Blend3	5.5	84.8	97.5	2376.4	2416.1	0.9
Blend4	6.0	85.3	98.5	2375.0	2419.2	0.8

Mixture Design for 19mm Granite with FAA of 44 and Gradation Plotting Through The Restricted Zone.

Project Name:	NPF	**N Initial:**	8
Workbook Name:		**N Design:**	96
Technician:	CP	**N Max:**	152
Date:		**Nom. Sieve Size:**	19mm
Asphalt Grade:	64-22	**Design Temperature:**	38°C
Compaction Temp:	150°C	**Design ESAL's (millions):**	3-10

Blend	%AC	%Gmm @ N = 8	%Gmm @ N = 96	%Gmm @ N = 152	%Air Voids @ NDesign	%VMA @ NDesign
Blend 1	3.5	83.1	91.4	92.7	8.6	14.6
Blend 2	4.0	85.2	93.4	94.8	6.6	14.0
Blend 3	4.5	86.0	94.7	96.0	5.3	14.0
Blend 4	5.0	86.8	96.6	98.0	3.4	13.5

	Blend 1	Blend 2	Blend 3	Blend 4	Design AC
Agg. Bulk Specific Gravity (Gsb):	2.647	2.647	2.647	2.647	**2.647**
Percent Binder by wt. of mix (Pbi):	3.5	4.0	4.5	5.0	**4.8**
Percent Aggregate (Ps):	96.5	96.0	95.5	95.0	**95.2**
Specific Gravity of Binder (Gb):	1.030	1.030	1.030	1.030	**1.030**
Fines (%Passing 0.075mm Sieve):	4.1	4.1	4.1	4.1	**4.1**
Rice Specific Gravity (Gmm):	2.562	2.539	2.516	2.494	**2.503**
Effective Specific Gravity (Gse):	2.7081	2.7041	2.6995	2.6957	**2.6975**
Effective % Binder (Pbe):	2.6	3.2	3.7	4.3	**4.1**
% Binder Absorption (Pba):	0.9	0.8	0.8	0.7	**0.7**
Dust Proportion (0.6-1.2%):	1.6	1.3	1.1	1.0	**1.0**
Surface Area(m^2/Kg):	4.71	4.71	4.71	4.71	**4.71**
Film Thickness(micron):	5.38	6.55	7.76	8.95	**8.46**

Mixture Design for 19mm Granite with FAA of 44 and Gradation Plotting Through The Restricted Zone.

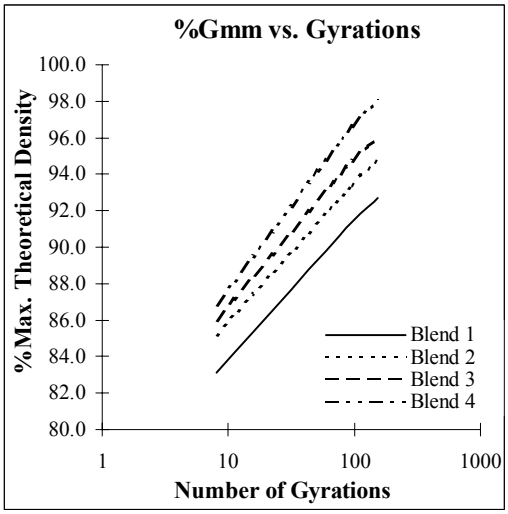

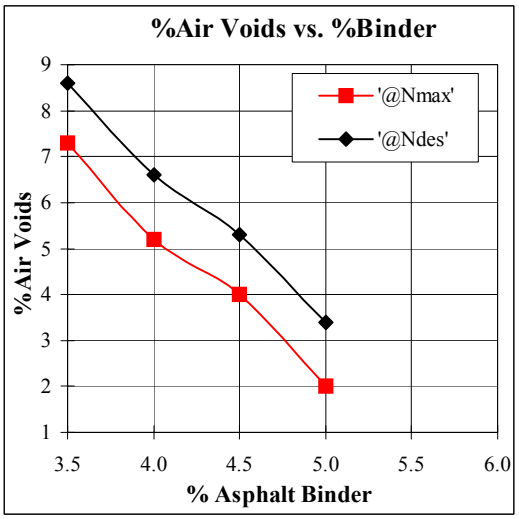

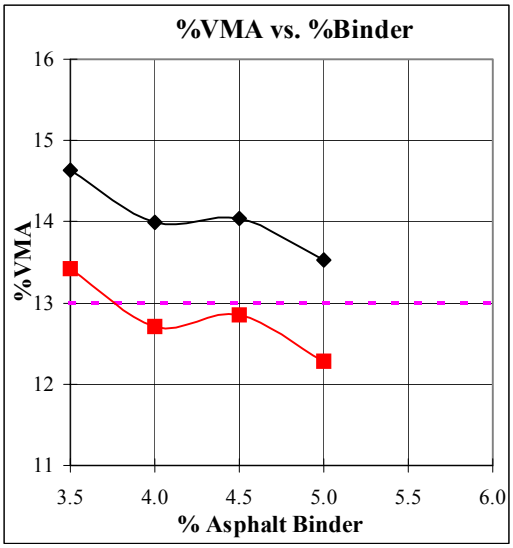

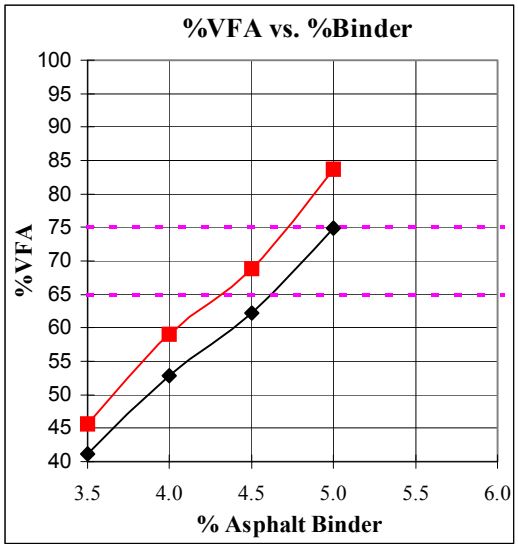

Blend	%AC	Air Voids @ NDesign	%VMA @ NDesign	%VFA @ NDesign	Air Voids @ NMax	%VMA @ Nmax	%VFA @ Nmax
Blend1	3.5	8.6	14.6	41.2	7.3	13.4	45.6
Blend2	4.0	6.6	14.0	52.8	5.2	12.7	59.1
Blend3	4.5	5.3	14.0	62.2	4.0	12.9	68.9
Blend4	5.0	3.4	13.5	74.9	2.0	12.3	83.7

Mixture Design for 19mm Granite with FAA of 44 and Gradation Plotting Through The Restricted Zone.

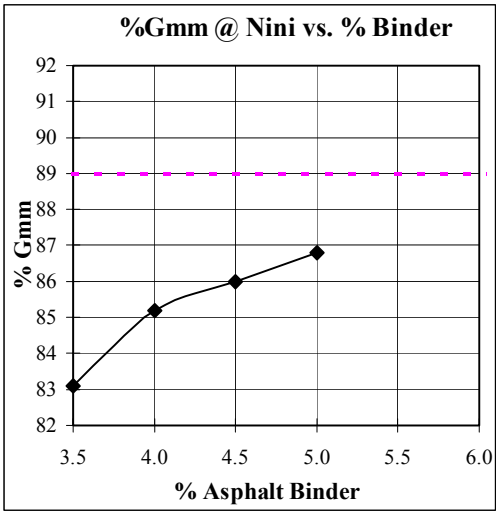

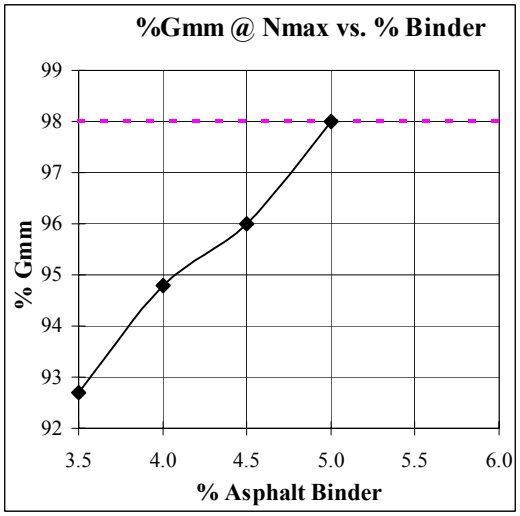

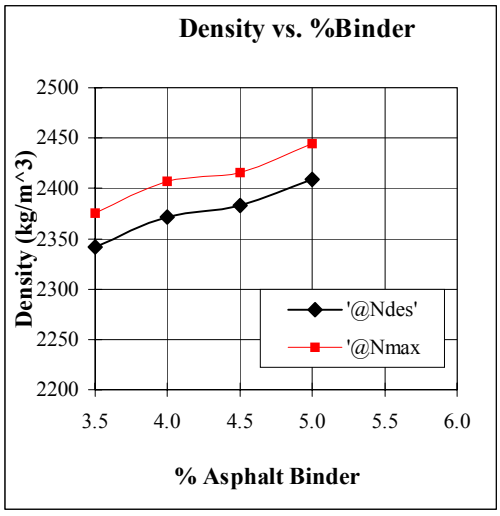

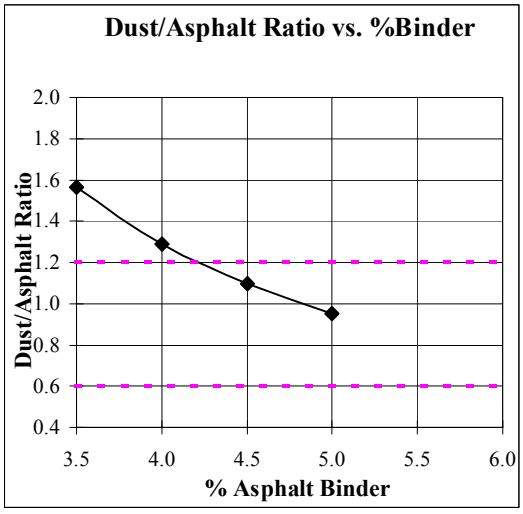

Blend	%AC	%Gmm @ Nini	%Gmm @ Nmax	Density @Ndes (kg/m3)	Density @Nmax (kg/m3)	D/A ratio
Blend1	3.5	83.1	92.7	2341.7	2375.0	1.6
Blend2	4.0	85.2	94.8	2371.4	2407.0	1.3
Blend3	4.5	86.0	96.0	2382.7	2415.4	1.1
Blend4	5.0	86.8	98.0	2409.2	2444.1	1.0

Mixture Design for 19mm Granite with FAA of 44 and Gradation Plotting Below The Restricted Zone.

Project Name:	NPF	**N Initial:**	8
Workbook Name:		**N Design:**	96
Technician:	CP	**N Max:**	152
Date:		**Nom. Sieve Size:**	19mm
Asphalt Grade:	64-22	**Design Temperature:**	38°C
Compaction Temp:	150°C	**Design ESAL's (millions):**	3-10

Blend	%AC	%Gmm @ N = 8	%Gmm @ N = 96	%Gmm @ N = 152	%Air Voids @ NDesign	%VMA @ NDesign
Blend 1	4.0	85.8	95.4	96.7	4.6	12.8
Blend 2	4.5	85.6	96.2	97.7	3.8	13.0
Blend 3	5.0	87.1	97.6	99.1	2.4	12.6
Blend 4	5.5	87.1	97.8	99.1	2.2	13.4

	Blend 1	Blend 2	Blend 3	Blend 4	Design AC
Agg. Bulk Specific Gravity (Gsb):	2.649	2.649	2.649	2.649	**2.649**
Percent Binder by wt. of mix (Pbi):	4.0	4.5	5.0	5.5	**4.4**
Percent Aggregate (Ps):	96.0	95.5	95.0	94.5	**95.6**
Specific Gravity of Binder (Gb):	1.030	1.030	1.030	1.030	**1.030**
Fines (%Passing 0.075mm Sieve):	4.2	4.2	4.2	4.2	**4.2**
Rice Specific Gravity (Gmm):	2.521	2.508	2.496	2.483	**2.510**
Effective Specific Gravity (Gse):	2.6828	2.6899	2.6981	2.7051	**2.6877**
Effective % Binder (Pbe):	3.5	3.9	4.3	4.7	**3.8**
% Binder Absorption (Pba):	0.5	0.6	0.7	0.8	**0.6**
Dust Proportion (0.6-1.2%):	1.2	1.1	1.0	0.9	**1.1**
Surface Area(m^2/Kg):	4.31	4.31	4.31	4.31	**4.31**
Film Thickness(micron):	7.91	8.85	9.77	10.74	**8.68**

Mixture Design for 19mm Granite with FAA of 44 and Gradation Plotting Below The Restricted Zone.

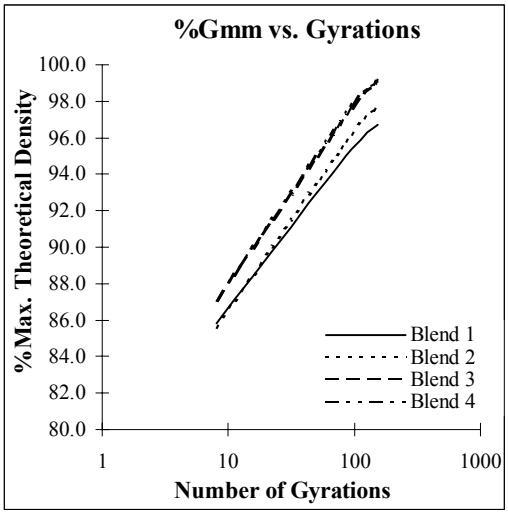

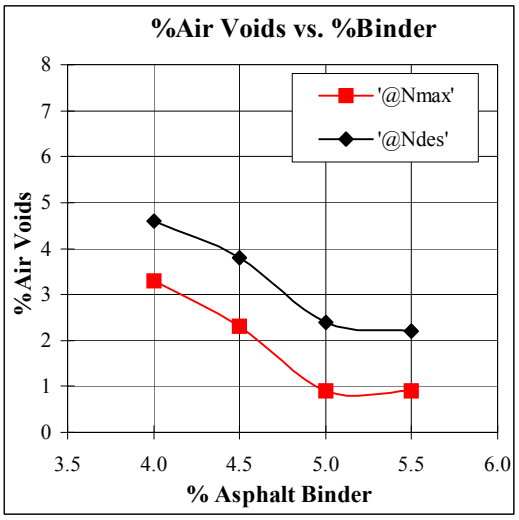

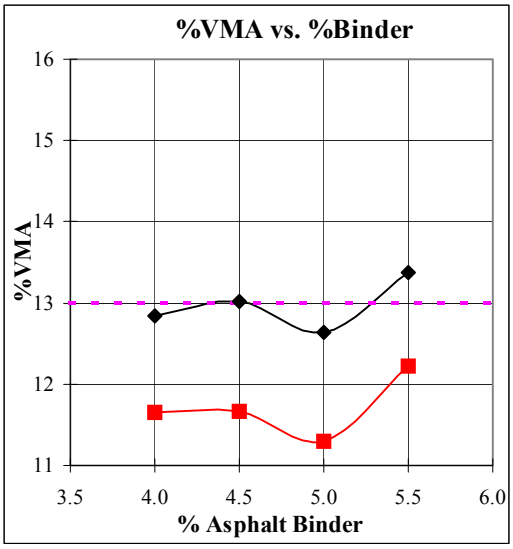

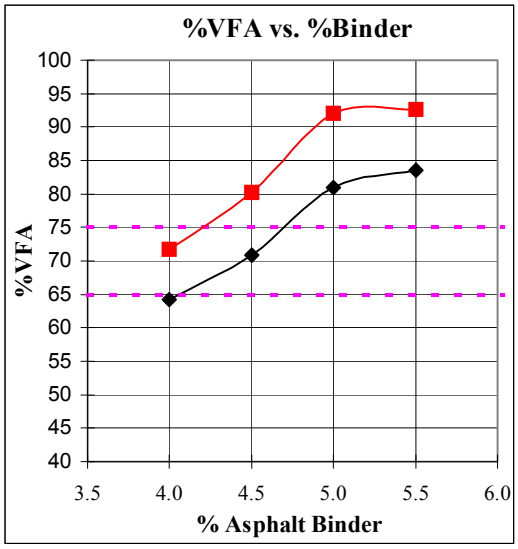

Blend	%AC	Air Voids @ NDesign	%VMA @ NDesign	%VFA @ NDesign	Air Voids @ NMax	%VMA @ Nmax	%VFA @ Nmax
Blend1	4.0	4.6	12.8	64.2	3.3	11.7	71.7
Blend2	4.5	3.8	13.0	70.8	2.3	11.7	80.3
Blend3	5.0	2.4	12.6	81.0	0.9	11.3	92.0
Blend4	5.5	2.2	13.4	83.5	0.9	12.2	92.6

Mixture Design for 19mm Granite with FAA of 44 and Gradation Plotting Below The Restricted Zone.

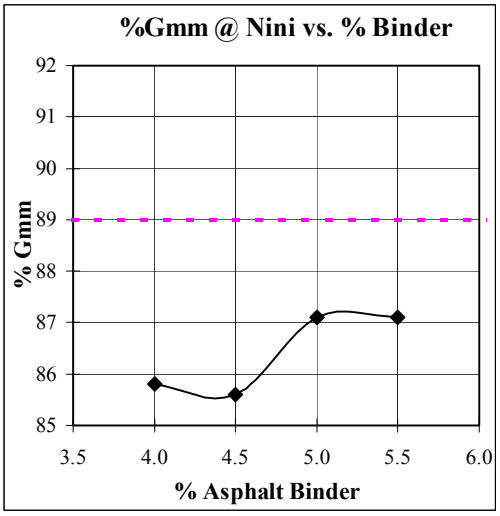

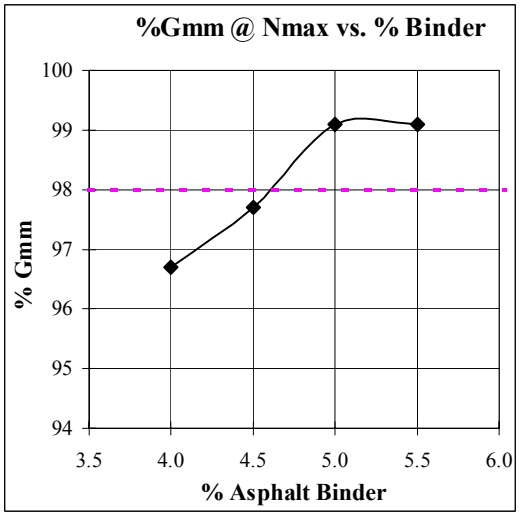

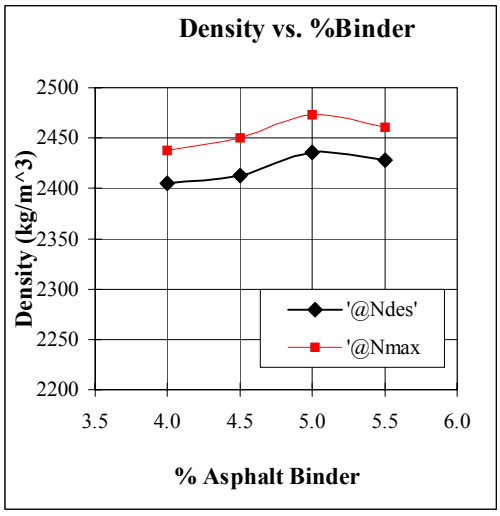

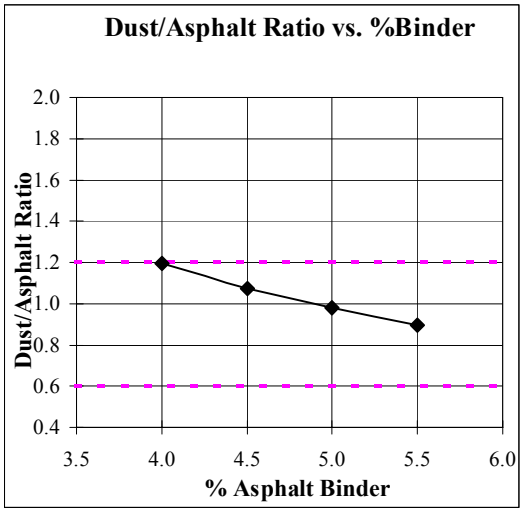

Blend	%AC	%Gmm @ Nini	%Gmm @ Nmax	Density @Ndes (kg/m3)	Density @Nmax (kg/m3)	D/A ratio
Blend1	4.0	85.8	96.7	2405.0	2437.8	1.2
Blend2	4.5	85.6	97.7	2412.7	2450.3	1.1
Blend3	5.0	87.1	99.1	2436.1	2473.5	1.0
Blend4	5.5	87.1	99.1	2428.4	2460.7	0.9

Mixture Design for 19mm Granite with FAA of 50 and Gradation Plotting Through The Restricted Zone.

Project Name:	NPF	**N Initial:**	8
Workbook Name:		**N Design:**	96
Technician:	CP	**N Max:**	152
Date:		**Nom. Sieve Size:**	19mm
Asphalt Grade:	64-22	**Design Temperature:**	38°C
Compaction Temp:	150°C	**Design ESAL's (millions):**	3-10

Blend	%AC	%Gmm @ N = 8	%Gmm @ N = 96	%Gmm @ N = 152	%Air Voids @ NDesign	%VMA @ NDesign
Blend 1	4.8	84.2	94.3	95.8	5.7	16.6
Blend 2	5.3	85.7	96.0	97.5	4.0	15.9
Blend 3	5.8	86.5	96.9	98.4	3.1	16.0
Blend 4	6.3	86.4	97.1	98.6	2.9	16.7

	Blend 1	Blend 2	Blend 3	Blend 4	Design AC
Agg. Bulk Specific Gravity (Gsb):	2.644	2.644	2.644	2.644	**2.644**
Percent Binder by wt. of mix (Pbi):	4.8	5.3	5.8	6.3	**5.3**
Percent Aggregate (Ps):	95.2	94.7	94.2	93.7	**94.7**
Specific Gravity of Binder (Gb):	1.030	1.030	1.030	1.030	**1.030**
Fines (%Passing 0.075mm Sieve):	5.5	5.5	5.5	5.5	**5.5**
Rice Specific Gravity (Gmm):	2.456	2.445	2.433	2.421	**2.445**
Effective Specific Gravity (Gse):	2.6403	2.6486	2.6557	2.6628	**2.6486**
Effective % Binder (Pbe):	4.9	5.2	5.6	6.0	**5.2**
% Binder Absorption (Pba):	-0.1	0.1	0.2	0.3	**0.1**
Dust Proportion (0.6-1.2%):	1.1	1.1	1.0	0.9	**1.1**
Surface Area(m^2/Kg):	5.27	5.27	5.27	5.27	**5.27**
Film Thickness(micron):	9.02	9.77	10.57	11.37	**9.77**

Mixture Design for 19mm Granite with FAA of 50 and Gradation Plotting Through The Restricted Zone.

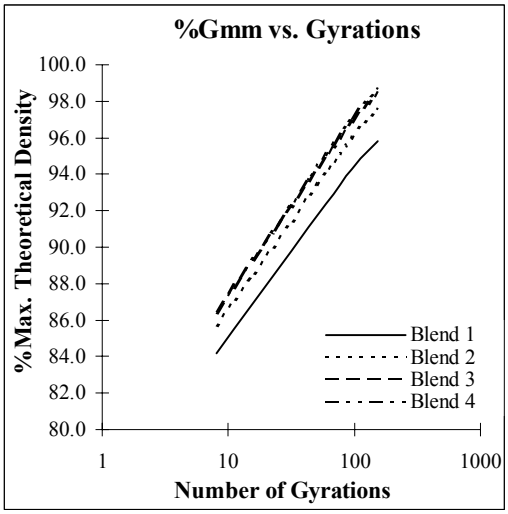

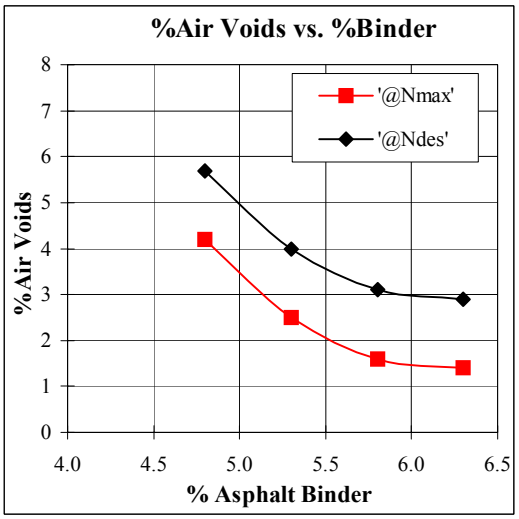

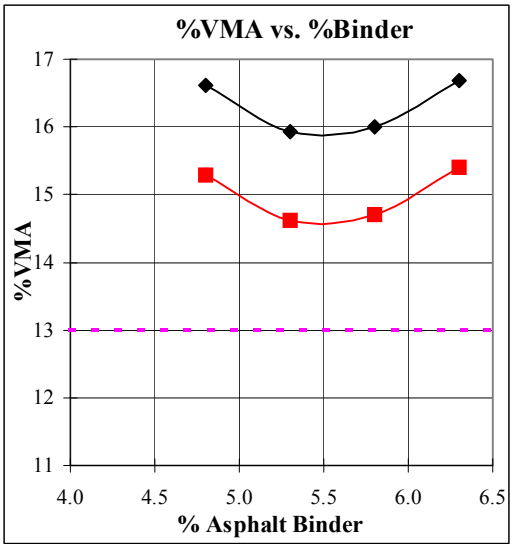

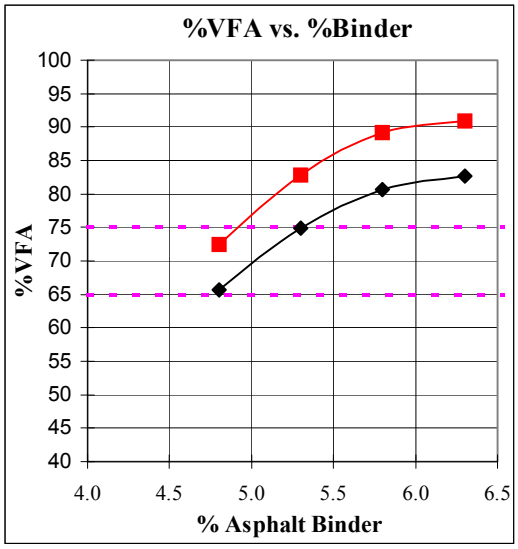

Blend	%AC	Air Voids @ NDesign	%VMA @ NDesign	%VFA @ NDesign	Air Voids @ NMax	%VMA @ Nmax	%VFA @ Nmax
Blend1	4.8	5.7	16.6	65.7	4.2	15.3	72.5
Blend2	5.3	4.0	15.9	74.9	2.5	14.6	82.9
Blend3	5.8	3.1	16.0	80.6	1.6	14.7	89.1
Blend4	6.3	2.9	16.7	82.6	1.4	15.4	90.9

Mixture Design for 19mm Granite with FAA of 50 and Gradation Plotting Through The Restricted Zone.

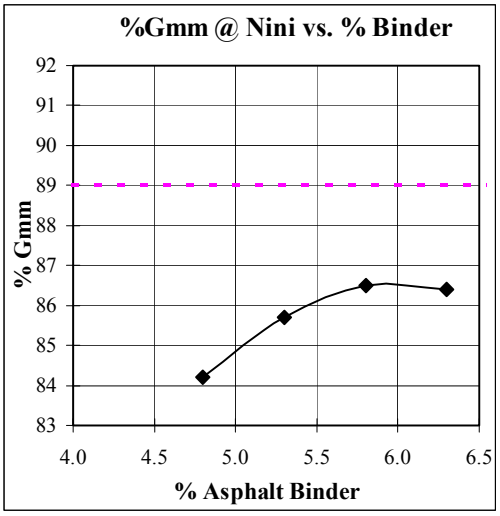

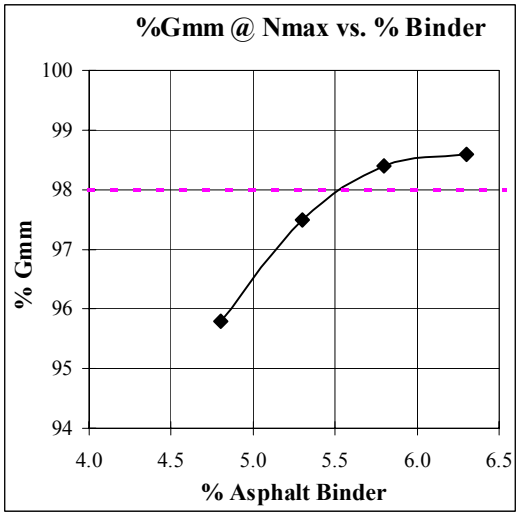

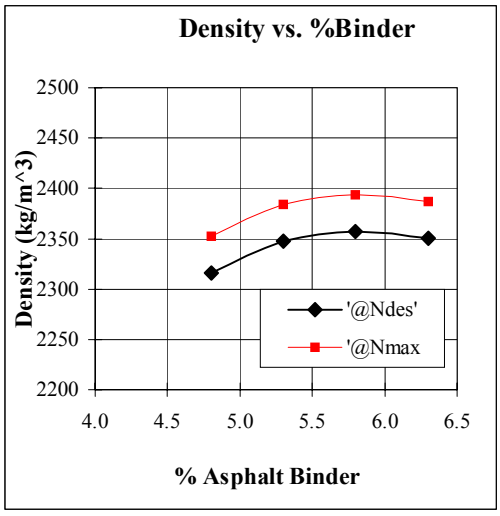

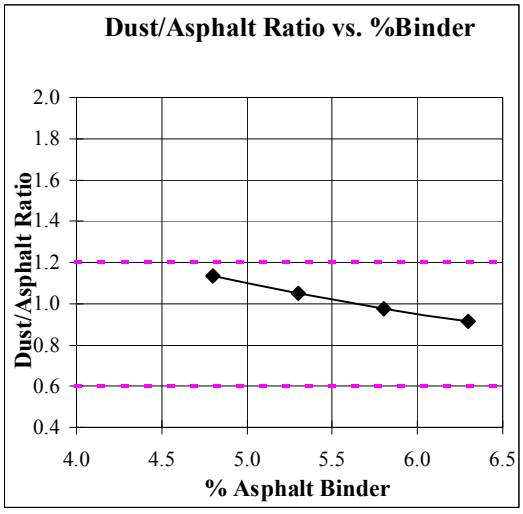

Blend	%AC	%Gmm @ Nini	%Gmm @ Nmax	Density @Ndes (kg/m3)	Density @Nmax (kg/m3)	D/A ratio
Blend1	4.8	84.2	95.8	2316.0	2352.8	1.1
Blend2	5.3	85.7	97.5	2347.2	2383.9	1.1
Blend3	5.8	86.5	98.4	2357.6	2394.1	1.0
Blend4	6.3	86.4	98.6	2350.8	2387.1	0.9

Mixture Design for 19mm Granite with FAA of 50 and Gradation Plotting Below The Restricted Zone.

Project Name:	NPF	**N Initial:**	8
Workbook Name:		**N Design:**	96
Technician:	CP	**N Max:**	152
Date:		**Nom. Sieve Size:**	19mm
Asphalt Grade:	64-22	**Design Temperature:**	38°C
Compaction Temp:	150°C	**Design ESAL's (millions):**	3-10

Blend	%AC	%Gmm @ N = 8	%Gmm @ N = 96	%Gmm @ N = 152	%Air Voids @ NDesign	%VMA @ NDesign
Blend 1	4.5	85.3	95.0	96.6	5.0	15.2
Blend 2	5.0	87.0	96.9	98.3	3.1	14.3
Blend 3	5.5	86.7	96.8	98.2	3.2	15.3
Blend 4	6.0	86.8	97.2	98.7	2.8	15.8

	Blend 1	Blend 2	Blend 3	Blend 4	Design AC
Agg. Bulk Specific Gravity (Gsb):	2.645	2.645	2.645	2.645	**2.645**
Percent Binder by wt. of mix (Pbi):	4.5	5.0	5.5	6.0	**4.8**
Percent Aggregate (Ps):	95.5	95.0	94.5	94.0	**95.2**
Specific Gravity of Binder (Gb):	1.030	1.030	1.030	1.030	**1.030**
Fines (%Passing 0.075mm Sieve):	4.6	4.6	4.6	4.6	**4.6**
Rice Specific Gravity (Gmm):	2.472	2.461	2.449	2.437	**2.466**
Effective Specific Gravity (Gse):	2.6466	2.6552	2.6625	2.6698	**2.6525**
Effective % Binder (Pbe):	4.5	4.9	5.2	5.6	**4.7**
% Binder Absorption (Pba):	0.0	0.1	0.3	0.4	**0.1**
Dust Proportion (0.6-1.2%):	1.0	0.9	0.9	0.8	**1.0**
Surface Area(m^2/Kg):	4.55	4.55	4.55	4.55	**4.55**
Film Thickness(micron):	9.60	10.46	11.37	12.29	**10.09**

Mixture Design for 19mm Granite with FAA of 50 and Gradation Plotting Below The Restricted Zone.

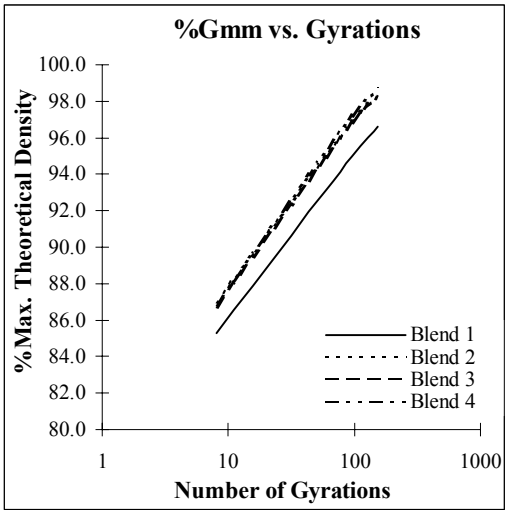

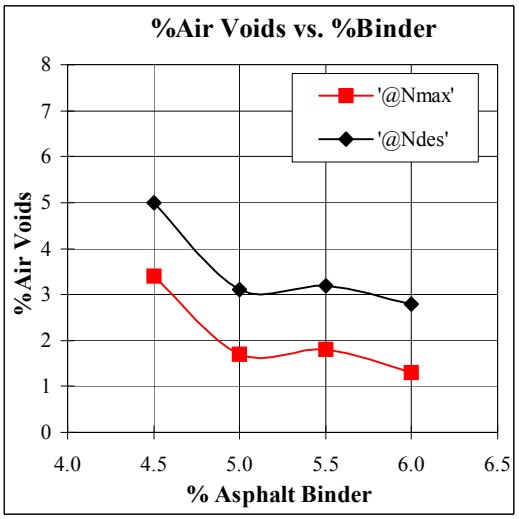

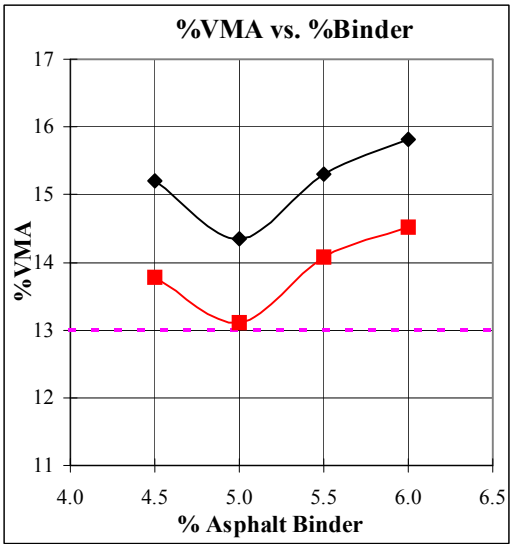

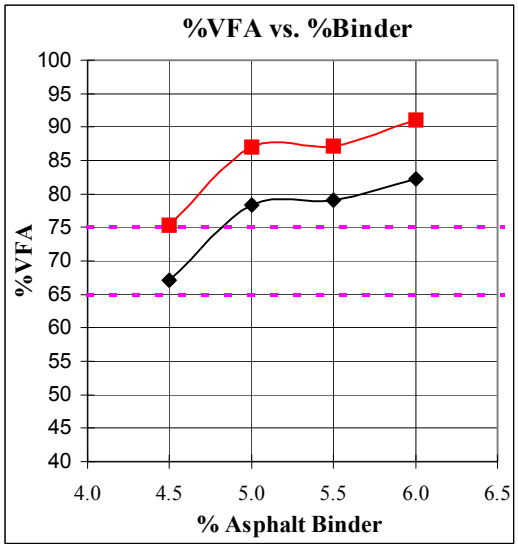

Blend	%AC	Air Voids @ NDesign	%VMA @ NDesign	%VFA @ NDesign	Air Voids @ NMax	%VMA @ Nmax	%VFA @ Nmax
Blend1	4.5	5.0	15.2	67.1	3.4	13.8	75.3
Blend2	5.0	3.1	14.3	78.4	1.7	13.1	87.0
Blend3	5.5	3.2	15.3	79.1	1.8	14.1	87.2
Blend4	6.0	2.8	15.8	82.3	1.3	14.5	91.0

Mixture Design for 19mm Granite with FAA of 50 and Gradation Plotting Below The Restricted Zone.

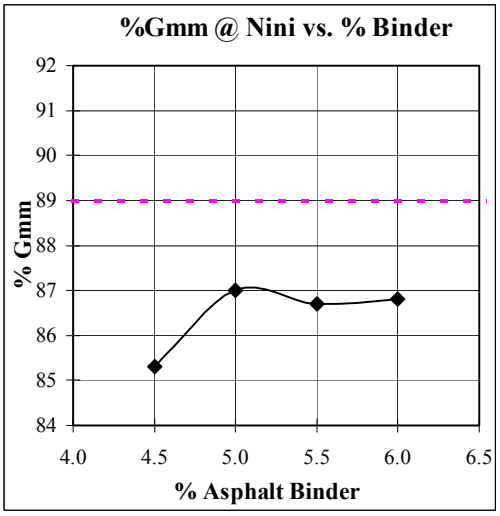

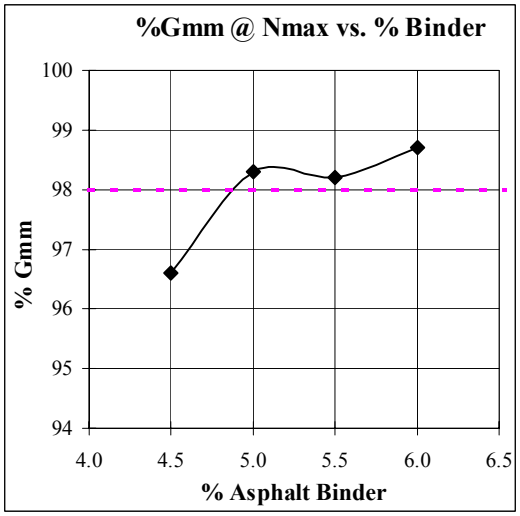

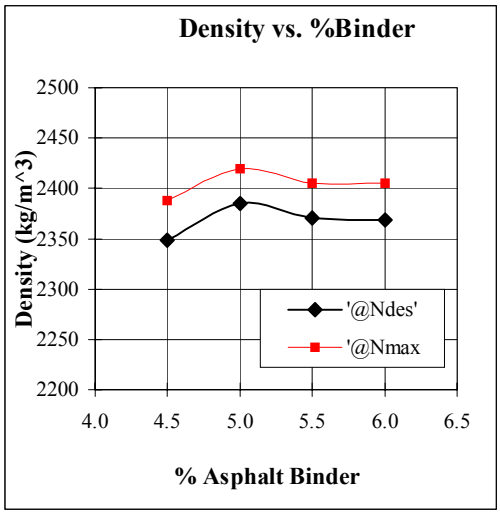

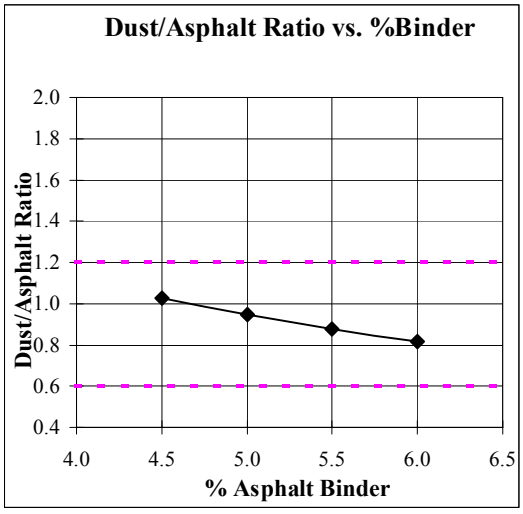

Blend	%AC	%Gmm @ Nini	%Gmm @ Nmax	Density @Ndes (kg/m3)	Density @Nmax (kg/m3)	D/A ratio
Blend1	4.5	85.3	96.6	2348.4	2388.0	1.0
Blend2	5.0	87.0	98.3	2384.7	2419.2	0.9
Blend3	5.5	86.7	98.2	2370.6	2404.9	0.9
Blend4	6.0	86.8	98.7	2368.8	2405.3	0.8

Mixture Design for 9.5mm Limestone with FAA of 44 and Gradation Plotting Above The Restricted Zone.

Project Name:	NPF	**N Initial:**	8
Workbook Name:		**N Design:**	96
Technician:	CP	**N Max:**	152
Date:		**Nom. Sieve Size:**	9.5mm
Asphalt Grade:	64-22	**Design Temperature:**	38°C
Compaction Temp:	150°C	**Design ESAL's (millions):**	3-10

Blend	%AC	%Gmm @ N = 8	%Gmm @ N = 96	%Gmm @ N = 152	%Air Voids @ NDesign	%VMA @ NDesign
Blend 1	5.0	83.7	93.1	94.5	6.9	16.5
Blend 2	5.5	85.8	95.7	97.1	4.3	15.3
Blend 3	6.0	87.4	97.5	98.5	2.5	14.8
Blend 4	6.5	88.3	98.4	99.1	1.6	15.1

	Blend 1	Blend 2	Blend 3	Blend 4	Design AC
Agg. Bulk Specific Gravity (Gsb):	2.646	2.646	2.646	2.646	**2.646**
Percent Binder by wt. of mix (Pbi):	5.0	5.5	6.0	6.5	**5.6**
Percent Aggregate (Ps):	95.0	94.5	94.0	93.5	**94.4**
Specific Gravity of Binder (Gb):	1.030	1.030	1.030	1.030	**1.030**
Fines (%Passing 0.075mm Sieve):	8.2	8.2	8.2	8.2	**8.2**
Rice Specific Gravity (Gmm):	2.497	2.479	2.461	2.443	**2.478**
Effective Specific Gravity (Gse):	2.6993	2.7001	2.7005	2.7005	**2.7035**
Effective % Binder (Pbe):	4.2	4.7	5.2	5.7	**4.8**
% Binder Absorption (Pba):	0.8	0.8	0.8	0.8	**0.8**
Dust Proportion (0.6-1.2%):	1.9	1.7	1.6	1.4	**1.7**
Surface Area(m^2/Kg):	8.22	8.22	8.22	8.22	**8.22**
Film Thickness(micron):	5.05	5.66	6.29	6.93	**5.73**

Mixture Design for 9.5mm Limestone with FAA of 44 and Gradation Plotting Above The Restricted Zone.

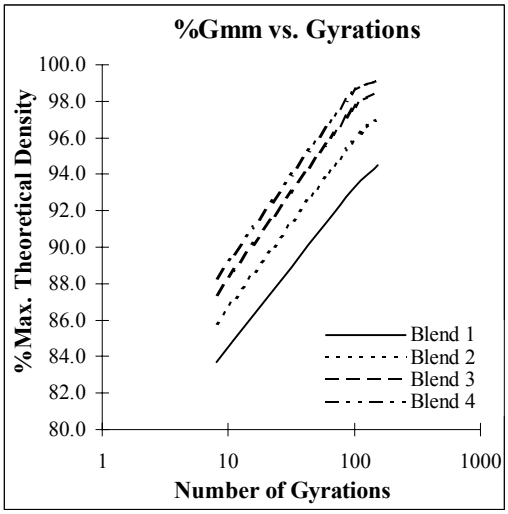

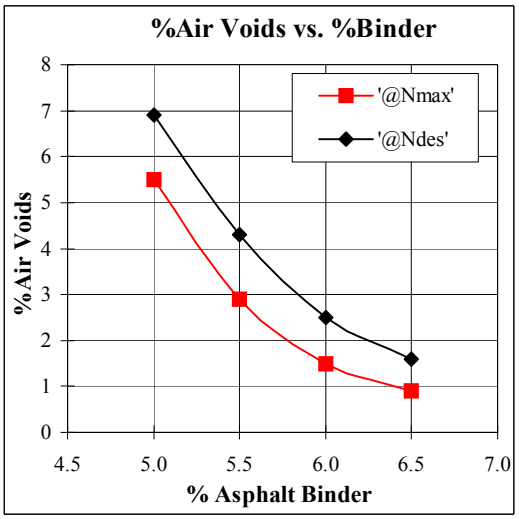

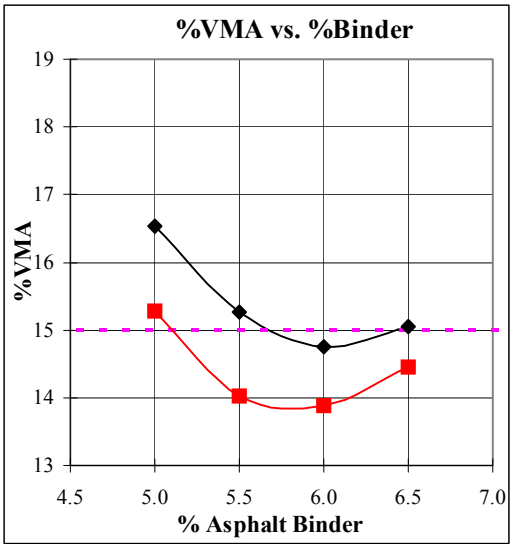

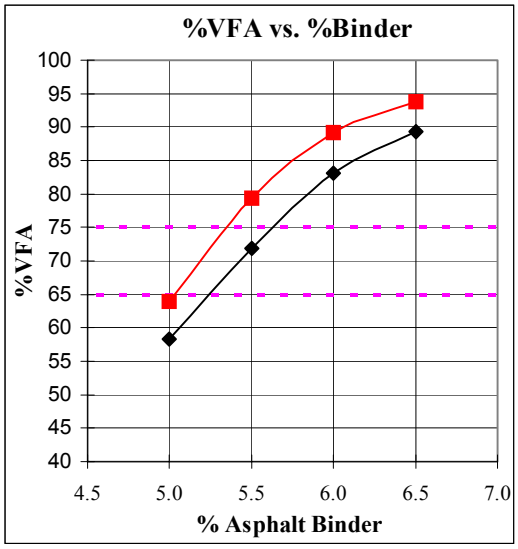

Blend	%AC	Air Voids @ NDesign	%VMA @ NDesign	%VFA @ NDesign	Air Voids @ NMax	%VMA @ Nmax	%VFA @ Nmax
Blend1	5.0	6.9	16.5	58.3	5.5	15.3	64.0
Blend2	5.5	4.3	15.3	71.8	2.9	14.0	79.3
Blend3	6.0	2.5	14.8	83.1	1.5	13.9	89.2
Blend4	6.5	1.6	15.1	89.4	0.9	14.5	93.8

Mixture Design for 9.5mm Limestone with FAA of 44 and Gradation Plotting Above The Restricted Zone.

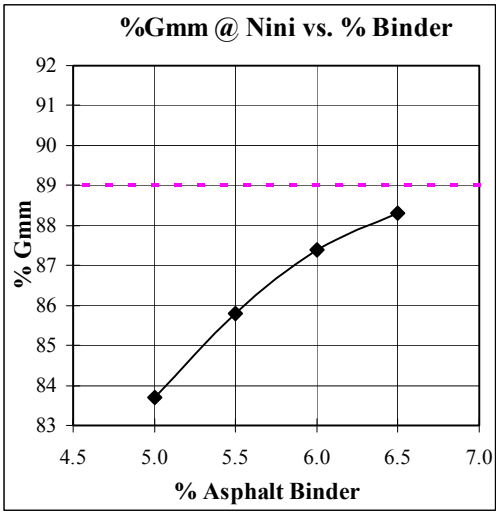

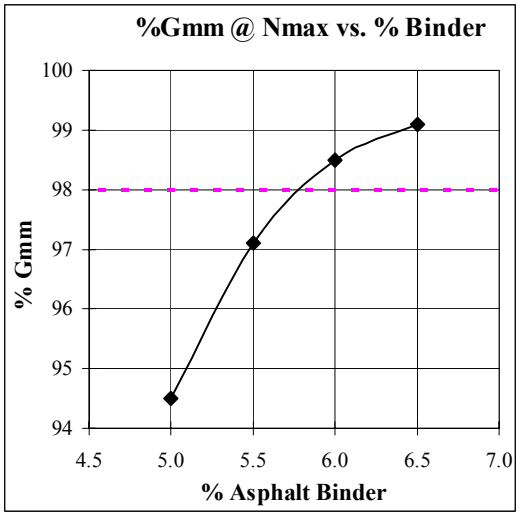

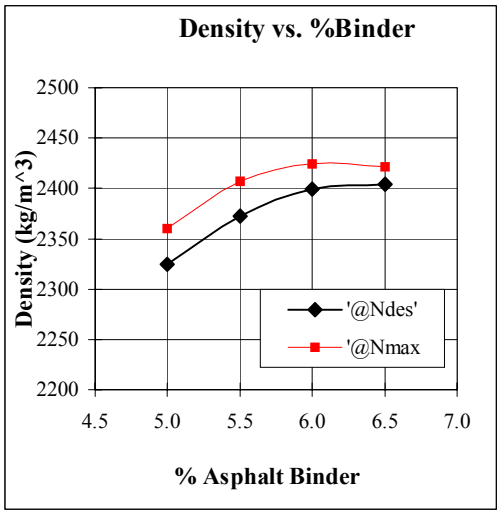

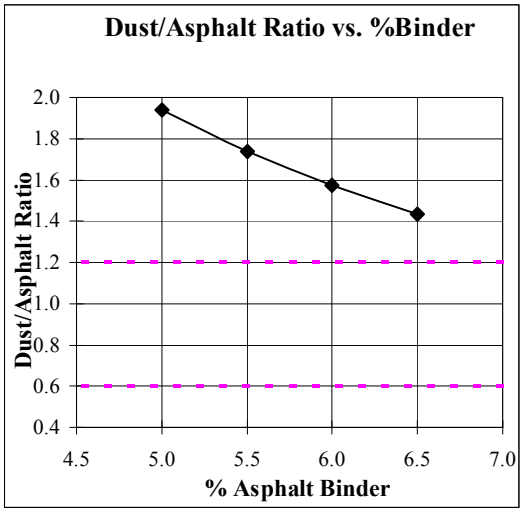

Blend	%AC	%Gmm @ Nini	%Gmm @ Nmax	Density @Ndes (kg/m3)	Density @Nmax (kg/m3)	D/A ratio
Blend1	5.0	83.7	94.5	2324.7	2359.7	1.9
Blend2	5.5	85.8	97.1	2372.4	2407.1	1.7
Blend3	6.0	87.4	98.5	2399.5	2424.1	1.6
Blend4	6.5	88.3	99.1	2403.9	2421.0	1.4

Mixture Design for 9.5mm Limestone with FAA of 44 and Gradation Plotting Through The Restricted Zone.

Project Name:	NPF	**N Initial:**	8
Workbook Name:		**N Design:**	96
Technician:	CP	**N Max:**	152
Date:		**Nom. Sieve Size:**	9.5mm
Asphalt Grade:	64-22	**Design Temperature:**	38°C
Compaction Temp:	150°C	**Design ESAL's (millions):**	3-10

Blend	%AC	%Gmm @ N = 8	%Gmm @ N = 96	%Gmm @ N = 152	%Air Voids @ NDesign	%VMA @ NDesign
Blend 1	5.0	82.1	91.8	93.2	8.2	18.1
Blend 2	5.5	83.5	93.7	95.2	6.3	17.5
Blend 3	6.0	84.3	94.9	96.5	5.1	17.6
Blend 4	6.5	85.6	96.6	98.2	3.4	17.2

	Blend 1	Blend 2	Blend 3	Blend 4	Design AC
Agg. Bulk Specific Gravity (Gsb):	2.644	2.644	2.644	2.644	**2.644**
Percent Binder by wt. of mix (Pbi):	5.0	5.5	6.0	6.5	**6.2**
Percent Aggregate (Ps):	95.0	94.5	94.0	93.5	**93.8**
Specific Gravity of Binder (Gb):	1.030	1.030	1.030	1.030	**1.030**
Fines (%Passing 0.075mm Sieve):	5.3	5.3	5.3	5.3	**5.3**
Rice Specific Gravity (Gmm):	2.484	2.463	2.443	2.423	**2.440**
Effective Specific Gravity (Gse):	2.6834	2.6800	2.6774	2.6744	**2.6827**
Effective % Binder (Pbe):	4.4	5.0	5.5	6.1	**5.6**
% Binder Absorption (Pba):	0.6	0.5	0.5	0.4	**0.6**
Dust Proportion (0.6-1.2%):	1.2	1.1	1.0	0.9	**0.9**
Surface Area(m^2/Kg):	5.96	5.96	5.96	5.96	**5.96**
Film Thickness(micron):	7.29	8.24	9.17	10.13	**9.40**

Mixture Design for 9.5mm Limestone with FAA of 44 and Gradation Plotting Through The Restricted Zone.

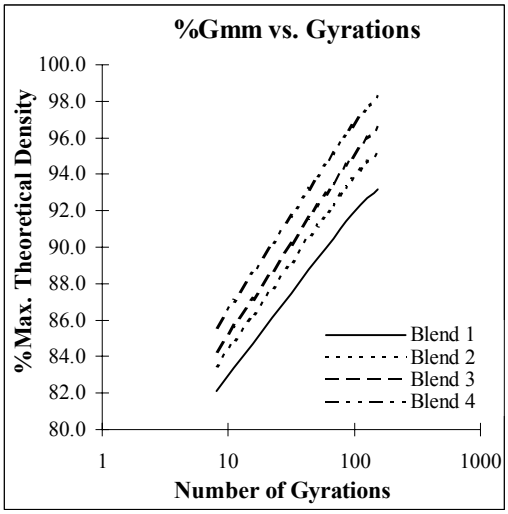

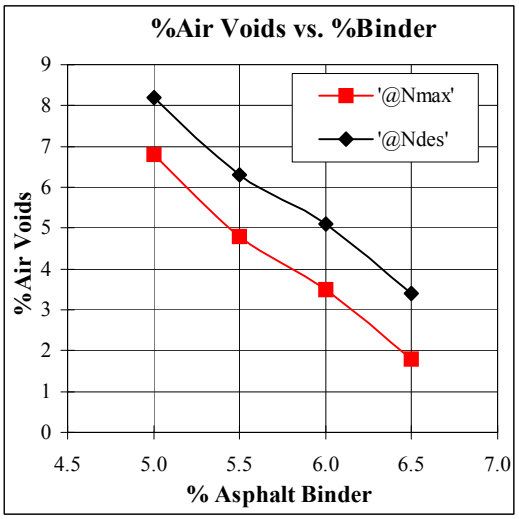

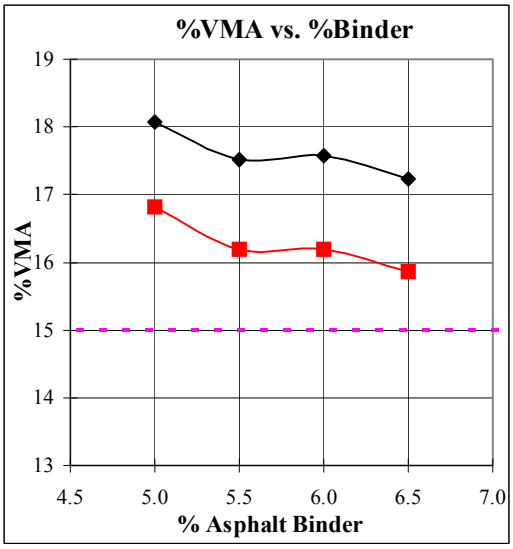

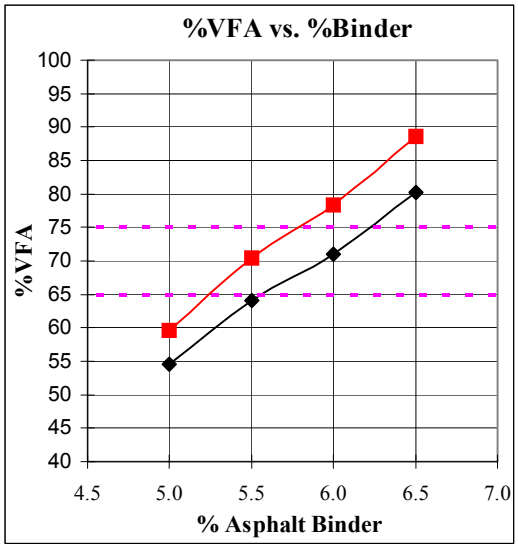

Blend	%AC	Air Voids @ NDesign	%VMA @ NDesign	%VFA @ NDesign	Air Voids @ NMax	%VMA @ Nmax	%VFA @ Nmax
Blend1	5.0	8.2	18.1	54.6	6.8	16.8	59.6
Blend2	5.5	6.3	17.5	64.0	4.8	16.2	70.4
Blend3	6.0	5.1	17.6	71.0	3.5	16.2	78.4
Blend4	6.5	3.4	17.2	80.3	1.8	15.9	88.6

Mixture Design for 9.5mm Limestone with FAA of 44 and Gradation Plotting Through The Restricted Zone.

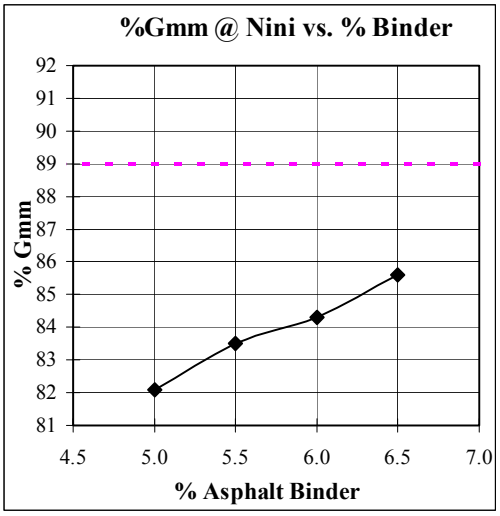

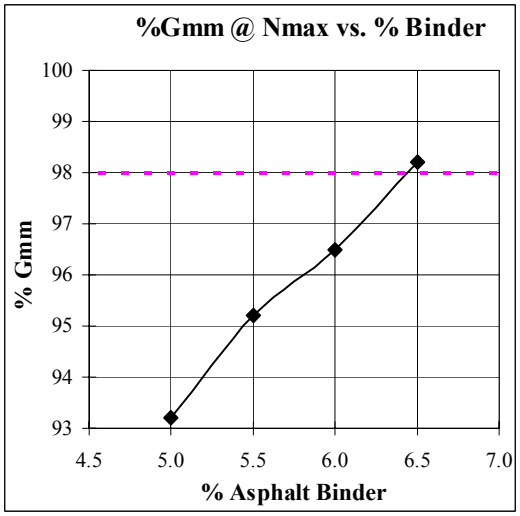

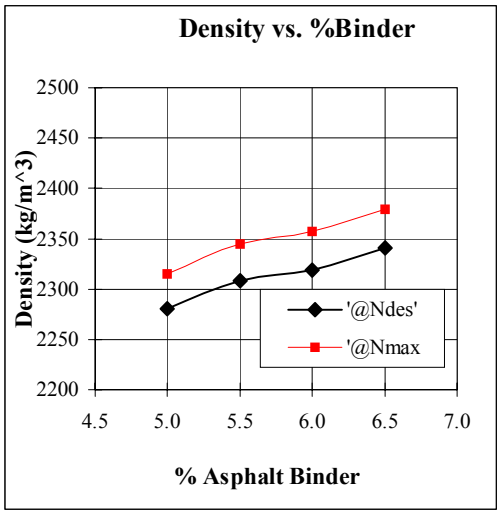

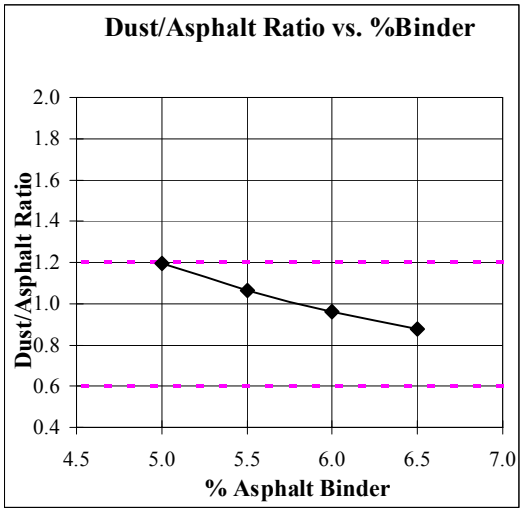

Blend	%AC	%Gmm @ Nini	%Gmm @ Nmax	Density @Ndes (kg/m3)	Density @Nmax (kg/m3)	D/A ratio
Blend1	5.0	82.1	93.2	2280.3	2315.1	1.2
Blend2	5.5	83.5	95.2	2307.8	2344.8	1.1
Blend3	6.0	84.3	96.5	2318.4	2357.5	1.0
Blend4	6.5	85.6	98.2	2340.6	2379.4	0.9

Mixture Design for 9.5mm Limestone with FAA of 44 and Gradation Plotting Below The Restricted Zone.

Project Name:	NPF	**N Initial:**	8
Workbook Name:		**N Design:**	96
Technician:	CP	**N Max:**	152
Date:		**Nom. Sieve Size:**	9.5mm
Asphalt Grade:	64-22	**Design Temperature:**	38°C
Compaction Temp:	150°C	**Design ESAL's (millions):**	3-10

Blend	%AC	%Gmm @ N = 8	%Gmm @ N = 96	%Gmm @ N = 152	%Air Voids @ NDesign	%VMA @ NDesign
Blend 1	5.0	82.7	93.2	94.8	6.8	16.7
Blend 2	5.5	82.7	93.7	95.6	6.3	17.3
Blend 3	6.0	83.6	95.2	96.9	4.8	17.1
Blend 4	6.5	85.0	96.8	98.6	3.2	16.3

	Blend 1	Blend 2	Blend 3	Blend 4	Design AC
Agg. Bulk Specific Gravity (Gsb):	2.643	2.643	2.643	2.643	**2.643**
Percent Binder by wt. of mix (Pbi):	5.0	5.5	6.0	6.5	**6.2**
Percent Aggregate (Ps):	95.0	94.5	94.0	93.5	**93.8**
Specific Gravity of Binder (Gb):	1.030	1.030	1.030	1.030	**1.030**
Fines (%Passing 0.075mm Sieve):	4.2	4.2	4.2	4.2	**4.2**
Rice Specific Gravity (Gmm):	2.486	2.467	2.447	2.443	**2.445**
Effective Specific Gravity (Gse):	2.6858	2.6850	2.6826	2.7005	**2.6892**
Effective % Binder (Pbe):	4.4	4.9	5.4	5.7	**5.5**
% Binder Absorption (Pba):	0.6	0.6	0.6	0.8	**0.7**
Dust Proportion (0.6-1.2%):	1.0	0.9	0.8	0.7	**0.8**
Surface Area(m^2/Kg):	4.7	4.7	4.7	4.7	**4.7**
Film Thickness(micron):	9.14	10.26	11.45	12.02	**11.69**

Mixture Design for 9.5mm Limestone with FAA of 44 and Gradation Plotting Below The Restricted Zone.

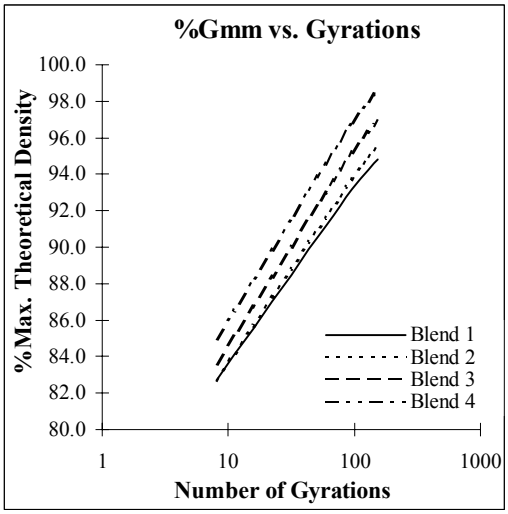

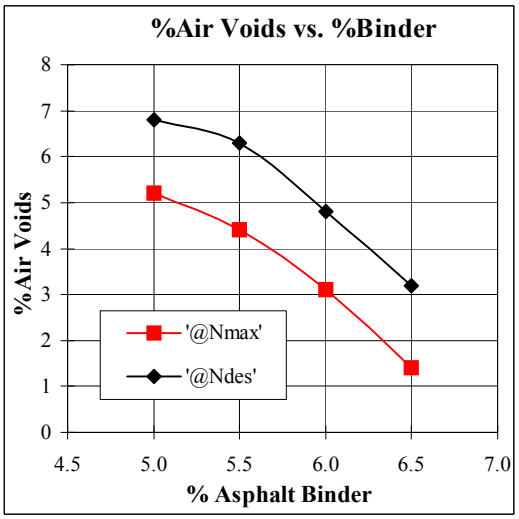

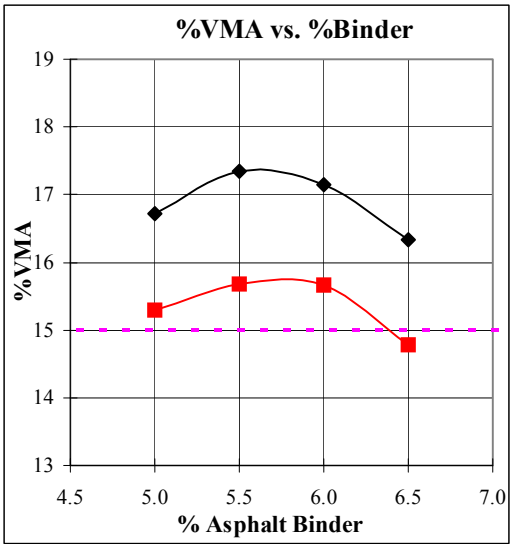

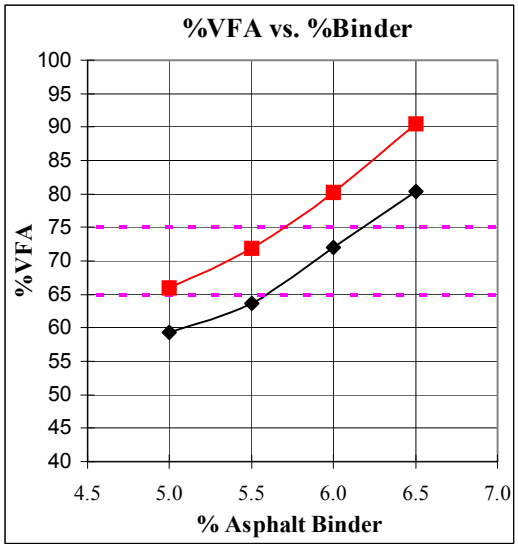

Blend	%AC	Air Voids @ NDesign	%VMA @ NDesign	%VFA @ NDesign	Air Voids @ NMax	%VMA @ Nmax	%VFA @ Nmax
Blend1	5.0	6.8	16.7	59.3	5.2	15.3	66.0
Blend2	5.5	6.3	17.3	63.7	4.4	15.7	71.9
Blend3	6.0	4.8	17.1	72.0	3.1	15.7	80.2
Blend4	6.5	3.2	16.3	80.4	1.4	14.8	90.5

Mixture Design for 9.5mm Limestone with FAA of 44 and Gradation Plotting Below The Restricted Zone.

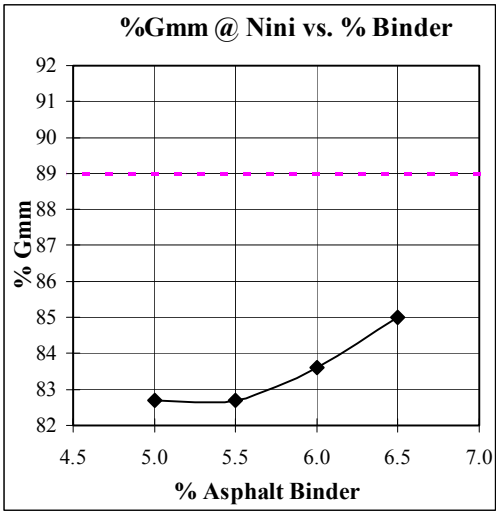

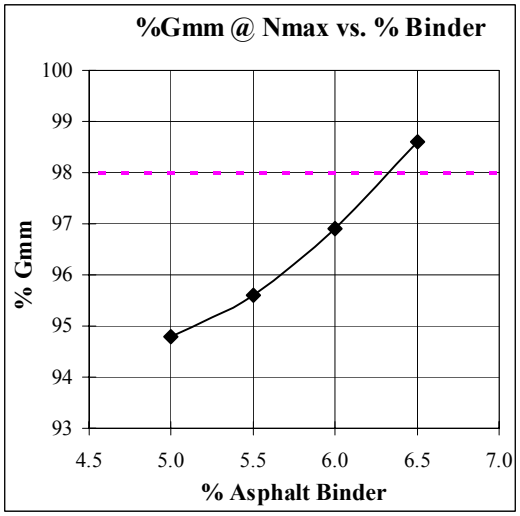

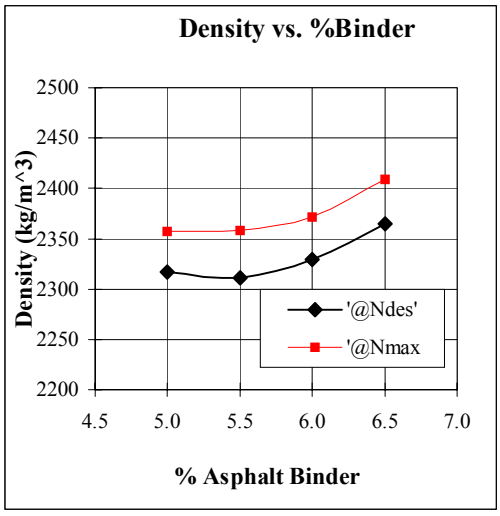

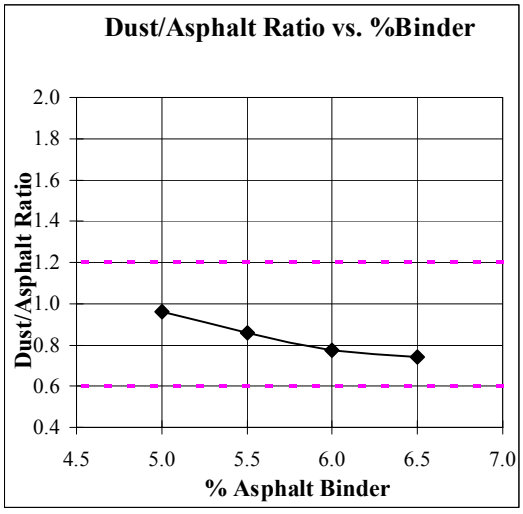

Blend	%AC	%Gmm @ Nini	%Gmm @ Nmax	Density @Ndes (kg/m3)	Density @Nmax (kg/m3)	D/A ratio
Blend1	5.0	82.7	94.8	2317.0	2356.7	1.0
Blend2	5.5	82.7	95.6	2311.6	2358.5	0.9
Blend3	6.0	83.6	96.9	2329.5	2371.1	0.8
Blend4	6.5	85.0	98.6	2364.8	2408.8	0.7

Mixture Design for 9.5mm Limestone with FAA of 50 and Gradation Plotting Through The Restricted Zone.

Project Name:	NPF	**N Initial:**	8
Workbook Name:		**N Design:**	96
Technician:	CP	**N Max:**	152
Date:		**Nom. Sieve Size:**	9.5mm
Asphalt Grade:	64-22	**Design Temperature:**	38°C
Compaction Temp:	150°C	**Design ESAL's (millions):**	3-10

Blend	%AC	%Gmm @ N = 8	%Gmm @ N = 96	%Gmm @ N = 152	%Air Voids @ NDesign	%VMA @ NDesign
Blend 1	5.5	81.5	92.5	94.1	7.5	18.2
Blend 2	6.0	83.1	94.3	96.0	5.7	17.6
Blend 3	6.5	83.9	95.4	97.0	4.6	17.6
Blend 4	7.0	85.6	96.8	97.9	3.2	17.3

	Blend 1	Blend 2	Blend 3	Blend 4	Design AC
Agg. Bulk Specific Gravity (Gsb):	2.640	2.640	2.640	2.640	**2.640**
Percent Binder by wt. of mix (Pbi):	5.5	6.0	6.5	7.0	**6.6**
Percent Aggregate (Ps):	94.5	94.0	93.5	93.0	**93.4**
Specific Gravity of Binder (Gb):	1.030	1.030	1.030	1.030	**1.030**
Fines (%Passing 0.075mm Sieve):	7.0	7.0	7.0	7.0	**7.0**
Rice Specific Gravity (Gmm):	2.469	2.454	2.440	2.426	**2.438**
Effective Specific Gravity (Gse):	2.6875	2.6915	2.6966	2.7016	**2.6987**
Effective % Binder (Pbe):	4.8	5.3	5.7	6.1	**5.8**
% Binder Absorption (Pba):	0.7	0.7	0.8	0.9	**0.8**
Dust Proportion (0.6-1.2%):	1.5	1.3	1.2	1.1	**1.2**
Surface Area(m^2/Kg):	5.85	5.85	5.85	5.85	**5.85**
Film Thickness(micron):	8.11	8.90	9.68	10.47	**9.81**

Mixture Design for 9.5mm Limestone with FAA of 50 and Gradation Plotting Through The Restricted Zone.

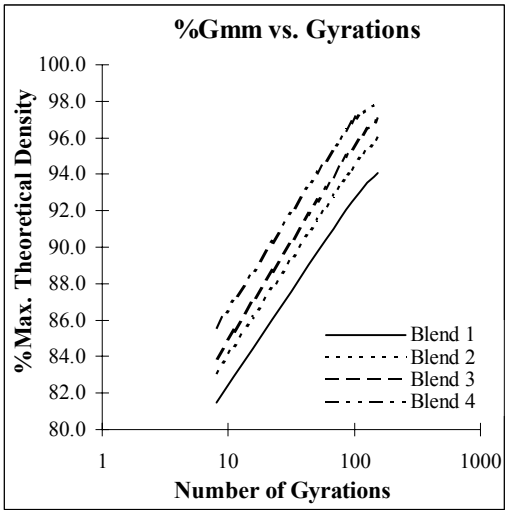

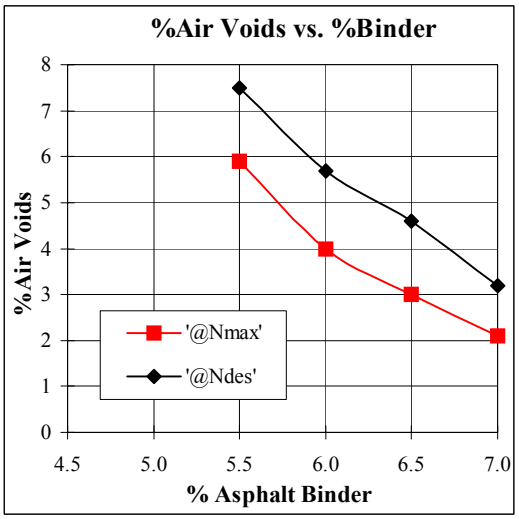

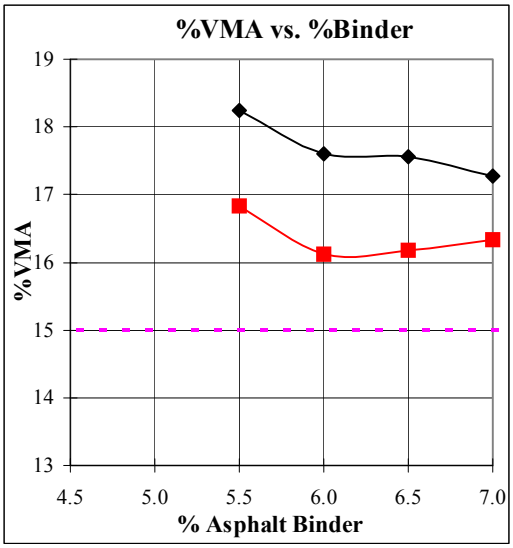

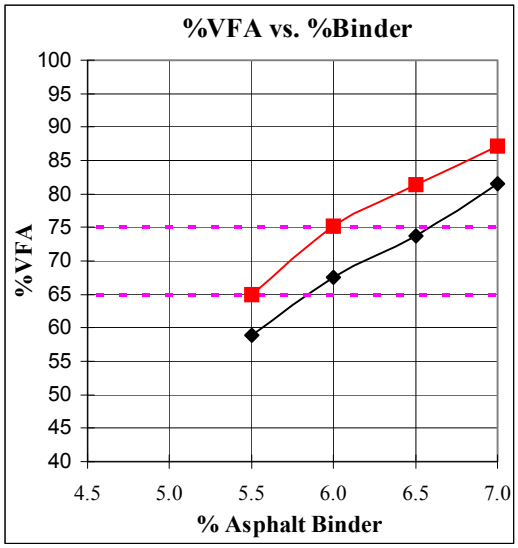

Blend	%AC	Air Voids @ NDesign	%VMA @ NDesign	%VFA @ NDesign	Air Voids @ NMax	%VMA @ Nmax	%VFA @ Nmax
Blend1	5.5	7.5	18.2	58.9	5.9	16.8	65.0
Blend2	6.0	5.7	17.6	67.6	4.0	16.1	75.2
Blend3	6.5	4.6	17.6	73.8	3.0	16.2	81.5
Blend4	7.0	3.2	17.3	81.5	2.1	16.3	87.1

Mixture Design for 9.5mm Limestone with FAA of 50 and Gradation Plotting Through The Restricted Zone.

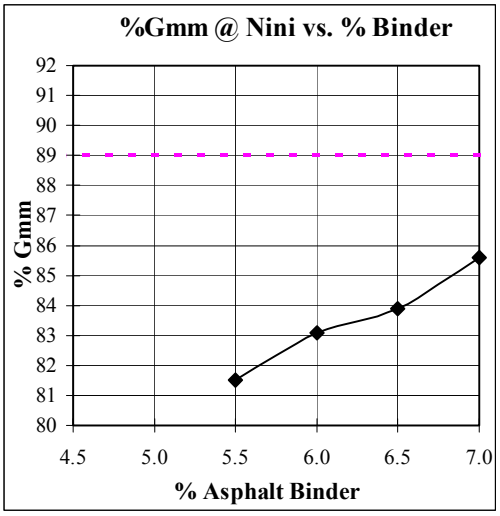

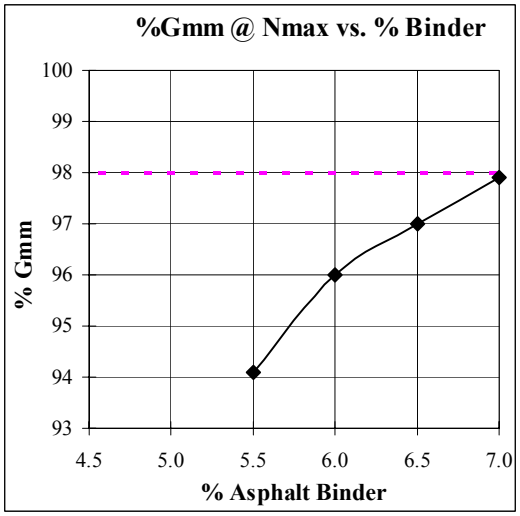

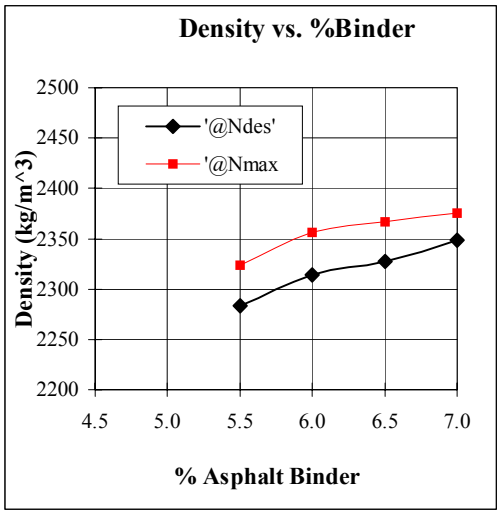

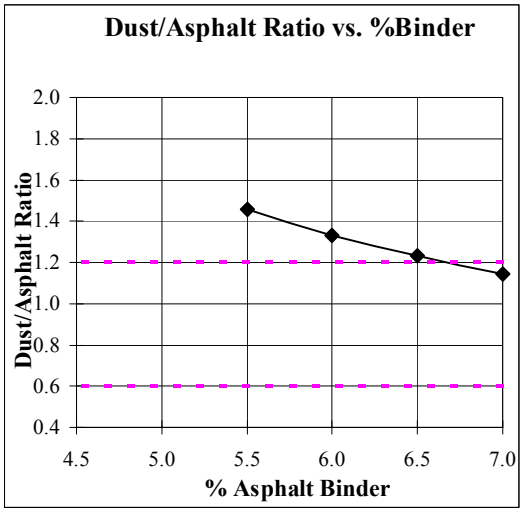

Blend	%AC	%Gmm @ Nini	%Gmm @ Nmax	Density @Ndes (kg/m3)	Density @Nmax (kg/m3)	D/A ratio
Blend1	5.5	81.5	94.1	2283.8	2323.3	1.5
Blend2	6.0	83.1	96.0	2314.1	2355.8	1.3
Blend3	6.5	83.9	97.0	2327.8	2366.8	1.2
Blend4	7.0	85.6	97.9	2348.4	2375.1	1.1

Mixture Design for 9.5mm Limestone with FAA of 50 and Gradation Plotting Below The Restricted Zone.

Project Name:	NPF	**N Initial:**	8
Workbook Name:		**N Design:**	96
Technician:	CP	**N Max:**	152
Date:		**Nom. Sieve Size:**	9.5mm
Asphalt Grade:	64-22	**Design Temperature:**	38°C
Compaction Temp:	150°C	**Design ESAL's (millions):**	3-10

Blend	%AC	%Gmm @ N = 8	%Gmm @ N = 96	%Gmm @ N = 152	%Air Voids @ NDesign	%VMA @ NDesign
Blend 1	5.5	81.7	92.6	94.3	7.4	18.2
Blend 2	6.0	83.1	94.4	96.1	5.6	17.5
Blend 3	6.5	83.1	94.5	96.3	5.5	18.3
Blend 4	7.0	86.0	96.8	98.5	3.2	17.3

	Blend 1	Blend 2	Blend 3	Blend 4	Design AC
Agg. Bulk Specific Gravity (Gsb):	2.640	2.640	2.640	2.640	**2.640**
Percent Binder by wt. of mix (Pbi):	5.5	6.0	6.5	7.0	**6.7**
Percent Aggregate (Ps):	94.5	94.0	93.5	93.0	**93.3**
Specific Gravity of Binder (Gb):	1.030	1.030	1.030	1.030	**1.030**
Fines (%Passing 0.075mm Sieve):	6.1	6.1	6.1	6.1	**6.1**
Rice Specific Gravity (Gmm):	2.469	2.453	2.440	2.426	**2.430**
Effective Specific Gravity (Gse):	2.6875	2.6902	2.6966	2.7016	**2.6928**
Effective % Binder (Pbe):	4.8	5.3	5.7	6.1	**5.9**
% Binder Absorption (Pba):	0.7	0.7	0.8	0.9	**0.8**
Dust Proportion (0.6-1.2%):	1.3	1.2	1.1	1.0	**1.0**
Surface Area(m^2/Kg):	5.9	5.9	5.9	5.9	**5.9**
Film Thickness(micron):	8.04	8.86	9.60	10.38	**10.05**

Mixture Design for 9.5mm Limestone with FAA of 50 and Gradation Plotting Below The Restricted Zone.

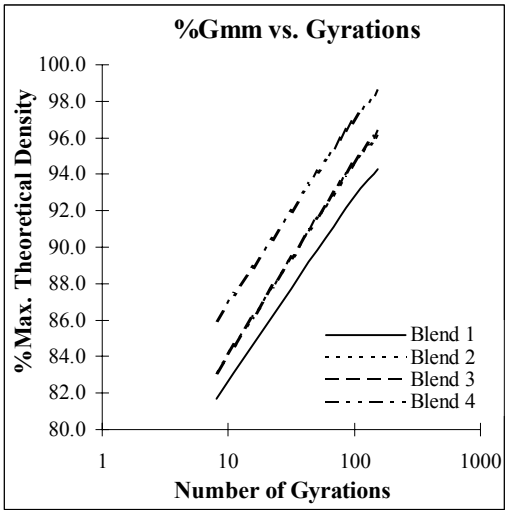

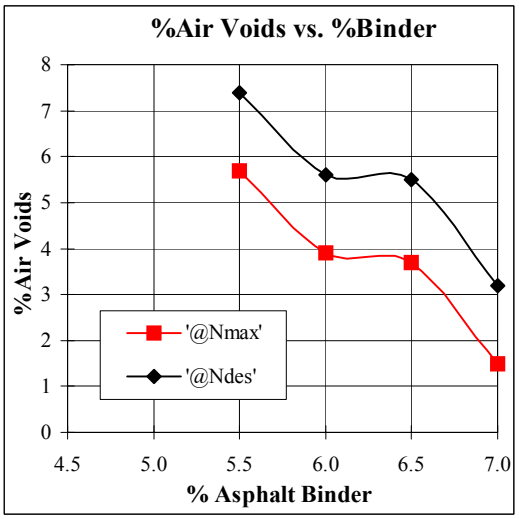

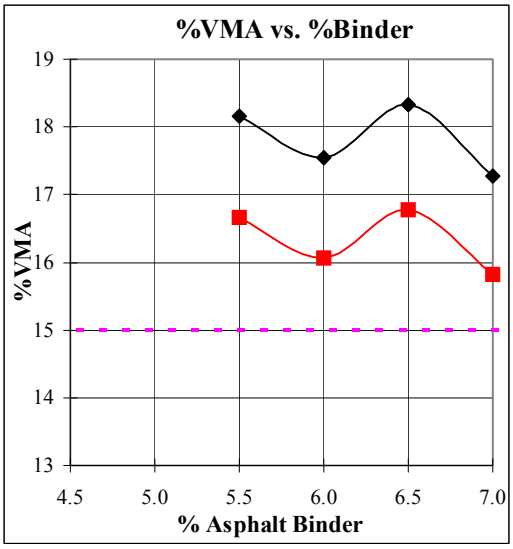

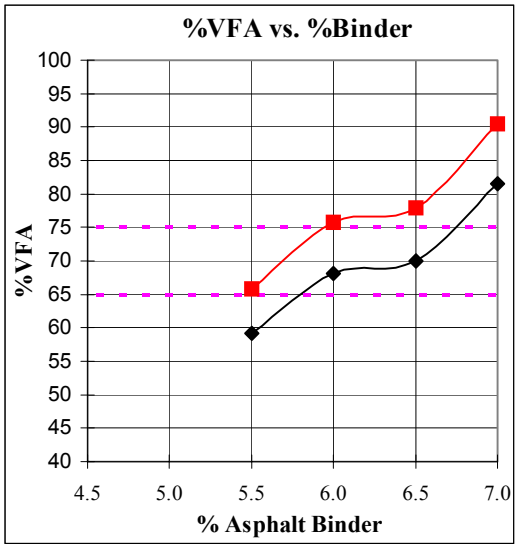

Blend	%AC	Air Voids @ NDesign	%VMA @ NDesign	%VFA @ NDesign	Air Voids @ NMax	%VMA @ Nmax	%VFA @ Nmax
Blend1	5.5	7.4	18.2	59.3	5.7	16.7	65.8
Blend2	6.0	5.6	17.5	68.1	3.9	16.1	75.7
Blend3	6.5	5.5	18.3	70.0	3.7	16.8	78.0
Blend4	7.0	3.2	17.3	81.5	1.5	15.8	90.5

Mixture Design for 9.5mm Limestone with FAA of 50 and Gradation Plotting Below The Restricted Zone.

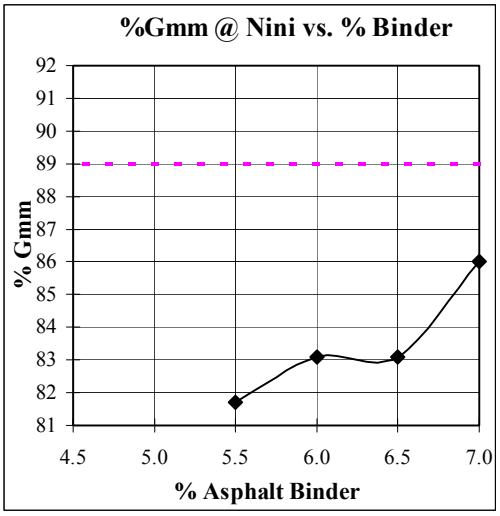

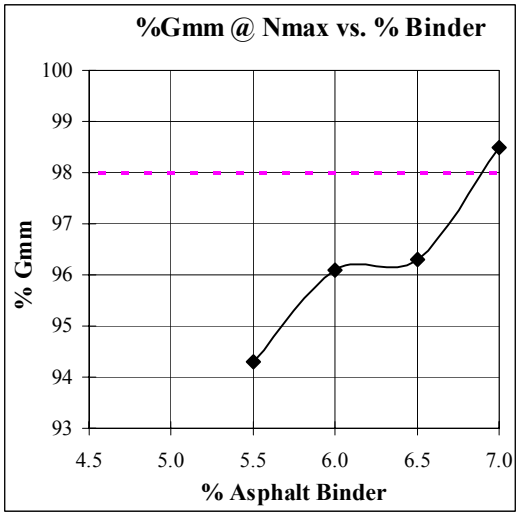

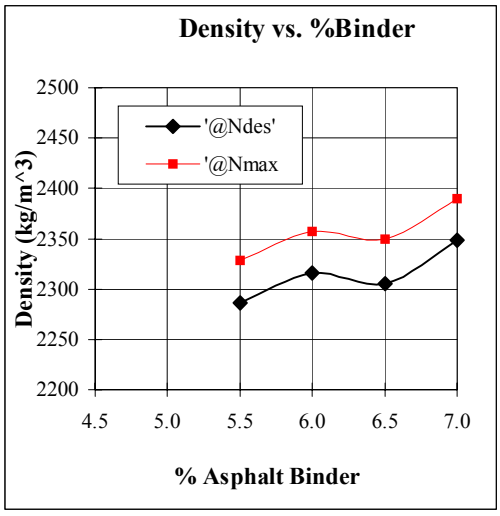

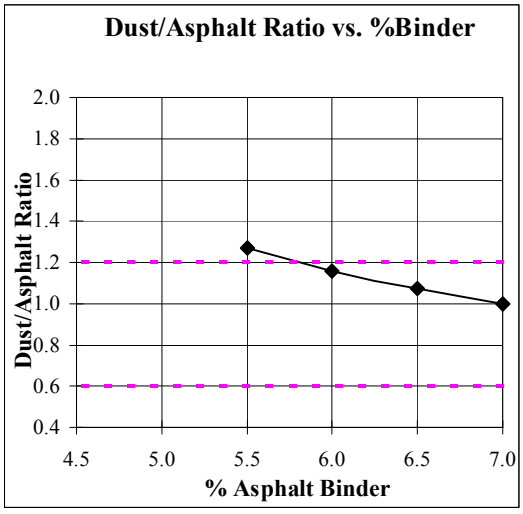

Blend	%AC	%Gmm @ Nini	%Gmm @ Nmax	Density @Ndes (kg/m3)	Density @Nmax (kg/m3)	D/A ratio
Blend1	5.5	81.7	94.3	2286.3	2328.3	1.3
Blend2	6.0	83.1	96.1	2315.6	2357.3	1.2
Blend3	6.5	83.1	96.3	2305.8	2349.7	1.1
Blend4	7.0	86.0	98.5	2348.4	2389.6	1.0

Mixture Design for 9.5mm Granite with FAA of 44 and Gradation Plotting Through The Restricted Zone

Project Name:	NPF	**N Initial:**	8
Workbook Name:		**N Design:**	96
Technician:	CP	**N Max:**	152
Date:		**Nom. Sieve Size:**	9.5mm
Asphalt Grade:	64-22	**Design Temperature:**	38°C
Compaction Temp:	150°C	**Design ESAL's (millions):**	3-10

Blend	%AC	%Gmm @ N = 8	%Gmm @ N = 96	%Gmm @ N = 152	%Air Voids @ NDesign	%VMA @ NDesign
Blend 1	4.5	84.9	93.6	94.9	6.4	15.3
Blend 2	5.0	86.5	95.2	96.5	4.8	14.8
Blend 3	5.5	87.4	96.7	97.9	3.3	14.2
Blend 4	6.0	88.4	98.1	98.7	1.9	13.9

	Blend 1	Blend 2	Blend 3	Blend 4	Design AC
Agg. Bulk Specific Gravity (Gsb):	2.647	2.647	2.647	2.647	**2.647**
Percent Binder by wt. of mix (Pbi):	4.5	5.0	5.5	6.0	**5.3**
Percent Aggregate (Ps):	95.5	95.0	94.5	94.0	**94.7**
Specific Gravity of Binder (Gb):	1.030	1.030	1.030	1.030	**1.030**
Fines (%Passing 0.075mm Sieve):	6.2	6.2	6.2	6.2	**6.2**
Rice Specific Gravity (Gmm):	2.507	2.495	2.484	2.471	**2.488**
Effective Specific Gravity (Gse):	2.6887	2.6969	2.7064	2.7133	**2.7021**
Effective % Binder (Pbe):	3.9	4.3	4.6	5.0	**4.5**
% Binder Absorption (Pba):	0.6	0.7	0.9	1.0	**0.8**
Dust Proportion (0.6-1.2%):	1.6	1.4	1.3	1.2	**1.4**
Surface Area(m^2/Kg):	6.64	6.64	6.64	6.64	**6.64**
Film Thickness(micron):	5.73	6.32	6.90	7.54	**6.68**

Mixture Design for 9.5mm Granite with FAA of 44 and Gradation Plotting Through The Restricted Zone

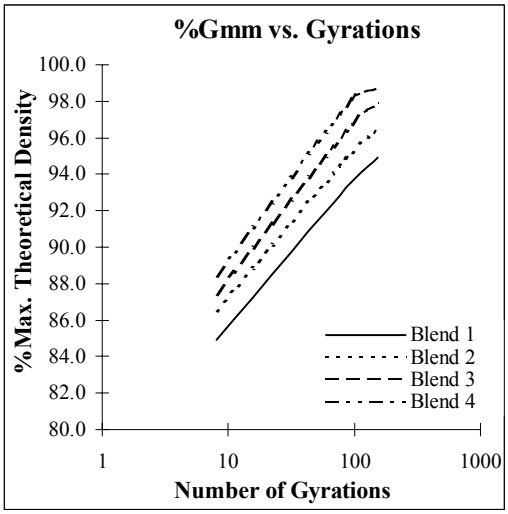

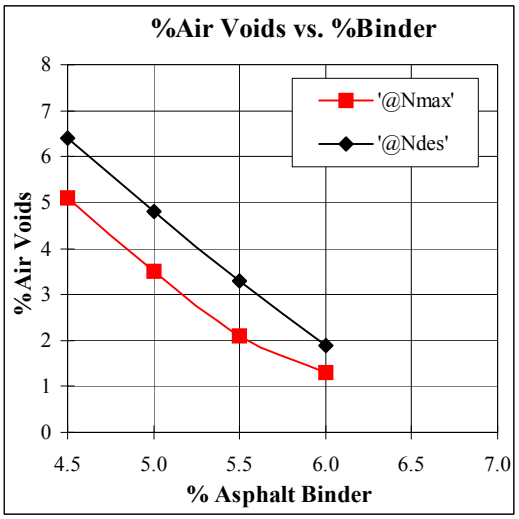

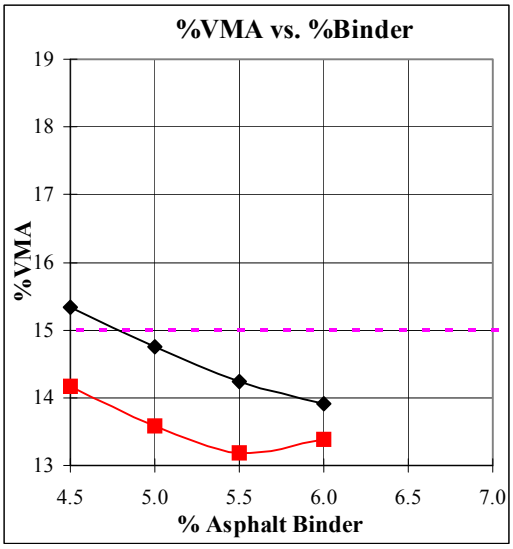

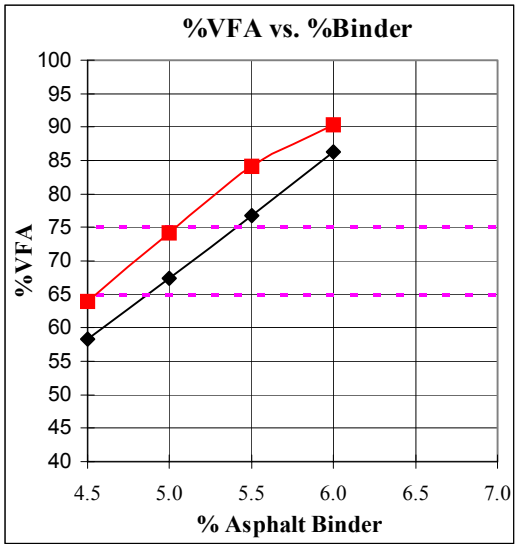

Blend	%AC	Air Voids @ NDesign	%VMA @ NDesign	%VFA @ NDesign	Air Voids @ NMax	%VMA @ Nmax	%VFA @ Nmax
Blend1	4.5	6.4	15.3	58.3	5.1	14.2	64.0
Blend2	5.0	4.8	14.8	67.5	3.5	13.6	74.2
Blend3	5.5	3.3	14.2	76.8	2.1	13.2	84.1
Blend4	6.0	1.9	13.9	86.3	1.3	13.4	90.3

Mixture Design for 9.5mm Granite with FAA of 44 and Gradation Plotting Through The Restricted Zone

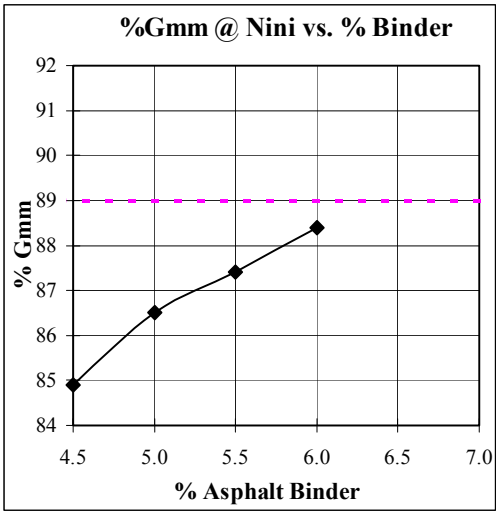

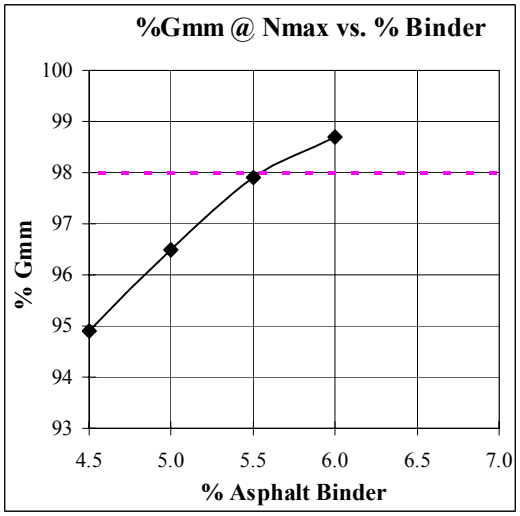

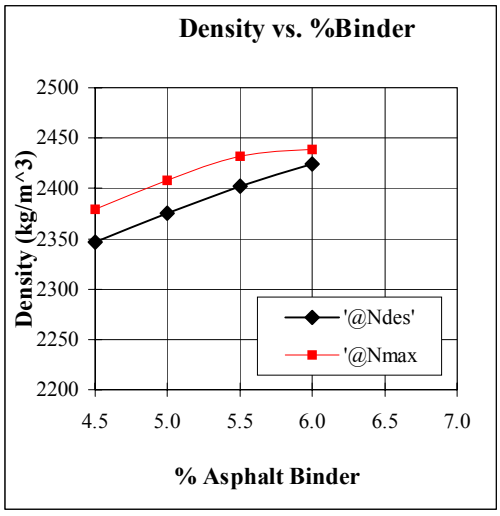

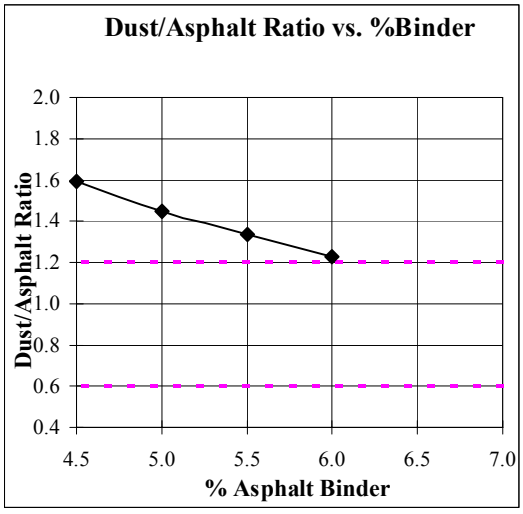

Blend	%AC	%Gmm @ Nini	%Gmm @ Nmax	Density @Ndes (kg/m3)	Density @Nmax (kg/m3)	D/A ratio
Blend1	4.5	84.9	94.9	2346.6	2379.1	1.6
Blend2	5.0	86.5	96.5	2375.2	2407.7	1.4
Blend3	5.5	87.4	97.9	2402.0	2431.8	1.3
Blend4	6.0	88.4	98.7	2424.1	2438.9	1.2

Mixture Design for 9.5mm Granite with FAA of 44 and Gradation Plotting Below The Restricted Zone

Project Name:	NPF	**N Initial:**	8
Workbook Name:		**N Design:**	96
Technician:	CP	**N Max:**	152
Date:		**Nom. Sieve Size:**	9.5mm
Asphalt Grade:	64-22	**Design Temperature:**	38°C
Compaction Temp:	150°C	**Design ESAL's (millions):**	3-10

Blend	%AC	%Gmm @ N = 8	%Gmm @ N = 96	%Gmm @ N = 152	%Air Voids @ NDesign	%VMA @ NDesign
Blend 1	5.0	86.0	95.4	96.7	4.6	14.6
Blend 2	5.5	87.0	96.8	98.0	3.2	14.3
Blend 3	6.0	87.8	98.0	98.9	2.0	13.7
Blend 4	6.5	89.1	99.2	99.6	0.8	13.7

	Blend 1	Blend 2	Blend 3	Blend 4	Design AC
Agg. Bulk Specific Gravity (Gsb):	2.647	2.647	2.647	2.647	**2.647**
Percent Binder by wt. of mix (Pbi):	5.0	5.5	6.0	6.5	**5.2**
Percent Aggregate (Ps):	95.0	94.5	94.0	93.5	**94.8**
Specific Gravity of Binder (Gb):	1.030	1.030	1.030	1.030	**1.030**
Fines (%Passing 0.075mm Sieve):	4.7	4.7	4.7	4.7	**4.7**
Rice Specific Gravity (Gmm):	2.495	2.480	2.479	2.464	**2.490**
Effective Specific Gravity (Gse):	2.6969	2.7013	2.7236	2.7280	**2.6999**
Effective % Binder (Pbe):	4.3	4.7	4.9	5.3	**4.4**
% Binder Absorption (Pba):	0.7	0.8	1.1	1.2	**0.8**
Dust Proportion (0.6-1.2%):	1.1	1.0	1.0	0.9	**1.1**
Surface Area(m^2/Kg):	5.04	5.04	5.04	5.04	**5.04**
Film Thickness(micron):	8.33	9.23	9.65	10.57	**8.66**

Mixture Design for 9.5mm Granite with FAA of 44 and Gradation Plotting Below The Restricted Zone

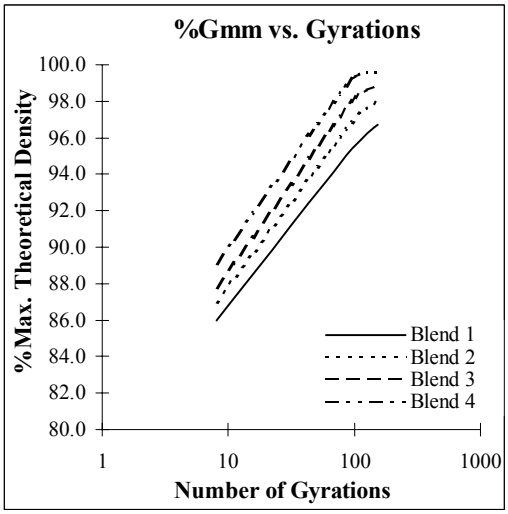

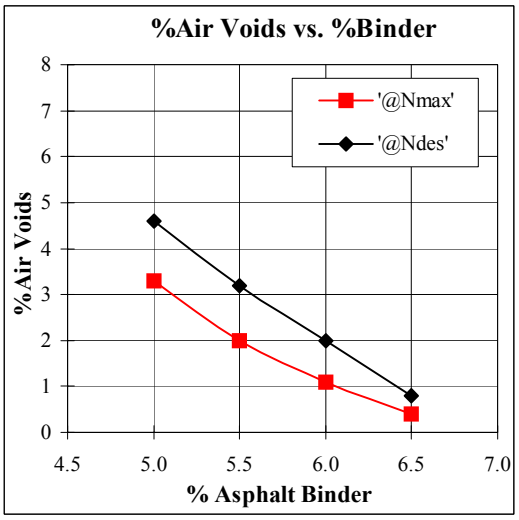

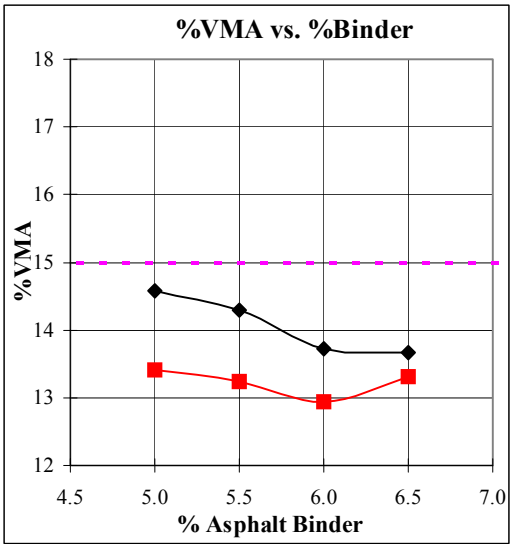

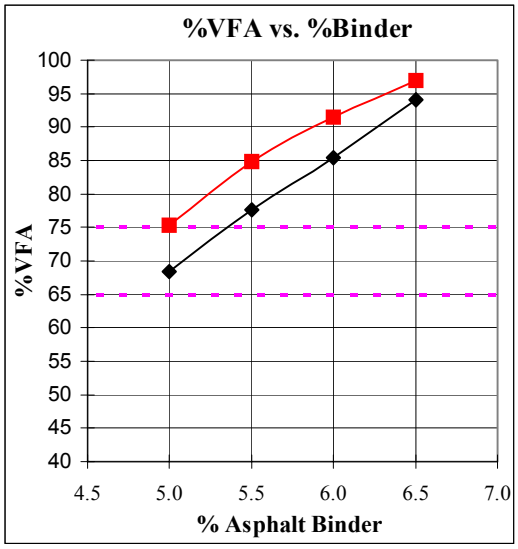

Blend	%AC	Air Voids @ NDesign	%VMA @ NDesign	%VFA @ NDesign	Air Voids @ NMax	%VMA @ Nmax	%VFA @ Nmax
Blend1	5.0	4.6	14.6	68.4	3.3	13.4	75.4
Blend2	5.5	3.2	14.3	77.6	2.0	13.2	84.9
Blend3	6.0	2.0	13.7	85.4	1.1	12.9	91.5
Blend4	6.5	0.8	13.7	94.1	0.4	13.3	97.0

Mixture Design for 9.5mm Granite with FAA of 44 and Gradation Plotting Below The Restricted Zone

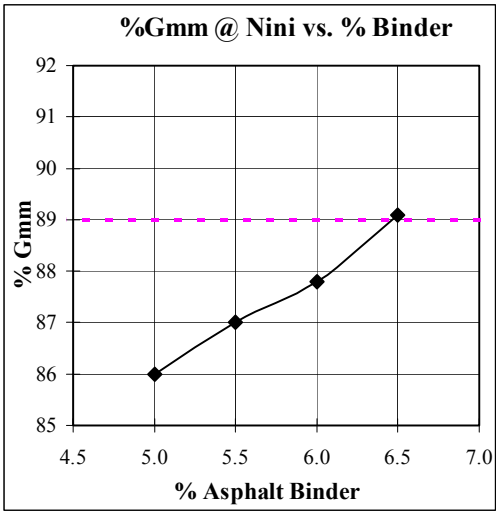

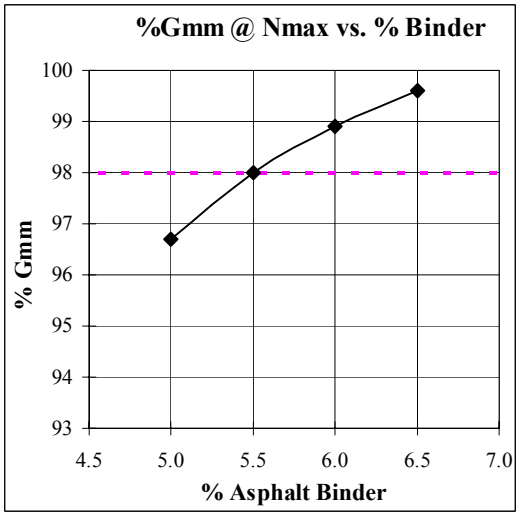

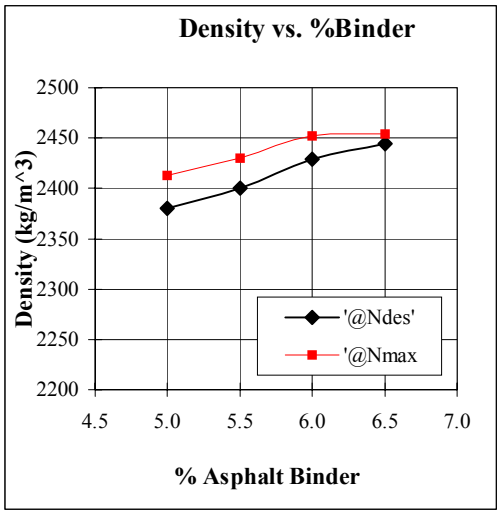

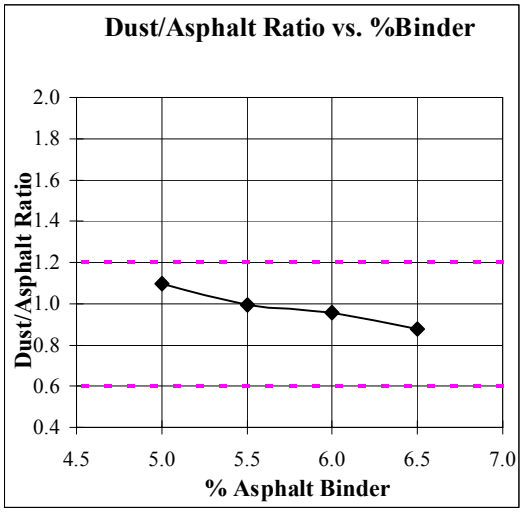

Blend	%AC	%Gmm @ Nini	%Gmm @ Nmax	Density @Ndes (kg/m3)	Density @Nmax (kg/m3)	D/A ratio
Blend1	5.0	86.0	96.7	2380.2	2412.7	1.1
Blend2	5.5	87.0	98.0	2400.6	2430.4	1.0
Blend3	6.0	87.8	98.9	2429.4	2451.7	1.0
Blend4	6.5	89.1	99.6	2444.3	2454.1	0.9

Mixture Design for 9.5mm Granite with FAA of 50 and Gradation Plotting Through The Restricted Zone

Project Name:	NPF	**N Initial:**	8
Workbook Name:		**N Design:**	96
Technician:	CP	**N Max:**	152
Date:		**Nom. Sieve Size:**	9.5mm
Asphalt Grade:	64-22	**Design Temperature:**	38°C
Compaction Temp:	150°C	**Design ESAL's (millions):**	3-10

Blend	%AC	%Gmm @ N = 8	%Gmm @ N = 96	%Gmm @ N = 152	%Air Voids @ NDesign	%VMA @ NDesign
Blend 1	5.2	84.3	94.0	95.5	6.0	16.1
Blend 2	5.7	85.2	95.5	96.9	4.5	15.7
Blend 3	6.2	86.0	96.5	97.9	3.5	16.0
Blend 4	6.7	88.0	98.3	99.0	1.7	15.5

	Blend 1	Blend 2	Blend 3	Blend 4	Design AC
Agg. Bulk Specific Gravity (Gsb):	2.642	2.642	2.642	2.642	**2.642**
Percent Binder by wt. of mix (Pbi):	5.2	5.7	6.2	6.7	**6.0**
Percent Aggregate (Ps):	94.8	94.3	93.8	93.3	**94.0**
Specific Gravity of Binder (Gb):	1.030	1.030	1.030	1.030	**1.030**
Fines (%Passing 0.075mm Sieve):	7.4	7.4	7.4	7.4	**7.4**
Rice Specific Gravity (Gmm):	2.487	2.472	2.453	2.434	**2.460**
Effective Specific Gravity (Gse):	2.6962	2.7005	2.6995	2.6981	**2.6992**
Effective % Binder (Pbe):	4.4	4.9	5.4	5.9	**5.2**
% Binder Absorption (Pba):	0.8	0.8	0.8	0.8	**0.8**
Dust Proportion (0.6-1.2%):	1.7	1.5	1.4	1.3	**1.4**
Surface Area(m^2/Kg):	6.98	6.98	6.98	6.98	**6.98**
Film Thickness(micron):	6.22	6.87	7.64	8.43	**7.35**

Mixture Design for 9.5mm Granite with FAA of 50 and Gradation Plotting Through The Restricted Zone

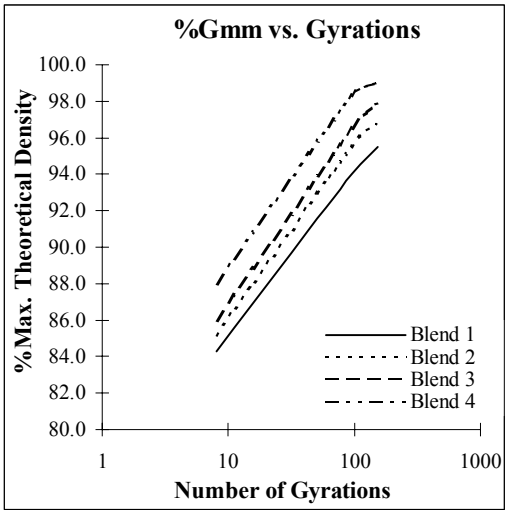

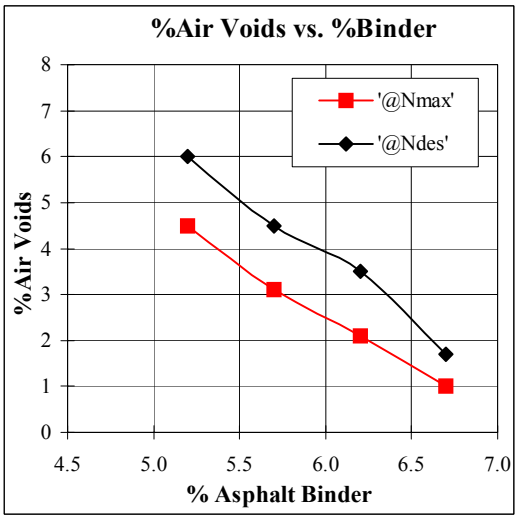

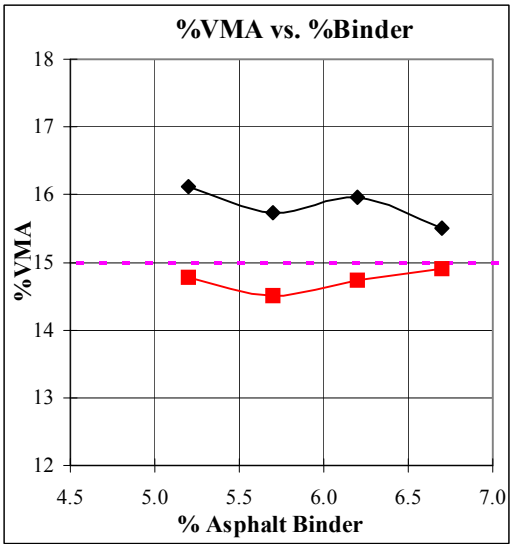

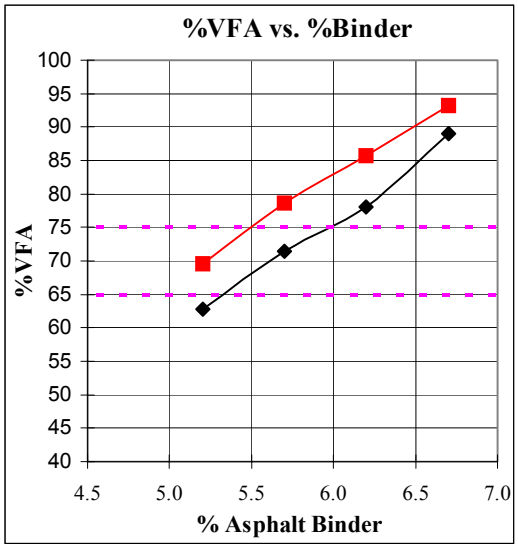

Blend	%AC	Air Voids @ NDesign	%VMA @ NDesign	%VFA @ NDesign	Air Voids @ NMax	%VMA @ Nmax	%VFA @ Nmax
Blend1	5.2	6.0	16.1	62.8	4.5	14.8	69.5
Blend2	5.7	4.5	15.7	71.4	3.1	14.5	78.6
Blend3	6.2	3.5	16.0	78.1	2.1	14.7	85.8
Blend4	6.7	1.7	15.5	89.0	1.0	14.9	93.3

Mixture Design for 9.5mm Granite with FAA of 50 and Gradation Plotting Through The Restricted Zone

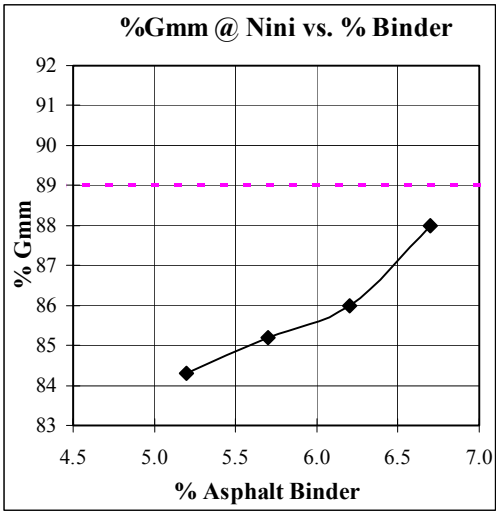

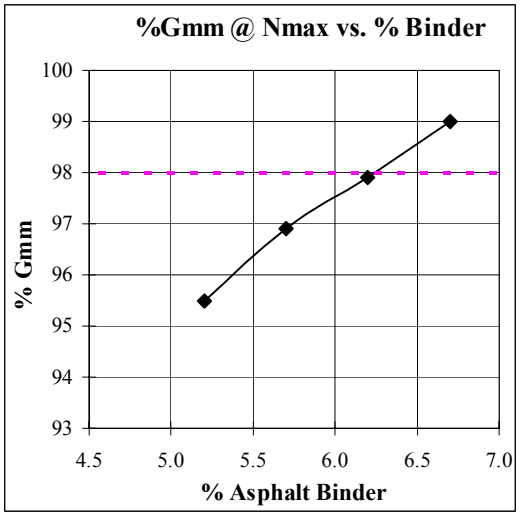

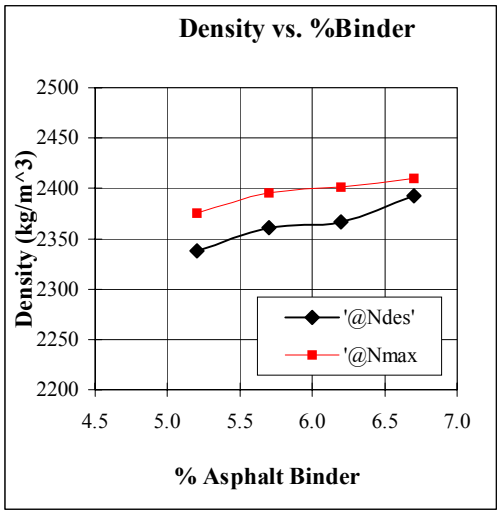

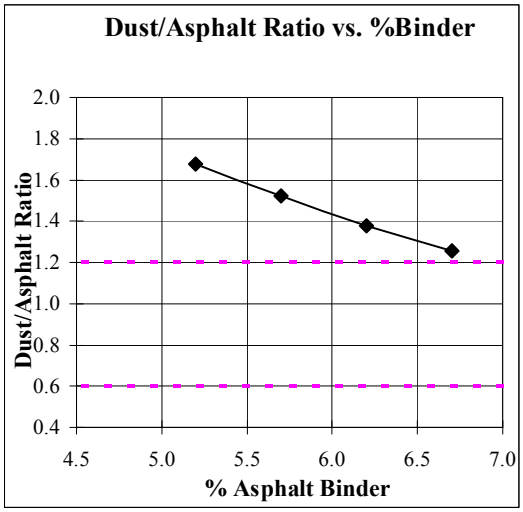

Blend	%AC	%Gmm @ Nini	%Gmm @ Nmax	Density @Ndes (kg/m3)	Density @Nmax (kg/m3)	D/A ratio
Blend1	5.2	84.3	95.5	2337.8	2375.1	1.7
Blend2	5.7	85.2	96.9	2360.8	2395.4	1.5
Blend3	6.2	86.0	97.9	2367.1	2401.5	1.4
Blend4	6.7	88.0	99.0	2392.6	2409.7	1.3

Mixture Design for 9.5mm Granite with FAA of 50 and Gradation Plotting Below The Restricted Zone

Project Name:	NPF	**N Initial:**	8
Workbook Name:		**N Design:**	96
Technician:	CP	**N Max:**	152
Date:		**Nom. Sieve Size:**	9.5mm
Asphalt Grade:	64-22	**Design Temperature:**	38°C
Compaction Temp:	150°C	**Design ESAL's (millions):**	3-10

Blend	%AC	%Gmm @ N = 8	%Gmm @ N = 96	%Gmm @ N = 152	%Air Voids @ NDesign	%VMA @ NDesign
Blend 1	5.5	85.6	95.6	97.2	4.4	15.2
Blend 2	6.0	87.0	97.3	98.4	2.7	14.8
Blend 3	6.5	87.2	97.9	99.0	2.1	15.4
Blend 4	7.0	87.2	98.1	99.2	1.9	16.4

	Blend 1	Blend 2	Blend 3	Blend 4	Design AC
Agg. Bulk Specific Gravity (Gsb):	2.643	2.643	2.643	2.643	**2.643**
Percent Binder by wt. of mix (Pbi):	5.5	6.0	6.5	7.0	**5.2**
Percent Aggregate (Ps):	94.5	94.0	93.5	93.0	**94.8**
Specific Gravity of Binder (Gb):	1.030	1.030	1.030	1.030	**1.030**
Fines (%Passing 0.075mm Sieve):	6.1	6.1	6.1	6.1	**6.1**
Rice Specific Gravity (Gmm):	2.480	2.461	2.442	2.423	**2.472**
Effective Specific Gravity (Gse):	2.7013	2.7005	2.6992	2.6976	**2.6776**
Effective % Binder (Pbe):	4.7	5.2	5.7	6.2	**4.7**
% Binder Absorption (Pba):	0.8	0.8	0.8	0.8	**0.5**
Dust Proportion (0.6-1.2%):	1.3	1.2	1.1	1.0	**1.3**
Surface Area(m^2/Kg):	5.88	5.88	5.88	5.88	**5.88**
Film Thickness(micron):	7.81	8.72	9.64	10.59	**7.85**

Mixture Design for 9.5mm Granite with FAA of 50 and Gradation Plotting Below The Restricted Zone

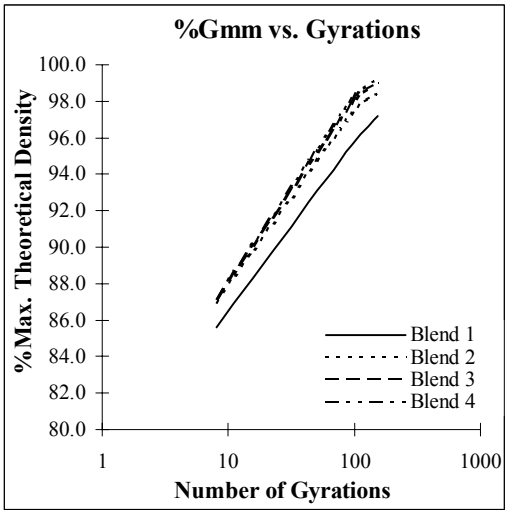

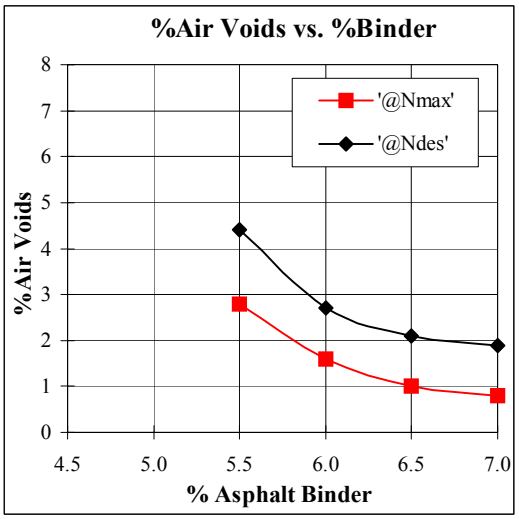

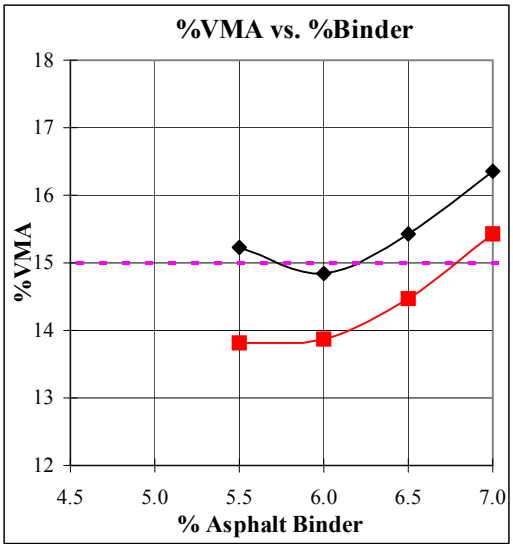

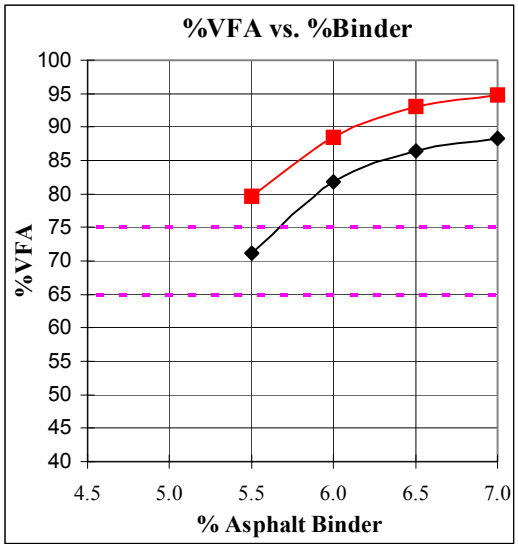

Blend	%AC	Air Voids @ NDesign	%VMA @ NDesign	%VFA @ NDesign	Air Voids @ NMax	%VMA @ Nmax	%VFA @ Nmax
Blend1	5.5	4.4	15.2	71.1	2.8	13.8	79.7
Blend2	6.0	2.7	14.8	81.8	1.6	13.9	88.5
Blend3	6.5	2.1	15.4	86.4	1.0	14.5	93.1
Blend4	7.0	1.9	16.4	88.4	0.8	15.4	94.8

Mixture Design for 9.5mm Granite with FAA of 50 and Gradation Plotting Below The Restricted Zone

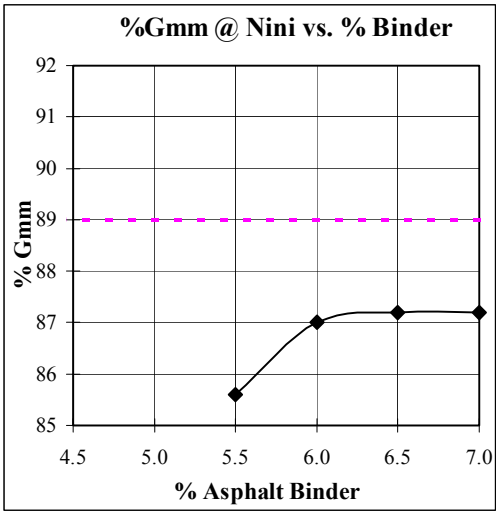

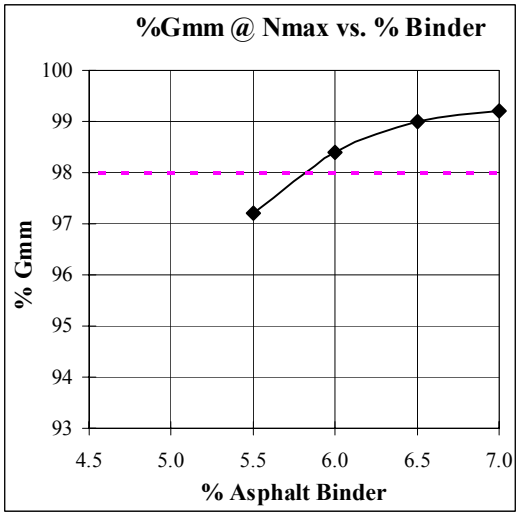

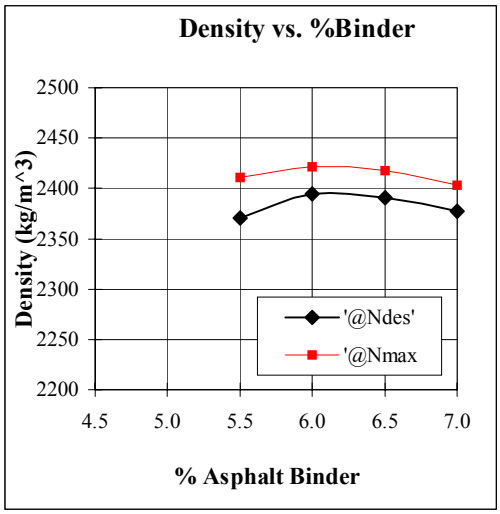

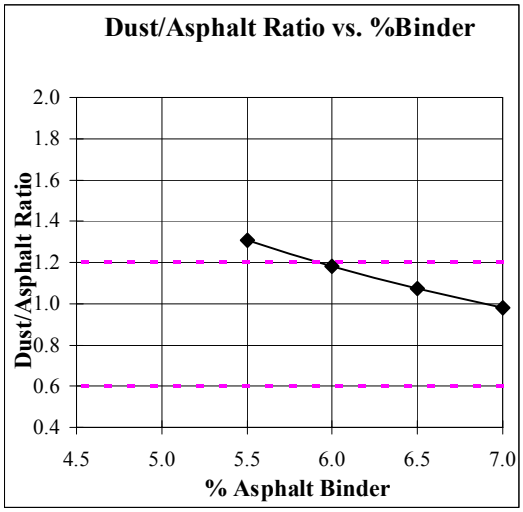

Blend	%AC	%Gmm @ Nini	%Gmm @ Nmax	Density @Ndes (kg/m3)	Density @Nmax (kg/m3)	D/A ratio
Blend1	5.5	85.6	97.2	2370.9	2410.6	1.3
Blend2	6.0	87.0	98.4	2394.6	2421.6	1.2
Blend3	6.5	87.2	99.0	2390.7	2417.6	1.1
Blend4	7.0	87.2	99.2	2377.0	2403.6	1.0

APPENDIX B Statistical Analysis (paired t-test results) on Effects of Experimental Variables on Volumetric Mixture Properties

Terminology

The following abbreviations are used to identify the aggregate characteristics associated with the individual mixtures listed in the first column of the tables in this appendix:

- 19 or 9.5 refer to nominal maximum size.
- LS or GR refer to coarse aggregate type, i.e. limestone or granite, respectively.
- 39, 44, or 50 refer to fine aggregate angularity, i.e. FAA of 39, FAA of 44, or FAA or 50, respectively.
- A, T, or B refer to gradation plotting above, through, or below the restricted zone, respectively.

For example the first entry in the first column of Table B.1, "LS44A" indicates the mixture which incorporates limestone coarse aggregate blended with the fine aggregate with a FAA of 44 (limestone sand) and a gradation that plots above the restricted zone.

Table B. 1 Test of Nominal Size Effect on Design AC

Mixture	19	9.5	Δ	Calculation
LS44A	4.6	5.6	-1.0	$\alpha = 0.05$
LS44T	5.4	6.2	-0.8	H_0 : AC 19 = AC 9.5
LS44B	4.6	6.2	-1.6	H_1 : AC 19 < AC 9.5
LS50T	5.9	6.6	-0.7	$\Delta_{average} = -0.9$
LS50B	5.5	6.7	-1.2	$\Delta_{std.dev.} = 0.328$
GR44T	4.8	5.3	-0.5	$t_0 = -8.235$, $t_\alpha = -2.306$, p = 3.54e-5
GR44B	4.4	5.2	-0.8	Conclusion:
GR50T	5.3	6.0	-0.7	**AC 19 < AC 9.5**
GR50B	4.8	5.6	-0.8	

Table B. 2 Test of Coarse Aggregate Type Effect on Design AC

Mixture	LS	GR	Δ	Calculation
9.5-44T	6.2	5.3	0.9	$\alpha = 0.05$
9.5-44B	6.2	5.2	1.0	H_0 : AC LS = AC GR
9.5-50T	6.6	6.0	0.6	H_1 : AC LS > AC GR
9.5-50B	6.7	5.6	1.1	$\Delta_{average} = 0.71$
19-44T	5.4	4.8	0.6	$\Delta_{std.dev.} = 0.285$
19-44B	4.6	4.4	0.2	$t_0 = 7.070$, $t_\alpha = 2.365$ p = 0.0002
19-50T	5.9	5.3	0.6	Conclusion:
19-50B	5.5	4.8	0.7	**AC LS > AC GR**

Table B. 3 Test of Fine Aggregate Angularity Effect on Design AC

Mixture	44	50	Δ	Calculation
9.5LS-T	6.2	6.6	-0.4	$\alpha = 0.05$
9.5LS-B	6.2	6.7	-0.5	H_0 : AC 44 = AC 50
9.5GR-T	5.3	6.0	-0.7	H_1 : AC 44 < AC 50
9.5GR-B	5.2	5.6	-0.4	$\Delta_{average} = -0.62$
19LS-A	4.6	5.9	-1.3	$\Delta_{std.dev.} = 0.303$
19LS-T	5.4	5.9	-0.5	$t_0 = -6.156$, $t_\alpha = -2.306$, p = 0.0003
19LS-B	4.6	5.5	-0.9	Conclusion:
19GR-T	4.8	5.3	-0.5	**AC 44 < AC 50**
19GR-B	4.4	4.8	-0.4	

Table B. 4 Test of Gradation Plotting Above And Through Restricted Zone Effect on Design AC

Mixture	Above	Through	Δ	Calculation
9.5LS44	5.6	6.2	-0.6	H_0 : AC Above = AC Through
19LS44	4.6	5.4	-0.8	H_1 : AC Above < AC Through
19LS50	5.9	5.9	0.0	$\Delta_{average} = -0.47$, $\Delta_{std.dev.} = 0.416$, $\alpha = 0.05$
				$t_0 = -1.941$, $t_\alpha = -4.303$, p = 0.1917
				Conclusion: **AC Above = AC Through**

Table B. 5 Test of Gradation Plotting Above and Below Restricted Zone Effect on Design AC

Mixture	Above	Below	Δ	Calculation
9.5LS44	5.6	6.2	-0.6	H_0 : AC Above = AC Below
19LS39	4.7	5.5	-0.8	H_1 : AC Above > AC Below
19LS44	4.6	4.6	0.0	$\Delta_{average}$ = -0.25, $\Delta_{std.dev.}$ = 0.551, α = 0.05
19LS50	5.9	5.5	0.4	t_0 = -0.908, t_α = -3.182, p = 0.4309
				Conclusion: **AC Above = AC Below**

Table B. 6 Test of Gradation Plotting Through And Below Restricted Zone Effect on Design AC

Mixture	Through	Below	Δ	Calculation
9.5LS44	6.2	6.2	0.0	α = 0.05
9.5GR44	5.3	5.2	0.1	H_0 : AC Through = AC Below
9.5LS50	6.6	6.7	-0.1	H_1 : AC Through > AC Below
9.5GR50	6.0	5.6	0.4	$\Delta_{average}$ = 0.31
19LS44	5.4	4.6	0.8	$\Delta_{std.dev.}$ = 0.295
19LS50	5.9	5.5	0.4	t_0 = 2.997, t_α = 2.365, p = 0.0200
19GR44	4.8	4.4	0.4	Conclusion:
19GR50	5.3	4.8	0.5	**AC Through > AC Below**

Table B. 7 Test of Nominal Size Effect on VMA

Mixture	19	9.5	Δ	Calculation
LS44A	12.9	15.1	-2.2	α = 0.05
LS44T	14.8	16.9	-2.1	H_0 : VMA 19 = VMA 9.5
LS44B	13.1	16.7	-3.6	H_1 : VMA 19 < VMA 9.5
LS50T	15.7	17.2	-1.5	$\Delta_{average}$ = -1.644
LS50B	15.0	17.6	-2.6	$\Delta_{std.dev.}$ = 1.108
GR44T	13.6	14.5	-0.9	t_0 = -4.452, t_α = -2.306, p = 0.0021
GR44B	13.0	14.4	-1.4	Conclusion:
GR50T	15.9	16.0	-0.1	**VMA 19 < VMA 9.5**
GR50B	14.8	15.2	-0.4	

Table B. 8 Test of Coarse Aggregate Type Effect on VMA

Mixture	LS	GR	Δ	Calculation
9.5-44T	16.9	14.5	2.4	$\alpha = 0.05$
9.5-44B	16.7	14.4	2.3	H_0 : VMA LS = VMA GR
9.5-50T	17.2	16.0	1.2	H_1 : VMA LS > VMA GR
9.5-50B	17.6	15.2	2.4	$\Delta_{average} = 1.2$
19-44T	14.8	13.6	1.2	$\Delta_{std.dev.} = 1.086$
19-44B	13.1	13.0	0.1	$t_0 = 3.125$, $t_\alpha = 2.365$, $p = 0.0167$
19-50T	15.7	15.9	-0.2	Conclusion:
19-50B	15.0	14.8	0.2	**VMA LS > VMA GR**

Table B. 9 Test of Fine Aggregate Angularity Effect on VMA

Mixture	44	50	Δ	Calculation
9.5LS-T	16.9	17.2	-0.3	$\alpha = 0.05$
9.5LS-B	16.7	17.6	-0.9	H_0 : VMA 44 = VMA 50
9.5GR-T	14.5	16.0	-1.5	H_1 : VMA 44 < VMA 50
9.5GR-B	14.4	15.2	-0.8	$\Delta_{average} = -0.62$
19LS-A	12.9	15.8	-2.9	$\Delta_{std.dev.} = 0.303$
19LS-T	14.8	15.7	-0.9	$t_0 = -6.156$, $t_\alpha = -2.306$, $p = 0.0007$
19LS-B	13.1	15.0	-1.9	Conclusion:
19GR-T	13.6	15.9	-2.3	**VMA 44 < VMA 50**
19GR-B	13.0	14.8	-1.8	

Table B. 10 Test of Gradation Plotting Above And Through Restricted Zone Effect on VMA

Mixture	Above	Through	Δ	Calculation
9.5LS44	15.1	16.9	-1.8	H_0 : VMA Above = VMA Through
19LS44	12.9	14.8	-1.9	H_1 : VMA Above < VMA Through
19LS50	15.8	15.7	0.1	$\Delta_{average} = -1.20$, $\Delta_{std.dev.} = 1.127$, $\alpha = 0.05$
				$t_0 = -1.844$, $t_\alpha = -4.303$, $p = 0.2064$
				Conclusion: **VMA Above = VMA Through**

Table B. 11 Test of Gradation Plotting Above and Below Restricted Zone Effect on VMA

Mixture	Above	Below	Δ	Calculation
9.5LS44	15.1	16.7	-1.6	H_0 : VMA Above = VMA Below
19LS39	13.3	15.7	-2.4	H_1 : VMA Above > VMA Below
19LS44	12.9	13.1	-0.2	$\Delta_{average}$ = -0.85, $\Delta_{std.dev.}$ = 1.427, α = 0.05
19LS50	15.8	15.0	0.8	t_0 = -1.191, t_α = -3.182, p = 0.3192
				Conclusion: **VMA Above = VMA Below**

Table B. 12 Test of Gradation Plotting Through And Below Restricted Zone Effect on VMA

Mixture	Through	Below	Δ	Calculation
9.5LS44	16.9	16.7	0.2	α = 0.05
9.5GR44	14.5	14.4	0.1	H_0 : VMA Through = VMA Below
9.5LS50	17.2	17.6	-0.4	H_1 : VMA Through > VMA Below
9.5GR50	16.0	15.2	0.8	$\Delta_{average}$ = 0.60
19LS44	14.8	13.1	1.7	$\Delta_{std.dev.}$ = 0.646
19LS50	15.7	15.0	0.7	t_0 = 2.628, t_α = 2.365, p = 0.0340
19GR44	13.6	13.0	0.6	Conclusion:
19GR50	15.9	14.8	1.1	**VMA Through > VMA Below**

Table B. 13 Test of Nominal Size Effect on VFA

Mixture	19	9.5	Δ	Calculation
LS44A	69.0	73.6	-4.6	α = 0.05
LS44T	72.9	76.3	-3.4	H_0 : VFA 19 = VFA 9.5
LS44B	69.5	76.0	-6.5	H_1 : VFA 19 < VFA 9.5
LS50T	74.6	76.7	-2.1	$\Delta_{average}$ = -2.89
LS50B	73.6	77.2	-3.6	$\Delta_{std.dev.}$ = 1.946
GR44T	70.5	72.5	-2.0	t_0 = -4.454, t_α = -2.306, p = 0.0021
GR44B	69.3	72.2	-2.9	Conclusion:
GR50T	74.9	75.0	-0.1	**VFA 19 < VFA 9.5**
GR50B	73.0	73.8	-0.8	

Table B. 14 Test of Coarse Aggregate Type Effect on VFA

Mixture	LS	GR	Δ	Calculation
9.5-44T	76.3	72.5	3.8	$\alpha = 0.05$
9.5-44B	76.0	72.2	3.8	H_0 : VFA LS = VFA GR
9.5-50T	76.7	75.0	1.7	H_1 : VFA LS > VFA GR
9.5-50B	77.2	73.8	3.4	$\Delta_{average} = 1.91$
19-44T	72.9	70.5	2.4	$\Delta_{std.dev.} = 1.692$
19-44B	69.5	69.3	0.2	$t_0 = 3.196$, $t_\alpha = 2.365$, $p = 0.0151$
19-50T	74.6	74.9	-0.3	Conclusion:
19-50B	73.3	73.0	0.3	**VFA LS > VFA GR**

Table B. 15 Test of Fine Aggregate Angularity Effect on VFA

Mixture	44	50	Δ	Calculation
9.5LS-T	76.3	76.7	-0.4	$\alpha = 0.05$
9.5LS-B	76.0	77.2	-1.2	H_0 : VFA 44 = VFA 50
9.5GR-T	72.5	75.0	-2.5	H_1 : VFA 44 < VFA 50
9.5GR-B	72.2	73.8	-1.6	$\Delta_{average} = -2.78$
19LS-A	69.0	74.7	-5.7	$\Delta_{std.dev.} = 1.726$
19LS-T	72.9	74.6	-1.7	$t_0 = -4.828$, $t_\alpha = -2.306$, $p = 0.0013$
19LS-B	69.5	73.3	-3.8	Conclusion:
19GR-T	70.5	74.9	-4.4	**VFA 44 < VFA 50**
19GR-B	69.3	73.0	-3.7	

Table B. 16 Test of Gradation Plotting Above And Through Restricted Zone Effect on VFA

Mixture	Above	Through	Δ	Calculation
9.5LS44	73.6	76.3	-2.7	H_0 : VFA Above = VFA Through
19LS44	69.0	72.9	-3.9	H_1 : VFA Above < VFA Through
19LS50	74.7	74.6	0.1	$\Delta_{average} = -2.16$, $\Delta_{std.dev.} = 2.053$, $\alpha = 0.05$
				$t_0 = -1.828$, $t_\alpha = -4.303$, $p = 0.2090$
				Conclusion: **VFA Above = VFA Through**

Table B. 17 Test of Gradation Plotting Above and Below Restricted Zone Effect on VFA

Mixture	Above	Below	Δ	Calculation
9.5LS44	73.6	76.0	-2.4	H_0 : VFA Above = VFA Below
19LS39	69.8	74.6	-4.8	H_1 : VFA Above < VFA Below
19LS44	69.0	69.5	-0.5	$\Delta_{average}$ = -1.58, $\Delta_{std.dev.}$ = 2.651, α = 0.05
19LS50	74.7	73.3	1.4	t_0 = -1.188, t_α = -3.183, p = 0.3203
				Conclusion: **VFA Above = VFA Below**

Table B. 18 Test of Gradation Plotting Through And Below Restricted Zone Effect on VFA

Mixture	Through	Below	Δ	Calculation
9.5LS44	76.3	76.0	0.3	α = 0.05
9.5GR44	72.5	72.2	0.3	H_0 : VFA Through = VFA Below
9.5LS50	76.7	77.2	-0.5	H_1 : VFA Through > VFA Below
9.5GR50	75.0	73.8	1.2	$\Delta_{average}$ = 0.60
19LS44	72.9	69.5	3.4	$\Delta_{std.dev.}$ = 0.646
19LS50	74.6	73.3	1.3	t_0 = 2.628, t_α = 2.365, p = 0.0299
19GR44	70.5	69.3	1.2	Conclusion:
19GR50	74.9	73.0	1.9	**VFA Through > VFA Below**

Table B. 19 Test of Nominal Size Effect on Dust Proportion

Mixture	19	9.5	Δ	Calculation
LS44A	1.57	1.72	-0.15	α = 0.05
LS44T	1.00	0.94	0.06	H_0 : DP 19 = DP 9.5
LS44B	1.12	0.76	0.36	H_1 : DP 19 < DP 9.5
LS50T	1.13	1.22	-0.09	$\Delta_{average}$ = -0.10
LS50B	0.91	1.03	-0.12	$\Delta_{std.dev.}$ = 0.235
GR44T	1.01	1.38	-0.37	t_0 = -1.335, t_α = -2.306, p = 0.2186
GR44B	1.09	1.06	0.03	Conclusion:
GR50T	1.05	1.43	-0.38	**DP 19 = DP 9.5**
GR50B	0.95	1.26	-0.28	

Table B. 20 Test of Coarse Aggregate Type Effect on Dust Proportion

Mixture	LS	GR	Δ	Calculation
9.5-44T	0.94	1.38	-0.44	$\alpha = 0.05$
9.5-44B	0.76	1.06	-0.30	H_0 : DP LS = DP GR
9.5-50T	1.22	1.43	-0.21	H_1 : DP LS < DP GR
9.5-50B	1.03	1.26	-0.23	$\Delta_{average} = -0.14$
19-44T	1.00	1.01	-0.01	$\Delta_{std.dev.} = 0.180$
19-44B	1.12	1.09	0.03	$t_0 = -2.255$, $t_\alpha = -2.365$, $p = 0.0588$
19-50T	1.13	1.05	0.08	Conclusion:
19-50B	0.91	0.98	-0.07	**DP LS = DP GR**

Table B. 21 Test of Fine Aggregate Angularity Effect on Dust Proportion

Mixture	44	50	Δ	Calculation
9.5LS-T	0.94	1.22	-0.28	$\alpha = 0.05$
9.5LS-B	0.76	1.03	-0.27	H_0 : DP 44 = DP 50
9.5GR-T	1.38	1.43	-0.05	H_1 : DP 44 < DP 50
9.5GR-B	1.06	1.26	-0.20	$\Delta_{average} = -0.05$
19LS-A	1.57	1.36	0.21	$\Delta_{std.dev.} = 0.191$
19LS-T	1.00	1.13	-0.13	$t_0 = -0.769$, $t_\alpha = -2.306$, $p = 0.4641$
19LS-B	1.12	0.91	0.21	Conclusion:
19GR-T	1.01	1.05	-0.04	**DP 44 = DP 50**
19GR-B	1.09	0.98	0.11	

Table B. 22 Test of Gradation Plotting Above And Through Restricted Zone Effect on Dust Proportion

Mixture	Above	Through	Δ	Calculation
9.5LS44	1.72	0.94	0.78	H_0 : DP Above = DP Through
19LS44	1.57	1.00	0.57	H_1 : DP Above > DP Through
19LS50	1.36	1.13	0.23	$\Delta_{average} = 0.53$, $\Delta_{std.dev.} = 0.278$, $\alpha = 0.05$
				$t_0 = 3.287$, $t_\alpha = 4.303$, $p = 0.0814$
				Conclusion: **DP Above = DP Through**

Table B. 23 Test of Gradation Plotting Above and Below Restricted Zone Effect on Dust Proportion

Mixture	Above	Below	Δ	Calculation
9.5LS44	1.72	0.76	0.96	H_0 : DP Above = DP Below
19LS39	1.22	0.61	0.61	H_1 : DP Above > DP Below
19LS44	1.57	1.12	0.45	$\Delta_{average} = 0.62$, $\Delta_{std.dev.} = 0.240$, $\alpha = 0.05$
19LS50	1.36	0.91	0.45	$t_0 = 5.136$, $t_\alpha = 3.183$, $p = 0.0143$
				Conclusion: **DP Above > DP Below**

Table B. 24 Test of Gradation Plotting Through And Below Restricted Zone Effect on Dust Proportion

Mixture	Through	Below	Δ	Calculation
9.5LS44	0.94	0.76	0.18	$\alpha = 0.05$
9.5GR44	1.38	1.06	0.32	H_0 : DP Through = DP Below
9.5LS50	1.22	1.03	0.19	H_1 : DP Through > DP Below
9.5GR50	1.43	1.26	0.17	$\Delta_{average} = 0.12$
19LS44	1.00	1.12	-0.12	$\Delta_{std.dev.} = 0.152$
19LS50	1.13	0.91	0.22	$t_0 = 2.214$, $t_\alpha = 2.365$, $p = 0.0624$
19GR44	1.01	1.09	-0.08	Conclusion:
19GR50	1.05	0.98	0.07	**DP Through = DP Below**

Table B. 25 Test of Nominal Size Effect on Film Thickness

Mixture	19	9.5	Δ	Calculation
LS44A	6.02	5.73	0.29	$\alpha = 0.05$
LS44T	8.62	9.40	-0.78	H_0 : FT 19 = FT 9.5
LS44B	8.94	11.69	-2.75	H_1 : FT 19 > FT 9.5
LS50T	9.23	9.81	-0.58	$\Delta_{average} = 0.42$
LS50B	11.45	10.05	1.40	$\Delta_{std.dev.} = 1.654$
GR44T	8.46	6.68	1.78	$t_0 = 0.760$, $t_\alpha = 2.306$, $p = 0.4691$
GR44B	8.68	8.66	0.02	Conclusion:
GR50T	9.77	7.35	2.42	**FT 19 = FT 9.5**
GR50B	10.09	8.12	1.97	

Table B. 26 Test of Coarse Aggregate Type Effect on Film Thickness

Mixture	LS	GR	Δ	Calculation
9.5-44T	9.40	6.68	2.72	$\alpha = 0.05$
9.5-44B	11.69	8.66	3.03	H_0 : FT LS = FT GR
9.5-50T	9.81	7.35	2.46	H_1 : FT LS > FT GR
9.5-50B	10.05	8.12	1.93	$\Delta_{average} = 1.42$
19-44T	8.62	8.46	0.16	$\Delta_{std.dev.} = 1.331$
19-44B	8.94	8.68	0.26	$t_0 = 3.023$, $t_\alpha = 2.365$, $p = 0.0193$
19-50T	9.23	9.77	-0.54	Conclusion:
19-50B	11.45	10.09	1.36	**FT LS > FT GR**

Table B. 27 Test of Fine Aggregate Angularity Effect on Film Thickness of 19 mm Mixtures

Mixture	44	50	Δ	Calculation
19LS-A	6.02	7.76	-1.74	H_0 : FT 44 (19 mm) = FT 50 (19 mm)
19LS-T	8.62	9.23	-0.61	H_1 : FT 44 (19 mm) < FT 50 (19 mm)
19LS-B	8.94	11.45	-2.51	$\Delta_{average} = -1.52$, $\Delta_{std.dev.} = 0.692$, $\alpha = 0.05$
19GR-T	8.46	9.77	-1.31	$t_0 = -4.902$, $t_\alpha = -2.777$, $p = 0.0080$
19GR-B	8.68	10.09	-1.41	Conclusion: **FT 44 (19mm) < FT 50 (19 mm)**

Table B. 28 Test of Fine Aggregate Angularity Effect on Film Thickness of 9.5 mm Mixtures

Mixture	44	50	Δ	Calculation
9.5LS-T	9.40	9.81	-0.4	H_0 : FT 44 (9.5 mm) = FT 50 (9.5 mm)
9.5LS-B	11.69	10.05	1.6	H_1 : FT 44 (9.5 mm) < FT 50 (9.5 mm)
9.5GR-T	6.68	7.35	-0.7	$\Delta_{average} = 0.28$, $\Delta_{std.dev.} = 1.048$, $\alpha = 0.05$
9.5GR-B	8.66	8.12	0.5	$t_0 = 0.525$, $t_\alpha = 3.182$, $p = 0.6361$
				Conclusion: **FT 44 (9.5mm) = FT 50 (9.5 mm)**

Table B. 29 Test of Gradation Plotting Above And Through Restricted Zone Effect on Film Thickness

Mixture	Above	Through	Δ	Calculation
9.5LS44	5.73	9.40	-3.67	H_0 : FT Above = FT Through
19LS44	6.02	8.62	-2.60	H_1 : FT Above < FT Through
19LS50	7.76	9.23	-1.47	$\Delta_{average}$ = -2.58, $\Delta_{std.dev.}$ = 1.100, α = 0.05
				t_0 = -4.062, t_α = -4.303, p = 0.0556
				Conclusion: **FT Above = FT Through**

Table B. 30 Test of Gradation Plotting Above and Below Restricted Zone Effect on Film Thickness

Mixture	Above	Below	Δ	Calculation
9.5LS44	5.73	11.69	-5.96	H_0 : FT Above = FT Below
19LS39	6.63	13.27	-6.64	H_1 : FT Above < FT Below
19LS44	6.02	8.94	-2.92	$\Delta_{average}$ = -4.80, $\Delta_{std.dev.}$ = 1.779, α = 0.05
19LS50	7.76	11.45	-3.69	t_0 = -5.398, t_α = -3.182, p = 0.0125
				Conclusion: **FT Above < FT Below**

Table B. 31 Test of Gradation Plotting Through And Below Restricted Zone Effect on Film Thickness

Mixture	Through	Below	Δ	Calculation
9.5LS44	9.40	11.69	-2.29	α = 0.05
9.5GR44	6.68	8.66	-1.98	H_0 : FT Through = FT Below
9.5LS50	9.81	10.05	-0.24	H_1 : FT Through < FT Below
9.5GR50	7.35	8.12	-0.77	$\Delta_{average}$ = -1.05
19LS44	8.62	8.94	-0.32	$\Delta_{std.dev.}$ = 0.946
19LS50	9.23	11.45	-2.22	t_0 = 3.125, t_α = -2.365, p = 0.0167
19GR44	8.46	8.68	-0.22	Conclusion:
19GR50	9.77	10.09	-0.32	**FT Through < FT Below**

Table B. 32 Test of Nominal Size Effect on Percent Gmm at $N_{initial}$

Mixture	19	9.5	Δ	Calculation
LS44A	87.44	86.12	1.32	$\alpha = 0.05$
LS44T	86.16	84.82	1.34	H_0 : %G@N_{ini} 19 = %G@N_{ini} 9.5
LS44B	85.72	84.16	1.56	H_1 : %G@N_{ini} 19 > %G@N_{ini} 9.5
LS50T	85.32	84.24	1.08	$\Delta_{average} = 0.55$
LS50B	84.80	84.26	0.54	$\Delta_{std.dev.} = 0.848$
GR44T	86.48	87.04	-0.56	$t_0 = 1.956$, $t_\alpha = 2.306$, p = 0.0861
GR44B	85.64	86.40	-0.76	Conclusion:
GR50T	85.70	85.68	0.02	**%G@N_{ini} 19 = %G@N_{ini} 9.5**
GR50B	86.32	85.88	0.44	

Table B. 33 Test of Coarse Aggregate Type Effect on Percent Gmm at $N_{initial}$

Mixture	LS	GR	Δ	Calculation
9.5-44T	84.82	87.04	-2.22	$\alpha = 0.05$
9.5-44B	84.16	86.40	-2.24	H_0 : %G@N_{ini} LS = %G@N_{ini} GR
9.5-50T	84.24	85.68	-1.44	H_1 : %G@N_{ini} LS < %G@N_{ini} GR
9.5-50B	84.26	85.88	-1.62	$\Delta_{average} = -1.21$
19-44T	86.16	86.48	-0.32	$\Delta_{std.dev.} = 0.890$
19-44B	85.72	85.64	0.08	$t_0 = -3.838$, $t_\alpha = -2.365$, p = 0.0064
19-50T	85.32	85.70	-0.38	Conclusion:
19-50B	84.80	86.32	-1.52	**%G@N_{ini} LS < %G@N_{ini} GR**

Table B. 34 Test of Fine Aggregate Angularity Effect on Percent Gmm at $N_{initial}$

Mixture	44	50	Δ	Calculation
9.5LS-T	84.82	84.24	0.58	$\alpha = 0.05$
9.5LS-B	84.16	84.26	-0.10	H_0 : %G@N_{ini} 44 = %G@N_{ini} 50
9.5GR-T	87.04	85.68	1.36	H_1 : %G@N_{ini} 44 > %G@N_{ini} 50
9.5GR-B	86.40	85.88	0.52	$\Delta_{average} = 0.74$
19LS-A	87.44	85.04	2.40	$\Delta_{std.dev.} = 0.865$
19LS-T	86.16	85.32	0.84	$t_0 = 2.552$, $t_\alpha = 2.306$, p = 0.0341
19LS-B	85.72	84.80	0.92	Conclusion:
19GR-T	86.48	85.70	0.78	**%G@N_{ini} 44 > %G@N_{ini} 50**
19GR-B	85.64	86.32	-0.68	

Table B. 35 Test of Gradation Plotting Above And Through Restricted Zone Effect on Percent Gmm at $N_{initial}$

Mixture	Above	Through	Δ	Calculation
9.5LS44	86.12	84.82	1.30	H_0 : %G@N_{ini} Above = %G@N_{ini} Through
19LS44	87.44	86.16	1.28	H_1 : %G@N_{ini} Above > %G@N_{ini} Through
19LS50	85.04	85.32	-0.28	$\Delta_{average}$ = 0.77, $\Delta_{std.dev.}$ = 0.906, α = 0.05
				t_0 = 1.465, t_α = 4.303, p = 0.2806
				Conclusion: **%G@N_{ini} Above = %G@N_{ini} Through**

Table B. 36 Test of Gradation Plotting Above and Below Restricted Zone Effect on Percent Gmm at $N_{initial}$

Mixture	Above	Below	Δ	Calculation
9.5LS44	86.12	84.16	1.96	H_0 : %G@N_{ini} Above = %G@N_{ini} Below
19LS39	88.48	85.80	2.68	H_1 : %G@N_{ini} Above > %G@N_{ini} Below
19LS44	87.44	85.72	1.72	$\Delta_{average}$ = 1.65, $\Delta_{std.dev.}$ = 1.025, α = 0.05
19LS50	85.04	84.80	0.24	t_0 = 3.220, t_α = 3.183, p = 0.0486
				Conclusion: **%G@N_{ini} Above > %G@N_{ini} Below**

Table B. 37 Test of Gradation Plotting Through And Below Restricted Zone Effect on Percent Gmm at $N_{initial}$

Mixture	Through	Below	Δ	Calculation
9.5LS44	84.82	84.16	0.66	α = 0.05
9.5GR44	87.04	86.40	0.64	H_0 : %G@N_{ini} Through = %G@N_{ini} Below
9.5LS50	84.24	84.26	-0.02	H_1 : %G@N_{ini} Through > %G@N_{ini} Below
9.5GR50	85.68	85.88	-0.20	$\Delta_{average}$ = 0.28
19LS44	86.16	85.72	0.44	$\Delta_{std.dev.}$ = 0.507
19LS50	85.32	84.80	0.52	t_0 = 1.575, t_α = 2.365, p = 0.1592
19GR44	86.48	85.64	0.84	Conclusion:
19GR50	85.70	86.32	-0.62	**%G@N_{ini} Through = %G@N_{ini} Below**

Table B. 38 Test of Nominal Size Effect on Percent Gmm at $N_{maximum}$

Mixture	19	9.5	Δ	Calculation
LS44A	97.34	97.38	-0.04	$\alpha = 0.05$
LS44T	97.36	97.18	0.18	H_0 : %G@N_{max} 19 = %G@N_{max} 9.5
LS44B	97.76	97.58	0.18	H_1 : %G@N_{max} 19 > %G@N_{max} 9.5
LS50T	97.36	97.18	0.18	$\Delta_{average} = 0.13$
LS50B	97.50	97.18	0.32	$\Delta_{std.dev.} = 0.153$
GR44T	97.20	97.34	-0.14	$t_0 = 2.484$, $t_\alpha = 2.306$, p = 0.0379
GR44B	97.50	97.22	0.28	Conclusion:
GR50T	97.50	97.50	0.00	**%G@N_{max} 19 > %G@N_{max} 9.5**
GR50B	97.62	97.44	0.18	

Table B. 39 Test of Coarse Aggregate Type Effect on Percent Gmm at $N_{maximum}$

Mixture	LS	GR	Δ	Calculation
9.5-44T	97.18	97.34	-0.16	$\alpha = 0.05$
9.5-44B	97.58	97.22	0.36	H_0 : %G@N_{max} LS = %G@N_{max} GR
9.5-50T	97.18	97.50	-0.32	H_1 : %G@N_{max} LS < %G@N_{max} GR
9.5-50B	97.18	97.44	-0.26	$\Delta_{average} = -0.03$
19-44T	97.36	97.20	0.16	$\Delta_{std.dev.} = 0.253$
19-44B	97.76	97.50	0.26	$t_0 = -0.308$, $t_\alpha = -2.365$, p = 0.7670
19-50T	97.36	97.50	-0.14	Conclusion:
19-50B	97.50	97.62	-0.12	**%G@N_{max} LS = %G@N_{max} GR**

Table B. 40 Test of Fine Aggregate Angularity Effect on Percent Gmm at $N_{maximum}$

Mixture	44	50	Δ	Calculation
9.5LS-T	97.18	97.18	0.00	$\alpha = 0.05$
9.5LS-B	97.58	97.18	0.40	H_0 : %G@N_{max} 44 = %G@N_{max} 50
9.5GR-T	97.34	97.50	-0.16	H_1 : %G@N_{max} 44 < %G@N_{max} 50
9.5GR-B	97.22	97.44	-0.22	$\Delta_{average} = -0.03$
19LS-A	97.34	97.48	-0.14	$\Delta_{std.dev.} = 0.228$
19LS-T	97.36	97.36	0.00	$t_0 = -0.409$, $t_\alpha = -2.306$, p = 0.6934
19LS-B	97.76	97.50	0.26	Conclusion:
19GR-T	97.20	97.50	-0.30	**%G@N_{max} 44 = %G@N_{max} 50**
19GR-B	97.50	97.62	-0.12	

Table B. 41 Test of Gradation Plotting Above And Through Restricted Zone Effect on Percent Gmm at $N_{maximum}$

Mixture	Above	Through	Δ	Calculation
9.5LS44	97.38	97.18	0.20	H_0 : %G@N_{max} Above = %G@N_{max} Through
19LS44	97.34	97.36	-0.02	H_1 : %G@N_{max} Above > %G@N_{max} Through
19LS50	97.48	97.36	0.12	$\Delta_{average}$ = 0.10, $\Delta_{std.dev.}$ = 0.111, α = 0.05
				t_0 = 1.555, t_α = 4.303, p = 0.2601
				Conclusion: **%G@N_{max} Above = %G@N_{max} Through**

Table B. 42 Test of Gradation Plotting Above and Below Restricted Zone Effect on Percent Gmm at $N_{maximum}$

Mixture	Above	Below	Δ	Calculation
9.5LS44	97.38	97.58	-0.20	H_0 : %G@N_{max} Above = %G@N_{max} Below
19LS39	97.00	97.60	-0.60	H_1 : %G@N_{max} Above < %G@N_{max} Below
19LS44	97.34	97.76	-0.42	$\Delta_{average}$ = -0.31, $\Delta_{std.dev.}$ = 0.253, α = 0.05
19LS50	97.48	97.50	-0.02	t_0 = -2.448, t_α = -3.182, p = 0.0918
				Conclusion: **%G@N_{max} Above < %G@N_{max} Below**

Table B. 43 Test of Gradation Plotting Through And Below Restricted Zone Effect on Percent Gmm at $N_{maximum}$

Mixture	Through	Below	Δ	Calculation
9.5LS44	97.18	97.58	-0.40	α = 0.05
9.5GR44	97.34	97.22	0.12	H_0 : %G@N_{max} Through = %G@N_{max} Below
9.5LS50	97.18	97.18	0.00	H_1 : %G@N_{max} Through < %G@N_{max} Below
9.5GR50	97.50	97.44	0.06	$\Delta_{average}$ = -0.15
19LS44	97.36	97.76	-0.40	$\Delta_{std.dev.}$ = 0.203
19LS50	97.36	97.50	-0.14	t_0 = -2.057, t_α = -2.365, p = 0.0787
19GR44	97.20	97.50	-0.30	Conclusion:
19GR50	97.50	97.62	-0.12	**%G@N_{max} Through = %G@N_{max} Below**

APPENDIX C APT DATA

Table C. 1 Regression Analysis of Total Rut and Rut Depth in APT

Dependent Variable: APT Total Rut Analysis of Variance					
Source	df	SS	MS	F	Pr > F
Model	1	883.486	883.486	43.611	5.28E-07
Error	26	526.713	20.258		
Total	27	1410.199			
R-square = 0.6265		Adjusted R-square = 0.6121			
Parameter Estimate					
Variable	df	Parameter Estimate	Standard Error	T for H_0	Pr > T
Intercept	1	-1.804	2.667	-0.676	0.5048
Rut Depth	1	1.850	0.280	6.604	5.28E-07

Table C. 2 Regression Analysis of Total Rut and Rise Height in APT.

Dependent Variable: APT Total Rut Analysis of Variance					
Source	df	SS	MS	F	Pr > F
Model	2	1323.097	661.549	189.878	7.66E-16
Error	25	87.102	3.484		
Total	27	1410.199			
R-square = 0.9382		Adjusted R-square = 0.9333			
Parameter Estimate					
Variable	df	Parameter Estimate	Standard Error	T for H_0	Pr > T
Intercept	1	3.192	0.914	3.492	0.0018
Rise Height	1	2.448	0.220	11.111	3.67E-11
Rise Height^2	1	-0.045	0.008	-5.457	1.15E-05

Table C. 3 Regression Analysis of Rise Height and Rut Depth in APT

Dependent Variable: APT Rise Height Analysis of Variance					
Source	df	SS	MS	F	Pr > F
Model	1	186.314	186.314	9.198	0.0054
Error	26	526.666	20.256		
Total	27	712.980			
R-square = 0.2613		Adjusted R-square = 0.2329			
Parameter Estimate					
Variable	df	Parameter Estimate	Standard Error	T for H_0	Pr > T
Intercept	1	-1.796	2.667	-0.674	0.5065
Rut Depth	1	0.850	0.280	3.033	0.0054

Table C. 4 ANOVA for Factor Effects on APT Total Rut.

Dependent Variable: APT Total Rut					
Source	df	SS	MS	F	Pr > F
Model	9	1053.351	117.039	5.88	0.0007
Error	18	358.513	19.9174		
Total	27	1411.864			
R-square = 0.7461 Adjusted R-square = 0.5873					
Parameter Estimate					
Source	df	Type I SS	MS	F	Pr > F
Nominal Max. Size	1	261.838	261.838	13.15	0.0019
Coarse Agg. Type	1	277.673	277.673	13.94	0.0015
Fine Agg. Angularity	2	280.905	140.452	7.05	0.0055
Gradation	2	158.331	79.166	3.97	0.0372
Nominal * Coarse	1	1.033	1.033	0.05	0.8224
Nominal * FAA	1	65.576	65.576	3.29	0.0863
Nominal * Gradation	0	0	.	.	.
Coarse * FAA	1	7.995	7.995	0.4	0.5343
Coarse * Gradation	0	0	.	.	.
FAA*Gradation	0	0	.	.	.
Source	df	Type III SS	MS	F	Pr > F
Nominal Max. Size	1	37.950	37.950	1.91	0.1844
Coarse Agg. Type	1	96.432	96.432	4.84	0.0411
Fine Agg. Angularity	2	137.443	68.722	3.45	0.0539
Gradation	2	220.329	110.165	5.53	0.0134
Nominal * Coarse	0	0	.	.	.
Nominal * FAA	0	0	.	.	.
Nominal * Gradation	0	0	.	.	.
Coarse * FAA	0	0	.	.	.
Coarse * Gradation	0	0	.	.	.
FAA*Gradation	0	0	.	.	.

Table C. 5 Regression Analysis of APT Total Rut and VMA for 19mm Mixtures.

Dependent Variable: APT Total Rut Analysis of Variance					
Source	df	SS	MS	F	Pr > F
Model	1	151.449	151.449	15.784	0.0165
Error	4	38.381	9.595		
Total	5	189.829			
R-square = 0.7978		Adjusted R-square = 0.7473			
Parameter Estimate					
Variable	df	Parameter Estimate	Standard Error	T for H_0	Pr > T
Intercept	1	-51.201	16.735	-3.059	0.0377
VMA	1	4.030	1.014	3.973	0.0165

Table C. 6 Regression Analysis of APT Total Rut and VMA for 9.5mm Mixtures.

Dependent Variable: APT Total Rut Analysis of Variance					
Source	df	SS	MS	F	Pr > F
Model	1	67.569	67.569	21.758	0.0096
Error	4	12.422	3.105		
Total	5	79.991			
R-square = 0.8447		Adjusted R-square = 0.8059			
Parameter Estimate					
Variable	df	Parameter Estimate	Standard Error	T for H_0	Pr > T
Intercept	1	-20.035	7.517	-2.665	0.0561
VMA	1	1.794	0.385	4.665	0.0096

Table C. 7 Regression Analysis of APT Total Rut and Dust Proportion for All Mixtures.

Dependent Variable: APT Total Rut Analysis of Variance					
Source	df	SS	MS	F	Pr > F
Model	2	296.239	148.120	3.320	0.0526
Error	25	1115.347	44.614		
Total	27	1411.587			
R-square = 0.2099		Adjusted R-square = 0.1467			
Parameter Estimate					
Variable	df	Parameter Estimate	Standard Error	T for H_0	Pr > T
Intercept	1	41.053	15.697	2.615	0.0149
DP		-46.211	32.338	-1.429	0.1654
DP^2	1	17.800	14.926	1.193	0.2442

Table C. 8 Regression Analysis of APT Total Rut and Selected In-Place Dust Proportion.

Dependent Variable: APT Total Rut Analysis of Variance					
Source	df	SS	MS	F	Pr > F
Model	2	472.974	236.487	17.632	0.0104
Error	4	53.650	13.412		
Total	6	526.623			
R-square = 0.8981		Adjusted R-square = 0.8472			
Parameter Estimate					
Variable	df	Parameter Estimate	Standard Error	T for H_0	Pr > T
Intercept	1	95.583	18.649	5.125	0.0069
DP		-134.325	36.744	-3.656	0.0217
DP^2	1	51.914	16.527	3.141	0.0348

Table C. 9 Regression Analysis of APT Total Rut and Film Thickness for All Mixtures.

Dependent Variable: APT Total Rut Analysis of Variance					
Source	df	SS	MS	F	Pr > F
Model	1	600.835	600.835	19.268	0.0002
Error	26	810.752	31.183		
Total	27	1411.587			
R-square = 0.4256		Adjusted R-square = 0.4036			
Parameter Estimate					
Variable	df	Parameter Estimate	Standard Error	T for H_0	Pr > T
Intercept	1	-6.789	5.050	-1.344	0.1904
FT	1	2.296	0.523	4.390	0.0002

Table C. 10 Regression Analysis of APT Total Rut and Film Thickness for 19mm Mixtures.

Dependent Variable: APT Total Rut Analysis of Variance					
Source	df	SS	MS	F	Pr > F
Model	1	713.593	713.593	30.262	0.0003
Error	10	235.803	23.580		
Total	11	949.396			
R-square = 0.7516		Adjusted R-square = 0.7268			
Parameter Estimate					
Variable	df	Parameter Estimate	Standard Error	T for H_0	Pr > T
Intercept	1	-14.053	6.067	-2.316	0.0430
FT	1	3.188	0.580	5.501	0.0003

Table C. 11 APT Rutting and Mixture Property Data.

Mixture Name	19LS39B	19LS39B	19LS44A	19LS44A
Traffic Wheel Loading	No Wander	No Wander	No Wander	No Wander
Thickness (cm)	10	10	10	10
Binder Layer Type	N/A	N/A	N/A	N/A
Nominal Max. Size (mm)	19	19	19	19
Coarse Agg. Type *	LS	LS	LS	LS
FAA	39	39	44	44
Gradation **	Below	Below	Above	Above
Rut Depth (mm)	11.00	10.00	9.05	7.87
Rise Height (mm)	14.25	27.00	2.79	1.67
Total Rut (mm)	25.25	37.00	11.85	9.54
AC (%)	5.7	5.7	4.7	4.7
AV (%)	6.6	2.8	9.9	6.6
VMA (%)	18.1	14.8	18.4	15.4
VFA (%)	63.5	81.0	46.1	57.1
Film Thickness (μm)	13.77	13.77	7.93	7.93
Surface Area (m^2/Kg)	3.67	3.67	4.69	4.69
Dust Proportion	0.60	0.60	0.86	0.86
Binder Absorption, Pba (%)	0.6	0.6	0.9	0.9
Effective Binder, Pbe (%)	5.1	5.1	3.8	3.8
Effective Spec. Gravity, Gse	2.685	2.685	2.714	2.714
Rice Specific Gravity, Gmm	2.460	2.460	2.520	2.520
Materials Passing #200 (%)	3.09	3.09	3.29	3.29
Agg. Bulk Spec. Gravity, Gsb	2.645	2.645	2.651	2.651
Bulk Specific Gravity, Gmb	2.298	2.391	2.271	2.354

Note: * LS = limestone, GR = granite

** gradation plotting with respect to the restricted zone

Table C. 11 APT Rutting and Mixture Property Data.(continue)

Mixture Name	19LS44B	19LS44B	19LS50A	19LS50A
Traffic Wheel Loading	No Wander	No Wander	No Wander	No Wander
Thickness (cm)	10	10	10	10
Binder Layer Type	N/A	N/A	N/A	N/A
Nominal Max. Size (mm)	19	19	19	19
Coarse Agg. Type *	LS	LS	LS	LS
FAA	44	44	50	50
Gradation **	Below	Below	Above	Above
Rut Depth (mm)	17.19	11.39	9.86	17.42
Rise Height (mm)	11.78	7.67	5.24	9.15
Total Rut (mm)	28.97	19.06	15.10	26.57
AC (%)	4.9	4.9	5.8	5.8
AV (%)	9.8	8.3	6.3	4.1
VMA (%)	18.8	17.4	17.5	15.6
VFA (%)	47.8	52.4	64.0	73.7
Film Thickness (μm)	12.70	12.70	10.42	10.42
Surface Area (m^2/Kg)	3.12	3.12	4.69	4.69
Dust Proportion	0.60	0.60	0.67	0.67
Binder Absorption, Pba (%)	0.9	0.9	0.9	0.9
Effective Binder, Pbe (%)	4.0	4.0	4.9	4.9
Effective Spec. Gravity, Gse	2.711	2.711	2.703	2.703
Rice Specific Gravity, Gmm	2.510	2.510	2.470	2.470
Materials Passing #200 (%)	2.41	2.41	3.29	3.29
Agg. Bulk Spec. Gravity, Gsb	2.651	2.651	2.643	2.643
Bulk Specific Gravity, Gmb	2.264	2.302	2.314	2.369

Note: * LS = limestone, GR = granite

** gradation plotting with respect to the restricted zone

Table C. 11 APT Rutting and Mixture Property Data.(continue)

Mixture Name	19GR44B	19GR44B	19GR50T	19GR50T
Traffic Wheel Loading	No Wander	No Wander	No Wander	No Wander
Thickness (cm)	10	10	10	10
Binder Layer Type	N/A	N/A	N/A	N/A
Nominal Max. Size (mm)	19	19	19	19
Coarse Agg. Type *	GR	GR	GR	GR
FAA	44	44	50	50
Gradation **	Below	Below	Through	Through
Rut Depth (mm)	6.79	12.09	5.10	7.64
Rise Height (mm)	2.84	6.80	2.05	4.49
Total Rut (mm)	9.63	18.89	7.15	12.13
AC (%)	4.5	5.6	4.5	5.4
AV (%)	7.9	5.5	9.4	4.0
VMA (%)	15.2	15.4	17.9	15.1
VFA (%)	48.0	64.6	47.6	73.5
Film Thickness (μm)	6.80	9.30	7.30	9.18
Surface Area (m^2/Kg)	4.50	4.50	5.13	5.13
Dust Proportion	1.66	1.23	1.42	1.14
Binder Absorption, Pba (%)	1.4	1.4	0.7	0.6
Effective Binder, Pbe (%)	3.1	4.2	3.8	4.8
Effective Spec. Gravity, Gse	2.745	2.745	2.690	2.687
Rice Specific Gravity, Gmm	2.554	2.511	2.508	2.472
Materials Passing #200 (%)	5.21	5.21	5.45	5.45
Agg. Bulk Spec. Gravity, Gsb	2.649	2.649	2.644	2.644
Bulk Specific Gravity, Gmb	2.352	2.374	2.272	2.373

Note: * LS = limestone, GR = granite
** gradation plotting with respect to the restricted zone

Table C. 11 APT Rutting and Mixture Property Data.(continue)

Mixture Name	9.5LS44T	9.5LS44T	9.5LS44T	9.5LS44T
Traffic Wheel Loading	No Wander	No Wander	No Wander	No Wander
Thickness (cm)	3.2	3.2	3.2	3.2
Binder Layer Type	12.5mm	12.5mm	9.5 mm	9.5 mm
Nominal Max. Size (mm)	9.5	9.5	9.5	9.5
Coarse Agg. Type *	LS	LS	LS	LS
FAA	44	44	44	44
Gradation **	Through	Through	Through	Through
Rut Depth (mm)	11.07	6.37	8.05	10.17
Rise Height (mm)	7.25	3.40	4.04	7.76
Total Rut (mm)	18.32	9.77	12.09	17.94
AC (%)	6.3	5.6	5.6	6.3
AV (%)	10.6	14.9	14.2	10.4
VMA (%)	21.8	24.5	23.9	21.6
VFA (%)	51.2	39.1	40.5	51.8
Film Thickness (μm)	9.90	8.86	8.86	9.90
Surface Area (m^2/Kg)	5.15	5.15	5.15	5.15
Dust Proportion	0.80	0.89	0.89	0.80
Binder Absorption, Pba (%)	1.2	1.0	1.0	1.2
Effective Binder, Pbe (%)	5.1	4.6	4.6	5.1
Effective Spec. Gravity, Gse	2.726	2.712	2.712	2.726
Rice Specific Gravity, Gmm	2.470	2.485	2.485	2.470
Materials Passing #200 (%)	4.09	4.09	4.09	4.09
Agg. Bulk Spec. Gravity, Gsb	2.644	2.644	2.644	2.644
Bulk Specific Gravity, Gmb	2.208	2.114	2.132	2.213

Note: * LS = limestone, GR = granite
** gradation plotting with respect to the restricted zone

Table C. 11 APT Rutting and Mixture Property Data.(continue)

Mixture Name	9.5LS50T	9.5LS50T	9.5LS50T	9.5LS50T
Traffic Wheel Loading	No Wander	No Wander	No Wander	No Wander
Thickness (cm)	3.2	3.2	3.2	3.2
Binder Layer Type	12.5mm	12.5mm	9.5 mm	9.5 mm
Nominal Max. Size (mm)	9.5	9.5	9.5	9.5
Coarse Agg. Type *	LS	LS	LS	LS
FAA	50	50	50	50
Gradation **	Through	Through	Through	Through
Rut Depth (mm)	10.00	10.98	8.36	7.74
Rise Height (mm)	5.47	8.12	3.49	2.66
Total Rut (mm)	15.47	19.10	11.84	10.40
AC (%)	6.0	6.8	6.8	6.0
AV (%)	11.7	6.9	5.2	11.1
VMA (%)	23.0	20.4	18.9	22.5
VFA (%)	49.1	66.2	72.7	50.7
Film Thickness (μm)	7.07	8.16	8.16	7.07
Surface Area (m^2/Kg)	7.50	7.50	7.50	7.50
Dust Proportion	1.51	1.32	1.32	1.51
Binder Absorption, Pba (%)	0.7	0.7	0.7	0.7
Effective Binder, Pbe (%)	5.3	6.1	6.1	5.3
Effective Spec. Gravity, Gse	2.685	2.687	2.687	2.685
Rice Specific Gravity, Gmm	2.449	2.422	2.422	2.449
Materials Passing #200 (%)	8.08	8.08	8.08	8.08
Agg. Bulk Spec. Gravity, Gsb	2.640	2.640	2.640	2.640
Bulk Specific Gravity, Gmb	2.162	2.255	2.297	2.178

Note: * LS = limestone, GR = granite

** gradation plotting with respect to the restricted zone

Table C. 11 APT Rutting and Mixture Property Data.(continue)

Mixture Name	9.5GR44B	9.5GR44B	9.5GR44B	9.5GR44B
Traffic Wheel Loading	No Wander	No Wander	No Wander	No Wander
Thickness (cm)	3.2	3.2	3.2	3.2
Binder Layer Type	12.5mm	12.5mm	9.5 mm	9.5 mm
Nominal Max. Size (mm)	9.5	9.5	9.5	9.5
Coarse Agg. Type *	GR	GR	GR	GR
FAA	44	44	44	44
Gradation **	Below	Below	Below	Below
Rut Depth (mm)	7.00	5.37	4.58	6.28
Rise Height (mm)	2.93	2.60	3.42	3.26
Total Rut (mm)	9.93	7.97	8.00	9.54
AC (%)	5.3	5.2	5.2	5.3
AV (%)	8.9	10.5	10.8	10.4
VMA (%)	18.9	20.2	20.5	20.2
VFA (%)	53.0	48.0	47.2	48.7
Film Thickness (μm)	10.93	10.75	10.75	10.93
Surface Area (m^2/Kg)	4.06	4.06	4.06	4.06
Dust Proportion	0.65	0.66	0.66	0.65
Binder Absorption, Pba (%)	0.8	0.8	0.8	0.8
Effective Binder, Pbe (%)	4.5	4.4	4.4	4.5
Effective Spec. Gravity, Gse	2.702	2.700	2.700	2.702
Rice Specific Gravity, Gmm	2.488	2.490	2.490	2.488
Materials Passing #200 (%)	2.94	2.94	2.94	2.94
Agg. Bulk Spec. Gravity, Gsb	2.647	2.647	2.647	2.647
Bulk Specific Gravity, Gmb	2.267	2.229	2.221	2.230

Note: * LS = limestone, GR = granite

** gradation plotting with respect to the restricted zone

Table C. 11 APT Rutting and Mixture Property Data.(continue)

Mixture Name	9.5GR50B	9.5GR50B	9.5GR50B	9.5GR50B
Traffic Wheel Loading	No Wander	No Wander	No Wander	No Wander
Thickness (cm)	3.2	3.2	3.2	3.2
Binder Layer Type	12.5mm	12.5mm	9.5 mm	9.5 mm
Nominal Max. Size (mm)	9.5	9.5	9.5	9.5
Coarse Agg. Type *	GR	GR	GR	GR
FAA	50	50	50	50
Gradation **	Below	Below	Below	Below
Rut Depth (mm)	9.23	6.33	5.77	6.92
Rise Height (mm)	2.69	3.18	5.17	3.16
Total Rut (mm)	11.92	9.50	13.94	10.08
AC (%)	5.5	6.2	6.2	5.5
AV (%)	6.9	3.4	2.9	6.2
VMA (%)	17.5	16.0	15.6	16.9
VFA (%)	60.4	78.8	81.4	63.2
Film Thickness (μm)	7.18	8.38	8.38	7.18
Surface Area (m^2/Kg)	6.45	6.45	6.45	6.45
Dust Proportion	1.55	1.34	1.34	1.55
Binder Absorption, Pba (%)	0.8	0.8	0.8	0.8
Effective Binder, Pbe (%)	4.7	5.4	5.4	4.7
Effective Spec. Gravity, Gse	2.699	2.696	2.696	2.699
Rice Specific Gravity, Gmm	2.478	2.450	2.450	2.478
Materials Passing #200 (%)	7.28	7.28	7.28	7.28
Agg. Bulk Spec. Gravity, Gsb	2.643	2.643	2.643	2.643
Bulk Specific Gravity, Gmb	2.306	2.367	2.379	2.324

Note: * LS = limestone, GR = granite

** gradation plotting with respect to the restricted zone

Table C. 11 APT Rutting and Mixture Property Data.(continue)

Mixture Name	19LS44B	19LS44B	19GR44B	19GR44B	19GR50T	19GR50T
Traffic Wheel Loading	Wander	Wander	Wander	Wander	Wander	Wander
Thickness (cm)	10	10	10	10	10	10
Binder Layer Type	N/A	N/A	N/A	N/A	N/A	N/A
Nominal Max. Size (mm)	19	19	19	19	19	19
Coarse Agg. Type *	LS	LS	GR	GR	GR	GR
FAA	44	44	44	44	50	50
Gradation **	Below	Below	Below	Below	Through	Through
Rut Depth (mm)	10.96	11.37	8.32	13.00	5.02	7.95
Rise Height (mm)	6.00	6.31	4.06	17.00	0.89	4.92
Total Rut (mm)	16.96	17.67	12.38	30.00	5.90	11.04
AC (%)	4.9	4.9	4.5	5.6	4.5	5.4
AV (%)	9.8	8.3	7.9	5.5	9.4	4.0
VMA (%)	18.8	17.4	15.2	15.4	17.9	15.1
VFA (%)	47.8	52.4	48.0	64.6	47.6	73.5
Film Thickness (μm)	12.70	12.70	6.80	9.30	7.30	9.18
Surface Area (m^2/Kg)	3.12	3.12	4.50	4.50	5.13	5.13
Dust Proportion	0.60	0.60	1.66	1.23	1.42	1.14
Binder Absorp., Pba (%)	0.9	0.9	1.4	1.4	0.7	0.6
Effective Binder, Pbe (%)	4.0	4.0	3.1	4.2	3.8	4.8
Effective Spec. Gravity, Gse	2.711	2.711	2.745	2.745	2.690	2.687
Rice Specific Gravity, Gmm	2.510	2.510	2.554	2.511	2.508	2.472
Materials Passing #200 (%)	2.41	2.41	5.21	5.21	5.45	5.45
Agg. Bulk Spec. Gravity, Gsb	2.651	2.651	2.649	2.649	2.644	2.644
Bulk Specific Gravity, Gmb	2.264	2.302	2.352	2.374	2.272	2.373

Note: * LS = limestone, GR = granite

** gradation plotting with respect to the restricted zone

Table C. 12 In-Wheel Path Mixture Properties.

Mixture Name	19LS39B	19LS39B	19LS44A	19LS44A
Traffic Wheel Loading	No Wander	No Wander	No Wander	No Wander
Thickness (cm)	10	10	10	10
Binder Layer Type	N/A	N/A	N/A	N/A
Nominal Max. Size (mm)	19	19	19	19
Coarse Agg. Type *	LS	LS	LS	LS
FAA	39	39	44	44
Gradation **	Below	Below	Above	Above
AC (%)	5.7	5.7	4.7	4.7
AV (%)	5.3	2.8	7.9	5.7
VMA (%)	16.9	14.7	16.6	14.6
VFA (%)	68.8	81.2	52.2	60.8
Film Thickness (μm)	13.77	13.77	7.93	7.93
Surface Area (m^2/Kg)	3.67	3.67	4.69	4.69
Dust Proportion	0.60	0.60	0.86	0.86
Binder Absorption, Pba (%)	0.6	0.6	0.9	0.9
Effective Binder, Pbe (%)	5.1	5.1	3.8	3.8
Effective Spec. Gravity, Gse	2.685	2.685	2.714	2.714
Rice Specific Gravity, Gmm	2.460	2.460	2.520	2.520
Materials Passing #200 (%)	3.09	3.09	3.29	3.29
Agg. Bulk Spec. Gravity, Gsb	2.645	2.645	2.651	2.651
Bulk Specific Gravity, Gmb	2.330	2.392	2.320	2.376

Note: * LS = limestone, GR = granite

** gradation plotting with respect to the restricted zone

Table C. 12 In-Wheel Path Mixture Properties. (continue)

Mixture Name	19LS44B	19LS44B	19LS50A	19LS50A
Traffic Wheel Loading	No Wander	No Wander	No Wander	No Wander
Thickness (cm)	10	10	10	10
Binder Layer Type	N/A	N/A	N/A	N/A
Nominal Max. Size (mm)	19	19	19	19
Coarse Agg. Type *	LS	LS	LS	LS
FAA	44	44	50	50
Gradation **	Below	Below	Above	Above
AC (%)	4.9	4.9	5.8	5.8
AV (%)	6.7	5.9	4.0	2.7
VMA (%)	16.0	15.3	15.5	14.4
VFA (%)	58.1	61.4	73.9	81.1
Film Thickness (μm)	12.70	12.70	10.42	10.42
Surface Area (m^2/Kg)	3.12	3.12	4.69	4.69
Dust Proportion	0.60	0.60	0.67	0.67
Binder Absorption, Pba (%)	0.9	0.9	0.9	0.9
Effective Binder, Pbe (%)	4.0	4.0	4.9	4.9
Effective Spec. Gravity, Gse	2.711	2.711	2.703	2.703
Rice Specific Gravity, Gmm	2.510	2.510	2.470	2.470
Materials Passing #200 (%)	2.41	2.41	3.29	3.29
Agg. Bulk Spec. Gravity, Gsb	2.651	2.651	2.643	2.643
Bulk Specific Gravity, Gmb	2.342	2.362	2.370	2.403

Note: * LS = limestone, GR = granite

** gradation plotting with respect to the restricted zone

Table C. 12 In-Wheel Path Mixture Properties. (continue)

Mixture Name	19GR44B	19GR44B	19GR50T	19GR50T
Traffic Wheel Loading	No Wander	No Wander	No Wander	No Wander
Thickness (cm)	10	10	10	10
Binder Layer Type	N/A	N/A	N/A	N/A
Nominal Max. Size (mm)	19	19	19	19
Coarse Agg. Type *	GR	GR	GR	GR
FAA	44	44	50	50
Gradation **	Below	Below	Through	Through
AC (%)	4.5	5.6	4.5	5.4
AV (%)	13.5	12.1	6.9	3.1
VMA (%)	20.4	21.3	15.6	14.3
VFA (%)	33.6	43.4	56.1	78.2
Film Thickness (μm)	6.80	9.30	7.30	9.18
Surface Area (m^2/Kg)	4.50	4.50	5.13	5.13
Dust Proportion	1.66	1.23	1.42	1.14
Binder Absorption, Pba (%)	1.4	1.4	0.7	0.6
Effective Binder, Pbe (%)	3.1	4.2	3.8	4.8
Effective Spec. Gravity, Gse	2.745	2.745	2.690	2.687
Rice Specific Gravity, Gmm	2.554	2.511	2.508	2.472
Materials Passing #200 (%)	5.21	5.21	5.45	5.45
Agg. Bulk Spec. Gravity, Gsb	2.649	2.649	2.644	2.644
Bulk Specific Gravity, Gmb	2.208	2.208	2.336	2.395

Note: * LS = limestone, GR = granite

** gradation plotting with respect to the restricted zone

Table C. 12 In-Wheel Path Mixture Properties. (continue)

Mixture Name	9.5LS44T	9.5LS44T	9.5LS44T	9.5LS44T
Traffic Wheel Loading	No Wander	No Wander	No Wander	No Wander
Thickness (cm)	3.2	3.2	3.2	3.2
Binder Layer Type	12.5mm	12.5mm	9.5 mm	9.5 mm
Nominal Max. Size (mm)	9.5	9.5	9.5	9.5
Coarse Agg. Type *	LS	LS	LS	LS
FAA	44	44	44	44
Gradation **	Through	Through	Through	Through
AC (%)	6.3	5.6	5.6	6.3
AV (%)	9.3	11.9	11.5	8.5
VMA (%)	20.6	21.8	21.5	19.9
VFA (%)	54.8	45.6	46.3	57.2
Film Thickness (μm)	9.90	8.86	8.86	9.90
Surface Area (m^2/Kg)	5.15	5.15	5.15	5.15
Dust Proportion	0.80	0.89	0.89	0.80
Binder Absorption, Pba (%)	1.2	1.0	1.0	1.2
Effective Binder, Pbe (%)	5.1	4.6	4.6	5.1
Effective Spec. Gravity, Gse	2.726	2.712	2.712	2.726
Rice Specific Gravity, Gmm	2.470	2.485	2.485	2.470
Materials Passing #200 (%)	4.09	4.09	4.09	4.09
Agg. Bulk Spec. Gravity, Gsb	2.644	2.644	2.644	2.644
Bulk Specific Gravity, Gmb	2.240	2.190	2.198	2.259

Note: * LS = limestone, GR = granite

** gradation plotting with respect to the restricted zone

Table C. 12 In-Wheel Path Mixture Properties. (continue)

Mixture Name	9.5LS50T	9.5LS50T	9.5LS50T	9.5LS50T
Traffic Wheel Loading	No Wander	No Wander	No Wander	No Wander
Thickness (cm)	3.2	3.2	3.2	3.2
Binder Layer Type	12.5mm	12.5mm	9.5 mm	9.5 mm
Nominal Max. Size (mm)	9.5	9.5	9.5	9.5
Coarse Agg. Type *	LS	LS	LS	LS
FAA	50	50	50	50
Gradation **	Through	Through	Through	Through
AC (%)	6.0	6.8	6.8	6.0
AV (%)	6.4	2.9	2.8	7.7
VMA (%)	18.4	17.0	16.9	19.5
VFA (%)	65.1	83.0	83.2	60.6
Film Thickness (μm)	7.07	8.16	8.16	7.07
Surface Area (m^2/Kg)	7.50	7.50	7.50	7.50
Dust Proportion	1.51	1.32	1.32	1.51
Binder Absorption, Pba (%)	0.7	0.7	0.7	0.7
Effective Binder, Pbe (%)	5.3	6.1	6.1	5.3
Effective Spec. Gravity, Gse	2.685	2.687	2.687	2.685
Rice Specific Gravity, Gmm	2.449	2.422	2.422	2.449
Materials Passing #200 (%)	8.08	8.08	8.08	8.08
Agg. Bulk Spec. Gravity, Gsb	2.640	2.640	2.640	2.640
Bulk Specific Gravity, Gmb	2.292	2.352	2.353	2.261

Note: * LS = limestone, GR = granite

** gradation plotting with respect to the restricted zone

Table C. 12 In-Wheel Path Mixture Properties. (continue)

Mixture Name	9.5GR44B	9.5GR44B	9.5GR44B	9.5GR44B
Traffic Wheel Loading	No Wander	No Wander	No Wander	No Wander
Thickness (cm)	3.2	3.2	3.2	3.2
Binder Layer Type	12.5mm	12.5mm	9.5 mm	9.5 mm
Nominal Max. Size (mm)	9.5	9.5	9.5	9.5
Coarse Agg. Type *	GR	GR	GR	GR
FAA	44	44	44	44
Gradation **	Below	Below	Below	Below
AC (%)	5.3	5.2	5.2	5.3
AV (%)	8.3	10.1	9.0	8.8
VMA (%)	18.4	19.8	18.9	18.8
VFA (%)	54.8	49.0	52.1	53.4
Film Thickness (μm)	10.93	10.75	10.75	10.93
Surface Area (m^2/Kg)	4.06	4.06	4.06	4.06
Dust Proportion	0.65	0.66	0.66	0.65
Binder Absorption, Pba (%)	0.8	0.8	0.8	0.8
Effective Binder, Pbe (%)	4.5	4.4	4.4	4.5
Effective Spec. Gravity, Gse	2.702	2.700	2.700	2.702
Rice Specific Gravity, Gmm	2.488	2.490	2.490	2.488
Materials Passing #200 (%)	2.94	2.94	2.94	2.94
Agg. Bulk Spec. Gravity, Gsb	2.647	2.647	2.647	2.647
Bulk Specific Gravity, Gmb	2.281	2.238	2.265	2.270

Note: * LS = limestone, GR = granite

** gradation plotting with respect to the restricted zone

Table C. 12 In-Wheel Path Mixture Properties. (continue)

Mixture Name	9.5GR50B	9.5GR50B	9.5GR50B	9.5GR50B
Traffic Wheel Loading	No Wander	No Wander	No Wander	No Wander
Thickness (cm)	3.2	3.2	3.2	3.2
Binder Layer Type	12.5mm	12.5mm	9.5 mm	9.5 mm
Nominal Max. Size (mm)	9.5	9.5	9.5	9.5
Coarse Agg. Type *	GR	GR	GR	GR
FAA	50	50	50	50
Gradation **	Below	Below	Below	Below
AC (%)	5.5	6.2	6.2	5.5
AV (%)	6.1	3.5	2.3	4.8
VMA (%)	16.8	16.1	15.1	15.7
VFA (%)	63.6	78.4	84.6	69.1
Film Thickness (μm)	7.18	8.38	8.38	7.18
Surface Area (m^2/Kg)	6.45	6.45	6.45	6.45
Dust Proportion	1.55	1.34	1.34	1.55
Binder Absorption, Pba (%)	0.8	0.8	0.8	0.8
Effective Binder, Pbe (%)	4.7	5.4	5.4	4.7
Effective Spec. Gravity, Gse	2.699	2.696	2.696	2.699
Rice Specific Gravity, Gmm	2.478	2.450	2.450	2.478
Materials Passing #200 (%)	7.28	7.28	7.28	7.28
Agg. Bulk Spec. Gravity, Gsb	2.643	2.643	2.643	2.643
Bulk Specific Gravity, Gmb	2.326	2.365	2.393	2.358

Note: * LS = limestone, GR = granite

** gradation plotting with respect to the restricted zone

Table C. 13 Asphalt Extraction Data.

Nom. Max. Size		19	19	19	19	19	19
Coarse Ag. Type		Limestone	Limestone	Limestone	Limestone	Granite	Granite
FAA		39	44	44	50	44	44
Gradation		Below	Above	Below	Above	Below	Below
Design AC (%)		5.5	4.6	4.6	5.9	4.4	4.4
Layer		Surface	Surface	Surface	Surface	Surface	Surface
Extraction	Method	Centrifuge	Centrifuge	Centrifuge	Centrifuge	Reflux	Reflux
	Average	5.7	4.7	4.9	5.8	4.5	5.6
	Sample 1	5.78	4.88	4.88	5.84	4.60	5.63
	Sample 2	5.55	4.59	4.85	5.79	4.19	5.50
	Sample 3					4.58	5.54

Note: Centrifuge = ASTM D2172 – Method A, Reflux = ASTM D2172 – Method B

Table C. 13 Asphalt Extraction Data. (continue)

Nom. Max. Size		19	19	9.5	9.5	9.5	9.5
Coarse Ag. Type		Granite	Granite	Limestone	Limestone	Limestone	Limestone
FAA		50	50	44	44	50	50
Gradation		Through	Through	Through	Through	Through	Through
Design AC (%)		5.3	5.3	6.2	6.2	6.6	6.6
Layer		Surface	Surface	Surface	Surface	Surface	Surface
Extraction	Method	Reflux	Reflux	Reflux	Reflux	Reflux	Reflux
	Average	4.5	5.4	5.6	6.3	6.0	6.8
	Sample 1	4.69	5.62	5.77	6.27	6.03	6.90
	Sample 2	4.32	5.18	5.46	6.27	5.91	6.72
	Sample 3		5.26	5.50		5.91	6.78

Note: Centrifuge = ASTM D2172 – Method A, Reflux = ASTM D2172 – Method B

Table C. 13 Asphalt Extraction Data. (continue)

Nom. Max. Size		9.5	9.5	9.5	9.5	12.5
Coarse Ag. Type		Granite	Granite	Granite	Granite	
FAA		44	44	50	50	
Gradation		Below	Below	Below	Below	
Design AC (%)		5.2	5.2	5.6	5.6	
Layer		Surface	Surface	Surface	Surface	Binder
Extraction	Method	Reflux	Reflux	Reflux	Reflux	Reflux
	Average	5.2	5.3	5.5	6.2	5.2
	Sample 1	5.27	5.42	5.52	6.29	5.36
	Sample 2	5.07	5.23	5.40	6.09	5.05
	Sample 3	5.21	5.28	5.45	6.23	5.22

Note: Centrifuge = ASTM D2172 – Method A, Reflux = ASTM D2172 – Method B

Table C. 14 In-Place Gradation Analysis of 19 mm Limestone with FAA of 39 and Gradation Plotting Below The Restricted Zone Mixtures.

Mixture Name: 19LS39B		Nominal. Max. Size: 19 mm						
Coarse Aggregate Type: Limestone		Gradation: Below the restricted zone						
Fine Aggregate Angularity: 39		AC = 5.7% (+0.1% Design AC)						
Sieve Size (mm)	Design	Washed Sieve Gradation Analysis (no. of sample = 2)						
		Average	Difference	Standard Deviation	C.O.V	No. 1	No. 2	No.3
25	100.0	100.0	0.0	0.0	0.0	100.00	100.00	
19	97.1	97.2	0.1	2.5	2.6	95.42	99.01	
12.5	87.8	91.1	3.3	7.4	8.2	85.82	96.32	
9.5	81.5	86.5	5.0	8.3	9.6	80.62	92.42	
4.75	52.7	60.9	8.2	5.9	9.7	56.70	65.00	
2.36	29.7	33.4	3.7	2.1	6.3	31.91	34.88	
1.18	22.0	21.5	-0.5	1.6	7.2	20.44	22.64	
0.6	15.0	14.7	-0.3	1.2	8.2	13.82	15.52	
0.3	8.1	7.4	-0.7	0.8	10.4	6.84	7.92	
0.15	4.5	4.1	-0.4	0.5	12.5	3.73	4.45	
0.075	3.1	3.1	0.0	0.5	14.4	2.78	3.41	

Table C. 15 In-Place Gradation Analysis of 19 mm Limestone with FAA of 44 and Gradation Plotting Above The Restricted Zone Mixtures.

Mixture Name: 19LS44A				Nominal. Max. Size: 19 mm				
Coarse Aggregate Type: Limestone				Gradation: Above the restricted zone				
Fine Aggregate Angularity: 44				AC = 4.7% (+0.1% Design AC)				
Sieve Size (mm)	Design	Washed Sieve Gradation Analysis (no. of sample = 2)						
		Average	Difference	Standard Deviation	C.O.V	No. 1	No. 2	No. 3
25	100.0	100.0	0.0	0.0	0.0	100.00	100.00	
19	95.5	97.2	1.7	2.6	2.6	95.37	98.99	
12.5	80.7	86.5	5.8	7.4	8.5	81.30	91.70	
9.5	73.1	79.0	5.9	6.6	8.3	74.32	83.64	
4.75	64.6	68.6	4.0	5.7	8.3	64.58	72.58	
2.36	48.9	51.5	2.6	4.9	9.5	48.02	54.91	
1.18	30.5	30.8	0.3	2.8	9.0	28.81	32.73	
0.6	20.8	19.4	-1.4	1.6	8.1	18.32	20.55	
0.3	14.4	11.7	-2.7	0.9	7.8	11.08	12.38	
0.15	9.0	5.9	-3.1	0.5	7.6	5.58	6.21	
0.075	5.9	3.3	2.6	0.3	9.5	3.07	3.51	

Table C. 16 In-Place Gradation Analysis of 19 mm Limestone with FAA of 44 and Gradation Plotting Below The Restricted Zone Mixtures.

Mixture Name: 19LS44B		Nominal. Max. Size: 19 mm						
Coarse Aggregate Type: Limestone		Gradation: Below the restricted zone						
Fine Aggregate Angularity: 44		AC = 4.9% (+0.3% Design AC)						
Sieve Size (mm)	Design	Washed Sieve Gradation Analysis (no. of sample = 2)						
		Average	Difference	Standard Deviation	C.O.V	No. 1	No. 2	No. 3
25	100.0	100.0	0.0	0.0	0.0	100.00	100.00	
19	94.3	89.4	-4.9	4.5	5.1	86.17	92.59	
12.5	75.7	71.0	-4.7	4.7	6.7	67.61	74.31	
9.5	65.5	63.4	-2.1	1.3	2.0	62.45	64.24	
4.75	46.5	45.3	-1.2	0.2	0.5	45.15	45.46	
2.36	29.0	28.3	-0.7	0.4	1.5	28.05	28.63	
1.18	18.2	17.2	-1.0	0.5	2.8	16.88	17.55	
0.6	12.8	11.4	-1.5	0.3	2.6	11.14	11.55	
0.3	9.3	7.0	-2.3	0.2	2.2	6.85	7.07	
0.15	6.5	3.9	-2.6	0.1	1.5	3.81	3.89	
0.075	4.3	2.4	-1.9	0.04	1.5	2.39	2.44	

Table C. 17 In-Place Gradation Analysis of 19 mm Limestone with FAA of 50 and Gradation Plotting Above The Restricted Zone Mixtures.

Mixture Name: 19LS50A				Nominal. Max. Size: 19 mm				
Coarse Aggregate Type: Limestone				Gradation: Above the restricted zone				
Fine Aggregate Angularity: 50				AC = 5.8% (-0.1% Design AC)				
Sieve Size (mm)	Design	Washed Sieve Gradation Analysis (no. of sample = 2)						
		Average	Difference	Standard Deviation	C.O.V	No. 1	No. 2	No. 3
25	100.0	100.0	0.0	0.0	0.0	100.00	100.00	
19	96.4	97.2	0.8	2.6	2.6	95.37	98.99	
12.5	84.8	86.5	1.7	7.4	8.5	81.30	91.70	
9.5	77.9	79.0	1.1	6.6	8.3	74.32	83.64	
4.75	57.4	68.6	11.2	5.7	8.3	64.58	72.58	
2.36	37.1	51.5	14.4	4.9	9.5	48.02	54.91	
1.18	24.6	30.8	6.2	2.8	9.0	28.81	32.73	
0.6	17.0	19.4	2.4	1.6	8.1	18.32	20.55	
0.3	11.5	11.7	0.2	0.9	7.8	11.08	12.38	
0.15	8.2	5.9	-2.3	0.5	7.6	5.58	6.21	
0.075	5.7	3.3	-2.4	0.3	9.5	3.07	3.51	

Table C. 18 In-Place Gradation Analysis of 19 mm Granite with FAA of 44, Gradation Plotting Below The Restricted Zone, and +0.1% Design AC Mixtures.

Mixture Name: 19GR44B		Nominal. Max. Size: 19 mm						
Coarse Aggregate Type: Granite		Gradation: Below the restricted zone						
Fine Aggregate Angularity: 44		AC = 4.5% (+0.1% Design AC)						
Sieve Size (mm)	Design	Washed Sieve Gradation Analysis (no. of sample = 3)						
		Average	Difference	Standard Deviation	C.O.V	No. 1	No. 2	No. 3
25	100.0	100.0	0.0	0.0	0.0	100.00	100.00	100.00
19	98.9	99.2	0.3	0.8	0.8	98.44	99.23	100.00
12.5	77.7	76.7	-1.0	5.4	7.0	70.53	79.84	79.76
9.5	58.5	58.0	-0.5	6.2	10.8	50.79	62.22	60.84
4.75	38.2	36.4	-1.8	4.2	11.6	31.51	39.14	38.48
2.36	28.3	24.8	-3.5	1.9	7.7	22.62	26.13	25.70
1.18	17.6	15.6	-2.0	0.8	4.8	14.75	16.13	15.94
0.6	12.8	11.1	-1.7	0.5	4.4	10.53	11.43	11.32
0.3	9.5	8.0	-1.5	0.4	4.9	7.51	8.22	8.14
0.15	6.5	5.6	-0.9	0.3	5.5	5.26	5.80	5.76
0.075	4.2	4.1	-0.1	0.3	6.0	3.84	4.27	4.26

Table C. 19 In-Place Gradation Analysis of 19 mm Granite with FAA of 44, Gradation Plotting Below The Restricted Zone, and +1.2% Design AC Mixtures.

Mixture Name: 19GR44B		Nominal. Max. Size: 19 mm						
Coarse Aggregate Type: Granite		Gradation: Below the restricted zone						
Fine Aggregate Angularity: 44		AC = 5.6% (+1.2% Design AC)						
Sieve Size (mm)	Design	Washed Sieve Gradation Analysis (no. of sample = 3)						
		Average	Difference	Standard Deviation	C.O.V	No. 1	No. 2	No. 3
25	100.0	100.0	0.0	0.0	0.0	100.00	100.00	100.00
19	98.9	98.6	-0.2	1.4	1.4	97.27	100.00	98.64
12.5	77.7	80.2	2.6	2.4	3.0	82.91	79.40	78.34
9.5	58.5	62.4	3.9	1.8	2.9	64.43	60.89	61.90
4.75	38.2	39.9	1.7	0.8	2.1	40.79	39.80	39.14
2.36	28.3	28.1	-0.2	0.3	1.0	28.37	28.10	27.80
1.18	17.6	18.0	0.4	0.2	0.9	18.22	17.92	17.98
0.6	12.8	13.2	0.4	0.1	1.1	13.35	13.08	13.15
0.3	9.5	10.2	0.7	0.1	1.1	10.35	10.13	10.22
0.15	6.5	8.0	1.5	0.1	1.2	8.06	7.88	8.01
0.075	4.2	6.4	2.1	0.1	1.5	6.33	6.19	6.35

Table C. 20 In-Place Gradation Analysis of 19 mm Granite with FAA of 50, Gradation Plotting Through The Restricted Zone, and –0.8% Design AC Mixtures.

Mixture Name: 19GR50T		Nominal. Max. Size: 19 mm						
Coarse Aggregate Type: Granite		Gradation: Below the restricted zone						
Fine Aggregate Angularity: 50		AC = 4.5% (-0.8% Design AC)						
Sieve Size (mm)	Design	Washed Sieve Gradation Analysis (no. of sample = 3)						
		Average	Difference	Standard Deviation	C.O.V	No. 1	No. 2	No. 3
25	100.0	100.0	0.0	0.0	0.0	100.00	100.00	100.00
19	99.6	99.2	-0.4	0.7	0.7	100.00	98.63	99.03
12.5	92.6	89.7	-2.9	6.8	7.6	96.29	90.05	82.72
9.5	83.2	79.6	-3.6	10.1	12.7	89.06	80.85	68.95
4.75	51.7	42.0	-9.6	8.4	20.1	49.85	43.16	33.10
2.36	36.8	25.9	-10.9	3.7	14.3	29.38	26.37	22.03
1.18	23.9	18.9	-5.1	1.9	10.0	20.56	19.14	16.84
0.6	16.8	14.6	-2.2	1.3	9.2	15.82	14.75	13.17
0.3	11.3	10.9	-0.4	1.0	9.3	11.89	11.04	9.86
0.15	8.0	7.5	-0.5	0.7	9.9	8.18	7.57	6.70
0.075	5.5	5.1	-0.4	0.6	11.2	5.61	5.15	4.48

Table C. 21 In-Place Gradation Analysis of 19 mm Granite with FAA of 50, Gradation Plotting Through The Restricted Zone, and +0.1% Design AC Mixtures.

Mixture Name: 19GR50T		Nominal. Max. Size: 19 mm						
Coarse Aggregate Type: Granite		Gradation: Below the restricted zone						
Fine Aggregate Angularity: 50		AC = 5.4% (+0.1% Design AC)						
Sieve Size (mm)	Design	Washed Sieve Gradation Analysis (no. of sample = 3)						
		Average	Difference	Standard Deviation	C.O.V	No. 1	No. 2	No. 3
25	100.0	100.0	0.0	0.0	0.0	100.00	100.00	100.00
19	99.6	99.4	-0.2	0.6	0.6	98.73	99.34	100.00
12.5	92.6	91.1	-1.5	4.2	4.6	88.70	88.77	95.91
9.5	83.2	83.9	0.7	4.4	5.2	81.92	80.81	88.87
4.75	51.7	52.1	0.4	4.2	7.9	51.29	48.38	56.54
2.36	36.8	33.6	-3.2	2.0	5.8	33.20	31.88	35.73
1.18	23.9	23.6	-0.3	0.9	3.8	23.33	22.78	24.53
0.6	16.8	17.2	0.4	0.6	3.4	17.00	16.71	17.84
0.3	11.3	12.4	1.1	0.5	3.6	12.32	12.05	12.93
0.15	8.0	8.6	0.6	0.3	4.0	8.53	8.30	8.97
0.075	5.5	5.8	0.4	0.3	4.4	5.81	5.58	6.10

Table C. 22 In-Place Gradation Analysis of 9.5 mm Limestone with FAA of 44, Gradation Plotting Through The Restricted Zone, and –0.6% Design AC Mixtures.

Mixture Name: 9.5LS44T		Nominal. Max. Size: 9.5 mm						
Coarse Aggregate Type: Limestone		Gradation: Through the restricted zone						
Fine Aggregate Angularity: 44		AC = 5.6% (-0.6% Design AC)						
Sieve Size (mm)	Design	Washed Sieve Gradation Analysis (no. of sample = 3)						
		Average	Difference	Standard Deviation	C.O.V	No. 1	No. 2	No. 3
12.5	100.0	100.0	0.0	0.0	0.0	100.00	100.00	100.00
9.5	99.0	99.8	0.8	0.0	0.0	99.78	99.76	99.71
4.75	83.0	85.0	2.0	0.7	0.9	85.22	84.17	85.57
2.36	55.8	58.1	2.3	1.0	1.7	58.28	57.06	59.04
1.18	33.3	34.9	1.6	0.4	1.1	35.18	34.51	35.13
0.6	21.6	21.8	0.2	0.3	1.3	22.08	21.53	21.77
0.3	14.2	11.1	-3.1	0.2	1.8	11.35	10.98	11.02
0.15	8.4	4.9	-3.5	0.2	4.9	5.20	4.79	4.78
0.075	5.3	3.1	-2.2	0.3	9.8	3.46	2.96	2.91

Table C. 23 In-Place Gradation Analysis of 9.5 mm Limestone with FAA of 44, Gradation Plotting Through The Restricted Zone, and +0.1% Design AC Mixtures.

Mixture Name: 9.5LS44T		Nominal. Max. Size: 9.5 mm						
Coarse Aggregate Type: Limestone		Gradation: Through the restricted zone						
Fine Aggregate Angularity: 44		AC = 6.3% (+0.1% Design AC)						
Sieve Size (mm)	Design	Washed Sieve Gradation Analysis (no. of sample = 3)						
		Average	Difference	Standard Deviation	C.O.V	No. 1	No. 2	No. 3
12.5	100.0	100.0	0.0	0.0	0.0	100.00	100.00	
9.5	99.0	99.7	0.7	0.1	0.1	99.72	99.62	
4.75	83.0	84.1	1.1	0.2	0.3	83.94	84.27	
2.36	55.8	55.3	-0.5	0.3	0.6	55.08	55.53	
1.18	33.3	32.0	-1.3	0.4	1.1	31.77	32.27	
0.6	21.6	20.2	-1.5	0.5	2.3	19.85	20.51	
0.3	14.2	12.2	-2.0	0.5	4.4	11.78	12.54	
0.15	8.4	7.5	-0.9	0.6	7.9	7.04	7.87	
0.075	5.3	5.6	0.3	0.6	11.1	5.12	5.99	

Table C. 24 In-Place Gradation Analysis of 9.5 mm Limestone with FAA of 50, Gradation Plotting Through The Restricted Zone, and –0.6% Design AC Mixtures.

Mixture Name: 9.5LS50T		Nominal. Max. Size: 9.5 mm						
Coarse Aggregate Type: Limestone		Gradation: Through the restricted zone						
Fine Aggregate Angularity: 50		AC = 6.0% (-0.6% Design AC)						
Sieve Size (mm)	Design	Washed Sieve Gradation Analysis (no. of sample = 3)						
		Average	Difference	Standard Deviation	C.O.V	No. 1	No. 2	No. 3
12.5	100.0	100.0	0.0	0.0	0.0	100.00	100.00	100.00
9.5	98.6	99.9	1.4	0.1	0.1	100.00	100.00	99.82
4.75	75.5	84.7	9.2	0.9	1.0	84.91	85.38	83.73
2.36	48.3	55.5	7.2	0.8	1.4	55.42	56.37	54.79
1.18	31.8	38.1	6.3	0.4	1.1	37.85	38.55	37.86
0.6	21.7	26.7	5.0	0.3	0.9	26.42	26.92	26.66
0.3	14.6	16.2	1.7	0.5	2.8	15.72	16.46	16.53
0.15	10.3	10.6	0.3	0.6	5.8	9.85	10.87	10.93
0.075	7.0	7.8	0.7	0.7	8.6	6.98	8.10	8.17

Table C. 25 In-Place Gradation Analysis of 9.5 mm Limestone with FAA of 50, Gradation Plotting Through The Restricted Zone, and +0.2% Design AC Mixtures.

Mixture Name: 9.5LS50T		Nominal. Max. Size: 9.5 mm						
Coarse Aggregate Type: Limestone		Gradation: Through the restricted zone						
Fine Aggregate Angularity: 50		AC = 6.8% (+0.2% Design AC)						
Sieve Size (mm)	Design	Washed Sieve Gradation Analysis (no. of sample = 3)						
		Average	Difference	Standard Deviation	C.O.V	No. 1	No. 2	No. 3
12.5	100.0	100.0	0.0	0.0	0.0	100.00	100.00	100.00
9.5	98.6	100.0	1.4	0.0	0.0	100.00	100.00	100.00
4.75	75.5	82.4	6.9	0.8	1.0	81.89	82.05	83.37
2.36	48.3	52.0	3.7	0.6	1.1	51.51	51.89	52.63
1.18	31.8	36.0	4.2	0.2	0.6	35.95	35.89	36.28
0.6	21.7	25.6	3.9	0.1	0.4	25.63	25.44	25.62
0.3	14.6	16.2	1.6	0.1	0.5	16.29	16.14	16.23
0.15	10.3	11.0	0.7	0.1	0.5	11.06	10.97	11.03
0.075	7.0	8.4	1.4	0.1	0.7	8.43	8.35	8.47

Table C. 26 In-Place Gradation Analysis of 9.5 mm Granite with FAA of 44, Gradation Plotting Below The Restricted Zone, and Design AC Mixtures.

Mixture Name: 9.5GR44B		Nominal. Max. Size: 9.5 mm						
Coarse Aggregate Type: Granite		Gradation: Below the restricted zone						
Fine Aggregate Angularity: 44		AC = 5.2% (Design AC)						
Sieve Size (mm)	Design	Washed Sieve Gradation Analysis (no. of sample = 3)						
		Average	Difference	Standard Deviation	C.O.V	No. 1	No. 2	No. 3
12.5	100.0	100.0	0.0	0.0	0.0	100.00	100.00	100.00
9.5	95.0	97.2	2.2	0.9	0.9	98.10	97.13	96.32
4.75	61.5	66.6	5.1	2.5	3.7	68.58	67.27	63.82
2.36	41.9	48.3	6.4	1.4	2.8	49.75	48.13	47.05
1.18	24.9	30.6	5.7	0.6	2.1	31.09	30.77	29.85
0.6	17.0	19.8	2.8	0.4	1.9	20.09	19.91	19.37
0.3	11.7	10.5	-1.2	0.3	2.6	10.68	10.64	10.18
0.15	7.3	4.8	-2.5	0.2	4.8	4.93	4.98	4.56
0.075	4.7	3.3	-1.4	0.2	6.4	3.40	3.42	3.05

Table C. 27 In-Place Gradation Analysis of 9.5 mm Granite with FAA of 44, Gradation Plotting Below The Restricted Zone, and +0.1% Design AC Mixtures.

Mixture Name: 9.5GR44B		Nominal. Max. Size: 9.5 mm						
Coarse Aggregate Type: Granite		Gradation: Below the restricted zone						
Fine Aggregate Angularity: 44		AC = 5.3% (+0.1%Design AC)						
Sieve Size (mm)	Design	Washed Sieve Gradation Analysis (no. of sample = 3)						
		Average	Difference	Standard Deviation	C.O.V	No. 1	No. 2	No. 3
12.5	100.0	100.0	0.0	0.0	0.0	100.00	100.00	100.00
9.5	95.0	96.0	0.1	0.6	0.6	96.00	96.52	95.43
4.75	61.5	63.0	1.5	2.3	3.7	61.41	61.89	65.65
2.36	41.9	43.6	1.7	1.1	2.5	43.21	42.76	44.79
1.18	24.9	25.8	0.8	0.4	1.5	25.63	25.44	26.18
0.6	17.0	15.5	-1.5	0.1	0.4	15.50	15.42	15.56
0.3	11.7	7.8	-3.9	0.02	0.3	7.83	7.83	7.80
0.15	7.3	3.7	-3.6	0.02	0.6	3.73	3.73	3.69
0.075	4.7	2.6	-2.1	0.02	0.7	2.58	2.60	2.57

Table C. 28 In-Place Gradation Analysis of 9.5 mm Granite with FAA of 50, Gradation Plotting Below The Restricted Zone, and -0.1% Design AC Mixtures.

Mixture Name: 9.5GR50B		Nominal. Max. Size: 9.5 mm						
Coarse Aggregate Type: Granite		Gradation: Below the restricted zone						
Fine Aggregate Angularity: 50		AC = 5.5% (-0.1%Design AC)						
Sieve Size (mm)	Design	Washed Sieve Gradation Analysis (no. of sample = 3)						
		Average	Difference	Standard Deviation	C.O.V	No. 1	No. 2	No. 3
12.5	100.0	100.0	0.0	0.0	0.0	100.00	100.00	100.00
9.5	94.7	95.9	1.2	0.9	0.9	95.03	96.74	95.98
4.75	58.7	56.9	-1.8	0.5	0.9	57.16	56.27	57.20
2.36	41.1	37.1	-4.0	0.1	0.4	37.23	36.95	37.09
1.18	26.8	25.9	-0.9	0.1	0.3	25.95	25.81	25.89
0.6	18.8	18.5	-0.3	0.1	0.6	18.47	18.45	18.65
0.3	12.7	12.6	-0.1	0.1	0.6	12.58	12.57	12.70
0.15	8.9	8.6	-0.3	0.1	0.6	8.58	8.57	8.67
0.075	6.1	6.1	0.0	0.04	0.7	6.09	6.01	6.09

Table C. 29 In-Place Gradation Analysis of 9.5 mm Granite with FAA of 50, Gradation Plotting Below The Restricted Zone, and +0.6% Design AC Mixtures.

Mixture Name: 9.5GR50B		Nominal. Max. Size: 9.5 mm						
Coarse Aggregate Type: Granite		Gradation: Below the restricted zone						
Fine Aggregate Angularity: 50		AC = 6.2% (+0.6%Design AC)						
Sieve Size (mm)	Design	Washed Sieve Gradation Analysis (no. of sample = 3)						
		Average	Difference	Standard Deviation	C.O.V	No. 1	No. 2	No. 3
12.5	100.0	100.0	0.0	0.0	0.0	100.00	100.00	100.00
9.5	94.7	97.5	2.8	1.4	1.4	96.31	97.30	98.98
4.75	58.7	59.9	1.2	2.9	4.8	56.72	60.81	62.26
2.36	41.1	38.4	-2.7	1.0	2.7	37.18	38.86	39.07
1.18	26.8	27.3	0.5	0.6	2.2	26.64	27.54	27.75
0.6	18.8	20.5	1.7	0.5	2.5	19.88	20.68	20.86
0.3	12.7	15.7	3.0	0.5	2.9	15.17	15.88	16.01
0.15	8.9	11.9	2.9	0.4	3.1	11.45	12.01	12.14
0.075	6.1	8.5	2.4	0.3	3.3	8.17	8.60	8.69

Table C. 30 In-Place Gradation Analysis of Superpave Intermediate Layer

Mixture Name: Intermediate Layer		Nominal. Max. Size: 12.5 mm						
Coarse Aggregate Type: Limestone		Gradation:						
Fine Aggregate Angularity:		AC = 5.2%						
Sieve Size (mm)	Design	Washed Sieve Gradation Analysis (no. of sample = 3)						
		Average	Difference	Standard Deviation	C.O.V	No. 1	No. 2	No. 3
19		100.0		0.0	0.0	100.0	100.0	100.0
12.5		94.4		1.5	1.6	96.1	94.1	93.1
9.5		85.5		1.4	1.6	86.7	83.9	85.8
4.75		55.8		1.3	2.3	56.1	54.5	57.0
2.36		39.8		0.6	1.5	40.2	39.2	40.2
1.18		28.6		0.5	1.7	28.9	28.0	28.8
0.6		19.3		0.3	1.3	19.6	19.1	19.4
0.3		9.0		0.1	1.4	9.1	8.9	9.0
0.15		4.3		0.1	2.3	4.4	4.2	4.2
0.075		3.0		0.1	2.4	3.1	2.9	2.9

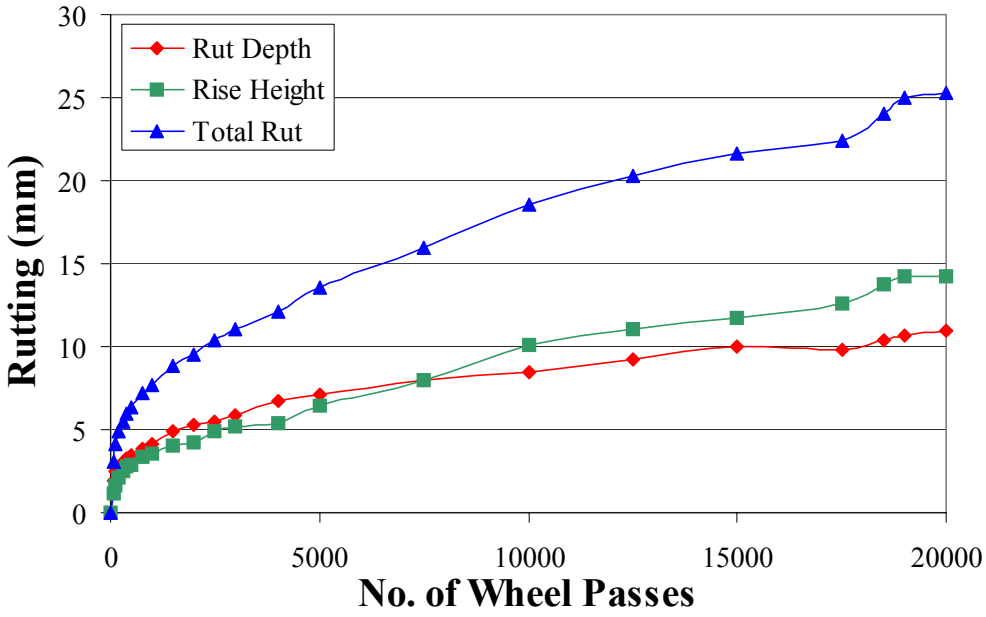

Figure C. 1 No Wander Rutting for 19 mm Limestone with FAA of 39, Gradation Plotting Below The Restricted Zone, Low Density Lane.

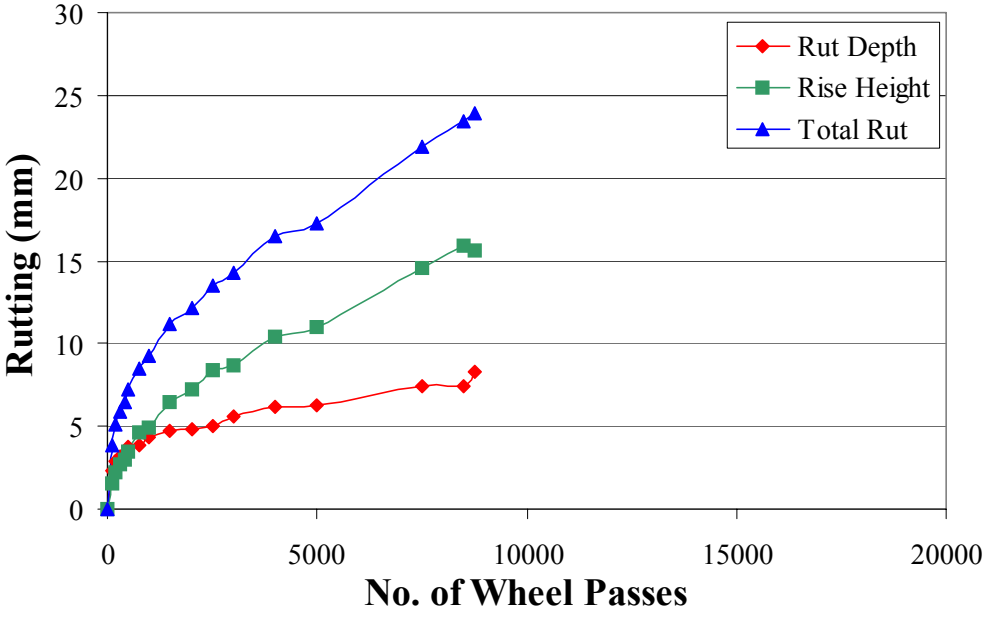

Figure C. 2 No Wander Rutting for 19 mm Limestone with FAA of 39, Gradation Plotting Below The Restricted Zone, High Density Lane.

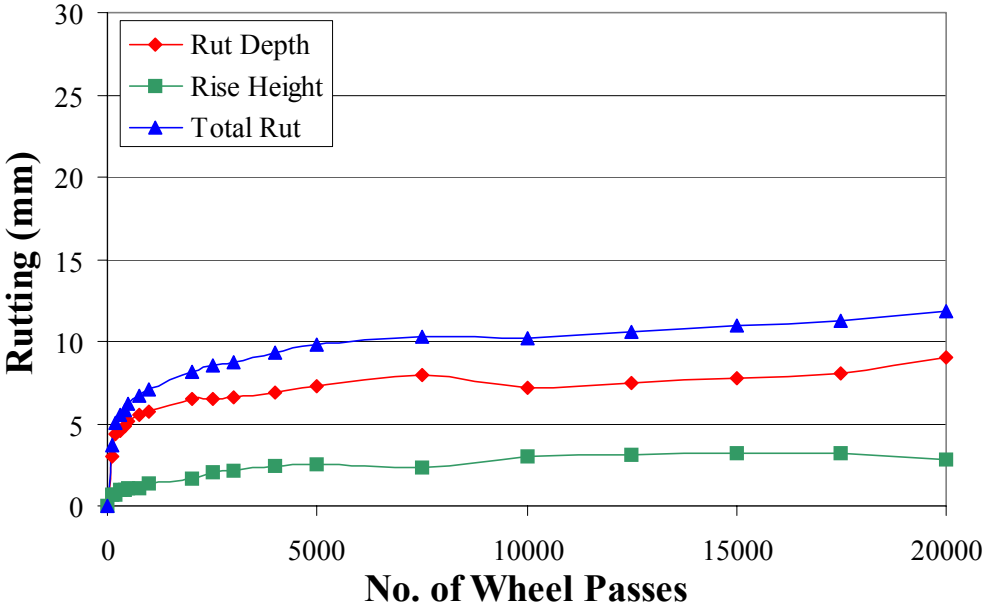

Figure C. 3 No Wander Rutting for 19 mm Limestone with FAA of 44, Gradation Plotting Above The Restricted Zone, Low Density Lane.

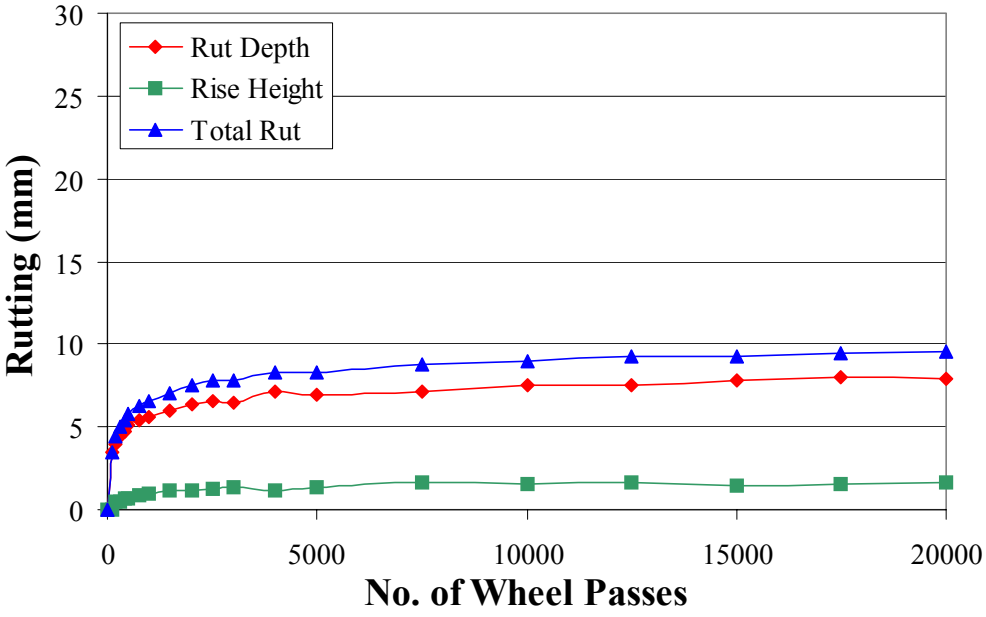

Figure C. 4 No Wander Rutting for 19 mm Limestone with FAA of 44, Gradation Plotting Above The Restricted Zone, High Density Lane.

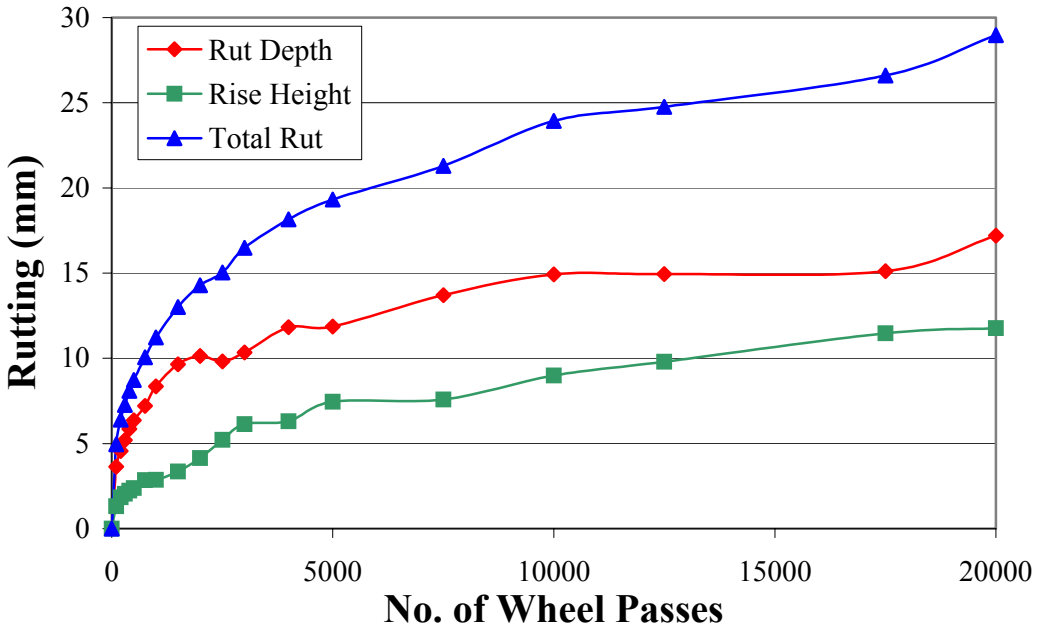

Figure C. 5 No Wander Rutting for 19 mm Limestone with FAA of 44, Gradation Plotting Below The Restricted Zone, Low Density Lane.

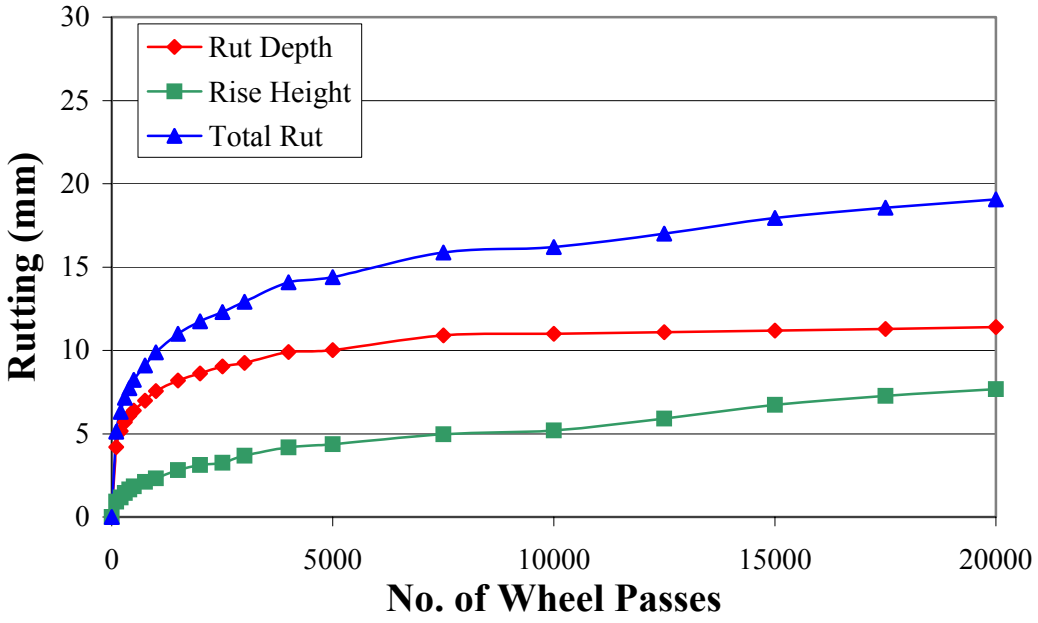

Figure C. 6 No Wander Rutting for 19 mm Limestone with FAA of 44, Gradation Plotting The Below Restricted Zone, High Density Lane.

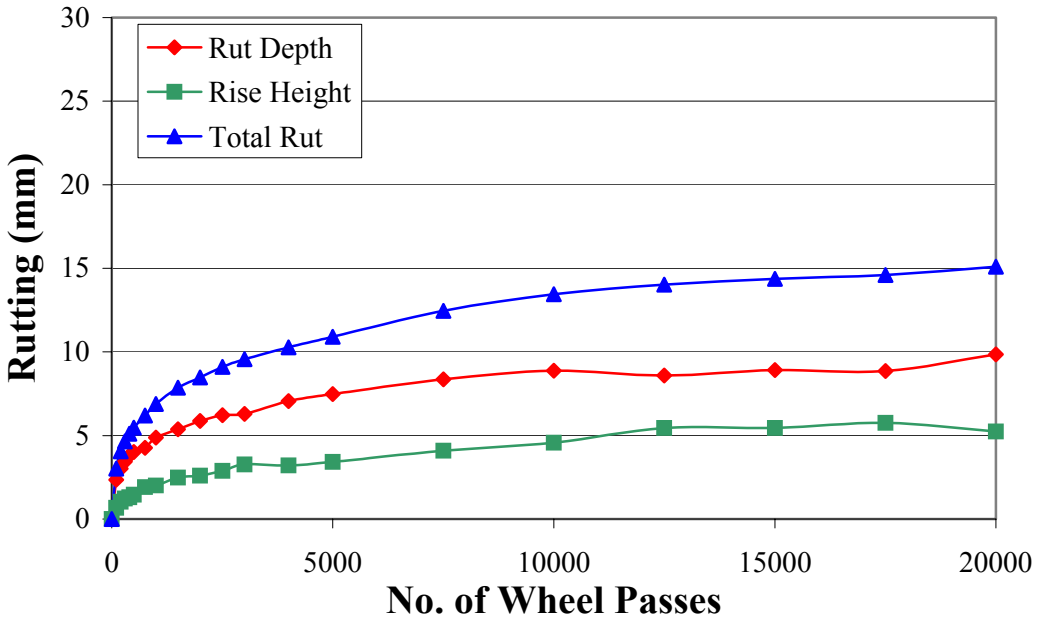

Figure C. 7 No Wander Rutting for 19 mm Limestone with FAA of 50, Gradation Plotting Above The Restricted Zone, Low Density Lane.

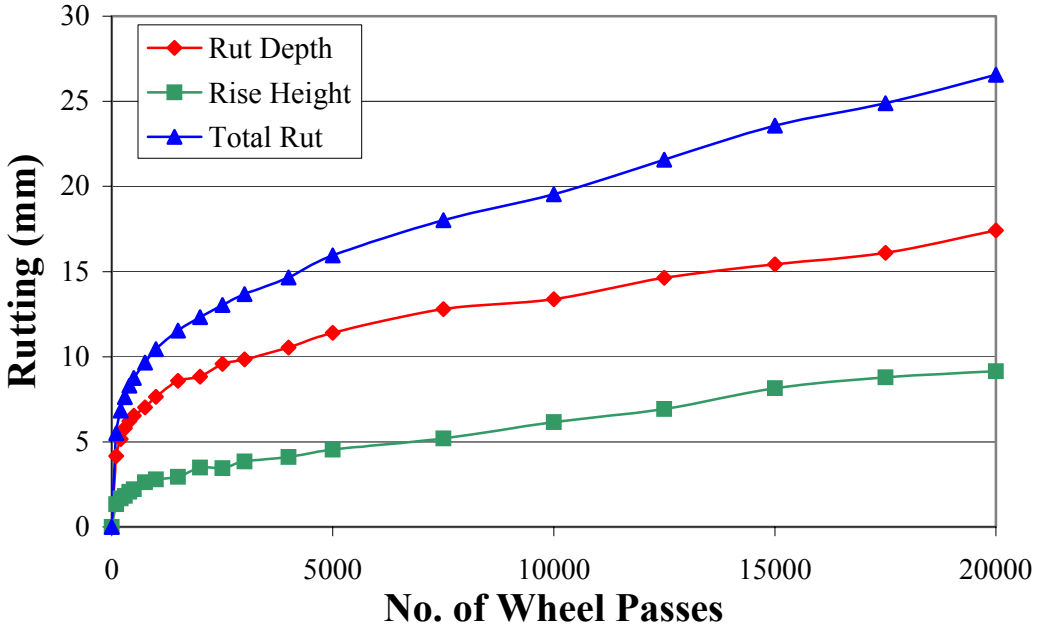

Figure C. 8 No Wander Rutting for 19 mm Limestone with FAA of 50, Gradation Plotting Above The Restricted Zone, High Density Lane.

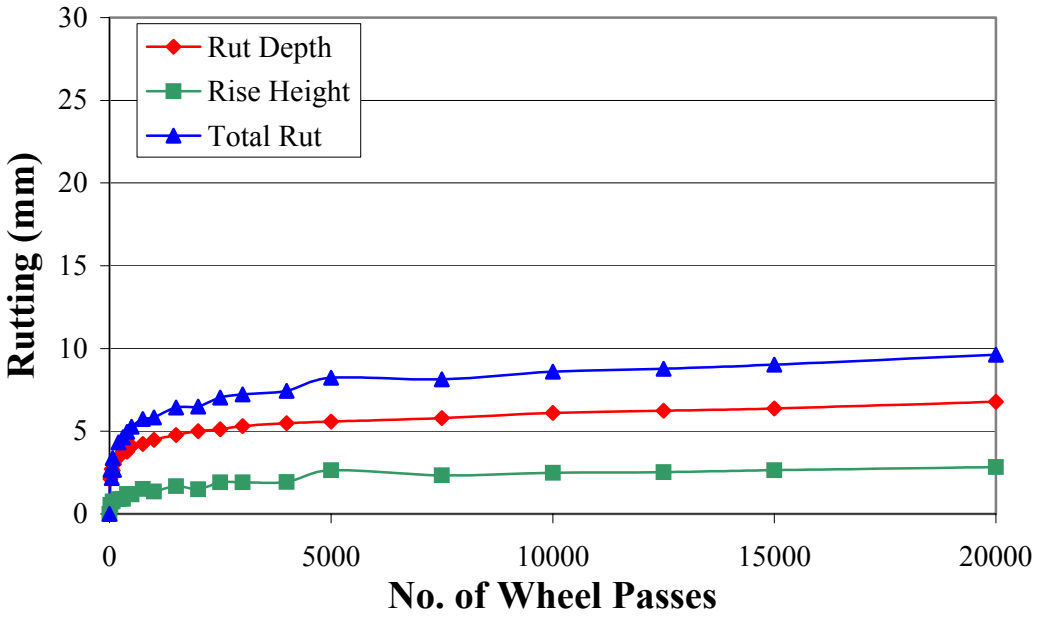

Figure C. 9 No Wander Rutting for 19 mm Granite with FAA of 44, Gradation Plotting Below The Restricted Zone, +0.1% Design AC Lane.

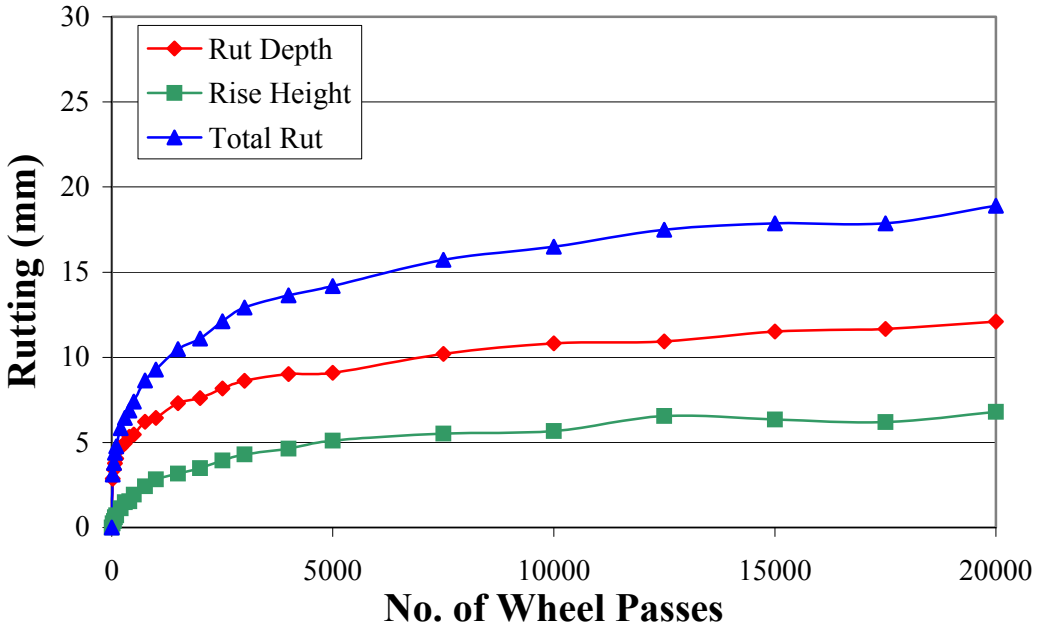

Figure C. 10 No Wander Rutting for 19 mm Granite with FAA of 44, Gradation Plotting Below The Restricted Zone, +1.2% Design AC Lane.

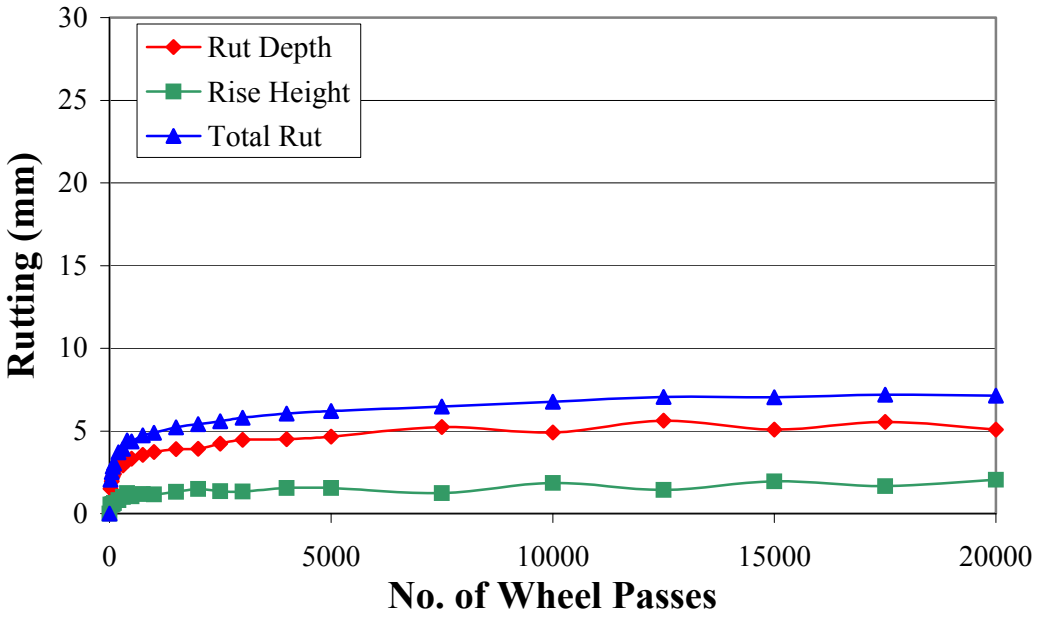

Figure C. 11 No Wander Rutting for 19 mm Granite with FAA of 50, Gradation Plotting Through The Restricted Zone, -0.8% Design AC Lane.

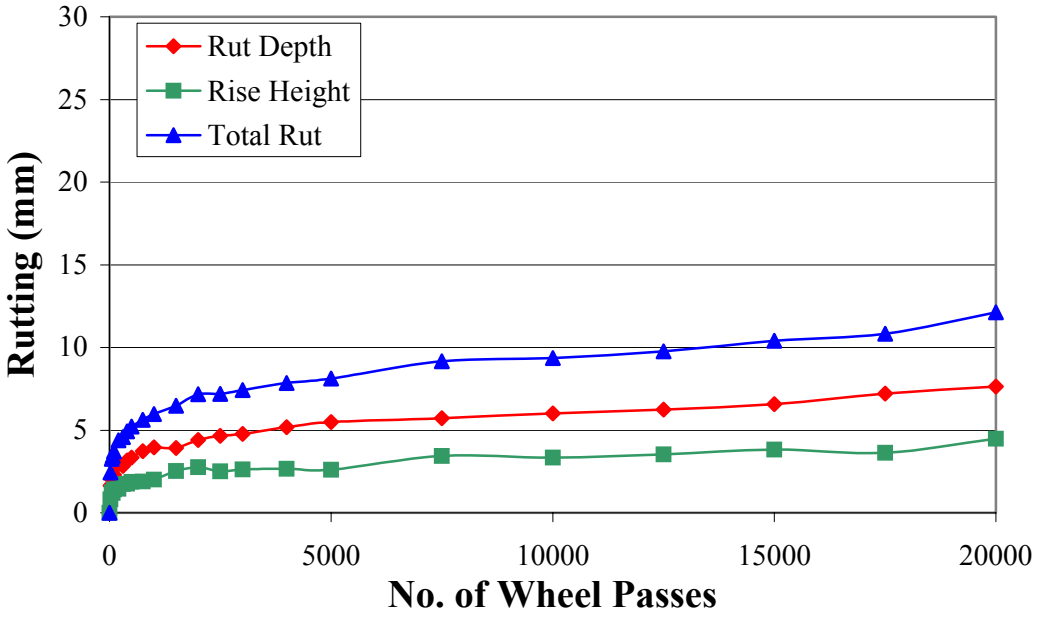

Figure C. 12 No Wander Rutting for 19 mm Granite with FAA of 50, Gradation Plotting Through The Restricted Zone, +0.1% Design AC Lane.

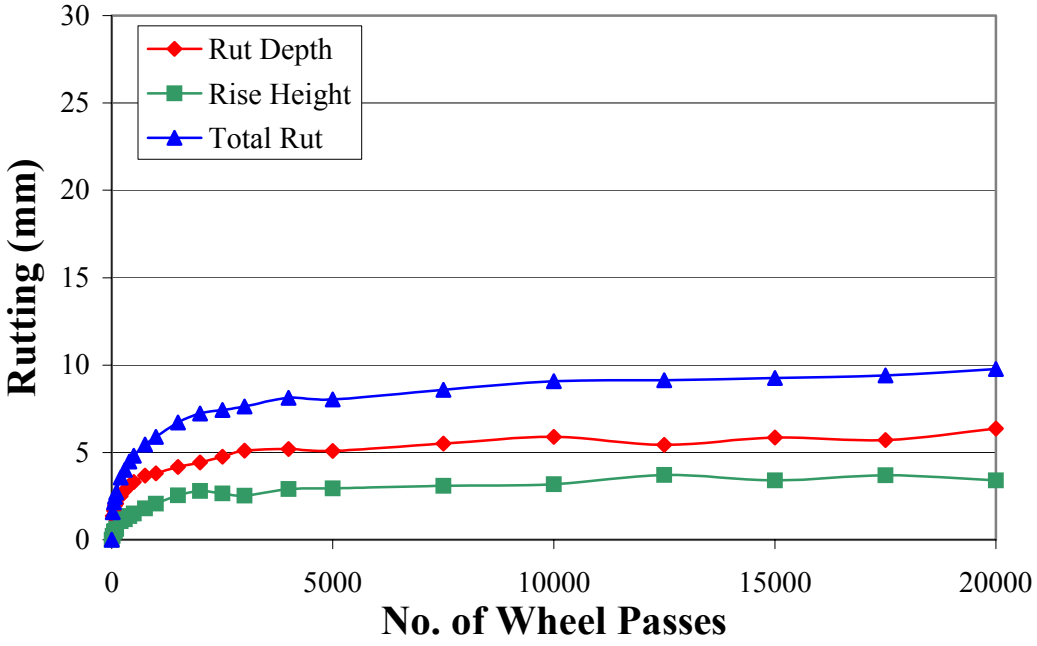

Figure C. 13 No Wander Rutting for 9.5 mm Limestone with FAA of 44, Gradation Plotting Through The Restricted Zone, -0.6% Design AC, on Top of Intermediate Layer Lane.

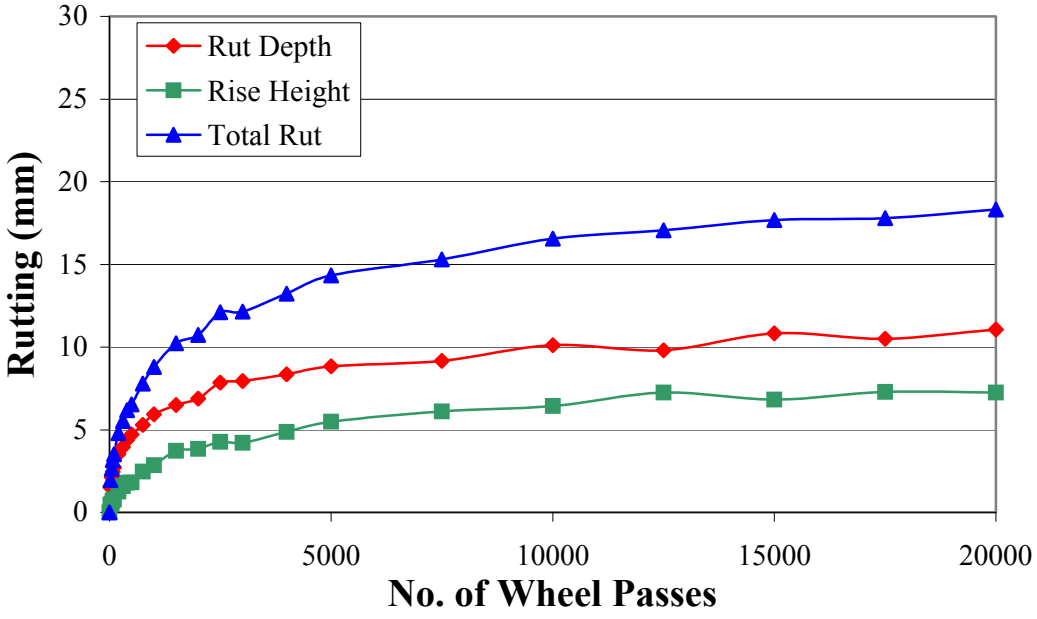

Figure C. 14 No Wander Rutting for 9.5 mm Limestone with FAA of 44, Gradation Plotting Through The Restricted Zone, +0.1% Design AC, on Top of Intermediate Layer Lane.

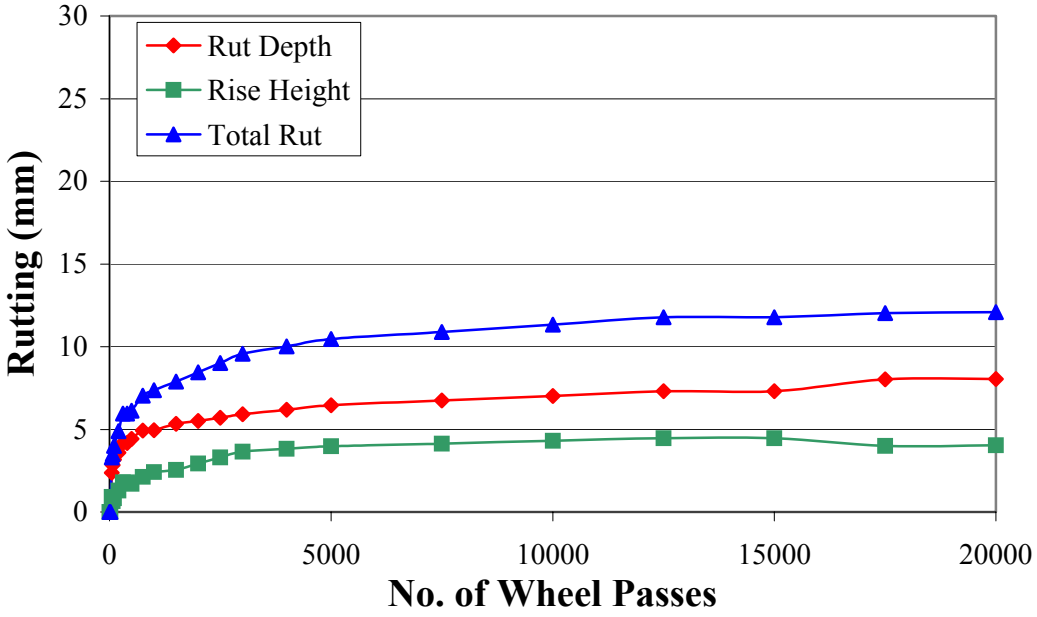

Figure C. 15 No Wander Rutting for 9.5 mm Limestone with FAA of 44, Gradation Plotting Through The Restricted Zone, -0.6% Design AC, on Top of 9.5 mm Layer Lane.

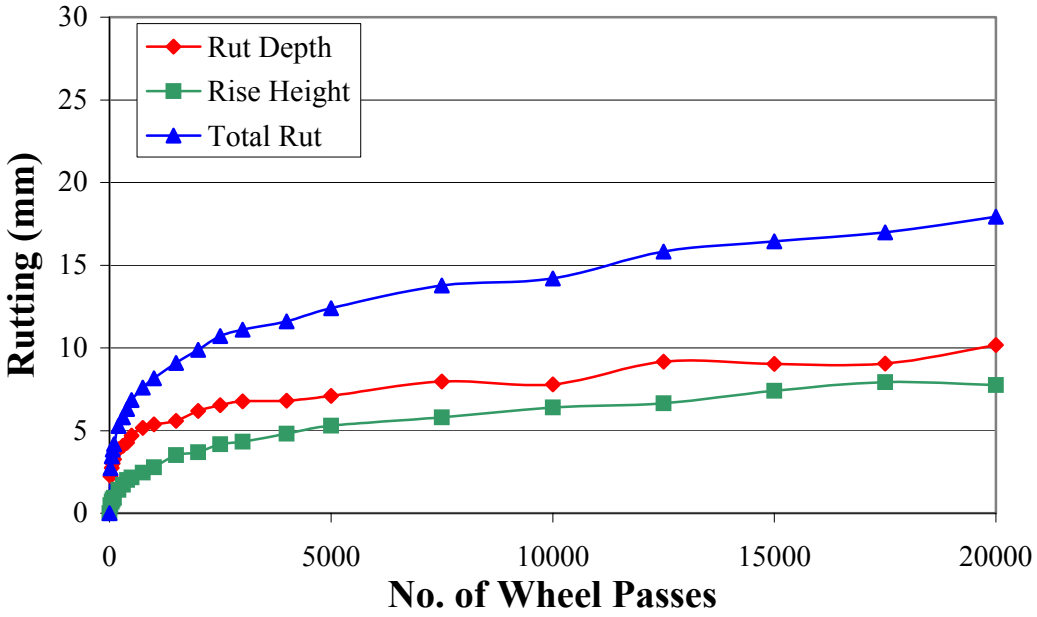

Figure C. 16 No Wander Rutting for 9.5 mm Limestone with FAA of 44, Gradation Plotting Through The Restricted Zone, +0.1% Design AC, on Top of 9.5 mm Layer Lane.

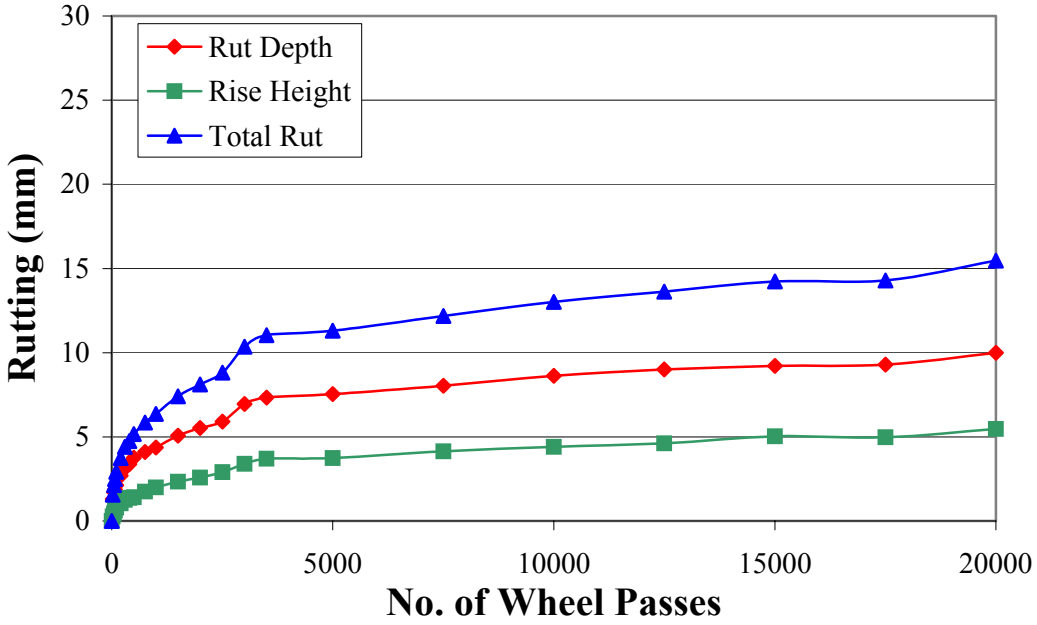

Figure C. 17 No Wander Rutting for 9.5 mm Limestone with FAA of 50, Gradation Plotting Through The Restricted Zone, -0.6% Design AC, on Top of Intermediate Layer Lane.

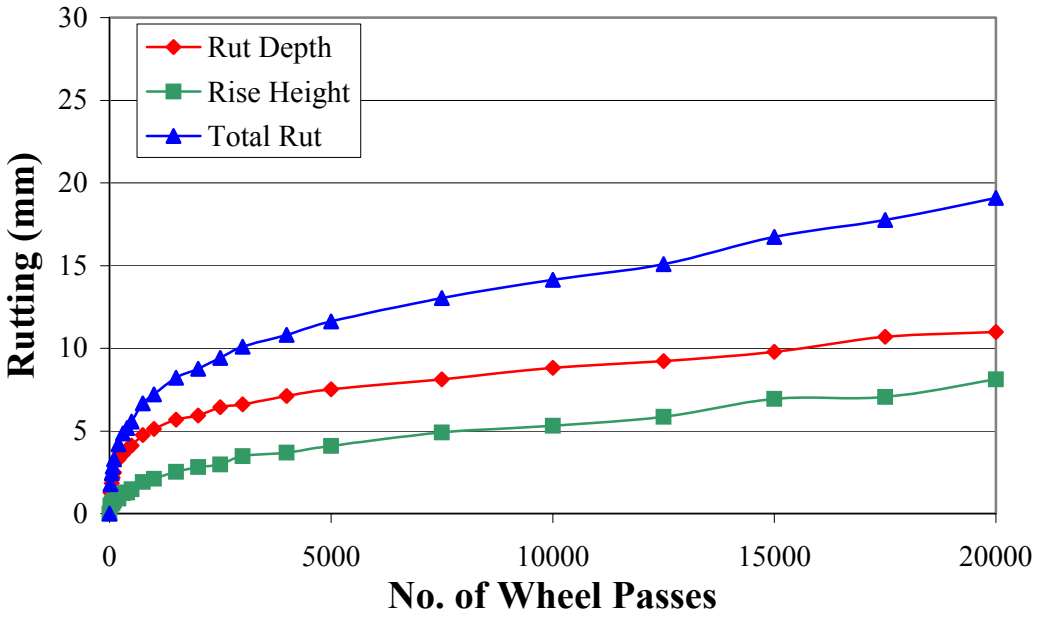

Figure C. 18 No Wander Rutting for 9.5 mm Limestone with FAA of 50, Gradation Plotting Through The Restricted Zone, +0.2% Design AC, on Top of Intermediate Layer Lane.

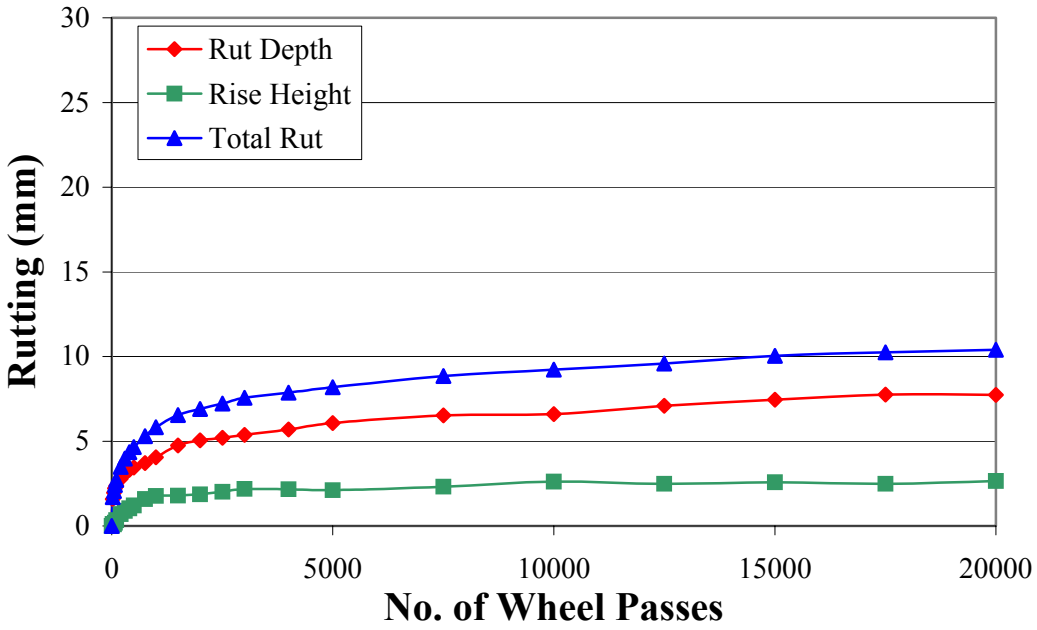

Figure C. 19 No Wander Rutting for 9.5 mm Limestone with FAA of 50, Gradation Plotting Through The Restricted Zone, -0.6% Design AC, on Top of 9.5 mm Layer Lane.

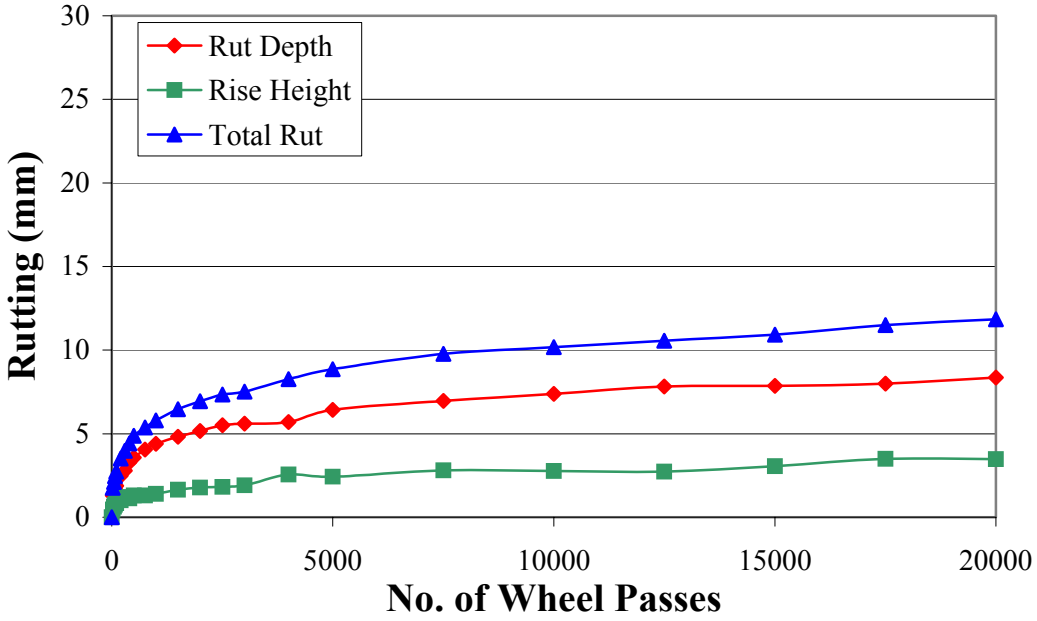

Figure C. 20 No Wander Rutting for 9.5 mm Limestone with FAA of 50, Gradation Plotting Through The Restricted Zone, +0.2% Design AC, on Top of 9.5 mm Layer Lane.

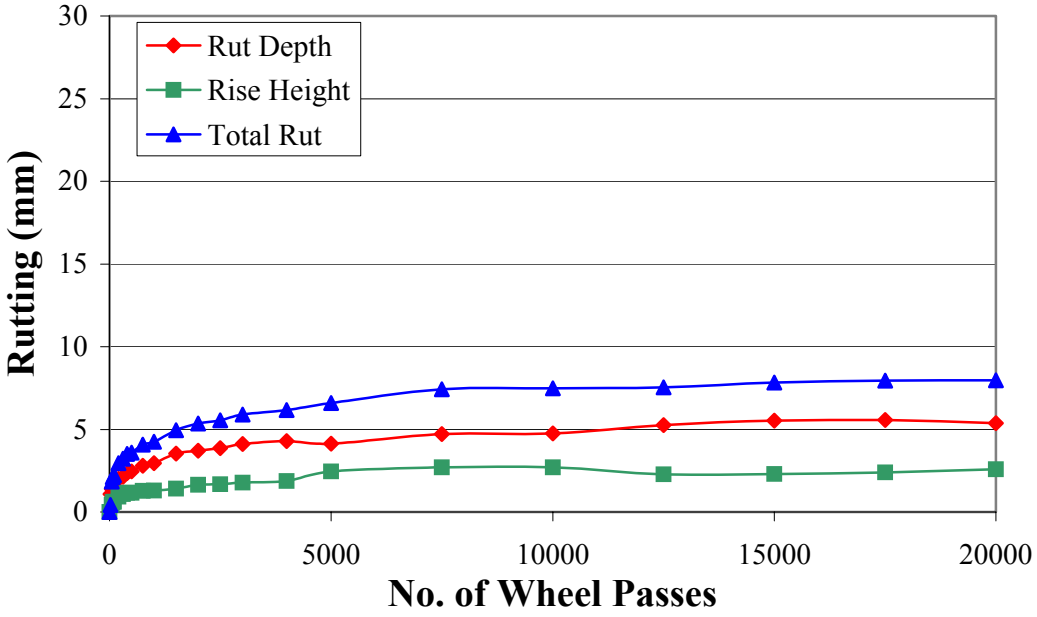

Figure C. 21 No Wander Rutting for 9.5 mm Granite with FAA of 44, Gradation Plotting Below The Restricted Zone, Design AC, on Top of Intermediate Layer Lane.

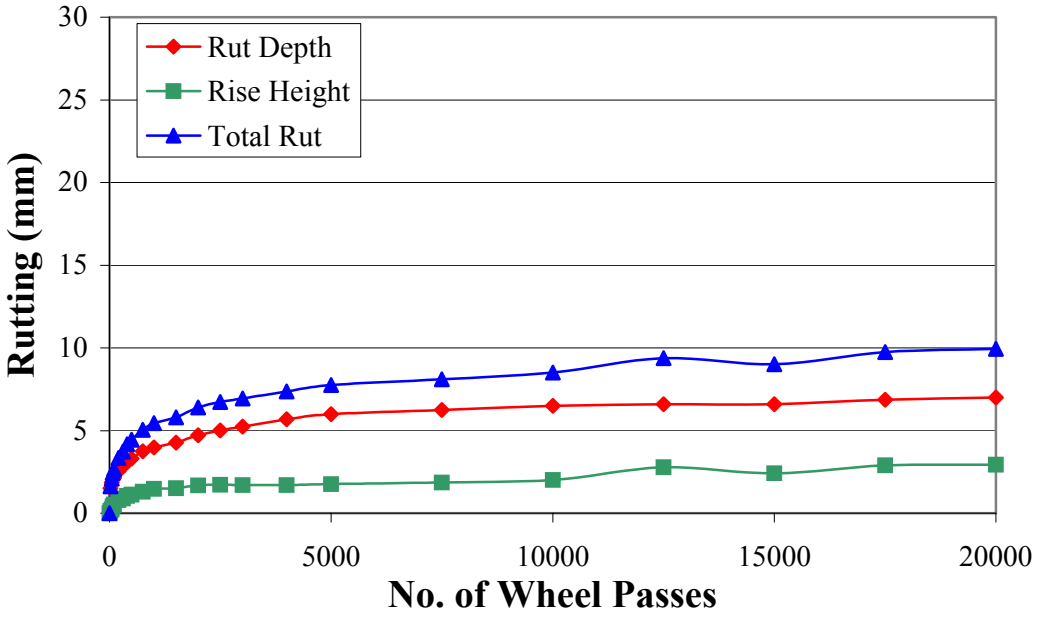

Figure C. 22 No Wander Rutting for 9.5 mm Granite with FAA of 44, Gradation Plotting Below The Restricted Zone, +0.1%Design AC, on Top of Intermediate Layer Lane

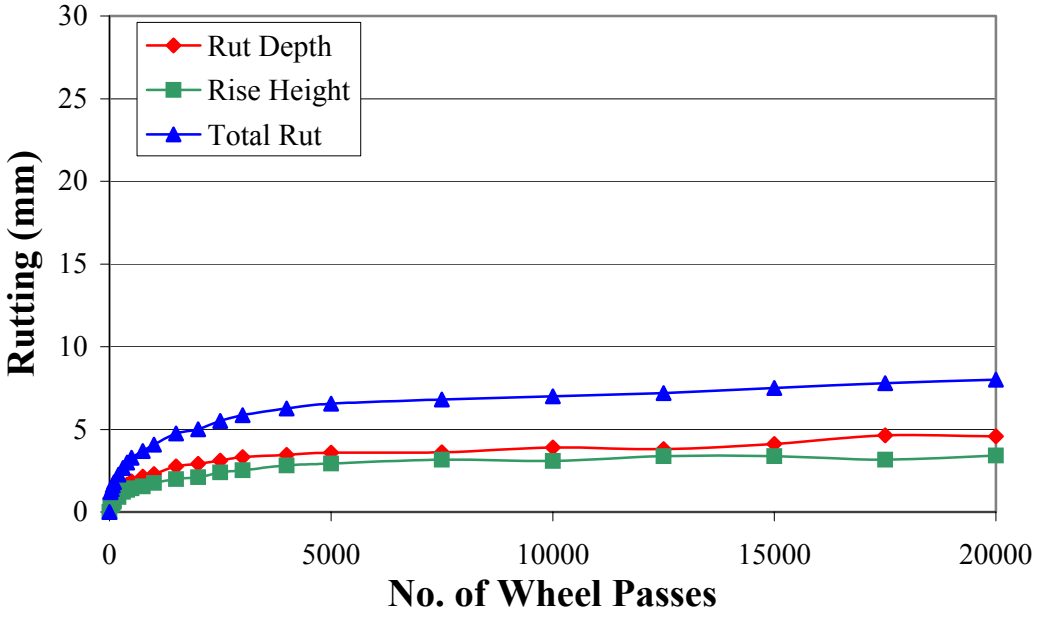

Figure C. 23 No Wander Rutting for 9.5 mm Granite with FAA of 44, Gradation Plotting Below The Restricted Zone, Design AC, on Top of 9.5 mm Layer Lane.

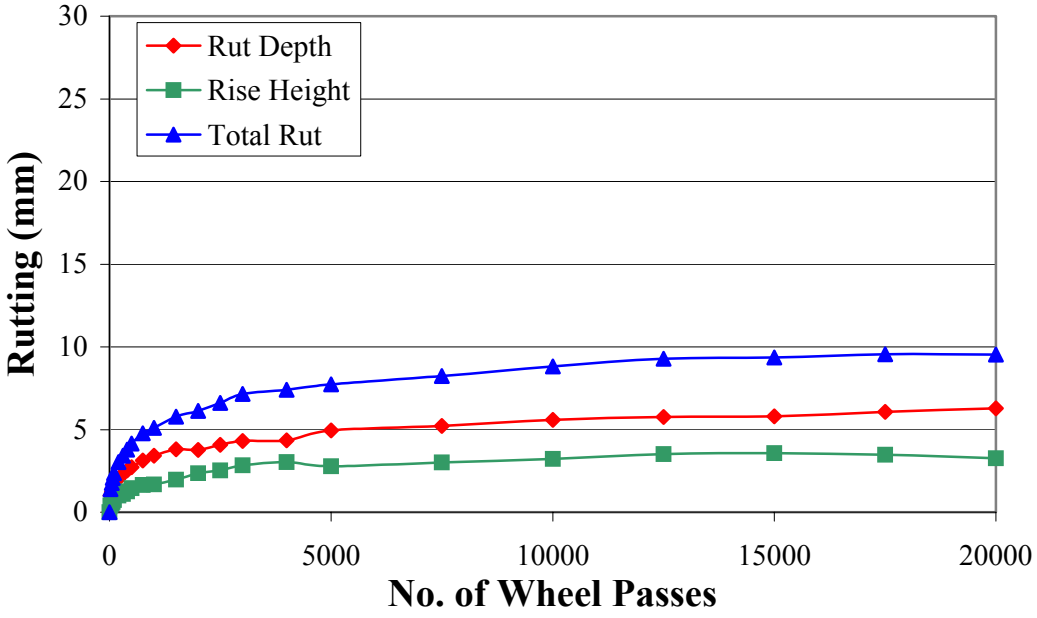

Figure C. 24 No Wander Rutting for 9.5 mm Granite with FAA of 44, Gradation Plotting Below The Restricted Zone, +0.1%Design AC, on Top of 9.5 mm Layer Lane.

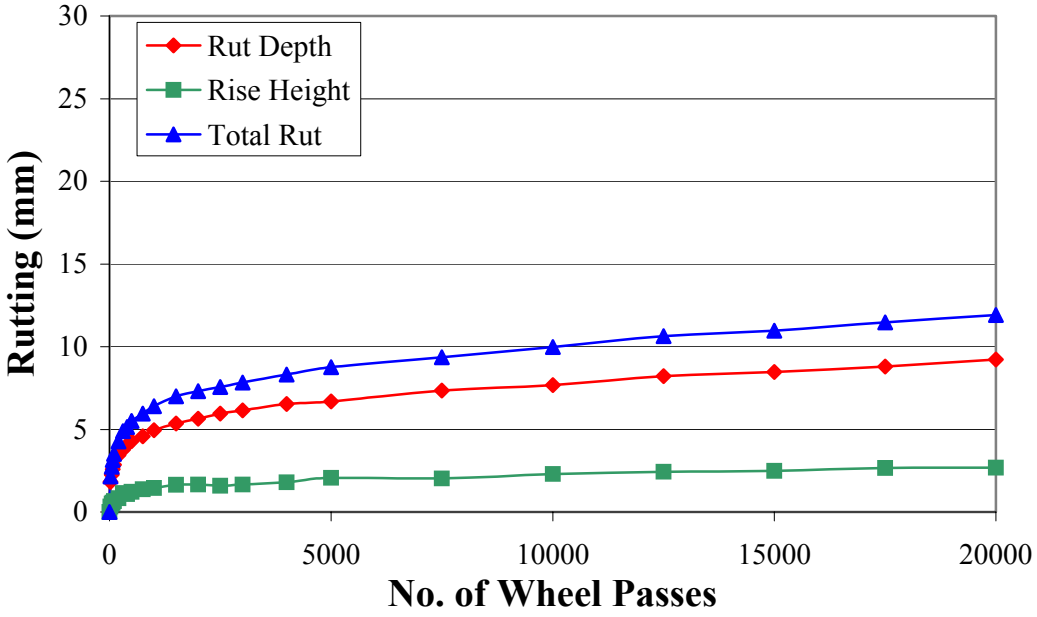

Figure C. 25 No Wander Rutting for 9.5 mm Granite with FAA of 50, Gradation Plotting Below The Restricted Zone, -0.1% Design AC, on Top of Intermediate Layer Lane.

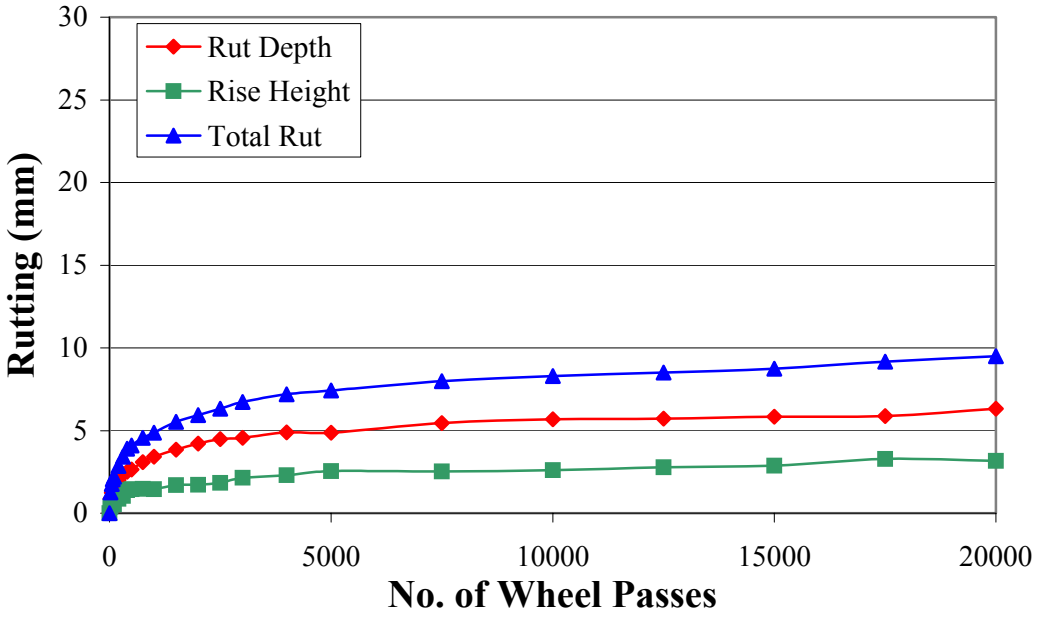

Figure C. 26 No Wander Rutting for 9.5 mm Granite with FAA of 50, Gradation Plotting Below The Restricted Zone, +0.6% Design AC, on Top of Intermediate Layer Lane.

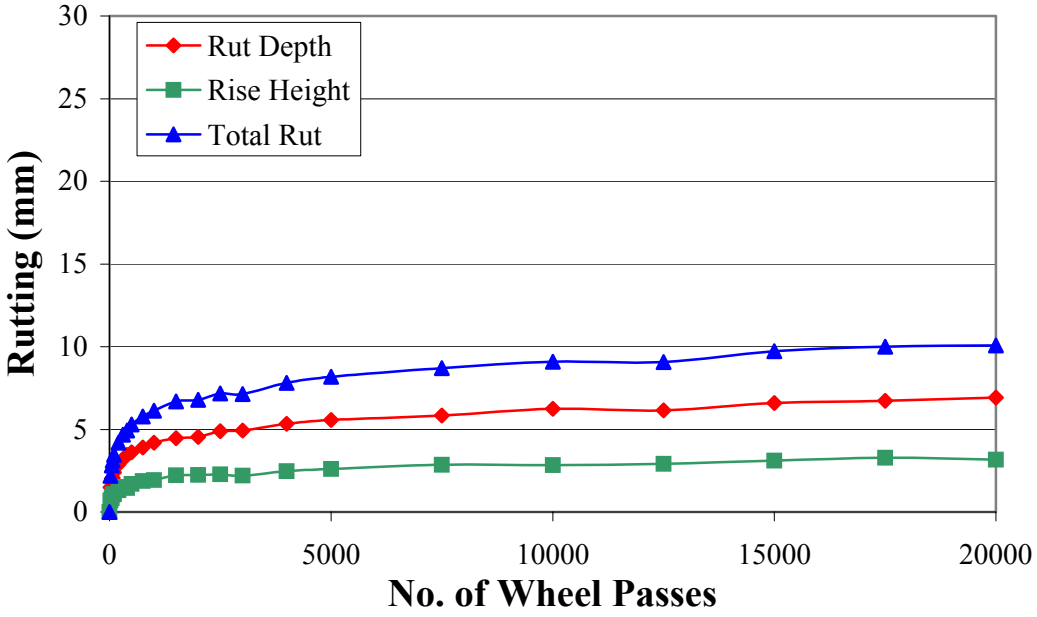

Figure C. 27 No Wander Rutting for 9.5 mm Granite with FAA of 50, Gradation Plotting Below The Restricted Zone, -0.1% Design AC, on Top of 9.5 mm Layer Lane.

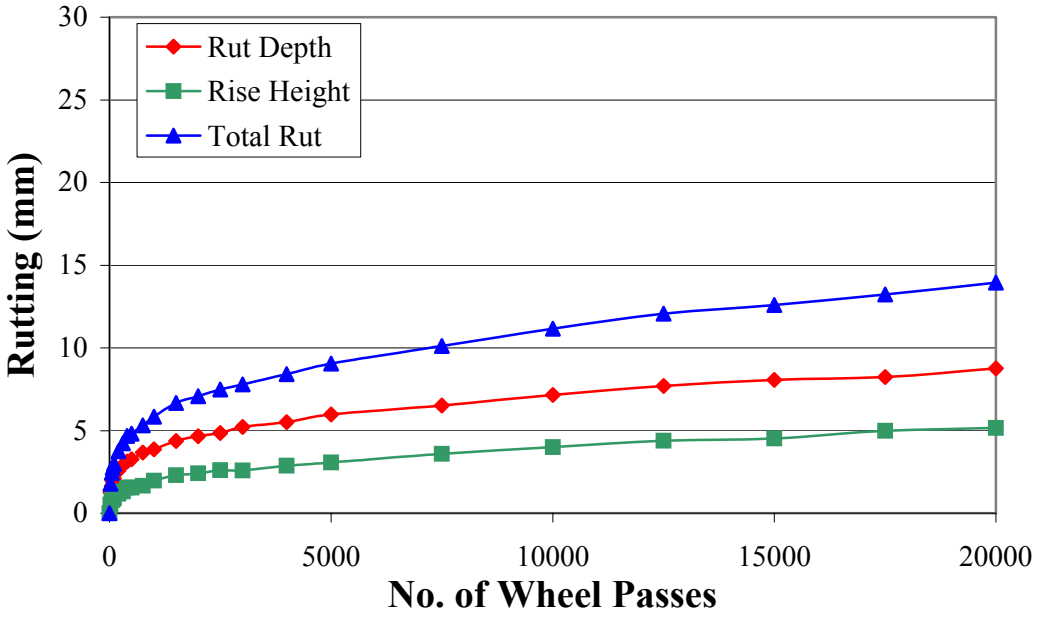

Figure C. 28 No Wander Rutting for 9.5 mm Granite with FAA of 50, Gradation Plotting Below The Restricted Zone, +0.6% Design AC, on Top of 9.5 mm Layer Lane.

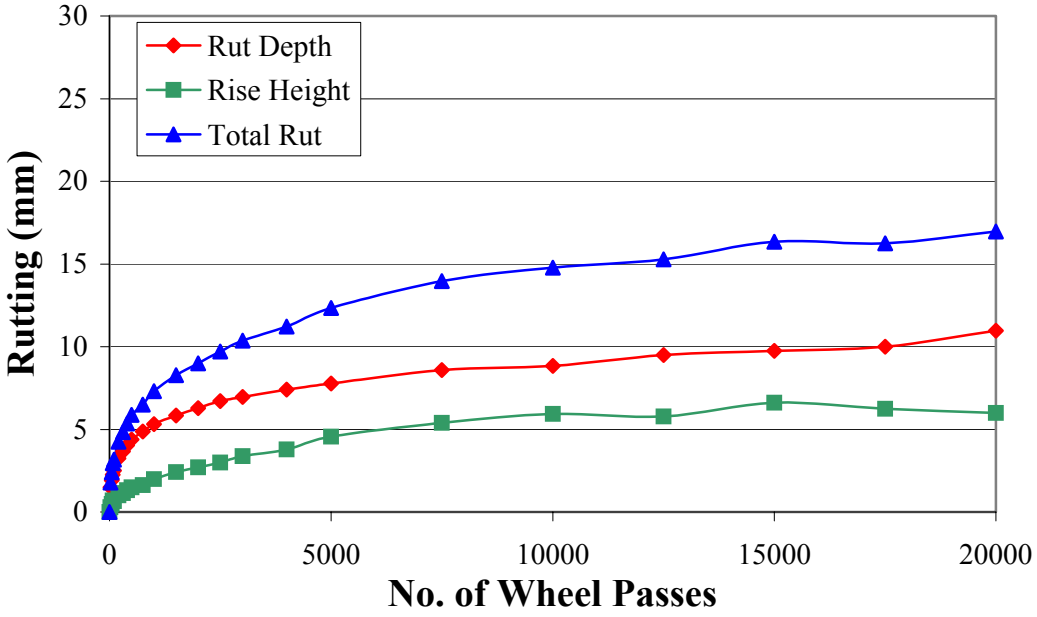

Figure C. 29 Wander Rutting for 19 mm Limestone with FAA of 44, Gradation Plotting Below The Restricted Zone, Low Density Lane.

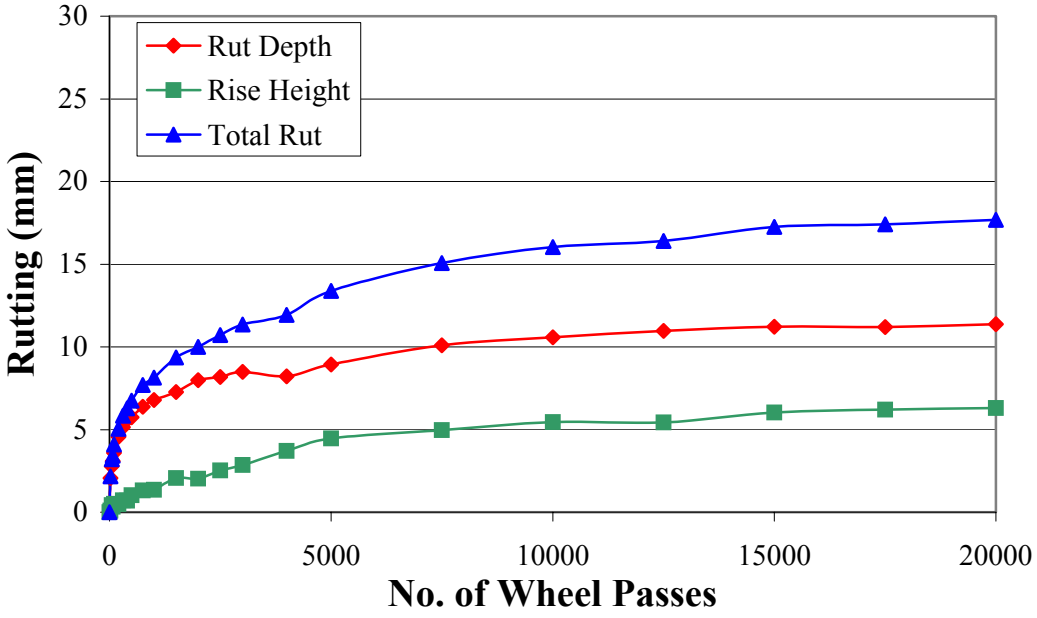

Figure C. 30 Wander Rutting for 19 mm Limestone with FAA of 44, Gradation Plotting Below The Restricted Zone, High Density Lane.

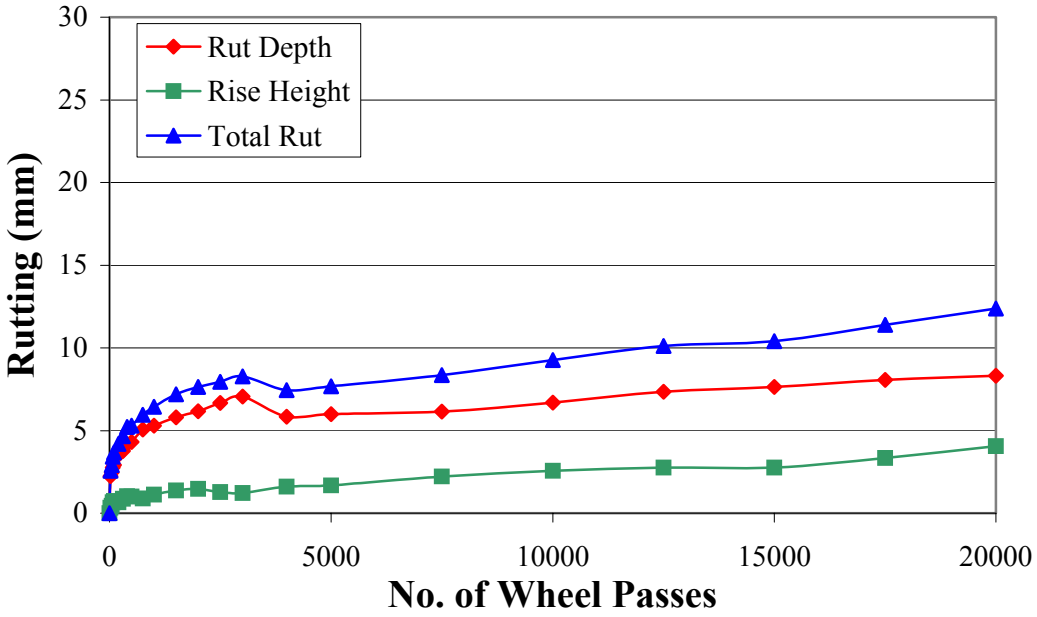

Figure C. 31 Wander Rutting for 19 mm Granite with FAA of 44, Gradation Plotting Below The Restricted Zone, +0.1% Design AC Lane.

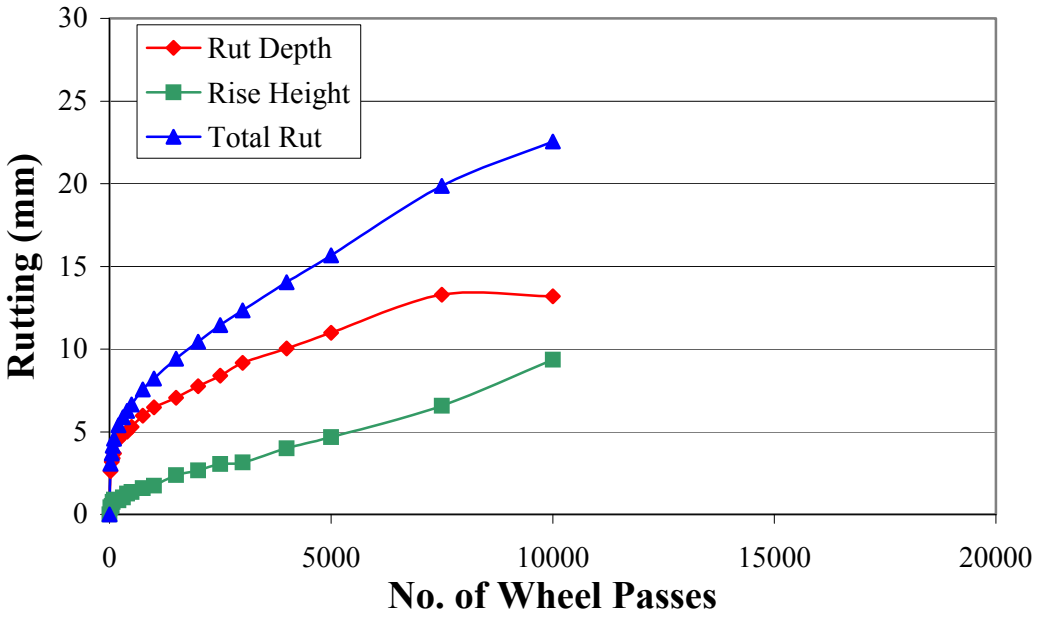

Figure C. 32 Wander Rutting for 19 mm Granite with FAA of 44, Gradation Plotting Below The Restricted Zone, +1.2% Design AC Lane.

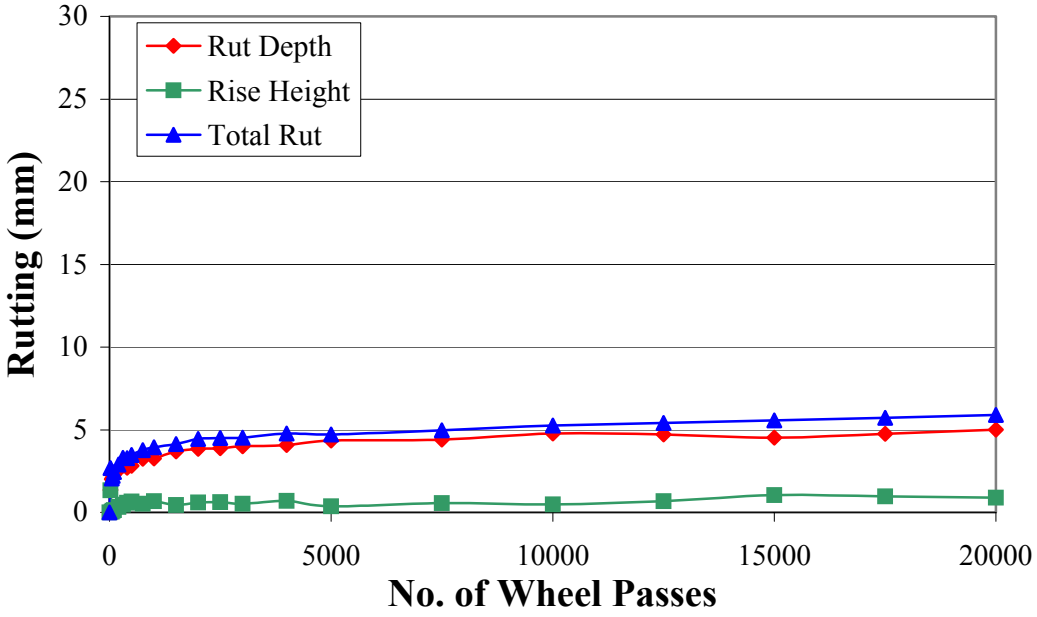

Figure C. 33 Wander Rutting for 19 mm Granite with FAA of 50, Gradation Plotting Through The Restricted Zone, -0.8% Design AC Lane.

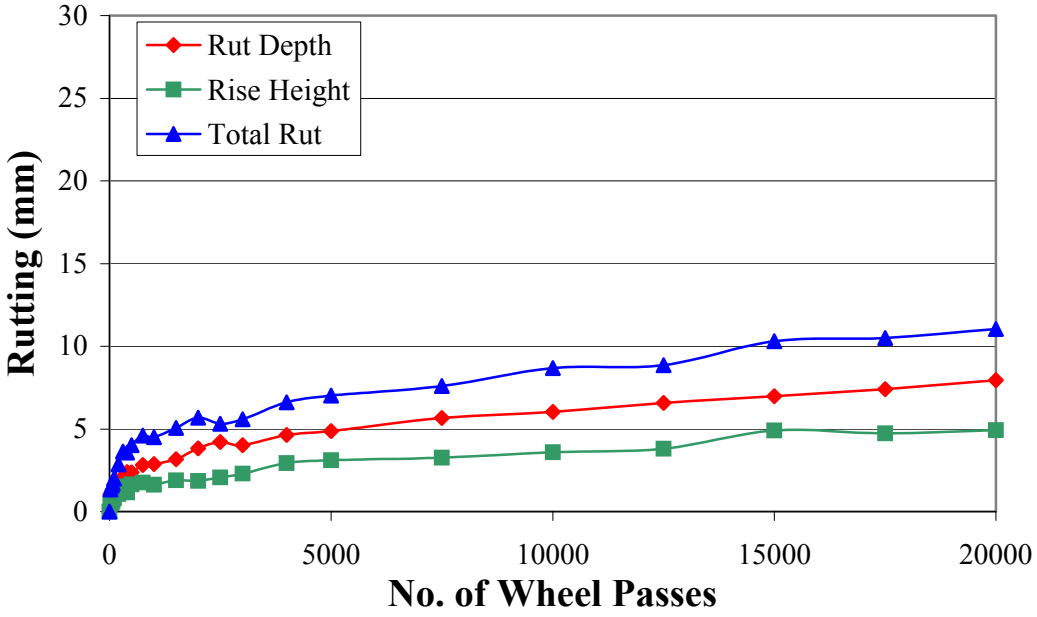

Figure C. 34 Wander Rutting for 19 mm Granite with FAA of 50, Gradation Plotting Through The Restricted Zone, +0.1% Design AC Lane.

APPENDIX D1 PURWheel Test Procedure

Standard Test Method for Determining Rutting Susceptibility of Bituminous Mixture Using Purdue Laboratory Wheel Track Test Device (PURWHeel)

1. Scope

1.1 *This method describes rut testing of bituminous paving mixtures using the Purdue Laboratory Wheel Track Test Device (PURWheel). This test method is for use with Field (Asphalt Plant) Mixture Field Compacted, Field Mixture Laboratory Compacted, and Laboratory Prepared Mixture Laboratory Compacted specimens under dry and wet conditions.*

1.2 *This standard may involve hazardous materials, operations, and equipment. This standard does not purport to address all of the safety problems associated with its use. It is the responsibility of the user of this standard to establish appropriate safety and health practices and determine the applicability of regulatory limitations prior to use*.

2. Referenced Documents

2.1 *ASTM Standards*:

2.1.1 D 8 Standard Terminology Relating to Materials for Roads and Pavements.

2.1.2 D 1559 Standard Test Method for Resistance to Plastic Flow of Bituminous Mixtures Using Marshall Apparatus.

2.1.3 D 2726 Test Method for Bulk Specific Gravity and Density of Non-Absorptive Compacted Bituminous Mixtures.

2.2 *Federal Highway Administration Report*:

2.2.1 FHWA-SA-95-003 Background of Superpave Asphalt Mixture Design and Analysis.

3. Terminology

3.1 *Definitions* – The definitions of terms used in this test method shall be in accordance with Terminology D 8.

3.2 *Description of Terms Specific to this Standard:*

3.2.1 *Purdue Laboratory Wheel Track Test Device (PURWheel)* – a laboratory scale device designed to test the rutting susceptibility of bituminous mixtures. The PURWheel consists of an environmental control chamber and cyclical loading mechanism that uses a pneumatic tire to apply repetitive loads on bituminous specimens.

3.2.2 *Linear Compactor* – a laboratory device designed to compact bituminous mixtures into 292 mm (11.5 in.) in width by 622 mm (24.5 in.) in length rectangle specimens. The thickness of the specimens is determined based on the nominal maximum size and is specified in section 7.3.

3.2.3 *Field Mixture Field Compacted specimens* – bituminous mixtures that were produced in the asphalt plant, compacted using field compaction equipments, cut into approximately 300 mm in length by 300 mm in width slabs.

3.2.4 *Field Mixture Laboratory Compacted specimens* – bituminous mixtures that were produced in the asphalt plant, compacted using laboratory linear compaction equipment.

3.2.5 *Laboratory Prepared Mixture Laboratory Compacted specimens* – bituminous mixtures that were prepared in the laboratory, compacted using laboratory linear compaction equipment.

3.2.6 *Volumetric Density* – the ratio of the dry weight and the geometric volume of a specimen. The geometric volume is calculated based on its dimension.

3.2.7 *Bulk Specific Gravity* – the bulk specific gravity of bituminous mixtures that is measured according to ASTM D 2726.

3.2.8 *Rut Depth* – vertical deformation along the wheel path measured from the original surface elevation downward.

3.2.9 *Stripping* – a distress that is characterized by the loss of bond between the aggregates and the bituminous materials.

3.2.10 *Dry condition* – a test condition that the specimen slabs are in air-dry condition.

3.2.11 *Wet condition* – a test condition that the specimen slabs are submerged completely under water. The distance between the mixture and water surface is about 25 mm.

3.2.12 *Full Slab* – a rectangle bituminous mixture specimen with 292 mm (11.5 in.) in width by 622 mm (24.5 in.) in length produced by linear compactor.

3.2.13 *Slab* – a rectangle bituminous mixture specimen with 292 mm (11.5 in.) in width by 311 mm (12.3 in.) in length.

4. Significance and use

4.1 In dry condition, this test method is used to evaluate the rutting potential of bituminous mixtures under different temperatures.

4.2 In wet condition, this test method is used to evaluate both rutting and stripping potential of bituminous mixtures under different temperatures.

5. Apparatus

5.1 *Linear Compactor*

5.1.1 *Compaction Mold Box* – The compaction mold box consists of two L-shape parts. When both parts are assembled, a box of 292 mm (11.5 in.) in width by 622 mm (24.5 in.) in length by 368 mm (14.5 in) in height shall conform to the details shown in Figure 1. A 25.4 mm (1 in.) thickness of the mold is recommended. One part of the mold shall be permanently fixed to the base.

5.1.2 *A Set of Base Plates* – The base steel plates shall consist of three pieces of 292 mm (11.5 in) in width by 622 mm (24.5 in.) in length by 12.5 mm (0.5 in) in thickness and two pieces of 292 mm (11.5 in) in width by 622 mm (24.5 in.) in length by 25.4 mm (1.0 in) in thickness. The base plates are to be used to adjust the thickness of the specimen.

5.1.3 *A Set of Compaction Plates* - The compaction steel plates shall consist of forty-nine pieces of 279.4 mm (11 in.) in width by 241 mm (9.5 in.) in length and 12.5 mm (0.5

in.) in thickness (Figure 2). The compaction plates are to be used vertically to compact the bituminous mixture.

5.1.4 *Cyclical Linear Movement Base* – The steel base shall have a cyclical linear movement mechanism and shall sit on top of a series of steel roller (Figure 3).

5.1.5 *Top Frame With Fixed Steel Roller* – A top frame with a fixed steel roller shall conform to the details shown in Figure 3.

5.1.6 *Infrared Heater* – The infrared heater must have the capability of heating the compaction mold box to the desired compaction temperature.

5.1.7 *Hydraulic Ram* – The hydraulic ram shall have the capacity to pull the top frame until the steel roller touches the compaction mold box during compaction operation. A capacity of 17250 kPa (2500 psi) is recommended.

5.2 *PURWheel*

5.2.1 *Environment Control Chamber* – The chamber shall be thermostatically controlled to maintain the test temperature at any set point between 25^0 and $65^0 \pm 1^0$ C in wet and dry conditions.

5.2.2 *Cyclical Linear Movement Mechanism* – The PURWheel shall have linear movement mechanism that extends and retracts the wheel at a constant speed of 330 mm/sec. The number of cycles shall be counted. Two units that operate independently are recommended.

5.2.3 *Alternate Tire No. 1: Steel Tire* – A steel tire of 150 mm (6 in.) in diameter by 102 mm (4 in.) in width shall conform to the details shown in Figure 4.

5.2.4 *Alternate Tire No. 2: Rubber Tire* – A pneumatic tire of 150 mm (6 in.) in diameter by 50 mm (2 in.) in width shall conform to the details shown in Figure 5.

5.2.5 *Loading Block* – A loading block shall be used to apply load to the tire to achieve a desired contact pressure. A 1470 N (330 lb.) load applied on 786 kPa (114 psi) rubber tire pressure gives 621 kPa (90 psi) contact pressure.

5.2.6 *Wheel Frame* – A wheel frame shall be connected to the cyclical linear movement mechanism. The loading block and the tire are assembled to the wheel frame.

5.2.7 *Vertical Movement Measurement* – The PURWheel shall have a vertical movement measurement of the wheel frame. It is recommended that the vertical measurement is simultaneously measured the horizontal position of the wheel with respect to the specimen position.

5.2.8 *Specimen Mounting Box* – The specimen-mounting box shall be able to contain different specimen thickness and have adequate length to maintain a constant wheel velocity. It is recommended that a heating system be installed in the box and a set of aluminum plates with different thickness are used to accommodate specimen thickness.

5.2.9 Mixing Apparatus – Mechanical mixing is recommended. Any type of mechanical mixer may be used provided it can be maintained the required mixing temperature and will provide a well-coated, homogeneous mixture of the required amount in the allowable time, and further provided that essentially all of the batch can be recovered. A metal pan or bowl of sufficient capacity and mixing may also be used.

5.2.10 *Circular Saw* – A mechanical circular saw that is capable of cutting concrete or rocks is recommended. The circular saw is to be used to cut the full slab (292 mm by 622 mm) in two slabs (292 mm by 311 mm) or to trim Field Mixture Field Compacted specimen to 292 mm in width by 311 mm in length slab.

5.3 Miscellaneous Equipment:

5.3.1 Infrared Heat Sensor

5.3.2 Brown paper

5.3.3 A flexible steel sheet of 290 mm in width by 310 mm in length.

6. Materials

6.1 Plaster of Paris – white powder materials that will harden in a relative short period of time (20 minutes) after being mixed with tap water.

7. Test Specimens

7.1 *Number of Specimens* – Prepare at least one full slab (292 mm (11.5 in.) in width by 622 mm (24.5 in.) in length) for each combination of aggregates and bitumen content.

The full slab shall be cut in two slabs (292 mm in width by 311 mm in length). The two slabs shall be tested in PURWheel.

7.2 *Size of Specimens* – The width of the specimen shall be 292 mm (11.5 in.) and the length of the specimen shall be 311 mm (12.3 in).

7.3 *Thickness of Specimens* – The thickness of the specimen shall be at least three times larger than the nominal maximum size of the aggregates. The recommended specimen thickness at a given nominal maximum size is given in Table 1

7.4 *Preparation of Specimens*.

7.4.1 *Field Mixture Field Compacted Specimens*.

The specimen shall be resized following section 7.4.5 in order to meet the size specification of section 7.2.

7.4.2 *Field Mixture Laboratory Compacted Specimens.*

7.4.2.1 Determine total amount of field mixture based on the thickness of the specimens according to section 7.3 and the target volumetric density. The target volumetric density can be calculated from the ratio of the measured bulk specific gravity to the correction factor. The appropriate correction factor for each mixture shall be used.

7.4.2.2 The compaction of the specimen shall follow section 7.4.4.

7.4.2.3 The specimen shall be resized following section 7.4.5 in order to meet the size specification of section 7.2.

7.4.3 *Laboratory Prepared Mixture Laboratory Compacted Specimens*.

7.4.3.1 Determine total amount of aggregates based on the thickness of the specimens according to section 7.3, the target volumetric density, and the asphalt content. The target volumetric density can be calculated from the ratio of the measured bulk specific gravity to the correction factor. The appropriate correction factor for each mixture shall be used.

7.4.3.2 The mixing method shall follow ASTM D 1559 or FHWA-SA-95-003.

7.4.3.3 The compaction of the specimen shall follow section 7.4.4.

7.4.3.4 The specimen shall be resized following section 7.4.5 in order to meet the size specification of section 7.2.

7.4.4 *Compaction of Specimens*

7.4.4.1 Determine the thickness of the specimens according to section 7.3. Place the appropriate number of base plates such that the total thickness of the steel plates and the specimens equals to 127 mm (5 in.).

7.4.4.2 Assemble the compaction mold box. The compaction mold box shall be heated by the infrared heater to the compaction temperature set point.

7.4.4.3 Place the hot bituminous mixture in the mold, spread homogenously, and level the mixture horizontally. The temperature of the mixture shall be measured by the infrared heat sensor.

7.4.4.4 Cover the hot bituminous mixture with a piece of brown paper and place the flexible steel sheet on top of the paper. Insert the compaction steel plates vertically. It is recommended to insert the forty-eight pieces of steel plates simultaneously with a hydraulic hoist. The last piece is to be inserted when the other forty-eight pieces have set properly inside the compaction mold box.

7.4.4.5 Lower and attach the top frame to the hydraulic ram.

7.4.4.6 Start the cyclical linear movement of the compaction mold box.

7.4.4.7 Lower the top frame until the steel roller is in contact with the compaction plates by increasing the pressure in the hydraulic ram. [1]

7.4.4.8 Stop the movement of compaction box when the top of the compaction plates is even with the top of the compaction box.

7.4.4.9 Release the pressure of the hydraulic ram, raise the top frame, and remove the vertical compaction plates from the compaction box, the flexible steel sheet, and the brown paper. When the temperature of the bituminous mixture is low enough, disassemble the compaction mold box and remove the bituminous mixture full slab.

7.4.5 *Specimen Resizing.* A circular saw shall be used to cut the compacted full slab (292 mm by 622 mm) in two slabs (292 mm by 311 mm) or to trim Field Mixture Field Compacted specimen to 292 mm in width by 311 mm in length slab.

[1] Note: When the steel roller is in contact with the compaction plates, it is important to lower the steel roller slowly and maintain the compaction plates horizontally.

7.4.6 *Measurement of Specimen Properties*. Weigh the dry specimen and measure the width, length, and thickness of the specimen. The bulk specific gravity of the specimen can be measured in accordance to ASTM D2726.

8. Calibration

8.1 *Tire Pressure*. When rubber tire is used, measure the tire pressure before each testing with a tire pressure gauge. Adjust the tire pressure when it is necessary.

8.2 *Wheel Velocity*. Calibrate the wheel velocity to 330 ± 20 mm/sec (13 ± 0.8 in./sec) by adjusting the extension and retraction mechanism.

8.3 *Vertical Movement Measurement*. Calibrate the vertical movement measurement reading to a standard material thickness. It is recommended that the position of the device be adjusted such that the measurement reading has a minimum range of 20 mm (0.79 in.).

9. Procedure

9.1 *Dry Test*

9.1.1 *Conditioning*. Place the specimen in the specimen-mounting box. Place a mixture of plaster and water along the sides of the specimen. A plaster to water ratio of seven to six gives adequate liquidity and reasonable hardening time. Turn on the heating system. It is recommended that the heating system consist of a temperature-controlled water that circulates underneath the specimen and an air heater. Wait until the temperature of the specimen reaches and stabilizes at the set point. Check the temperature of the specimen by using the infrared heat sensor.

9.1.2 *Testing.* Count the number of wheel cycles and measure the vertical deformation of the wheel simultaneously. Stop the testing when the total number of wheel cycles has reached the target or the rut depth has reached the predetermined maximum rut depth. It takes about 8 hours to accomplish 20000 wheel cycles. It is recommended that the predetermined maximum rut depth be set to 20 mm (0.79 in.).

9.2 *Wet Test*

9.2.1 *Conditioning.* Place the specimen in the specimen-mounting box. Place a mixture of plaster and water along the sides of the specimen. A plaster to water ratio of seven to four gives adequate solidity when submerged under water. Fill in the chamber with water until the specimen is completely submerged. It is recommended that the distance between the water and specimen surface be 25.4 mm (1 in.). Turn on the heating system. A separate heating system from the dry test system is required. It is recommended that the heating system consist of a high capacity water heater equipped with a temperature sensor feedback. [2]Wait until the temperature of the specimen reaches and stabilizes at the set point.

9.2.2 *Testing.* Count the number of wheel cycles and measure the vertical deformation of the wheel simultaneously. Stop the testing when the total number of wheel cycles has reached the target or the rut depth has reached the predetermined maximum rut depth. It takes about 8 hours to accomplish 20000 wheel cycles. It is recommended that the predetermined maximum rut depth be set to 20 mm (0.79 in.).

10. Report

10.1 The report shall include the following information:

10.1.1 Type of sample tested, i.e. Field Mixture Field Compacted, Field Mixture Laboratory Compacted, or Laboratory Prepared Mixture Laboratory Compacted specimen.

10.1.2 Type of testing condition, i.e. Wet Test or Dry Test.

10.1.3 Type of tire, i.e. Rubber Tire or Steel Tire.

10.1.4 Contact pressure between the tire and the specimen.

10.1.5 Test temperature.

10.1.6 Thickness of the specimen.

10.1.7 Volumetric density of the specimen.

10.1.8 Historical plot between rut depth and number of wheel cycles.

[2] Note: Due to high humidity in wet test condition, it is necessary to protect the dry-test heating system.

11. Precision and Bias

11.1 The precision and bias of this test method have not been established by an interlaboratory test program. However, based on the test data that are available, the following may serve as a guide to the variability of rutting susceptibility of bituminous materials by PURWheel.

11.2 Tests were performed in a single laboratory on Mixture Laboratory Compacted specimens, under dry condition, using rubber tire with 90 psi contact pressure, at 50^0C. The sample nominal maximum size is 9.5 mm ($^3/_8$ in.) and the thickness of the specimen is 37.5 mm (1.5 in.). Results of tests are given in Table 2.

12. Keywords

PURWheel, tracking device, accelerated loading, rut tester, rutting, stripping, rut depth.

Table 1. Recommended Specimen Thickness

Nominal Maximum Size (mm) (in.)	Specimen Thickness (mm) (in.)
37.5 ($1^1/_2$)	127 (5)
25 (1)	102 (4)
19 ($^3/_4$)	76 (3)
12.5 ($^1/_2$)	51 (2)
9.5 ($^3/_8$)	37.5 ($1^1/_2$)

Table 2. Precision

Correction Factor: 1.040					
Maximum Theoretical Specific Gravity (Gmm): 2.478					
	Asphalt Content (%)	Volumetric Density (gr/cm^3)	Bulk Specific Gravity (Gmb)	Air Void (%)	Rut Depth after 20000 Wheel Cycles (mm)
Specimen 1	5.5	2.203	2.292	7.5	1.4
Specimen 2	5.5	2.219	2.308	6.9	1.2
Specimen 3	5.5	2.229	2.319	6.4	2.0
Specimen 4	5.5	2.193	2.281	7.9	1.9
Average	5.5	2.210	2.300	7.19	1.63
Standard Deviation	0	0.016	0.017	0.67	0.4
Coefficient of Variation (%)	0	0.7	0.7	9.3	25

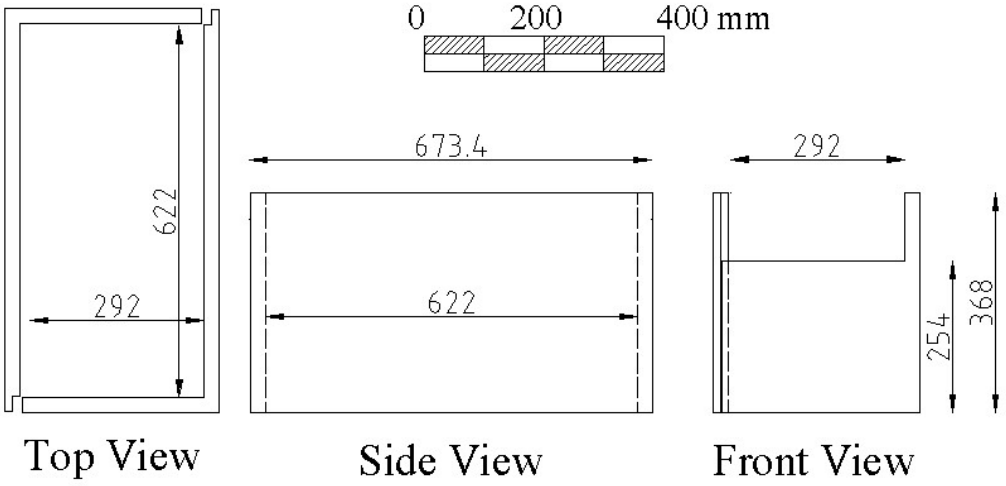

Figure 1. Compaction Mold

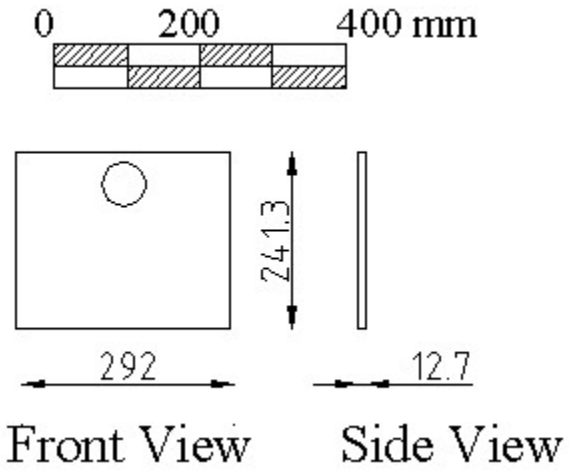

Figure 2. Compaction Plate

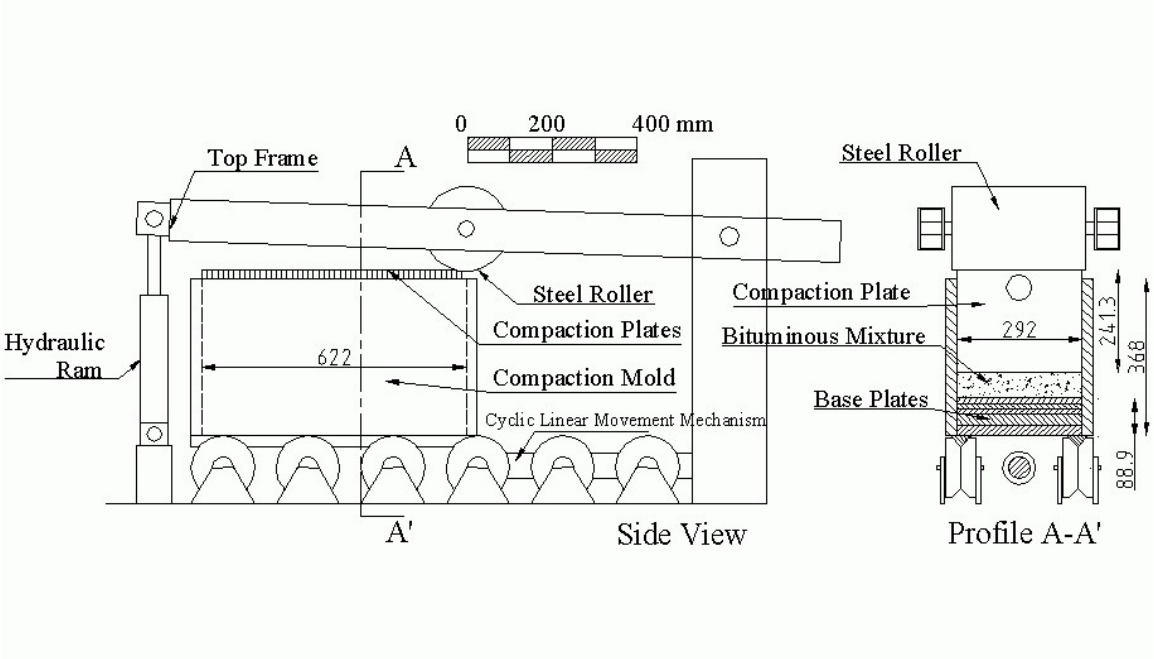

Figure 3. Linear Compactor

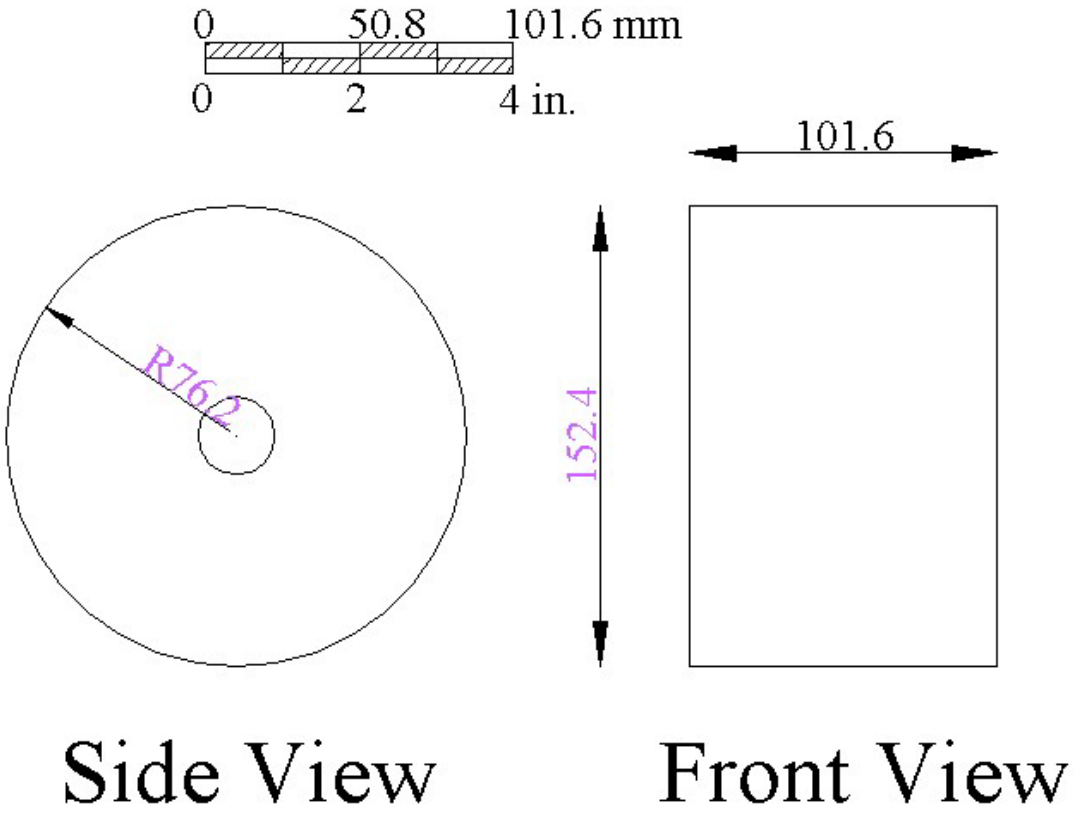

Figure 4. Steel Tire

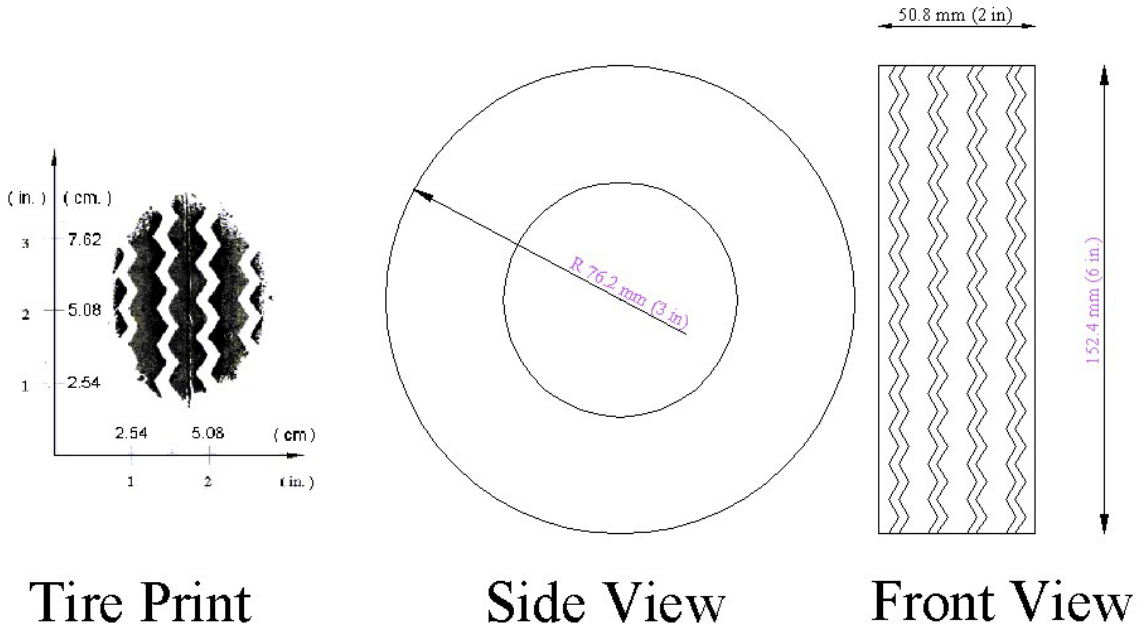

Figure 5. Rubber Tire

APPENDIX D2 PURWheel Test Results

Table D2. 1 PURWheel FMFC Data

Nom. Size (mm)	Coarse Agg. Type	FAA	Gradation	Rut Depth (mm)	Temp. (° C)	AC (%)	Air Voids (%)	VMA (%)	VFA (%)	Film Thick. (µm)	Surface Area (m^2/Kg)	Dust Prop.	Binder Abs. (Pba, %)	Effective Binder (Pbe, %)	Gse	Gmm	p200 (%)	Gsb	Bsg
19	LS	44	Below	6.63	50	4.9	9.8	18.8	47.8	12.70	3.12	0.60	0.9	4.0	2.7107	2.510	2.4	2.651	2.264
19	LS	44	Below	6.01	50	4.9	9.8	18.8	47.8	12.70	3.12	0.60	0.9	4.0	2.7107	2.510	2.4	2.651	2.264
19	LS	44	Below	6.24	50	4.9	8.3	17.4	52.4	12.70	3.12	0.60	0.9	4.0	2.7107	2.510	2.4	2.651	2.302
19	LS	44	Below	4.79	50	4.9	8.3	17.4	52.4	12.70	3.12	0.60	0.9	4.0	2.7107	2.510	2.4	2.651	2.302
19	GR	44	Below	4.47	50	4.5	7.9	15.2	48.0	6.80	4.50	1.66	1.4	3.1	2.7454	2.554	5.2	2.649	2.352
19	GR	44	Below	4.02	50	4.5	7.9	15.2	48.0	6.80	4.50	1.66	1.4	3.1	2.7454	2.554	5.2	2.649	2.352
19	GR	44	Below	6.36	50	5.6	5.5	15.4	64.6	9.30	4.50	1.23	1.4	4.2	2.7452	2.511	5.2	2.649	2.374
19	GR	44	Below	5.46	50	5.6	5.5	15.4	64.6	9.30	4.50	1.23	1.4	4.2	2.7452	2.511	5.2	2.649	2.374
19	GR	50	Through	4.69	50	4.5	9.4	17.9	47.6	7.30	5.13	1.42	0.7	3.8	2.6899	2.508	5.5	2.644	2.272
19	GR	50	Through	4.70	50	4.5	9.4	17.9	47.6	7.30	5.13	1.42	0.7	3.8	2.6899	2.508	5.5	2.644	2.272
19	GR	50	Through	6.49	50	5.4	4.0	15.1	73.5	9.18	5.13	1.14	0.6	4.8	2.6867	2.472	5.5	2.644	2.373
19	GR	50	Through	5.85	50	5.4	4.0	15.1	73.5	9.18	5.13	1.14	0.6	4.8	2.6867	2.472	5.5	2.644	2.373
9.5	LS	44	Through	7.65	50	6.3	10.6	21.8	51.2	9.90	5.15	0.80	1.2	5.1	2.7263	2.470	4.1	2.644	2.208
9.5	LS	44	Through	6.38	50	5.6	14.9	24.5	39.1	8.86	5.15	0.89	1.0	4.6	2.7123	2.485	4.1	2.644	2.114
9.5	LS	44	Through	15.06	50	5.6	14.2	23.9	40.5	8.86	5.15	0.89	1.0	4.6	2.7123	2.485	4.1	2.644	2.132
9.5	LS	44	Through	14.24	50	6.3	10.4	21.6	51.8	9.90	5.15	0.80	1.2	5.1	2.7263	2.470	4.1	2.644	2.213
9.5	LS	50	Through	8.59	50	5.9	11.1	22.4	50.5	7.01	7.50	1.52	0.6	5.3	2.6805	2.449	8.1	2.640	2.178
9.5	LS	50	Through	8.19	50	5.9	11.1	22.4	50.5	7.01	7.50	1.52	0.6	5.3	2.6805	2.449	8.1	2.640	2.178
9.5	LS	50	Through	12.27	50	6.6	6.9	20.2	65.9	8.05	7.50	1.34	0.5	6.1	2.6777	2.422	8.1	2.640	2.255
9.5	LS	50	Through	19.09	50	6.6	6.9	20.2	65.9	8.05	7.50	1.34	0.5	6.1	2.6777	2.422	8.1	2.640	2.255
9.5	GR	44	Below	1.40	50	5.2	10.5	20.2	48.0	10.75	4.06	0.66	0.8	4.4	2.6999	2.490	2.9	2.647	2.229
9.5	GR	44	Below	3.98	50	5.2	10.5	20.2	48.0	10.75	4.06	0.66	0.8	4.4	2.6999	2.490	2.9	2.647	2.229
9.5	GR	44	Below	4.03	50	5.3	10.4	20.2	48.7	10.93	4.06	0.65	0.8	4.5	2.7021	2.488	2.9	2.647	2.230
9.5	GR	44	Below	5.06	50	5.3	10.4	20.2	48.7	10.93	4.06	0.65	0.8	4.5	2.7021	2.488	2.9	2.647	2.230
9.5	GR	50	Below	5.89	50	5.5	6.9	17.5	60.4	7.18	6.45	1.55	0.8	4.7	2.6988	2.478	7.3	2.643	2.306
9.5	GR	50	Below	2.81	50	6.2	3.4	16.0	78.8	8.38	6.45	1.34	0.8	5.4	2.6956	2.450	7.3	2.643	2.367
9.5	GR	50	Below	6.44	50	6.2	2.9	15.6	81.4	8.38	6.45	1.34	0.8	5.4	2.6956	2.450	7.3	2.643	2.379
9.5	GR	50	Below	5.86	50	5.5	6.2	16.9	63.2	7.18	6.45	1.55	0.8	4.7	2.6988	2.478	7.3	2.643	2.324

Table D2. 2 PURWheel FMLC Data

Nom. Size (mm)	Coarse Agg. Type	FAA	Gradation	Rut Depth (mm)	Temp. (° C)	AC (%)	Air Voids (%)	VMA (%)	VFA (%)	Film Thick. (µm)	Surface Area (m^2/Kg)	Dust Prop.	Binder Abs. (Pba, %)	Effective Binder (Pbe, %)	Gse	Gmm	p200 (%)	Gsb	Bsg
19	GR	44	Below	2.02	50	4.5	6.5	13.9	53.2	6.80	4.50	1.66	1.4	3.1	2.7454	2.554	5.2	2.649	2.387
19	GR	44	Below	2.13	50	4.5	5.9	13.3	56.0	6.80	4.50	1.66	1.4	3.1	2.7454	2.554	5.2	2.649	2.404
19	GR	44	Below	1.31	50	4.5	6.2	13.6	54.5	6.80	4.50	1.66	1.4	3.1	2.7454	2.554	5.2	2.649	2.396
19	GR	44	Below	1.64	50	4.5	6.2	13.6	54.5	6.80	4.50	1.66	1.4	3.1	2.7454	2.554	5.2	2.649	2.396
19	GR	44	Below	1.67	50	5.6	3.2	13.4	75.8	9.30	4.50	1.23	1.4	4.2	2.7452	2.511	5.2	2.649	2.430
19	GR	44	Below	2.19	50	5.6	4.0	14.1	71.5	9.30	4.50	1.23	1.4	4.2	2.7452	2.511	5.2	2.649	2.410
19	GR	44	Below	2.08	50	5.6	2.8	13.0	78.6	9.30	4.50	1.23	1.4	4.2	2.7452	2.511	5.2	2.649	2.441
19	GR	44	Below	2.11	50	5.6	4.4	14.4	69.8	9.30	4.50	1.23	1.4	4.2	2.7452	2.511	5.2	2.649	2.401
19	GR	50	Through	1.65	50	4.5	9.0	17.5	48.9	7.30	5.13	1.42	0.7	3.8	2.6899	2.508	5.5	2.644	2.283
19	GR	50	Through	2.10	50	4.5	7.0	15.8	55.5	7.30	5.13	1.42	0.7	3.8	2.6899	2.508	5.5	2.644	2.332
19	GR	50	Through	1.62	50	5.4	3.2	14.4	77.6	9.18	5.13	1.14	0.6	4.8	2.6867	2.472	5.5	2.644	2.392
19	GR	50	Through	2.67	50	5.4	2.7	13.9	80.6	9.18	5.13	1.14	0.6	4.8	2.6867	2.472	5.5	2.644	2.405
9.5	LS	44	Through	1.49	50	5.6	8.2	18.6	55.8	8.86	5.15	0.89	1.0	4.6	2.7123	2.485	4.1	2.644	2.281
9.5	LS	44	Through	2.09	50	5.6	9.8	20.0	50.8	8.86	5.15	0.89	1.0	4.6	2.7123	2.485	4.1	2.644	2.241
9.5	LS	44	Through	1.96	50	5.6	9.5	19.7	51.8	8.86	5.15	0.89	1.0	4.6	2.7123	2.485	4.1	2.644	2.249
9.5	LS	44	Through	1.64	50	5.6	5.2	15.9	67.4	8.86	5.15	0.89	1.0	4.6	2.7123	2.485	4.1	2.644	2.356
9.5	LS	44	Through	1.15	50	6.3	2.8	14.9	81.4	9.90	5.15	0.80	1.2	5.1	2.7263	2.470	4.1	2.644	2.401
9.5	LS	44	Through	3.55	50	6.3	8.4	19.8	57.6	9.90	5.15	0.80	1.2	5.1	2.7263	2.470	4.1	2.644	2.262
9.5	LS	44	Through	1.42	50	6.3	5.3	17.1	69.1	9.90	5.15	0.80	1.2	5.1	2.7263	2.470	4.1	2.644	2.340
9.5	LS	44	Through	2.52	50	6.3	7.7	19.2	60.1	9.90	5.15	0.80	1.2	5.1	2.7263	2.470	4.1	2.644	2.281
9.5	LS	50	Through	2.25	50	5.9	7.8	19.5	60.2	7.01	7.50	1.52	0.6	5.3	2.6805	2.449	8.1	2.640	2.259
9.5	LS	50	Through	4.08	50	5.9	11.8	23.0	48.8	7.01	7.50	1.52	0.6	5.3	2.6805	2.449	8.1	2.640	2.161
9.5	LS	50	Through	6.09	50	5.9	9.2	20.7	55.7	7.01	7.50	1.52	0.6	5.3	2.6805	2.449	8.1	2.640	2.224
9.5	LS	50	Through	4.83	50	5.9	8.2	19.8	58.8	7.01	7.50	1.52	0.6	5.3	2.6805	2.449	8.1	2.640	2.249

Table D2. 2 PURWheel FMLC Data (continue)

Nom. Size (mm)	Coarse Agg. Type	FAA	Gradation	Rut Depth (mm)	Temp. (° C)	AC (%)	Air Voids (%)	VMA (%)	VFA (%)	Film Thick. (µm)	Surface Area (m^2/Kg)	Dust Prop.	Binder Abs. (Pba, %)	Effective Binder (Pbe, %)	Gse	Gmm	p200 (%)	Gsb	Bsg
9.5	LS	50	Through	10.90	50	6.6	8.6	21.7	60.2	8.05	7.50	1.34	0.5	6.1	2.6777	2.422	8.1	2.640	2.213
9.5	LS	50	Through	6.98	50	6.6	8.7	21.8	60.0	8.05	7.50	1.34	0.5	6.1	2.6777	2.422	8.1	2.640	2.211
9.5	LS	50	Through	18.77	50	6.6	10.5	23.4	54.8	8.05	7.50	1.34	0.5	6.1	2.6777	2.422	8.1	2.640	2.167
9.5	LS	50	Through	9.25	50	6.6	5.9	19.4	69.4	8.05	7.50	1.34	0.5	6.1	2.6777	2.422	8.1	2.640	2.278
9.5	GR	44	Below	4.85	50	5.2	12.2	21.7	43.7	10.75	4.06	0.66	0.8	4.4	2.6999	2.490	2.9	2.647	2.186
9.5	GR	44	Below	2.45	50	5.2	8.3	18.3	54.3	10.75	4.06	0.66	0.8	4.4	2.6999	2.490	2.9	2.647	2.282
9.5	GR	44	Below	3.86	50	5.2	9.9	19.7	49.6	10.75	4.06	0.66	0.8	4.4	2.6999	2.490	2.9	2.647	2.243
9.5	GR	44	Below	3.44	50	5.2	9.1	18.9	52.0	10.75	4.06	0.66	0.8	4.4	2.6999	2.490	2.9	2.647	2.264
9.5	GR	44	Below	2.16	50	5.3	11.3	21.0	46.4	10.93	4.06	0.65	0.8	4.5	2.7021	2.488	2.9	2.647	2.208
9.5	GR	44	Below	4.61	50	5.3	12.8	22.3	42.9	10.93	4.06	0.65	0.8	4.5	2.7021	2.488	2.9	2.647	2.171
9.5	GR	44	Below	5.25	50	5.3	11.3	21.0	46.3	10.93	4.06	0.65	0.8	4.5	2.7021	2.488	2.9	2.647	2.207
9.5	GR	44	Below	7.67	50	5.3	12.3	22.0	43.9	10.93	4.06	0.65	0.8	4.5	2.7021	2.488	2.9	2.647	2.182
9.5	GR	50	Below	1.21	50	5.5	5.9	16.6	64.7	7.18	6.45	1.55	0.8	4.7	2.6988	2.478	7.3	2.643	2.333
9.5	GR	50	Below	2.21	50	5.5	7.5	18.0	58.5	7.18	6.45	1.55	0.8	4.7	2.6988	2.478	7.3	2.643	2.293
9.5	GR	50	Below	3.53	50	5.5	9.4	19.8	52.2	7.18	6.45	1.55	0.8	4.7	2.6988	2.478	7.3	2.643	2.244
9.5	GR	50	Below	2.18	50	5.5	5.9	16.7	64.4	7.18	6.45	1.55	0.8	4.7	2.6988	2.478	7.3	2.643	2.331
9.5	GR	50	Below	1.22	50	6.2	2.4	15.1	84.3	8.38	6.45	1.34	0.8	5.4	2.6956	2.450	7.3	2.643	2.392
9.5	GR	50	Below	2.24	50	6.2	3.6	16.2	77.6	8.38	6.45	1.34	0.8	5.4	2.6956	2.450	7.3	2.643	2.361
9.5	GR	50	Below	2.57	50	6.2	3.7	16.3	77.1	8.38	6.45	1.34	0.8	5.4	2.6956	2.450	7.3	2.643	2.359
9.5	GR	50	Below	0.80	50	6.2	2.7	15.4	82.4	8.38	6.45	1.34	0.8	5.4	2.6956	2.450	7.3	2.643	2.384

Table D2. 3 PURWheel LMLCF Data

Nom. Size (mm)	Coarse Agg. Type	FAA	Gradation	Rut Depth (mm)	Temp. (° C)	AC (%)	Air Voids (%)	VMA (%)	VFA (%)	Film Thick. (μm)	Surface Area (m^2/Kg)	Dust Prop.	Binder Abs. (Pba, %)	Effective Binder (Pbe, %)	Gse	Gmm	p200 (%)	Gsb	Bsg
19	GR	44	Below	1.55	50	4.5	6.4	13.9	53.5	6.80	4.50	1.66	1.4	3.1	2.7454	2.554	5.2	2.649	2.390
19	GR	44	Below	2.24	50	4.5	8.5	15.8	46.0	6.80	4.50	1.66	1.4	3.1	2.7454	2.554	5.2	2.649	2.337
19	GR	44	Below	2.36	50	5.6	6.6	16.4	60.0	9.30	4.50	1.23	1.4	4.2	2.7452	2.511	5.2	2.649	2.346
19	GR	44	Below	2.20	50	5.6	3.9	14.0	72.2	9.30	4.50	1.23	1.4	4.2	2.7452	2.511	5.2	2.649	2.413
19	GR	50	Through	1.14	50	4.5	9.0	17.6	48.6	7.30	5.13	1.42	0.7	3.8	2.6899	2.508	5.5	2.644	2.281
19	GR	50	Through	1.56	50	4.5	9.9	18.4	46.2	7.30	5.13	1.42	0.7	3.8	2.6899	2.508	5.5	2.644	2.260
19	GR	50	Through	1.08	50	5.4	5.2	16.2	67.8	9.18	5.13	1.14	0.6	4.8	2.6867	2.472	5.5	2.644	2.343
19	GR	50	Through	1.95	50	5.4	4.3	15.4	71.9	9.18	5.13	1.14	0.6	4.8	2.6867	2.472	5.5	2.644	2.365
9.5	LS	44	Through	1.38	50	5.6	14.9	24.5	39.1	8.86	5.15	0.89	1.0	4.6	2.7123	2.485	4.1	2.644	2.114
9.5	LS	44	Through	2.06	50	5.6	15.0	24.6	38.9	8.86	5.15	0.89	1.0	4.6	2.7123	2.485	4.1	2.644	2.111
9.5	LS	44	Through	1.30	50	5.6	11.5	21.5	46.5	8.86	5.15	0.89	1.0	4.6	2.7123	2.485	4.1	2.644	2.200
9.5	LS	44	Through	3.72	50	5.6	15.0	24.6	39.0	8.86	5.15	0.89	1.0	4.6	2.7123	2.485	4.1	2.644	2.113
9.5	LS	44	Through	1.89	50	6.3	9.8	21.0	53.4	9.90	5.15	0.80	1.2	5.1	2.7263	2.470	4.1	2.644	2.228
9.5	LS	44	Through	2.35	50	6.3	9.9	21.1	53.1	9.90	5.15	0.80	1.2	5.1	2.7263	2.470	4.1	2.644	2.225
9.5	LS	44	Through	2.69	50	6.3	11.6	22.6	48.7	9.90	5.15	0.80	1.2	5.1	2.7263	2.470	4.1	2.644	2.183
9.5	LS	44	Through	1.62	50	6.3	8.3	19.7	57.9	9.90	5.15	0.80	1.2	5.1	2.7263	2.470	4.1	2.644	2.265
9.5	LS	50	Through	3.09	50	5.9	13.5	24.5	44.8	7.01	7.50	1.52	0.6	5.3	2.6805	2.449	8.1	2.640	2.117
9.5	LS	50	Through	2.26	50	5.9	9.2	20.8	55.5	7.01	7.50	1.52	0.6	5.3	2.6805	2.449	8.1	2.640	2.223
9.5	LS	50	Through	4.93	50	5.9	13.9	24.9	44.0	7.01	7.50	1.52	0.6	5.3	2.6805	2.449	8.1	2.640	2.107
9.5	LS	50	Through	2.31	50	5.9	8.7	20.3	57.1	7.01	7.50	1.52	0.6	5.3	2.6805	2.449	8.1	2.640	2.236
9.5	LS	50	Through	2.32	50	6.6	5.4	18.9	71.7	8.05	7.50	1.34	0.5	6.1	2.6777	2.422	8.1	2.640	2.292
9.5	LS	50	Through	4.66	50	6.6	7.5	20.7	63.9	8.05	7.50	1.34	0.5	6.1	2.6777	2.422	8.1	2.640	2.241
9.5	LS	50	Through	1.64	50	6.6	4.6	18.3	74.6	8.05	7.50	1.34	0.5	6.1	2.6777	2.422	8.1	2.640	2.310
9.5	LS	50	Through	3.81	50	6.6	8.2	21.4	61.5	8.05	7.50	1.34	0.5	6.1	2.6777	2.422	8.1	2.640	2.223

Table D2. 3 PURWheel LMLCF Data (continue).

Nom. Size (mm)	Coarse Agg. Type	FAA	Gradation	Rut Depth (mm)	Temp. (° C)	AC (%)	Air Voids (%)	VMA (%)	VFA (%)	Film Thick. (µm)	Surface Area (m^2/Kg)	Dust Prop.	Binder Abs. (Pba, %)	Effective Binder (Pbe, %)	Gse	Gmm	p200 (%)	Gsb	Bsg
9.5	GR	44	Below	1.50	50	4.5	10.0	19.1	47.9	10.07	4.06	0.70	0.3	4.2	2.6682	2.490	2.9	2.647	2.242
9.5	GR	44	Below	1.12	50	4.5	9.4	18.6	49.4	10.07	4.06	0.70	0.3	4.2	2.6682	2.490	2.9	2.647	2.256
9.5	GR	44	Below	1.16	50	4.5	9.4	18.6	49.6	10.07	4.06	0.70	0.3	4.2	2.6682	2.490	2.9	2.647	2.257
9.5	GR	44	Below	1.27	50	4.5	9.2	18.4	50.1	10.07	4.06	0.70	0.3	4.2	2.6682	2.490	2.9	2.647	2.261
9.5	GR	44	Below	1.63	50	5.2	11.2	20.9	46.3	10.83	4.06	0.66	0.7	4.5	2.6974	2.488	2.9	2.647	2.209
9.5	GR	44	Below	1.18	50	5.2	9.7	19.5	50.4	10.83	4.06	0.66	0.7	4.5	2.6974	2.488	2.9	2.647	2.247
9.5	GR	44	Below	1.50	50	5.2	11.0	20.7	46.8	10.83	4.06	0.66	0.7	4.5	2.6974	2.488	2.9	2.647	2.214
9.5	GR	44	Below	1.20	50	5.2	9.4	19.3	51.1	10.83	4.06	0.66	0.7	4.5	2.6974	2.488	2.9	2.647	2.253
9.5	GR	50	Below	1.39	50	5.5	7.5	18.1	58.3	7.18	6.45	1.55	0.8	4.7	2.6988	2.478	7.3	2.643	2.292
9.5	GR	50	Below	1.16	50	5.5	6.9	17.5	60.7	7.18	6.45	1.55	0.8	4.7	2.6988	2.478	7.3	2.643	2.308
9.5	GR	50	Below	2.01	50	5.5	6.4	17.1	62.4	7.18	6.45	1.55	0.8	4.7	2.6988	2.478	7.3	2.643	2.319
9.5	GR	50	Below	1.89	50	5.5	7.9	18.4	56.9	7.18	6.45	1.55	0.8	4.7	2.6988	2.478	7.3	2.643	2.281
9.5	GR	50	Below	2.26	50	6.2	3.7	16.2	77.4	8.38	6.45	1.34	0.8	5.4	2.6956	2.450	7.3	2.643	2.360
9.5	GR	50	Below	1.74	50	6.2	1.7	14.5	88.5	8.38	6.45	1.34	0.8	5.4	2.6956	2.450	7.3	2.643	2.409
9.5	GR	50	Below	1.37	50	6.2	2.5	15.2	83.7	8.38	6.45	1.34	0.8	5.4	2.6956	2.450	7.3	2.643	2.389
9.5	GR	50	Below	1.69	50	6.2	3.4	16.0	78.8	8.38	6.45	1.34	0.8	5.4	2.6956	2.450	7.3	2.643	2.367

Table D2. 4 PURWheel LMLCD Data.

Nom. Size (mm)	Coarse Agg. Type	FAA	Gradation	Rut Depth (mm)	Temp. (° C)	AC (%)	Air Voids (%)	VMA (%)	VFA (%)	Film Thick. (µm)	Surface Area (m^2/Kg)	Dust Prop.	Binder Abs. (Pba, %)	Effective Binder (Pbe, %)	Gse	Gmm	p200 (%)	Gsb	Bsg
19	LS	39	Above	2.14	57.5	4.7	3.9	13.2	70.4	6.63	5.79	1.22	0.8	3.9	2.6978	2.507	4.8	2.644	2.409
19	LS	39	Above	1.10	57.5	4.7	3.9	13.2	70.4	6.63	5.79	1.22	0.8	3.9	2.6978	2.507	4.8	2.644	2.409
19	LS	39	Above	1.73	57.5	4.7	4.4	13.6	67.9	6.63	5.79	1.22	0.8	3.9	2.6978	2.507	4.8	2.644	2.398
19	LS	39	Above	3.53	57.5	4.7	4.4	13.6	67.6	6.63	5.79	1.22	0.8	3.9	2.6978	2.507	4.8	2.644	2.396
19	LS	39	Below	6.87	57.5	5.5	4.6	16.3	71.7	13.27	3.79	0.61	0.4	5.1	2.6725	2.457	3.1	2.645	2.344
19	LS	39	Below	3.55	57.5	5.5	5.4	17.0	68.1	13.27	3.79	0.61	0.4	5.1	2.6725	2.457	3.1	2.645	2.324
19	LS	39	Below	4.55	57.5	5.5	2.5	14.4	82.8	13.27	3.79	0.61	0.4	5.1	2.6725	2.457	3.1	2.645	2.396
19	LS	39	Below	2.87	57.5	5.5	3.3	15.1	78.3	13.27	3.79	0.61	0.4	5.1	2.6725	2.457	3.1	2.645	2.376
19	LS	44	Above	2.16	57.5	4.6	5.0	13.8	63.8	6.02	6.09	1.57	0.8	3.8	2.7102	2.521	5.9	2.651	2.395
19	LS	44	Above	2.10	57.5	4.6	3.2	12.1	74.0	6.02	6.09	1.57	0.8	3.8	2.7102	2.521	5.9	2.651	2.441
19	LS	44	Above	2.16	57.5	4.6	4.4	13.3	66.8	6.02	6.09	1.57	0.8	3.8	2.7102	2.521	5.9	2.651	2.410
19	LS	44	Below	2.50	57.5	4.6	5.3	14.3	62.9	8.94	4.21	1.12	0.7	3.9	2.7029	2.515	4.3	2.651	2.382
19	LS	44	Below	1.92	57.5	4.6	3.7	12.9	71.1	8.94	4.21	1.12	0.7	3.9	2.7029	2.515	4.3	2.651	2.421
19	LS	44	Below	1.58	57.5	4.6	3.8	12.9	70.8	8.94	4.21	1.12	0.7	3.9	2.7029	2.515	4.3	2.651	2.420
19	LS	44	Below	2.46	57.5	4.6	4.2	13.3	68.7	8.94	4.21	1.12	0.7	3.9	2.7029	2.515	4.3	2.651	2.411
19	LS	50	Above	2.56	57.5	5.9	3.0	14.9	79.8	7.76	6.49	1.36	0.8	5.1	2.6997	2.464	6.9	2.643	2.390
19	LS	50	Above	3.55	57.5	5.9	4.4	16.1	72.7	7.76	6.49	1.36	0.8	5.1	2.6997	2.464	6.9	2.643	2.355
19	LS	50	Above	2.10	57.5	5.9	4.2	15.9	73.9	7.76	6.49	1.36	0.8	5.1	2.6997	2.464	6.9	2.643	2.362
19	LS	50	Above	2.13	57.5	5.9	3.6	15.4	76.6	7.76	6.49	1.36	0.8	5.1	2.6997	2.464	6.9	2.643	2.375
19	LS	50	Below	2.55	57.5	5.5	3.5	14.6	75.7	11.45	4.07	0.91	0.8	4.7	2.6988	2.478	4.3	2.645	2.390
19	LS	50	Below	2.52	57.5	5.5	6.1	16.8	63.9	11.45	4.07	0.91	0.8	4.7	2.6988	2.478	4.3	2.645	2.327
19	LS	50	Below	1.72	57.5	5.5	3.9	14.9	74.0	11.45	4.07	0.91	0.8	4.7	2.6988	2.478	4.3	2.645	2.382
19	LS	50	Below	2.39	57.5	5.5	4.1	15.1	72.6	11.45	4.07	0.91	0.8	4.7	2.6988	2.478	4.3	2.645	2.375

Table D2. 4 PURWheel LMLCD Data.(continue)

Nom. Size (mm)	Coarse Agg. Type	FAA	Gradation	Rut Depth (mm)	Temp. (° C)	AC (%)	Air Voids (%)	VMA (%)	VFA (%)	Film Thick. (µm)	Surface Area (m^2/Kg)	Dust Prop.	Binder Abs. (Pba, %)	Effective Binder (Pbe, %)	Gse	Gmm	p200 (%)	Gsb	Bsg
19	LS	44	Through	1.15	60	4.4	5.1	13.6	62.2	7.46	4.71	1.14	0.8	3.6	2.7022	2.522	4.1	2.647	2.392
19	LS	44	Through	1.82	60	4.4	7.7	15.9	51.6	7.46	4.71	1.14	0.8	3.6	2.7022	2.522	4.1	2.647	2.328
19	LS	44	Through	1.41	60	4.9	4.3	13.9	69.3	8.54	4.71	1.00	0.8	4.1	2.7021	2.503	4.1	2.647	2.396
19	LS	44	Through	1.41	60	4.9	4.3	14.0	69.0	8.54	4.71	1.00	0.8	4.1	2.7021	2.503	4.1	2.647	2.395
19	LS	44	Through	1.82	60	5.4	3.9	14.7	73.3	9.65	4.71	0.89	0.8	4.6	2.7017	2.484	4.1	2.647	2.386
19	LS	44	Through	2.26	60	5.4	3.0	13.9	78.3	9.65	4.71	0.89	0.8	4.6	2.7017	2.484	4.1	2.647	2.409
19	LS	44	Through	1.94	60	5.9	2.5	14.5	82.9	10.74	4.71	0.80	0.8	5.1	2.7022	2.466	4.1	2.647	2.405
19	LS	44	Through	1.78	60	5.9	0.4	12.7	96.8	10.74	4.71	0.80	0.8	5.1	2.7022	2.466	4.1	2.647	2.456
19	LS	44	Through	1.87	60	6.4	0.3	13.7	97.5	11.84	4.71	0.73	0.8	5.6	2.7024	2.448	4.1	2.647	2.440
19	LS	44	Through	1.98	60	6.4	1.0	14.3	92.8	11.84	4.71	0.73	0.8	5.6	2.7024	2.448	4.1	2.647	2.423
19	LS	50	Through	2.09	60	4.9	4.5	15.2	70.4	8.44	5.43	1.22	0.2	4.7	2.6593	2.468	5.7	2.644	2.357
19	LS	50	Through	1.83	60	4.9	3.7	14.5	74.6	8.44	5.43	1.22	0.2	4.7	2.6593	2.468	5.7	2.644	2.377
19	LS	50	Through	1.92	60	5.4	4.8	16.5	71.1	9.39	5.43	1.10	0.2	5.2	2.6593	2.450	5.7	2.644	2.333
19	LS	50	Through	1.38	60	5.4	1.2	13.4	91.2	9.39	5.43	1.10	0.2	5.2	2.6593	2.450	5.7	2.644	2.421
19	LS	50	Through	2.81	60	5.9	2.8	15.9	82.4	10.40	5.43	1.00	0.2	5.7	2.6577	2.431	5.7	2.644	2.363
19	LS	50	Through	3.19	60	5.9	-0.4	13.2	102.7	10.40	5.43	1.00	0.2	5.7	2.6577	2.431	5.7	2.644	2.440
19	LS	50	Through	3.81	60	6.4	0.3	14.8	98.0	11.39	5.43	0.92	0.2	6.2	2.6569	2.413	5.7	2.644	2.406
19	LS	50	Through	3.20	60	6.4	0.3	14.8	98.0	11.39	5.43	0.92	0.2	6.2	2.6569	2.413	5.7	2.644	2.406
19	LS	50	Through	5.16	60	6.9	0.2	15.8	98.9	12.37	5.43	0.85	0.2	6.7	2.6572	2.396	5.7	2.644	2.392
19	LS	50	Through	4.12	60	6.9	-0.1	15.5	100.9	12.37	5.43	0.85	0.2	6.7	2.6572	2.396	5.7	2.644	2.399

Table D2. 4 PURWheel LMLCD Data.(continue)

Nom. Size (mm)	Coarse Agg. Type	FAA	Gradation	Rut Depth (mm)	Temp. (^{o} C)	AC (%)	Air Voids (%)	VMA (%)	VFA (%)	Film Thick. (μm)	Surface Area (m^2/Kg)	Dust Prop.	Binder Abs. (Pba, %)	Effective Binder (Pbe, %)	Gse	Gmm	p200 (%)	Gsb	Bsg
19	LS	50	Below	1.59	60	4.5	5.5	14.1	60.8	8.78	4.07	1.17	0.8	3.7	2.7031	2.519	4.3	2.645	2.380
19	LS	50	Below	1.81	60	4.5	6.3	14.8	57.4	8.78	4.07	1.17	0.8	3.7	2.7031	2.519	4.3	2.645	2.361
19	LS	50	Below	2.11	60	5	4.0	13.8	71.0	10.04	4.07	1.03	0.8	4.2	2.7030	2.500	4.3	2.645	2.400
19	LS	50	Below	1.83	60	5	4.8	14.6	66.7	10.04	4.07	1.03	0.8	4.2	2.7030	2.500	4.3	2.645	2.379
19	LS	50	Below	1.87	60	5.5	2.2	13.3	83.7	11.32	4.07	0.92	0.8	4.7	2.7026	2.481	4.3	2.645	2.427
19	LS	50	Below	2.03	60	5.5	4.6	15.4	70.3	11.32	4.07	0.92	0.8	4.7	2.7026	2.481	4.3	2.645	2.368
19	LS	50	Below	2.26	60	6	3.0	15.1	80.0	12.58	4.07	0.83	0.8	5.2	2.7030	2.463	4.3	2.645	2.388
19	LS	50	Below	2.88	60	6	1.9	14.2	86.3	12.58	4.07	0.83	0.8	5.2	2.7030	2.463	4.3	2.645	2.415
19	LS	50	Below	4.19	60	6.5	2.0	15.3	86.7	13.87	4.07	0.76	0.8	5.7	2.7032	2.445	4.3	2.645	2.395
19	LS	50	Below	2.97	60	6.5	0.9	14.3	94.0	13.87	4.07	0.76	0.8	5.7	2.7032	2.445	4.3	2.645	2.424
19	GR	44	Through	1.82	60	3.8	10.7	17.4	38.7	6.22	4.71	1.36	0.8	3.0	2.7008	2.544	4.1	2.647	2.273
19	GR	44	Through	2.26	60	3.8	9.0	15.8	43.4	6.22	4.71	1.36	0.8	3.0	2.7008	2.544	4.1	2.647	2.316
19	GR	44	Through	1.64	60	4.3	9.0	16.9	46.9	7.28	4.71	1.16	0.8	3.5	2.7012	2.525	4.1	2.647	2.299
19	GR	44	Through	1.52	60	4.3	7.4	15.5	52.1	7.28	4.71	1.16	0.8	3.5	2.7012	2.525	4.1	2.647	2.338
19	GR	44	Through	1.58	60	4.8	6.9	16.1	57.2	8.36	4.71	1.02	0.8	4.0	2.7012	2.506	4.1	2.647	2.333
19	GR	44	Through	1.19	60	4.8	5.6	15.0	62.2	8.36	4.71	1.02	0.8	4.0	2.7012	2.506	4.1	2.647	2.364
19	GR	44	Through	1.71	60	5.3	3.8	14.3	73.5	9.31	4.71	0.92	0.8	4.5	2.7058	2.491	4.1	2.647	2.397
19	GR	44	Through	1.68	60	5.3	7.3	17.4	57.8	9.31	4.71	0.92	0.8	4.5	2.7058	2.491	4.1	2.647	2.308
19	GR	44	Through	2.98	60	5.8	2.9	14.7	80.1	10.54	4.71	0.82	0.8	5.0	2.7014	2.469	4.1	2.647	2.397
19	GR	44	Through	2.56	60	5.8	2.3	14.1	83.8	10.54	4.71	0.82	0.8	5.0	2.7014	2.469	4.1	2.647	2.412

Table D2. 4 PURWheel LMLCD Data. (continue)

Nom. Size (mm)	Coarse Agg. Type	FAA	Gradation	Rut Depth (mm)	Temp. (° C)	AC (%)	Air Voids (%)	VMA (%)	VFA (%)	Film Thick. (µm)	Surface Area (m^2/Kg)	Dust Prop.	Binder Abs. (Pba, %)	Effective Binder (Pbe, %)	Gse	Gmm	p200 (%)	Gsb	Bsg
19	GR	44	Below	1.53	60	3.4	9.7	16.3	40.1	6.51	4.31	1.44	0.5	2.9	2.6828	2.544	4.2	2.649	2.296
19	GR	44	Below	1.65	60	3.4	9.2	15.7	41.7	6.51	4.31	1.44	0.5	2.9	2.6828	2.544	4.2	2.649	2.311
19	GR	44	Below	1.47	60	3.9	5.6	13.5	58.5	7.67	4.31	1.23	0.5	3.4	2.6830	2.525	4.2	2.649	2.383
19	GR	44	Below	1.54	60	3.9	9.1	16.7	45.7	7.67	4.31	1.23	0.5	3.4	2.6830	2.525	4.2	2.649	2.296
19	GR	44	Below	1.36	60	4.4	5.8	14.8	60.7	8.84	4.31	1.07	0.5	3.9	2.6830	2.506	4.2	2.649	2.360
19	GR	44	Below	1.72	60	4.4	6.0	15.0	59.9	8.84	4.31	1.07	0.5	3.9	2.6830	2.506	4.2	2.649	2.355
19	GR	44	Below	1.79	60	4.9	3.8	14.1	73.1	10.00	4.31	0.96	0.5	4.4	2.6837	2.488	4.2	2.649	2.394
19	GR	44	Below	1.85	60	4.9	5.4	15.5	65.1	10.00	4.31	0.96	0.5	4.4	2.6837	2.488	4.2	2.649	2.353
19	GR	44	Below	2.41	60	5.4	2.4	14.0	82.6	11.22	4.31	0.86	0.5	4.9	2.6830	2.469	4.2	2.649	2.409
19	GR	44	Below	2.58	60	5.4	3.0	14.5	79.2	11.22	4.31	0.86	0.5	4.9	2.6830	2.469	4.2	2.649	2.395
19	GR	50	Through	1.93	60	4.3	9.0	17.1	47.7	6.74	5.27	1.51	0.7	3.6	2.6892	2.515	5.5	2.644	2.290
19	GR	50	Through	1.74	60	4.3	7.4	15.7	52.7	6.74	5.27	1.51	0.7	3.6	2.6892	2.515	5.5	2.644	2.328
19	GR	50	Through	1.99	60	4.8	6.7	16.2	58.4	7.71	5.27	1.33	0.7	4.1	2.6890	2.496	5.5	2.644	2.328
19	GR	50	Through	2.21	60	4.8	7.7	17.0	54.9	7.71	5.27	1.33	0.7	4.1	2.6890	2.496	5.5	2.644	2.304
19	GR	50	Through	1.90	60	5.3	4.3	15.1	71.4	8.70	5.27	1.18	0.6	4.7	2.6884	2.477	5.5	2.644	2.370
19	GR	50	Through	1.54	60	5.3	5.4	16.1	66.2	8.70	5.27	1.18	0.6	4.7	2.6884	2.477	5.5	2.644	2.342
19	GR	50	Through	2.47	60	5.8	2.4	14.5	83.2	9.67	5.27	1.07	0.6	5.2	2.6887	2.459	5.5	2.644	2.399
19	GR	50	Through	1.81	60	5.8	3.4	15.3	78.0	9.67	5.27	1.07	0.6	5.2	2.6887	2.459	5.5	2.644	2.376
19	GR	50	Through	2.92	60	6.3	2.1	15.3	86.2	10.67	5.27	0.97	0.6	5.7	2.6886	2.441	5.5	2.644	2.389
19	GR	50	Through	2.18	60	6.3	1.7	14.9	88.8	10.67	5.27	0.97	0.6	5.7	2.6886	2.441	5.5	2.644	2.400

Table D2. 4 PURWheel LMLCD Data.(continue).

Nom. Size (mm)	Coarse Agg. Type	FAA	Gradation	Rut Depth (mm)	Temp. (° C)	AC (%)	Air Voids (%)	VMA (%)	VFA (%)	Film Thick. (µm)	Surface Area (m^2/Kg)	Dust Prop.	Binder Abs. (Pba, %)	Effective Binder (Pbe, %)	Gse	Gmm	p200 (%)	Gsb	Bsg
19	GR	50	Below	0.75	60	3.8	9.8	17.5	43.9	7.41	4.55	1.32	0.3	3.5	2.6669	2.515	4.6	2.645	2.268
19	GR	50	Below	2.82	60	3.8	10.3	17.9	42.7	7.41	4.55	1.32	0.3	3.5	2.6669	2.515	4.6	2.645	2.257
19	GR	50	Below	2.08	60	4.3	7.0	16.0	56.4	8.53	4.55	1.15	0.3	4.0	2.6665	2.496	4.6	2.645	2.322
19	GR	50	Below	1.64	60	4.3	7.1	16.1	56.0	8.53	4.55	1.15	0.3	4.0	2.6665	2.496	4.6	2.645	2.320
19	GR	50	Below	2.39	60	4.8	2.4	13.0	81.4	9.64	4.55	1.03	0.3	4.5	2.6670	2.478	4.6	2.645	2.418
19	GR	50	Below	2.48	60	4.8	7.9	17.8	55.8	9.64	4.55	1.03	0.3	4.5	2.6670	2.478	4.6	2.645	2.283
19	GR	50	Below	2.52	60	5.3	2.7	14.3	81.0	10.76	4.55	0.92	0.3	5.0	2.6672	2.460	4.6	2.645	2.393
19	GR	50	Below	3.56	60	5.3	3.0	14.5	79.7	10.76	4.55	0.92	0.3	5.0	2.6672	2.460	4.6	2.645	2.387
19	GR	50	Below	8.48	60	5.8	1.9	14.7	86.8	11.91	4.55	0.84	0.3	5.5	2.6671	2.442	4.6	2.645	2.394
19	GR	50	Below	3.86	60	5.8	2.1	14.8	86.0	11.91	4.55	0.84	0.3	5.5	2.6671	2.442	4.6	2.645	2.391
9.5	LS	44	Above	1.72	60	4.6	8.9	17.5	49.0	4.53	8.22	2.15	0.8	3.8	2.7005	2.513	8.2	2.646	2.289
9.5	LS	44	Above	1.88	60	4.6	8.5	17.1	50.2	4.53	8.22	2.15	0.8	3.8	2.7005	2.513	8.2	2.646	2.299
9.5	LS	44	Above	2.03	60	5.1	5.2	15.2	65.7	5.16	8.22	1.90	0.8	4.3	2.7003	2.494	8.2	2.646	2.364
9.5	LS	44	Above	2.12	60	5.1	8.3	18.0	53.9	5.16	8.22	1.90	0.8	4.3	2.7003	2.494	8.2	2.646	2.287
9.5	LS	44	Above	2.00	60	5.6	4.4	15.6	71.9	5.80	8.22	1.70	0.8	4.8	2.6997	2.475	8.2	2.646	2.367
9.5	LS	44	Above	1.63	60	5.6	4.7	15.9	70.3	5.80	8.22	1.70	0.8	4.8	2.6997	2.475	8.2	2.646	2.358
9.5	LS	44	Above	1.66	60	6.1	2.6	15.1	82.8	6.43	8.22	1.54	0.8	5.3	2.7000	2.457	8.2	2.646	2.393
9.5	LS	44	Above	2.95	60	6.1	3.8	16.2	76.2	6.43	8.22	1.54	0.8	5.3	2.7000	2.457	8.2	2.646	2.363
9.5	LS	44	Above	2.34	60	6.6	2.5	16.1	84.2	7.07	8.22	1.41	0.8	5.8	2.7000	2.439	8.2	2.646	2.377
9.5	LS	44	Above	1.46	60	6.6	2.0	15.7	87.0	7.07	8.22	1.41	0.8	5.8	2.7000	2.439	8.2	2.646	2.389

Table D2. 4 PURWheel LMLCD Data. (continue)

Nom. Size (mm)	Coarse Agg. Type	FAA	Gradation	Rut Depth (mm)	Temp. (° C)	AC (%)	Air Voids (%)	VMA (%)	VFA (%)	Film Thick. (μm)	Surface Area (m^2/Kg)	Dust Prop.	Binder Abs. (Pba, %)	Effective Binder (Pbe, %)	Gse	Gmm	p200 (%)	Gsb	Bsg
9.5	LS	44	Through	1.40	60	5.2	5.4	16.1	66.3	7.68	5.96	1.14	0.5	4.7	2.6813	2.475	5.3	2.644	2.341
9.5	LS	44	Through	1.01	60	5.2	4.2	15.0	72.2	7.68	5.96	1.14	0.5	4.7	2.6813	2.475	5.3	2.644	2.372
9.5	LS	44	Through	1.87	60	5.7	4.3	16.1	73.5	8.55	5.96	1.03	0.5	5.2	2.6816	2.457	5.3	2.644	2.352
9.5	LS	44	Through	1.35	60	5.7	3.8	15.7	76.0	8.55	5.96	1.03	0.5	5.2	2.6816	2.457	5.3	2.644	2.365
9.5	LS	44	Through	1.93	60	6.2	5.7	18.4	69.1	9.43	5.96	0.94	0.5	5.7	2.6815	2.439	5.3	2.644	2.300
9.5	LS	44	Through	1.40	60	6.2	0.3	13.7	97.9	9.43	5.96	0.94	0.5	5.7	2.6815	2.439	5.3	2.644	2.432
9.5	LS	44	Through	2.33	60	6.7	2.0	16.3	87.5	10.30	5.96	0.86	0.6	6.1	2.6823	2.422	5.3	2.644	2.373
9.5	LS	44	Through	1.41	60	6.7	1.5	15.8	90.5	10.30	5.96	0.86	0.6	6.1	2.6823	2.422	5.3	2.644	2.386
9.5	LS	44	Through	2.14	60	7.2	0.6	16.1	96.5	11.21	5.96	0.80	0.5	6.7	2.6815	2.404	5.3	2.644	2.391
9.5	LS	44	Through	1.23	60	7.2	0.5	16.0	96.9	11.21	5.96	0.80	0.5	6.7	2.6815	2.404	5.3	2.644	2.392
9.5	LS	44	Below	2.43	60	5.2	10.0	18.8	46.6	8.18	4.70	1.07	1.3	3.9	2.7335	2.517	4.2	2.643	2.265
9.5	LS	44	Below	1.27	60	5.2	5.4	14.6	63.1	8.18	4.70	1.07	1.3	3.9	2.7335	2.517	4.2	2.643	2.382
9.5	LS	44	Below	2.26	60	5.7	7.3	17.4	57.7	9.24	4.70	0.96	1.3	4.4	2.7348	2.499	4.2	2.643	2.315
9.5	LS	44	Below	1.35	60	5.7	4.1	14.5	71.7	9.24	4.70	0.96	1.3	4.4	2.7348	2.499	4.2	2.643	2.396
9.5	LS	44	Below	2.04	60	6.2	4.6	16.0	71.0	10.31	4.70	0.86	1.3	4.9	2.7357	2.481	4.2	2.643	2.366
9.5	LS	44	Below	1.37	60	6.2	4.2	15.6	73.4	10.31	4.70	0.86	1.3	4.9	2.7357	2.481	4.2	2.643	2.378
9.5	LS	44	Below	2.30	60	6.7	1.9	14.7	87.2	11.41	4.70	0.78	1.3	5.4	2.7364	2.463	4.2	2.643	2.416
9.5	LS	44	Below	1.90	60	6.7	4.5	17.0	73.5	11.41	4.70	0.78	1.3	5.4	2.7364	2.463	4.2	2.643	2.352
9.5	LS	44	Below	3.03	60	7.2	3.3	16.9	80.7	12.49	4.70	0.72	1.4	5.8	2.7380	2.446	4.2	2.643	2.366
9.5	LS	44	Below	2.56	60	7.2	1.9	15.7	88.2	12.49	4.70	0.72	1.4	5.8	2.7380	2.446	4.2	2.643	2.401

Table D2. 4 PURWheel LMLCD Data.(continue).

Nom. Size (mm)	Coarse Agg. Type	FAA	Gradation	Rut Depth (mm)	Temp. (° C)	AC (%)	Air Voids (%)	VMA (%)	VFA (%)	Film Thick. (µm)	Surface Area (m^2/Kg)	Dust Prop.	Binder Abs. (Pba, %)	Effective Binder (Pbe, %)	Gse	Gmm	p200 (%)	Gsb	Bsg
9.5	LS	50	Through	1.93	60	5.6	8.2	18.8	56.4	8.06	5.85	1.47	0.8	4.8	2.6972	2.473	7.0	2.640	2.270
9.5	LS	50	Through	1.42	60	5.6	6.0	16.9	64.4	8.06	5.85	1.47	0.8	4.8	2.6972	2.473	7.0	2.640	2.324
9.5	LS	50	Through	2.67	60	6.1	6.3	18.2	65.5	8.97	5.85	1.32	0.8	5.3	2.6961	2.454	7.0	2.640	2.300
9.5	LS	50	Through	1.50	60	6.1	3.9	16.1	75.7	8.97	5.85	1.32	0.8	5.3	2.6961	2.454	7.0	2.640	2.358
9.5	LS	50	Through	2.33	60	6.6	3.9	17.1	77.5	9.84	5.85	1.21	0.8	5.8	2.6974	2.437	7.0	2.640	2.343
9.5	LS	50	Through	1.76	60	6.6	2.9	16.3	82.0	9.84	5.85	1.21	0.8	5.8	2.6974	2.437	7.0	2.640	2.365
9.5	LS	50	Through	3.36	60	7.1	3.3	17.7	81.3	10.76	5.85	1.12	0.8	6.3	2.6970	2.419	7.0	2.640	2.339
9.5	LS	50	Through	2.61	60	7.1	2.0	16.6	87.9	10.76	5.85	1.12	0.8	6.3	2.6970	2.419	7.0	2.640	2.371
9.5	LS	50	Through	4.74	60	7.6	1.8	17.5	89.8	11.70	5.85	1.03	0.8	6.8	2.6962	2.401	7.0	2.640	2.358
9.5	LS	50	Through	2.75	60	7.6	2.2	17.9	87.4	11.70	5.85	1.03	0.8	6.8	2.6962	2.401	7.0	2.640	2.347
9.5	LS	50	Below	1.67	60	5.7	5.3	16.4	67.9	8.14	5.90	1.25	0.8	4.9	2.6980	2.470	6.1	2.640	2.340
9.5	LS	50	Below	1.28	60	5.7	5.3	16.5	67.7	8.14	5.90	1.25	0.8	4.9	2.6980	2.470	6.1	2.640	2.339
9.5	LS	50	Below	2.27	60	6.2	6.3	18.3	65.8	9.02	5.90	1.14	0.8	5.4	2.6982	2.452	6.1	2.640	2.298
9.5	LS	50	Below	1.42	60	6.2	2.2	14.8	85.1	9.02	5.90	1.14	0.8	5.4	2.6982	2.452	6.1	2.640	2.398
9.5	LS	50	Below	1.87	60	6.7	3.6	17.1	78.9	9.92	5.90	1.04	0.8	5.9	2.6981	2.434	6.1	2.640	2.346
9.5	LS	50	Below	1.44	60	6.7	3.2	16.7	80.8	9.92	5.90	1.04	0.8	5.9	2.6981	2.434	6.1	2.640	2.356
9.5	LS	50	Below	3.87	60	7.2	4.0	18.5	78.3	10.84	5.90	0.96	0.8	6.4	2.6976	2.416	6.1	2.640	2.319
9.5	LS	50	Below	3.48	60	7.2	1.3	16.2	92.0	10.84	5.90	0.96	0.8	6.4	2.6976	2.416	6.1	2.640	2.385
9.5	LS	50	Below	5.20	60	7.7	0.8	16.8	95.4	11.74	5.90	0.89	0.8	6.9	2.6982	2.399	6.1	2.640	2.381
9.5	LS	50	Below	3.90	60	7.7	2.8	18.5	84.7	11.74	5.90	0.89	0.8	6.9	2.6982	2.399	6.1	2.640	2.331

Table D2. 4 PURWheel LMLCD Data.(continue).

Nom. Size (mm)	Coarse Agg. Type	FAA	Gradation	Rut Depth (mm)	Temp. (° C)	AC (%)	Air Voids (%)	VMA (%)	VFA (%)	Film Thick. (µm)	Surface Area (m^2/Kg)	Dust Prop.	Binder Abs. (Pba, %)	Effective Binder (Pbe, %)	Gse	Gmm	p200 (%)	Gsb	Bsg
9.5	GR	44	Through	1.49	60	4.3	11.1	18.9	41.0	5.16	6.64	1.76	0.8	3.5	2.7012	2.525	6.2	2.647	2.244
9.5	GR	44	Through	0.79	60	4.3	10.2	18.0	43.5	5.16	6.64	1.76	0.8	3.5	2.7012	2.525	6.2	2.647	2.268
9.5	GR	44	Through	1.53	60	4.8	8.2	17.3	52.4	5.93	6.64	1.54	0.8	4.0	2.7012	2.506	6.2	2.647	2.300
9.5	GR	44	Through	1.65	60	4.8	9.1	18.1	49.6	5.93	6.64	1.54	0.8	4.0	2.7012	2.506	6.2	2.647	2.278
9.5	GR	44	Through	1.77	60	5.3	8.5	18.6	54.3	6.71	6.64	1.37	0.8	4.5	2.7008	2.487	6.2	2.647	2.276
9.5	GR	44	Through	1.44	60	5.3	7.4	17.6	57.9	6.71	6.64	1.37	0.8	4.5	2.7008	2.487	6.2	2.647	2.302
9.5	GR	44	Through	1.03	60	5.8	5.7	17.2	66.5	7.48	6.64	1.24	0.8	5.0	2.7014	2.469	6.2	2.647	2.327
9.5	GR	44	Through	1.61	60	5.8	5.6	17.0	67.4	7.48	6.64	1.24	0.8	5.0	2.7014	2.469	6.2	2.647	2.332
9.5	GR	44	Through	2.94	60	6.3	4.4	17.1	74.0	8.26	6.64	1.12	0.8	5.5	2.7016	2.451	6.2	2.647	2.342
9.5	GR	44	Through	1.40	60	6.3	3.0	15.8	81.2	8.26	6.64	1.12	0.8	5.5	2.7016	2.451	6.2	2.647	2.378
9.5	GR	44	Below	1.37	60	4.2	10.0	17.9	44.0	6.82	5.04	1.33	0.7	3.5	2.6930	2.522	4.7	2.647	2.270
9.5	GR	44	Below	0.85	60	4.2	8.1	16.1	49.9	6.82	5.04	1.33	0.7	3.5	2.6930	2.522	4.7	2.647	2.319
9.5	GR	44	Below	1.38	60	4.7	8.5	17.4	51.0	7.63	5.04	1.20	0.8	3.9	2.7002	2.509	4.7	2.647	2.295
9.5	GR	44	Below	1.09	60	4.7	6.5	15.5	58.2	7.63	5.04	1.20	0.8	3.9	2.7002	2.509	4.7	2.647	2.346
9.5	GR	44	Below	1.10	60	5.2	7.0	16.9	58.5	8.49	5.04	1.08	0.9	4.3	2.7061	2.495	4.7	2.647	2.320
9.5	GR	44	Below	1.39	60	5.2	5.3	15.3	65.7	8.49	5.04	1.08	0.9	4.3	2.7061	2.495	4.7	2.647	2.364
9.5	GR	44	Below	2.21	60	5.7	4.9	15.9	69.1	9.32	5.04	0.99	0.9	4.8	2.7132	2.482	4.7	2.647	2.360
9.5	GR	44	Below	1.60	60	5.7	5.4	16.3	67.1	9.32	5.04	0.99	0.9	4.8	2.7132	2.482	4.7	2.647	2.349
9.5	GR	44	Below	2.28	60	6.2	3.4	15.5	77.9	10.16	5.04	0.91	1.0	5.2	2.7202	2.469	4.7	2.647	2.384
9.5	GR	44	Below	1.97	60	6.2	3.2	15.3	79.0	10.16	5.04	0.91	1.0	5.2	2.7202	2.469	4.7	2.647	2.390

Table D2. 4 PURWheel LMLCD Data.(continue).

Nom. Size (mm)	Coarse Agg. Type	FAA	Gradation	Rut Depth (mm)	Temp. (° C)	AC (%)	Air Voids (%)	VMA (%)	VFA (%)	Film Thick. (μm)	Surface Area (m^2/Kg)	Dust Prop.	Binder Abs. (Pba, %)	Effective Binder (Pbe, %)	Gse	Gmm	p200 (%)	Gsb	Bsg
9.5	GR	50	Through	1.66	60	5	5.7	16.7	65.6	6.86	6.98	1.52	0.1	4.9	2.6503	2.457	7.4	2.642	2.316
9.5	GR	50	Through	2.23	60	5	6.1	17.1	64.0	6.86	6.98	1.52	0.1	4.9	2.6503	2.457	7.4	2.642	2.306
9.5	GR	50	Through	2.59	60	5.5	3.3	15.7	79.1	7.63	6.98	1.37	0.1	5.4	2.6487	2.438	7.4	2.642	2.358
9.5	GR	50	Through	1.75	60	5.5	4.2	16.5	74.4	7.63	6.98	1.37	0.1	5.4	2.6487	2.438	7.4	2.642	2.335
9.5	GR	50	Through	2.68	60	6	2.5	16.1	84.3	8.40	6.98	1.25	0.1	5.9	2.6481	2.420	7.4	2.642	2.359
9.5	GR	50	Through	1.88	60	6	1.6	15.3	89.6	8.40	6.98	1.25	0.1	5.9	2.6481	2.420	7.4	2.642	2.382
9.5	GR	50	Through	4.22	60	6.5	-0.4	14.7	102.6	9.17	6.98	1.15	0.1	6.4	2.6471	2.402	7.4	2.642	2.411
9.5	GR	50	Through	2.44	60	6.5	1.8	16.6	88.9	9.17	6.98	1.15	0.1	6.4	2.6471	2.402	7.4	2.642	2.358
9.5	GR	50	Through	6.51	60	7	-0.4	15.7	102.7	9.97	6.98	1.07	0.1	6.9	2.6458	2.384	7.4	2.642	2.394
9.5	GR	50	Through	5.40	60	7	-0.3	15.8	101.8	9.97	6.98	1.07	0.1	6.9	2.6458	2.384	7.4	2.642	2.391
9.5	GR	50	Below	1.46	60	4.6	5.4	14.7	63.1	6.66	5.88	1.52	0.6	4.0	2.6835	2.499	6.1	2.643	2.364
9.5	GR	50	Below	1.16	60	4.6	8.4	17.4	51.7	6.66	5.88	1.52	0.6	4.0	2.6835	2.499	6.1	2.643	2.289
9.5	GR	50	Below	1.35	60	5.1	5.6	15.7	64.3	7.34	5.88	1.39	0.7	4.4	2.6916	2.487	6.1	2.643	2.348
9.5	GR	50	Below	1.30	60	5.1	4.9	15.1	67.4	7.34	5.88	1.39	0.7	4.4	2.6916	2.487	6.1	2.643	2.365
9.5	GR	50	Below	1.98	60	5.6	6.0	17.0	64.5	8.12	5.88	1.26	0.8	4.8	2.6959	2.472	6.1	2.643	2.323
9.5	GR	50	Below	1.95	60	5.6	2.3	13.7	83.3	8.12	5.88	1.26	0.8	4.8	2.6959	2.472	6.1	2.643	2.415
9.5	GR	50	Below	3.42	60	6.1	2.5	15.0	83.6	9.03	5.88	1.14	0.7	5.4	2.6949	2.453	6.1	2.643	2.393
9.5	GR	50	Below	2.99	60	6.1	1.3	14.0	90.7	9.03	5.88	1.14	0.7	5.4	2.6949	2.453	6.1	2.643	2.421
9.5	GR	50	Below	3.79	60	6.6	1.8	15.4	88.4	9.84	5.88	1.05	0.8	5.8	2.6987	2.438	6.1	2.643	2.394
9.5	GR	50	Below	3.20	60	6.6	1.6	15.2	89.4	9.84	5.88	1.05	0.8	5.8	2.6987	2.438	6.1	2.643	2.399

APPENDIX D3 Statistical Analysis of PURWheel Test Results

Table D3. 1 Regression Analysis of Total Rut and Rut Depth in PURWheel Relationship.

Dependent Variable: PURWheel Total Rut Analysis of Variance					
Source	df	SS	MS	F	Pr > F
Model	1	909.884	909.884	888.028	4.28E-71
Error	178	182.381	1.025		
Total	179	1092.264			
R-square = 0.8330 Adjusted R-square = 0.8320					
Parameter Estimate					
Variable	df	Parameter Estimate	Standard Error	T for H_0	Pr > T
Intercept	1	-0.008	0.162	-0.051	0.9592
Rut Depth	1	1.889	0.063	29.800	4.28E-71

Table D3. 2 Regression Analysis of APT Total Rut and PURWheel Rut Depth on FMFC Specimens (All mixtures).

Dependent Variable: APT Total Rut Analysis of Variance					
Source	df	SS	MS	F	Pr > F
Model	1	145.705	145.705	4.855	0.0478
Error	12	360.115	30.010		
Total	13	505.820			
R-square = 0.2881 Adjusted R-square = 0.2287					
Parameter Estimate					
Variable	df	Parameter Estimate	Standard Error	T for H_0	Pr > T
Intercept	1	7.751	3.021	2.566	0.0247
FMFC	1	0.873	0.396	2.203	0.0478

Table D3. 3 Regression Analysis of APT Total Rut and PURWheel Rut Depth on FMLC Specimens (All mixtures).

Dependent Variable: APT Total Rut Analysis of Variance					
Source	df	SS	MS	F	Pr > F
Model	1	64.744	64.744	4.708	0.0552
Error	10	137.508	13.751		
Total	11	202.252			
R-square = 0.3201 Adjusted R-square = 0.2521					
Parameter Estimate					
Variable	df	Parameter Estimate	Standard Error	T for H_0	Pr > T
Intercept	1	8.094	2.028	3.991	0.0026
FMLC	1	1.195	0.551	2.170	0.0552

Table D3. 4 Regression Analysis of APT Total Rut and PURWheel Rut Depth on LMLCF Specimens (All mixtures).

Dependent Variable: APT Total Rut Analysis of Variance					
Source	df	SS	MS	F	Pr > F
Model	1	67.341	67.341	5.108	0.0502
Error	9	118.642	13.182		
Total	10	185.983			
R-square = 0.3621 Adjusted R-square = 0.2912					
Parameter Estimate					
Variable	df	Parameter Estimate	Standard Error	T for H_0	Pr > T
Intercept	1	4.052	3.760	1.078	0.3092
LMLCF	1	3.757	1.662	2.260	0.0502

Table D3. 5 Regression Analysis of APT Total Rut and PURWheel Rut Depth on FMFC Specimens (19 mm mixtures only).

Dependent Variable: APT Total Rut Analysis of Variance					
Source	df	SS	MS	F	Pr > F
Model	1	295.009	295.009	44.589	0.0026
Error	4	26.464	6.616		
Total	5	321.473			
R-square = 0.9177 Adjusted R-square = 0.8971					
Parameter Estimate					
Variable	df	Parameter Estimate	Standard Error	T for H_0	Pr > T
Intercept	1	-11.762	4.281	-2.748	0.0515
FMFC	1	5.068	0.759	6.678	0.0026

Table D3. 6 Regression Analysis of APT Total Rut and PURWheel Rut Depth on FMLC Specimens (19 mm mixtures only).

Dependent Variable: APT Total Rut Analysis of Variance					
Source	df	SS	MS	F	Pr > F
Model	1	57.764	57.764	5.9346	0.1352
Error	2	19.467	9.734		
Total	3	77.231			
R-square = 0.7479 Adjusted R-square = 0.6219					
Parameter Estimate					
Variable	df	Parameter Estimate	Standard Error	T for H_0	Pr > T
Intercept	1	-8.073	8.353	-0.967	0.4358
FMLC	1	10.718	4.400	2.436	0.1352

Table D3. 7 Regression Analysis of APT Total Rut and PURWheel Rut Depth on LMLCF Specimens (19 mm mixtures only).

Dependent Variable: APT Total Rut Analysis of Variance					
Source	df	SS	MS	F	Pr > F
Model	1	44.276	44.276	2.687	0.2428
Error	2	32.955	16.477		
Total	3	77.231			
R-square = 0.5733 Adjusted R-square = 0.3599					
Parameter Estimate					
Variable	df	Parameter Estimate	Standard Error	T for H_0	Pr > T
Intercept	1	-4.710	10.344	-0.455	0.6935
LMLCF	1	8.394	5.120	1.639	0.2428

Table D3. 8 Regression Analysis of APT Total Rut and PURWheel Rut Depth on FMFC Specimens (9.5 mm mixtures only).

Dependent Variable: APT Total Rut Analysis of Variance					
Source	df	SS	MS	F	Pr > F
Model	1	116.756	116.756	85.213	0.0001
Error	6	8.221	1.370		
Total	7	124.977			
R-square = 0.9342 Adjusted R-square = 0.9233					
Parameter Estimate					
Variable	df	Parameter Estimate	Standard Error	T for H_0	Pr > T
Intercept	1	5.415	0.805	6.726	0.0005
FMFC	1	0.842	0.091	9.231	0.0001

Table D3. 9 Regression Analysis of APT Total Rut and PURWheel Rut Depth on FMLC Specimens (9.5 mm mixtures only).

Dependent Variable: APT Total Rut Analysis of Variance					
Source	df	SS	MS	F	Pr > F
Model	1	69.314	69.314	7.472	0.0340
Error	6	55.663	9.277		
Total	7	124.977			
R-square = 0.5546 Adjusted R-square = 0.4804					
Parameter Estimate					
Variable	df	Parameter Estimate	Standard Error	T for H_0	Pr > T
Intercept	1	6.518	2.209	2.951	0.0256
FMLC	1	1.402	0.513	2.733	0.0340

Table D3. 10 Regression Analysis of APT Total Rut and PURWheel Rut Depth on LMLCF Specimens (9.5 mm mixtures only).

Dependent Variable: APT Total Rut Analysis of Variance					
Source	df	SS	MS	F	Pr > F
Model	1	38.761	38.761	2.787	0.1559
Error	5	69.548	13.910		
Total	6	108.309			
R-square = 0.4187 Adjusted R-square = 0.3218					
Parameter Estimate					
Variable	df	Parameter Estimate	Standard Error	T for H_0	Pr > T
Intercept	1	5.210	4.495	1.159	0.2988
LMLCF	1	3.140	1.881	1.669	0.1559

Table D3. 11 Regression Analysis of APT Rut Depth and PURWheel Rut Depth on FMFC Specimens (19 mm mixtures only).

Dependent Variable: APT Rut Depth Analysis of Variance					
Source	df	SS	MS	F	Pr > F
Model	1	22.280	22.280	5.811	0.0735
Error	4	15.335	3.834		
Total	5	37.616			
R-square = 0.5923 Adjusted R-square = 0.4904					
Parameter Estimate					
Variable	df	Parameter Estimate	Standard Error	T for H_0	Pr > T
Intercept	1	1.204	3.259	0.370	0.7304
FMFC	1	1.393	0.578	2.411	0.0735

Table D3. 12 Regression Analysis of APT Total Rut and PURWheel Rut Depth on FMLC Specimens (19 mm mixtures only).

Dependent Variable: APT Rut Depth Analysis of Variance					
Source	df	SS	MS	F	Pr > F
Model	1	17.767	17.767	3.991	0.1838
Error	2	8.904	4.452		
Total	3	26.671			
R-square = 0.6661 Adjusted R-square = 0.4992					
Parameter Estimate					
Variable	df	Parameter Estimate	Standard Error	T for H_0	Pr > T
Intercept	1	-3.169	5.649	-0.561	0.6313
FMLC	1	5.944	2.976	1.998	0.1838

Table D3. 13 Regression Analysis of APT Rut Depth and PURWheel Rut Depth on LMLCF Specimens (19 mm mixtures only).

Dependent Variable: APT Rut Depth Analysis of Variance					
Source	df	SS	MS	F	Pr > F
Model	1	14.766	14.766	2.481	0.2559
Error	2	11.905	5.953		
Total	3	26.671			
R-square = 0.5536 Adjusted R-square = 0.3304					
Parameter Estimate					
Variable	df	Parameter Estimate	Standard Error	T for H_0	Pr > T
Intercept	1	-1.685	6.217	-0.271	0.8118
LMLCF	1	4.847	3.078	1.575	0.2559

Table D3. 14 Regression Analysis of APT Rut Depth and PURWheel Rut Depth on FMFC Specimens (9.5 mm mixtures only).

Dependent Variable: APT Rut Depth Analysis of Variance					
Source	df	SS	MS	F	Pr > F
Model	1	17.068	17.068	19.520	0.0045
Error	6	5.246	0.874		
Total	7	22.314			
R-square = 0.7648 Adjusted R-square = 0.7257					
Parameter Estimate					
Variable	df	Parameter Estimate	Standard Error	T for H_0	Pr > T
Intercept	1	5.513	0.643	8.573	0.0001
FMFC	1	0.322	0.073	4.418	0.0045

Table D3. 15 Regression Analysis of APT Rut Depth and PURWheel Rut Depth on FMLC Specimens (9.5 mm mixtures only).

Dependent Variable: APT Rut Depth Analysis of Variance					
Source	df	SS	MS	F	Pr > F
Model	1	5.687	5.687	2.052	0.2020
Error	6	16.627	2.771		
Total	7	22.314			
R-square = 0.2549 Adjusted R-square = 0.1307					
Parameter Estimate					
Variable	df	Parameter Estimate	Standard Error	T for H_0	Pr > T
Intercept	1	6.440	1.207	5.335	0.0018
FMLC	1	0.402	0.280	1.433	0.2020

Table D3. 16 Regression Analysis of APT Rut Depth and PURWheel Rut Depth on LMLCF Specimens (9.5 mm mixtures only).

Dependent Variable: APT Rut Depth Analysis of Variance					
Source	df	SS	MS	F	Pr > F
Model	1	5.205	5.205	3.775	0.1096
Error	5	6.893	1.379		
Total	6	12.097			
R-square = 0.4302 Adjusted R-square = 0.3163					
Parameter Estimate					
Variable	df	Parameter Estimate	Standard Error	T for H_0	Pr > T
Intercept	1	5.766	1.415	4.075	0.0096
LMLCF	1	1.150	0.592	1.943	0.1096

Table D3. 17 Regression Analysis of PURWheel FMFC and FMLC.

Dependent Variable: PURWheel FMFC Rut Depth Analysis of Variance					
Source	df	SS	MS	F	Pr > F
Model	1	116.293	116.293	16.022	0.0025
Error	10	72.584	7.258		
Total	11	188.876			
R-square = 0.6157 Adjusted R-square = 0.5773					
Parameter Estimate					
Variable	df	Parameter Estimate	Standard Error	T for H_0	Pr > T
Intercept	1	1.602	1.474	1.087	0.3023
FMLC	1	1.601	0.400	4.003	0.0025

Table D3. 18 Regression Analysis of PURWheel FMFC and LMLCF.

Dependent Variable: PURWheel FMFC Rut Depth Analysis of Variance					
Source	df	SS	MS	F	Pr > F
Model	1	88.812	88.812	9.761	0.0122
Error	9	81.886	9.098		
Total	10	170.698			
R-square = 0.5203 Adjusted R-square = 0.4670					
Parameter Estimate					
Variable	df	Parameter Estimate	Standard Error	T for H_0	Pr > T
Intercept	1	-2.354	3.124	-0.754	0.4704
LMLCF	1	4.314	1.381	3.124	0.0122

Table D3. 19 Regression Analysis of PURWheel FMLC and LMLCF.

Dependent Variable: PURWheel FMLC Rut Depth Analysis of Variance					
Source	df	SS	MS	F	Pr > F
Model	1	22.532	22.532	8.959	0.0151
Error	9	22.634	2.515		
Total	10	45.165			
R-square = 0.4989 Adjusted R-square = 0.4432					
Parameter Estimate					
Variable	df	Parameter Estimate	Standard Error	T for H_0	Pr > T
Intercept	1	-1.538	1.642	-0.936	0.3735
LMLCF	1	2.173	0.726	2.993	0.0151

Table D3. 20 Regression Analysis of PURWheel LMLCF and LMLCD.

Dependent Variable: PURWheel LMLCF Rut Depth Analysis of Variance					
Source	df	SS	MS	F	Pr > F
Model	1	0.996	0.996	2.345	0.1766
Error	6	2.548	0.425		
Total	7	3.545			
R-square = 0.2810 Adjusted R-square = 0.1612					
Parameter Estimate					
Variable	df	Parameter Estimate	Standard Error	T for H_0	Pr > T
Intercept	1	0.835	0.799	1.044	0.3366
LMLCD	1	0.557	0.364	1.531	0.1766

Table D3. 21 Regression Analysis of APT Total Rut and PURWheel Rut Depth on LMLCD Specimens (19 mm mixtures only).

Dependent Variable: APT Total Rut Analysis of Variance					
Source	df	SS	MS	F	Pr > F
Model	1	213.982	213.982	7.201	0.0364
Error	6	178.304	29.717		
Total	7	392.286			
R-square = 0.5455 Adjusted R-square = 0.4697					
Parameter Estimate					
Variable	df	Parameter Estimate	Standard Error	T for H_0	Pr > T
Intercept	1	2.035	5.554	0.366	0.7266
LMLCD	1	5.919	2.206	2.683	0.0364

Table D3. 22 Regression Analysis of APT Total Rut and PURWheel Rut Depth on LMLCD Specimens (9.5 mm mixtures only).

Dependent Variable: APT Total Rut Analysis of Variance					
Source	df	SS	MS	F	Pr > F
Model	1	9.532	9.532	0.336	0.6210
Error	2	56.810	28.405		
Total	3	66.342			
R-square = 0.1437 Adjusted R-square = -0.2845					
Parameter Estimate					
Variable	df	Parameter Estimate	Standard Error	T for H_0	Pr > T
Intercept	1	7.391	8.485	0.871	0.4756
LMLCD	1	2.018	3.483	0.579	0.6210

Table D3. 23 Test of Nominal Size Effect on LMLCD Specimens in PURWheel.

Mixture	19	9.5	Δ	Calculation
LS44A	2.14	2.12	0.02	$\alpha = 0.05$
LS44T	1.42	1.56	-0.14	H_0 : RD 19 = RD 9.5
LS50T	2.01	1.71	0.30	H_1 : RD 19 > RD 9.5
LS50B	3.00	1.80	1.20	$\Delta_{average} = 0.10$, $\Delta_{std.dev.} = 0.516$
GR44T	1.95	1.65	0.30	$t_0 = 0.569$, $t_\alpha = 2.306$, p = 0.5851
GR44B	1.23	1.61	-0.38	Conclusion: ($\alpha = 0.05$)
GR50T	1.54	1.24	0.30	**RD 19 = RD 9.5**
GR50B	1.72	2.28	-0.56	

Table D3. 24 Test of Coarse Aggregate Type Effect on LMLCD Specimens in PURWheel.

Mixture	LS	GR	Δ	Calculation
9.5-44T	1.56	1.61	-0.05	$\alpha = 0.05$
9.5-44B	1.71	1.24	0.47	H_0 : RD LS = RD GR
9.5-50T	1.80	2.28	-0.48	H_1 : RD LS > RD GR
9.5-50B	1.65	1.97	-0.32	$\Delta_{average} = 0.21$, $\Delta_{std.dev.} = 0.549$
19-44T	1.42	1.23	0.19	$t_0 = 1.095$, $t_\alpha = 0.310$, p = 0.3099
19-50T	2.01	1.54	0.47	Conclusion:
19-50B	3.00	1.72	1.28	**RD LS = RD GR**

Table D3. 25 Test of Fine Aggregate Angularity Effect on LMLCD Specimens in PURWheel.

Mixture	44	50	Δ	Calculation
9.5LS-T	1.56	1.80	-0.24	$\alpha = 0.05$
9.5LS-B	1.71	1.65	0.06	H_0 : RD 44 = RD 50
9.5GR-T	1.61	2.28	-0.67	H_1 : RD 44 < RD 50
9.5GR-B	1.24	1.97	-0.73	$\Delta_{average} = -0.489$, $\Delta_{std.dev.} = 0.500$
19LS-A	2.14	2.68	-0.54	$t_0 = -2.936$, $t_\alpha = -2.306$, p = 0.0188
19LS-T	1.42	3.00	-1.58	Conclusion:
19GR-T	2.01	1.95	0.06	**RD 44 < RD 50**
19GR-B	1.23	1.72	-0.49	

Table D3. 26 Test of Gradation Plotting Above And Through Restricted Zone Effect on LMLCD Specimens in PURWheel.

Mixture	Above	Through	Δ	Calculation
9.5LS44	2.12	1.56	0.56	H_0 : RD Above = RD Through
19LS44	2.14	1.42	0.72	H_1 : RD Above > RD Through
19LS50	2.68	3.00	-0.32	$\Delta_{average} = 0.32$, $\Delta_{std.dev.} = 0.560$, $\alpha = 0.05$
				$t_0 = 0.990$, $t_\alpha = 4.303$, p =0.4266
				Conclusion: **RD Above = RD Through**

Table D3. 27 Test of Gradation Plotting Above and Below Restricted Zone Effect on LMLCD Specimens in PURWheel.

Mixture	Above	Below	Δ	Calculation
9.5LS44	2.12	1.71	0.41	H_0 : RD Above = RD Below
19LS39	2.71	4.47	-1.76	H_1 : RD Above < RD Below
19LS44	2.14	2.01	0.13	$\Delta_{average} = -0.12$, $\Delta_{std.dev.} = 1.119$, $\alpha = 0.05$
19LS50	2.68	1.95	0.73	$t_0 = -0.219$, $t_\alpha = 3.182$, p =0.8407
				Conclusion: **RD Above = RD Below**

Table D3. 28 Test of Gradation Plotting Through And Below Restricted Zone Effect on LMLCD Specimens in PURWheel.

Mixture	Through	Below	Δ	Calculation
9.5LS44	1.56	1.71	-0.15	$\alpha = 0.05$
9.5GR44	1.61	1.24	0.37	H_0 : RD Through = RD Below
9.5LS50	1.80	1.65	0.15	H_1 : RD Through > RD Below
9.5GR50	2.28	1.97	0.31	$\Delta_{average} = 0.095$
19LS44	1.42	2.01	-0.59	$\Delta_{std.dev.} = 0.502$
19LS50	3.00	1.95	1.05	$t_0 = 0.521$, $t_\alpha = 2.364$, p =0.6184
19GR44	1.23	1.54	-0.31	Conclusion:
19GR50	1.72	1.81	-0.09	**RD Through = RD Below**

Table D3. 29 ANOVA for Factor Effects on PURWheel Rut Depth.

Dependent Variable: PURWheel LMLCD Rut Depth					
Source	df	SS	MS	F	Pr > F
Model	12	9.383	0.782	5.61	0.0072
Error	9	1.254	0.139		
Total	21	10.637			
R-square = 0.8821 Adjusted R-square = 0.7642					
Parameter Estimate					
Source	df	Type I SS	MS	F	Pr > F
Nominal Max. Size	1	1.097	1.097	6.10	0.0565
Coarse Agg. Type	1	1.340	1.340	7.45	0.0413
Fine Agg. Angularity	2	4.551	2.275	12.65	0.0111
Gradation	2	0.012	0.006	0.03	0.9665
Nominal * Coarse	1	0.372	0.372	2.07	0.2102
Nominal * FAA	1	0.072	0.072	0.40	0.5537
Nominal * Gradation	1	0.421	0.421	2.34	0.1866
Coarse * FAA	1	0.036	0.036	0.20	0.675
Coarse * Gradation	1	0.006	0.006	0.04	0.8575
FAA*Gradation	1	1.475	1.475	8.20	0.0353
Source	df	Type III SS	MS	F	Pr > F
Nominal Max. Size	1	0.090	0.090	0.50	0.5111
Coarse Agg. Type	1	0.031	0.031	0.17	0.6942
Fine Agg. Angularity	2	2.927	1.463	8.13	0.0268
Gradation	2	0.223	0.112	0.62	0.5748
Nominal * Coarse	1	0.006	0.006	0.03	0.8600
Nominal * FAA	1	0.128	0.128	0.71	0.4369
Nominal * Gradation	1	0.004	0.004	0.02	0.8918
Coarse * FAA	1	0.019	0.019	0.10	0.7603
Coarse * Gradation	1	0.215	0.215	1.19	0.3242
FAA*Gradation	1	0.557	0.364	1.531	0.1766

Table D3. 30 Regression Analysis of PURWheel Rut Depth and Design VMA on LMLCD Specimens (19mm mixtures only).

Dependent Variable: PURWheel Rut Depth Analysis of Variance					
Source	df	SS	MS	F	Pr > F
Model	2	4.403	2.202	5.056	0.0304
Error	10	4.355	0.435		
Total	12	8.758			
R-square = 0.503 Adjusted R-square = 0.403					
Parameter Estimate					
Variable	df	Parameter Estimate	Standard Error	T for H_0	Pr > T
Intercept	1	139.061	51.889	2.680	0.0231
VMA	1	-19.498	7.262	-2.685	0.0229
VMA^2	1	0.691	0.253	2.730	0.0212

Table D3. 31 Regression Analysis of PURWheel Rut Depth and VFA on LMLCD Specimens.

Dependent Variable: PURWheel Rut Depth Analysis of Variance					
Source	df	SS	MS	F	Pr > F
Model	1	48.102	48.102	52.575	0.0001
Error	181	165.603	0.915		
Total	182	213.705			
R-square = 0.225 Adjusted R-square = 0.221					
Parameter Estimate					
Variable	df	Parameter Estimate	Standard Error	T for H_0	Pr > T
Intercept	1	-0.276	0.356	-0.776	0.4389
VFA	1	0.035	0.005	7.251	0.0001

Table D3. 32 Regression Analysis of PURWheel Rut Depth and Dust Proportion on LMLCD Specimens.

Dependent Variable: PURWheel Rut Depth Analysis of Variance					
Source	df	SS	MS	F	Pr > F
Model	2	31.586	15.793	15.609	5.61E-07
Error	180	182.119	1.012		
Total	182	213.705			
R-square = 0.148 Adjusted R-square = 0.138					
Parameter Estimate					
Variable	df	Parameter Estimate	Standard Error	T for H_0	Pr > T
Intercept	1	6.262	0.966	6.483	8.37E-10
DP	1	-5.575	1.569	-3.553	0.0005
DP^2	1	1.702	0.617	2.757	0.0064

Table D3. 33 Regression Analysis of PURWheel Rut Depth and Design Dust Proportion on LMLCD Specimens.

Dependent Variable: PURWheel Rut Depth Analysis of Variance					
Source	df	SS	MS	F	Pr > F
Model	2	3.454	1.727	4.562	0.0241
Error	19	7.192	0.379		
Total	21	10.646			
R-square = 0.324 Adjusted R-square = 0.253					
Parameter Estimate					
Variable	df	Parameter Estimate	Standard Error	T for H_0	Pr > T
Intercept	1	8.464	2.132	3.969	0.0008
DP	1	-10.923	3.674	-2.973	0.0078
DP^2	1	4.429	1.549	2.859	0.0100

Table D3. 34 Regression Analysis of PURWheel Rut Depth and Film Thickness on LMLCD Specimens.

Dependent Variable: PURWheel Rut Depth Analysis of Variance					
Source	df	SS	MS	F	Pr > F
Model	2	62.445	31.222	37.155	3.1E-14
Error	180	151.260	0.840		
Total	182	213.705			
R-square = 0.292 Adjusted R-square = 0.284					
Parameter Estimate					
Variable	df	Parameter Estimate	Standard Error	T for H_0	Pr > T
Intercept	1	3.498	1.151	3.040	0.0027
FT	1	-0.573	0.256	-2.236	0.0266
FT^2	1	0.046	0.014	3.317	0.0011

Table D3. 35 Regression Analysis of PURWheel Rut Depth and Design Film Thickness on LMLCD Specimens.

Dependent Variable: PURWheel Rut Depth Analysis of Variance					
Source	df	SS	MS	F	Pr > F
Model	2	5.999	3.000	12.265	0.0004
Error	19	4.647	0.245		
Total	21	10.646			
R-square = 0.564 Adjusted R-square = 0.518					
Parameter Estimate					
Variable	df	Parameter Estimate	Standard Error	T for H_0	Pr > T
Intercept	1	9.414	2.011	4.682	0.0002
FT	1	-1.808	0.442	-4.087	0.0006
FT^2	1	0.106	0.024	4.427	0.0003

APPENDIX E1 Air Dry Triaxial Test Procedure

Standard Test Method for Triaxial Compressive Strength of Bituminous Mixtures In Air-Dry Condition

1. Scope

1.1 This test method covers the determination of strength and stress-strain relationships for a cylindrical specimen of bituminous mixtures at a predetermined temperature in air-dry condition when it is isotropically confined and sheared drained in compression at a constant rate of axial deformation (strain controlled).[1]

1.2 The test method provides for the calculation of total stresses by measurement of axial load and axial deformation.

1.3 The test provides data useful in determining strength and deformation properties of bituminous mixtures such as Mohr strength envelopes and Young's modulus. Generally, three specimens are tested at different confining stresses to define a strength envelope.

1.4 The determination of strength envelopes and the development of relationships to aid in interpreting and evaluating test results are left to the engineer or office requesting the test.

1.5 The values stated in either SI or non-SI units shall be regarded separately as standard. The values in each system may not be exact equivalents, therefore, each system must be used independently of the other, without combining values in any way.

1.6 This standard may involve hazardous materials, operations, and equipment. This standard does not purport to address all of the safety problems associated with its use. It is the responsibility of the user of this standard to establish appropriate safety and health practices and determine the applicability of regulatory limitations prior to its use.

---

[1] This test method does not include a procedure for obtaining pore pressure measurements. Furthermore, at the rapid strain rates used in this test method such measurements could be inaccurate.

2. Referenced Documents

2.1 ASTM Standards:

2.1.1 D 8 Standard Terminology Relating to Materials for Roads and Pavements.

2.1.2 D1559 Standard Test Method for Resistance to Plastic Flow of Bituminous Mixtures Using Marshall Apparatus.

2.1.3 D 1561 Standard Practice for Preparation of Bituminous Mixture Test Specimens by Means of California Kneading Compactor.

2.1.4 D 2664 Standard Test Method for Triaxial Compressive Strength of Undrained Rock Core Specimens Without Pore Pressure Measurements.

2.1.5 D 2726 Test Method for Bulk Specific Gravity and Density of Non-Absorptive Compacted Bituminous Mixtures.

2.1.6 D 2850 Test Method for Unconsolidated, Undrained Compressive Strength of Cohesive Soils in Triaxial Compression.

2.1.7 D 3387 Compaction and Shear Properties of Bituminous Mixtures by Means of U.S. Corps of Engineers Gyratory Testing Machine (GTM).

2.1.8 D 4767 Standard Test Method for Consolidated-Undrained Triaxial Compression Test on Cohesive Soils.

2.1.9 C 617 Standard Practice for Capping Cylindrical Concrete Specimens.

2.2 Federal Highway Administration Report

2.2.1 FHWA-SA-95-003 Background of Superpave Asphalt Mixture Design and Analysis.

3. Terminology

3.1 Definitions – The definitions of terms used in this test method shall be in accordance with Terminology D8.

3.2 Description of Terms Specific to this Standard:

3.2.1 *confining stress* – the cell pressure applied to the specimen prior to shearing the specimen.

3.2.2 *failure* – the stress condition at failure for a test specimen. Failure is often taken as the stresses in the specimen corresponding to the maximum principal stress difference (deviator stress) attained or the principal stress difference (deviator stress) at 15% axial strain, whichever is obtained first during the performance of a test. failure – the stress condition at failure for a test specimen. Failure is often taken to correspond to the maximum principal stress difference (deviator stress) attained or the principal stress difference (deviator stress) at 15% axial strain, whichever is obtained first during the performance of a test. Depending in the mixture behavior and application, other suitable failure criteria may be defined, for example, the principal stress difference (deviator stress) at a selected axial strain other than 15 %.

4. Significance and Use

4.1 The shear strength of an air-dry bituminous mixture in triaxial compression depends on the stresses applied, strain rate, and the stress history experienced by the bituminous mixture.

4.2 In this test method, the compressive strength of a bituminous mixture is determined in terms of the total stress. The air flow is permitted from and into the bituminous specimen as the load is applied.

4.2 If the specimen is in air-dry condition and the strain rate is low enough such that the specimen does not generate excessive pore pressure, the total stresses are close to the effective stresses.

5. Apparatus

5.1 Axial Loading Device – The axial compression device may be a screw jack driven by an electric motor through a geared transmission, a hydraulic or pneumatic loading device, or any other compression device with sufficient capacity and control to provide the rate

loading prescribed in 7.6. When the loading device is set to advance at a certain rate of strain, the actual strain rate shall not deviate by more than ± 1 %. [2]

5.2 Axial Loading-Measuring Device – The axial load-measuring device shall be a load ring, electronic load cell, hydraulic load cell, or any other load-measuring device capable of the accuracy prescribed in this section and may be a part of the axial loading device. The axial load-measuring device shall be capable of measuring the axial load to an accuracy of 1 % of the estimated axial load at failure. If the load-measuring device is located inside the triaxial compression chamber, it shall be insensitive to horizontal forces and to the magnitude of the chamber pressure.

5.1 Chamber Pressure Maintaining and Measurement Device – The chamber pressure-maintaining and measurement device shall be capable of applying and controlling the chamber pressure to within ± 1% of the applied chamber pressure. This device may consist of a reservoir connected to the triaxial chamber and partially filled with the chamber media (usually water), with the upper part of the reservoir connected to a compressed gas supply; the gas pressure being controlled by a pressure regulator and measured by a pressure gage, electronic pressure transducer, or any other device capable of measuring to the prescribed tolerance.

5.2 Triaxial Compression Chamber – The triaxial chamber must be able to withstand a chamber pressure equal to the confining pressure. It shall consist of a top plate and a base plate separated by a cylinder. The cylinder may be constructed of any material capable of withstanding the applied pressure. It is desirable to use a transparent material or have a cylinder provided with viewing ports so the behavior of the specimen may be observed. The top plate shall have a vent valve such that air can be forced out of the chamber. The base plate shall have an inlet through which the pressure liquid is supplied to the chamber, and inlets that lead to the specimen base and provide for connection to the cap to allow drainage of the specimen.

---

[2] A loading device may be said to provide sufficiently small vibrations if there are no visible ripples in a glass of water placed on the loading platen when the device is operating at the speed at which the test is performed.

5.3 Environmental Control Chamber – The environmental control chamber must be able to achieve and maintain the temperature set point within ± 1^0 C during the whole testing procedure.

5.4 Axial Load Piston – The piston passing through the top of the chamber and its seal must be designed so the variation in axial load due to friction does not exceed 0.1 % of the axial load at failure and so there is negligible lateral bending of the piston during loading.[3]

5.5 Specimen Cap and Base – The specimen cap and base shall be designed to provide drainage from both ends of the specimen. They shall be constructed of a rigid, noncorrosive, impermeable material, and each shall, except for the drainage provision, have a circular plane surface of contact with the porous discs and a circular cross section. The weight of the specimen cap shall be less than 0.5% of the applied axial load at failure or shall produce an axial stress on the specimen of less than 3.45 kPa (0.5 psi). The diameter of the cap and base shall be equal to the initial diameter of the specimen. The specimen base shall be connected to the triaxial compression chamber to prevent lateral motion or tilting, and the specimen cap shall be designed such that eccentricity of the piston-to-cap contact relative to the vertical axis of the specimen does not exceed 1.3 mm (0.05 in). The end of the piston and specimen cap contact area shall be designed so that tilting of the specimen cap during the test is minimal. The cylindrical surface of the specimen base and cap that contacts the membrane to form a seal shall be smooth and free of scratches.

5.6 Deformation Indicator – The vertical deformation of the specimen is usually determined from the travel of the piston acting on the top of the specimen. The piston travel shall be measured with an accuracy of at least ± 0.02% of the initial specimen height. The deformation indicator shall have a travel range of at least 20% of the initial height of the specimen and may be a dial indicator, linear variable differential

[3] The use of two linear ball bushings to guide the piston is recommended to minimize friction and maintain alignment. A minimum piston diameter of $^1/_6$ the specimen diameter has been used successfully in many laboratories to minimize lateral bending.

transformer (LVDT), extensiometer, or other measuring device meeting the requirements for accuracy and range.

5.7 Rubber Membranes – The rubber membrane used to encase the specimen shall provide reliable protection against leakage. To check a membrane for leakage, the membrane shall be placed around a cylindrical form, sealed at both ends with rubber O-rings, subjected to a small air pressure on the inside, and immersed in water. If air bubbles appear from any point on the membrane it shall be rejected. To offer minimum restraint to the specimen, the unstretched membrane diameter shall be between 90 and 95 % of that of the specimen. The membrane thickness shall not exceed 1% of the diameter of the specimen. The membrane shall be sealed to the specimen cap and base with rubber O-rings for which the unstressed inside diameter is between 75 and 85 % of the diameter cap and base, or by other means that will provide a positive seal. An equation for correcting the principal stress difference (deviator stress) for the effect of the stiffness of the membrane is given in 8.6.

5.8 Specimen Size Measurement Devices – Devices used to determine the height and diameter of the specimen shall measure the respective dimensions to within ± 0.1% of the total dimension and shall be constructed such that their use will not disturb the specimen.

5.9 Timer – A timing device indicating the elapsed testing time to the nearest 1 s shall be used to verify the rate of strain.

5.10 Miscellaneous Apparatus – Circular saw, mixing, and compaction apparatus shall be provided as required.

6. Test Specimens

a. Specimen Size – Specimens shall be cylindrical and have a minimum diameter at least four times larger than the nominal maximum size. The height-to-diameter ratio shall be between 2 and 2.5.

b. Preparation of Specimens

6.2.1 Compaction to A Target Volumetric Density

6.2.1.1 Determine the total amount of aggregates based on the volume of the mold, the target volumetric density, and the asphalt content. The target volumetric density can be calculated from the ratio of the measured bulk specific gravity to a correction factor. The appropriate correction factor for each mixture shall be used.

6.2.1.2 The mixing method shall follow ASTM D 1559 or FHWA-SA-95-003.

6.2.1.3 The specimen may be compacted by kneading action or by gyration. The California Kneading Compactor (ASTM D1561) can be modified to compact different sizes of specimen by kneading action. The number of blows and the foot pressure shall be adjusted in order to meet the target density. In order to insure the smoothness and flatness of the specimen surface, the specimens may be trimmed by circular saw or capped following ASTM C 617. The Superpave Gyratory Compactor or The U.S. Corps of Engineers Gyratory Testing Machine (ASTM D3387) can be used to compact the specimen by gyration. The number of gyrations shall be adjusted in order to meet the target density. When the gyratory compactor is used, two or three identical specimens need to be stacked in order to meet the height-to-diameter ratio criterion (section 6.1). The difference of the stacked specimen densities shall be less than 0.4%. Figure 1 illustrates the stacking of two specimens.

6.2.1.4 After the specimen temperature is low enough, jack the specimen out of the mold and measure the density of the specimen following ASTM D2726.

6.2.2 Compaction with A Certain Level of Compaction Energy.

6.2.2.1 Determine the total amount of aggregates that satisfy the height-to-diameter ratio criterion (section 6.1) under a predetermined level of compaction energy.

6.2.2.2 The mixing method shall follow ASTM D 1559 or FHWA-SA-95-003.

6.2.2.3 The specimen may be compacted by kneading action or by gyration. The California Kneading Compactor (ASTM D 1561) can be modified to compact different sizes of specimen by kneading action. The number of blows and the foot pressure shall be determined as the level of compaction energy. In order to insure the smoothness and

flatness of the specimen surface, the specimens may be trimmed by circular saw or capped following ASTM C 617. The Superpave Gyratory Compactor or The U.S. Corps of Engineers Gyratory Testing Machine (ASTM D 3387) can be used to compact the specimen by gyration. The number of gyrations shall be determined as the level of compaction energy. When the gyratory compactor is used, two or three identical specimens need to be stacked in order to meet the height-to-diameter ratio criterion (section 6.1). The difference of the stacked specimen densities shall be less than 0.4%. Figure 1 illustrates the stacking of two specimens.

6.2.2.4 After the specimen temperature is low enough, jack the specimen out of the mold and measure the density of the specimen following ASTM D2726.

7. Procedure

7.1 Place the membrane on the membrane expander or, if it is rolled onto the specimen, roll the membrane onto the cap or base. Place the specimen on the base. Place the rubber membrane around the specimen and seal it at the cap and base with O-rings or other positive seals at each end. When air is used as the confining media, double membranes are recommended to minimize air penetration to the specimen. A thin coating of silicon grease on the vertical surfaces of the cap and base will aid in sealing the membrane.

7.2 With the specimen encased in the rubber membrane, which is sealed to the specimen cap and base and positioned in the chamber, assemble the triaxial chamber. Attach the top and base drainage lines and check the alignment of the specimen and the specimen cap. The top and base drainage lines shall be in contact with free air in order that no pore pressure is generated inside the specimen during shear.

7.3 Bring the axial load piston into contact with the specimen cap several times to permit proper seating and alignment of the piston with the cap. When the piston is brought into contact the final time, record the reading on the deformation indicator. During this procedure, take care not to apply an axial stress to the specimen exceeding approximately 0.5 % of the estimated compressive strength. If the weight of the piston is sufficient to apply an axial stress exceeding approximately 0.5 % of the estimated compressive

strength, lock the piston in place above the specimen cap after checking the seating and alignment and keep locked until application of the chamber pressure.

7.4 Place the chamber in position in the axial loading device. Be careful to align the axial loading device, the axial loading-measuring device, and the triaxial chamber to prevent the application of a lateral force to the piston during testing. Attach the pressure-maitaining and measurement device and fill the chamber with the confining media. Adjust the pressure-maintaining and measurement device to the desired chamber pressure and apply the pressure to the chamber media. Wait approximately 5 min. after the application of chamber pressure before continuing the test.[4]

7.5 If the axial load-measuring device is located outside of the triaxial chamber, the chamber pressure will produce an upward force on the piston that will react against the axial loading device. In this case, start the test with the piston slightly above the specimen cap, and before the piston comes in contact with the specimen cap, either: (1) measure and record the initial piston friction and upward thrust of the piston produced by the chamber pressure and later correct the measured axial load, or (2) adjust the axial load-measuring device to compensate for the friction and thrust. If the axial load-measuring device is located inside the chamber, it will not necessary to correct or compensate for the uplift force acting on the axial loading device or for piston friction. Record the initial reading on the deformation indicator when the piston contacts the specimen cap.

7.6 Apply the axial load to produce axial strain at a rate of approximately 1%/min that achieves maximum deviator stress at approximately 3 to 6 % strain. At these rates, the elapsed time to reach maximum deviator stress will be approximately 15 to 20 min. Continue the loading to 15 % axial strain, except loading may be stopped when the deviator stress has peaked then dropped 20 % or the axial strain has reached 5 % beyond the strain at which the peak in deviator stress occurred.

---

[4] In some cases the chamber will be filled and the chamber pressure is applied before placement in the axial loading device. Make sure the piston is locked or held in place by the axial loading device before applying the chamber pressure. The purpose of the waiting period is to allow the specimen to stabilize under the chamber pressure prior to application of the axial load.

7.7 Record load and deformation values at about 0.1, 0.2, 0.3, 0.4, and 0.5 % strain; then at increments of about 0.5 % strain to 3 %; and, thereafter at every 1 %. Take sufficient readings to define the stress – strain curve; hence more frequent readings may be required in the early stages of the test and as failure is approached. [5]

7.8 After completion of tests, remove the axial load and reduce the chamber pressure to zero. Remove the test specimen from the chamber. Make a sketch, or take a photo, of the test specimen at failure and show the slope angle of the failure surface if the angle is visible and measurable.

8. Calculations

8.1 Calculate the axial strain, ε (expressed as a decimal), for a given applied axial load, as follows:

$$\varepsilon = \frac{\Delta L}{L_0} \qquad \text{Eqn. 1}$$

where:

ΔL = change in length of specimen as read from deformation indicator, and

L_0 = initial length of test specimen minus any change in length prior to loading.

8.2 Calculate the average cross-sectional area, A, for a given applied axial load as follows:

$$A = \frac{A_0}{(1-\varepsilon)} \qquad \text{Eqn. 2}$$

where:

A_0 = initial average cross-sectional area of the specimen, and

ε = axial strain for the given axial load (expressed as a decimal).

[5] Alternate intervals for the readings may be used provided sufficient points are obtained to define the stress – strain curve.

8.3 Calculate the principal stress difference (deviator stress), σ_1 - σ_3, for a given applied axial load as follows:

$$\sigma_1 - \sigma_3 = \frac{P}{A} \qquad \text{Eqn. 3}$$

where:

P = measured applied axial load (corrected for uplift and piston friction, if required see 7.4), and

A = corresponding average cross-sectional area.

8.4 Stress – Strain Curve – Prepare a graph showing the relationship between principal stress difference (deviator stress) and axial strain, plotting deviator stress as ordinate and axial strain (in percent) as abscissa. Select the compressive strength and axial strain at failure in accordance with the definitions in 3.2.2.

8.5 Correction of Strength Due to Stiffness of Rubber Membrane – Assuming units are consistent, the following equation, or other acceptable equations, shall be used to correct the principal stress difference or deviator stress for the effect of the rubber membrane if the error in principal stress difference due to the stiffness of the membrane exceeds 5 %:

$$\Delta(\sigma_1 - \sigma_3) = \frac{4E_m t\varepsilon_1}{D} \qquad \text{Eqn. 4}$$

where:

$\Delta(\sigma_1 - \sigma_3)$ = correction to be subtracted from the measured principal stress difference,

D = $\sqrt{\frac{4A}{\pi}}$ = diameter of specimen,

E_m = Young's modulus for the membrane material,

t = thickness of the membrane, and

ε_1 = axial strain.

8.6 The Young's modulus of the membrane material may be determined by hanging a 10.0 mm wide strip of membrane over a thin rod, placing another rod along the bottom of

the hanging membrane, and measuring the force per unit strain obtained by stretching the membrane. The modulus value may be computed using the following equation assuming units are consistent:

$$E_m = \frac{FL}{A_m \Delta L} \qquad \text{Eqn. 5}$$

where:

E_m = Young's modulus for the membrane material,

F = force applied to stretch the membrane,

A_m = twice the initial thickness of the membrane multiplied by the width of the membrane strip,

L = unstretched length of the membrane, and

ΔL = change in length of the membrane due to application of F.

A typical value of E_m for latex membrane is 1400 kN/m^2.[6]

8.7 Calculate the major and minor principal total stresses at failure as follows:

σ_3 = minor principal total stress = chamber pressure, and

σ_1 = major principal total stress = deviator stress at failure plus chamber pressure.

9. Report

9.1 The report shall include the following:

9.1.1 Identification of specimen, including nominal maximum size of aggregates, aggregate types, asphalt content, method of mixing, and method of compaction.

9.1.2 Volumetric density and bulk specific gravity according to ASTM D2726.

9.1.3 Initial height and diameter of the specimen.

9.1.4 Initial height to diameter ratio.

[6] The effect of the stiffness of the membrane on the lateral stress is usually assumed to be negligible. The correction for rubber membranes is based on simplified assumptions concerning their behavior during shear. Their actual behavior is complex and there is not a consensus on more exact corrections.

9.1.5 The value of the compressive strength and the values of the minor and major principal stresses at failure.

9.1.6 Stress – strain curve as described in 8.4.

9.1.7 Axial strain at failure, in percent.

9.1.8 Average rate of axial strain to failure, percent per minute.

9.1.9 Sketch or photo showing type of failure, that is, bulge, diagonal shear, and the like.

9.1.10 If a membrane correction was used, the report shall state that a membrane correction was used to adjust the compressive strength and must indicate the membrane correction equation that was used.

9.1.11 In a remarks section note any unusual conditions or other data that would be considered necessary to properly interpret the results obtained.

10. Precision and Bias

10.1 No method presently exists to evaluate the precision of a group of triaxial compression tests on undisturbed specimens, due to specimen variability.

10.2 A suitable test material and method of specimen preparation have not been developed for the determination of laboratory variances of compacted specimens. No estimates of precision for this test method are available.

11. Keywords

Triaxial, air-dry condition, stress strain, shear strength.

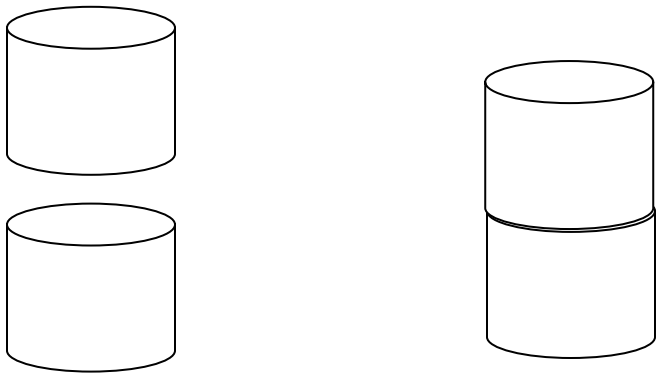

Figure 1. Stacking of Two Specimens

APPENDIX E2 Triaxial Test Results

Triaxial Test Results for 19mm Limestone with FAA of 44 and Gradation Plotting Above the Restricted zone.

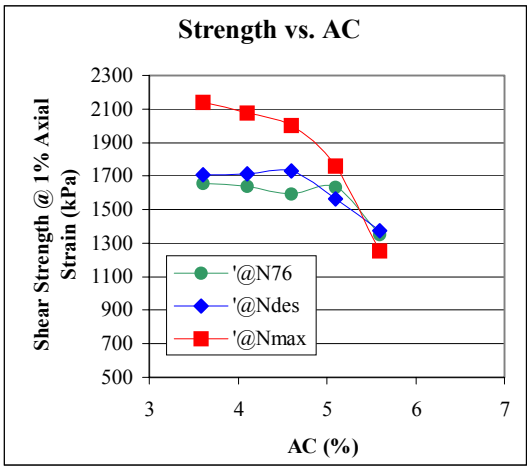

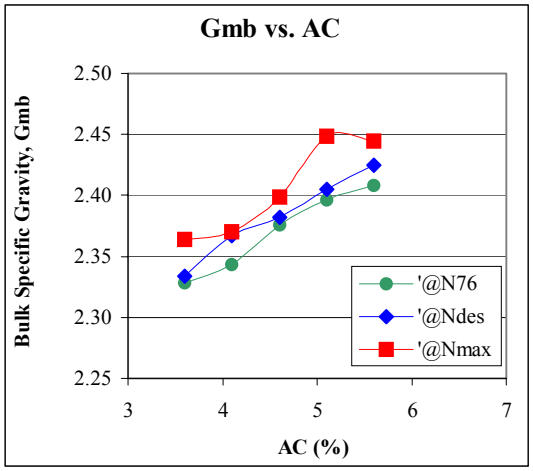

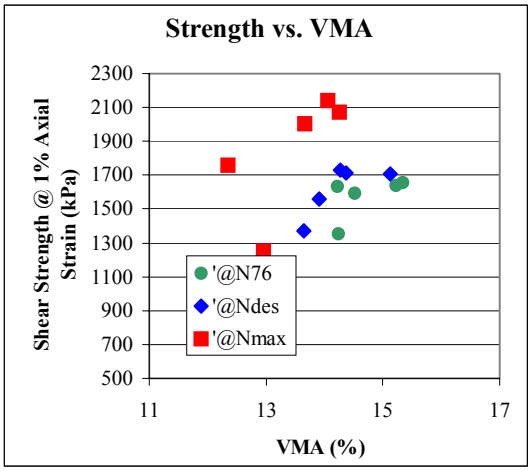

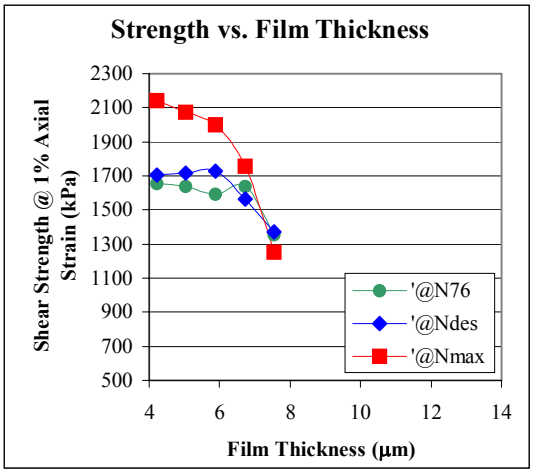

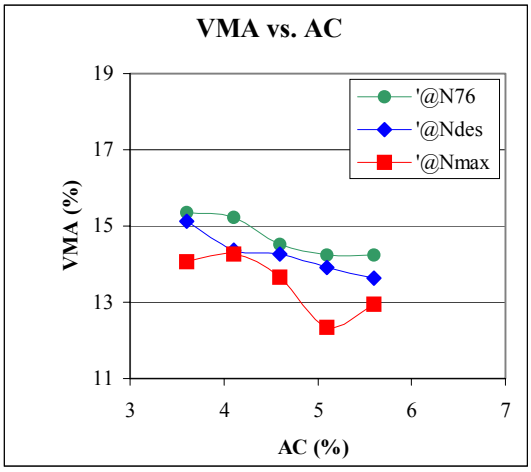

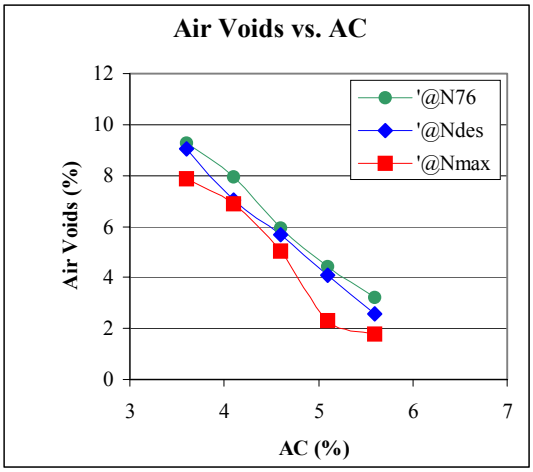

Triaxial Test Results for 19mm Limestone with FAA of 44 and Gradation Plotting Through the Restricted zone.

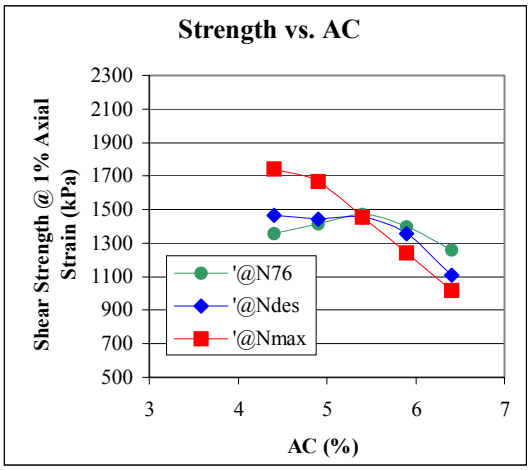

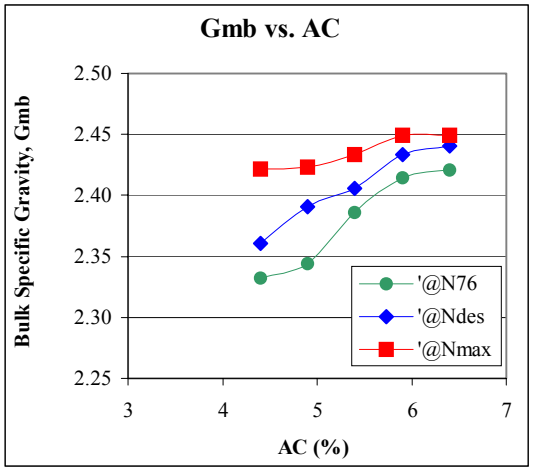

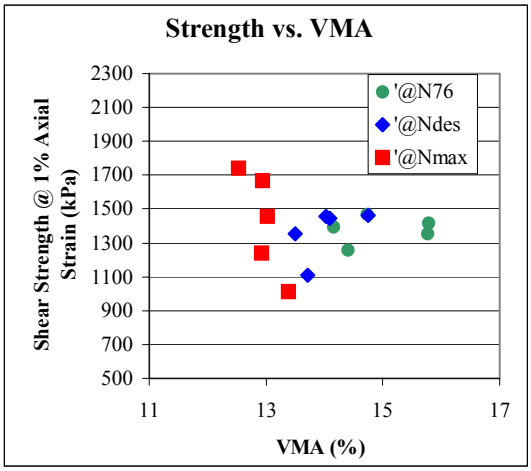

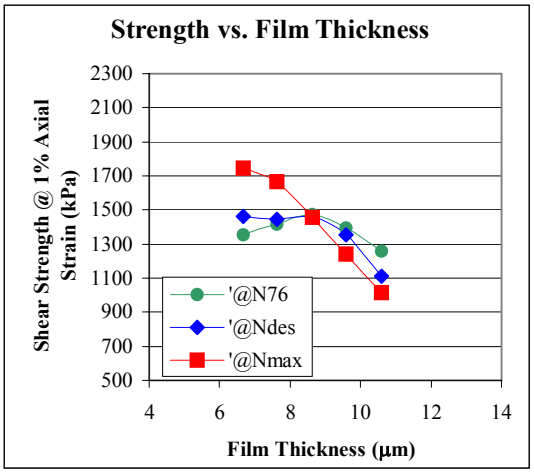

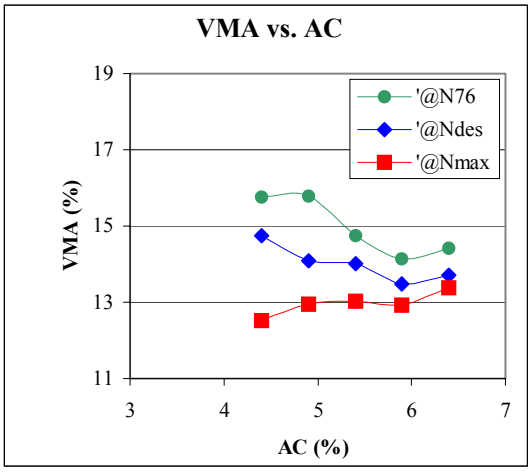

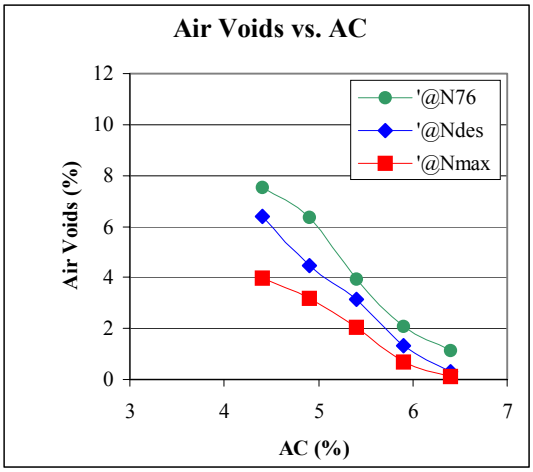

Triaxial Test Results for 19mm Limestone with FAA of 44 and Gradation Plotting Below the Restricted zone.

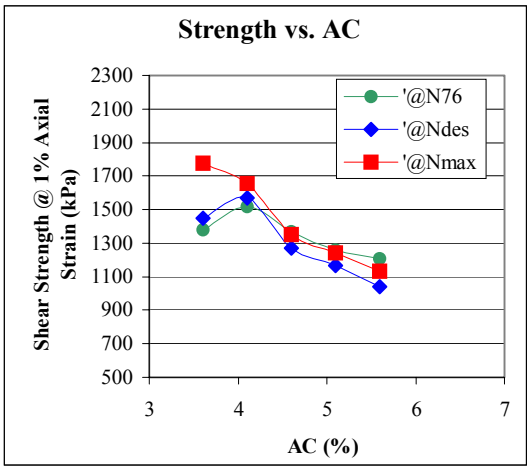

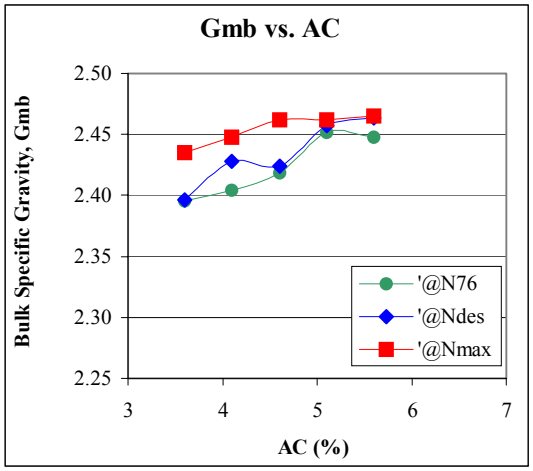

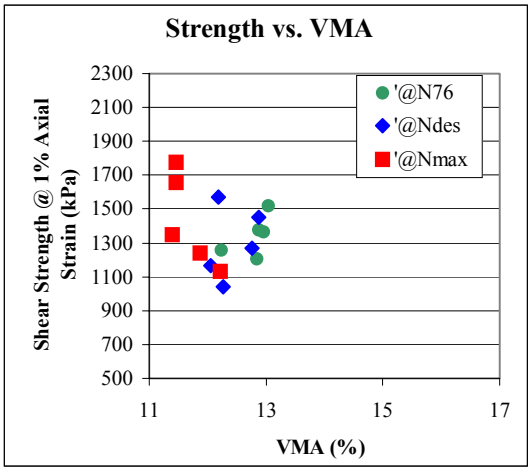

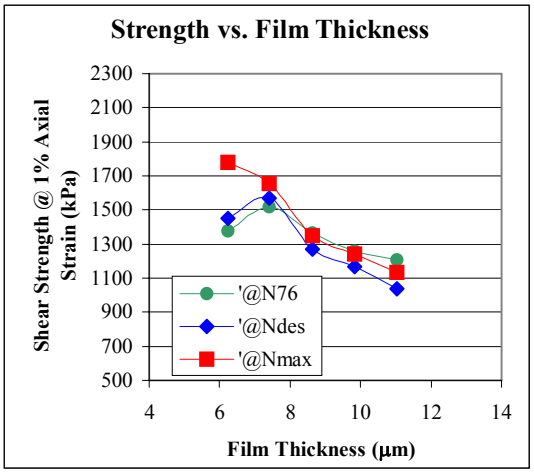

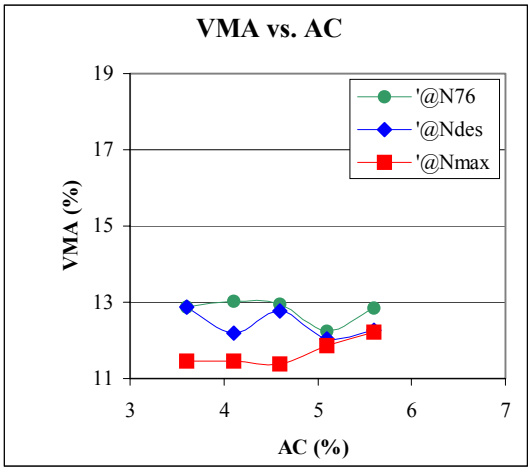

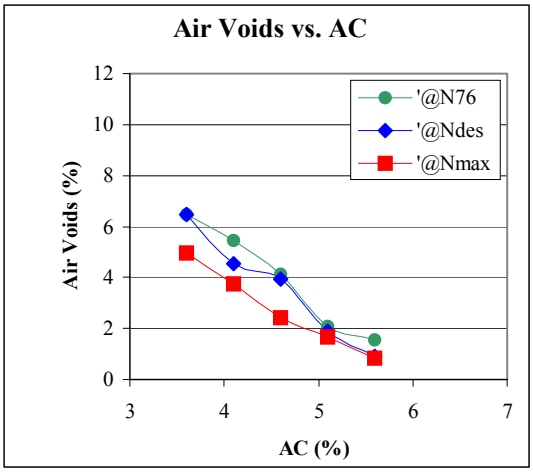

Triaxial Test Results for 19mm Limestone with FAA of 50 and Gradation Plotting Above the Restricted zone.

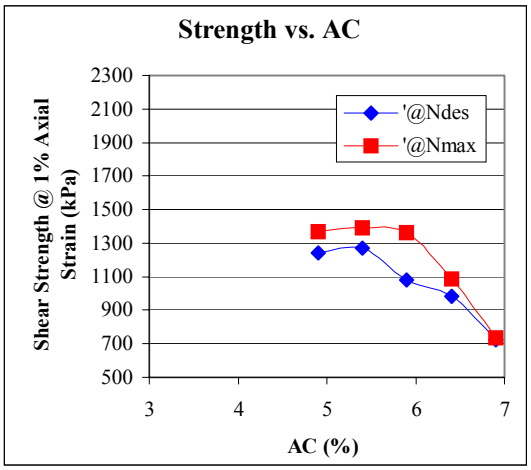

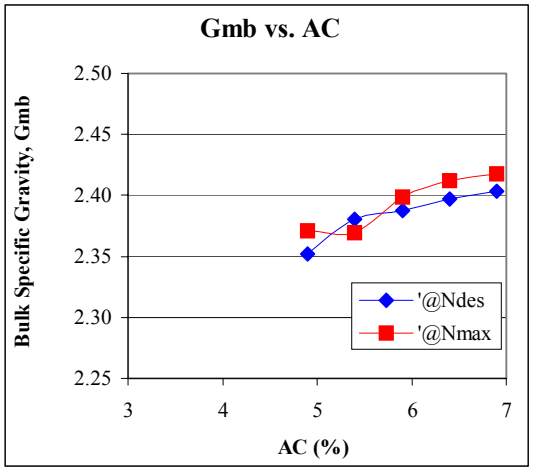

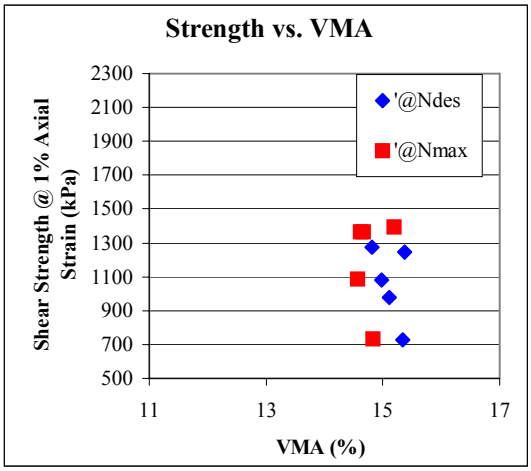

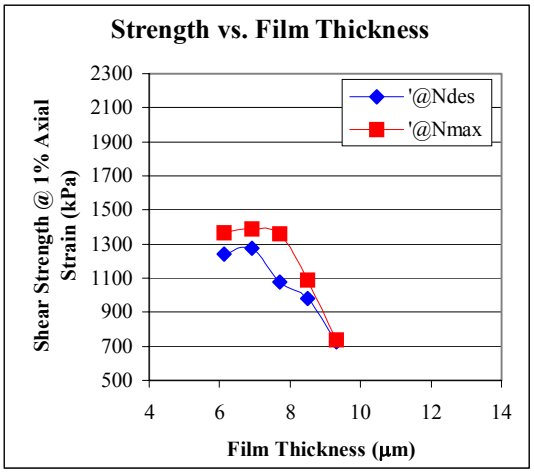

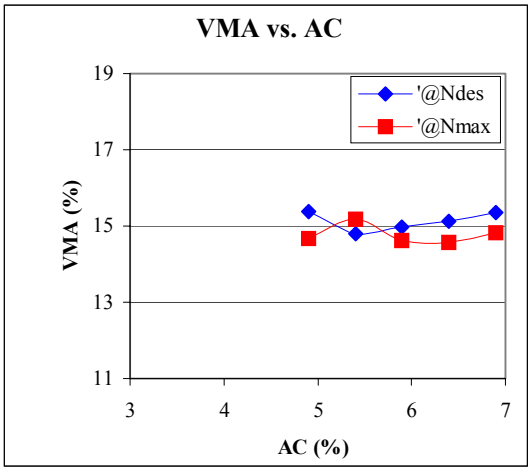

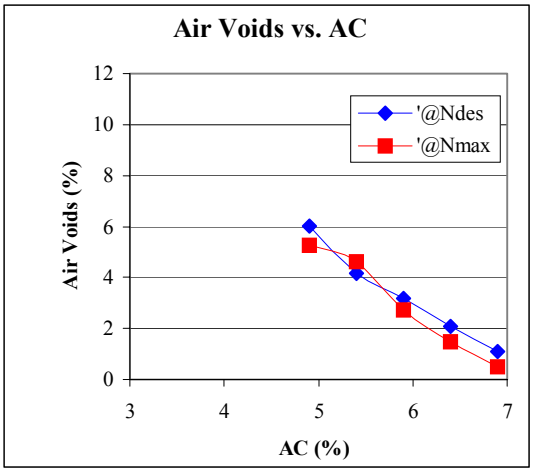

Triaxial Test Results for 19mm Limestone with FAA of 50 and Gradation Plotting Through the Restricted zone.

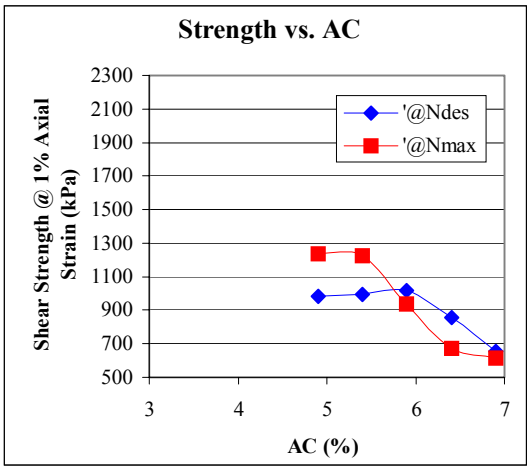

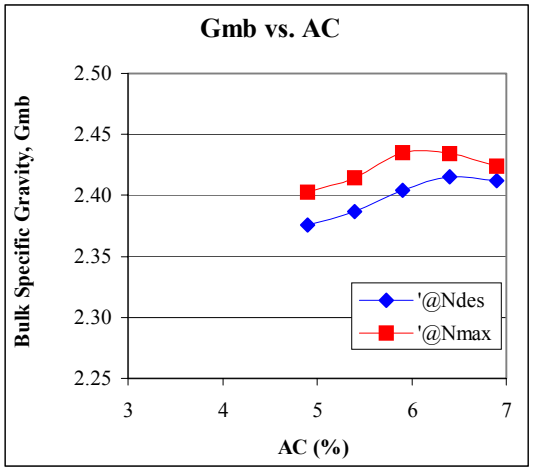

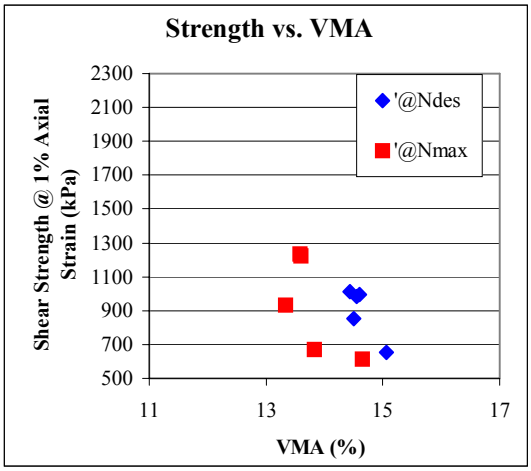

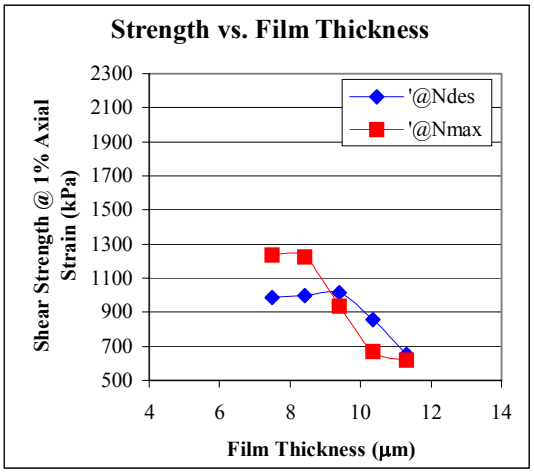

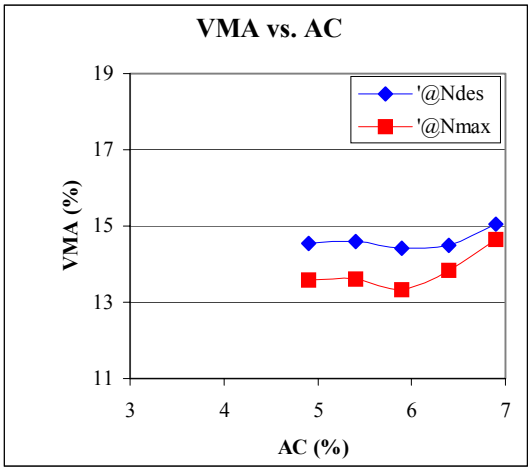

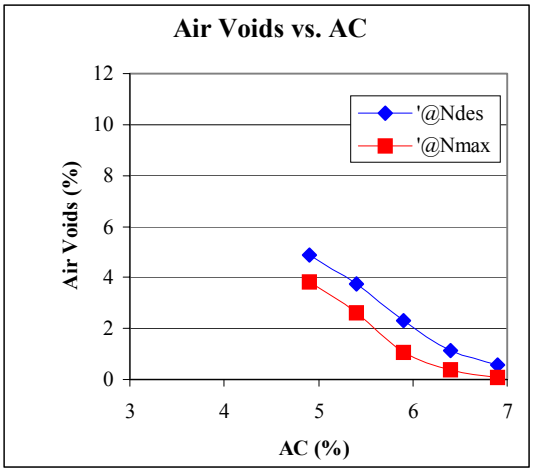

Triaxial Test Results for 19mm Limestone with FAA of 50 and Gradation Plotting Below the Restricted zone.

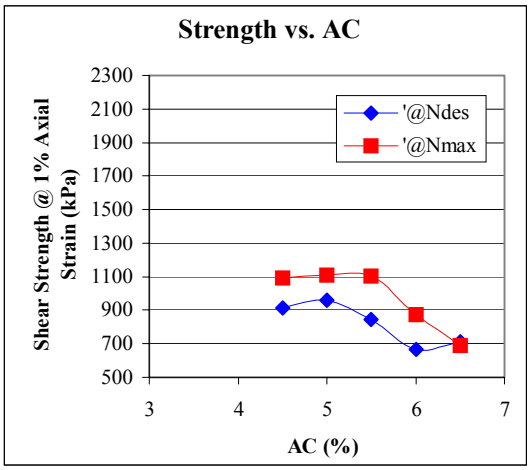

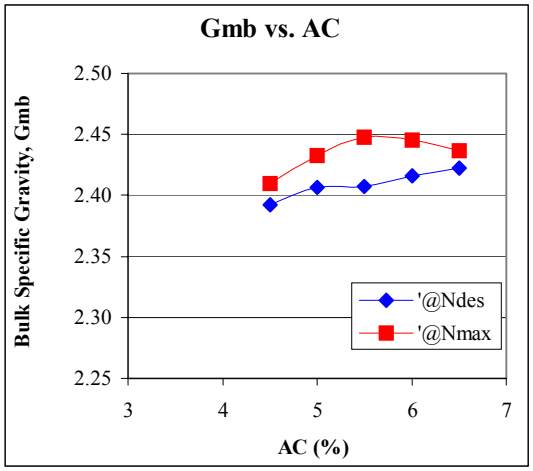

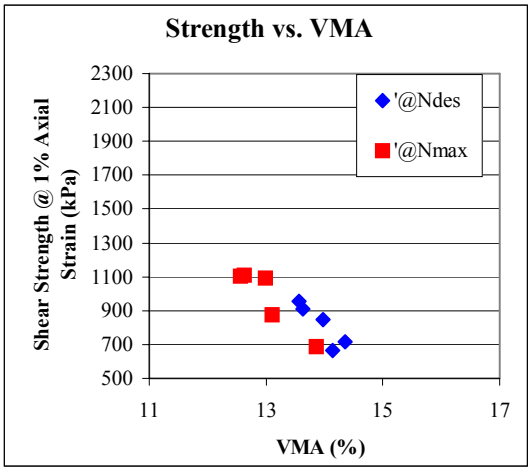

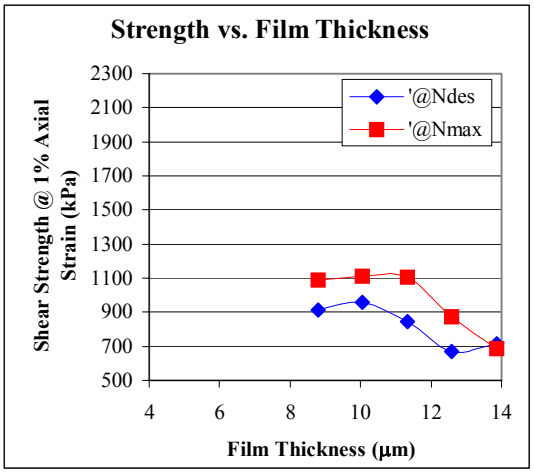

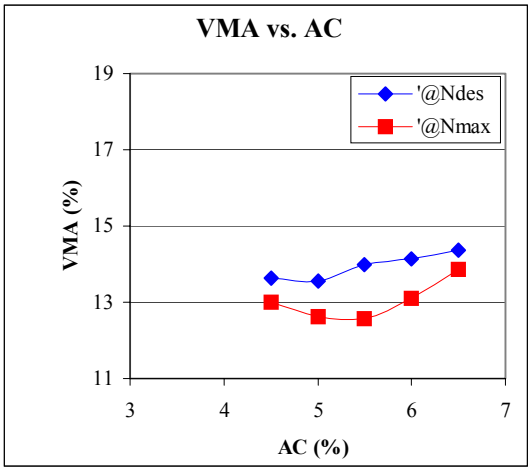

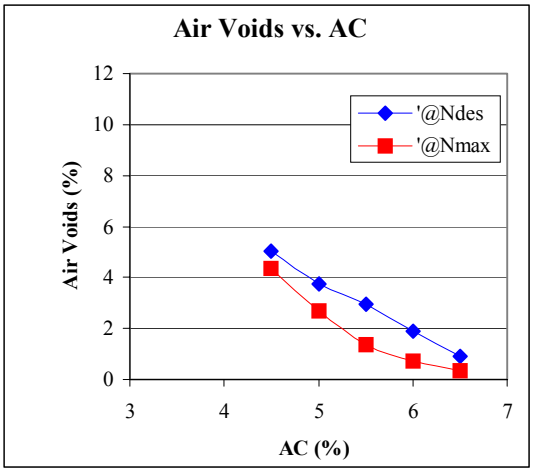

Triaxial Test Results for 19mm Granite with FAA of 44 and Gradation Plotting Through the Restricted zone.

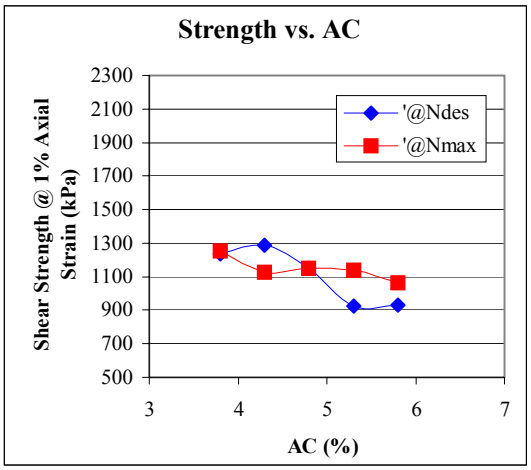

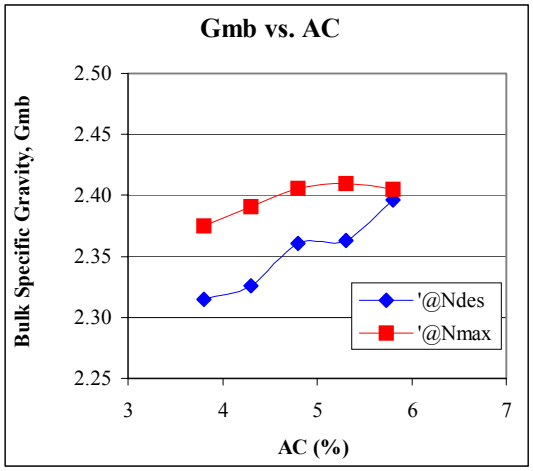

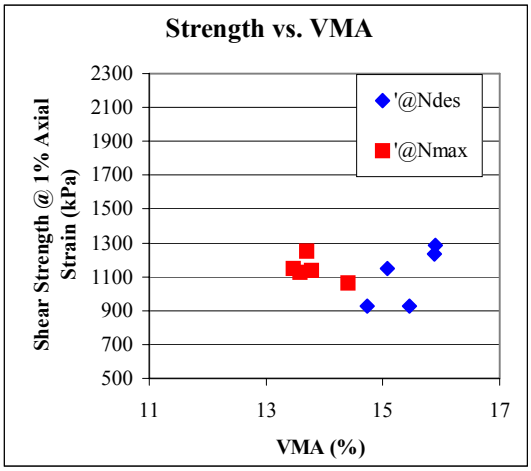

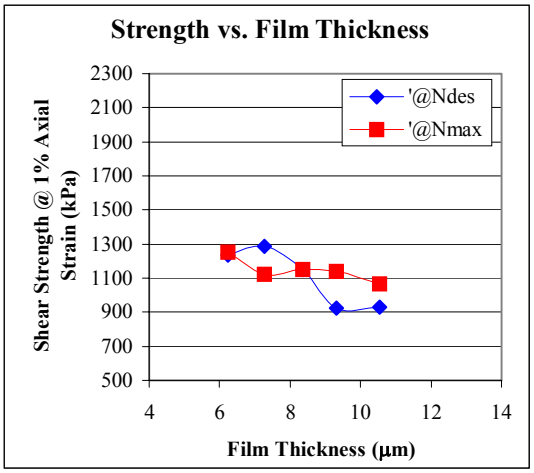

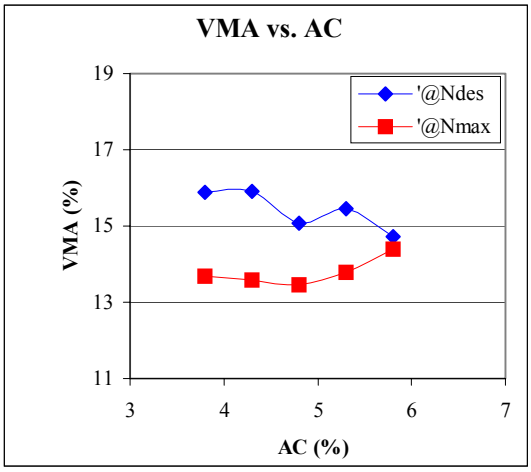

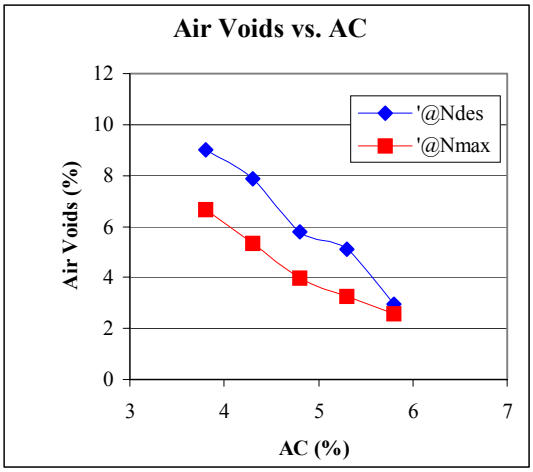

Triaxial Test Results for 19mm Granite with FAA of 44 and Gradation Plotting Below the Restricted zone.

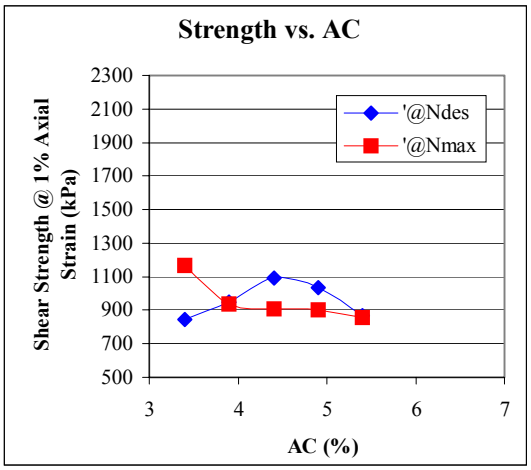

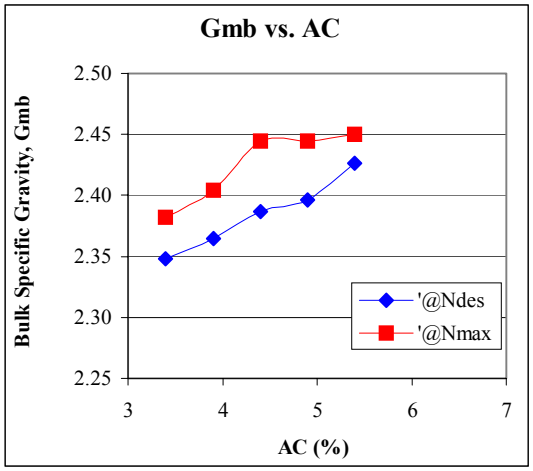

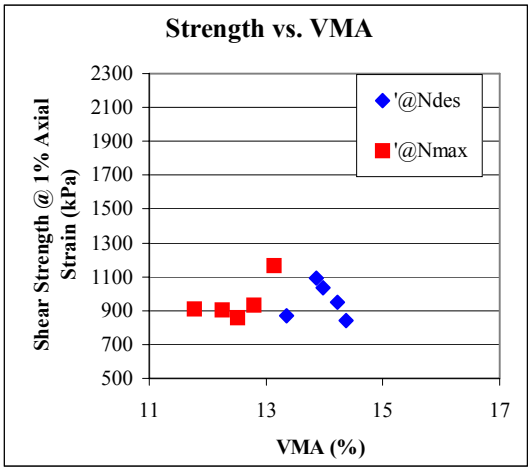

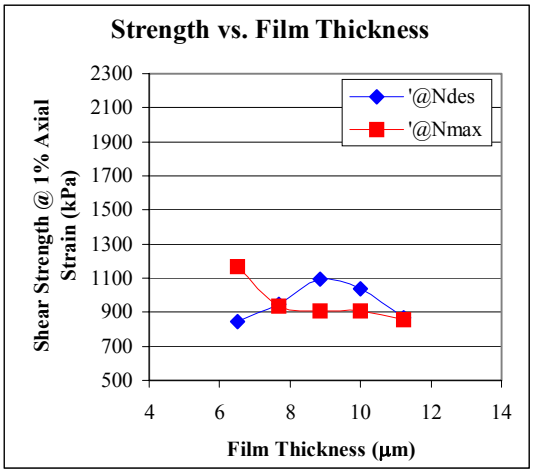

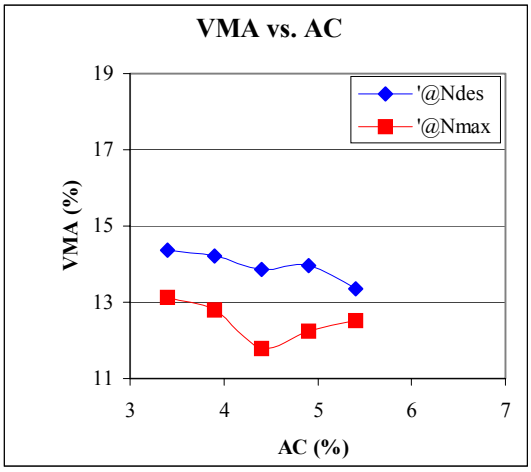

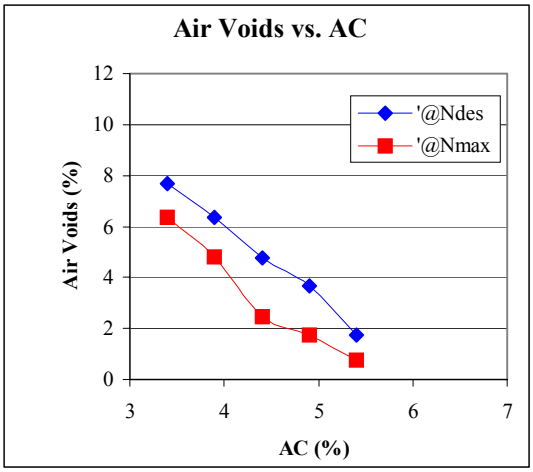

Triaxial Test Results for 19mm Granite with FAA of 50 and Gradation Plotting Through the Restricted zone.

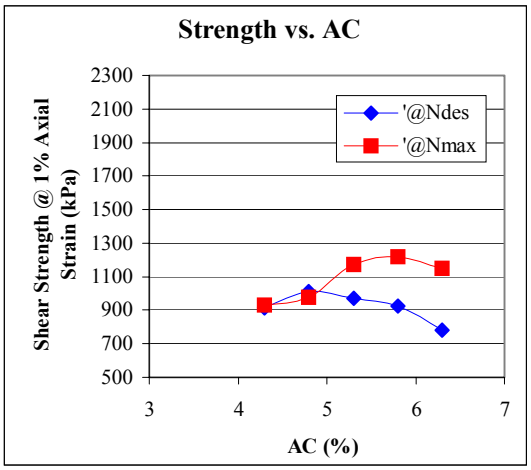

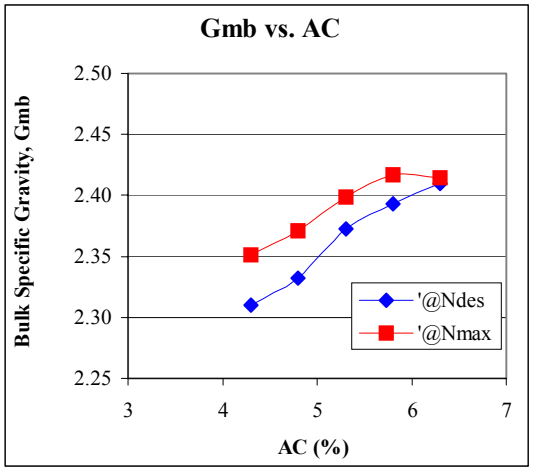

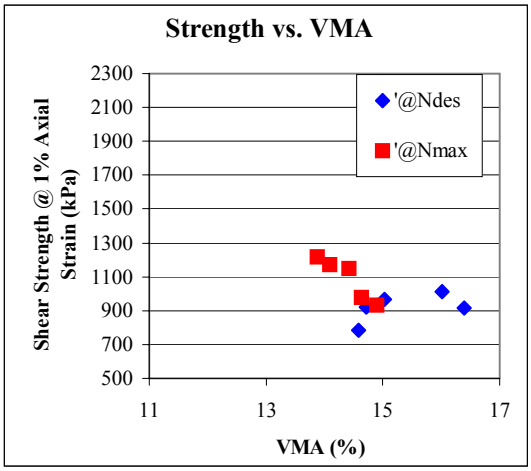

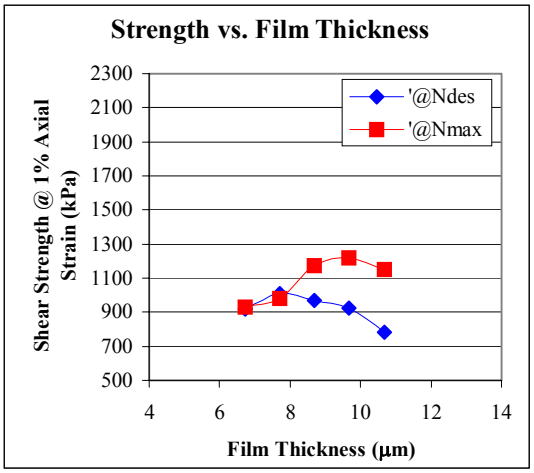

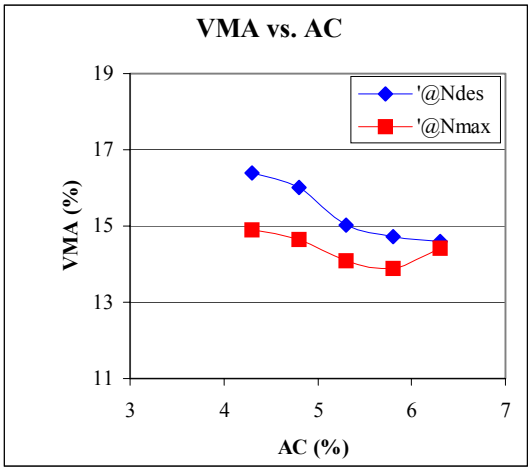

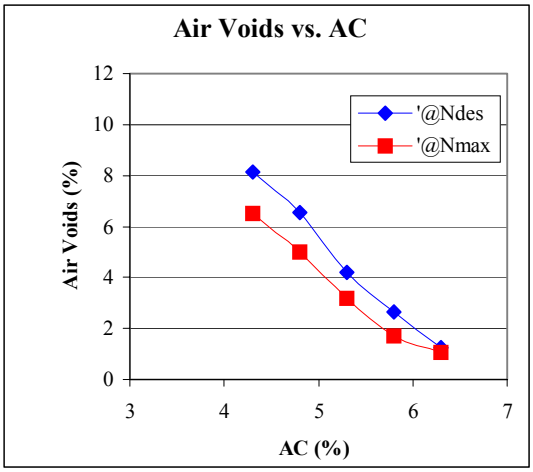

Triaxial Test Results for 19mm Granite with FAA of 50 and Gradation Plotting Below the Restricted zone.

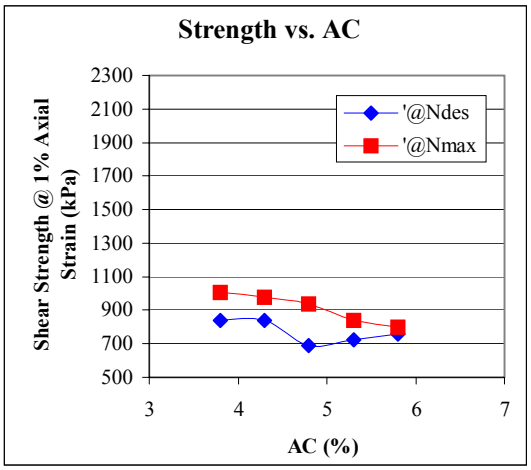

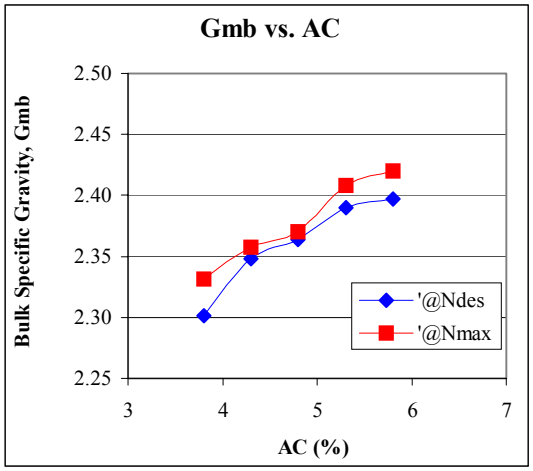

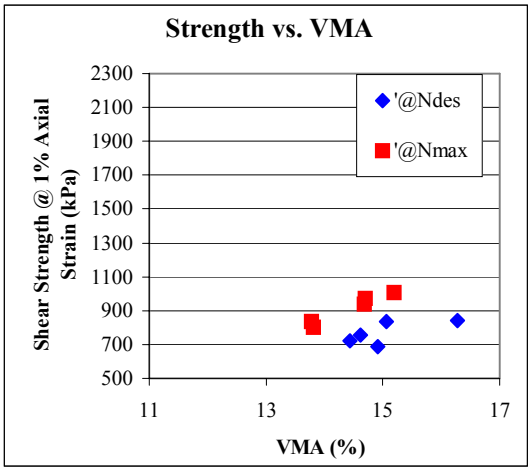

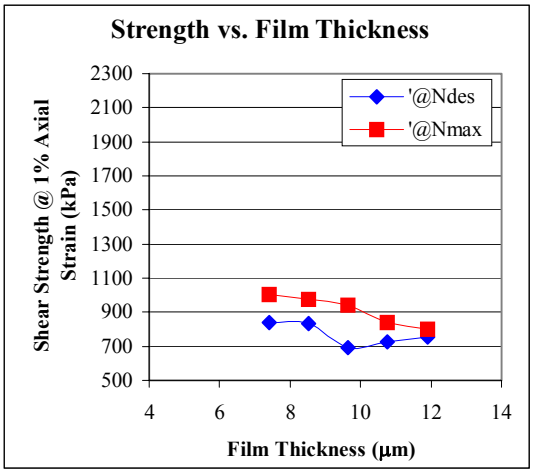

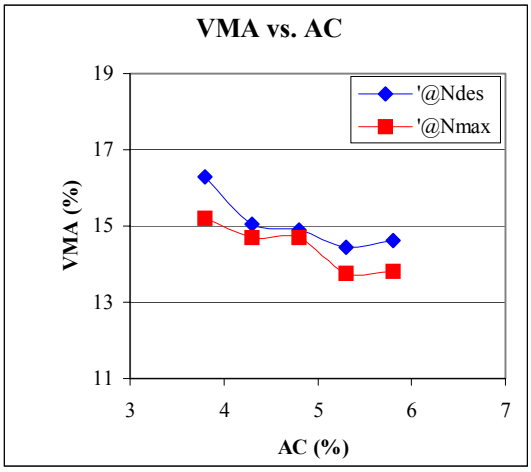

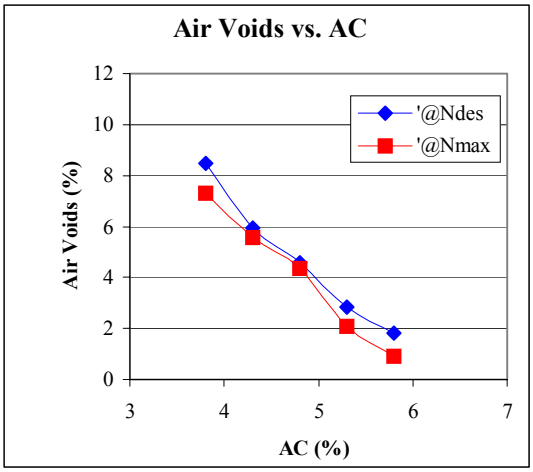

Triaxial Test Results for 9.5mm Limestone with FAA of 44 and Gradation Plotting Above the Restricted zone.

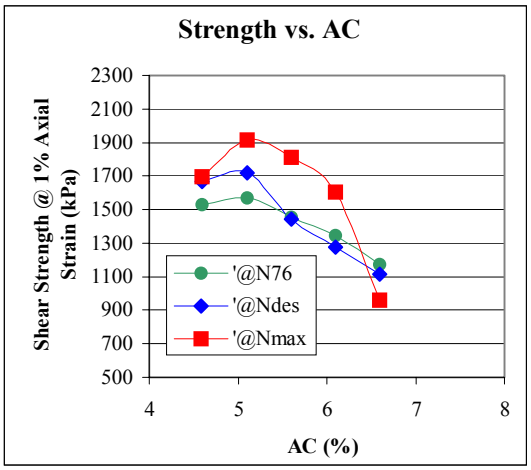

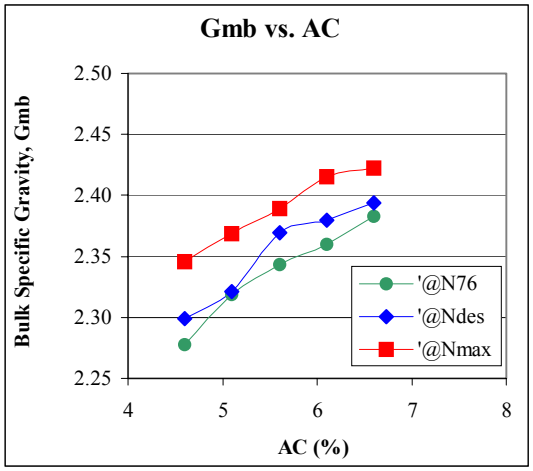

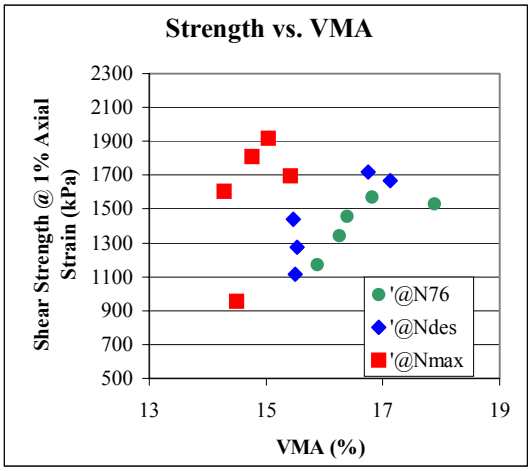

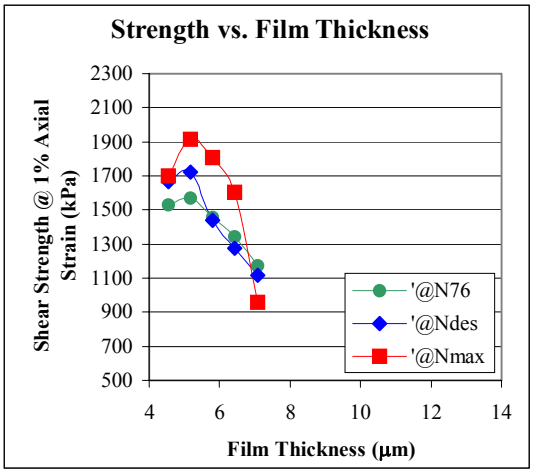

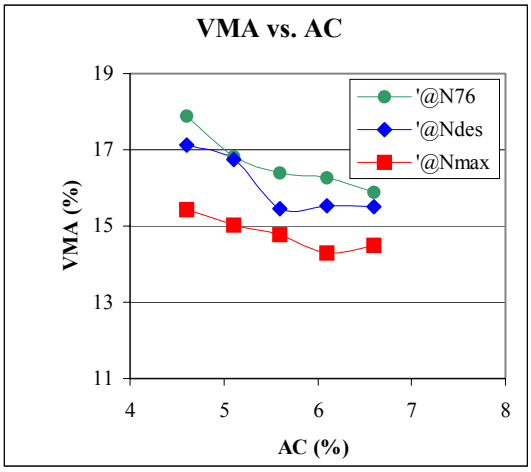

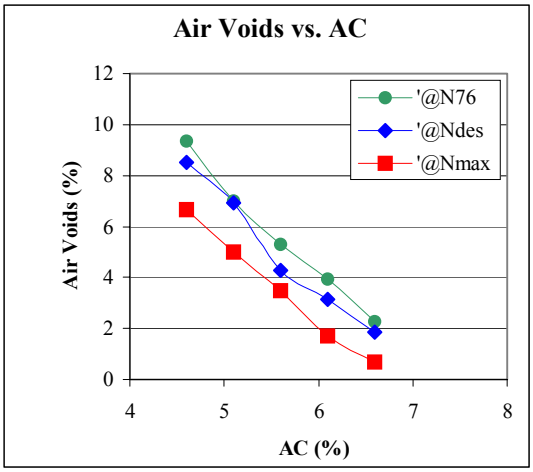

Triaxial Test Results for 9.5mm Limestone with FAA of 44 and Gradation Plotting Through the Restricted zone.

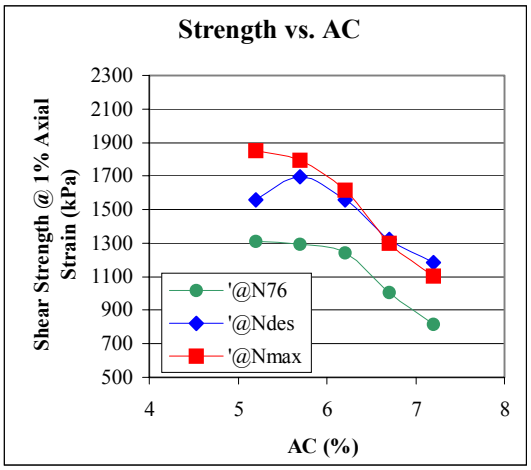

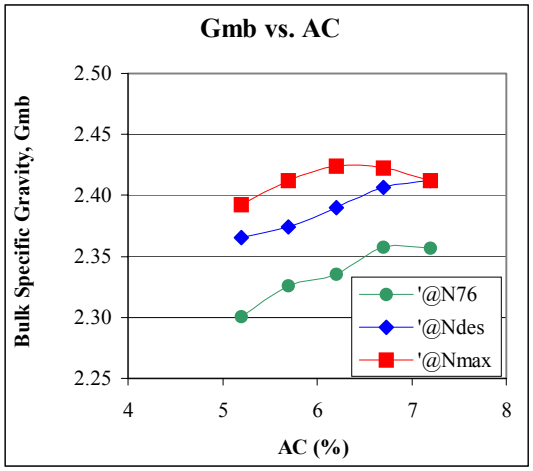

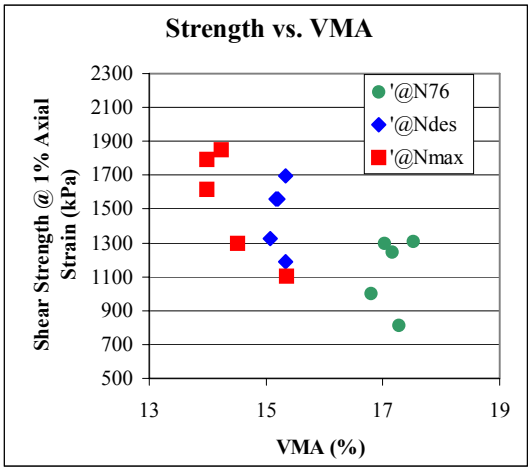

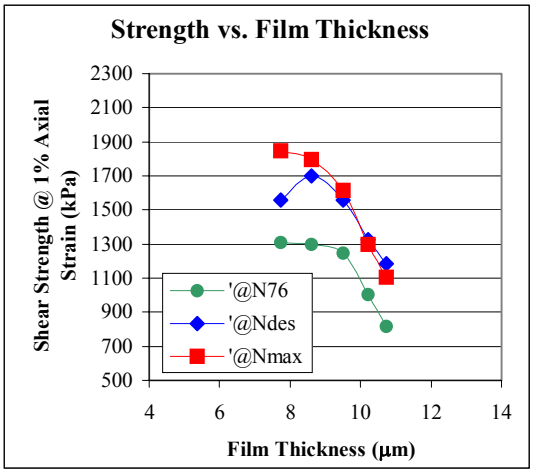

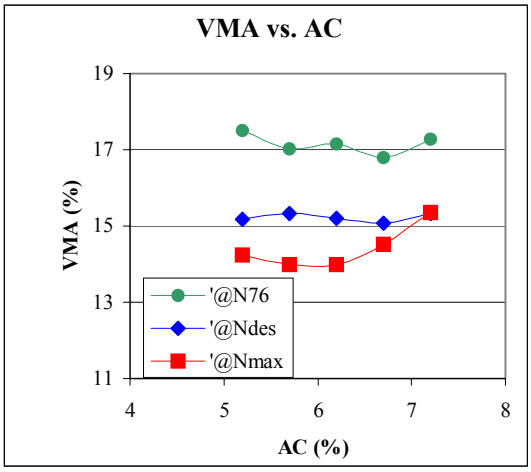

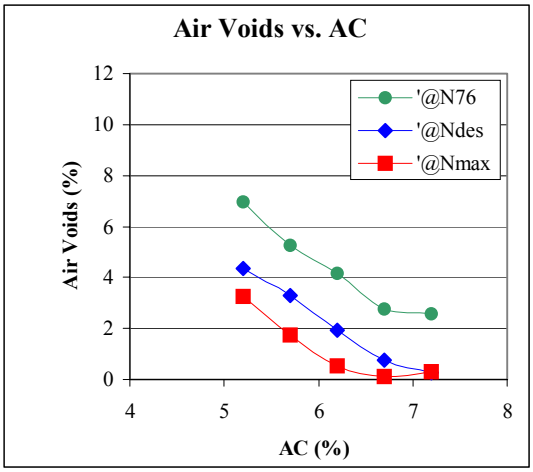

Triaxial Test Results for 9.5mm Limestone with FAA of 44 and Gradation Plotting Below the Restricted zone.

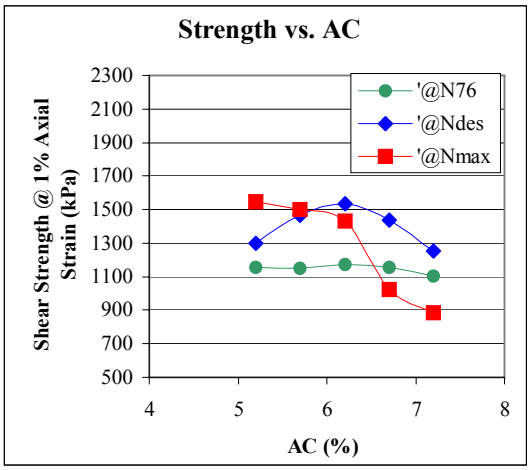

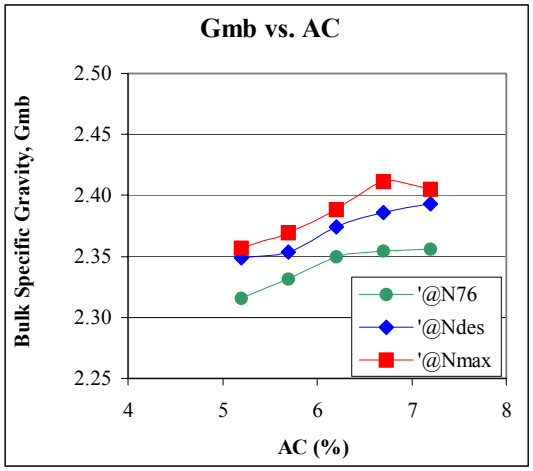

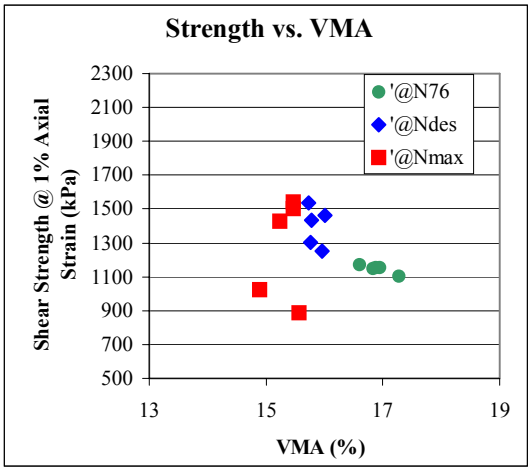

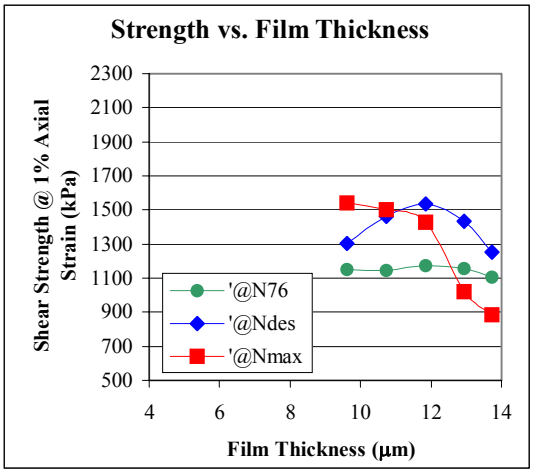

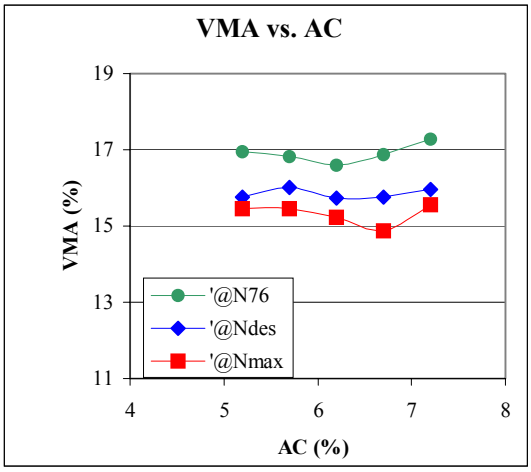

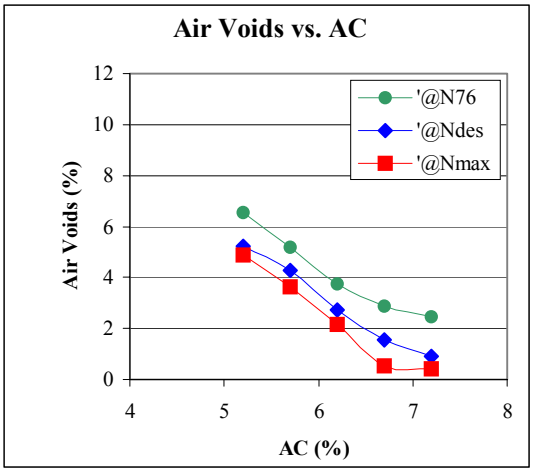

Triaxial Test Results for 9.5mm Limestone with FAA of 50 and Gradation Plotting Through the Restricted zone.

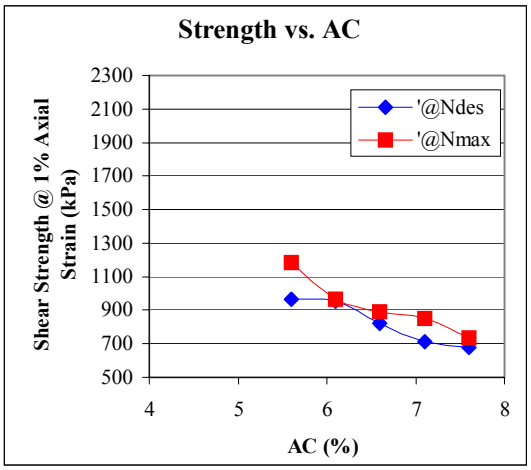

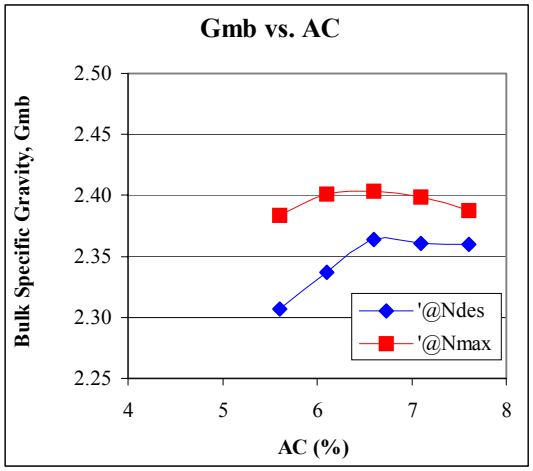

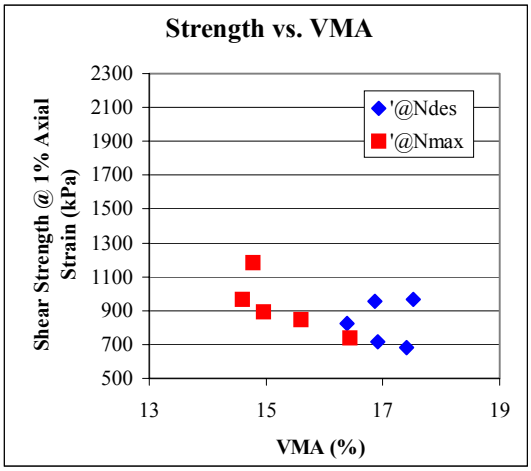

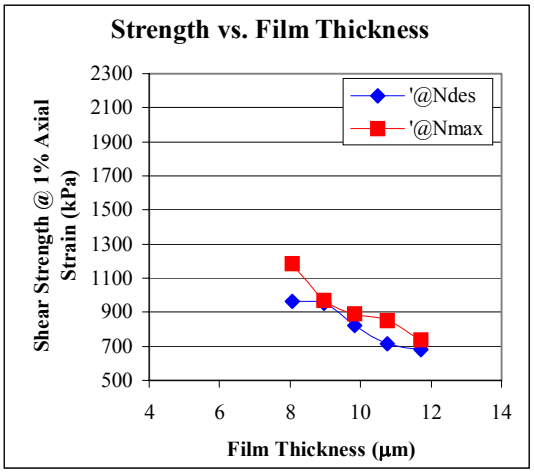

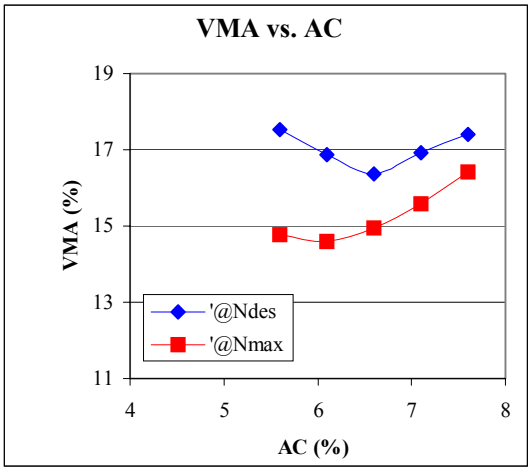

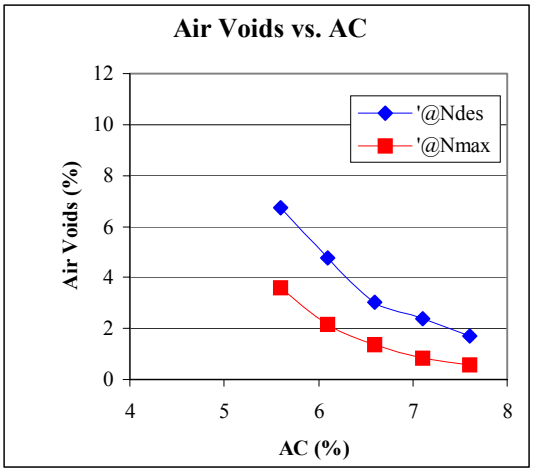

Triaxial Test Results for 9.5mm Limestone with FAA of 50 and Gradation Plotting Below the Restricted zone.

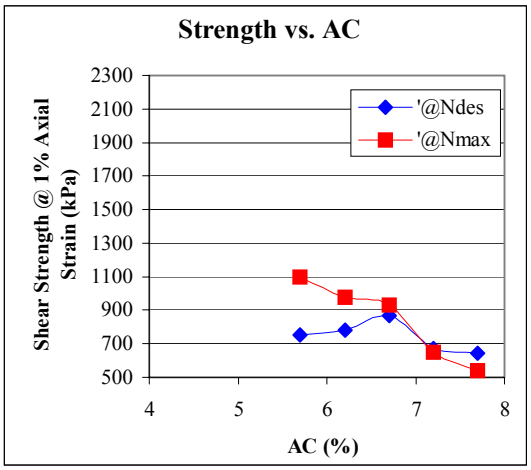

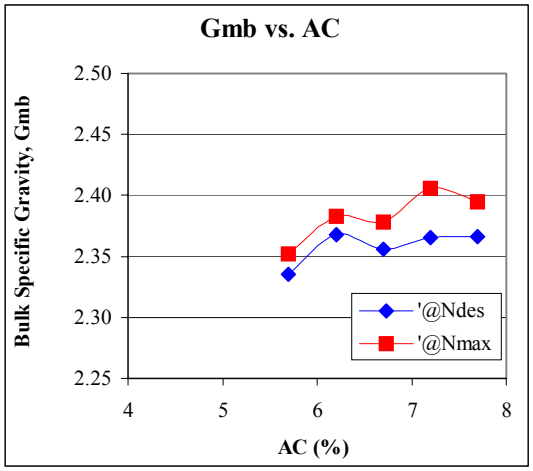

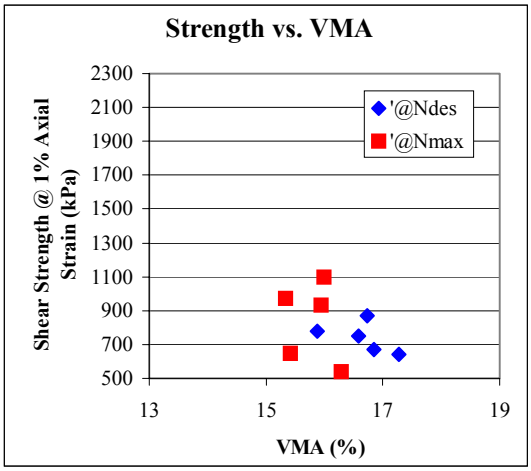

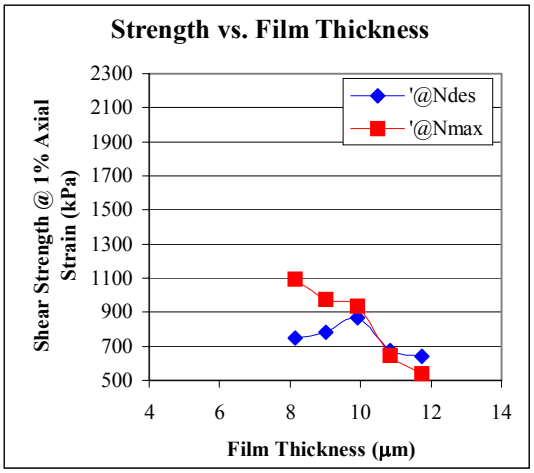

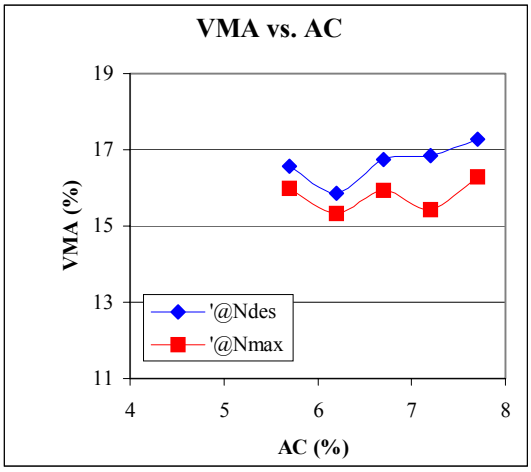

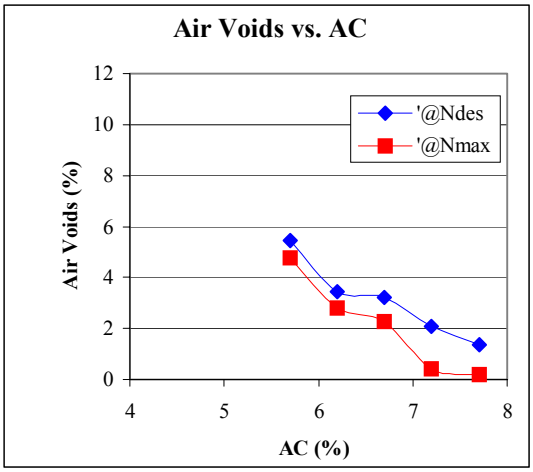

Triaxial Test Results for 9.5mm Granite with FAA of 44 and Gradation Plotting Through the Restricted zone.

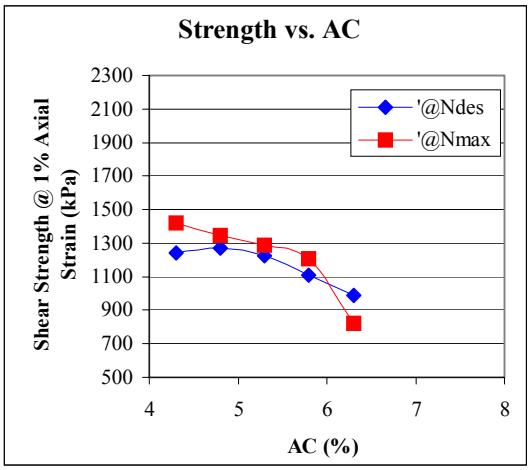

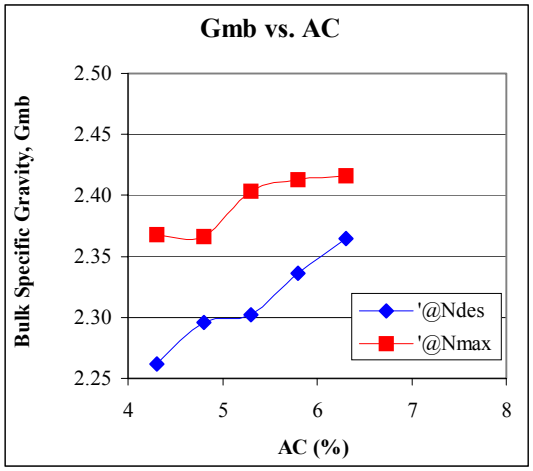

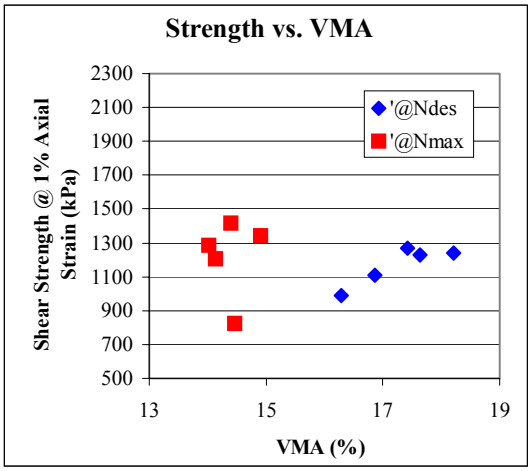

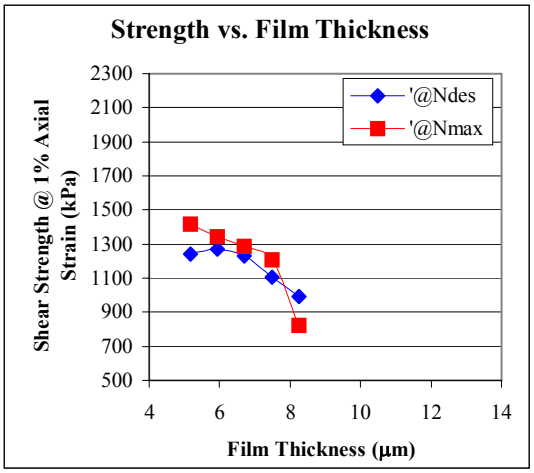

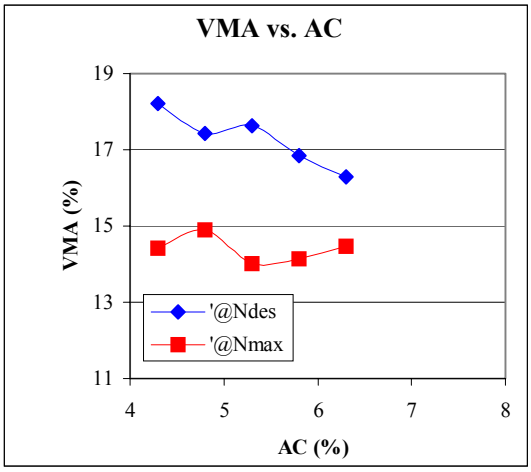

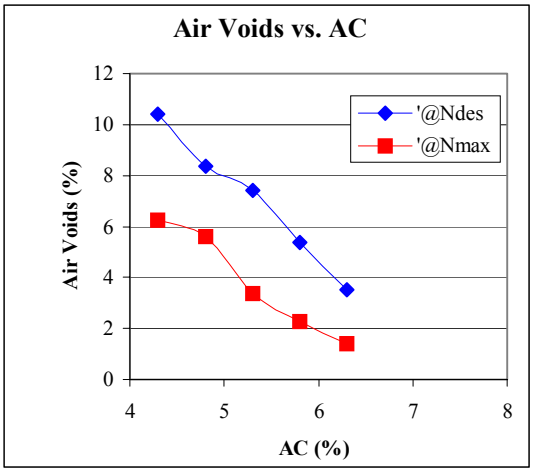

Triaxial Test Results for 9.5mm Granite with FAA of 44 and Gradation Plotting Below the Restricted zone.

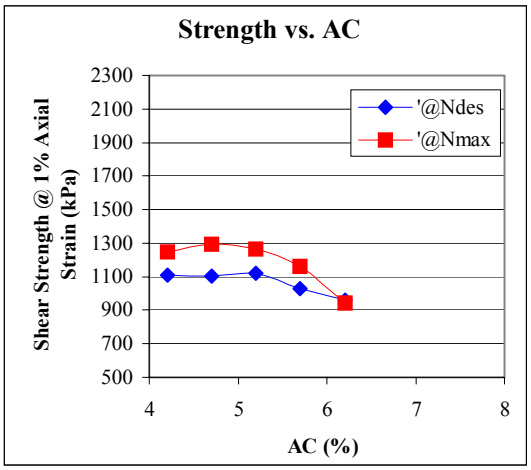

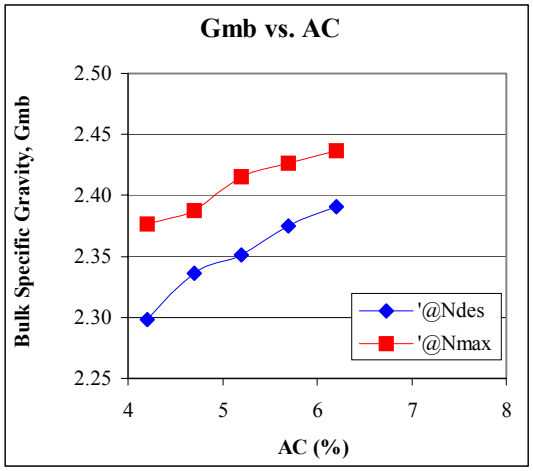

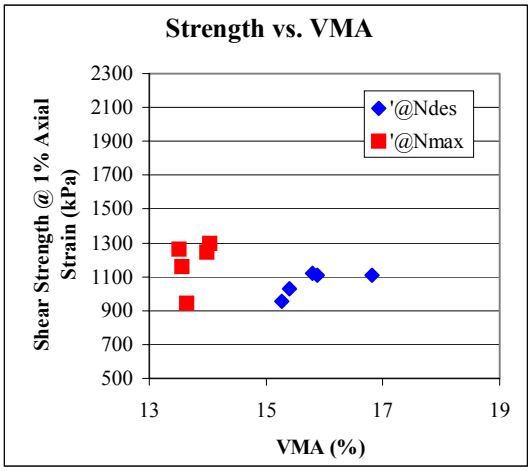

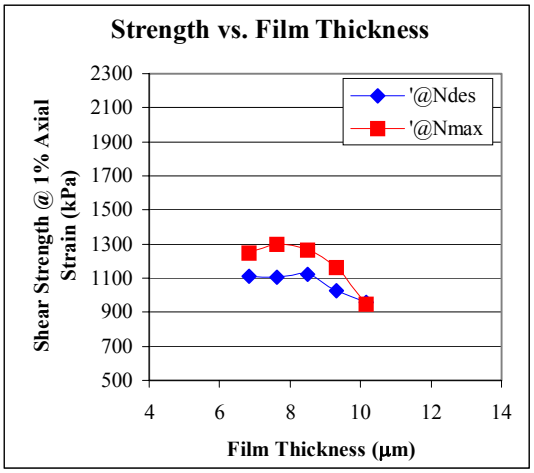

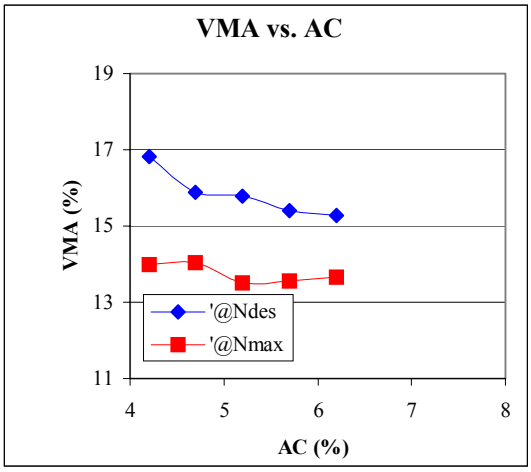

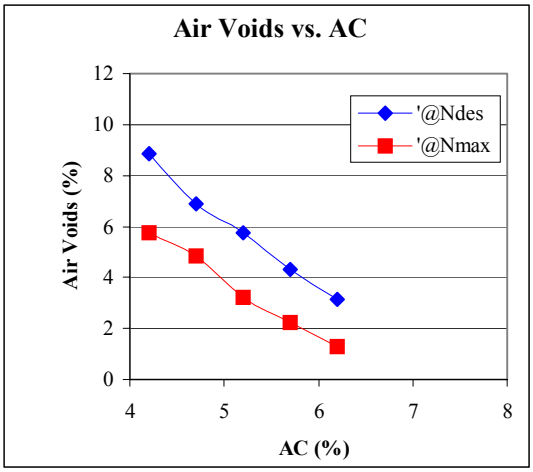

Triaxial Test Results for 9.5mm Granite with FAA of 50 and Gradation Plotting Through the Restricted zone.

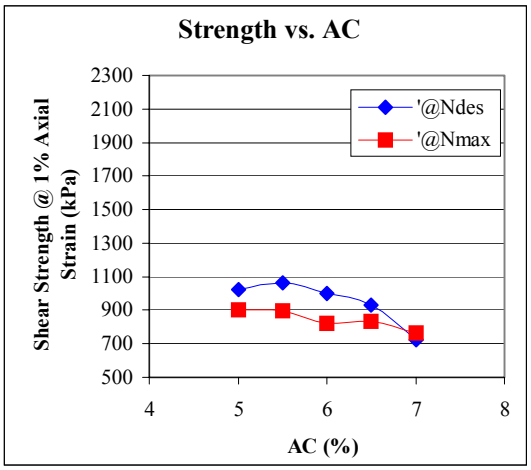

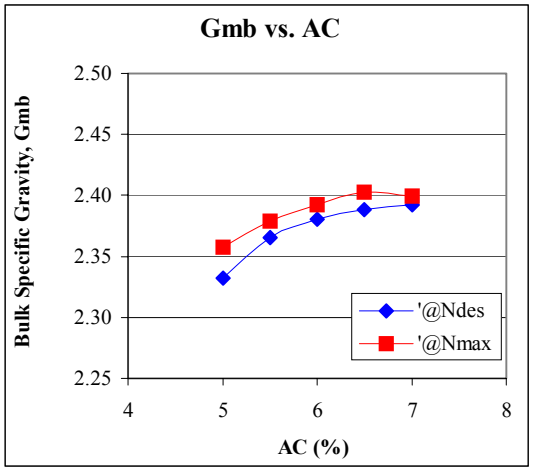

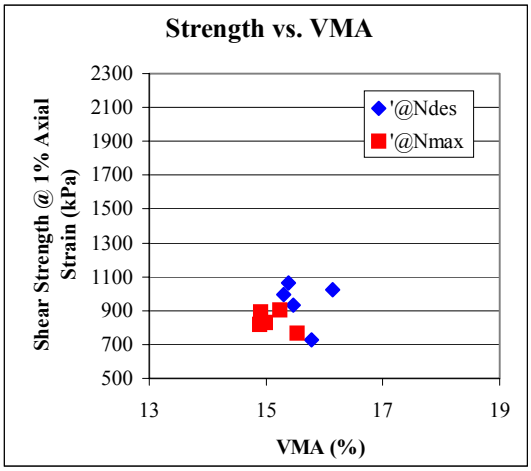

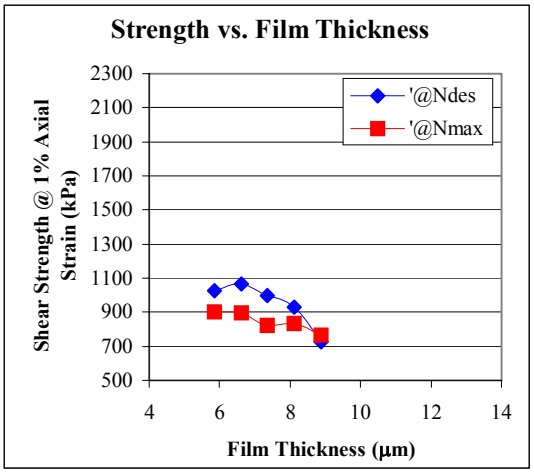

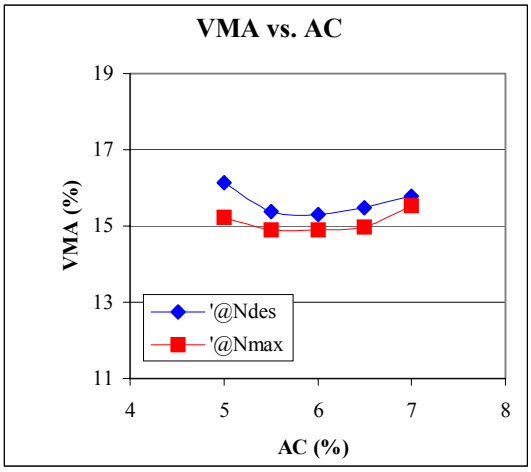

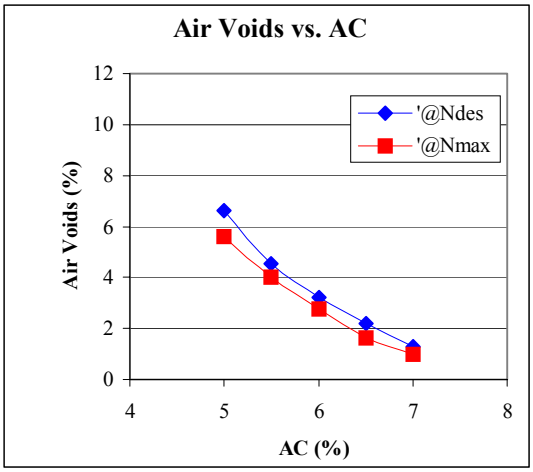

Triaxial Test Results for 9.5mm Granite with FAA of 50 and Gradation Plotting Below the Restricted zone.

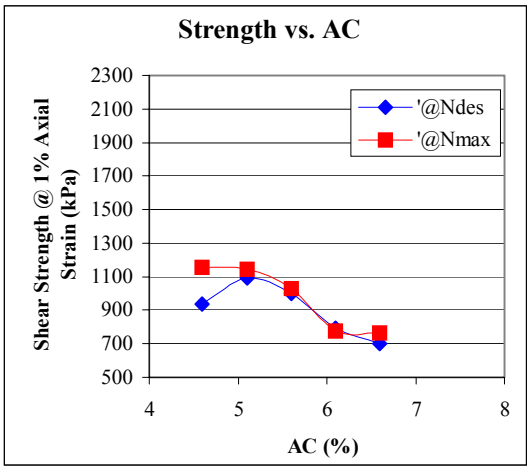

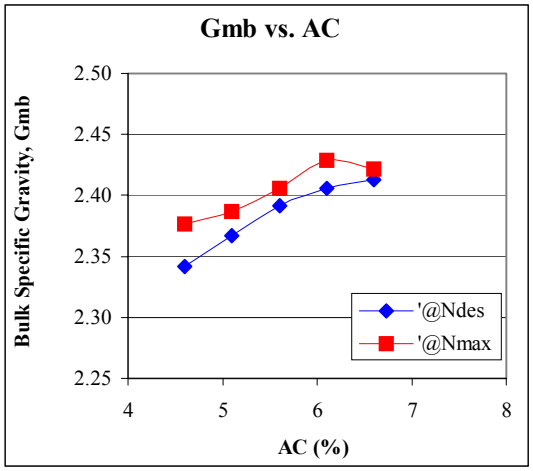

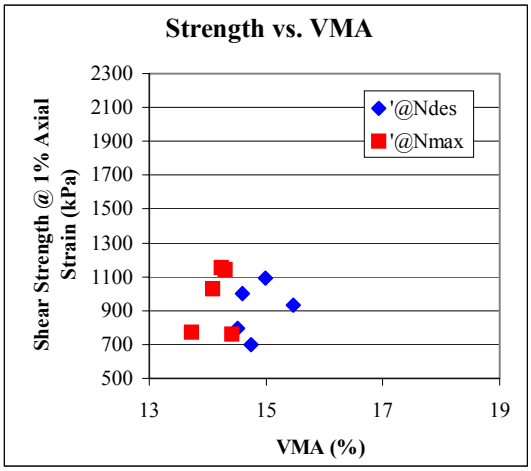

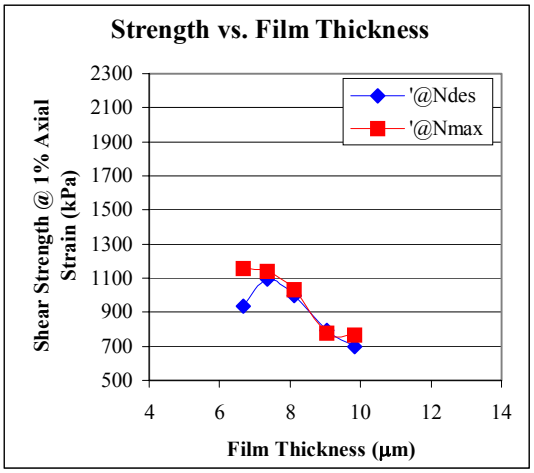

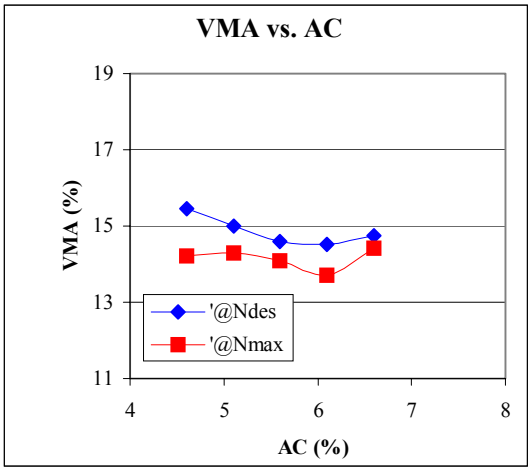

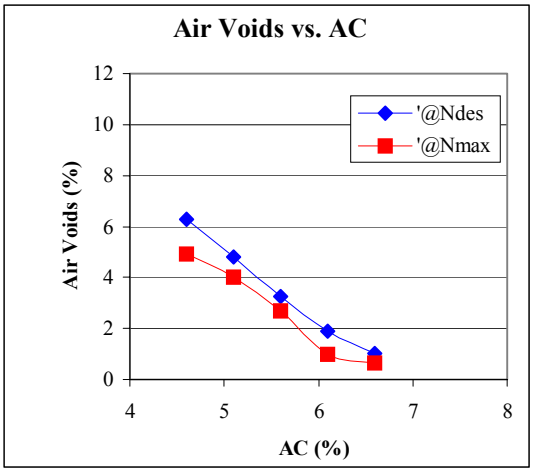

APPENDIX E3 Statistical Analysis of Triaxial Test Results

Table E3. 1 Regression Analysis of Shear Strength and Height to Diameter Ratio in Triaxial Test.

Dependent Variable: Shear Strength @ 1%Strain Analysis of Variance					
Source	df	SS	MS	F	Pr > F
Model	1	119330.532	119330.532	10.562	0.0117
Error	8	90387.709	11298.464		
Total	9	209718.241			
R-square = 0.5690	Adjusted R-square = 0.5151				
Parameter Estimate					
Variable	df	Parameter Estimate	Standard Error	T for H_0	Pr > T
Intercept	1	603.585	109.963	5.489	0.0006
H/D	1	247.932	76.290	3.250	0.0117

Table E3. 2 Regression Analysis of Triaxial Shear Strength and PURWheel Rut Depth.

Dependent Variable: Shear Strength @ 1%Strain Analysis of Variance					
Source	df	SS	MS	F	Pr > F
Model	1	0.312	0.312	37.265	3.75E-08
Error	78	0.653	0.008		
Total	79	0.965			
R-square = 0.3233	Adjusted R-square = 0.3146				
Parameter Estimate					
Variable	df	Parameter Estimate	Standard Error	T for H_0	Pr > T
Log(Intercept)	1	3.126	0.022	141.974	6.45E-96
Rut Depth	1	-0.396	0.065	-6.104	3.75E-08

Table E3. 3 ANOVA for Factor Effects on Triaxial Test Results.

Dependent Variable: Triaxial Shear Strength at 1 percent axial strain					
Source	df	SS	MS	F	Pr > F
Model	39	21476019	550667	36.94	0.0001
Error	280	4173909	14907		
Total	319	25649928			
R-square = 0.8373					
Parameter Estimate					
Source	df	Type I SS	MS	F	Pr > F
Nominal Max. Size	1	28309	28309	1.90	0.1693
Coarse Agg. Type	1	1252676	1252676	84.03	0.0001
Fine Agg. Angularity	1	10029599	10029599	672.82	0.0001
Gradation	1	544005	544005	36.49	0.0001
Gyration	1	309321	309321	20.75	0.0001
AC level	4	5010502	1252626	84.03	0.0001
Nominal * Coarse	1	108339	108339	7.27	0.0074
Nominal * FAA	1	270514	270514	18.15	0.0001
Nominal * Gradation	1	15172	15172	1.02	0.3139
Nominal*Gyration	1	65083	65083	4.37	0.0376
Nominal * AC level	4	74221	18555	1.24	0.2922
Coarse * FAA	1	2443564	2443564	163.92	0.0001
Coarse * Gradation	1	4493	4493	0.30	0.5835
Coarse * Gyration	1	469	469	0.03	0.8594
Coarse * AC level	4	679957	169989	11.40	0.0001
FAA * Gradation	1	49129	49129	3.30	0.0705
FAA * Gyration	1	31450	31450	2.11	0.1475
FAA * AC level	4	132657	33164	2.22	0.0665
Gradation * Gyration	1	9277	9277	0.62	0.4308
Gradation * AC level	4	32844	8211	0.55	0.6986
Gyration * AC level	4	384439	96110	6.45	0.0001

Table E3. 4 SNK for Main Factors on Triaxial Test Results.

Variable	Value	Mean	Results
Nominal Maximum Size	19mm	1081.84	19mm = 9.5mm
	9.5mm	1063.03	
Coarse Aggregate Type	Limestone	1135.00	Limestone > Granite
	Granite	1009.87	
Fine Aggregate Angularity	44	1249.47	44 > 50
	50	895.40	
Gradation	Through	1113.67	Through > Below
	Below	1031.20	
No. of Gyrations	152	1103.53	152 > 96
	96	1041.34	
AC Level	1	1191.69	1=2>3>4>5
	2	1189.81	
	3	1122.44	
	4	987.04	
	5	871.20	

Table E3. 5 Regression Analysis of Triaxial Shear Strength and VFA.

Dependent Variable: Shear Strength @ 1%Strain Analysis of Variance					
Source	df	SS	MS	F	Pr > F
Model	2	8511115	4255558	49.220	5.27E-20
Error	437	37782656	86459.17		
Total	439	46293771			
R-square = 0.1839 Adjusted R-square = 0.1801					
Parameter Estimate					
Variable	df	Parameter Estimate	Standard Error	T for H_0	Pr > T
Intercept	1	1471.958	313.700	4.692	3.62E-06
VFA	1	1.767	8.737	0.202	0.8398
VFA^2	1	-0.075	0.059	-1.264	0.2068

Table E3. 6 Regression Analysis of Triaxial Shear Strength and Film Thickness.

Dependent Variable: Shear Strength @ 1%Strain Analysis of Variance					
Source	df	SS	MS	F	Pr > F
Model	2	16034176	8017088	115.780	4.49E-41
Error	437	30259596	69243.93		
Total	439	46293771			
R-square = 0.3464 Adjusted R-square = 0.3434					
Parameter Estimate					
Variable	df	Parameter Estimate	Standard Error	T for H_0	Pr > T
Intercept	1	2851.907	172.258	16.556	3.84E-48
FT	1	-313.823	39.433	-7.958	1.51E-14
FT^2	1	12.946	2.185	5.925	6.35E-09